INTERACTIONS OF PLANTS WITH BACTERIA AND FUNGI: MOLECULAR AND EPIGENETIC PLASTICITY OF THE HOST

EDITED BY: Valentina Fiorilli, Marco Catoni, Luisa Lanfranco and Nicolae Radu Zabet

PUBLISHED IN: Frontiers in Plant Science and Frontiers in Microbiology

frontiers Research Topics

frontiers

ISSN 1664-8714
ISBN 978-2-88963-654-9
DOI 10.3389/978-2-88963-654-9

About Frontiers

Frontiers is more than just an open-access publisher of scholarly articles: it is a pioneering approach to the world of academia, radically improving the way scholarly research is managed. The grand vision of Frontiers is a world where all people have an equal opportunity to seek, share and generate knowledge. Frontiers provides immediate and permanent online open access to all its publications, but this alone is not enough to realize our grand goals.

Frontiers Journal Series

The Frontiers Journal Series is a multi-tier and interdisciplinary set of open-access, online journals, promising a paradigm shift from the current review, selection and dissemination processes in academic publishing. All Frontiers journals are driven by researchers for researchers; therefore, they constitute a service to the scholarly community. At the same time, the Frontiers Journal Series operates on a revolutionary invention, the tiered publishing system, initially addressing specific communities of scholars, and gradually climbing up to broader public understanding, thus serving the interests of the lay society, too.

Dedication to Quality

Each Frontiers article is a landmark of the highest quality, thanks to genuinely collaborative interactions between authors and review editors, who include some of the world's best academicians. Research must be certified by peers before entering a stream of knowledge that may eventually reach the public - and shape society; therefore, Frontiers only applies the most rigorous and unbiased reviews.
Frontiers revolutionizes research publishing by freely delivering the most outstanding research, evaluated with no bias from both the academic and social point of view. By applying the most advanced information technologies, Frontiers is catapulting scholarly publishing into a new generation.

What are Frontiers Research Topics?

Frontiers Research Topics are very popular trademarks of the Frontiers Journals Series: they are collections of at least ten articles, all centered on a particular subject. With their unique mix of varied contributions from Original Research to Review Articles, Frontiers Research Topics unify the most influential researchers, the latest key findings and historical advances in a hot research area! Find out more on how to host your own Frontiers Research Topic or contribute to one as an author by contacting the Frontiers Editorial Office: researchtopics@frontiersin.org

INTERACTIONS OF PLANTS WITH BACTERIA AND FUNGI: MOLECULAR AND EPIGENETIC PLASTICITY OF THE HOST

Topic Editors:
Valentina Fiorilli, University of Turin, Italy
Marco Catoni, University of Birmingham, United Kingdom
Luisa Lanfranco, University of Turin, Italy
Nicolae Radu Zabet, University of Essex, United Kingdom

Citation: Fiorilli, V., Catoni, M., Lanfranco, L., Zabet, N. R., eds. (2020). Interactions of Plants With Bacteria and Fungi: Molecular and Epigenetic Plasticity of the Host. Lausanne: Frontiers Media SA. doi: 10.3389/978-2-88963-654-9

Table of Contents

05 ***Editorial: Interactions of Plants With Bacteria and Fungi: Molecular and Epigenetic Plasticity of the Host***
Valentina Fiorilli, Marco Catoni, Luisa Lanfranco and Nicolae Radu Zabet

08 ***The* Botrytis cinerea *Xylanase BcXyl1 Modulates Plant Immunity***
Yuankun Yang, Xiufen Yang, Yijie Dong and Dewen Qiu

21 ***Dominant and Recessive Major R Genes Lead to Different Types of Host Cell Death During Resistance to* Xanthomonas oryzae *in Rice***
Jianbo Cao, Meng Zhang, Jinghua Xiao, Xianghua Li, Meng Yuan and Shiping Wang

35 **GmDAD1*, a Conserved* Defender Against Cell Death 1 *(*DAD1*) From Soybean, Positively Regulates Plant Resistance Against* Phytophthora *Pathogens***
Qiang Yan, Jierui Si, Xiaoxia Cui, Hao Peng, Maofeng Jing, Xin Chen, Han Xing and Daolong Dou

47 ***Differences in Ear Rot Resistance and* Fusarium verticillioides*-Produced Fumonisin Contamination Between Polish Currently and Historically Used Maize Inbred Lines***
Elżbieta Czembor, Agnieszka Waśkiewicz, Urszula Piechota, Marta Puchta, Jerzy H. Czembor and Łukasz Stępień

61 ***Cytoprotective Co-chaperone BcBAG1 is a Component for Fungal Development, Virulence, and Unfolded Protein Response (UPR) of* Botrytis cinerea**
Honghong Zhang, Yurong Li, Martin B. Dickman and Zonghua Wang

76 ***Spatial Effects and GWA Mapping of Root Colonization Assessed in the Interaction Between the Rice Diversity Panel 1 and an Arbuscular Mycorrhizal Fungus***
Hazel Davidson, Roshi Shrestha, Thomas Cornulier, Alex Douglas, Tony Travis, David Johnson† and Adam H. Price

90 ***Plant Aquaporins in Infection by and Immunity Against Pathogens – A Critical Review***
Liyuan Zhang, Lei Chen and Hansong Dong

106 ***Comparative Transcriptomics and Proteomics of* Atractylodes lancea *in Response to Endophytic Fungus* Gilmaniella *sp. AL12 Reveals Regulation in Plant Metabolism***
Jie Yuan, Wei Zhang, Kai Sun, Meng-Jun Tang, Piao-Xue Chen, Xia Li and Chuan-Chao Dai

124 ***Diazotrophic* Paenibacillus beijingensis *BJ-18 Provides Nitrogen for Plant and Promotes Plant Growth, Nitrogen Uptake and Metabolism***
Yongbin Li, Yunlong Li, Haowei Zhang, Minyang Wang and Sanfeng Chen

142 ***Arbuscular Mycorrhizal Symbiosis: Plant Friend or Foe in the Fight Against Viruses?***
Laura Miozzi, Anna Maria Vaira, Marco Catoni, Valentina Fiorilli, Gian Paolo Accotto and Luisa Lanfranco

151 **Streptomyces *Strains Induce Resistance to* Fusarium oxysporum *f. sp.* lycopersici *Race 3 in Tomato Through Different Molecular Mechanisms***
Sakineh Abbasi, Naser Safaie, Akram Sadeghi and Masoud Shamsbakhsh

167 ***Plant Host-Associated Mechanisms for Microbial Selection***
Piet Jones, Benjamin J. Garcia, Anna Furches, Gerald A. Tuskan and Daniel Jacobson

181 ***Improved Powdery Mildew Resistance of Transgenic Nicotiana* benthamiana *Overexpressing the* Cucurbita moschata CmSGT1 *Gene***
Wei-Li Guo, Bi-Hua Chen, Yan-Yan Guo, He-Lian Yang, Jin-Yan Mu, Yan-Li Wang, Xin-Zheng Li and Jun-Guo Zhou

frontiers in Plant Science

EDITORIAL
published: 04 March 2020
doi: 10.3389/fpls.2020.00274

Editorial: Interactions of Plants With Bacteria and Fungi: Molecular and Epigenetic Plasticity of the Host

Valentina Fiorilli[1]*, *Marco Catoni*[2]*, *Luisa Lanfranco*[1]* and *Nicolae Radu Zabet*[3]*

[1] Department of Life Sciences and Systems Biology, University of Turin, Turin, Italy, [2] School of Biosciences, University of Birmingham, Birmingham, United Kingdom, [3] School of Life Sciences, University of Essex, Colchester, United Kingdom

Keywords: plant-bacterial interactions, plant-fungal interactions, molecular mechanisms, omics tools, genotypes

Editorial on the Research Topic

Interactions of Plants with Bacteria and Fungi: Molecular and Epigenetic Plasticity of the Host

In both natural and agricultural environments plants live in association with a multitude of microorganisms belonging to different microbial types, mainly bacteria and fungi. Some of these microbes regulate positively plant growth and productivity, while others can damage the host with important ecological and economic consequences. During the last decades, many studies contributed to unravel the multifaceted process at the basis of plant microbe-interactions (Cheng et al., 2019). However, many issues remain still unsolved, as for example how plants could discriminate between beneficial and pathogenic microbes or between different pathogen attackers, or which gene regulatory networks are responsible for host-microbe interactions and their degree of conservation among species.

When challenged by pathogens, plants trigger highly complex defense system, in order to recognize invader organisms and translate this signal into defense such as the expression of defense response genes. This plant immune system relies on a wide variety of different strategies, showing high plasticity in the response depending on the attacker lifestyle. These processes involve the regulation of genes, small RNAs, signal molecules, plant hormones, which can act locally or systemically through plant organs.

On the other hand, plants are strictly associated with microbial symbionts in natural environments, often poor in nutrients (van der Heijden et al., 2008). Beneficial microbes in the soil could help the host to overcome the nutritional and abiotic stresses, boost plant growth and fitness, and sustain plant productivity. In addition, beneficial associations can enhance the defensive ability of plants, resulting in faster and stronger defense activation upon pathogens attacks. While these phenomena have been widely described, the underling molecular mechanisms remain elusive. Changes in transcription, protein regulation and phytohormones accumulation have been reported during plant-beneficial microbe interactions. Moreover, epigenetic modifications triggering stable changes in plant's transcriptional capacity are emerging as relevant modulator of plant's responses to microbes, with potential role in memory and priming (Alonso et al., 2019).

With 13 original contributions, this Research Topic provides an overview of the current state of the art on the field of plant microbe-interactions. This Topic includes a combination of Reviews, Mini Reviews and Original Research Articles, focused on the role of the molecular infrastructures evolved by plants to manage different microbe-interactions, revealing that a complex plant–microorganism genotype and environment combinations could determine the outcome of the interaction.

Recently, genome wide RNA sequencing has become a popular approach to study transcriptional changes also in non-model organisms. Yuan et al. investigated the increased growth and

OPEN ACCESS

Edited by:
Victor Flors,
University of Jaume I, Spain

Reviewed by:
Juan Antonio Lopez Raez,
Experimental Station of Zaidín (EEZ), Spain

***Correspondence:**
Valentina Fiorilli
valentina.fiorilli@unito.it
Marco Catoni
m.catoni@bham.ac.uk
Luisa Lanfranco
luisa.lanfranco@unito.it
Nicolae Radu Zabet
nzabet@essex.ac.uk

Specialty section:
This article was submitted to Plant Microbe Interactions, a section of the journal Frontiers in Plant Science

Received: *14 January 2020*
Accepted: *21 February 2020*
Published: *04 March 2020*

Citation:
Fiorilli V, Catoni M, Lanfranco L and Zabet NR (2020) Editorial: Interactions of Plants With Bacteria and Fungi: Molecular and Epigenetic Plasticity of the Host. Front. Plant Sci. 11:274. doi: 10.3389/fpls.2020.00274

sesquiterpenoids accumulation induced by the endophyte *Gilmaniella* in the medicinal herb *Atractylodes lancea* combining transcriptomic (RNAseq) and proteomic approaches. Authors observed that the presence of the endophyte induced in the host suppression of genes involved in plant immunity and signaling, while genes involve in both primary and secondary metabolism such as phenylpropanoid and zeatin biosynthesis were upregulated.

An emerging theme is the significance of genetic variation in differentiating the biological response to harmful and beneficial microorganisms. In this Research Topic a number of contributions addressed the role of different host genotypes in plant-microbe interactions. Czembor et al. studied 98 maize inbreed lines, historically used in Poland, in relation to resistance to *Fusarium*, across a 2 year in-field experiment. They coupled HPLC analysis for the detection of fumolisin content to NGS approach (ddRADseq) to infer genetic distances across the lines; they then correlate genetic distance with resistance to *Fusarium*. Authors observed large differences in resistance and fumolisin accumulation across the lines and concluded that old lines represent a valuable source of resistant traits against *Fusarium*.

Another emerging and powerful approach to identify novel genes involved in plant-microbe interactions is represented by Genome-Wide Association (GWA) studies. The contribution of plant genetic variability to the positive effects of arbuscular mycorrhizal (AM) symbiosis have been investigated in different crops (Diedhiou et al., 2016; Lehnert et al., 2017; Watts-Williams et al., 2019), and, in this line, Davidson et al. tested the responsiveness to AM colonization of 334 rice cultivars inoculated with the AM fungus *Rhizophagus irregularis*. GWA mapping for hyphal colonization revealed 23 quantitative trait loci (QTLs) with putative impact on AM fungal colonization and identified candidate genes associated to three QTLs.

More specific topics on plant-pathogen interactions are addressed by Cao et al. who investigated the hypersensitive response (HR) against *Xanthomonas oryzae* pv. *oryzae* (*Xoo*) in rice mediated by genes ascribed to the major disease resistance pathway. By observing the physiological response to infection in the xylem parenchyma, authors concluded that dominant resistant genes mediate HR by prevalent autophagy-like cell death, while recessive genes induce HR by vacuole-mediated cell death.

Legumes and vegetables pathogens affect field-grown and greenhouse-grown crops worldwide. Two works investigated, in different host plants, the role of a key component of the plant disease-associated signal transduction pathway (Guo et al.) and a negative regulator of programmed cell death (PCD) process (Yan et al.). Both reports highlighted how manipulating the expression of a specific gene of interest, using a genetic approach, could determine the biological function of genes in the plant resistance process. These results pave the way for the identification of molecular targets potentially useful for breeding programs to control pathogen resistance in crops.

Two studies, Zhang H. et al. and Yang et al., focused on the study of the microbial partner, characterizing two genes which contribute to *Botrytis cinerea* virulence, one of the most notorious pathogenic species, in different host plants.

An emerging theme in the field of plant-microbe interactions is the relevance of mineral nutrients availability. Mineral nutrients are not only important for the growth and development of plants and microorganisms but they also play a key role in the dynamics and the outcome of plant -pathogenic/beneficial microbes interactions. Li et al. studied the association of the diazotrophic bacteria *Paenibacillus beijingensis* with wheat, maize and cucumber in conditions of high and low nitrogen in the soil, and they observed beneficial effects on plant growth related to improved nitrogen uptake and assimilation, in line to previous findings from other bacterial/host combinations (Xie et al., 2016; Hao and Chen, 2017). Zhang L. et al. reviewed current knowledge on the roles of plant aquaporins (AQPs) of the plasma membrane intrinsic protein family. The authors highlighted that AQPs are not only involved in maintaining the plant water or mineral nutrition status, but they also contribute to control plant immune system and pathogen susceptibility.

In nature, plants are very likely subjected to multiple complex interactions involving several organisms, rather than single bipartite relationships. Although less investigated, multiple interactions represent a system more similar to the natural environment, and their study can assist to select or design optimal bio-fertilization or bio-control procedures. In this Research Topic, different contributions addressed this issue. Abbasi et al. compared the ability of different plant growth promoting rhizobacteria (PGPR) and the application of a chemical fungicide to antagonize *Fusarium oxysporum* f. sp. *lycopersici* race 3 (*FOL*) in tomato plants. Interestingly, all bacterial treatments mitigated *FOL* disease symptoms at the same level or better than chemical treatments. In a mini-review, Miozzi et al. provided an overview of the impact of the arbuscular mycorrhizal symbiosis on plant viral diseases. The authors proposed the term "Mycorrhizal-Induced Susceptibility" (MIS) to describe the enhanced viral infection reported in many tripartite interactions (plant-mycorrhiza-virus), in opposition to the Mycorrhizal-Induced Resistance (MIR) that is often observed in response to infection by bacterial and fungal pathogens. Finally, Jones et al. summarized recent research that expands upon the role of keystone microbial species, phytohormones, and abiotic stress and how they relate to plant driven dynamic microbial structuring.

Plants are extremely plastic in their interaction with microorganisms, and the heterogeneous composition of the works published in this Research Topic well-represents the variety of responses, model and non-model organisms and experimental approaches used to investigate this subject. The knowledge of the determinants and the mechanisms that regulate plant-microbe interactions with different level of complexity can be instrumental for the development of new agro-biotechnological strategies of crop protection, with the aim to improve food security and environmental sustainability.

AUTHOR CONTRIBUTIONS

All authors listed have made a substantial, direct and intellectual contribution to the work, and approved it for publication.

FUNDING

Research in the laboratories of the Topic Editors was supported by the European Union's Horizon 2020 research and innovation programme under grant agreement no. 727929 (TOMRES) and from Competitive Research Grant CRG2017 given to LL from King Abdullah University of Science and Technology and 60% Project (University of Turin) given to VF.

REFERENCES

Alonso, C., Ramos-Cruz, D., and Becker, C. (2019). The role of plant epigenetics in biotic interactions. *New Phytol.* 221, 731–737. doi: 10.1111/nph.15408

Cheng, Y. T., Zhang, L., and He, S. Y. (2019). Plant-microbe interactions facing environmental challenge. *Cell Host Microbe.* 26, 183–192. doi: 10.1016/j.chom.2019.07.009

Diedhiou, A. G, Mbaye, F. K, Mbodj, D., Faye, M. N, Pignoly, S., Ndoye, I., et al. (2016). Field trials reveal ecotype-specific responses to mycorrhizal inoculation in rice. *PLoS ONE* 11:e0167014. doi: 10.1371/journal.pone.0167014

Hao, T., and Chen, S. (2017). Colonization of wheat, maize and cucumber by *Paenibacillus polymyxa* WLY78. *PLoS ONE* 12:e0169980. doi: 10.1371/journal.pone.0169980

Lehnert, H., Serfling, A., Enders, M., Friedt, W., and Ordon, F. (2017). Genetics of mycorrhizal symbiosis in winter wheat (*Triticum aestivum*). *New Phytol.* 215, 779–791. doi: 10.1111/nph.14595

van der Heijden, M. G., Bardgett, R. D., and van Straalen, N. M. (2008). The unseen majority: soil microbes as drivers of plant diversity and productivity in terrestrial ecosystems. *Ecol. Lett.* 11, 296–310. doi: 10.1111/j.1461-0248.2007.01139.x

Watts-Williams, S. J., Emmett, B. D., Levesque-Tremblay, V., MacLean, A. M., Sun, X., Satterlee, J. W., et al. (2019). Diverse Sorghum bicolor accessions show marked variation in growth and transcriptional responses to arbuscular mycorrhizal fungi. *Plant Cell Env.* 42, 1758–1774. doi: 10.1111/pce.13509

Xie, J., Shi, H., Du, Z., Wang, T., Liu, X., and Chen, S. (2016). Comparative genomic and functional analysis reveal conservation of plant growth promoting traits in *Paenibacillus polymyxa* and its closely related species. *Sci. Rep.* 6:21329. doi: 10.1038/srep21329

Conflict of Interest: The authors declare that the research was conducted in the absence of any commercial or financial relationships that could be construed as a potential conflict of interest.

frontiers in Microbiology

ORIGINAL RESEARCH
published: 23 October 2018
doi: 10.3389/fmicb.2018.02535

The *Botrytis cinerea* Xylanase BcXyl1 Modulates Plant Immunity

Yuankun Yang, Xiufen Yang, Yijie Dong and Dewen Qiu**

The State Key Laboratory for Biology of Plant Diseases and Insect Pests, Institute of Plant Protection, Chinese Academy of Agricultural Sciences, Beijing, China

Botrytis cinerea is one of the most notorious pathogenic species that causes serious plant diseases and substantial losses in agriculture throughout the world. We identified BcXyl1 from *B. cinerea* that exhibited xylanase activity. Expression of the *BcXyl1* gene was strongly induced in *B. cinerea* infecting *Nicotiana benthamiana* and tomato plants, and *BcXyl1* deletion strains severely compromised the virulence of *B. cinerea*. BcXyl1 induced strong cell death in several plants, and cell death activity of BcXyl1 was independent of its xylanase activity. Purified BcXyl1 triggered typically PAMP-triggered immunity (PTI) responses and conferred resistance to *B. cinerea* and TMV in tobacco and tomato plants. A 26-amino acid peptide of BcXyl1 was sufficient for elicitor function. Furthermore, the BcXyl1 death-inducing signal was mediated by the plant LRR receptor-like kinases (RLKs) BAK1 and SOBIR1. Our data suggested that BcXyl1 contributed to *B. cinerea* virulence and induced plant defense responses.

Keywords: *Botrytis cinerea*, xylanase, BcXyl1, plant immunity, virulence

OPEN ACCESS

Edited by:
Luisa Lanfranco,
Università degli Studi di Torino, Italy

Reviewed by:
Franco Faoro,
Università degli Studi di Milano, Italy
Mario Serrano,
Universidad Nacional Autónoma de México, Mexico

****Correspondence:***
Yijie Dong
nkdongyijie@163.com
Dewen Qiu
qiudewen@caas.cn

Specialty section:
This article was submitted to Plant Microbe Interactions, a section of the journal Frontiers in Microbiology

Received: *01 August 2018*
Accepted: *04 October 2018*
Published: *23 October 2018*

Citation:
Yang Y, Yang X, Dong Y and Qiu D (2018) The Botrytis cinerea Xylanase BcXyl1 Modulates Plant Immunity. Front. Microbiol. 9:2535. doi: 10.3389/fmicb.2018.02535

INTRODUCTIONS

Botrytis cinerea is a necrotrophic pathogen, causing widespread plant diseases and enormous economic losses in a large number of important crops throughout the world (Prins et al., 2000). *B. cinerea* can infect various organs in plants, including leaves, bulb, flowers, fruits, and root tubers. The infection process of *B. cinerea* mainly includes two typical stages: local lesions at an early stage and a late stage of fast-spreading lesions.

The plant cell wall is a natural barrier, which provides mechanical strength and rigidity to prevent pathogen infection. To establish successful colonization, *B. cinerea*, like other fungal pathogen, secretes a large number of cell wall-degrading enzymes (CWDEs) to degrade the plant defensive barriers during the infection process, thereby to permit pathogens to invade plant tissue and supply pathogens with nutrients (Cantarel et al., 2009; Kubicek et al., 2014). These CWDEs, including pectinases, cellulases, cutinases, and xylanases, are generally regarded as important virulence factors through the maceration of host tissues and the degradation of host macromolecules (Prins et al., 2000). The effects of targeted deletion of some genes encoding CWDEs support their direct involvement in the infection process. For example, deletion of the pectate lyase gene *CcpelA* and the pectate lyase gene *PelB* in *Colletotrichum coccodes*, resulted in a substantial loss of virulence on green tomato fruit and reduced virulence on avocado, respectively (Yakoby et al., 2001; Ben-Daniel et al., 2011). Targeted deletion of VdCUT11, a cutinase in *V. dahliae*, significantly compromised virulence on cotton plants (Gui Y. et al., 2017). However, the specific roles of the majority of CWDEs in pathogen virulence remain largely unknown, especially in *B. cinerea*.

To ward off microorganisms infection, plants have evolved elaborate systems to provide better immunity against pathogens (Zipfel, 2008). Recognition of conserved pathogen-associated molecular patterns (PAMPs) *via* pattern recognition receptors (PRRs) located on the cell surface constitutes the first layer of plant innate immunity and is termed as PAMP-triggered immunity (PTI). Intracellular responses associated with PTI include Ca^{2+} influx, the burst of reactive oxygen species (ROS), the accumulation of defense hormone, the expression of defense-related genes and callose deposition (Boller and Felix, 2009; Couto and Zipfel, 2016). In turn, during the coevolution of hosts and microbes, pathogens also employ numerous effectors to interfere with PTI and establish successful infection, which is regarded as effector-triggered susceptibility (ETS) (Chisholm et al., 2006; Jones and Dangl, 2006; Saijo et al., 2017). As a countermeasure, some plants recruit R proteins to recognize these effectors directly or indirectly termed effector-triggered immunity (ETI) (Houterman et al., 2008; Stergiopoulos and de Wit, 2009). Generally, ETI is often accompanied with stronger immune responses, such as hypersensitive response (HR).

Apart from the role of virulence factor, some CWDEs also function as PAMPs to activate the plant immune responses independent of their enzymatic activity. For instance, VdEG1, VdEG3 and VdVUT11 from *Verticillium dahliae*, XEG1 from *Phytophthora sojae* and BcXYG1, a secreted xyloglucanase from *B. cinerea* contributed to virulence and triggered plant immunity as PAMPs simultaneously (Ma et al., 2015; Gui Y. et al., 2017; Gui Y.-J. et al., 2017; Zhu et al., 2017).

Plants recognizes characteristic microbial molecules classically known as PAMPs by employing a multitier surveillance system, including PRRs (Couto and Zipfel, 2016). Plant PRRs include RLKs and receptor-like proteins (RLPs) (Boutrot and Zipfel, 2017). Currently, a handful of PRRs have been identified as receptors to participate in the recognition of PAMPs. The brassinosteroid insensitive 1 (BRI1)-associated receptor kinase 1 (BAK1) and the LRR receptor-like kinase (LRR-RLK) SUPPRESSOR OF BIR1-1 (SOBIR1) are involved in multiple PRR pathways and signal activation (Liebrand et al., 2014). For example, BcSpl1, XEG1, and VdCUT11 could trigger cell death in the plants, and the resulting immunity signal was mediated by the plant LRR RLKs BAK1 and SOBIR1 (Frías et al., 2011; Ma et al., 2015; Gui Y. et al., 2017).

Xylan is the major component of hemicellulose of the plant cell wall (Collins et al., 2005). Due to the complexity, the degradation of xylan requires several hydrolytic enzymes, of which xylanase is a crucial component for hydrolyzing the 1,4-β-d-xylosidic linkages in xylan. Xylanase has received more attention because of the special role in fungi pathogenicity. For example, a mutation in the *xynB* endoxylanase gene from *Xanthomonas oryzae* pv. *oryzae* resulted in attenuated virulence in rice (Pandey and Sonti, 2010). Moreover, the deletion of xylanases *Xyn11A* gene had a marked effect on the ability of *B. cinerea* to infect tomato leaves and grape (Brito et al., 2006). In addition to their roles in virulence, xylanases are regarded as elicitors to induce defense responses in plants. For example, ethylene-inducing xylanase (EIX) is a potent elicitor in tobacco and tomato. However, the function of the majority of xylanases in *B. cinerea* remains mostly undiscovered. Here, we reported on the identification and characterization of BcXyl1, a xylanase from *B. cinerea*. BcXyl1 contributes to *B. cinerea* virulence and triggers PTI responses in plants. Furthermore, a small peptide of BcXyl1 is sufficient for elicitor function. We found that the cell death signal is mediated by BAK1 and SOBIR1, and the xylanases activity is not necessary for the induction of necrosis.

MATERIALS AND METHODS

Fungal Cultures, Plants Grown

Botrytis cinerea B05.10 was used as wild-type strain and control strain in this study. All *B. cinerea* strains, including two independent *BcXyl1* knockout mutants and two complementary transformants, were routinely maintained in 15% glycerol at −80°C and grown on PDA at 22°C, respectively. *Agrobacterium tumefaciens* AGL-1 were grown on LB (Kan and Rif) medium at 28°C. To obtain conidia, *B. cinerea* grown on tomato-PDA plates (39 g of potato dextrose agar plus 250 g of homogenized tomato fruits per liter) as explained previously (Benito et al., 1998). *N. benthamiana* and tomato (*Solanum lycopersicum*) plants were grown at 27 °C in a greenhouse with a day/night period of 14/10 h and 60% relative humidity (RH).

Expression and Purification of Recombinant Protein

The open reading frame of *BcXyl1* (amplified with primers BcXyl1 F/BcXyl1 R; **Supplementary Table S2**) and $C^{130-155}$ were amplified by PCR from cDNA of the wild-type strain B05.10 and the fragment fused with a myc tag and a 6xHis tag at the C terminus was cloned into the pPICZαA vector at the *Bam*HI and *Eco*RI sites. The recombinant plasmid pPICZαA-BcXyl1 and pPICZαA-$C^{130-155}$ were linearized with *Pme*I and transformed into *Pichia pastoris* KM71H for expression. The transformed yeasts were grown and induced in BMGY (buffered glycerol complex medium) and BMMY (buffered methanol complex medium), respectively (Easy Select Pichia expression kit; Invitrogen). Then, the supernatant was collected (3000 *g* for 10 min at 4°C) and purified using nickel affinity chromatography. The purified $C^{130-155}$, $BcXyl1^{rec}$, or BcXyl1 were kept in protein buffer (20 mM Tris, pH 8.0) and further detected *via* SDS-PAGE and Western blotting. The concentration of the purified protein was measured using Easy II Protein Quantitative Kit (BCA) and the protein was then stored at −80°C.

Truncated Mutant Construction and Agroinfiltration Assay

To transiently express truncated mutants of the BcXyl1 protein in leaves, DNA sequences encoding different fragments (BcXyl1, N^{80}, N^{130}, N^{155} C^{80}, C^{130}, C^{155}, and $C^{130-155}$) were amplified by PCR from cDNA of the wild-type strain B05.10 and inserted into pYBA1132 vector at the *Xba*I and *Bam*HI sites and then transformed into the *A. tumefaciens* strain GV3101. Agroinfiltration assays were performed on *N. benthamiana* plants. *Agrobacterium*-mediated transient expression was

performed as described (Ma et al., 2015). Leaves were scored and photographed 6 days after initial inoculation. Each assay was performed on six leaves from three individual plants, and repeated at least three times.

Site-Directed Mutagenesis

To determine the relationship between the enzymatic activity and cell death-inducing activity of BcXyl1, we constructed BcXyl1^{rec} mutant, which abolished the enzymatic activity. According to multiple sequence alignment, two potentially highly conserved catalytic residues (E104 and E157) were the critical catalytic sites of BcXyl1. Next, two glutamic acid residues were substituted by Gln using the Quick Change^{TM} Site-Directed Mutagenesis Kit (Stratagene, United States). BcXyl1^{rec} was expressed in *P. pastoris* and carried out the enzyme assay.

Xylanase Assay

The xylanase activity was assayed *via* the method as described previously (Biely et al., 1988). The purified BcXyl1^{rec} or BcXyl1 (500 ng) and substrate (1% beechwood xylan) were co-incubated in citrate phosphate McIlvaine buffer, pH 5, at 35°C for 10 min (total volume: 125 μl). All samples were incubated at 100°C for 10 min to end the assays reactions. The amount of reducing sugars released from xylan was quantified using a standard calibration curve obtained with the dinitrosalicylic acid procedure. The experiment was replicated three times.

Immunoblot Analysis

To confirm whether BcXyl1 was secreted into the apoplast and the relationship between enzymatic activity of BcXyl1 and cell death-inducing activity, transient expression in *N. benthamiana* was performed. Three sequences (BcXyl1, BcXyl1$^{-\Delta SP}$, and BcXyl1^{rec}) were cloned into the pYBA1132 vector which contained a C-terminal GFP tag at the *Xba*I and *Bam*HI sites, and then transformed into the *A. tumefaciens* strain GV3101. All primers are listed in **Supplementary Table S2**. Plant total protein extractions and immunoblots were assessed as previously described (Yu et al., 2012). All proteins were analyzed by immunoblots using anti-GFP-tag primary monoclonal antibody. The blots were visualized using the Odyssey® LI-COR Imaging System. Rubisco was used to confirm the equal protein loading.

Protein Infiltration Assays and Induction of PTI by BcXyl1

To test the induction of cell death or PTI responses, BcXyl1 and C$^{130-155}$ were dissolved in PBS and infiltrated into the leaves of *N. benthamiana* and tomato plants using a syringe. Plants were grown in a greenhouse with a day/night period of 14/10 h. The cell-death response was investigated after 48 h treated with BcXyl1, C$^{130-155}$, or PEVC (*P. pastoris* culture supernatant from an empty vector control strain, purified in the same way as BcXyl1). To further investigate cell death, trypan blue staining was performed by boiling leaf tissues in a mixture of phenol, lactic acid, glycerol, and distilled water containing 1 mg/ml trypan blue (1:1:1:1) for 1 min. The samples were then soaked in 2.5 mg/ml chloral hydrate overnight. The accumulation of ROS in plant leaves was stained by 3′3-diaminobenzidine (DAB) and Nitroblue Tetrazolium (NBT) solution as described previously (Bindschedler et al., 2006). To visualize callose deposition, 4-week-old *N. benthamiana* leaves were infiltrated with 1 μM recombinant proteins and stained with aniline blue at 24 h post-treatment, as described previously (Chen et al., 2012). To assay electrolyte leakage, the *N. benthamiana* leaves treated with proteins were harvested at different time points and submerged in sterile water at 4°C. Ion conductivity was measured using a conductivity meter. To test whether BcXyl1 could confer plants disease resistance, the purified BcXyl1, C$^{130-155}$, or PEVC was individually syringe-infiltrated into 4-week-old *N. benthamiana* and tomato leaves. Five microliters of 2 × 10^6 conidia/ml *B. cinerea* and TMV-GFP were placed on the systemic leaves, respectively. The inoculated plants were placed in a greenhouse at 25°C with a day/night period of 14/10 h. Lesion diameter of *B. cinerea* and the number of TMV-GFP lesions on *N. benthamiana* leaves were evaluated at 2 and 4 days post-inoculation, respectively. All experiments were performed three times.

Pathogenicity Assays

To test whether BcXyl1 functioned as a virulence factor of *B. cinerea*, the wild-type strain and derived mutants, including the BcXyl1 deletion (Δ*BcXyl1*-1 and Δ*BcXyl1*-2) and complementary mutants (Δ*BcXyl1*-1-C and Δ*BcXyl1*-2-C) were used in this study. Four-week-old *N. benthamiana* leaves were inoculated with 5 μL of 2 × 10^6 conidia/ml *B. cinerea*. The inoculated plants were placed in a greenhouse with a day/night period of 14/10 h. The lesion development of *B. cinerea* on the *N. benthamiana* leaves was evaluated at 2 days post-inoculation by determining the average lesion diameter. Tomato, grape, and apple fruits (commercially obtained) were washed under running tap water and surface sterilized by immersion for 5 min in ethanol. After air drying, fruits were inoculated with 5 μL of 2 × 10^6 conidia/ml *B. cinerea*. Fruits were incubated at 25°C under conditions of high humidity on water-soaked filter paper in closed containers. The lesion development of *B. cinerea* on the fruits was evaluated at 3 days post-inoculation by determining the average lesion diameter. All the experiments were performed three times.

VIGS in *N. benthamiana*

To determine whether BAK1 or SOBIR1 participate in induction of cell death by BcXyl1, VIGS was performed. *NbBAK1* or *NbSOBIR1* gene was silenced using VIGS, as described previously (Kettles et al., 2016). *A. tumefaciens* strain harboring constructs (pTRV1, pTR::*BAK1* or pTRV1, pTRV2::*SOBIR1*) were infiltrated into the *N. benthamiana* leaves. pTRV2::*GFP* was used as the control and the expression levels of *BAK1* and *SOBIR1* were determined by qRT-PCR. Agroinfiltration assays were performed on *N. benthamiana* plants using Bcl-2-associated X protein (BAX) as positive controls. Phenotypes were photographed 6 days after infiltration. All the experiments were performed three times.

RNA Extraction and qRT-PCR

To measure the expression of *BcXyl1* during infection, 4-week-old *N. benthamiana* or 4-week-old tomato plants were inoculated with *B. cinerea* 2×10^6 conidia/ml. We selected 10 indicated time points during different stages of post-inoculation to determine expression patterns of *BcXyl1* by qPCR. All samples were stored at −80°C. Total RNA of *B. cinerea* was extracted with the E.Z.N.A.® Total RNA Kit I according to the manufacturer's instructions and stored at −80°C. For the measurement of defense-related genes expression, leaves of 4-week-old *N. benthamiana* plants were treated with 1 μM purified BcXyl1, $C^{130-155}$, or PEVC. The leaves were obtained at the indicated time points, immediately frozen in liquid nitrogen, and stored at −80°C. The EasyPure Plant RNA Kit (TransGen Biotech) was used to extract total RNA. After isolation of total RNA, qPCR was performed using a TransStart Green qPCR SuperMix UDG according to the manufacturer's instructions (TransGen Biotech). qRT-PCR was performed under the following conditions: an initial 95°C denaturation step for 10 min followed by 40 cycles of 95°C for 15 s and 60°C for 1 min. *N. benthamiana* EF-1a (P43643.1) and *B. cinerea Bcgpdh* gene (BC1G_05277) were used as endogenous plant controls and used to quantify fungal colonization, respectively. qPCR assays were repeated at least twice, each repetition with three independent replicates (Livak and Schmittgen, 2001). All primers are listed in **Supplementary Table S2**. The relative transcript levels among various samples were determined using the $2^{-\Delta\Delta CT}$ method with three independent determinations (Livak and Schmittgen, 2001).

Generation of *BcXyl1* Deletion and Complementary Mutants

BcXyl1 gene and 500 bp flanking sequences of the target gene were amplified from *B. cinerea* B05.10 wild-type strain genomic DNA. Two flanking sequences of the target gene and hygromycin resistance cassette were constructed into a fusion fragment using a nested PCR reaction, which is subsequently introduced into the binary vector pGKO2 gateway. To generated complementary transformants, the donor vector pCT-HN containing *BcXyl1* gene was integrated into the mutant transformants using a previously described *Agrobacterium*-mediated transformation method (Liu et al., 2013). All mutants were identified using PCR with the corresponding primers. All primers are listed in **Supplementary Table S2**.

Statistical Analysis

All the experiments and data presented here were performed at least three repeats. The data are presented as the means and standard deviations. Statistical Analysis System (SAS) software was used to perform the statistical analysis *via* Student's *t*-test.

RESULTS

Amino Acid Sequence Analysis of VdCP1 BcXyl1

BcXyl1 was identified by searching the *B. cinerea* genome sequence. The open reading frame of BcXyl1 (GenBank: ATZ53308.1) is 987 bp encoding a 329 aa protein with a predicted N-terminal signal peptide (1–20 aa), and no transmembrane helices of BcXyl1 were found, suggesting that it may be secreted into extracellular space. The bioinformatics analysis suggested that BcXyl1 belongs to SGNH hydrolase subfamily and has a highly strong similarity to fungal endo-β-1,4-xylanases.

BcXyl1 Contributes to *B. cinerea* Virulence

Previous studies showed that xylanases in pathogenic microorganisms were implicated in the pathogenicity. In

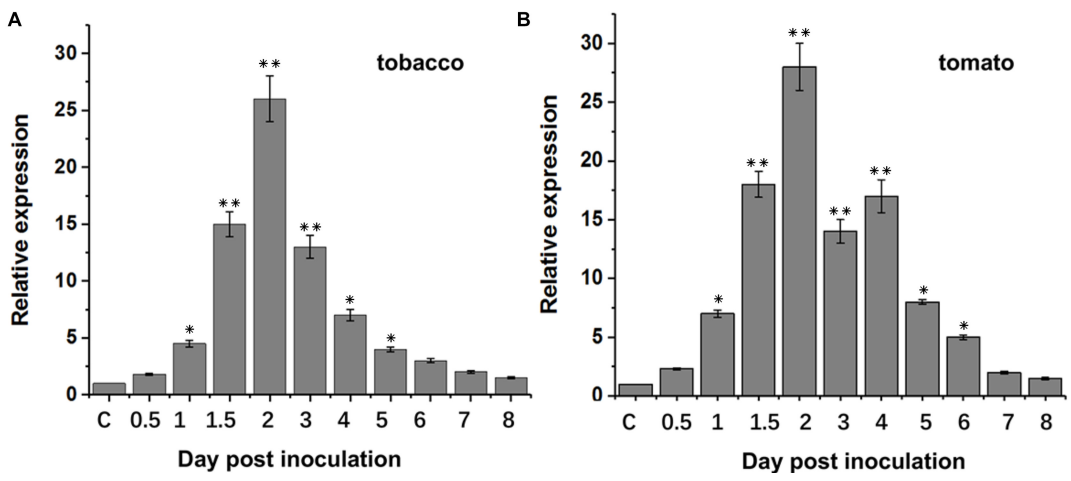

FIGURE 1 | *BcXyl1* expression analysis during infection of tobacco and tomato plants. Tobacco and tomato leaves were inoculated with *B. cinerea* spores, and the expression of *BcXyl1* was detected by qPCR. The control (C) was mixed with non-inoculated conidia tobacco or tomato leaves. *B. cinerea Bcgpdh* gene (BC1G_05277) was used as an endogenous control. Error bars represent standard deviation of three independent replicates. Asterisks indicate significant differences with based on Student's *t*-test (*$p < 0.05$ and **$p < 0.01$).

order to assess the role of BcXyl1 to *B. cinerea* virulence, we first analyzed the expression patterns of *BcXyl1* during different stages of post-inoculation. qRT-PCR results suggested that when the spore suspension of *B. cinerea* was inoculated onto leaves of *N. benthamiana* and tomato, transcript level of *BcXyl1* increased rapidly and reached a maximum of about 26-fold to 28-fold at 2 days post-inoculation, and then rapidly declined and maintained a level that was slightly higher than the initial level during later stages (**Figure 1**).

To more directly explore the biological roles of BcXyl1 during infection, we constructed two *BcXyl1* deletion mutants in *B. cinerea* (Δ*BcXyl1*-1 and Δ*BcXyl1*-2) and two rescued strains (Δ*BcXyl1*-1-C and Δ*BcXyl1*-2-C), and the ability of the resulting mutants to infect various plant organisms was evaluated. All mutants showed no significant differences with the wild-type stain in growth rate and colony morphology on PDA plates (**Supplementary Figure S2**). *N. benthamiana* leaves were inoculated with spore suspension of the wild type and mutants, and lesion size was measured 48 h after inoculation. Interestingly, the deletion of *BcXyl1* displayed significantly reduced virulence and produced much smaller lesions on leaves of *N. benthamiana* than the WT strain at 48 hpi (**Figures 2A,B**). The rescued strains recovered the high virulence phenotypes. And two *BcXyl1* deletion mutants displayed much weaker disease symptoms and lesion diameter than the wild-type strain and the complement strains (Δ*BcXyl1*-1-C and Δ*BcXyl1*-2-C) on grape, tomato, and apple fruits 72 h post-inoculation (**Figures 2A,B**). These results indicated that BcXyl1 functioned as a virulence factor that contributes to *B. cinerea* virulence on host plants.

BcXyl1 Is a Secreted Protein to Induce Cell Death in Several Plant Species

To further confirm whether BcXyl1 could induce cell death in *N. benthamiana*, we expressed BcXyl1 in the yeast *P. pastoris* using the pPICZαA vector (pPICZαA: *BcXyl1*). Moreover, the recombinant protein BcXyl1, with a size of 35 kDa, was infiltrated into the mesophyll of *N. benthamiana* leaves with different concentrations (**Supplementary Figure S3**). The area of necrosis occurred and increased with increasing concentrations of BcXyl1 from 800 nM to 2 μM after infiltration 3 days, whereas no cell death activity was detected in the leaves treated with PEVC (*P. pastoris* culture supernatant from an empty vector control strain, purified in the same way as BcXyl1) (**Figures 3A,B**).

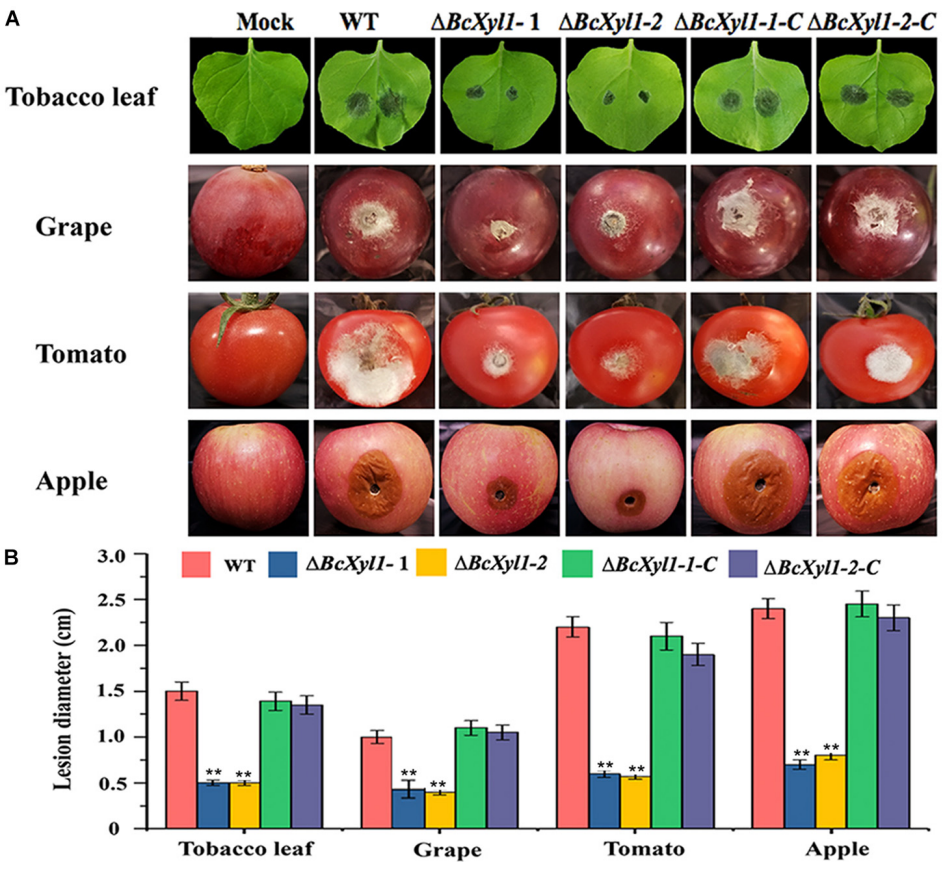

FIGURE 2 | Virulence analysis of *BcXyl1* mutants on plant organs. **(A)** Disease symptoms on wounded tobacco leaves, grape fruits, tomato fruits, and apple fruits after 72 h inoculation. **(B)** Diameter of disease lesion on leaves and fruits was determined. Error bars represent standard deviation of three independent replicates. Student's *t*-test was performed to determine the significant differences between mutants and WT stain. Asterisks "**" indicate statistically significant differences at a *p*-value <0.01.

To examined the cell death-inducing activity of BcXyl1 in plants other than *N. benthamiana*, we infiltrated BcXyl1 (1 μM) into the leaves of several plants, including tomato, soybean, and cotton. BcXyl1 could induce significant cell death in these plants while PEVC did not (**Figure 3C**). So, BcXyl1 has ability to induce cell death in several plant species.

BcXyl1 has a signal peptide with 20 amino acids and no transmembrane helices, implying that BcXyl1 might be a secreted protein. In order to check if, as previously hypothesized, BcXyl1 was secreted into the apoplast to induce cell death response, we transiently expressed the full length BcXyl1 and BcXyl1$^{-\Delta SP}$ (lacking the signal peptide) in *N. benthamiana* by agroinfiltration. The results showed that BcXyl1 containing signal peptide induced cell death in *N. benthamiana*, whereas BcXyl1$^{-\Delta SP}$ lacking signal peptide abolished the ability to trigger cell death at 5 days after agroinfiltration (**Supplementary Figure S4A**). The protein expression level of BcXyl1 and BcXyl1$^{-\Delta SP}$ in *N. benthamiana* were detected by immunoblot (**Supplementary Figure S4B**). So, all results showed BcXyl1 was delivered into the apoplast to induce cell death in several plant species.

The Cell Death-Inducing Activity Is Independent of the Xylanase Activity of BcXyl1

Previous reports showed that xylanases from fungi had ability to degrade xylan (Brutus et al., 2005). Interestingly, purified BcXyl1 had a xylanase activity using low viscosity xylane (LVX) as substrate (**Supplementary Table S1**). The sequence alignment results showed that BcXyl1 included two potentially highly conserved catalytic residues (E104 and E157), which are essential for the xylanase activity (**Supplementary Figure S1**). In addition, the enzymatic activity of CWDEs was required for cell death activity, and in a few cases, the cell death-inducing activity was found to be independent of the enzymatic activity. To determine the relationship between the enzymatic activity and cell death-inducing activity of BcXyl1, we generated a site-directed mutant (BcXyl1^{rec}) that two glutamic acid residues were substituted by Gln using site-directed mutagenesis and expressed the mutant protein in *P. pastoris* (**Figure 4A**). Enzymatic assays with purified BcXyl1^{rec} showed the xylan-degrading xylanase activity was abolished (**Supplementary Table S1**). Surprisingly, although BcXyl1^{rec} absent the ability of xylanase activity, retained the same cell death-inducing activity as the wild-type (BcXyl1) (**Figure 4B**). Further, *A. tumefaciens* infiltration assays showed that BcXyl1^{rec} and BcXyl1 induced similar visible cell death symptoms in *N. benthamiana* leaves 4 days post-inoculation (**Figure 4B**). Western blot assays showed that the accumulation of BcXyl1 and BcXyl1^{rec} was similar (**Figure 4C**). These results confirmed that BcXyl1 did not need to xylanase activity to induce cell death in *N. benthamiana*.

BcXyl1 Triggers the PTI Responses

Some cell death-inducing proteins are recognized by plant immune system and activate host PTI responses, bring a series of typical characteristics such as accumulation of ROS, leakage

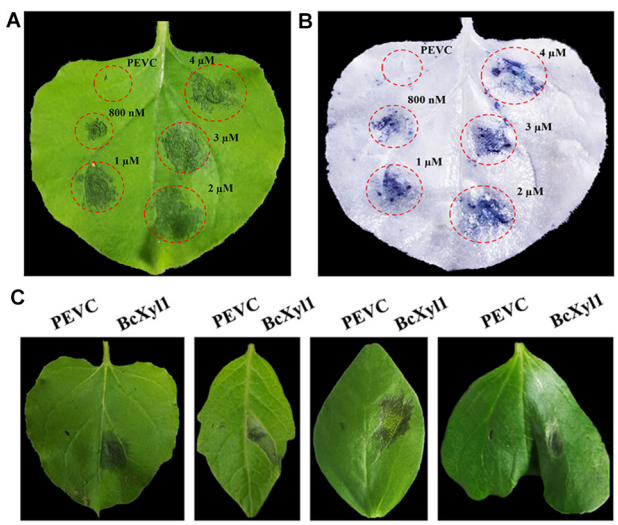

FIGURE 3 | BcXyl1 induces cell death in several plants. **(A,B)** *N. benthamiana* leaves were infiltrated with purified BcXyl1 protein (800 nM to 2 μM), and PEVC (*P. pastoris* culture supernatant from an empty vector control strain, purified in the same way as BcXyl1). Two days post-infiltration, the leaves were photographed and stained with trypan blue. **(C)** The leaves of tomato, soybean, and cotton were infiltrated with purified BcXyl1 (1 μM) and PEVC (1 μM). Two days post-infiltration, different plants leaves were photographed. All the experiments were replicated three times.

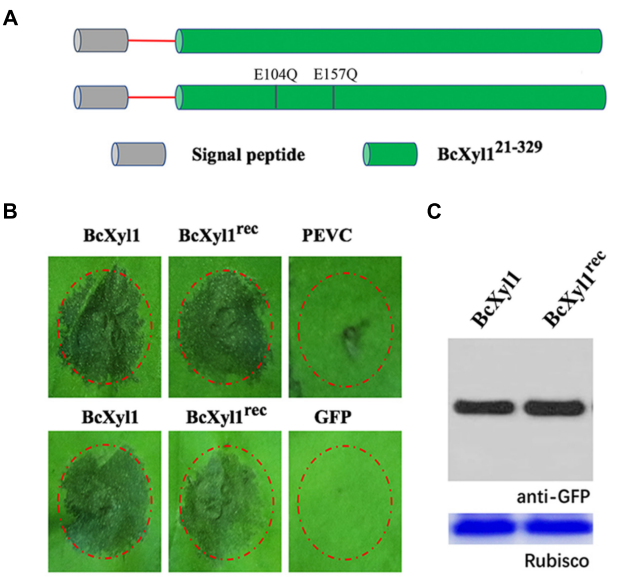

FIGURE 4 | Cell death activity of BcXyl1 is independent of its xylanase activity in *N. benthamiana*. **(A)** Schematic presentation of the examined constructs. BcXyl1 (the native protein) and BcXyl1^{rec} (replaced E104 and E157 with Gln). **(B)** Upper pictures: treatment of tomato leaves with 1 μM purified BcXyl1 or BcXyl1^{rec}. Lower pictures: analysis of cell death produced by *A. tumefaciens* strains transiently expressing BcXyl1 or BcXyl1^{rec}. **(C)** Immunoblot analysis of proteins from *N. benthamiana* leaves transiently expressing the examined proteins using a pYBA1132 vector. All the experiments were replicated three times.

of ion electrolytes, expression of defense genes, and callose deposition (Frías et al., 2012; Zhang et al., 2014, 2015). To examine whether BcXyl1 could induce typical PTI responses, the leaves of *N. benthamiana* and tomato plants were infiltrated with 1 μM BcXyl1. The ability of BcXyl1 to induce the accumulation of ROS in the infiltrated leaves was studied. The hydrogen peroxide (H_2O_2) and superoxide anion (O_{2-}) production levels were assayed using DAB and NBT, respectively. A clear brown and blue precipitate was observed in leaves treated with BcXyl1, whereas the leaves treated with PEVC showed opposite patterns of DAB and NBT signal (**Figure 5A**). Meanwhile, BcXyl1 also induced electrolyte leakage and displayed an increase in conductivity, while PEVC exhibited barely change at the same concentration (**Figure 5B**). BcXyl1 was shown to cause significantly upregulation of seven genes associated with PTI and defense response in *N. benthamiana* leaves 12 h after treatment with BcXyl1; these genes included *PR-1a* and *PR-5*, which are involved in the SA-dependent defense pathway, *PAL* (phenylalanine ammonia lyase), *NPR1* (the non-expressor of pathogenesis related 1), *HSR203J* and *HIN1*, which are two HR marker genes in *tobacco*, and *COI1* (CORONATINE INSENSITIVE 1), which is JA responsive (**Figure 5C**). We finally examined callose deposition in leaves treated with BcXyl1, PEVC, or flg22. Furthermore, *N. benthamiana* leaves infiltrated with BcXyl1 or flg22 exhibited strong callose deposition compared with those infiltrated with PEVC, which exhibited undetectable levels of callose deposition (**Figure 5D**). These data indicated that BcXyl1 could induce typical PTI responses.

BcXyl1 Confers Plants Disease Resistance

Recent reports showed that fungi CWDEs could confer plants disease resistance (Gui Y. et al., 2017; Gui Y.-J. et al., 2017; Zhu et al., 2017). To further confirm the role of BcXyl1 in conferring resistance to plant diseases, the *N. benthamiana* leaves were treated with 1 μM BcXyl1or PEVC, and after 2 days, the systemic leaves were inoculated with TMV-GFP and *B. cinerea* spore suspension. BcXyl1-treated tobacco plants enhanced disease resistance against TMV, and the number of TMV-GFP lesions of BcXyl1-treated leaves was significantly decreased than that of the leaves treated with PEVC (**Figure 6A**). Meanwhile, BcXyl1 led to more resistance to the *B. cinerea* infection in *N. benthamiana*, as significantly lower lesions size on leaves compared with the leaves treated with PEVC controls (**Figure 6B**). Furthermore, in tomato plants that were pre-infiltrated with BcXyl1, lesion size on the *B. cinerea*-infected leaves was significant smaller compared with lesions size on leaves in plants that were pre-infiltrated with PEVC (**Figure 6C**). Together, these results strongly suggested that BcXyl1 conferred plants disease resistance.

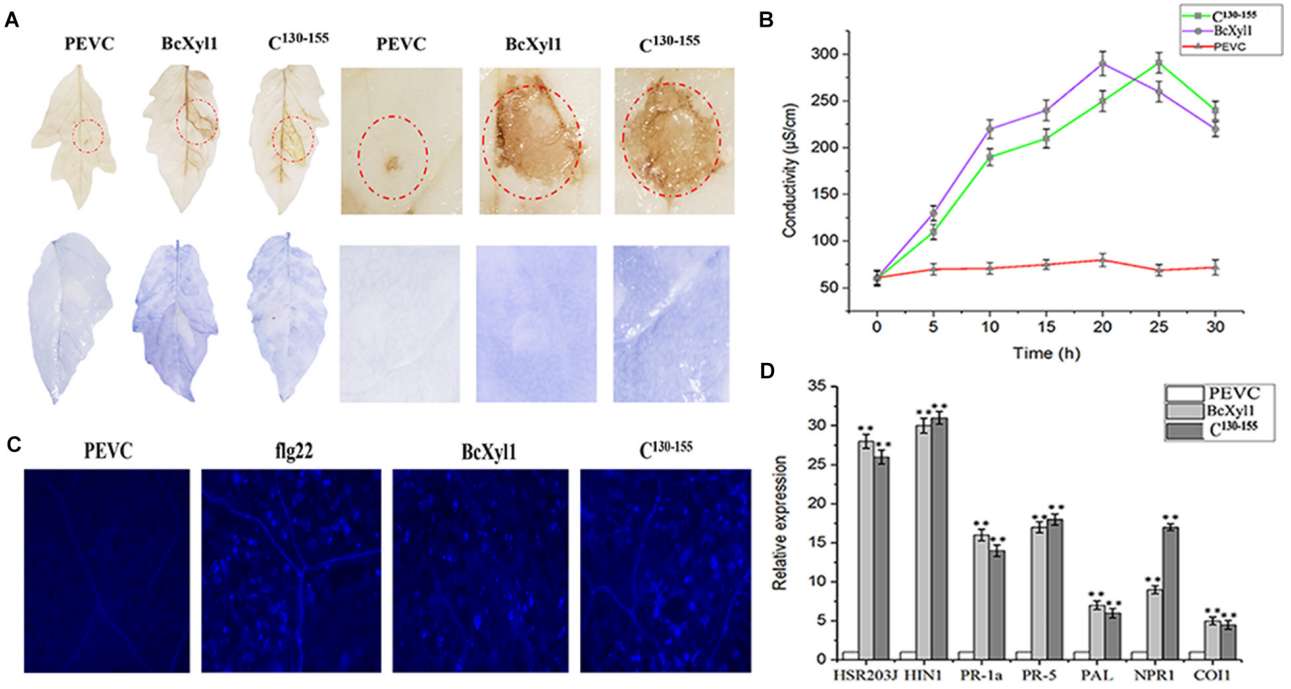

FIGURE 5 | BcXyl1 induces PTI responses in plants. *N. benthamiana* or tomato leaves were infiltrated with 1 μM purified BcXyl1, $C^{130-155}$, or PEVC. **(A)** ROS accumulation was detected in tobacco and tomato leaves 12 h after infiltration. The treated leaves were stained with DAB and NBT. All the experiments were replicated three times. **(B)** The conductivity was measured at the indicated time points. Error bars represent standard errors. All the experiments were replicated three times. **(D)** The expression of defense response genes was measured in *N. benthamiana* leaves by qPCR. Error bars represent standard deviation of three independent replicates. Student's *t*-test was performed to determine the significant differences between BcXyl1, $C^{130-155}$, and PEVC. Asterisks "**" indicate statistically significant differences at a *p*-value <0.01. **(C)** Callose deposition in *N. benthamiana* leaves were detected 2 days after infiltration; the treated leaves were stained with aniline blue. All the experiments were replicated three times.

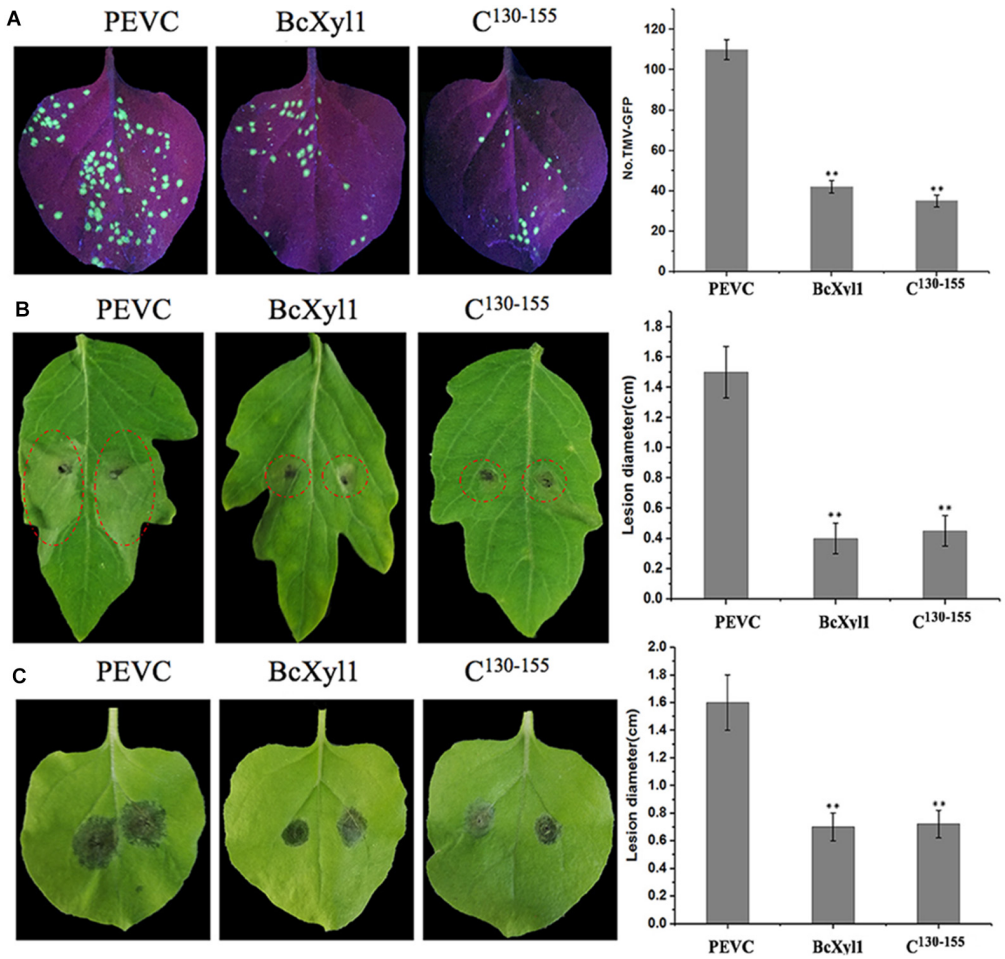

FIGURE 6 | BcXyl1 confers disease resistance in plants. *N. benthamiana* or tomato leaves were infiltrated with 0.5 μM purified BcXyl1, $C^{130-155}$, or PEVC. **(A)** The systemic leaves were inoculated with TMV-GFP, and the number of TMV-GFP lesions were measured. **(B,C)** The *N. benthamiana* or tomato systemic leaves were inoculated with 5 μL of 2 × 10^6 conidia/ml *Botrytis cinerea*. Lesions symptoms and diameter were observed and measured at 2 days post-inoculation, respectively. Error bars represent standard deviation of three independent replicates. Student's *t*-test was performed to determine the significant differences between BcXyl1, $C^{130-155}$, and PEVC. Asterisks "**" indicate statistically significant differences at a *p*-value <0.01.

A Small Peptide of BcXyl1 Is Sufficient for Elicitor Function

The plant receptors often recognize specific small protein epitopes of PAMP to induce plant immunity (Rotblat et al., 2002). To delineate the elicitor active peptide of BcXyl1, we generated N-terminal and C-terminal truncated mutants and detected the ability to induce cell death by agroinfiltration in *N. benthamiana* leaves (**Figure 7A**). We found that the N-terminal truncated mutant (N^{155}) maintained the ability of cell death-inducing, whereas expression of N^{80} and N^{130} did not trigger cell death. The C-terminal truncated mutants (C^{80} and C^{130}) induced cell death, but C^{155} resulted in the loss of cell death-inducing activity in *N. benthamiana*. Further, $C^{130-155}$ induced the same cell death symptom compared with full-length BcXyl1 in *N. benthamiana* (**Figure 7B**). Hence, $C^{130-155}$ was identified as the functional peptide of BcXyl1 to induce cell death in *N. benthamiana*. To probe whether $C^{130-155}$ induced plant immune responses, purified $C^{130-155}$ was used to infiltrate plants leaves. We found that like BcXyl1, $C^{130-155}$ could induce typical PTI responses, including accumulation of ROS, leakage of ion electrolytes, expression of defense genes, and callose deposition (**Figure 5**). Meanwhile, $C^{130-155}$ could also enhance resistance to *B. cinerea* and TMV in plants (**Figure 6**). These results suggested that a small peptide of BcXyl1 was sufficient for elicitor function.

BAK1 and SOBIR1 Mediates BcXyl1-Triggered Cell Death in *N. benthamiana*

The plant PRRs, such as the LRR RLKs BAK1 and SOBIR1, were employed to participate in multiple PRR pathways, including cell death induction (Monaghan and Zipfel, 2012; Liebrand et al., 2014; Gravino et al., 2016). For example, BAK1 was required for cell death inducing of GH12 members (Ma et al., 2015;

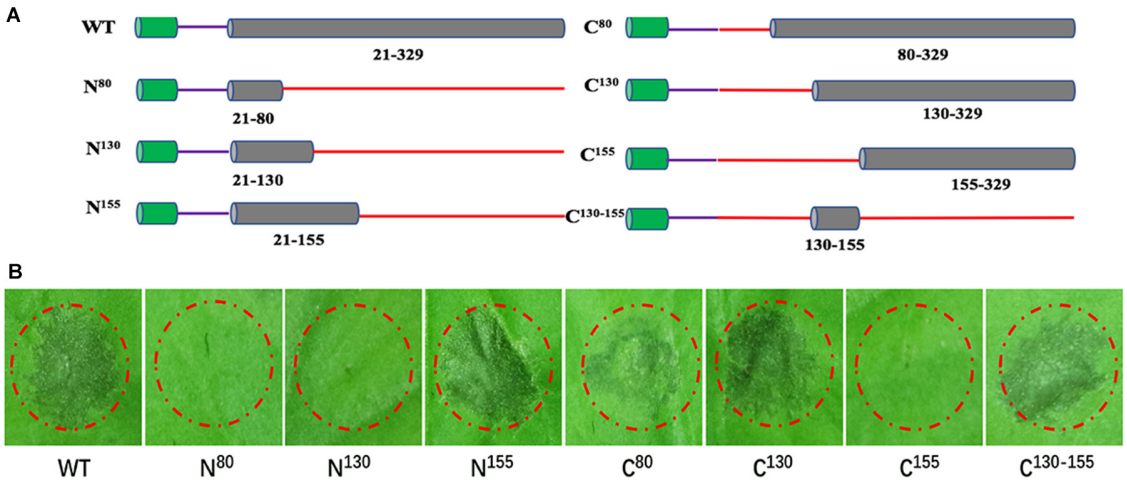

FIGURE 7 | A small peptide of BcXyl1 is sufficient for inducing cell death. **(A)** Schematic presentation of the examined constructs, including N^{80}, N^{130}, N^{155}, C^{80}, C^{130}, C^{155}, and $C^{130-155}$. **(B)** Analysis of cell death produced by *A. tumefaciens* strains transiently expressing various truncated mutants in *N. benthamiana* leaves. All the experiments were replicated three times.

Zhu et al., 2017). As demonstrated above, BcXyl1 was secreted into the apoplast to induce cell death. To determine whether BAK1 and SOBIR1 participated in induction of cell death by BcXyl1, we used virus-induced gene silencing (VIGS) to induce the gene silencing of *BAK1* or *SOBIR1* in *N. benthamiana* leaves. Three weeks after viral inoculation to silence *BAK1*, transient expression of BcXyl1 in *N. benthamiana* did not result in cell death after agroinfiltration with BcXyl1 expression constructs. Treatment of *BAK1*-silenced plants with Bcl-2-associated protein X (BAX) was used as a control, which resulted in cell death induction (**Figure 8A**). The results of *SOBIR1*-silenced plants were in accordance with BAK1-silenced plants, BcXyl1 did not trigger cell death, while BAX was still capable of inducing cell death (**Figure 8A**). Immunoblotting confirmed that BcXyl1 were successfully expressed at the expected size in *N. benthamiana* plants inoculated with TRV::*BAK*, TRV::*SOBIR1*, or TRV::*GFP* (**Figure 8B**). qPCR analysis confirmed that the expression of *BAK1* or *SOBIR1* expression was markedly reduced upon inoculation with the TRV::*BAK* or TRV::*SOBIR1*, with an expression level about 20% in comparison with inoculation with TRV::GFP (**Figure 8C**). From these results, we inferred that BAK1 and SOBIR1 (a LRR-RLP/SOBIR1/BAK1 complex) were required for BcXyl1-triggered cell death in *N. benthamiana*.

DISCUSSION

Botrytis cinerea, a necrotrophic plant pathogen, attacks the plant organs, including leaves, flowers, fruits, bulb, and root tubers, and causes serious plant diseases and substantial losses in agriculture throughout the world (Williamson et al., 2007; Ky et al., 2012). Like other phytopathogenic fungi, *B. cinerea* secretes vast array of proteins during infection process (Fillinger and Elad, 2016). Cell wall-degrading enzymes (CWDEs) are the largest class of *B. cinerea*-secreted proteins (Kubicek et al., 2014). Recent studies have revealed that several CWDEs functioned as virulence factors in plant pathogens and were also recognized as PAMPs by plant PRRs to trigger the PTI responses, during plant–pathogen interactions (Ma et al., 2015). In this study, we described the identification and analysis of BcXyl1, a secreted xylanase from *B. cinerea*. BcXyl1 had the ability to induce cell death and plant PTI responses independent of its enzymatic activity. Furthermore, our study also found that a small peptide from BcXyl1 was sufficient for elicitor activity. VIGS assays showed that a LRR-RLP/SOBIR1/BAK1 complex modulates BcXyl1-triggered cell death in *N. benthamiana*. We also found that BcXyl1 functions as a virulence factor that contributes to *B. cinerea* virulence on host plants.

Increasing evidence demonstrated that xylanases are responsible for the pathogenesis of necrotrophic phytopathogens, including *B. cinerea* (Schouten et al., 2007; Frías et al., 2011). For instance, xyn11A was an endo-β-1,4-xylanase belonging to family 11 of glycoside hydrolase and required for virulence in *B. cinerea*, and the deletion of the *xynB* gene encoding an endo-xylanase distinctly reduced the virulence of *Xanthomonas oryzae* pv. *oryzae* (Brito et al., 2006; Pandey and Sonti, 2010). In this study, we found BcXyl1 appeared to be a major virulence factor. Strikingly, *BcXyl1* was strongly induced and accumulated during the early stage of infection, and the mutation of *BcXyl1* had a severe effect on pathogenicity (**Figures 1**, **2**). It is noteworthy that not all fungal xylanases have been conclusively involved in pathogenicity and virulence. So far, gene deletion experiments in *Fusarium oxysporum*, *Fusarium graminearum*, *Magnaporthe grisea*, and *Cochliobolus carbonum* did not support an essential role for xylanases in fungal pathogenesis (Apel, 1993; Wu et al., 1997; Gómez-Gómez et al., 2002; Santhanam et al., 2013; Sella et al., 2013). In addition, previously study showed that a xylanase from *B. cinerea* could contribute to virulence by promoting the necrosis of the plant tissue surrounding the infection (Noda et al., 2010). Interestingly, a few nanograms of purified BcXyl1

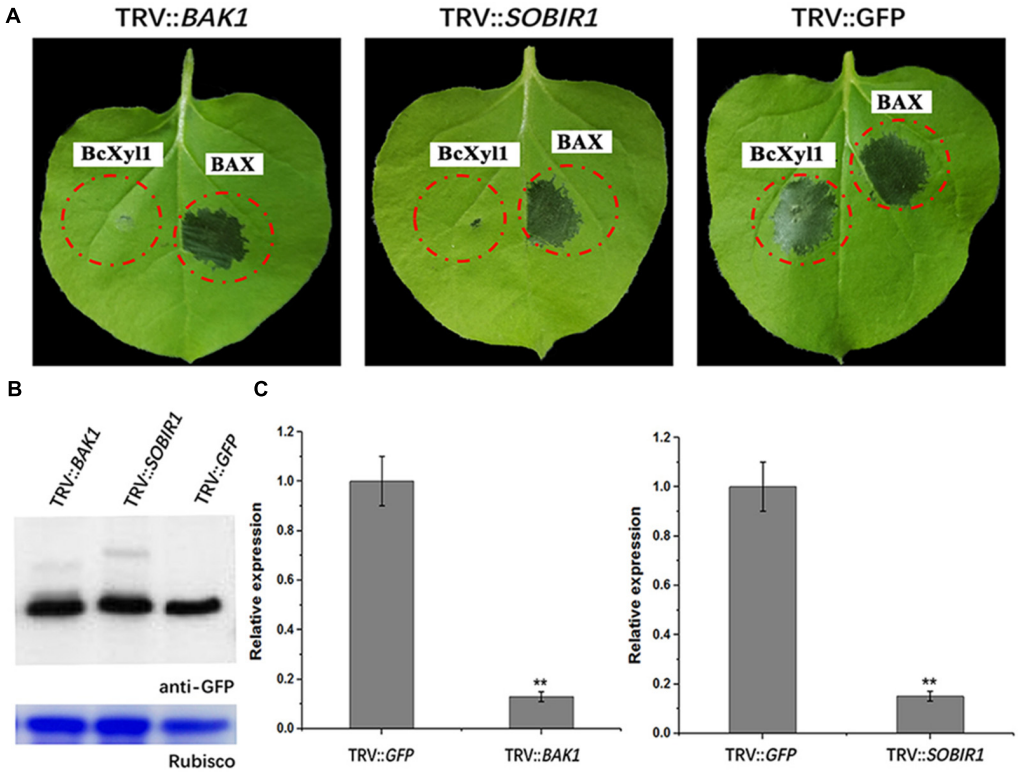

FIGURE 8 | BAK1 and SOBIR1 mediates BcXyl1-triggered cell death in *N. benthamiana*. Three silence constructs (TRV::*BAK1*, TRV::*SOBIR1*, and TRV::*GFP*) were generated. **(A)** BcXyl1 and BAX (the positive control) were transiently expressed in *BAK1* and *SOBIR1* silenced tobacco leaves, respectively. The cell death induction was detected and photographed in *N. benthamiana* leaves 4 days after infiltration. **(B)** Immunoblot analysis of BcXyl1 transiently expressed in genes-silenced *N. benthamiana* leaves. **(C)** The silencing efficiency of *BAK1* and *SOBIR1* was examined by qPCR. Error bars represent standard errors. Error bars represent standard deviation of three independent replicates. Student's *t*-test was performed to determine the significant differences between mutants and WT. Asterisks "**" indicate statistically significant differences at a *p*-value <0.01.

resulted in a rapid leaf tissue necrosis in soybean, tomato, cotton, and *N. benthamiana* (**Figure 3C**). The range of plant species responding to BcXyl1 may be larger than we detected.

Previous studies showed that the enzymatic activity of many fungal CWDEs was required for cell death-inducing activity (Gui Y. et al., 2017). However, in certain cases, the cell death inducing activity was found to be unrelated to the enzymatic activity (Ma et al., 2014, 2015). For instance, Xyn11A, a xylanase from *B. cinerea*, and the *Trichoderma viride* EIX could induce cell death in plants independent of the xylanase activity (Furman-Matarasso et al., 1999; Noda et al., 2010). Although BcXyl1 is a xylanase, induction of cell death did not require the enzymatic activity (**Figure 4**).

Our results showed that BcXyl1 was localized to the plant apoplast by a signal peptide experiment, suggesting that the cell death-inducing activity may be mediated by surface-localized PRRs (**Supplementary Figure S5**). Plant surface-localized PRRs such as RLKs and RLPs were involved in the recognition of PAMPs (Boutrot and Zipfel, 2017). In addition, BAK1, as a co-receptor, plays a regulatory role in receptor complexes that mediate PTI (Schulze et al., 2010; Liu et al., 2013; Gravino et al., 2016; Yamada et al., 2016). And SOBIR1 is also specifically required for the function of receptor complexes (Liebrand et al., 2014). VIGS assays confirmed that tobacco BAK1 was required for BcXyl1-induced cell death, and the cell-death response also disappeared in VIGS-*SOBIR1* plants (**Figure 8**). Hence, the RLP–SOBIR1–BAK1 complex mediated the cell death-inducing activity of BcXyl1.

The detection of PAMPs by plant PRRs to trigger PTI is a major component of plant defense responses. We confirmed that BcXyl1 triggered typical defense responses, including accumulation of ROS, leakage of ion electrolytes, deposition of callose, and expression of defense genes (**Figure 5**). We also found that the recombinant BcXyl1 proteins conferred systemic resistance in *N. benthamiana*, which offered protection against TMV and *B. cinerea* (**Figure 6**).

Generally, PAMPs are perceived by PRRs *via* specific epitopes, and the small peptides located on the surface of the proteins are sufficient to stimulate immune responses. For example, a 35-amino acid peptide of BcIEB1 could trigger necrosis and the PTI responses (González et al., 2017). Similarly, a 30-amino acid peptide of Xyn11A mediated the induction of cell death (Noda et al., 2010). The small peptide of VdEG3 from the GH12 domain was sufficient to induce cell death in *N. benthamiana* (Gui Y.-J. et al., 2017). In this study, progressive truncation of BcXyl1

confirmed that a region with 26 amino acids was sufficient for elicitor function (**Figures 5–7**).

Previous studies showed that many fungal xylanases involved in inducing plant defense responses immunity. For instance, the xylanase EIX from *T. viride* was an elicitor to induce defense responses in tomato, pepper and tomato plants (Rotblat et al., 2002). A xylanase from *F. graminearum* could induce cell death and hydrogen peroxide accumulation in wheat leaves (Sella et al., 2013; Moscetti et al., 2014). We have also determined that BcXyl1 induced plant defense responses and conferred tobacco and tomato plants disease resistance. Therefore, we speculated that fungal xylanases have the ability to trigger immunity in dicot and monocot plants.

Successful pathogens deliver effectors to interference the host PTI response and establish infection (Jones and Dangl, 2006; Gimenez-Ibanez et al., 2009). For example, a RXLR effector and CBM1 effector suppressed XEG1-triggered immunity in oomycetes and suppressed the GH12 protein and BcXyl1-triggered immunity in *V. dahlia*, respectively. Whether effectors mediate the suppression of BcXyl1, needs further investigation.

AUTHOR CONTRIBUTIONS

YD and DQ designed the experiments. YY performed most of the experiments and wrote the paper. XY participated in some part of the study and the Graduate Student Innovation Scientific Research Subject of Hainan Province (Hyb2017-17).

FUNDING

This study was supported by the National Natural Science Foundation of China (no. 31701782 and no. 31371984).

ACKNOWLEDGMENTS

We are grateful to X. F. Dai from the Institute of Food Science and Technology, Chinese Academy of Agricultural Sciences, for the generous gift of the vectors for gene knockout and complementation. We also thank L. Yao from Beijing Academy of Agriculture and Forestry for providing the pYBA1132 plasmid and pPICZαA plasmid. And YY thanks the meticulous care and selfless support of Ms. Nianhua Jiang over the past 4 years.

SUPPLEMENTARY MATERIAL

The Supplementary Material for this article can be found online at: https://www.frontiersin.org/articles/10.3389/fmicb.2018.02535/full#supplementary-material

FIGURE S1 | Sequence alignment of BcXyl1 and xylanases from other fungi. Two red triangles indicated possible catalytic residues of BcXyl1 (E104 and E157). Sequence data of all proteins can be found in the GenBank/EMBL data libraries under accession numbers: XynBc1 (ACF16413.1), BcXyl1 (ATZ53308.1), XynG1 (XP_001258363.1), BcXyl2 (XP_001546507.1), BcXyl3 (ATZ58346.1), BcXyl4 (ATZ51455.1), NpGH11 (EOD46026.1), and SsGH11 (XP_001588545).

FIGURE S2 | *BcXyl1* deletion strains do not show developmental defects. *BcXyl1* deletion mutants (Δ*BcXyl1*-1 and Δ*BcXyl1*-2), rescued strains (Δ*BcXyl1*-1-C and Δ*BcXyl1*-2-C). **(A)** The radial growth and colony morphology were observed after 8 days of incubation on PDA medium at 25°C. **(B)** Conidial germination rate of each strain was determined after cultivated on Water-Agar media at 25°C for 15 h. **(C)** Fungi were grown on PDA plates at 25°C. Radial growth was measured every day, and the growth rate was calculated. All the experiments were replicated three times.

FIGURE S3 | SDS-PAGE analysis of BcXyl1 and BcXyl1^{rec} recombinant proteins. BcXyl1 is the native protein; BcXyl1^{rec} is the site-directed mutagenized protein, which E104 and E157 were substituted with Gln. Two recombinant proteins were stained with Coomassie blue.

FIGURE S4 | BcXyl1 is secreted into the apoplast to induce cell death. **(A)** BcXyl1 (the native protein) and BcXyl1$^{-\Delta SP}$ (deleted the signal peptide). Cell death induction was detected in *N. benthamiana* leaves 5 days after infiltration with the examined various *A. tumefaciens* strains. **(B)** Immunoblot analysis of proteins from *N. benthamiana* leaves transiently expressing the examined proteins using a pYBA1132 vector. All the experiments were replicated three times.

FIGURE S5 | BcXyl1 confers disease resistance in plants. *N. benthamiana* or tomato leaves were infiltrated with 0.5 μM purified BcXyl1, C$^{130-155}$, or PEVC. **(A)** The local leaves were inoculated with TMV-GFP, and the number of TMV-GFP lesions were measured. **(B,C)** The *N. benthamiana* or tomato local leaves were inoculated with 5 μL of 2 × 10^6 conidia/ml *Botrytis cinerea*. Lesions symptoms and diameter were observed and measured at 2 days post-inoculation, respectively. Error bars represent standard deviation of three independent replicates. Student's *t*-test was performed to determine the significant differences between BcXyl1, C$^{130-155}$ and PEVC. Asterisks "**" indicate statistically significant differences at a p-value <0.01.

TABLE S1 | Hydrolysis activity test.

TABLE S2 | Primers used in this study.

REFERENCES

Apel, P. C. (1993). Cloning and targeted gene disruption of XYL1,a β1,4-Xylanase gene from the maize pathogen *Cochliobolus carbonum*. *Mol. Plant Microbe Interact.* 6, 467–473. doi: 10.1094/MPMI-6-467

Ben-Daniel, B.-H., Bar-Zvi, D., and Tsror Lahkim, L. (2011). Pectate lyase affects pathogenicity in natural isolates of *Colletotrichum coccodes* and in pelA gene-disrupted and gene-overexpressing mutant lines. *Mol. Plant Pathol.* 13, 187–197. doi: 10.1111/j.1364-3703.2011.00740.x

Benito, E. P., ten Have, A., van 't Klooster, J. W., and van Kan, J. A. L. (1998). Fungal and plant gene expression during synchronized infection of tomato leaves by *Botrytis cinerea*. *Eur. J. Plant Pathol.* 104, 207–220. doi: 10.1023/A:1008698116106

Biely, P., Mislovičová, D., and Toman, R. (1988). Remazol brilliant blue-xylan: a soluble chromogenic substrate for xylanases. *Meth. Enzymol.* 160, 536–541. doi: 10.1016/0076-6879(88)60165-0

Bindschedler, L. V., Dewdney, J., Blee, K. A., Stone, J. M., Asai, T., Plotnikov, J., et al. (2006). Peroxidase-dependent apoplastic oxidative burst in *Arabidopsis* required for pathogen resistance. *Plant J.* 47, 851–863. doi: 10.1111/j.1365-313X.2006.02837.x

Boller, T., and Felix, G. (2009). A renaissance of elicitors: perception of microbe-associated molecular patterns and danger signals by pattern-recognition receptors. *Annu. Rev. Plant Biol.* 60, 379–406. doi: 10.1146/annurev.arplant.57.032905.105346

Boutrot, F., and Zipfel, C. (2017). Function, discovery, and exploitation of plant pattern recognition receptors for broad-spectrum disease resistance. *Annu. Rev. Phytopathol.* 55, 257–286. doi: 10.1146/annurev-phyto-080614-120106

Brito, N., Espino, J. J., and González, C. (2006). The endo-beta-1,4-xylanase xyn11A is required for virulence in *Botrytis cinerea*. *MPMI* 19, 25–32. doi: 10.1094/MPMI-19-0025

Brutus, A., Reca, I. B., Herga, S., Mattei, B., Puigserver, A., Chaix, J.-C., et al. (2005). A family 11 xylanase from the pathogen *Botrytis cinerea* is inhibited by plant endoxylanase inhibitors XIP-I and TAXI-I. *Biochem. Biophys. Res. Commun.* 337, 160–166. doi: 10.1016/j.bbrc.2005.09.030

Cantarel, B. L., Coutinho, P. M., Rancurel, C., Bernard, T., Lombard, V., and Henrissat, B. (2009). The carbohydrate-active enzymes database (CAZy): an expert resource for glycogenomics. *Nucleic Acids Res.* 37, D233–D238. doi: 10.1093/nar/gkn663

Chisholm, S. T., Coaker, G., Day, B., and Staskawicz, B. J. (2006). Host-microbe interactions: shaping the evolution of the plant immune response. *Cell* 124, 803–814. doi: 10.1016/j.cell.2006.02.008

Chen, M., Zeng, H., Qiu, D., Guo, L., Yang, X., Shi, H., et al. (2012). Purification and characterization of a novel hypersensitive response-inducing elicitor from *Magnaporthe oryzae* that triggers defense response in rice. *PLoS One* 7:e37654. doi: 10.1371/journal.pone.0037654

Collins, T., Gerday, C., and Feller, G. (2005). Xylanases, xylanase families and extremophilic xylanases. *FEMS Microbiol. Rev.* 29, 3–23. doi: 10.1016/j.femsre.2004.06.005

Couto, D., and Zipfel, C. (2016). Regulation of pattern recognition receptor signalling in plants. *Nat. Rev. Immunol.* 16, 537–552. doi: 10.1038/nri.2016.77

Fillinger, S., and Elad, Y. (2016). *Botrytis – the Fungus, the Pathogen and its Management in Agricultural Systems*. Berlin: Springer International Publishing. doi: 10.1007/978-3-319-23371-0

Frías, M., Brito, N., and González, C. (2012). The *Botrytis cinerea* cerato-platanin BcSpl1 is a potent inducer of systemic acquired resistance (SAR) in tobacco and generates a wave of salicylic acid expanding from the site of application. *Mol. Plant Pathol.* 14, 191–196. doi: 10.1111/j.1364-3703.2012.00842.x

Frías, M., González, C., and Brito, N. (2011). BcSpl1, a cerato-platanin family protein, contributes to *Botrytis cinerea* virulence and elicits the hypersensitive response in the host. *New Phytol.* 192, 483–495. doi: 10.1111/j.1469-8137.2011.03802.x

Furman-Matarasso, N., Cohen, E., Du, Q., Chejanovsky, N., Hanania, U., and Avni, A. (1999). A point mutation in the ethylene-inducing xylanase elicitor inhibits the beta-1-4-endoxylanase activity but not the elicitation activity. *Plant Physiol.* 121, 345–351. doi: 10.1104/pp.121.2.345

Gimenez-Ibanez, S., Hann, D. R., Ntoukakis, V., Petutschnig, E., Lipka, V., and Rathjen, J. P. (2009). AvrPtoB targets the LysM receptor kinase CERK1 to promote bacterial virulence on plants. *Curr. Biol.* 19, 423–429. doi: 10.1016/j.cub.2009.01.054

Gómez-Gómez, E., Ruíz-Roldán, M. C., Di Pietro, A., Roncero, M. I. G., and Hera, C. (2002). Role in pathogenesis of two endo-β-1,4-xylanase genes from the vascular wilt fungus *Fusarium oxysporum*. *Fungal Genet. Biol.* 35, 213–222. doi: 10.1006/fgbi.2001.1318

González, M., Brito, N., and González, C. (2017). The *Botrytis cinerea* elicitor protein BcIEB1 interacts with the tobacco PR5-family protein osmotin and protects the fungus against its antifungal activity. *New Phytol.* 215, 397–410. doi: 10.1111/nph.14588

Gravino, M., Locci, F., Tundo, S., Cervone, F., Savatin, D. V., and De Lorenzo, G. (2016). Immune responses induced by oligogalacturonides are differentially affected by AvrPto and loss of BAK1/BKK1 and PEPR1/PEPR2. *Mol. Plant Pathol.* 18, 582–595. doi: 10.1111/mpp.12419

Gui, Y., Zhang, W., Zhang, D., Zhou, L., Short, D. P. G., Wang, J., et al. (2017). A *Verticillium dahliae* extracellular cutinase modulates plant immune responses. *Mol. Plant Microbe Interact.* 31, 260–273. doi: 10.1094/MPMI-06-17-0136-R

Gui, Y.-J., Chen, J.-Y., Zhang, D.-D., Li, N.-Y., Li, T.-G., Zhang, W.-Q., et al. (2017). *Verticillium dahliae* manipulates plant immunity by glycoside hydrolase 12 proteins in conjunction with carbohydrate-binding module 1. *Environ. Microbiol.* 19, 1914–1932. doi: 10.1111/1462-2920.13695

Houterman, P. M., Cornelissen, B. J. C., and Rep, M. (2008). Suppression of plant resistance gene-based immunity by a fungal effector. *PLoS Pathog.* 4:e1000061. doi: 10.1371/journal.ppat.1000061

Jones, J. D. G., and Dangl, J. L. (2006). The plant immune system. *Nature* 444, 323–329. doi: 10.1038/nature05286

Kettles, G. J., Bayon, C., Canning, G., Rudd, J. J., and Kanyuka, K. (2016). Apoplastic recognition of multiple candidate effectors from the wheat pathogen *Zymoseptoria triticiin* the nonhost plant *Nicotiana benthamiana*. *New Phytol.* 213, 338–350. doi: 10.1111/nph.14215

Kubicek, C. P., Starr, T. L., and Glass, N. L. (2014). Plant cell wall–degrading enzymes and their secretion in plant-pathogenic fungi. *Annu. Rev. Phytopathol.* 52, 427–451. doi: 10.1146/annurev-phyto-102313-045831

Ky, I., Lorrain, B., Jourdes, M., Pasquier, G., Fermaud, M., Gény, L., et al. (2012). Assessment of grey mould (*Botrytis cinerea*) impact on phenolic and sensory quality of *Bordeaux grapes*, musts and wines for two consecutive vintages. *Aust. J. Grape Wine Res.* 18, 215–226. doi: 10.1111/j.1755-0238.2012.00191.x

Liebrand, T. W. H., van den Burg, H. A., and Joosten, M. H. A. J. (2014). Two for all: receptor-associated kinases SOBIR1 and BAK1. *Trends Plant Sci.* 19, 123–132. doi: 10.1016/j.tplants.2013.10.003

Liu, Z., Wu, Y., Yang, F., Zhang, Y., Chen, S., Xie, Q., et al. (2013). BIK1 interacts with PEPRs to mediate ethylene-induced immunity. *Proc. Natl. Acad. Sci. U.S.A.* 110, 6205–6210. doi: 10.1073/pnas.1215543110

Livak, K. J., and Schmittgen, T. D. (2001). Analysis of relative gene expression data using real-time quantitative PCR and the $2-\Delta\Delta CT$ method. *Methods* 25, 402–408. doi: 10.1006/meth.2001.1262

Ma, Y., Han, C., Chen, J., Li, H., He, K., Liu, A., et al. (2014). Fungal cellulase is an elicitor but its enzymatic activity is not required for its elicitor activity. *Mol. Plant Pathol.* 16, 14–26. doi: 10.1111/mpp.12156

Ma, Z., Song, T., Zhu, L., Ye, W., Wang, Y., Shao, Y., et al. (2015). A *Phytophthora sojae* glycoside hydrolase 12 protein is a major virulence factor during soybean infection and is recognized as a PAMP. *Plant Cell* 27, 2057–2072. doi: 10.1105/tpc.15.00390

Monaghan, J., and Zipfel, C. (2012). Plant pattern recognition receptor complexes at the plasma membrane. *Curr. Opin. Plant Biol.* 15, 349–357. doi: 10.1016/j.pbi.2012.05.006

Moscetti, I., Faoro, F., Moro, S., Sabbadin, D., Sella, L., Favaron, F., et al. (2014). The xylanase inhibitor TAXI-III counteracts the necrotic activity of a *Fusarium graminearum* xylanase in vitroand in durum wheat transgenic plants. *Mol. Plant Pathol.* 16, 583–592. doi: 10.1111/mpp.12215

Noda, J., Brito, N., and González, C. (2010). The *Botrytis cinerea* xylanase Xyn11A contributes to virulence with its necrotizing activity, not with its catalytic activity. *BMC Plant Biol.* 10:38. doi: 10.1186/1471-2229-10-38

Pandey, A., and Sonti, R. V. (2010). Role of the FeoB protein and siderophore in promoting virulence of *Xanthomonas oryzae* pv. *oryzae on Rice. J. Bacteriol.* 192, 3187–3203. doi: 10.1128/JB.01558-09

Prins, T. W., Tudzynski, P., von Tiedemann, A., Tudzynski, B., ten Have, A., Hansen, M. E., et al. (2000). "Infection strategies of *Botrytis cinerea* and related necrotrophic pathogens," in *Fungal Pathology*, ed. J. W. Kronstad (Dordrecht: Kluwer Academic Publishers Group), 33–64.

Rotblat, B., Enshell-Seijffers, D., Gershoni, J. M., Schuster, S., and Avni, A. (2002). Identification of an essential component of the elicitation active site of the EIX protein elicitor. *Plant J.* 32, 1049–1055. doi: 10.1046/j.1365-313X.2002.01490.x

Saijo, Y., Loo, E. P.-I., and Yasuda, S. (2017). Pattern recognition receptors and signaling in plant-microbe interactions. *Plant J.* 93, 592–613. doi: 10.1111/tpj.13808

Santhanam, P., van Esse, H. P., Albert, I., Faino, L., Nürnberger, T., and Thomma, B. P. H. J. (2013). Evidence for functional diversification within a fungal NEP1-Like protein family. *MPMI* 26, 278–286. doi: 10.1094/MPMI-09-12-0222-R

Schouten, A., van Baarlen, P., and van Kan, J. A. L. (2007). Phytotoxic Nep1-like proteins from the necrotrophic fungus *Botrytis cinerea* associate with membranes and the nucleus of plant cells. *New Phytol.* 177, 493–505.

Schulze, B., Mentzel, T., Jehle, A. K., Mueller, K., Beeler, S., Boller, T., et al. (2010). Rapid heteromerization and phosphorylation of ligand-activated plant transmembrane receptors and their associated kinase BAK1. *J. Biol. Chem.* 285, 9444–9451. doi: 10.1074/jbc.M109.096842

Sella, L., Gazzetti, K., Faoro, F., Odorizzi, S., D'Ovidio, R., Schäfer, W., et al. (2013). A *Fusarium graminearum* xylanase expressed during wheat infection

is a necrotizing factor but is not essential for virulence. *Plant Physiol. Biochem.* 64, 1–10. doi: 10.1016/j.plaphy.2012.12.008

Stergiopoulos, I., and de Wit, P. J. G. M. (2009). Fungal effector proteins. *Annu. Rev. Phytopathol.* 47, 233–263. doi: 10.1146/annurev.phyto.112408.132637

Williamson, B., Tudzynski, B., Tudzynski, P., and van Kan, J. A. L. (2007). *Botrytis cinerea*: the cause of grey mould disease. *Mol. Plant Pathol.* 8, 561–580. doi: 10.1111/j.1364-3703.2007.00417.x

Wu, S.-C., Ham, K.-S., Darvill, A. G., and Albersheim, P. (1997). Deletion of two endo-β-1,4-Xylanase genes reveals additional isozymes secreted by the rice blast fungus. *MPMI* 10, 700–708. doi: 10.1094/MPMI.1997.10.6.700

Yakoby, N., Beno-Moualem, D., Keen, N. T., Dinoor, A., Pines, O., and Prusky, D. (2001). *Colletotrichum gloeosporioides* pelBIs an important virulence factor in avocado fruit-fungus interaction. *MPMI* 14, 988–995. doi: 10.1094/MPMI.2001.14.8.988

Yamada, K., Yamashita-Yamada, M., Hirase, T., Fujiwara, T., Tsuda, K., Hiruma, K., et al. (2016). Danger peptide receptor signaling in plants ensures basal immunity upon pathogen-induced depletion of BAK1. *EMBO J.* 35, 46–61. doi: 10.15252/embj.201591807

Yu, X., Tang, J., Wang, Q., Ye, W., Tao, K., Duan, S., et al. (2012). The RxLR effector Avh241 from *Phytophthora sojae* requires plasma membrane localization to induce plant cell death. *New Phytol.* 196, 247–260. doi: 10.1111/j.1469-8137.2012.04241.x

Zhang, H., Wu, Q., Cao, S., Zhao, T., Chen, L., Zhuang, P., et al. (2014). A novel protein elicitor (SsCut) from *Sclerotinia sclerotiorum* induces multiple defense responses in plants. *Plant Mol. Biol.* 86, 495–511. doi: 10.1007/s11103-014-0244-3

Zhang, Y., Zhang, Y., Qiu, D., Zeng, H., Guo, L., and Yang, X. (2015). BcGs1, a glycoprotein from *Botrytis cinerea*, elicits defence response and improves disease resistance in host plants. *Biochem. Biophys. Res. Commun.* 457, 627–634. doi: 10.1016/j.bbrc.2015.01.038

Zhu, W., Ronen, M., Gur, Y., Minz-Dub, A., Masrati, G., Ben-Tal, N., et al. (2017). BcXYG1, a secreted xyloglucanase from *Botrytis cinerea*, triggers both cell death and plant immune responses. *Plant Physiol.* 175, 438–456. doi: 10.1104/pp.17.00375

Zipfel, C. (2008). Pattern-recognition receptors in plant innate immunity. *Curr. Opin. Immunol.* 20, 10–16. doi: 10.1016/j.coi.2007.11.003

Conflict of Interest Statement: The authors declare that the research was conducted in the absence of any commercial or financial relationships that could be construed as a potential conflict of interest.

frontiers in Plant Science

ORIGINAL RESEARCH
published: 21 November 2018
doi: 10.3389/fpls.2018.01711

Dominant and Recessive Major *R* Genes Lead to Different Types of Host Cell Death During Resistance to *Xanthomonas oryzae* in Rice

*Jianbo Cao[1,2], Meng Zhang[1], Jinghua Xiao[1], Xianghua Li[1], Meng Yuan[1] and Shiping Wang[1]**

[1] National Key Laboratory of Crop Genetic Improvement, National Center of Plant Gene Research (Wuhan), Huazhong Agricultural University, Wuhan, China, [2] Public Laboratory of Electron Microscopy, Huazhong Agricultural University, Wuhan, China

OPEN ACCESS

Edited by:
Marco Catoni,
University of Birmingham,
United Kingdom

Reviewed by:
Philip Carella,
University of Cambridge,
United Kingdom
Davide Pacifico,
Istituto di Bioscienze e Biorisorse (IBBR), Italy
Angela Feechan,
University College Dublin, Ireland

***Correspondence:**
Shiping Wang
swang@mail.hzau.edu.cn

Specialty section:
This article was submitted to Plant Microbe Interactions, a section of the journal Frontiers in Plant Science

Received: 09 August 2018
Accepted: 02 November 2018
Published: 21 November 2018

Citation:
Cao J, Zhang M, Xiao J, Li X, Yuan M and Wang S (2018) Dominant and Recessive Major R Genes Lead to Different Types of Host Cell Death During Resistance to Xanthomonas oryzae in Rice. Front. Plant Sci. 9:1711. doi: 10.3389/fpls.2018.01711

The bacterial blight caused by *Xanthomonas oryzae* pv. *oryzae* (*Xoo*) is the most devastating bacterial disease of rice worldwide. A number of dominant major disease resistance (*MR*) genes and recessive *MR* genes against *Xoo* have been cloned and molecularly characterized in the last two decades. However, how these *MR* genes mediated-resistances occur at the cytological level is largely unknown. Here, by ultrastructural examination of xylem parenchyma cells, we show that resistances to *Xoo* conferred by dominant *MR* genes and recessive *MR* genes resulted in different types of programmed cell death (PCD). Three dominant *MR* genes *Xa1*, *Xa4*, and *Xa21* and two recessive *MR* genes *xa5* and *xa13* that encode very different proteins were used in this study. We observed that *Xa1*-, *Xa4*-, and *Xa21*-mediated resistances to *Xoo* were associated mainly with autophagy-like cell death featured by the formation of autophagosome-like bodies in the xylem parenchyma cells. In contrast, the *xa5*- and *xa13*-mediated resistances to *Xoo* were associated mainly with vacuolar-mediated cell death characterized by tonoplast disruption of the xylem parenchyma cells. Application of autophagy inhibitor 3-methyladenine partially compromised *Xa1*-, *Xa4*-, and *Xa21*-mediated resistances, as did Na_2HPO_4 alkaline solution to *xa5*- and *xa13*-mediated resistances. These results suggest that autophagy-like cell death is a feature of the dominant *MR* gene-mediated resistance to *Xoo* and vacuolar-mediated cell death is a characteristic of the recessive *MR* gene-mediated resistance.

Keywords: major disease resistance gene, bacteria blight, autophagy-like cell death, vacuolar-mediated cell death, ultrastructure

INTRODUCTION

Plant resistance against pathogens can be genetically classified into two classes based on the strength of resistance: qualitative or complete resistance conferred by major disease resistance (*MR*) genes and quantitative or partial resistance mediated by multiple genes or quantitative trait loci (Kou and Wang, 2010; Zhang and Wang, 2013). The molecular mechanisms of plant disease resistance are explained, in general, with a two-tiered innate immune system: pathogen-associated molecular

pattern-triggered immunity (PTI) or plant-derived damage-associated molecular PTI or basal resistance, and effector-triggered immunity (ETI) or gene-for-gene resistance (Jones and Dangl, 2006; Thomma et al., 2011; Monaghan and Zipfel, 2012). PTI is initiated by plasma membrane-localized plant pattern recognition receptors (PRRs), which are receptor-kinase proteins or receptor-like proteins, and ETI is initiated by cytoplasmic nucleotide-binding (NB)–leucine-rich repeat (LRR)-type resistance proteins (Jones and Dangl, 2006; Macho and Zipfel, 2014). Thus, in general, PTI is quantitative resistance and ETI is qualitative resistance in many plant–pathogen pathosystems (Zhang and Wang, 2013). However, rice and biotrophic *Xanthomonas oryzae* pv. *oryzae* (*Xoo*), which causes the most devastating bacterial disease of rice worldwide, are a unique pathosystem for rice qualitative resistance against *Xoo* (Zhang and Wang, 2013). The rice *MR* genes resistant to *Xoo* can be an ETI or a PTI or other mechanisms that cannot be explained by ETI and PTI (Zhang and Wang, 2013; Ke et al., 2017).

Except for the rice-*Xoo* pathosystem, earlier studies have shown that plant qualitative resistance to biotrophic pathogens frequently featured a rapid hypersensitive response (HR), which is characterized by rapid and localized cell death to restrict pathogen replication during the early stage of the plant–pathogen interaction (Pontier et al., 1998; Mur et al., 2008). Further studies have revealed that HR is often, but not always, a part of ETI initiated by NB-LRR proteins (Coll et al., 2011). HR-associated cell death is a kind of programmed cell death (PCD). Evolutionarily conserved autophagy, which is intracellular self-digestion of cytoplasmic components characterized by the formation of membrane-bound autophagosomes carrying a portion of the cytoplasm to be degraded or organelle permeabilization, has been observed to be involved in plant PCD (Dickman and Fluhr, 2013; Kabbage et al., 2017). The autophagosomes have different ultrastructures: (1) the vacuolar membrane (tonoplast)-bound body (microautophagy) formed by a portion of the cytoplasm, cytoplasmic vesicles or organelles in the vacuole; (2) the double-membrane body (macroautophagy) formed by a portion of cytoplasm bound by an endoplasmic reticulum-like tubule derived double-membrane in the cytoplasm; (3) the multilamellar body formed by many membranes bound by a single membrane in the cytoplasm (van Doorn and Papini, 2013). In addition, vacuolar-mediated PCD, in which the tonoplast integrity is compromised or the tonoplast is fused with the plasma membrane resulting in the release of vacuolar components into the cytoplasm or the extracellular space leading to cell death, also occurs in HR (Hara-Nishimura and Hatsugai, 2011; Dickman and Fluhr, 2013). In contrast, plant necrosis is characterized by shrinkage of the protoplast and rupture of the plasma membrane (van Doorn et al., 2011).

One of the features that makes the qualitative resistance of rice to *Xoo* unique from other pathosystems is that one third of the 41 *MR* genes identified thus far are genetically recessive (Zhang and Wang, 2013; Ke et al., 2017). Eleven (*Xa1*, *Xa3/Xa26*, *Xa4*, *xa5*, *Xa10*, *xa13*, *Xa21*, *Xa23*, *xa25*, *Xa27*, and *xa41*) of these 41 genes, which have been cloned and molecularly characterized at present, are shown to encode diverse types of proteins. Among the dominant genes, *Xa1* encodes a classic NB-LRR-type protein (Yoshimura et al., 1998), *Xa3/Xa26* and *Xa21* encode plasma membrane-localized LRR receptor kinase-type proteins (Song et al., 1995; Sun et al., 2004), *Xa4* encodes a cell wall-associated protein kinase (Hu et al., 2017). The recessive gene *xa5* encodes a mutated basal transcriptional factor IIA gamma (TFIIAγ) subunit 5 (TFIIAγ5^{V39E}) (Iyer and McCouch, 2004; Yuan et al., 2016), and *xa13*, *xa25*, and *xa41* encode MtN3/saliva/SWEET-type membrane proteins with XA13 and XA25 localized in the plasma membrane (Chu et al., 2006; Liu et al., 2011; Hutin et al., 2015; Cheng et al., 2017). The dominant *MR* genes *Xa1*, *Xa4*, *Xa21* and the recessive *MR* genes *xa5*, *xa13* are race-specifically resistant to *Xoo*, while the recessive genes *xa1*, *xa4*, *xa21* and the dominant *Xa5*, *Xa13* are susceptible to *Xoo* (Zhang and Wang, 2013).

Xa27, *xa13*, and *xa5* can trigger a HR (although the HR of *xa5* is weak) leading to the brown symptoms on infected rice leaves after infiltrating inoculation with avirulent *Xoo* strains (Gu et al., 2005; Yang et al., 2006; Iyer-Pascuzzi et al., 2008). The ectopically expressed *Xa10* and *Xa23* can only induce HR in *Nicotiana benthamiana* (Tian et al., 2014; Wang et al., 2015). Nonetheless, the formation of HR in rice xylem vessel tissue against *Xoo* bacteria, which multiply in xylem vessels of rice leaves under natural infection conditions (Kou and Wang, 2010), needs to be investigated.

To address the HR of rice *MR* gene-mediated resistance to *Xoo*, we compared tissue phenotypes and ultrastructural morphologies of rice leaves from lines containing the dominant *Xa1*, *Xa4*, and *Xa21 MR* genes and the recessive *xa5* and *xa13 MR* genes. We found that autophagy-like cell death is the major characteristic in dominant *MR* gene-mediated resistance and that vacuolar-mediated cell death is the main feature in recessive *MR* gene-mediated resistance. These findings suggest that the different types of HR-PCD contribute to the resistance of rice against *Xoo* by different *MR* genes.

MATERIALS AND METHODS

Rice Materials

IRBB1, IRBB4, IRBB21, IRBB5, and IRBB13 are near-isogenic rice lines (NILs) carrying dominant *MR* genes *Xa1*, *Xa4*, and *Xa21* and recessive *MR* genes *xa5* and *xa13*, respectively, in the genetic background of the rice variety IR24. Each of these five lines confers race-specific resistance to *Xoo* bacteria with different resistance spectra (Zhang and Wang, 2013; Hu et al., 2017).

Pathogen Inoculation

Rice plants were inoculated with 10^9 cells ml^{-1} of *Xoo* strains T7174 (Japanese race (1), PXO61, PXO86, PXO112, PXO99, or PXO341 (Philippine race 1, 2, 5, 6 or 10) suspension at either the 4-leaf stage (rice lines IRBB4, IRBB5, IRBB13, and IR24) or 7-leaf stage (rice lines IRBB1, IRBB21, and IR24) by the leaf-clipping method (Chen et al., 2002). For mock treatment, water without *Xoo* was used by clipping rice leaves. Disease was scored by measuring the lesion length at 2 weeks after inoculation. To study the cell responses to *Xoo* and the effects of 3-methyladenine (3-MA) and Na_2HPO_4 on resistance, rice plants

were inoculated by infiltrating leaves with a bacterial suspension of *Xoo* using a needleless syringe method (Schaad et al., 1996). The bacterial suspension with 10^9 cells ml^{-1} contained 5 mM 3-MA (Sigma, SIGMA-ALDRICH, St. Louis, MO, United States) or 2 mM Na_2HPO_4 (Sinopharm, Signopharm Chemical Reagent Co., Ltd., Shanghai, China). For mock treatment, leaves were infiltrated only by 5 mM 3-MA or 2 mM Na_2HPO_4 solution. Disease was scored by counting the number of infiltrating sites with water-soaked symptom at 3 days after inoculation. The inoculated leaves were photographed using scientific scanner (Image Scanner III, GE, Sweden). All the inoculation of plants with *Xoo* was biologically repeated at least twice with similar results, and one replicate was shown.

Transmission Electron Microscopy

The ultrastructure of rice leaf cells was studied by transmission electron microscopy. The leaves were sampled at 0 day after inoculation (sampling at 1 h after inoculation) (0 DAI), 3 DAI, 5 DAI, and 14 DAI. The leaf tissues at the inoculation sites were cut into 1 × 3 mm pieces and fixed in 2.5% (w/v) glutaraldehyde in 0.1 M phosphate buffer solution (PBS) (pH 7.2) at 4°C overnight. The fixed tissues were washed in PBS three times for 30 min each at room temperature (20–25°C), postfixed for 2 h in 1% osmium tetroxide, dehydrated in a graded series of acetone, infiltrated with Spurr resin (SPI, SPI Chem, West Chester, PA, United States), and polymerized at 65°C for 48 h. The samples were cut into ultrathin sections (60–70 nm thick), stained with 2% uranyl acetate, and examined with a Hitachi transmission electron microscope (H-7650; Hitachi, Japan) at 80 kv. Each sample had 3 biological replicates with each replicate having at least 3 ultrathin sections observed under the electron microscope. To quantify the cells containing autophagosome-like body, tonoplast disruption and protoplast shrinkage, 208–520 xylem parenchyma cells were observed from at least six or nine leaf xylem veins of six or nine plants in two or three independent inoculations. In each xylem vein, the total xylem parenchyma cells of one vein were observed, then the frequencies (%) of the cells with the above three structures in the total xylem parenchyma cells were calculated. 57–80 mesophyll cells (approximately 10 cells from each plant) were observed and calculated for the frequencies (%) of cells with the above three structures from six leaves of six plants in two independent inoculations.

Expression Analysis of Autophagy-Related Genes and Vacuolar Processing Enzyme Gene

The 3-cm leaf fragments next to the inoculation sites were used for RNA isolation. Quantitative reverse transcription-PCR (qRT-PCR) was conducted as described previously using gene-specific primers (**Supplementary Table S1**; Qiu et al., 2007). The expression level of actin gene was used to standardize the RNA sample for each qRT-PCR, and then the expression level relative to the control was calculated. The assays were biologically repeated twice with similar results, and only one replicate was presented.

Statistical Analysis

The significant differences of lesion length, gene expression level and the number of cells with autophagosome-like body, tonoplast disruption or protoplast shrinkage ultrastructures between resistant and susceptible plants, were assessed using pairwise Student's *t*-test in Excel (Microsoft[1]).

RESULTS

The Leaf Tissue Morphology at Rice–*Xoo* Interaction Sites

Leaf tissue is a major infection site of *Xoo* (Niño-Liu et al., 2006). To study whether different types of rice *MR* gene-mediated resistance against *Xoo* have different types of cell death, we first analyzed the leaf morphology of rice–*Xoo* interaction sites in resistant IRBB1, IRBB4, IRBB5, IRBB13 and IRBB21 lines each carrying a different *MR* gene and susceptible line IR24 against *Xoo* strains T7174, PXO61, or PXO99 (**Figure 1**). At 5 days after infection (DAI), the brown HR-like lesions appeared on all the inoculation sites of rice leaves of the NILs carrying *MR* genes, while the inoculation sites of susceptible IR24 leaves formed approximately 0.5-cm-long chlorotic water-soaked symptoms (**Figure 1A**). At 14 DAI, all the infection sites of leaf tissue turned into yellow lesions in the resistant rice lines and the susceptible rice line (**Figure 1B**). The average lesion length of IR24 was about 6-fold longer than that of IRBB1, IRBB4, IRBB5, IRBB13, and IRBB21 at 14 DAI (**Figure 1C**).

Ultrastructural Morphotypes of Xylem Parenchyma Cells in Different *MR* Gene-Mediated Resistances to *Xoo*

Xoo multiply and spread in the xylem vessels of rice leaves (Kou and Wang, 2010). The leaf xylem parenchyma cells surrounding xylem vessels are in direct contact with *Xoo* (Niño-Liu et al., 2006). Thus, we examined the ultrastructure of xylem parenchyma cells in the process of cell death after *Xoo* infection in NILs by transmission electron microscopy. We observed three types of abnormal ultrastructures in xylem parenchyma cells of infection sites at 3 DAI (**Figures 2A–C**). The first type of abnormal ultrastructure was observed mostly in resistant IRBB4 and IRBB21 lines, which showed autophagosome-like bodies formed by autophagy processes including double-membrane-like bodies in the cytoplasm, single-membrane-bound bodies containing multiple small vesicles in the cytoplasm, and tonoplast-bound bodies in vacuoles (**Figure 2A**). The second type of abnormal ultrastructure was tonoplast disruption that was commonly observed in the resistant IRBB13 line (**Figure 2B**). The third type of abnormal structure was protoplast shrinkage and rupture of the plasma membrane observed in the susceptible IR24 line (**Figure 2C**).

To study whether the dominant or recessive *MR* gene-mediated resistance and the susceptible reaction are associated with different abnormal structures in rice-*Xoo* interactions,

[1]http://www.microsoftstore.com

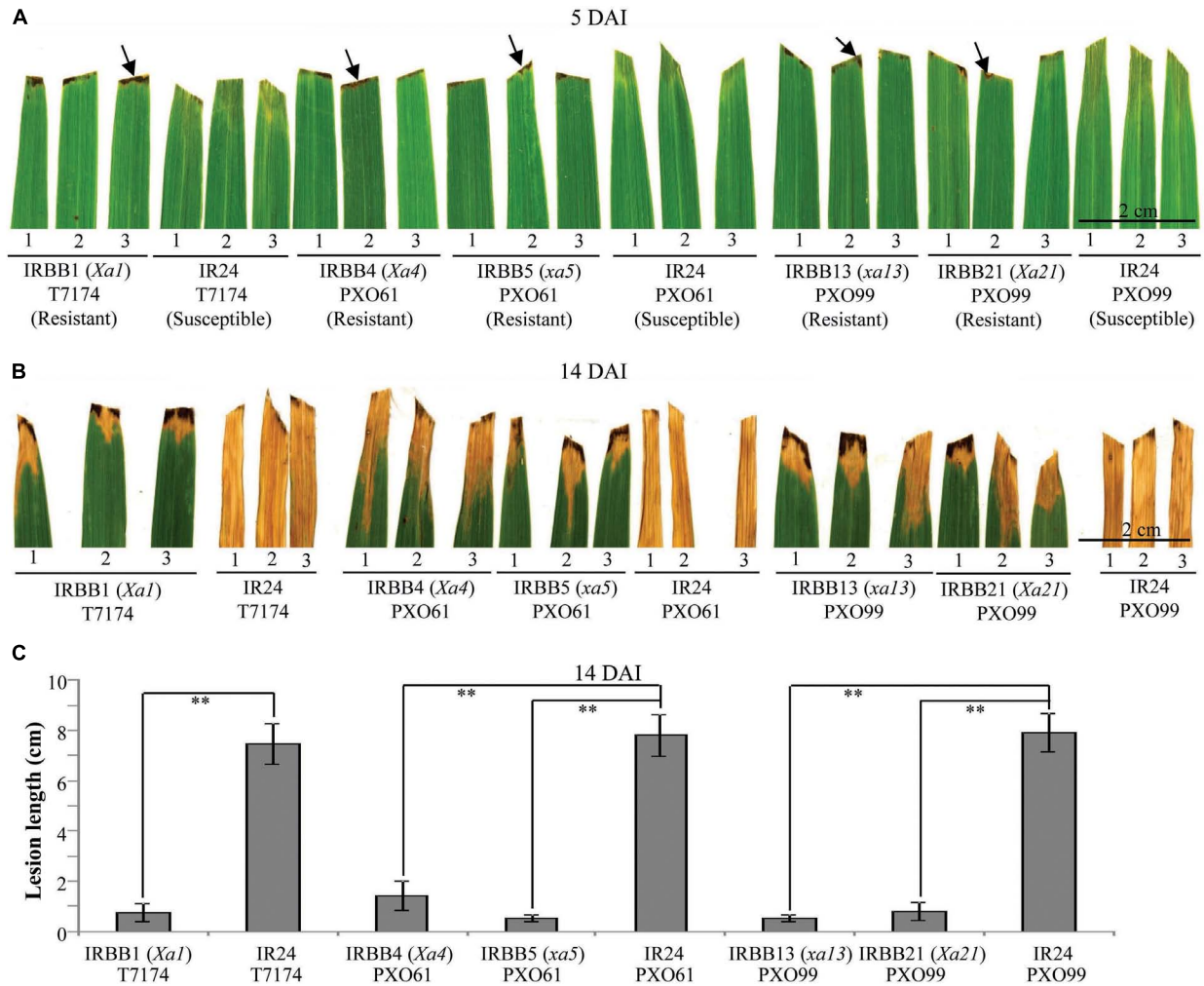

FIGURE 1 | Phenotypes of different rice line–*Xoo* strain interactions. DAI, day after infection; arrow, hypersensitive response-like lesion. **(A,B)** Leaf responses of resistant rice lines IRBB1, IRBB4, IRBB5, IRBB13, and IRBB21 and susceptible rice line IR24 inoculated with *Xoo* strain T7174, PXO61, or PXO99 at 5 and 14 DAI. **(C)** Lesion length of different rice lines infected with *Xoo* at 14 DAI. Bars represent mean (12 to 16 leaves from four plants) ± standard deviation (SD). The double asterisk (**) stands for the significant difference between resistant and susceptible plants at $P < 0.01$.

we counted the xylem parenchyma cells containing the three abnormal ultrastructures in all the rice lines at 0 and 5 DAI. There were integrated protoplasts and intact organelles in xylem parenchyma cells of all the rice lines and no significant difference in the numbers of xylem parenchyma cells with the three abnormal ultrastructures at 0 DAI among different lines (**Figures 3A,C,E**, **4A,C**, **5A–C** and **Supplementary Figures S1**, **S2**). However, at 5 DAI, autophagosome-like bodies, tonoplast disruption, and protoplast shrinkage were observed in xylem parenchyma cells of all the rice lines, but the frequencies of cells with the three ultrastructures were very different among these rice–*Xoo* interactions (**Figures 3–5** and **Supplementary Figure S2**). In IRBB1, IRBB4, and IRBB21 lines resistant to *Xoo* strains T7174, PXO61 or PXO112, PXO99, or PXO61, autophagosome-like bodies were the major feature in xylem parenchyma cells (**Figures 3A,C,E** and **Supplementary Figures S2A–B**). The number of rice cells containing autophagosome-like bodies was 4- and 3-fold higher than the number of cells containing tonoplast disruption and plasmolysis, respectively, in IRBB1; was 5- and 4-fold higher than the number of cells containing tonoplast disruption and plasmolysis, respectively, in IRBB4; and was 5- and 3-fold higher than the number of cells containing tonoplast disruption and plasmolysis, respectively, in IRBB21 (**Figure 3G** and **Supplementary Figure S2D**). However, protoplast shrinkage was the major features in xylem parenchyma cells in IRBB1, IRBB4 and IRBB21 lines susceptible to compatible *Xoo* strain PXO99, PXO341 (**Figures 3B,D,F**). The number of cells with protoplast shrinkage was 4- and 6-fold higher than the number of cells containing autophagosome-like bodies and tonoplast disruption (**Figure 3G**).

In contrast, tonoplast disruption was observed to be the major feature in xylem parenchyma cells during the IRBB5, IRBB13 lines resistant to *Xoo* strains PXO61 or PXO86, PXO99

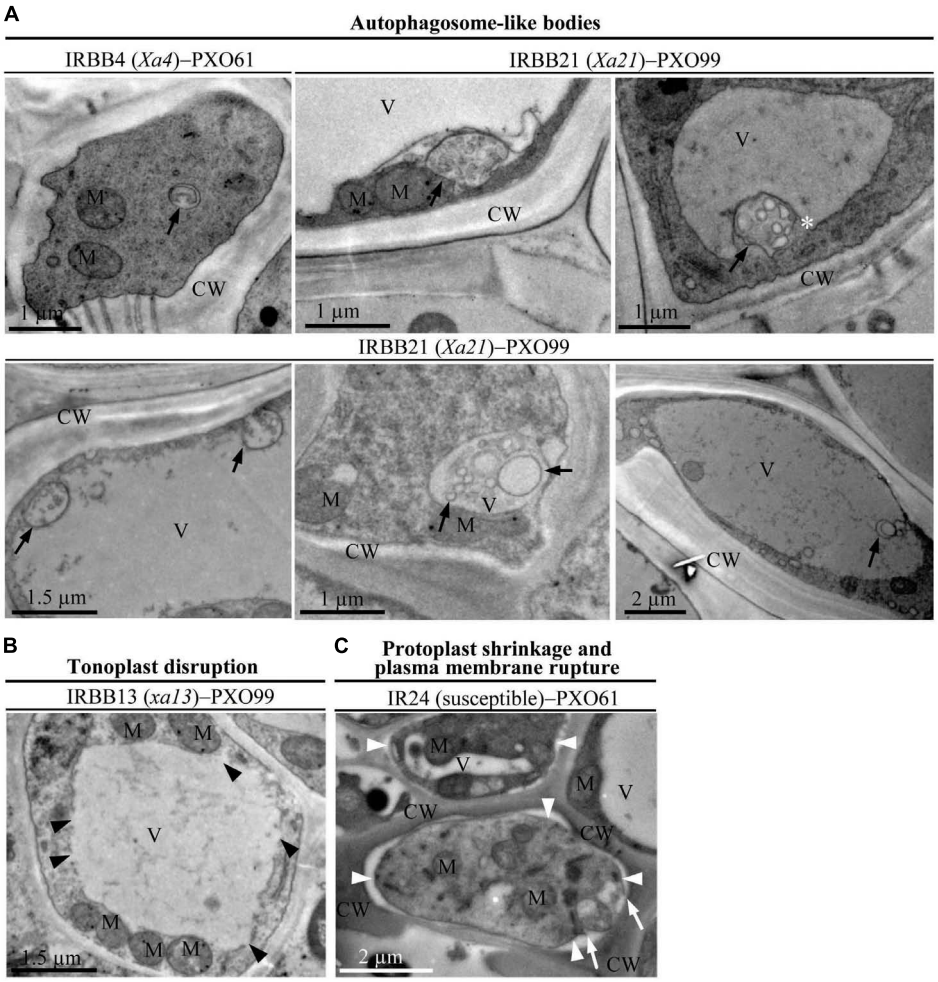

FIGURE 2 | The abnormal ultrastructures in rice xylem parenchyma cells after *Xoo* infection at 3 DAI. XV, xylem vessel; V, vacuole; CW, cell wall; M, mitochondrion. **(A)** Autophagosome-like bodies (dark arrows showing double-membrane-like body or single-membrane-like body) in the cytoplasm and vacuoles during resistant reactions. **(B)** Tonoplast disruption (dark arrowheads) in the resistant reaction. **(C)** Protoplast shrinkage (white arrowheads) and plasma membrane rupture (white arrows) in the susceptible reaction.

(**Figures 4A,C** and **Supplementary Figure S2C**). The number of rice cells containing tonoplast disruption was 3-fold higher than the number of cells containing autophagosome-like bodies or cells showing protoplast shrinkage in IRBB5, and was 3-fold higher than the number of cells containing autophagosome-like bodies and 6-fold higher than cells showing protoplast shrinkage in IRBB13 (**Figure 4E** and **Supplementary Figure S2D**). However, protoplast shrinkage was also the major features in xylem parenchyma cells in IRBB5, IRBB13 lines susceptible to compatible *Xoo* strains PXO99, PXO341 (**Figures 4B,D**). The number of cells with protoplast shrinkage was 4- and 6-fold higher than the number of cells containing autophagosome-like bodies and tonoplast disruption (**Figure 4E**). Meanwhile, the average lesion length of rice lines containing *MR* genes inoculated with compatible strains all exceeded 6 cm at 14 DAI (**Supplementary Figure S3**).

Furthermore, protoplast shrinkage was observed to be the major ultrastructure feature in xylem parenchyma cells in rice susceptible reactions to *Xoo* (**Figure 5**). Many xylem parenchyma cells showed protoplast shrinkage in IR24 that was susceptible to *Xoo* strains T7174, PXO61, and PXO99 (**Figures 5A–C**). The number of cells with protoplast shrinkage was 4- and 7-fold higher than the number of cells containing autophagosome-like bodies and tonoplast disruption, respectively, in all IR24–*Xoo* interactions (**Figure 5D**).

Expression of Autophagy-Related Genes and Vacuolar Processing Enzyme Gene in Different Resistances to *Xoo*

Autophagy-related genes (*ATG*) control the formation of autophagosome-like body in plants (Liu et al., 2005; Xia et al., 2011). Vacuolar processing enzyme genes (*VPE*) regulate vacuolar mediated cell death in plant-pathogens interactions and H_2O_2-induced PCD (Hatsugai et al., 2004; Deng et al., 2011). We analyzed transcription level of autophagy-related genes *OsATG5*

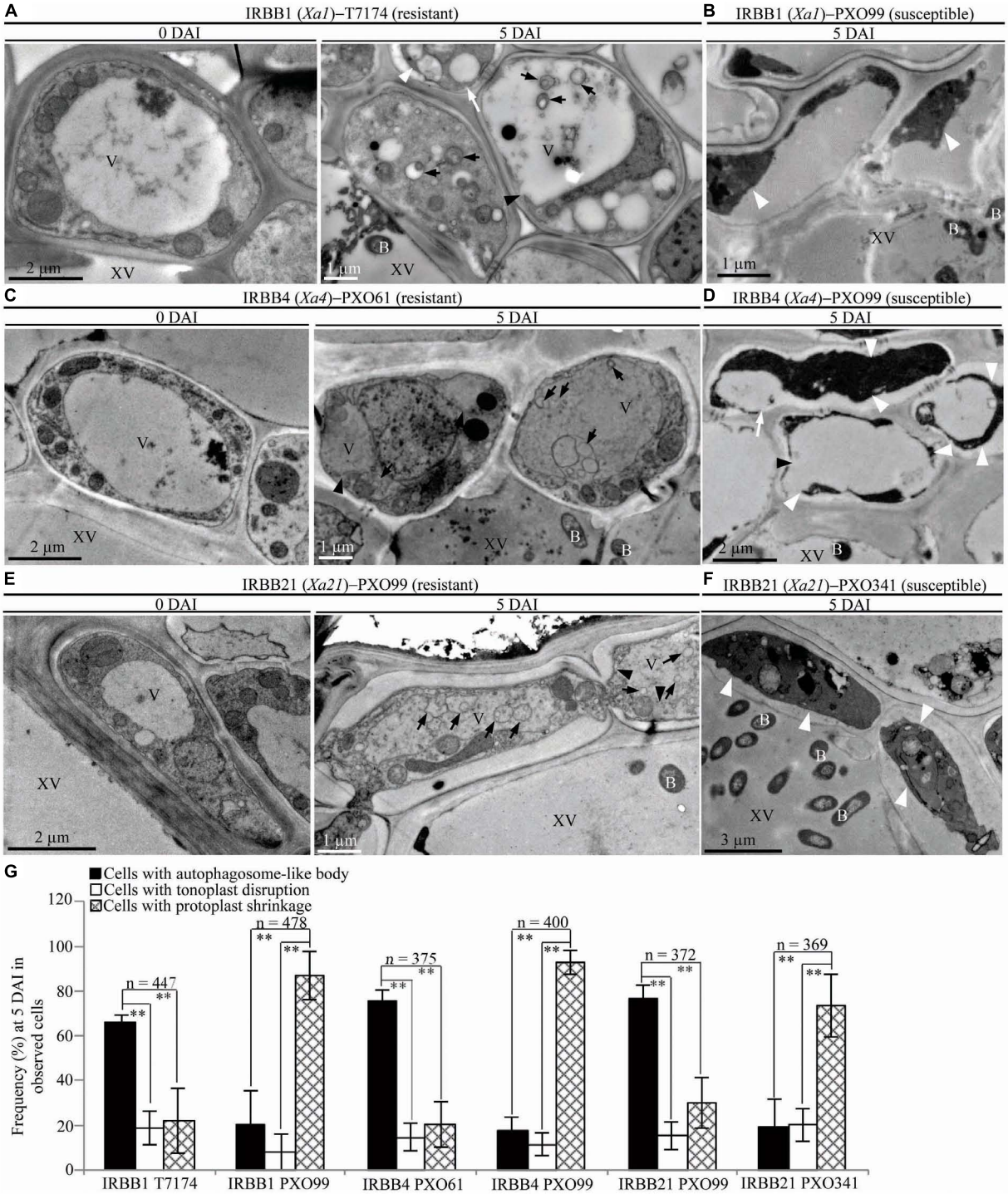

FIGURE 3 | Autophagosome-like body ultrastructural feature of xylem parenchyma cells in dominant *MR* genes *Xa1*, *Xa4*, or *Xa21* mediated-resistance. B, *Xoo* bacterium; V, vacuole; XV, xylem vessel; dark arrow, autophagosome-like body; dark arrowhead, tonoplast disruption; white arrowhead, protoplast shrinkage; white arrow, rupture of plasma membrane. **(A–F)** Many autophagosome-like bodies in xylem parenchyma cells of IRBB1, IRBB4, and IRBB21 plants at 5 days after inoculation (DAI) with *Xoo* strains T7174, PXO61, or PXO99 comparison with plants at 0 DAI and plants susceptible reaction to compatible strains PXO99, PXO341. **(G)** The percentage of cells with autophagosome-like bodies, tonoplast disruption, and protoplast shrinkage in micrographs of xylem parenchyma cell in rice leaves at 5 DAI. Data represent mean (at least nine leaf xylem parenchyma cells were observed from nine different plants in two or three independent inoculations) ± SD. The double asterisk (**) stands for a significant difference between frequency of cells with autophagosome-like body and frequency of cells with tonoplast disruption or protoplast shrinkage at $P < 0.01$. *n*, the total number of observed cells.

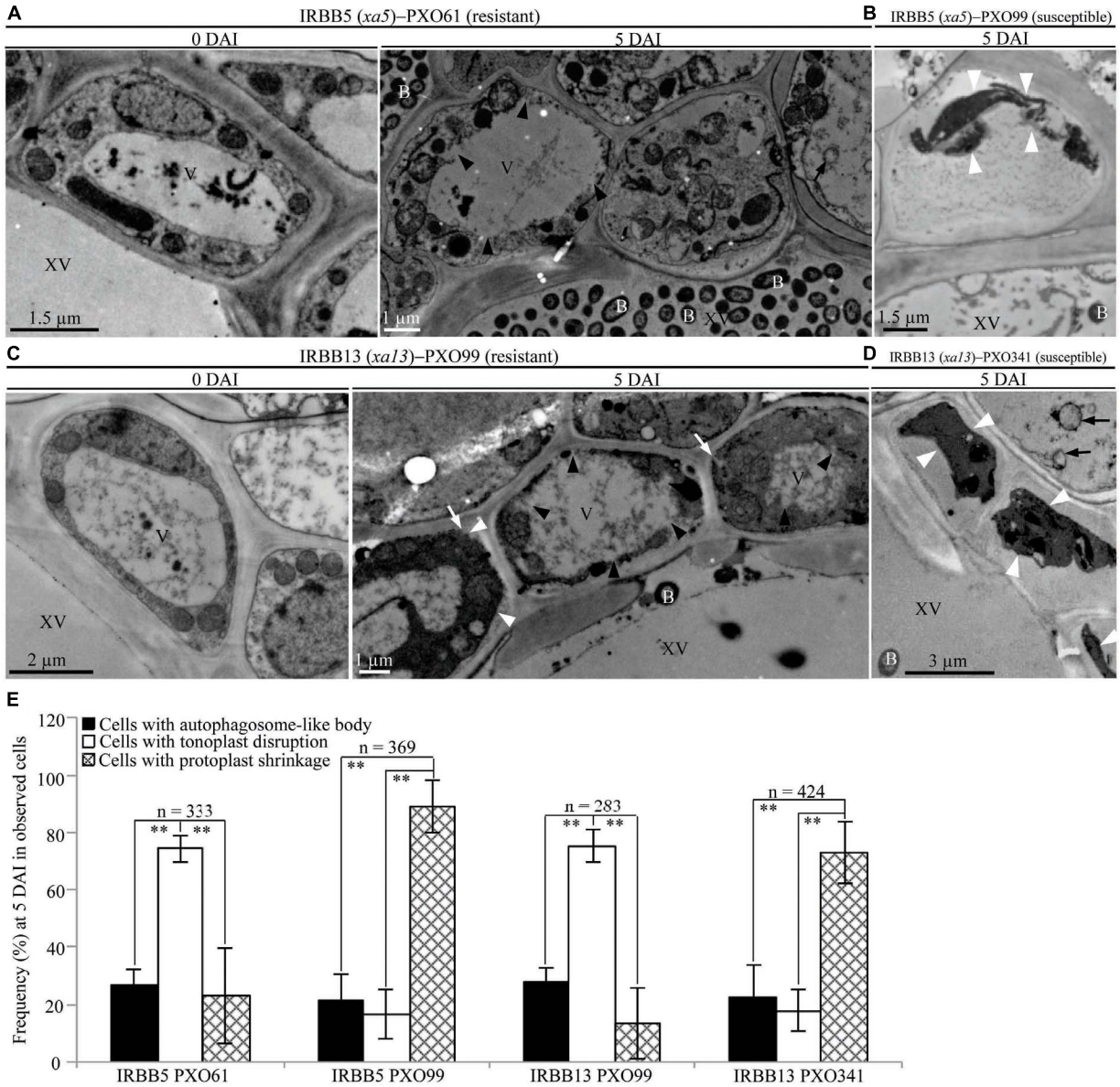

FIGURE 4 | Tonoplast disruption ultrastructure of xylem parenchyma cells in recessive *MR* genes *xa5* and *xa13* mediated-resistance. V, vacuole; XV, xylem vessel; and B, *Xoo* bacterium. Dark arrow, autophagosome-like body; dark arrowhead, tonoplast disruption; white arrowhead, protoplast shrinkage; and white arrow, rupture of plasma membrane. **(A–D)** Many xylem parenchyma cells with tonoplast disruption in IRBB5 and IRBB13 plants at 5 days after inoculation (DAI) with *Xoo* strains PXO61 and PXO99 comparison with plants at 0 DAI and plants susceptible reaction to compatible strains PXO99, PXO341. **(E)** The percentage of cells with autophagosome-like bodies, tonoplast disruption and protoplast shrinkage in micrographs of xylem parenchyma cell in rice leaves at 5 DAI. Data represents mean (at least nine leaf xylem parenchyma cells were observed from nine different plants in two or three independent inoculations) ± SD. The double asterisk (**) stands for a significant difference between frequency of cells with tonoplast disruption and frequency of cells with autophagosome-like body or protoplast shrinkage at $P < 0.01$. *n*, the total number of observed cells.

and *OsATG7*, *VPE* gene *OsVPE2* in IRBB1, IRBB4, IRBB21, and IRBB13 lines resistant to *Xoo* strains T7174, PXO61, and PXO99 (**Supplementary Figure S4**). On 8 and 24 h after inoculation, *OsATG5* and *OsATG7* were markedly induced to higher levels in IRBB1, IRBB4, and IRBB21 lines than that in susceptible IR24 control lines; *OsVPE2* was not induced in IRBB1, IRBB21 lines but was markedly induced to higher levels in IRBB13 plants compared to IR24 (**Supplementary Figure S4**).

Ultrastructural Morphotypes of Xylem Parenchyma Cells at Late Stage of Rice–*Xoo* Interaction and at Mock Treatment

To study the ultrastructure of xylem parenchyma cells at the late stage of the rice–*Xoo* interaction and the ultrastucture of xylem parenchyma cells of rice lines at mock treatment

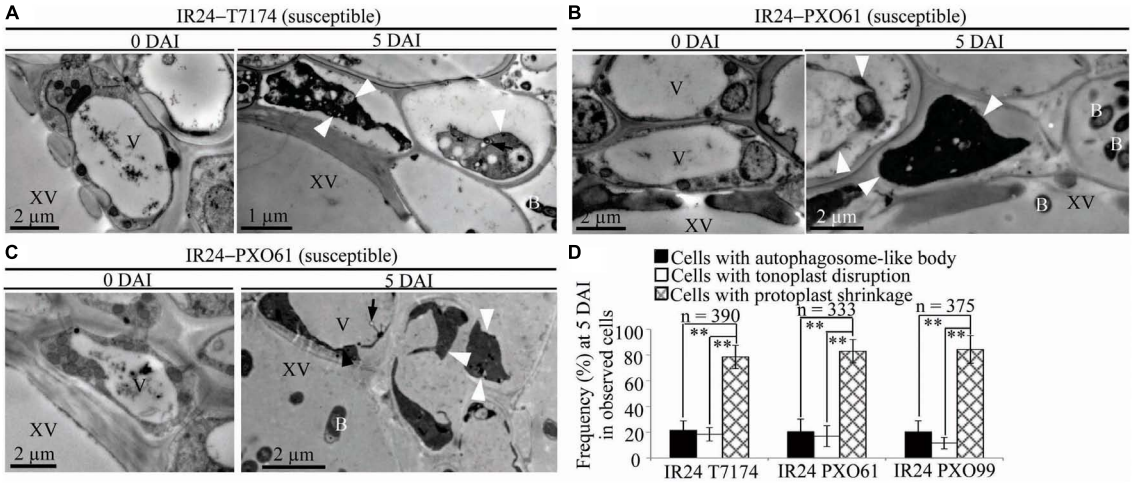

FIGURE 5 | Necrosis ultrastructural features of xylem parenchyma cells in susceptible reactions after *Xoo* infection. V, vacuole; XV, xylem vessel; and B, *Xoo* bacterium. Dark arrow, autophagosome-like body; dark arrowhead, tonoplast disruption; white arrowhead, protoplast shrinkage; and white arrow, rupture of plasma membrane. **(A–C)** Many xylem parenchyma cells with protoplast shrinkage in IR24 plants at 5 days after inoculation (DAI) susceptible to *Xoo* strains T7174, PXO61, PXO99 comparison with plants at 0 DAI. **(D)** The percentage of cells with autophagosome-like bodies, tonoplast disruption, and protoplast shrinkage in micrographs of xylem parenchyma cells in rice leaves at 5 DAI. Data represent mean (at least nine leaf xylem parenchyma cells were observed from nine different plants in two or three independent inoculations) ± SD. The double asterisk (**) stands for a significant difference between frequency of cells with protoplast shrinkage and frequency of cells with tonoplast disruption or autophagosome-like body at $P < 0.01$. *n*, the total number of observed cells.

(clipping leaf only with water), we examined the three abnormal structures, autophagosome-like bodies, tonoplast disruption, and protoplast shrinkage, in the infection sites of the rice lines at 14 DAI and the mock inoculation sites at 3, 5, 14 DAI (**Figure 6** and **Supplementary Figure S5**). Protoplast shrinkage was observed to be the major ultrastructural feature in xylem parenchyma cells at 14 DAI of all the rice–*Xoo* interactions and all the mock treatments (**Figures 6A–H** and **Supplementary Figures S5A–F**). The number of rice cells containing protoplast shrinkage was 3- to 6-fold higher than the number of cells with autophagosome-like bodies or tonoplast disruption, respectively, in all rice lines (**Figure 6I** and **Supplementary Figures S5G,H**). However, the number of rice cells containing autophagosome-like bodies was still 2- to 3-fold higher than the number of cells containing tonoplast disruption in dominant genes *Xa1*-, *Xa4*-, and *Xa21*-mediated resistance (**Figure 6I**). The number of rice cells containing tonoplast disruption was still 2- and 3-fold higher than the number of cells containing autophagosome-like bodies in recessive genes *xa5*- and *xa13*-mediated resistance (**Figure 6I**). Furthermore, at 3 and 5 DAI, there were integrated protoplasts and intact organelles in xylem parenchyma cells and no significant difference among the numbers of xylem parenchyma cell with the three abnormal ultrastructures at mock treatment (**Supplementary Figure S5**).

Effects of Autophagy Inhibitor 3-Methyladenine and Na_2HPO_4 Alkaline Solution on Different *MR* Gene-Mediated Resistances to *Xoo*

The infiltrated inoculation sites on rice leaves with deep ink-colored water-soaked symptoms defined the rice susceptibility to *Xoo* (Sugio et al., 2005; Yang et al., 2005). Na_2HPO_4 alkaline solution could neutralize the low pH (5.2–6.0) liquid released from disrupted vacuole (Martiniere et al., 2013). To determine if the autophagy inhibitor 3-methyladenine (3-MA) and Na_2HPO_4 alkaline solution could influence the resistance of rice lines with different *MR* genes, we observed whether there were water-soaked symptoms on the infiltrated inoculation sites (susceptible reaction) when the rice lines with *MR* genes were inoculated with *Xoo* bacteria in 3-MA solution or Na_2HPO_4 alkaline solution at 3 DAI (**Figures 7A–E**). The infiltration sites appeared water-soaked (deep inky color) in IRBB1, IRBB4, and IRBB21 inoculated with *Xoo* in 3-MA solution and IRBB5 and IRBB13 inoculated with *Xoo* in Na_2HPO_4 alkaline solution (**Figures 7A–E**). However, all the corresponding IRBB lines with *MR* genes inoculated with only the incompatible *Xoo* strain bacteria (resistant reaction) did not have water-soaked symptoms (**Figures 7A–E**). Furthermore, all the numbers of infiltration site with water-soaked symptom (susceptible reaction) in the inoculation of IRBB1, IRBB4 and IRBB21 with *Xoo* in 3-MA solution and the inoculation of IRBB5 and IRBB13 with *Xoo* in Na_2HPO_4 alkaline solution were significantly ($P < 0.01$) more than that in each rice lines inoculated only with *Xoo* (**Supplementary Table S2**). In contrast, the susceptible line IR24, when inoculated with *Xoo*, *Xoo* in 3-MA solution and *Xoo* in Na_2HPO_4 alkaline solution, had water-soaked symptoms on all infiltration sites (**Figures 7F–H**). Whereas there was no water-soaked symptom on infiltration sites in the rice lines only injected with 3-MA solution or Na_2HPO_4 alkaline solution (**Figure 7**).

To investigate whether the 3-MA and Na_2HPO_4 alkaline solution affected the ultrastructure of mesophyll cell in rice–*Xoo* interaction, we analyzed the mesophyll cell with the three

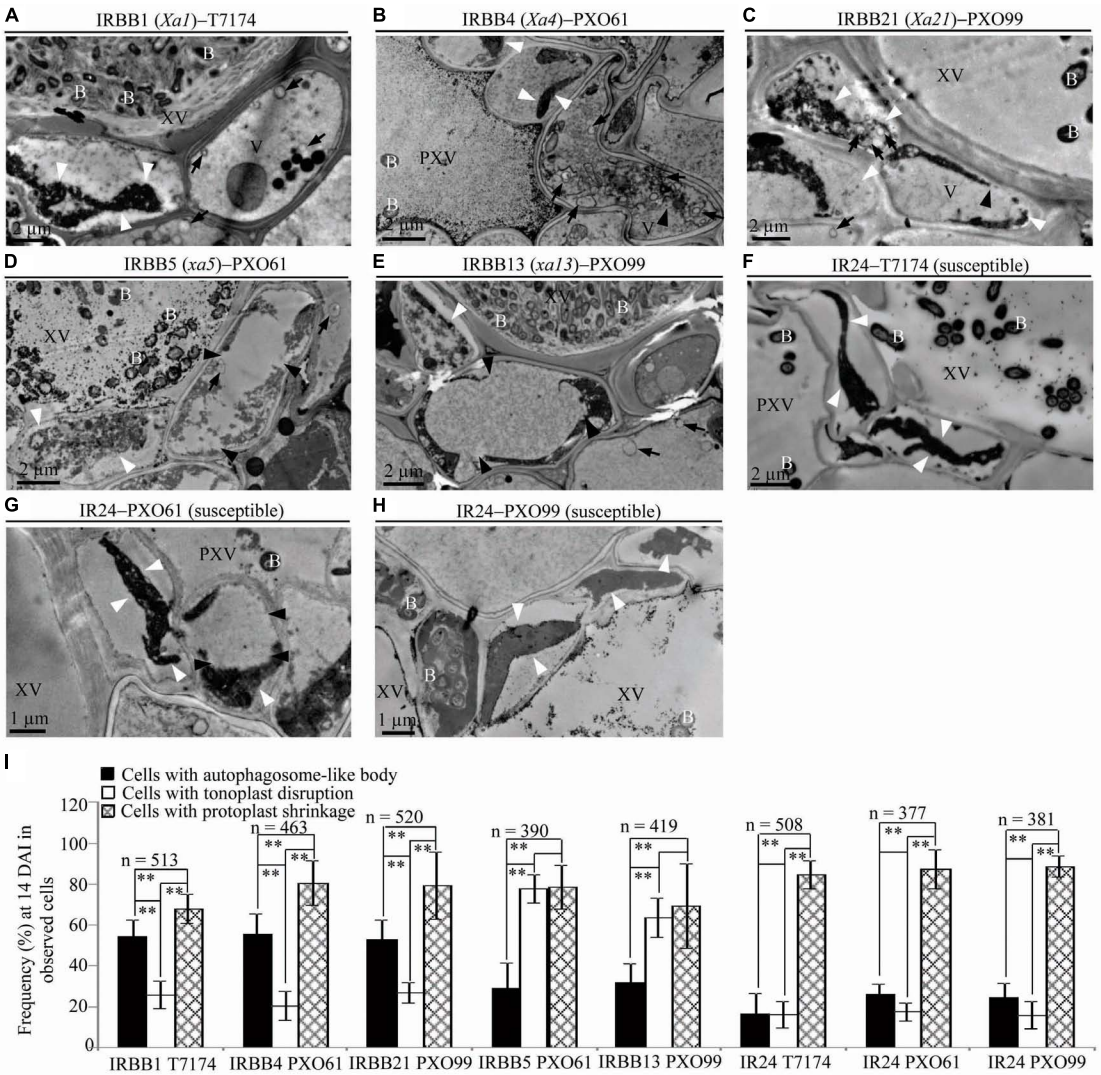

FIGURE 6 | Ultrastructural features of xylem parenchyma cells in dominant *MR* genes *Xa1*, *Xa4*, and *Xa21* and recessive *MR* genes *xa5* and *xa13* mediated-resistance compared with the susceptible control at 14 DAI with *Xoo*. B, *Xoo* bacterium; PXV, protoxylem vessel; V, vacuole; XV, xylem vessel; dark arrow, autophagosome-like body; dark arrowhead, tonoplast disruption; and white arrowhead, protoplast shrinkage. **(A–C)** Xylem parenchyma cells with most autophagosome-like bodies and with most protoplast shrinkage in IRBB1, IRBB4, IRBB21 plants. **(D,E)** Xylem parenchyma cells with most tonoplast disruption and with most protoplast shrinkage in IRBB5 and IRBB13 plants. **(F–H)** Xylem parenchyma cells with most protoplast shrinkage in IR24 plants. (**I**) Percentage of cells with autophagosome-like bodies, tonoplast disruption, and protoplast shrinkage in micrographs of xylem parenchyma cell in rice leaves at 14 DAI with *Xoo*. Data represent mean (at least nine leaf xylem parenchyma cells were observed from nine different plants in two or three independent inoculations) ± SD. The double asterisk (**) stands for a significant difference between frequency of cells with protoplast shrinkage and frequency of cells with autophagosome-like body or tonoplast disruption, between frequency of cells with autophagosome-like body and frequency of cells with tonoplast disruption in resistant plants, at $P < 0.01$. *n*, the total number of observed cells.

abnormal structures in rice lines with *MR* genes inoculated with *Xoo* bacteria in 3-MA solution or Na_2HPO_4 alkaline solution at 3 DAI (**Supplementary Figure S6**). In rice lines with *MR* genes infiltrated by only 3-MA or Na_2HPO_4 alkaline solution, the mesophyll cells represented intact protoplast and the numbers of mesophyll cell with three abnormal ultrastructures did not have difference (**Supplementary Figures S6A–E,I–J**). However, in IRBB1, IRBB4, IRBB21 lines inoculated with *Xoo* strains, the auphagosome-like bodies were the major ultrastructural features in mesophyll cells and the numbers of mesophyll cells with autophagosome-like bodies were 3- and 4-fold higher than the number of cells containing tonoplast disruption or protoplast shrinkage (**Supplementary Figures S6A–C,I**). In the IRBB1, IRBB4, and IRBB21 lines inoculated with *Xoo* strains in 3-MA solution, the IRBB5, IRBB13 lines inoculated with *Xoo* strains in Na_2HPO_4 alkaline solution and the IR24 lines only inoculated with *Xoo* strains, there were significantly more mesophyll cells with protoplast shrinkage than the mesophyll cells with autophagosome-like body or tonoplast disruption (**Supplementary Figure S6**). More mesophyll cells with tonoplast

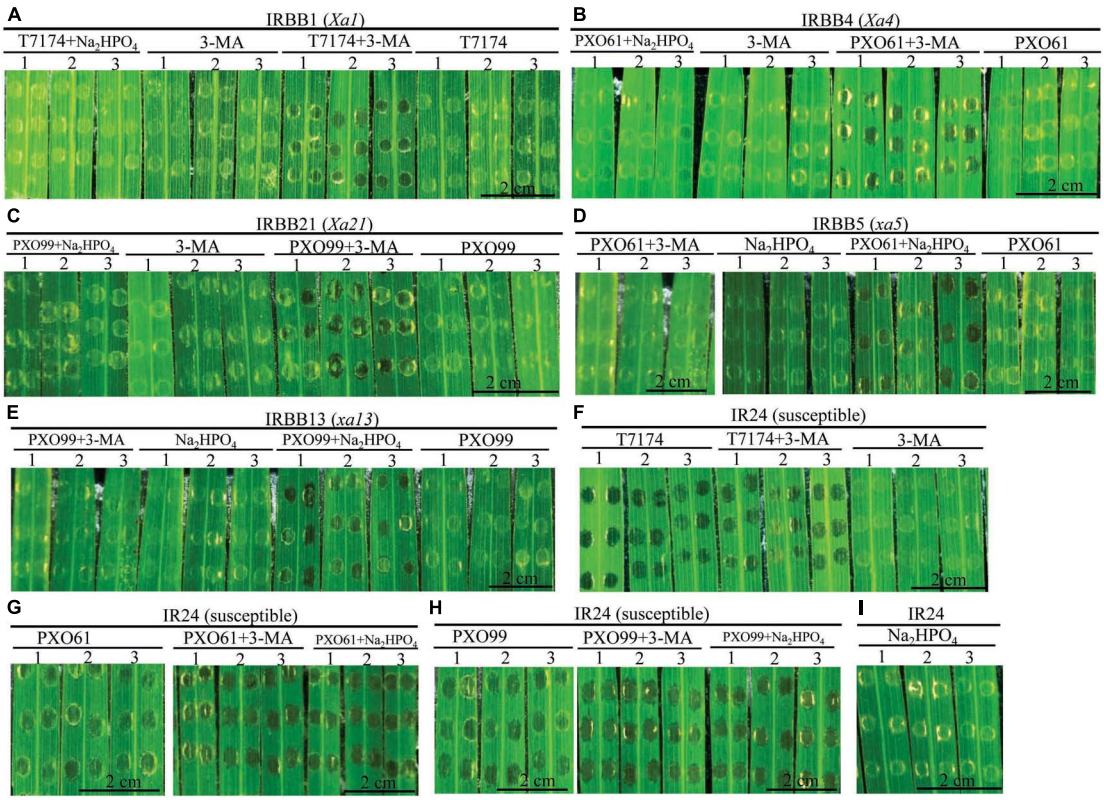

FIGURE 7 | Effects of 3-methyladenine and Na_2HPO_4 on water-soaked symptoms in rice lines infiltrated with *Xoo* strains in different solutions at the 3rd day. **(A–I)** The symptom of IRBB1, IRBB4, IRBB21, IRBB5, IRBB13, and IR24 leaf infiltration sites with *Xoo* strains T7174, PXO61, and PXO99 (nephelometry) in H_2O solution (T7174/PXO61/PXO99), in 5 mM 3-methyladenine (3-MA) solution (T7174/PXO61/PXO99 + 3-MA), in 2 mM Na_2HPO_4 solution (T7174/PXO61/PXO99 + Na_2HPO_4) and with only 5 mM 3-MA or 2 mM Na_2HPO_4 solution.

disruption were observed in IRBB5 and IRBB13 lines inoculated with only *Xoo* strains, even in IRBB5 and IRBB13 lines inoculated with *Xoo* strains in Na_2HPO_4 alkaline solution (**Supplementary Figures S6D–E,J**).

These results indicated that the mixing *Xoo* bacteria in 3-MA and Na_2HPO_4 alkaline solution significantly reduced the dominant genes *Xa1*-, *Xa4*-, and *Xa21*- mediated resistance and the recessive genes *xa5*- and *xa13*- mediated resistance, respectively.

DISCUSSION

A wide variety of pathogens can lead to lesion formation on infected plant tissue and trigger hypersensitive response-programmed cell death (HR-PCD) during plant resistance against pathogens (Mur et al., 2008; Kabbage et al., 2017). Most research on HR-PCD focused on the pathogens which grow and spread in the intercellular spaces of plant cells (Kabbage et al., 2017). However, the *Xoo* bacteria multiply and spread in the xylem vessels, a vascular structure surrounded by xylem parenchyma cells in rice leaves (Niño-Liu et al., 2006; Kou and Wang, 2010). In comparison with the chlorotic water-soaked symptoms of inoculated sites of susceptible rice line, the brown HR-like lesions on the *Xoo*-infected leaves of resistant rice lines (**Figure 1**) indicate that *Xoo* triggered the HR-PCD of resistant rice leaf cells. The xylem parenchyma cells, which directly interact with the *Xoo* bacterium (Niño-Liu et al., 2006), and the mesophyll cells appeared to have many classic autophagosome-like bodies and tonoplast rupture structures in resistant rice lines–*Xoo* interactions (**Figures 2–6** and **Supplementary Figures S2**, **S6**). *OsATG5* and *OsATG7* were only markedly induced expression in *Xa1*-, *Xa4*-, and *Xa21*-mediated resistance, as did *OsVPE2* only in *xa13*-mediated resistances (**Supplementary Figure S4**). Autophagy inhibitor 3-MA partially impaired the *Xa1*-, *Xa4*-, and *Xa21*-mediated resistances through reducing the number of mesophyll cells with autophagosome-like bodies (**Figure 7** and **Supplementary Figure S6**). Meanwhile, in all the susceptible reactions, the xylem parenchyma cells showed protoplast shrinkage and plasma membrane disruption (**Figures 3–6**). In all the resistant rice lines, there were little cells with autophagosome-like bodies and tonoplast rupture structures in control treatment (0 DAI) and mock treatment (3, 5, 14 DAI) (**Figures 3–5** and **Supplementary Figures S1**, **S5**), Therefore, the HR-PCD of xylem parenchyma cells belongs to autophagy-like cell death in *Xa1*-, *Xa4*-, and *Xa21*-mediated resistance and vacuolar-mediated cell death in *xa5*- and *xa13*-mediated resistance. However, there were approximately 70%

of xylem parenchyma cells that had autophagy-like cell death and vacuolar-mediated cell death at 5 DAI (**Figures 3**, **4** and **Supplementary Figure S2**). Thus, these findings suggest that autophagy-like cell death and vacuolar-mediated cell death are the major types partly mixed with other types in resistances against *Xoo*.

The dominant *Xa1*, *Xa4*, and *Xa21* encode a NB-LRR-type protein, a cell wall-associated kinase and a plasma membrane-localized LRR receptor kinase, respectively (Yoshimura et al., 1998; Chen et al., 2010; Hu et al., 2017). The *Arabidopsis thaliana MR* genes *Cf9*, *Pto*, *PRS2*, and *RPS4* encode a membrane-anchored glycoprotein, a cytoplasmic serine-threonine protein kinase, a CC-NB-LRR-type protein and a TIR-NB-LRR-type protein, respectively (Pedley and Martin, 2003; Hofius et al., 2009; Chakrabarti et al., 2016). The Cf9, Pto, PRS2 and RPS4 proteins as receptors can trigger autophagy cell death to mediate *A. thaliana* resistance to *Pseudomonas syringae pathovar* (pv) *tomato*, *Pst* (Liu et al., 2005; Hofius et al., 2009; Gururani et al., 2012). Although XA1, XA4, and XA21 belong to different types of receptor proteins, they can accept and transfer resistance signals into rice cells during the resistance response (Yoshimura et al., 1998; Wang et al., 2006; Hu et al., 2017). As receptors, XA1, XA4, and XA21 proteins presumably have triggered autophagy-like cell death to partially mediate rice resistance against *Xoo*. The xylem parenchyma cells with autophagy-like cell death still had intact morphologies in *Xa1*-, *Xa4*-, and *Xa21*-mediated resistance (**Figure 3** and **Supplementary Figure S2**). The intact xylem parenchyma cells possibly provide a vital cell environment to facilitate rice resistance against *Xoo*.

The low expression level of susceptible genes such as *SWEET11*/*Xa13*, *SWEET13*, and *SWEET14*/*Xa41* limits the growth of *Xoo* bacteria in *xa5*-, *xa13*-, and *xa41*- mediated resistances (Chen et al., 2010; Hutin et al., 2015; Huang et al., 2016; Yuan et al., 2016). The above *SWEET* genes encode glucose transporters which localize on plasma membrane and take part in pumping glucose to extracellular space (Chen et al., 2010; Hutin et al., 2015; Huang et al., 2016). A lot of other glucose transporters on tonoplast play important roles in uptake glucose into vacuole in *A. thaliana* and rice plant cells (Cho et al., 2010; Hedrich et al., 2015). The *SWEET* genes such as wheat leaf rust *R* genes *Lr67* and *Lr34* can lead to the intracellular glucose accumulation and the leaf senescence in resistance reactions (Krattinger et al., 2009; Chen et al., 2010; Moore et al., 2015). Therefore, in *xa5*- and *xa13*-mediated resistances, glucose may accumulate in xylem parenchyma cell where it is pumped into vacuole. Consequently, the tonoplast is disrupted by the high concentration of glucose in vacuole. The vacuole of plants has a low pH (5.2–6.0) to maintain the activity of acid hydrolytic enzymes and defense proteins (Neuhaus et al., 1991; Martiniere et al., 2013). These hydrolytic enzymes can inhibit *Pst* bacteria growth after being released into the extracellular matrix by tonoplast fusion with the plasma membrane in *A. thaliana* (Hatsugai et al., 2009). Meanwhile, the destructive vacuolar-mediated cell death mediated by VPE, which is characterized by vacuole collapse by tonoplast disruption and vacuole collapse leading to cytoplasmic content degradation and rapid cell death, is involved in *N. benthamiana* resistance to tobacco mosaic virus and *A. thaliana* resistance to *Pst* or *Botrytis cinerea* (Hatsugai et al., 2004; Rojo et al., 2004). We also found the tonoplast disintegration of most xylem parenchyma cells in *xa5*- and *xa13*-mediated resistances and the higher expression level of *OsVPE2* in *xa13*-mediated resistance (**Figures 4**, **6** and **Supplementary Figure S4**). Based on our results, vacuolar-mediated cell death is a form of destructive cell death. The Na_2HPO_4 alkaline solution (pH 9.0) dramatically increased the susceptibility but did not change the number of mesophyll cells with tonoplast disruption in *xa5*- and *xa13*-mediated resistances (**Figure 7**, **Supplementary Figure S6** and **Supplementary Table S2**), which suggests that the alkaline solution partially impairs *xa5*- and *xa13*-mediated resistance against *Xoo*. Destructive vacuolar-mediated cell death may depend on the low pH created by vacuole collapse to inhibit *Xoo* growth. Alternatively, hydrolytic enzymes and defense proteins released into the cytoplasm possibly participate in *xa5*- and *xa13*-mediated resistance.

The plant cells with shrinkage of protoplast and rupture of plasma membrane is regarded as necrosis cell death (van Doorn et al., 2011). The necrosis cell death typically happens under abiotic stress (van Doorn et al., 2011; Gao et al., 2015). However, the protoplast shrinkage also occurs in fungal toxin victorin-induced cell death (van Doorn et al., 2011). Meanwhile, the cell wall deformation, protoplast shrinkage and swelling of chloroplasts are observed in susceptible reaction of a black-rot-susceptible cultivar (Golden Acre) inoculated with *Xanthomonas campestris pv.campestri* (Bretschneider et al., 1989). At 3 and 5 DAI, the xylem parenchyma cells appeared protoplast shrinkage and plasma membrane rupture only in rice susceptible line IR24–*Xoo* interactions and the rice lines with *MR* genes but susceptible to compatible *Xoo* strains (**Figures 3–5**). Therefore, the cell death of xylem parenchyma cells in rice lines susceptible to *Xoo* can be categorized into necrosis at early stage of infection. At 14 DAI of resistant reaction, susceptible reaction or mock treatment, most parenchyma cells of rice line all represented protoplast shrinkage (**Figure 6** and **Supplementary Figure S5**), which indicates that the necrosis may be the general features of cell death in rice during late stages of pathogen infection and wound stress. In rice susceptible to *Xoo*, there are more bacteria in infection site than that in resistant reaction (Song et al., 1995; Yoshimura et al., 1998; Iyer and McCouch, 2004; Chu et al., 2006; Hu et al., 2017). The high bacterial population in xylem vessel of susceptible rice line may damage the xylem parenchyma cells to form necrosis. The necrosis of xylem parenchyma cells with plasma membrane rupture can possibly release nutrients into xylem vessels where *Xoo* bacteria multiply.

Plant cell often represents protoplast shrinkage and cell corpse at late stage of PCD (van Doorn et al., 2011). At 14 DAI, the leaves of infection site becoming yellow lesion (**Figure 1B**) indicated that the cell death of xylem parenchyma cells reached to late stage in resistant rice plants. Meanwhile, most xylem parenchyma cells appeared protoplast shrinkage and cell corpse in resistant rice plants at 14 DAI (**Figure 6**). But, most xylem parenchyma cells also represented autophagosome-like bodies and tonoplast disruption ultrastructures in resistant reactions (**Figures 6A–E,I**). Based on our results, the cell death progression in resistant rice lines happens as the following steps. Firstly,

the xylem parenchyma cells always keep autophagy-like cell death or vacuolar-mediated cell death from 3 DAI to 14 DAI. Secondly, the long-time autophagosome-like body formation or tonoplast disruption processes possibly lead to the rupture of plasma membrane. Lastly, the protoplast shrinkage leads to cell corpse at late stage. However, the cell death progression of xylem parenchyma cells in susceptible rice line is always keeping necrosis i.e., protoplast shrinkage from 3 DAI to 14 DAI (**Figures 2**, **5**, **6F–H**).

AUTHOR CONTRIBUTIONS

JC designed and performed most of the experiments, analyzed the data, and drafted the manuscript. MZ performed the qRT-PCR assays. JX and XL provided biochemical analysis support and field management. MY revised part of the manuscript. SW supervised the project, interpreted the data, and revised the manuscript. All authors read and approved the manuscript.

FUNDING

This work was supported by grants from the National Key Research and Development Program of China (2016YFD0100903) and the National Natural Science Foundations of China (31500977 and 31821005).

SUPPLEMENTARY MATERIAL

The Supplementary Material for this article can be found online at: https://www.frontiersin.org/articles/10.3389/fpls.2018.01711/full#supplementary-material

FIGURE S1 | Percentage of cells with autophagosome-like bodies, tonoplast disruption, and protoplast shrinkage in micrographs of xylem parenchyma cells in rice leaves at 0 DAI. Data represent mean (at least nine leaf xylem parenchyma cells were observed from nine different plants in two or three independent inoculations) ± SD. No difference between frequency of cells with protoplast shrinkage and frequency of cells with tonoplast disruption or autophagosome-like body at $P < 0.05$. *n*, the total number of observed cells.

FIGURE S2 | Autophagosome-like body and tonoplast disruption ultrastructural features of xylem parenchyma cells in rice lines with *MR* genes resistant to another incompatible *Xoo* strains. V, vacuole; XV, xylem vessel; and B, *Xoo* bacterium. Dark arrow, autophagosome-like body; dark arrowhead, tonoplast disruption; white arrowhead, protoplast shrinkage; and white arrow, rupture of plasma membrane. **(A–C)** Many autophagosome-like bodies and tonoplast disruption in xylem parenchyma cells of IRBB4, IRBB21, and IRBB5 plants at 5 days after inoculation (DAI) with *Xoo* strains PXO112, PXO61, and PXO86 comparison with plants at 0 DAI. **(D)** The percentage of cells with autophagosome-like bodies, tonoplast disruption, and protoplast shrinkage in micrographs of xylem parenchyma cell in rice leaves at 0 and 5 DAI. Data represent mean (at least six leaf xylem parenchyma cells were observed from six different plants in two independent inoculations) ± SD. The double asterisk (**) stands for a significant difference between frequency of cells with autophagosome-like body and frequency of cells with tonoplast disruption or protoplast shrinkage in at $P < 0.01$. *n*, the total number of observed cells.

FIGURE S3 | Lesion length of rice lines with *MR* genes *Xa1*, *Xa4*, *xa5*, *xa13*, and *Xa21* infected by compatible *Xoo* strains at 14 DAI. Bars represent mean (10 to 15 leaves from four plants) ± standard deviation (SD).

FIGURE S4 | Expression pattern of *OsATG5*, *OsATG7*, and *OsVPE2* in resistant (IRBB1, IRBB21, IRBB4, and IRBB13) and susceptible (IR24) rice lines–*Xoo* interactions. The expression of autophagy-related genes (*OsATG5*, *OsATG7*) and a vacuolar processing enzyme (*OsVPE2*) were analyzed by qRT-PCR in IRBB1/IR24 rice plants inoculated with *Xoo* strain T7174, IRBB21/IR24, and IRBB13/IR24 rice plants inoculated with *Xoo* strain PXO99, IRBB4/IR24 rice plants inoculated with *Xoo* strain PXO61. The rice plants were sampled on ck, 8 and 24 h after inoculation. Data are means (three replicates) ± standard deviations. ck, before inoculation. The letters "a" indicates statistically significant differences between ck and inoculated plants of the same rice plant at $P < 0.01$. Double astericks (**$P < 0.01$) indicate statistically significant differences resistant rice plant and susceptible rice plant inoculated at same time.

FIGURE S5 | Ultrastructural features of xylem parenchyma cell in rice lines with mock treatment. V, vacuole; XV, xylem vessel; and B, *Xoo* bacterium. White arrowhead, protoplast shrinkage; and white arrow, rupture of plasma membrane. **(A–F)** Many xylem parenchyma cells with protoplast shrinkage at 14 day after inoculation (DAI) comparison with the normal xylem parenchyma cells without three abnormal ultrastructures at 3 DAI and 5 DAI in IRBB1, IRBB4, IRBB21, IRBB5, IRBB13, and IR24 plants. **(G,H)** Percentage of cells with autophagosome-like bodies, tonoplast disruption, and protoplast shrinkage in micrographs of xylem parenchyma cell in rice leaves at 3, 5, and 14 DAI. Data represent mean (at least six leaf xylem parenchyma cells were observed from six different plants in two independent inoculations) ± SD. The double asterisk (**) stands for a significant difference between frequency of cells with protoplast shrinkage and frequency of cells with tonoplast disruption or autophagosome-like body at $P < 0.01$. *n*, the total number of observed cells.

FIGURE S6 | Effects of 3-methyladenine and Na_2HPO_4 on the ultrastructural features of mesophyll cell in rice lines infiltrated with *Xoo* strains in different solutions at the 3rd day. B, *Xoo* bacterium; V, vacuole; IS, intercellular space; Ch, chloroplast; N, nucleus; dark arrow, autophagosome-like body; dark arrowhead, tonoplast disruption; white arrowhead, protoplast shrinkage; and white arrow, rupture of plasma membrane. **(A–H)** the ultrastructural features of mesophyll cell in IRBB1, IRBB4, IRBB21, IRBB5, IRBB13, and IR24 leaf infiltration sites with *Xoo* strains T7174, PXO61, and PXO99 in H_2O solution (T7174/PXO61/PXO99), in 5 mM 3-methyladenine (3-MA) solution (T7174/PXO61/PXO99 + 3-MA), in 2 mM Na_2HPO_4 solution (T7174/PXO61/PXO99 + Na_2HPO_4) and with only 5 mM 3-MA or 2 mM Na_2HPO_4 solution. **(I,J)** percentage of cells with autophagosome-like bodies, tonoplast disruption, and protoplast shrinkage in micrographs of xylem parenchyma cell in rice leaves at 14 DAI with *Xoo*. Data represent mean (at least six leaf mesohyll cells were observed from six different plants in two independent inoculations) ± SD. The double asterisk (**) stands for a significant difference between frequency of cells with protoplast shrinkage and frequency of cells with autophagosome-like body or tonoplast disruption, between frequency of cells with autophagosome-like body and frequency of cells with tonoplast disruption in resistant plants, at $P < 0.01$. *n*, the total number of observed cells.

TABLE S1 | PCR primers used for quantitative RT-PCR assays.

TABLE S2 | Effect of 3-methyladenine and Na2HPO4 on the percentage of infiltrating inoculation site with water-soaked symptoms.

REFERENCES

Bretschneider, K. E., Gonella, M. P., and Robeson, D. J. (1989). A comparative light and electron microscopical study of compatible and incompatible interactions between *Xanthomonas campestris* pv. campestris and cabbage *(Brassica oleracea)*. *Mol. Plant Pathol.* 34, 285–297. doi: 10.1016/0885-5765(89)90026-X

Chakrabarti, A., Velusamy, T., Tee, C. Y., and Jones, D. (2016). A mutational analysis of the cytosolic domain of the tomato Cf-9 disease-resistance protein shows that membrane-proximal residues are important for

Avr9-dependent necrosis. *Mol. Plant Pathol.* 17, 565–576. doi: 10.1111/mpp.12315

Chen, H., Wang, S., and Zhang, Q. (2002). New gene for bacterial blight resistance in rice located on chromosome 12 identified from minghui 63, an elite restorer line. *Phytopathology* 92, 750–754. doi: 10.1094/PHYTO.2002.92.7.750

Chen, L. Q., Hou, B. H., Lalonde, S., Takanaga, H., Hartung, M. L., Qu, X. Q., et al. (2010). Sugar transporters for intercellular exchange and nutrition of pathogens. *Nature* 468, 527–532. doi: 10.1038/nature09606

Cheng, Q., Mao, W., Xie, W., Liu, Q., Cao, J., Yuan, M., et al. (2017). Characterization of a disease susceptibility locus for exploring an efficient way to improve rice resistance against bacterial blight. *Sci. China Life Sci.* 60, 298–306. doi: 10.1007/s11427-016-0299-x

Cho, J. I., Burla, B., Lee, D. W., Ryoo, N., Hong, S. K., Kim, H. B., et al. (2010). Expression analysis and functional characterization of the monosaccharide transporters, OsTMTs, involving vacuolar sugar transport in rice (*Oryza sativa*). *New Phytol.* 186, 657–668. doi: 10.1111/j.1469-8137.2010.03194.x

Chu, Z., Yuan, M., Yao, J., Ge, X., Yuan, B., Xu, C., et al. (2006). Promoter mutations of an essential gene for pollen development result in disease resistance in rice. *Genes Dev.* 20, 1250–1255. doi: 10.1101/gad.1416306

Coll, N. S., Epple, P., and Dangl, J. L. (2011). Programmed cell death in the plant immune system. *Cell Death Differ.* 18, 1247–1256. doi: 10.1038/cdd.2011.37

Deng, M., Bian, H., Xie, Y., Kim, Y., Wang, W., Lin, E., et al. (2011). Bcl-2 suppresses hydrogen peroxide-induced programmed cell death via OsVPE2 and OsVPE3, but not via OsVPE1 and OsVPE4, in rice. *FEBS J.* 278, 4797–4810. doi: 10.1111/j.1742-4658.2011.08380.x

Dickman, M. B., and Fluhr, R. (2013). Centrality of host cell death in plant-microbe interactions. *Annu. Rev. Phytopathol.* 51, 543–570. doi: 10.1146/annurev-phyto-081211-173027

Gao, H. J., Yang, H. Y., Bai, J. P., Liang, X. Y., Lou, Y., Zhang, J. L., et al. (2015). Ultrastructural and physiological responses of potato (*Solanum tuberosum* L.) plantlets to gradient saline stress. *Front. Plant Sci.* 5:787. doi: 10.3389/fpls.2014.00787

Gu, K., Yang, B., Tian, D., Wu, L., Wang, D., Sreekala, C., et al. (2005). R gene expression induced by a type-III effector triggers disease resistance in rice. *Nature* 435, 1122–1125. doi: 10.1038/nature03630

Gururani, M. A., Venkatesh, J., Upadhyaya, C. P., Nookaraju, A., Pandey, S. K., and Park, S. W. (2012). Plant disease resistance genes: current status and future directions. *Physiol. Mol. Plant Pathol.* 78, 51–65. doi: 10.1016/j.pmpp.2012.01.002

Hara-Nishimura, I., and Hatsugai, N. (2011). The role of vacuole in plant cell death. *Cell Death Differ.* 18, 1298–1304. doi: 10.1038/cdd.2011.70

Hatsugai, N., Iwasaki, S., Tamura, K., Kondo, M., Fuji, K., Ogasawara, K., et al. (2009). A novel membrane fusion-mediated plant immunity against bacterial pathogens. *Genes Dev.* 23, 2496–2506. doi: 10.1101/gad.1825209

Hatsugai, N., Kuroyanagi, M., Yamada, K., Meshi, T., Tsuda, S., Kondo, M., et al. (2004). A plant vacuolar protease, VPE, mediates virus-induced hypersensitive cell death. *Science* 305, 855–858. doi: 10.1126/science.1099859

Hedrich, R., Sauer, N., and Neuhaus, H. E. (2015). Sugar transport across the plant vacuolar membrane: nature and regulation of carrier proteins. *Curr. Opin. Plant Biol* 25, 63–70. doi: 10.1016/j.pbi.2015.04.008

Hofius, D., Schultz-Larsen, T., Joensen, J., Tsitsigiannis, D. I., Petersen, N. H., Mattsson, O., et al. (2009). Autophagic components contribute to hypersensitive cell death in Arabidopsis. *Cell* 137, 773–783. doi: 10.1016/j.cell.2009.02.036

Hu, K., Cao, J., Zhang, J., Xia, F., Ke, Y., Zhang, H., et al. (2017). Improvement of multiple agronomic traits by a disease resistance gene via cell wall reinforcement. *Nat. Plants* 3, 17009–17018. doi: 10.1038/nplants.2017.9

Huang, S., Antony, G., Li, T., Obasa, K., Yang, B., and White, F. F. (2016). The broadly effective recessive resistance gene xa5 of rice is a virulence effector-dependent quantitative trait for bacterial blight. *Plant J.* 86, 186–194. doi: 10.1111/tpj.13164

Hutin, M., Perez-Quintero, A., Lopez, C., and Szurek, B. (2015). MorTAL Kombat: the story of defense against TAL effectors through loss-of-susceptibility. *Front. Plant Sci.* 6:535. doi: 10.3389/fpls.2015.00535

Iyer, A. S., and McCouch, S. R. (2004). The rice bacterial blight resistance gene xa5 encodes a novel form of disease resistance. *Mol. Plant Microbe Interact.* 17, 1348–1354. doi: 10.1094/MPMI.2004.17.12.1348

Iyer-Pascuzzi, A. S., Jiang, H., Huang, L., and McCouch, S. R. (2008). Genetic and functional characterization of the rice bacterial blight disease resistance gene xa5. *Phytopathology* 98, 289–295. doi: 10.1094/PHYTO-98-3-0289

Jones, J. D., and Dangl, J. L. (2006). The plant immune system. *Nature* 444, 323–329. doi: 10.1038/nature05286

Kabbage, M., Kessens, R., Bartholomay, L. C., and Williams, B. (2017). The life and death of a plant cell. *Annu. Rev. Plant Biol.* 68, 375–404. doi: 10.1146/annurev-arplant-043015-111655

Ke, Y., Deng, H., and Wang, S. (2017). Advances in understanding broad-spectrum resistance to pathogens in rice. *Plant J.* 90, 738–748. doi: 10.1111/tpj.13438

Kou, Y., and Wang, S. (2010). Broad-spectrum and durability: understanding of quantitative disease resistance. *Curr. Opin. Plant Biol.* 13, 181–185. doi: 10.1016/j.pbi.2009.12.010

Krattinger, S. G., Lagudah, E. S., Spielmeyer, W., Singh, R. P., Huerta-Espino, J., McFadden, H., et al. (2009). A putative ABC transporter confers durable resistance to multiple fungal pathogens in wheat. *Science* 323, 1360–1363. doi: 10.1126/science.1166453

Liu, Q., Yuan, M., Zhou, Y., Li, X., Xiao, J., and Wang, S. (2011). A paralog of the MtN3/saliva family recessively confers race-specific resistance to Xanthomonas oryzae in rice. *Plant Cell Environ.* 34, 1958–1969. doi: 10.1111/j.1365-3040.2011.02391.x

Liu, Y., Schiff, M., Czymmek, K., Talloczy, Z., Levine, B., and Dinesh-Kumar, S. P. (2005). Autophagy regulates programmed cell death during the plant innate immune response. *Cell* 121, 567–577. doi: 10.1016/j.cell.2005.03.007

Macho, A. P., and Zipfel, C. (2014). Plant PRRs and the activation of innate immune signaling. *Mol. Cell.* 54, 263–272. doi: 10.1016/j.molcel.2014.03.028

Martiniere, A., Desbrosses, G., Sentenac, H., and Paris, N. (2013). Development and properties of genetically encoded pH sensors in plants. *Front. Plant Sci.* 4:523. doi: 10.3389/fpls.2013.00523

Monaghan, J., and Zipfel, C. (2012). Plant pattern recognition receptor complexes at the plasma membrane. *Curr. Opin. Plant Biol.* 15, 349–357. doi: 10.1016/j.pbi.2012.05.006

Moore, J. W., Herrera-Foessel, S., Lan, C., Schnippenkoetter, W., Ayliffe, M., Huerta-Espino, J., et al. (2015). A recently evolved hexose transporter variant confers resistance to multiple pathogens in wheat. *Nat. Genet.* 47, 1494–1498. doi: 10.1038/ng.3439

Mur, L. A., Kenton, P., Lloyd, A. J., Ougham, H., and Prats, E. (2008). The hypersensitive response; the centenary is upon us but how much do we know? *J. Exp. Bot.* 59, 501–520. doi: 10.1093/jxb/erm239

Neuhaus, J. M., Sticher, L., Meins, F. Jr., and Boller, T. (1991). A short C-terminal sequence is necessary and sufficient for the targeting of chitinases to the plant vacuole. *Proc. Natl. Acad. Sci. U.S.A.* 88, 10362–10366. doi: 10.1073/pnas.88.22.10362

Niño-Liu, D. O., Ronald, P. C., and Bogdanove, A. J. (2006). *Xanthomonas oryzae* pathovars: model pathogens of a model crop. *Mol. Plant Pathol.* 7, 303–324. doi: 10.1111/j.1364-3703.2006.00344.x

Pedley, K. F., and Martin, G. B. (2003). Molecular basis of Pto-mediated resistance to bacterial speck disease in tomato. *Annu. Rev. Phytopathol.* 41, 215–243. doi: 10.1146/annurev.phyto.41.121602.143032

Pontier, D., Balague, C., and Roby, D. (1998). The hypersensitive response. A programmed cell death associated with plant resistance. *C. R. Acad. Sci. III* 321, 721–734. doi: 10.1016/S0764-4469(98)80013-9

Qiu, D., Xiao, J., Ding, X., Xiong, M., Cai, M., Cao, Y., et al. (2007). OsWRKY13 mediates rice disease resistance by regulating defense-related genes in salicylate- and jasmonate-dependent signaling. *Mol. Plant Microbe Interact.* 20, 492–499. doi: 10.1094/MPMI-20-5-0492

Rojo, E., Martin, R., Carter, C., Zouhar, J., Pan, S., Plotnikova, J., et al. (2004). VPEγ exhibits a caspase-like activity that contributes to defense against pathogens. *Curr. Biol.* 14, 1897–1906. doi: 10.1016/j.cub.2004.09.056

Schaad, N., Wang, Z., Di, M., McBeath, J., Peterson, G., and Bonde, M. (1996). An improved infiltration technique to test the pathogenicity of *Xanthomonas oryzae* pv. oryzae in rice seedlings. *Seed Sci. Technol.* 24, 449–456.

Song, W., Wang, G., Chen, L., Kim, H., Pi, L., Holsten, T., et al. (1995). A receptor kinase-like protein encoded by the rice disease resistance gene, Xa21. *Science* 270, 1804–1806. doi: 10.1126/science.270.5243.1804

Sugio, A., Yang, B., and White, F. F. (2005). Characterization of the hrpF pathogenicity peninsula of *Xanthomonas oryzae* pv. oryzae. *Mol. Plant Microbe Interact.* 18, 546–554. doi: 10.1094/MPMI-18-0546

Sun, X., Cao, Y., Yang, Z., Xu, C., Li, X., Wang, S., et al. (2004). Xa26, a gene conferring resistance to *Xanthomonas oryzae* pv. oryzae in rice, encodes an LRR receptor kinase-like protein. *Plant J.* 37, 517–527. doi: 10.1046/j.1365-313X.2003.01976.x

Thomma, B. P., Nurnberger, T., and Joosten, M. H. (2011). Of PAMPs and effectors: the blurred PTI-ETI dichotomy. *Plant Cell* 23, 4–15. doi: 10.1105/tpc.110.082602

Tian, D., Wang, J., Zeng, X., Gu, K., Qiu, C., Yang, X., et al. (2014). The rice TAL effector-dependent resistance protein XA10 triggers cell death and calcium depletion in the endoplasmic reticulum. *Plant Cell* 26, 497–515. doi: 10.1105/tpc.113.119255

van Doorn, W. G., Beers, E., Dangl, J., Franklin-Tong, V., Gallois, P., Hara-Nishimura, I., et al. (2011). Morphological classification of plant cell deaths. *Cell Death Differ.* 18, 1241–1246. doi: 10.1038/cdd.2011.36

van Doorn, W. G., and Papini, A. (2013). Ultrastructure of autophagy in plant cells. *Autophagy* 9, 1922–1936. doi: 10.4161/auto.26275

Wang, C., Zhang, X., Fan, Y., Gao, Y., Zhu, Q., Zheng, C., et al. (2015). XA23 is an executor R protein and confers broad-spectrum disease resistance in rice. *Mol. Plant* 8, 290–302. doi: 10.1016/j.molp.2014.10.010

Wang, Y. S., Pi, L. Y., Chen, X. H., Chakrabarty, P. K., Jiang, J., De Leon, A. L., et al. (2006). Rice XA21 binding protein 3 is a ubiquitin ligase required for full Xa21-mediated disease resistance. *Plant Cell* 18, 3635–3646. doi: 10.1105/tpc.106.046730

Xia, K., Liu, T., Quyang, J., Wang, R., Fan, T., and Zhang, M. (2011). Genome-wide identification, classification, and expression analysis of autophagy-associated gene homologues in rice (*Oryza sativa* L.). *DNA Res.* 18, 363–377. doi: 10.1093/dnares/dsr024

Yang, B., Sugio, A., and White, F. F. (2005). Avoidance of host recognition by alterations in the repetitive and C-terminal regions of AvrXa7, a type III effector of *Xanthomonas oryzae* pv. oryzae. *Mol. Plant Microbe Interact.* 18, 142–149. doi: 10.1094/MPMI-18-0142

Yang, B., Sugio, A., and White, F. F. (2006). Os8N3 is a host disease-susceptibility gene for bacterial blight of rice. *Proc. Natl. Acad. Sci. U.S.A.* 103, 10503–10508. doi: 10.1073/pnas.0604088103

Yoshimura, S., Yamanouchi, U., Katayose, Y., Toki, S., Wang, Z. X., Kono, I., et al. (1998). Expression of Xa1, a bacterial blight-resistance gene in rice, is induced by bacterial inoculation. *Proc. Natl. Acad. Sci. U.S.A.* 95, 1663–1668. doi: 10.1073/pnas.95.4.1663

Yuan, M., Ke, Y., Huang, R., Ma, L., Yang, Z., Chu, Z., et al. (2016). A host basal transcription factor is a key component for infection of rice by TALE-carrying bacteria. *eLife* 5:e19605. doi: 10.7554/eLife.19605

Zhang, H., and Wang, S. (2013). Rice versus Xanthomonas oryzae pv oryzae: a unique pathosystem. *Curr. Opin. Plant Biol.* 16, 188–195. doi: 10.1016/j.pbi.2013.02.008

Conflict of Interest Statement: The authors declare that the research was conducted in the absence of any commercial or financial relationships that could be construed as a potential conflict of interest.

frontiers in Plant Science

ORIGINAL RESEARCH
published: 08 February 2019
doi: 10.3389/fpls.2019.00107

GmDAD1, a Conserved *Defender Against Cell Death 1* (*DAD1*) From Soybean, Positively Regulates Plant Resistance Against *Phytophthora* Pathogens

*Qiang Yan[1,2], Jierui Si[2], Xiaoxia Cui[1], Hao Peng[3], Maofeng Jing[2], Xin Chen[1], Han Xing[4] and Daolong Dou[2]**

[1] Institute of Industrial Crops, Jiangsu Academy of Agricultural Sciences/Jiangsu Key Laboratory for Horticultural Crop Genetic Improvement, Nanjing, China, [2] Department of Plant Pathology, Nanjing Agricultural University, Nanjing, China, [3] Department of Crop and Soil Sciences, Washington State University, Pullman, WA, United States, [4] National Center for Soybean Improvement, Nanjing Agricultural University, Nanjing, China

OPEN ACCESS

Edited by:
Valentina Fiorilli, University of Turin, Italy

Reviewed by:
Fabiano Sillo, University of Turin, Italy
Marino Moretti, Max-Planck-Institut für Terrestrische Mikrobiologie, Germany
Ivan Fernandez Lopez, Helmholtz-Zentrum für Umweltforschung (UFZ), Germany

***Correspondence:**
Daolong Dou
ddou@njau.edu.cn

Specialty section:
This article was submitted to Plant Microbe Interactions, a section of the journal Frontiers in Plant Science

Received: *10 September 2018*
Accepted: *23 January 2019*
Published: *08 February 2019*

Citation:
Yan Q, Si J, Cui X, Peng H, Jing M, Chen X, Xing H and Dou D (2019) GmDAD1, a Conserved Defender Against Cell Death 1 (DAD1) From Soybean, Positively Regulates Plant Resistance Against Phytophthora Pathogens. Front. Plant Sci. 10:107. doi: 10.3389/fpls.2019.00107

Initially identified as a mammalian apoptosis suppressor, defender against apoptotic death 1 (DAD1) protein has conserved plant orthologs acting as negative regulators of cell death. The potential roles and action mechanisms of plant DADs in resistance against *Phytophthora* pathogens are still unknown. Here, we cloned *GmDAD1* from soybean and performed functional dissection. *GmDAD1* expression can be induced by *Phytophthora sojae* infection in both compatible and incompatible soybean varieties. By manipulating *GmDAD1* expression in soybean hairy roots, we showed that *GmDAD1* transcript accumulations are positively correlated with plant resistance levels against *P. sojae*. Heterologous expression of *GmDAD1* in *Nicotiana benthamiana* enhanced its resistance to *Phytophthora parasitica*. *NbDAD1* from *N. benthamiana* was shown to have similar role in conferring *Phytophthora* resistance. As an endoplasmic reticulum (ER)-localized protein, GmDAD1 was demonstrated to be involved in ER stress signaling and to affect the expression of multiple defense-related genes. Taken together, our findings reveal that *GmDAD1* plays a critical role in defense against *Phytophthora* pathogens and might participate in the ER stress signaling pathway. The defense-associated characteristic of *GmDAD1* makes it a valuable working target for breeding *Phytophthora* resistant soybean varieties.

Keywords: *Glycine max*, *Phytophthora* resistant, *defender against apoptotic death 1* (*DAD1*), programmed cell death (PCD), ER stress

INTRODUCTION

As sessile organisms, plants are continually exposed to various biotic and abiotic stresses. Therefore, complex stress perception, signal transduction and adaptation strategies have evolved in plants to cope with adverse environmental conditions. In particular, the programmed cell death (PCD) pathway has been demonstrated to play key roles in plant responses to both abiotic and biotic stresses (Dickman et al., 2001; Lam et al., 2001; Williams et al., 2010). In plant defense against

pathogens, PCD restricts microbe growth and spreading in host tissue by eliminating excessive damaged cells (Kimchi, 2007).

Several PCD repressors have been identified in plants, including Bax inhibitor 1 (BI-1), B-cell lymphoma2 (Bcl-2)-associated athanogene (BAG), ER-luminal binding immunoglobulin protein (BiP), and defender against apoptotic death 1 (DAD1) (Gallois et al., 1997; Matsumura et al., 2003; Doukhanina et al., 2006; Williams et al., 2010; Jing et al., 2016; Li et al., 2016a,b). These repressors may increase or decrease plant resistance to different pathogens (Kawai-Yamada et al., 2004, 2009; Babaeizad et al., 2009; Watanabe and Lam, 2009; Eichmann et al., 2010; Ishikawa et al., 2011).

Among these PCD repressors, DAD1 is unique as it is conserved from yeast to mammals (Nakashima et al., 1993). Initially identified in a temperature-sensitive mutant hamster tsBN7 cell line, DAD1 is a subunit in the oligosaccharyltransferase (OST) complex, which is a core component for catalyzing *N*-glycosylation in ER (Yan et al., 2005; Peristera and Stephen, 2012). *N*-glycosylation is the attachment of oligosaccharides to certain asparagine residues of specific nascent proteins, which ensures their successful folding and export from ER. In *Drosophila melanogaster*, *DmDAD1* is essential for efficient *N*-glycosylation in developing tissues (Zhang et al., 2016). Disruption of *DmDAD1* increases accumulation of unfolded or misfolded proteins, which triggers stress signaling in ER and initiates PCD. In contrast, its overexpression stabilizes or increases *N*-glycosylation (Zhang et al., 2016).

Different hypotheses have been proposed for the roles of *DAD1* in maintaining cell viability. DAD1 may facilitate the targeting of OST complex to proteins directly responsible for cell viability. On the other hand, since DAD1 interacts with Mcl1, a Bcl2-family protein acting as an apoptosis inhibitor (Makishima et al., 2000), DAD1 may also affect cell viability in an OST-independent manner.

Plant *DAD1* orthologs from *Arabidopsis thaliana* and rice can rescue hamster tsBN7 cells from apoptosis (Gallois et al., 1997; Tanaka et al., 1997), which indicates they may also function as cell death repressors. Subsequent studies demonstrate that *AtDAD1* protects *Arabidopsis* protoplast cells against ultraviolet-C-induced PCD (Danon et al., 2004) and *DAD1* expression in *Gladiolus* decreases drastically during petal senescence (Yamada et al., 2004). Regarding the roles of *DAD1* proteins in plant defense, Wang X. J. et al. (2011) reported that *TaDAD2*-silenced wheat leaves have attenuated resistance to *Puccinia striiformis* with down-regulated expression of several defense-related genes. However, how this protein modulates plant-pathogen interactions has not been well characterized overall.

In this study, a *DAD1* orthologous gene was identified from soybean (*Glycine max*). Spatial and temporal expression of *GmDAD1* upon *P. sojae* infection, as well as its protein subcellular localization, were investigated. The function of *GmDAD1* in conferring *Phytophthora* resistance was dissected in soybean hairy roots with *GmDAD1* specifically silenced by RNAi, and *Nicotiana benthamiana* transgenic lines overexpressing *GmDAD1* or suppressing native *NbDAD1*. Our findings demonstrate that *GmDAD1* plays a critical role in *Phytophthora* resistance probably via regulating ER stress signaling.

MATERIALS AND METHODS

Plant Materials and Growth Conditions

Two soybean varieties were used in this research: Williams 82 carrying the gene *Rps*1k, which confers resistance to *P. sojae* race 2 (Bernard and Cremeens, 1988) and Williams which does not carry any known *Rps* resistance gene (Bernard and Lindahl, 1972). Seeds of Williams 82 and Williams were sown in small plastic pots containing disinfected soil and maintained in greenhouse at 25°C and 16h:8h light/dark photoperiod. *N. benthamiana* plants were grown under identical conditions as described above.

Culture of *Phytophthora* Pathogens

Phytophthora sojae isolates P6497 and P6497-RFP, which is a *P. sojae* strain constitutively expressing red fluorescence protein (RFP) (Xiong et al., 2014) were routinely cultured on 10% V8 juice agar plates at 25°C in the dark. *Phytophthora parasitica* was grown under the same conditions.

P. sojae Inoculation and Soybean Samples Collection

Root, stem and leaf samples of the soybean varieties Williams 82 and Williams were collected at seedling and pod-filling stages. Hypocotyl inoculation of *P. sojae* was performed on Williams 82 and Williams plants as described previously (Sun et al., 2014). Agar disks containing hyphae were cut from fresh cultures and inoculated onto hypocotyl incision. After inoculation, the seedlings were placed in growth chamber to keep moisture. Inoculated stems were collected at 0, 6, 12, 24, and 48 h post inoculation (hpi). All samples were frozen immediately in liquid nitrogen and stored at −70°C. Three biological replicates were performed for each time point.

DNA and RNA Extraction and RT-qPCR

Following supplier instructions, all DNA and RNA samples were extracted using the Hi-DNAsecure plant kit and the RNA simple Total RNA kit (Tiangen, China), respectively. For RNA samples, elimination of genomic DNA contamination and reverse transcription were performed using the HiScript II Q RT SuperMix reagent Kit (Vazyme, China).

qPCR reactions were performed on an ABI PRISM 7500 real-time PCR system (Applied Biosystems, United States) using the ChamQ^{TM} SYBR qPCR Master Mix reagent (Vazyme, China). Relative gene expression levels were calculated using the comparative $2^{-\Delta\Delta CT}$ method (Livak and Schmittgen, 2001). Statistical analysis was conducted using the Student's *t*-test with Excel 2010 software and the data were considered statistically significant for $P < 0.05$. qPCR primers for *GmDAD1* were designed from its conserved region. *PsTEF* (GenBank ID EU079791) was selected for determining *P. sojae* biomass (Yan et al., 2014). *GmCons4* (GenBank ID BU578186.1) was selected as

endogenous reference in soybean (Libault et al., 2008). *NbEF1a* (GenBank ID AY206004) was used as *N. benthamiana* reference in the VIGS (virus-induced gene silencing) assay.

Defense-related genes analyzed in this research include five pathogenesis-related (PR) genes: *PR1a*, *PR2*, *PR3*, *PR4* and *PR5* (Bertini et al., 2003; Chen et al., 2007; Mazarei et al., 2007; Maldonado et al., 2014); the JA-regulated defense gene *plant defensin 1.2* (*PDF1.2*) (Lorenzo and Solano, 2005); the ethylene (ET) signaling marker gene *ethylene response factor 1* (*ERF1*) (Lorenzo et al., 2003); the reactive oxygen species (ROS) biosynthetic gene *NADP oxidase* (*NADPHOX*) and two ROS scavenging genes: *catalase* (*CAT*) and *ascorbate peroxidase* (*APX*) (Perez and Brown, 2014). We employed the sequences of *G. max* if the genes have been reported already, or obtained them by searching in the soybean EST and genome databases[1] using orthologous sequences from *A. thaliana* as queries. All primers were designed using the Primer Premier 5 software. Primer specificity was evaluated by sequence similarity comparison and melting curve results of RT-qPCR. The primers of ER related genes were designed used the same strategy. The analyzed ER-stress related genes were the *binding immunoglobulin protein* (*Bip*), the *protein disulphide isomerase* (*PDI*), the *calnexin1* (*CNX1*), the *ER lumen-localized Dnaj protein3a* (*ERdj3A*), the *luminal binding domain/glucose-regulated protein 94* (*GRP94*), the *basic region/leucine zipper motif 17* (*bZIP17*) and the downstream gene *vacuolar processing enzyme* (*VPE*) (Rojo et al., 2004; Cai et al., 2014; Tiziana and Roberto, 2014). All primers used in this study and detailed information were listed in **Supplementary Table S1**.

Subcellular Localization of the GmDAD1 Protein

For subcellular localization, the full-length coding sequence (CDS) of *GmDAD1* was amplified from cDNAs of the Williams variety using primer pair pBIN-G-DAD-F/R (**Supplementary Table S1**). The 351-bp *GmDAD1* CDS was then translationally fused with GFP after cloning into pBIN-GFP (Zhang et al., 2014) using *Kpn*I and *Xba*I sites. After sequencing validation, *GmDAD1-GFP* and *mCherry-HDEL* constructs were introduced into *Agrobacterium* tumefaciens stain GV3101. The two *Agrobacterium* liquid cultures were mixed and co-infiltrated into *N. benthamiana* leaves using a blunt syringe. After maintained for 48 h in greenhouse, agroinfiltrated leaves were detached and visualized with a laser scanning confocal microscope (Zeiss, GERMANY) at 488 and 591 nm for GFP and mCherry detection, respectively.

Plasmid Construction for Soybean Cotyledon Transformation

The pBIN-GFP-*GmDAD1* construct which was used to determine GmDAD1 subcellular localization was also used to overexpress *GmDAD1* in soybean hairy roots, and the pBIN-GFP empty vector was used as control which allows expression of the *GFP* only. To make the *GmDAD1*-RNAi construct, partial *GmDAD1* gene was amplified (using primers p12-DAD-F and p12-DAD-R) and cloned into pDONR221 (Invitrogen, United States) and then entered in pHellsGate12:GFP via Gateway LR reaction. Modified from pHellsGate12 (Wesley et al., 2001), pHellsGate12:GFP harbors a 35S:*GFP*:nos expression cassette (Yan et al., 2014). After sequence validation, the pBIN-GFP-*GmDAD1*, *GmDAD1*-RNAi, the empty pBIN-GFP and pHellsGate12:GFP vectors were introduced into *Agrobacterium rhizogenes* strain K599 by electroporation.

Plasmid Construction for *N. benthamiana* Transformation

To overexpress *GmDAD1* in *N. benthamiana*, the full length of *GmDAD1* CDS was obtained from cDNAs of the Williams variety using primer pair pDONR-DAD-F/R (**Supplementary Table S1**) and then cloned into the entry vector pDONR221 via Gateway BP reaction. After sequencing validation, the fragment was then entered in pEarlyGate202 via LR recombination reaction between the entry clone and the destination vector (Invitrogen, United States) (Earley et al., 2006). To make Tobacco Rattle Virus (TRV)-based VIGS construct targeting *NbDAD1*, partial fragment of *NbDAD1* was amplified using primer pair TRV:NbDAD-F/R and cloned into pTRV2 (Liu et al., 2002) using *Kpn*I and *Eco*RI sites. All constructs were validated by sequencing and transformed into *A. tumefaciens* strain EHA105 for *N. benthamiana* transformation and GV3101 for VIGS experiment.

Soybean Cotyledon Transformation

Surface-sterilized soybean seeds were soaked in sterilized water overnight and then germinated on medium containing 0.5% sucrose and 1.2% agar in growth chamber with 16h:8h light/dark photoperiod. About 5 days after germination, unblemished cotyledons were harvested for *A. rhizogenes*-mediated transformation. Transformation was performed as described previously (Yan et al., 2014). After about 3 weeks of cultivation, transformed hairy roots became abundant at inoculated cotyledons. Positive transformants were selected by detecting GFP signal under fluorescence microscopy, cut off from cotyledons, and cultivated on White medium (**Supplementary Table S2**) for further verification and resistance level test.

N. benthamiana Transformation and Virus-Induced Gene Silencing (VIGS)

Nicotiana benthamiana plants overexpressing *GmDAD1* were generated via *A. tumefaciens* mediated leaf disk transformation (Horsch et al., 1985). The T1 seeds harvested from self-pollinated T0 plants were surface-sterilized with 70% ethanol for 30 s, and 10% sodium hypochlorite solution for 5 min, then washed by sterilized water for five times. The sterilized seeds were germinated on MS medium with 100 mg/L glufosinate ammonium (Sigma, United States). T2 seeds were collected and sown in small plastic pots. After 2 weeks, the seedlings were sprayed with 100 mg/L glufosinate ammonium solution. Resistant were transplanted to new pots and confirmed by both genomic DNA and cDNA PCR using gene-specific

[1] https://www.soybase.org/GlycineBlastPages/

primers (DAD-Test-F/R). The T2 plants were used for functional characterization.

For TRV-VIGS assay, *Agrobacterium* cultures harboring pTRV1 and pTRV2-VIGS (TRV2-NbDAD1, TRV2 empty vector or TRV2-NbPDS used as positive control of silencing) were mixed and infiltrated into *N. benthamiana* leaves using a blunt syringe (Fu et al., 2002). Inoculated plants were maintained at 20°C in greenhouse for effective virus infection and spread.

Resistance Assay of *N. benthamiana* Against *Phytophthora parasitica*

Leaves from 5 to 6-week-old *N. benthamiana* plants were detached and inoculated with 20 μl *P. parasitica* zoospores (10^4 ml^{-1}) per leaf. Inoculated leaves were then kept in a moist chamber and lesion diameters were measured at 36 and 60 hpi. Representative infected leaves were photographed at 60 hpi under a UV lamp and then stained with trypan blue to visualize the infected area. The experiment was repeated three times with similar results and at least 20 leaves were inoculated for each biological replicate. Two weeks after infiltration, leaves from TRV and NbDAD1-VIGS plants were inoculated with *P. parasitica* using the same strategy. Lesion diameters were measured at 36 and 48 hpi due to the semi-dwarf phenotype of NbDAD1-VIGS plants. At least 10 lesions per construct were measured with three biological repeats. Student's *t*-test was used to analyze the significance of differences. Difference were considered as significant when $P < 0.05$.

Root Infection and Observation

After verification by detection of GFP fluorescence and qPCR, transgenic hairy roots of similar length (approximately 3 cm) were excised and dipped in the zoospore suspension (10^4 zoospores per ml) of *P. sojae* race P6497-RFR for 5 min as described previously (Xiong et al., 2014). Inoculated roots were placed in Petri dishes containing 0.6% agar in the dark at room temperature. At 12, 24, and 36 hpi, the infection progression was monitored under an OLYMPUS MVX10 (OLYMPUS, Japan) fluorescence microscope via RFP fluorescence detection at 535 nm. The *P. sojae*-specific gene *PsTEF* was used for qPCR quantification of the relative biomass of *P. sojae*. For each sample, about 10 infected hairy roots were collected and pooled for DNA/RNA extraction which helps to reduce bias and increase statistical accuracy (Graham, 1991; Subramanian et al., 2005; Graham et al., 2007).

Western Blotting Assay

About 10 transgenic roots with GFP fluorescence were collected and ground in liquid nitrogen. Total proteins were extracted with the extraction buffer (50 mM Tris-HCl, pH 7.5, 5 mM EDTA, 2 mM DTT, 1% triton, 2% polyvinylpolypyrrolidone and Roche complete protein inhibitor tablets). The samples were boiled for 10 min in 6× sodium dodecyl sulfate (SDS) loading buffer. SDS-PAGE and immunoblotting were performed in a mini-gel apparatus and submarine gel transfer systems (Bio-Rad, United States), respectively. Proteins were then transferred onto polyvinylidene fluoride (PVDF) membranes and then membranes were blocked with 5% non-fat dry milk in 0.01 M PBST for 1 h and then incubated with anti-GFP (1:1,000) (Sigma, United States) for 2 h at room temperature. After washing by TBST three times, the membrane was incubated with IRDye®800CW Goat anti-rabbit IgG (LI-COR, United States) secondary antibody at room temperature for 1 h. Protein bands were detecting using the Odyssey® CLx quantitative fluorescence imaging system (LI-COR, United States).

Sequence Analysis and Alignment

The conserved and transmembrane domains of GmDAD1 were analyzed with InterProScan and TMPRED respectively (Hofmann and Stoel, 1993; Jones et al., 2014). Multiple sequence alignment was performed using the BioEdit software (Hall, 1999).

RESULTS

ER-Located GmDAD1 Shares Conserved Regions With Other Plant DAD1 Orthologs

GmDAD1 (Gma.7542.2.S1_at) was identified from an Affymetrix Genechip microarray data analysis on soybean and *P. sojae* interaction (Zhou et al., 2009). *GmDAD1* was up-regulated in soybean varieties with different degrees of resistance to *P. sojae* (Zhou et al., 2009). Sequence analysis of *GmDAD1* (cloned from the Williams variety) revealed that its open reading frame (ORF) encodes a protein of 117 amino acid residues. GmDAD1 shares 91, 54, and 36% identities with DAD1 orthologs in *Arabidopsis thaliana*, *Homo sapiens*, and *Saccharomyces cerevisiae*, respectively. Similar to other plant DAD1 orthologs, GmDAD1 contains three transmembrane regions (residues 27–52, 61–81, and 95–115) and a subunit of OST (residues 13–116) (**Figure 1A**). To investigate the subcellular localization of GmDAD1, a *GmDAD1-GFP* fusion construct driven by the CaMV 35S promoter was expressed in *N. benthamiana* leaves. GmDAD1-GFP co-localized in the cytoplasm with mCherry-HDEL, an endoplasmic reticulum (ER) marker, demonstrating the ER localization of GmDAD1 (**Figure 1B**).

GmDAD1 Expression Is Induced Upon *P. sojae* Infection

GmDAD1 transcript can be detected ubiquitously in roots, stems and leaves during plant development in cv Williams, with root being the organ exhibiting highest expression (**Figure 2A**). Interestingly, leaves showed much higher *GmDAD1* transcript accumulation at pod filling stage than seedling stage (**Figure 2A**). Similar *GmDAD1* expression pattern was detected in Williams 82 variety in the seedling stage (**Supplementary Figure S1**). On the contrary, the expression of *GmDAD1* is higher in roots at the pod filling stage in Williams 82 than in Williams.

After inoculation with P6497, a *P. sojae* isolate of race 2, the compatible variety Williams showed

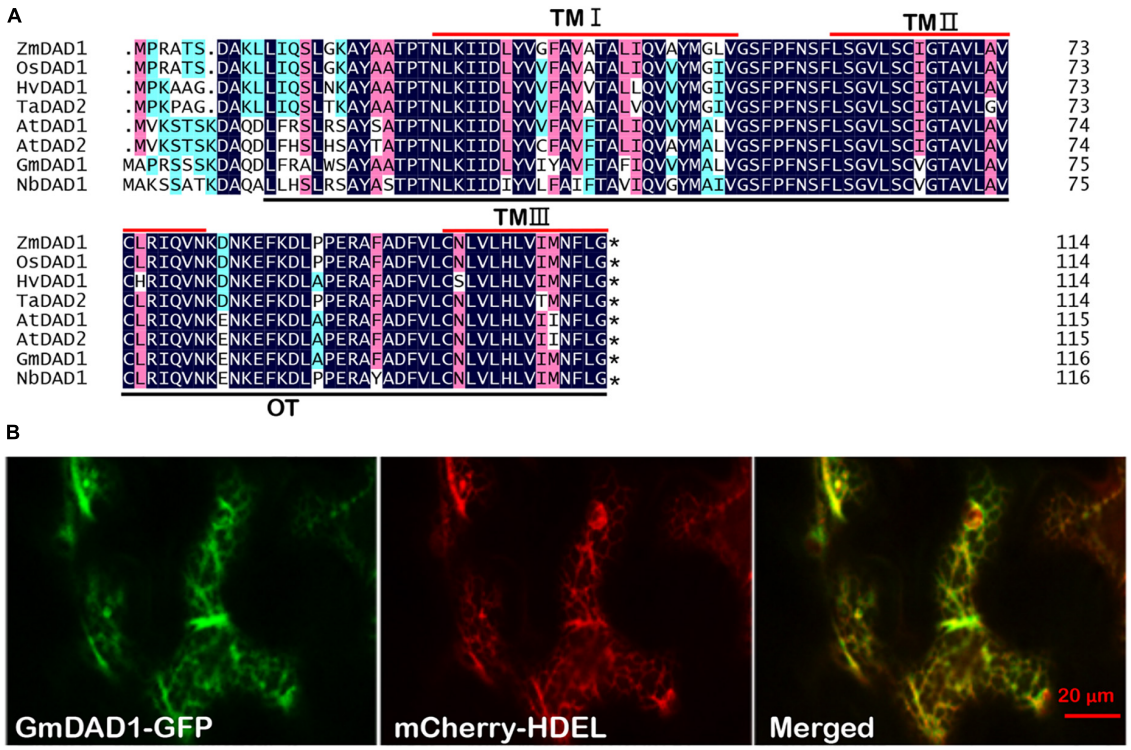

FIGURE 1 | Molecular characterization and subcellular localization of GmDAD1 protein. **(A)** Sequence alignment of GmDAD1 and other defender against cell death (DAD) proteins. The darkblue (100%), pink (75%), and cyan (50%) boxes represent levels of amino acid identity or similarity. TM, transmembrane domain; OT, oligosaccharyltransferase domain. At, *Arabidopsis thaliana*; Hv, *Hordeum vulgare*; Zm, *Zea mays*; Os, *Oryza sativa*; Ta, *Triticum aestivum*. The asterisk indicates the stop codon. **(B)** Subcellular localization of GmDAD1 was performed via transient expression system in *Nicotiana benthamiana*. Green and red fluorescence represent the signal of GFP fusion protein and ER marker mCherry-HDEL, respectively. The reticulate fluorescence pattern of GmDAD1-GFP and its co-localization with mCherry-HDEL indicate accumulation in the ER.

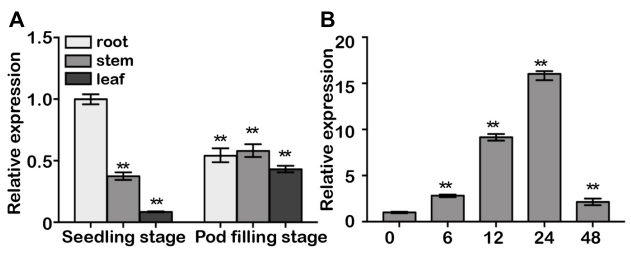

FIGURE 2 | Gene expression analysis of *GmDAD1*. **(A)** *GmDAD1* mRNA levels in various tissues of soybean cultivar Williams. Leaves, roots, and stems were harvested from plants at the seedling and pod filling stage. **(B)** Expression profiles of *GmDAD1* in Williams (compatible interaction) at 0, 6, 12, 24, 48 h post inoculation (hpi) with *P. sojae* (P6497). The relative expression level was normalized to soybean *GmCons4* (GenBank: BU578186.1). Means and standard deviations were calculated from three independent biological replicates. Data were analyzed by using Student's *t*-tests (**$P < 0.01$).

elevated *GmDAD1* expression which peaked at 24 hpi and subsequently decreased (**Figure 2B**). In the incompatible variety Williams 82, *GmDAD1* was also significantly induced by *P. sojae* infection at 24 hpi (**Supplementary Figure S1**).

GmDAD1 Enhances Resistance to *P. sojae* in Soybean Hairy Roots

RT-qPCR analysis of ten mixed hairy roots displaying GFP fluorescence indicated that expression of *GmDAD1* in *GmDAD1-GFP* overexpression (OE) plants was nearly 14-fold higher that in the control (GFP) (**Figure 3A**). Western blotting also showed the accumulation of the GmDAD1-GFP fusion protein (**Figure 3B**). When OE and GFP hairy roots were inoculated with *P. sojae* P6497-RFP (Xiong et al., 2014), the biomass of *P. sojae* was significantly and consistently less in OE hairy roots than in GFP samples at 12, 24, and 36 hpi (**Figure 3C**). In the GFP control, the invasion hyphae emerged at 12 hpi, rapidly extended at 24 hpi, and almost filled the entire tissue at 36 hpi (**Figure 3D**). In contrast, hyphal growth was limited and the invasion hyphae were much sparser in *GmDAD1-GFP* overexpression roots (**Figure 3D**), which is consistent with the lower accumulation of *P. sojae* biomass (**Figure 3C**).

Silencing of *GmDAD1* Reduces Resistance to *P. sojae* in Soybean Hairy Roots

RNAi-directed silencing of *GmDAD1* in soybean hairy roots (**Figure 4A**) was performed as described previously

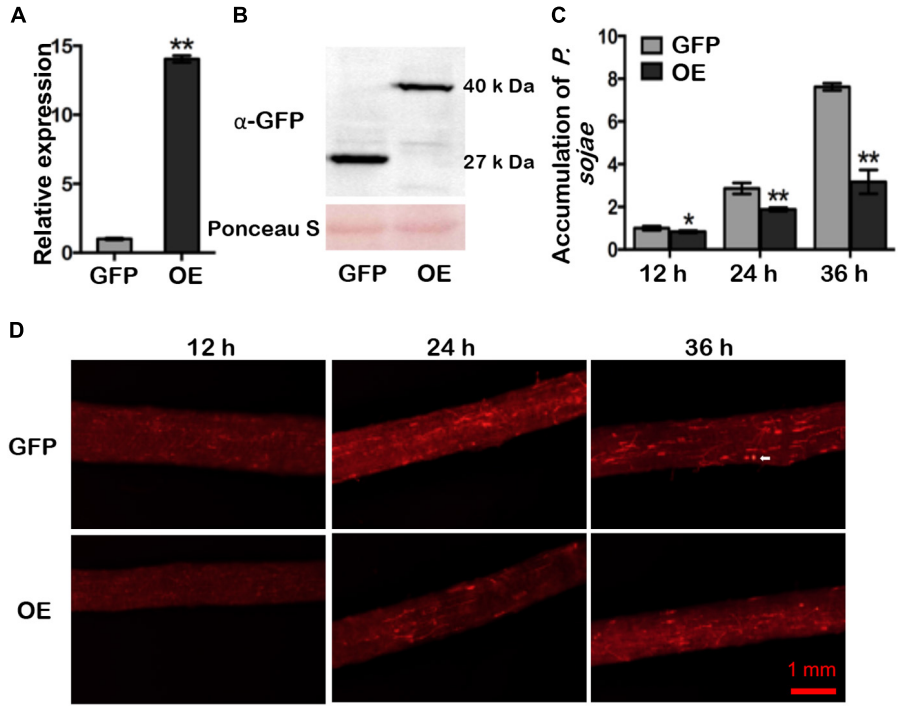

FIGURE 3 | *GmDAD1* overexpression enhances resistance to *P. sojae* in soybean hairy roots. **(A)** Expression of *GmDAD1* in the *GmDAD1-GFP* overexpressing (OE) and control (*GFP*) hairy roots without *P. sojae* infection. Samples derived from different pooled root materials. Control has been transformed with the empty vector which allows expression of the GFP only. **(B)** Western blotting of proteins from hairy roots expressing GFP (control) and GmDAD1 fused with GFP tag. **(C)** Relative biomass of *P. sojae* determined by qPCR in inoculated OE and GFP hairy roots at 12, 24, and 36 hpi. Values represent the means of three replicates and 10 hairy roots were used for each biological replicate. Data were analyzed by using Student's *t*-tests (*$P < 0.05$, **$P < 0.01$ compared with the control). **(D)** Microscopic analysis of *P. sojae* colonization in infected soybean hairy roots. The OE and control GFP hairy roots were inoculated with zoospore suspension (10^4 zoospore/ml) of the *P. sojae* P6497-RFP. Photos were taken at 12, 24, 36 hpi. The white arrow indicates a germinating oospore.

(Yan et al., 2014). Both *GmDAD1*-RNAi (RNAi) and EV control (EV) roots were inoculated with *P. sojae* P6497-RFP. Compared with control, *GmDAD1*-RNAi roots showed gradually increased *P. sojae* biomass accumulation over time (**Figure 4B**). Furthermore, a greater hyphal growth and higher oospore germination can be observed in *GmDAD1*-RNAi roots (**Figure 4C**). Our results indicated that *GmDAD1* is important for soybean resistance against *P. sojae*.

GmDAD1 Affects the Expression of Multiple Defense-Related Genes

To further determine whether the expression of defense-related genes was affected by *GmDAD1* silencing, we assessed the expression of several genes in hairy roots inoculated with *P. sojae*, including the marker genes of SA, and JA/ET signaling pathways, ROS generation and scavenging. The expression of *PR1a*, *PR2*, *PR3*, *PR5* and *ERF1* were decreased in *GmDAD1*-RNAi roots after *P. sojae* inoculation. It is to note that the expression of *PR1a* was also dramatically suppressed without inoculation (**Figure 5**). In contrast, the expression of *PDF1.2*, *PR4*, and two ROS scavenging genes, *CAT* and *APX*, were induced in the *GmDAD1* silencing roots infected with *P. sojae* (**Figure 5**). No significant change of *NADPHOX* expression was observed when *GmDAD1* was silenced (**Figure 5**).

GmDAD1 Is Involved in *P. sojae*-Activated ER Stress Signaling

Since DAD1 catalyzes the first step of protein N-linked glycosylation, disruption of *GmDAD1* is expected to trigger unfolded protein response (UPR), which facilitates proper protein folding in ER via inducing the expression of a series of relevant genes (Li et al., 2011). After *P. sojae* inoculation, the transcript accumulations of six UPR marker genes were examined in soybean hairy roots, including *Bip*, *PDI*, *CNX1*, *ERdj3A*, *GRP94*, and *bZIP17*. All these genes are induced at the onset of ER stress and mark the activation of adaptive UPR. Expression changes of *VPE* were also monitored since its protein product possesses caspase-1-like activity and acts downstream of UPR and is part of the ER-PCD pathway. Compared to EV control, *GmDAD1*-RNAi roots showed significantly higher transcript accumulations of all seven UPR/ER stress marker genes at both 24 and 36 hpi (**Figure 6**). *VPE* was upregulated at 12 hpi and its expression decreased at 24 and 36 hpi in EV hairy roots, On the contrary, different trend was observed in *GmDAD1* silencing hairy roots. The expression increased continuously through the selected time course, and was significantly higher at 24 and 36 hpi (**Figure 6**).

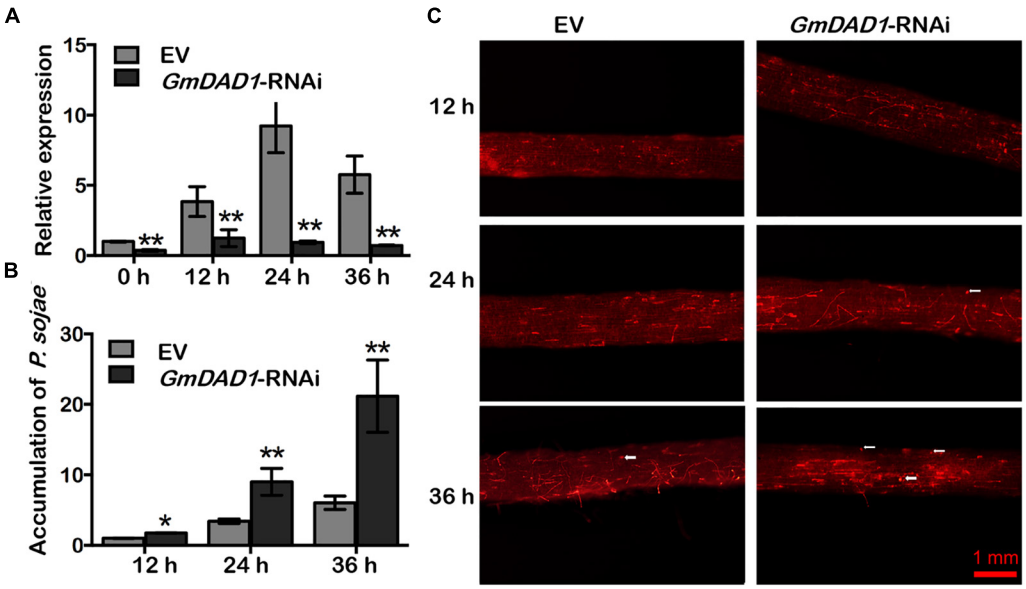

FIGURE 4 | Silencing of *GmDAD1* reduces resistance to *P. sojae* in soybean hairy roots. **(A)** Relative expression of *GmDAD1* was determined by RT-qPCR in inoculated hairy roots in which *GmDAD1* was silenced via RNAi (*GmDAD1*-RNAi) or empty vector (EV) at 0, 12, 24, and 36 hpi. **(B)** Relative biomass of *P. sojae* was determined in inoculated hairy roots *GmDAD1*-RNAi or EV at 12, 24, and 36 hpi. Values represent the means of three replicates ± SD. Data were analyzed by using Student's *t*-tests (*$P < 0.05$, **$P < 0.01$ compared with the control). **(C)** Microscopic analysis of *P. sojae* colonization in soybean hairy roots. The control EV and *GmDAD1*-RNAi hairy roots were inoculated with zoospore suspension (10^4 zoospore/ml) of the *P. sojae* P6497-RFP. Photos were taken at 12, 24, 36 hpi. The white arrows indicate germinating oospores.

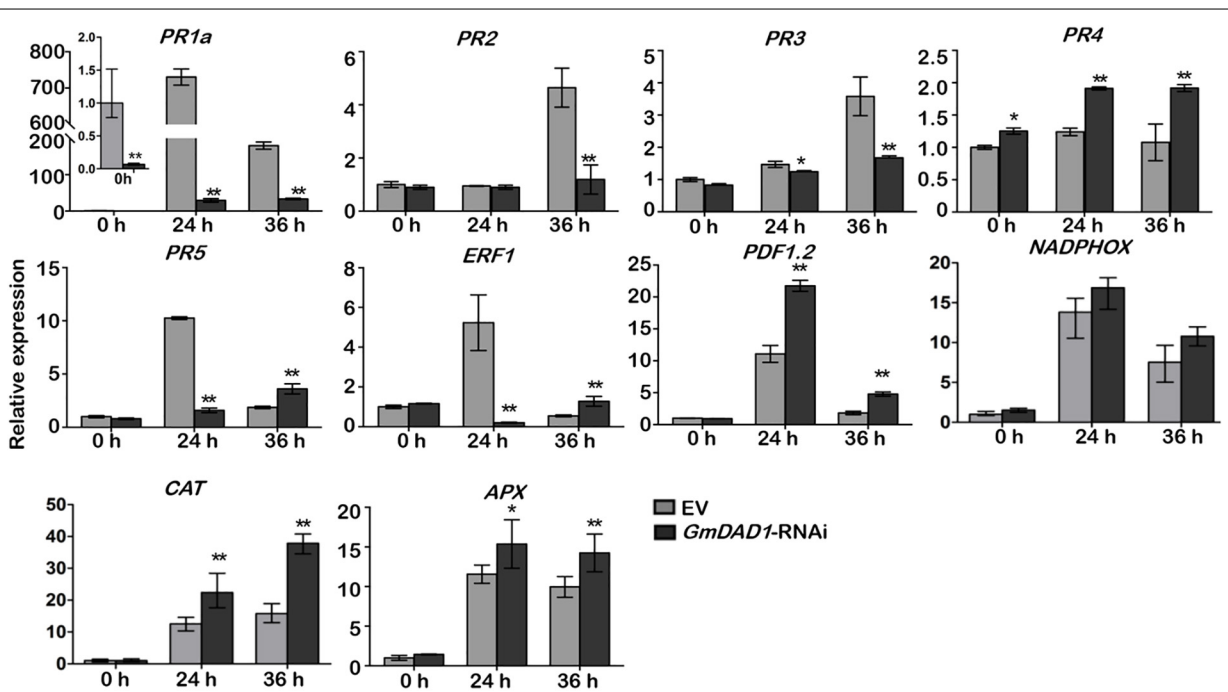

FIGURE 5 | *GmDAD1* affects the expression of multiple defense-related genes. RT-qPCR analysis of the expression patterns of defense-related genes in the EV and *GmDAD1*-RNAi transgenic hairy roots after inoculation with *P. sojae*. Values represent the means of three replicates ± SD. Data were analyzed by using Student's *t*-tests (*$P < 0.05$, **$P < 0.01$ compared with the control).

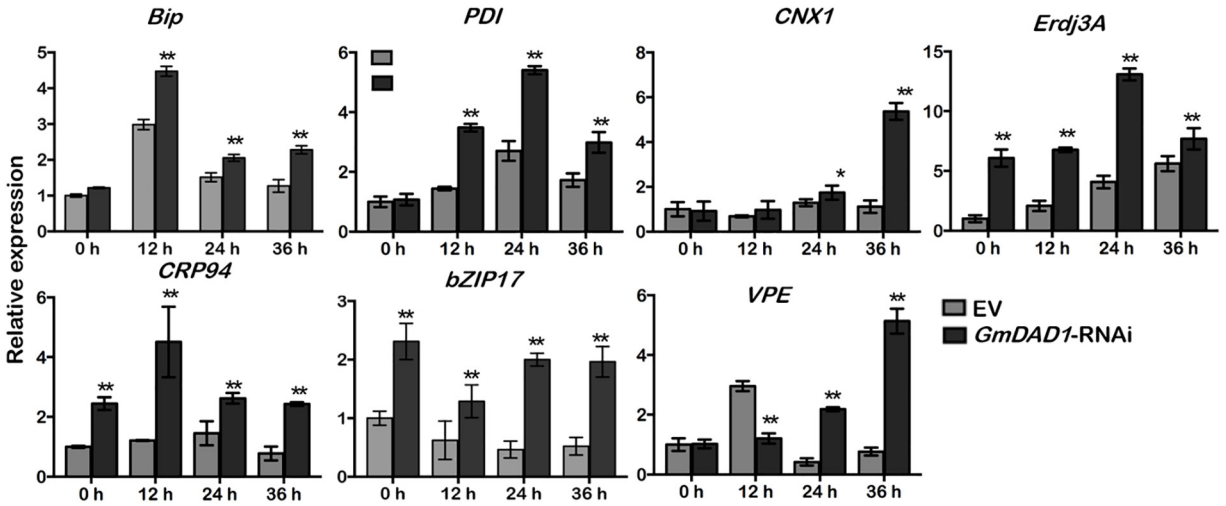

FIGURE 6 | *GmDAD1* is involved in *P. sojae*-activated ER stress signaling. Expression patterns of ER stress-related genes in the EV and *GmDAD1*-RNAi transgenic hairy roots after inoculation with *P. sojae* at 0, 12, 24, 36 hpi. Values represent the means of three replicates ± SD. Data were analyzed by using Student's *t*-tests (*$P < 0.05$, **$P < 0.01$ compared with the control).

GmDAD1 Enhances Resistance to *P. parasitica* in *N. benthamiana*

To test whether *GmDAD1* confers resistance against other *Phytophthora* pathogens, transgenic *N. benthamiana* plants overexpressing *GmDAD1* were generated and verified (**Supplementary Figure S2**). Compared to wild-type (WT) and empty vector controls (EV) both *GmDAD1* overexpression lines tested (4-1 and 8-4) showed reduced disease symptoms (**Figures 7A,B**) and significantly smaller lesion diameters on leaves (**Figure 7C**) when infected with *P. parasitica* zoospores. The results suggest that *GmDAD1* overexpression enhances *N. benthamiana* resistance against *P. parasitica*.

Silencing of *NbDAD1* in *N. benthamiana* Reduces Resistance to *P. parasitica*

Since plant DADs are highly conserved, the native *NbDAD1* in *N. benthamiana* was silenced via TRV-based VIGS system for functional analysis. Compared to TRV-infected controls, plants infiltrated with *TRV-NbDAD1* displayed a semi-dwarf phenotype with increased branching (**Figures 8A,B**), which implies a possible role of *NbDAD1* in modulating growth and development. Three verified *NbDAD1* knock-down lines and TRV-infected controls were challenged with *P. parasitica* zoospores on detached leaves (**Figure 8C**). Silencing of *NbDAD1* led to significantly larger lesion diameters at both 36 and 48 hpi (**Figures 8D–F**), which indicates that *NbDAD1* is similar as *GmDAD1* in the function of conferring resistance against *P. parasitica*.

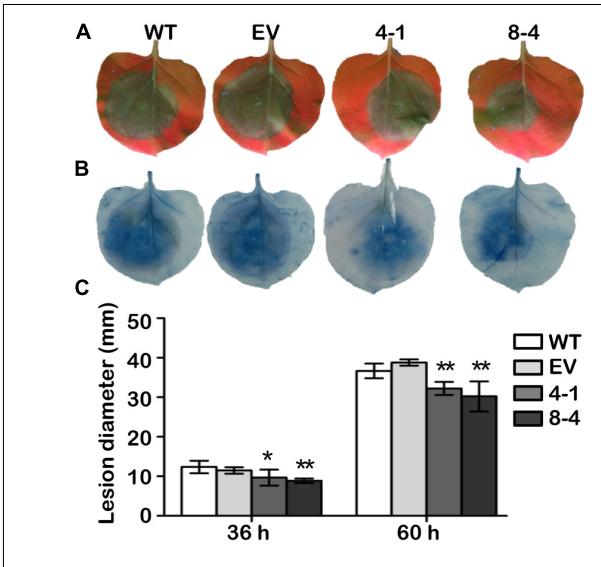

FIGURE 7 | *GmDAD1* enhances resistance to *P. parasitica* in *N. benthamiana*. **(A)** Detached leaves from wild type (WT), empty vector control (EV) and *GmDAD1* overexpression plants (4-1 and 8-4) were inoculated with *P. parasitica* zoospores. Photographs were taken at 60 hpi under a UV lamp. **(B)** Trypan blue staining of the *P. parasitica* inoculated *N. benthamiana* leaves. **(C)** Lesion diameter of inoculated leaves measured at 36 and 60 hpi. The lesion size was calculated from 20 leaves ± SD with three biological repeats. Data were analyzed by using Student's *t*-tests (*$P < 0.05$, **$P < 0.01$ compared with the control).

DISCUSSION

Being one of the most important crops worldwide, soybean can be infected by several major diseases, including the *Phytophthora* stem and root rot caused by *P. sojae* (Tyler, 2007). Continual efforts have been made to characterize novel defense genes against *Phytophthora* pathogens (Sugimoto et al., 2012). Here we identified GmDAD1, an ER-membrane protein from soybean, and dissected its function in plant–*Phytophthora* interactions.

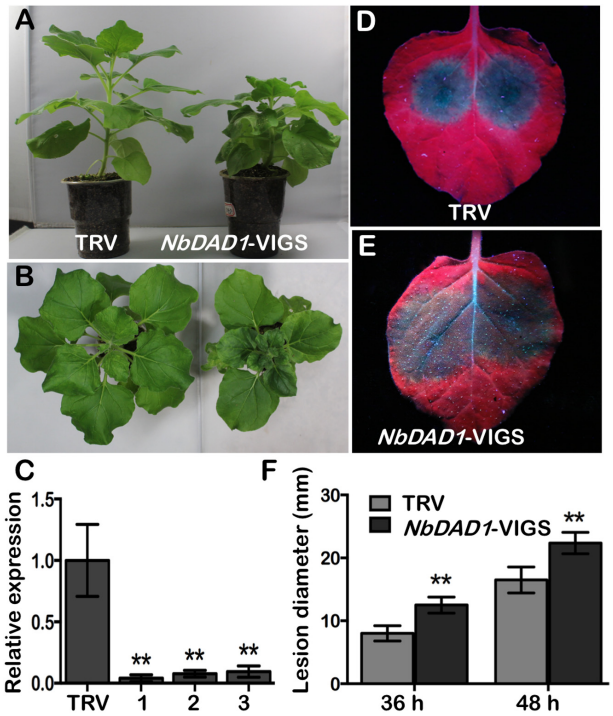

FIGURE 8 | Silencing of *NbDAD1* in *N. benthamiana* reduces resistance to *P. parasitica*. **(A,B)** Side- and top- view of the TRV-infected control and *NbDAD1* silencing plants. **(C)** Relative expression of *NbDAD1* in *N. benthamiana* plants inoculated with TRV and three *NbDAD1* knock-down plants. The samples were collected 2 weeks after infection. *N. benthamiana NbEF1*α gene was used as reference for normalization. Data are the means ± SD calculated from three replicates. $^{**}P < 0.01$. **(D,E)** Leaf phenotypes of TRV control and *NbDAD1*-VIGS after *P. parasitica* zoospores inoculation. Pictures were taken under UV illumination at 48 hpi. The experiments were repeated three times with similar results and representative images are shown. **(F)** Average lesion size of *NbDAD1* knock-down leaves and TRV control after *P. parasitica* zoospores inoculation. Averages were calculated from at least 10 lesions per construct. Data are the means ± SD. Data were analyzed by using Student's *t*-tests ($^{**}P < 0.01$).

Being evolutionary conserved across plant and animal species, DAD1 is a subunit of the OST complex, which catalyzes the first step of protein N-linked glycosylation in ER (Kelleher and Gilmore, 1997; Sanjay et al., 1998). In both animals and plants, the expression of *DAD1* orthologs responds to a wide range of adverse environmental stimuli, including injury (Zhu et al., 2008), temperature (Lee et al., 2003), and pathogen infection (Wang X. J. et al., 2011). *DAD1* inhibits undesired cell death triggered by host defense.

N-glycosylation has been reported to play a critical role in plant–pathogen interactions. For example, site-mutation on the *N*-glycosylation motif of *A. thaliana* receptor kinase EFR bleaches its ligand binding and results in oxidative burst elicitation capacity resulting in higher susceptibility of the plant to bacterial pathogens (Haweker et al., 2010). Several reports on the role of DAD proteins in plant defense have been published so far. The Arabidopsis *dad1* mutant shows reduced secretion of PR proteins and resistance against pathogens (Wang et al., 2005). In wheat, knock-down of *TaDAD2* suppresses the expression of *PR1*, *PR2,* and *PR5* in response to the infection of *Puccinia striiformis* f. sp. *tritici* (Wang X. J. et al., 2011). We hence propose that *GmDAD1* may also play a role in soybean disease resistance.

In soybean, *GmDAD1* expression can be induced by *P. sojae* infection in both compatible and incompatible varieties, which indicates that *GmDAD1* serves as a non-specific defense gene to some extent. However, *GmDAD1* has consistently higher expression after *P. sojae* inoculation in the incompatible variety Williams 82, and its expression does not drop dramatically afterward at 48 hpi, as it happens in the compatible variety Williams. Therefore, *GmDAD1* may be subjected to distinct transcriptional regulations in *P. sojae* compatible and incompatible soybean varieties.

Since *GmDAD1* has highest transcript accumulation in roots, we adopted the soybean hairy root infection system for *P. sojae* resistance test. *GmDAD1* gain- and loss-of-function mutants exhibit opposite *P. sojae* resistance phenotypes, which indicates that *GmDAD1* contributes to the resistance of soybean against *P. sojae*. Similarly, knock-down of *NbDAD1*, the native *DAD1* ortholog in *N. benthamiana*, reduces plant resistance to another *Phytophthora* pathogen, *P. parasitica*. Heterologous expression of *GmDAD1* in *N. benthamiana* enhances resistance to *P. parasitica*. Our results reveal that *DAD1* is a potential valuable defense gene against *Phytophthora* pathogens and this disease resistance function is conserved across plant species.

Phytohormone signaling, which is mediated by SA during biotrophic and hemibiotrophic plant–pathogen interactions and JA and ET for necrotrophic plant pathogens, plays important roles in plant resistance (Glazebrook, 2005). Previously studies demonstrated that the resistance to *P. sojae* is mediated by the SA and ET signaling pathways (Moy et al., 2004; Sugano et al., 2014). Therefore, we assessed the expression of several key defense related genes by RT-qPCR. When *GmDAD1* silencing hairy roots were inoculated with *P. sojae*, the transcription of *PR1a*, *PR2*, *PR3*, *PR5*, and *ERF1* were significantly reduced. Since the PR genes are generally regarded as early markers of resistance response, the suppressed expression of these genes may be responsible for the compromised resistance at the begin of the infection process (from 0 to 24 hpi). Moreover, the two JA-dependent signal marker genes *PDF1.2* and *PR4* were up-regulated after *P. sojae* infection in the silenced hairy roots (later than 24 hpi). We inferred that this JA resistance signaling activation might be lately induced, and the up-regulation might be caused by the antagonistic effect of JA and SA pathways.

Reactive oxygen species are important messenger molecules in defense signal regulation. The expression of ROS-generating gene *NADPHOX* showed no difference between EV and *GmDAD1*-RNAi hairy roots, however, the ROS-scavenging genes *CAT* and *APX* were statistically significant up-regulated after *P. sojae* infection in the silencing roots, this means that the ROS signaling was not completely affected by *GmDAD1* silencing.

AS a core subunit of OST complex, DAD1 plays an important role in protein *N*-glycosylation (Peristera and Stephen, 2012), the defeat of protein *N*-glycosylation cause accumulation of misfolded proteins in ER and subsequently ER stress (Li et al., 2011; Cai et al., 2014). In soybean hairy roots infected by *P. sojae*,

we found that *GmDAD1* acts as a repressor for multiple UPR marker genes. In detail, all tested genes become up-regulated at later stages of the infection when *GmDAD1* is silenced, indicating severe ER stress. We believe that this situation is caused by a less efficient or delayed defense signaling transduction. However, whether the suppression of defense-related genes was directly caused by the ER stress due to *GmDAD1* silencing need to be further investigated.

Under extreme condition such as pathogen infection, a prolonged ER stress is known to eventually activate the ER-PCD pathway. *Phytophthora* pathogens are hemibiotrophic. They initially establish a biotrophic relationship with their hosts, and switch to necrotrophic phase later than 15 hpi (Enkerli et al., 1997). In EV hairy roots, a sharp increase of *VPE*, a cystein proteinase mediating PCD via the maturation and activation of vacuolar proteins, was observed at 12 hpi most likely to limit and overcome the biotrophic phase of *P. sojae* infection. In *GmDAD1*-RNAi roots, *VPE* expression was relatively suppressed at the same infection stage, suggesting the failure of PCD induction. However, elevated expression of *VPE* was detected at 24 and 36 hpi indicating a later activation of ER-PCD pathway. This late apoptosis overlaps with the necrotrophic phase of *P. sojae*, which may be one of the reasons of the increased *P. sojae* accumulation in *GmDAD1* silencing hairy roots.

Disruption of *DAD1* causes growth defect or even embryonic lethality in animal systems (Brewster et al., 2000; Zhang et al., 2016). In this study, we have observed significantly reduced transformation rate when silencing *GmDAD1* in soybean hairy roots (**Supplementary Figure S3**). Moreover, knock-down of *NbDAD1* by VIGS caused a semi-dwarf phenotype in *N. benthamiana*. These results suggest that *DAD1* may play a similar role of regulating growth in plants most likely by acting on the *N*-glycosylation pathway of key proteins involved in plant development.

CONCLUSION

We observed that GmDAD1, a conserved component of the OST complex, via participating in the ER-PCD and UPR pathways and affecting the expression of multiple defense-related genes, confers resistance to *Phytophthora* pathogens. Moreover, *GmDAD1* regulates plant growth and development likely by the effect on the *N*-glycosylation pathway. Taken together, *GmDAD1* can be considered as a promising target for the molecular breeding of *Phytophthora*-resistant soybean varieties.

AUTHOR CONTRIBUTIONS

DD and QY designed the project. QY, JS, and XaC performed the experiments and analyzed the data. XnC, HX, and DD guided the experimental work. DD, QY, HP, and MJ wrote the manuscript. All authors read and approved the final manuscript.

FUNDING

This work was supported by grants from the National Natural Science Foundation of China (31625023, 31721004, and 31672008) and Special Fund for Agro-scientific Research in the Public Interest (201503112).

SUPPLEMENTARY MATERIAL

The Supplementary Material for this article can be found online at: https://www.frontiersin.org/articles/10.3389/fpls.2019.00107/full#supplementary-material

REFERENCES

Babaeizad, V., Imani, J., Kogel, K. H., Eichmann, R., and Huckelhoven, R. (2009). Over-expression of the cell death regulator BAX inhibitor-1 in barley confers reduced or enhanced susceptibility to distinct fungal pathogens. *Theor. Appl. Genet.* 118, 455–463. doi: 10.1007/s00122-008-0912-2

Bernard, R. L., and Cremeens, C. R. (1988). Registration of 'Williams 82' soybean. *Crop Sci.* 28, 1027–1028. doi: 10.2135/cropsci1988.0011183X002800060049x

Bernard, R. L., and Lindahl, D. A. (1972). Registration of williams soybean1 (reg. no. 94). *Crop Sci.* 12:716. doi: 10.2135/cropsci1972.0011183X001200050067x

Bertini, L., Leonardi, L., Caporale, C., Tucci, M., Cascone, N., Di Berardino, I., et al. (2003). Pathogen-responsive wheat PR4 genes are induced by activators of systemic acquired resistance and wounding. *Plant Sci.* 164, 1067–1078. doi: 10.1016/s0168-9452(03)00112-2

Brewster, J. L., Martin, S. L., Toms, J., Goss, D., Wang, K., Zachrone, K., et al. (2000). Deletion of Dad1 in mice induces an apoptosis-associated embryonic death. *Genesis* 26, 271–278. doi: 10.1002/(SICI)1526-968X(200004)26:4<271::AID-GENE90>3.0.CO;2-E

Cai, Y. M., Jia, Y., and Patrick, G. (2014). Endoplasmic reticulum stress-induced PCD and caspase-like activities involved. *Front. Plant Sci.* 5:41. doi: 10.3389/fpls.2014.00041

Chen, Y. P., Xing, L. P., Wu, G. J., Wang, H. Z., Wang, X. E., Cao, A. Z., et al. (2007). Plastidial glutathione reductase from *Haynaldia villosa* is an enhancer of powdery mildew resistance in wheat (*Triticum aestivum*). *Plant Cell Physiol.* 48, 1702–1712. doi: 10.1093/pcp/pcm142

Danon, A., Rotari, V. I., Gordon, A., Mailhac, N., and Gallois, P. (2004). Ultraviolet-C overexposure induces programmed cell death in Arabidopsis, which is mediated by caspase-like activities and which can be suppressed by caspase inhibitors, p35 and defender against apoptotic death. *J. Biol. Chem.* 279, 779–787. doi: 10.1074/jbc.M304468200

Dickman, M. B., Park, Y. K., Oltersdorf, T., Li, W., Clemente, T., and French, R. (2001). Abrogation of disease development in plants expressing animal antiapoptotic genes. *Proc. Natl. Acad. Sci. U.S.A.* 98, 6957–6962. doi: 10.1073/Pnas.091108998

Doukhanina, E. V., Chen, S., Van Der Zalm, E., Godzik, A., Reed, J., and Dickman, M. B. (2006). Identification and functional characterization of the BAG protein family in *Arabidopsis thaliana*. *J. Biol. Chem.* 281, 18793–18801. doi: 10.1074/jbc.M511794200

Earley, K. W., Haag, J. R., Pontes, O., Opper, K., Juehne, T., Song, K., et al. (2006). Gateway-compatible vectors for plant functional genomics and proteomics. *Plant J.* 45, 616–629. doi: 10.1111/j.1365-313X.2005.02617.x

Eichmann, R., Bischof, M., Weis, C., Shaw, J., Lacomme, C., Schweizer, P., et al. (2010). BAX INHIBITOR-1 is required for full susceptibility of barley to powdery mildew. *Mol. Plant Microbe Interact.* 23, 1217–1227. doi: 10.1094/Mpmi-23-9-1217

Enkerli, K., Mims, C. W., and Hahn, M. G. (1997). Ultrastructure of compatible and incompatible interactions of soybean roots infected with the plant pathogenic oomycete *Phytophthora sojae*. *Can. J. Bot.* 75, 1493–1508. doi: 10.1139/b97-864

Fu, D. Q., Zhu, B. Z., Zhu, H. L., Jiang, W. B., and Luo, Y. B. (2002). Virus-induced gene silencing in tomato. *Plant J.* 43, 299–308. doi: 10.1111/j.1365-313X.2005.02441.x

Gallois, P., Makishima, T., Hecht, V., Despres, B., Laudie, M., Nishimoto, T., et al. (1997). An *Arabidopsis thaliana* cDNA complementing a hamster apoptosis suppressor mutant. *Plant J.* 11, 1325–1331. doi: 10.1046/j.1365-313X.1997.11061325.x

Glazebrook, J. (2005). Contrasting mechanisms of defense against biotrophic and necrotrophic pathogens. *Annu. Rev. Phytopathol.* 43, 205–227. doi: 10.1146/annurev.phyto.43.040204.135923

Graham, T. L. (1991). A rapid, high resolution high performance liquid chromatography profiling procedure for plant and microbial aromatic secondary metabolites. *Plant Physiol.* 95, 584–593. doi: 10.1104/pp.95.2.584

Graham, T. L., Graham, M. Y., Subramanian, S., and Yu, O. (2007). RNAi silencing of genes for elicitation or biosynthesis of 5-deoxyisoflavonoids suppresses race-specific resistance and hypersensitive cell death in *Phytophthora sojae* infected tissues. *Plant Physiol.* 144, 728–740. doi: 10.1104/pp.107.097865

Hall, T. A. (1999). Bioedit: a user-friendly biological sequence alignment editor and analysis program for windows 95/98/nt. *Nucleic Acids Symp. Ser.* 41, 95–98. doi: 10.1021/bk-1999-0734.ch008

Haweker, H., Rips, S., Koiwa, H., Salomon, S., Saijo, Y., Chinchilla, D., et al. (2010). Pattern recognition receptors require N-glycosylation to mediate plant immunity. *J. Biol. Chem.* 285, 4629–4636. doi: 10.1074/jbc.M109.063073

Hofmann, K., and Stoel, W. (1993). Tmbase-A database of membrane spanning protein segments. *Biol. Chem. Hoppe Seyler* 374:166. doi: 10.1056/NEJM199001043220121

Horsch, R. B., Rogers, S. G., and Fraley, R. T. (1985). Transgenic Plants. *Cold Spring Harb. Symp. Quant. Biol.* 50, 433–437. doi: 10.1101/SQB.1985.050.01.054

Ishikawa, T., Watanabe, N., Nagano, M., Kawai-Yamada, M., and Lam, E. (2011). Bax inhibitor-1: a highly conserved endoplasmic reticulum-resident cell death suppressor. *Cell Death Differ.* 18, 1271–1278. doi: 10.1038/cdd.2011.59

Jing, M., Guo, B., Li, H., Bo, Y., Wang, H., Kong, G., et al. (2016). A *Phytophthora sojae* effector suppresses endoplasmic reticulum stress-mediated immunity by stabilizing plant binding immunoglobulin proteins. *Nat. Commun.* 7:11685. doi: 10.1038/ncomms11685

Jones, P., Binns, D., Chang, H. Y., Fraser, M., Li, W., Mcanulla, C., et al. (2014). InterProScan 5: genome-scale protein function classification. *Bioinformatics* 30, 1236–1240. doi: 10.1093/bioinformatics/btu031

Kawai-Yamada, M., Hori, Z., Ogawa, T., Ihara-Ohori, Y., Tamura, K., Nagano, M., et al. (2009). Loss of calmodulin binding to Bax inhibitor-1 affects *Pseudomonas*-mediated hypersensitive response-associated cell death in *Arabidopsis thaliana*. *J. Biol. Chem.* 284, 27998–28003. doi: 10.1074/jbc.M109.037234

Kawai-Yamada, M., Ohori, Y., and Uchimiya, H. (2004). Dissection of *Arabidopsis* Bax inhibitor-1 suppressing Bax-, hydrogen peroxide-, and salicylic acid-induced cell death. *Plant Cell* 16, 21–32. doi: 10.1105/tpc.014613

Kelleher, D. J., and Gilmore, R. (1997). DAD1, the defender against apoptotic cell death, is a subunit of the mammalian oligosaccharyltransferase. *Proc. Natl. Acad. Sci. U.S.A.* 94, 4994–4999. doi: 10.1073/pnas.94.10.4994

Kimchi, A. (2007). Programmed cell death: from novel gene discovery to studies on network connectivity and emerging biomedical implications. *Cytokine Growth Factor Rev.* 18, 435–440. doi: 10.1016/j.cytogfr.2007.06.004

Lam, E., Kato, N., and Lawton, M. (2001). Programmed cell death, mitochondria and the plant hypersensitive response. *Nature* 411, 848–853. doi: 10.1038/35081184

Lee, K. S., Han, J. H., Sohn, H. D., and Jin, B. R. (2003). cDNA cloning of a defender against apoptotic cell death 1 (DAD1) homologue, responsive to external temperature stimulus from the spider, *Araneus ventricosus*. *Comp. Biochem. Physiol. B Biochem. Mol. Biol.* 135, 117–123. doi: 10.1016/S1096-4959(03)00055-1

Li, K., Ouyang, H., Lü, Y., Liang, J., Wilson, I. B., and Jin, C. (2011). Repression of N-glycosylation triggers the unfolded protein response (UPR) and overexpression of cell wall protein and chitin in *Aspergillus fumigatus*. *Microbiology* 157:1968. doi: 10.1099/mic.0.047712-0

Li, Y., Kabbage, M., Liu, W., and Dickman, M. B. (2016a). Aspartyl protease mediated cleavage of AtBAG6 is necessary for autophagy and fungal resistance in plants. *Plant Cell* 28, 233–247. doi: 10.1105/tpc.15.00626

Li, Y., Williams, B., and Dickman, M. (2016b). *Arabidopsis* B-cell lymphoma2 (Bcl-2)-associated athanogene 7 (BAG7)-mediated heat tolerance requires translocation, sumoylation and binding to WRKY29. *New Phytol.* 214, 695–705. doi: 10.1111/nph.14388

Libault, M., Thibivilliers, S., Bilgin, D. D., Radwan, O., Benitez, M., Clough, S. J., et al. (2008). Identification of four soybean reference genes for gene expression normalization. *Plant Genome* 1, 44–54. doi: 10.3835/plantgenome2008.02.0091

Liu, Y., Schiff, M., Marathe, R., and Dinesh-Kumar, S. P. (2002). Tobacco Rar1, EDS1 and NPR1/NIM1 like genes are required for N-mediated resistance to tobacco mosaic virus. *Plant J.* 30, 415–429. doi: 10.1046/j.1365-313X.2002.01297.x

Livak, K. J., and Schmittgen, T. D. (2001). Analysis of relative gene expression data using real-time quantitative PCR and the $2^{-\Delta\Delta C_T}$ method. *Methods* 25, 402–408. doi: 10.1006/meth.2001.1262

Lorenzo, O., Piqueras, R., Sánchezserrano, J. J., and Solano, R. (2003). Ethylene response factor1 integrates signals from ethylene and jasmonate pathways in plant defense. *Plant Cell* 15, 165–178. doi: 10.1105/tpc.007468

Lorenzo, O., and Solano, R. (2005). Molecular players regulating the jasmonate signalling network. *Curr. Opin. Plant Biol.* 8, 532–540. doi: 10.1016/j.pbi.2005.07.003

Makishima, T., Yoshimi, M., Komiyama, S., Hara, N., and Nishimoto, T. (2000). A Subunit of the mammalian oligosaccharyltransferase, DADI, interacts with Mcl-1, one of the bcl-2 protein family1. *J. Biochem.* 128, 399–405. doi: 10.1093/oxfordjournals.jbchem.a022767

Maldonado, A., Youssef, R., Mcdonald, M., Brewer, E., Beard, H., Matthews, B. J. P., et al. (2014). Overexpression of four *Arabidopsis thaliana* NHL genes in soybean (*Glycine max*) roots and their effect on resistance to the soybean cyst nematode (*Heterodera glycines*). *Physiol. Mol. Plant P* 86, 1–10. doi: 10.1016/j.pmpp.2014.02.001

Matsumura, H., Nirasawa, S., Kiba, A., Urasaki, N., Saitoh, H., Ito, M., et al. (2003). Overexpression of Bax inhibitor suppresses the fungal elicitor-induced cell death in rice (*Oryza sativa* L.) cells. *Plant J.* 33, 425–434. doi: 10.1046/J.1365-313x.2003.01639.X

Mazarei, M., Elling, A. A., Maier, T. R., Puthoff, D. P., and Baum, T. J. (2007). GmEREBP1 is a transcription factor activating defense genes in soybean and *Arabidopsis*. *Mol. Plant Microbe Interact.* 20, 107–119. doi: 10.1094/MPMI-20-2-0107

Moy, P., Qutob, D., Chapman, B. P., Atkinson, I., and Gijzen, M. (2004). Patterns of gene expression upon infection of soybean plants by *Phytophthora sojae*. *Mol. Plant Microbe Interact.* 17, 1051–1062. doi: 10.1094/MPMI.2004.17.10.1051

Nakashima, T., Sekiguchi, T., Kuraoka, A., Fukushima, K., Shibata, Y., Komiyama, S., et al. (1993). Molecular-cloning of a human cDNA-encoding a novel protein, Dad1, whose defect causes apoptotic cell-death in hamster BHK-21-cells. *Mol. Cell Biol.* 13, 6367–6374. doi: 10.1128/MCB.13.10.6367

Perez, I. B., and Brown, P. J. (2014). The role of ROS signaling in cross-tolerance: from model to crop. *Front. Plant Sci.* 5:754. doi: 10.3389/fpls.2014.00754

Peristera, R., and Stephen, H. (2012). The oligosaccharyltransferase subunits OST48, DAD1 and KCP2 function as ubiquitous and selective modulators of mammalian N-glycosylation. *J. Cell Sci.* 125, 3474–3484. doi: 10.1242/jcs.103952

Rojo, E., Martin, R., Carter, C., Zouhar, J., Pan, S., Plotnikova, J., et al. (2004). VPE gamma exhibits a caspase-like activity that contributes to defense against pathogens. *Curr. Biol.* 14, 1897–1906. doi: 10.1016/j.cub.2004.09.056

Sanjay, A., Fu, J., and Kreibich, G. (1998). DAD1 is required for the function and the structural integrity of the oligosaccharyltransferase complex. *J. Biol. Chem.* 273, 26094–26099. doi: 10.1074/jbc.273.40.26094

Subramanian, S., Graham, M. Y., Yu, O., and Graham, T. L. (2005). RNA interference of soybean isoflavone synthase genes leads to silencing in tissues distal to the transformation site and to enhanced susceptibility to *Phytophthora sojae*. *Plant Physiol.* 137, 1345–1353. doi: 10.1104/pp.104.057257

Sugano, S., Sugimoto, T., Takatsuji, H., and Jiang, C. J. (2014). Induction of resistance to *Phytophthora sojae* in soyabean (*Glycine Max*) by salicylic acid and ethylene. *Plant Pathol.* 62, 1048–1056. doi: 10.1111/ppa.12011

Sugimoto, T., Kato, M., Yoshida, S., Matsumoto, I., Kobayashi, T., Kaga, A., et al. (2012). Pathogenic diversity of *Phytophthora sojae* and breeding strategies to develop phytophthora-resistant soybeans. *Breed. Sci.* 61, 511–522. doi: 10.1270/jsbbs.61.511

Sun, J., Li, L., Zhao, J., Huang, J., Yan, Q., Xing, H., et al. (2014). Genetic analysis and fine mapping of RpsJS, a novel resistance gene to *Phytophthora sojae* in soybean [*Glycine max* (L.) *Merr*]. *Theor. Appl. Genet.* 127, 913–919. doi: 10.1007/s00122-014-2266-2

Tanaka, Y., Makishima, T., Sasabe, M., Ichinose, Y., Shiraishi, T., Nishimoto, T., et al. (1997). dad-1, a putative programmed cell death suppressor gene in rice. *Plant Cell Physiol.* 38, 379–383. doi: 10.1093/oxfordjournals.pcp.a029179

Tiziana, A., and Roberto, S. (2014). Protein quality control in the early secretory pathway. *Embo J.* 27, 315–327. doi: 10.1038/sj.emboj.7601974

Tyler, B. M. (2007). *Phytophthora sojae*: root rot pathogen of soybean and model oomycete. *Mol. Plant Pathol.* 8, 1–8. doi: 10.1111/j.1364-3703.2006.00373.x

Wang, D., Weaver, N. D., Kesarwani, M., and Dong, X. (2005). Induction of protein secretory pathway is required for systemic acquired resistance. *Science* 308, 1036–1040. doi: 10.1126/science.1108791

Wang, X. J., Tang, C. L., Zhang, H. C., Xu, J. R., Liu, B., Lv, J., et al. (2011). TaDAD2, a negative regulator of programmed cell death, is important for the interaction between wheat and the stripe rust fungus. *Mol. Plant Microbe Interact.* 24, 79–90. doi: 10.1094/MPMI-06-10-0131

Watanabe, N., and Lam, E. (2009). Bax Inhibitor-1, a conserved cell death suppressor, is a key molecular switch downstream from a variety of biotic and abiotic stress signals in plants. *Int. J. Mol. Sci.* 10, 3149–3167. doi: 10.3390/ijms10073149

Wesley, S. V., Helliwell, C. A., Smith, N. A., Wang, M., Rouse, D. T., Liu, Q., et al. (2001). Construct design for efficient, effective and high-throughput gene silencing in plants. *Plant J.* 27, 581–590. doi: 10.1046/j.1365-313X.2001.01105.x

Williams, B., Kabbage, M., Britt, R., and Dickman, M. B. (2010). AtBAG7, an *Arabidopsis* Bcl-2-associated athanogene, resides in the endoplasmic reticulum and is involved in the unfolded protein response. *Proc. Natl. Acad. Sci. U.S.A.* 107, 6088–6093. doi: 10.1073/pnas.0912670107

Xiong, Q., Ye, W., Choi, D., Wong, J., Qiao, Y., Tao, K., et al. (2014). Phytophthora suppressor of RNA silencing 2 is a conserved RxLR effector that promotes infection in soybean and *Arabidopsis thaliana*. *Mol. Plant Microbe Interact.* 27, 1379–1389. doi: 10.1094/MPMI-06-14-0190-R

Yamada, T., Takatsu, Y., Kasumi, M., Marubashi, W., and Ichimura, K. (2004). A homolog of the defender against apoptotic death gene (DAD1) in senescing gladiolus petals is down-regulated prior to the onset of programmed cell death. *J. Plant Physiol.* 161, 1281–1283. doi: 10.1016/j.jplph.2004.06.005

Yan, A., Wu, E., and Lennarz, W. J. (2005). Studies of yeast oligosaccharyl transferase subunits using the split-ubiquitin system: topological features and in vivo interactions. *Proc. Natl. Acad. Sci. U.S.A.* 102, 7121–7126. doi: 10.1073/pnas.0502669102

Yan, Q., Cui, X., Su, L., Xu, N., Guo, N., Xing, H., et al. (2014). GmSGT1 is differently required for soybean Rps genes-mediated and basal resistance to *Phytophthora sojae*. *Plant Cell Rep.* 33, 1275–1288. doi: 10.1007/s00299-014-1615-6

Zhang, M., Rajput, N. A., Shen, D., Sun, P., Zeng, W., Liu, T., et al. (2014). A *Phytophthora sojae* cytoplasmic effector mediates disease resistance and abiotic stress tolerance in *Nicotiana benthamiana*. *Sci. Rep.* 5:10837. doi: 10.1038/srep10837

Zhang, Y., Chang, C., and Lai, Z. C. (2016). The defender against apoptotic cell death 1 gene is required for tissue growth and efficient N-glycosylation in *Drosophila melanogaster*. *Dev. Biol.* 420:186. doi: 10.1016/j.ydbio.2016.09.021

Zhou, L., Mideros, S. X., Bao, L., Hanlon, R., Arredondo, F. D., Tripathy, S., et al. (2009). Infection and genotype remodel the entire soybean transcriptome. *BMC Genomics* 10:49. doi: 10.1186/1471-2164-10-49

Zhu, L., Song, L., Zhang, H., Zhao, J., Li, C., and Xu, W. (2008). Molecular cloning and responsive expression to injury stimulus of a defender against cell death 1 (DAD1) gene from bay scallops *Argopecten irradians*. *Mol. Biol. Rep.* 35, 125–132. doi: 10.1007/s11033-007-9061-y

Conflict of Interest Statement: The authors declare that the research was conducted in the absence of any commercial or financial relationships that could be construed as a potential conflict of interest.

frontiers in Microbiology

ORIGINAL RESEARCH
published: 18 March 2019
doi: 10.3389/fmicb.2019.00449

Differences in Ear Rot Resistance and *Fusarium verticillioides*-Produced Fumonisin Contamination Between Polish Currently and Historically Used Maize Inbred Lines

Elżbieta Czembor[1], Agnieszka Waśkiewicz[2], Urszula Piechota[3], Marta Puchta[3], Jerzy H. Czembor[3] and Łukasz Stępień[4]*

[1] Department of Grasses, Legumes and Energy Plants, Plant Breeding and Acclimatization Institute – NRI, Radzikow, Blonie, Poland, [2] Department of Chemistry, Poznań University of Life Sciences, Poznań, Poland, [3] National Centre for Genetic Resources, Plant Breeding and Acclimatization Institute – NRI, Radzikow, Blonie, Poland, [4] Department of Pathogen Genetics and Plant Resistance, Institute of Plant Genetics, Polish Academy of Sciences, Poznań, Poland

OPEN ACCESS

Edited by:
Marco Catoni, University of Birmingham, United Kingdom

Reviewed by:
Javier Plasencia, National Autonomous University of Mexico, Mexico
John Laurie, Agriculture and Agri-Food Canada, Canada
Alessandra Lanubile, Catholic University of Sacred Heart, Italy

***Correspondence:**
Elżbieta Czembor
e.czembor@ihar.edu.pl

Specialty section:
This article was submitted to Plant Microbe Interactions, a section of the journal Frontiers in Microbiology

Received: *17 October 2018*
Accepted: *20 February 2019*
Published: *18 March 2019*

Citation:
Czembor E, Waśkiewicz A, Piechota U, Puchta M, Czembor JH and Stępień Ł (2019) Differences in Ear Rot Resistance and Fusarium verticillioides-Produced Fumonisin Contamination Between Polish Currently and Historically Used Maize Inbred Lines. Front. Microbiol. 10:449. doi: 10.3389/fmicb.2019.00449

Poland is the fifth largest European country, in terms of maize production. Ear rots caused by *Fusarium* spp. are significant diseases affecting yield and causing grain mycotoxin contamination. Inbred lines, which are commonly used in Polish breeding programs, belong, mostly, to two distinct genetic categories: flint and dent. However, historically used lines belonging to the heterotic Lancaster, IDT and SSS groups were also present in previous Polish breeding programs. In the current study, 98 inbred lines were evaluated across a 2-year-long experiment, after inoculation with *F. verticillioides* and under natural infection conditions. Lancaster, IDT, SSS and SSS/IDT groups were characterized as the most susceptible ones and flint as the more resistant. Based on the results obtained, the moderately resistant and most susceptible genotypes were defined to determine the content of fumonisins (FBs) in kernel and cob fractions using the HPLC method. Fumonisin's content was higher in the grain samples collected from inoculated plants than in cobs. The association of visible *Fusarium* symptoms with fumonisin concentration in grain samples was significant. Conversely, the cobs contained more FB_1 under natural infection, which may be related to a pathogen's type of growth, infection time or presence of competitive species. Using ddRADseq genome sampling method it was possible to distinguish a basal relationship between moderately resistant and susceptible genotypes. Genetic distance between maize genotypes was high. Moderately resistant inbreed lines, which belong to IDT and IDT/SSS belong to one haplotype. Genotypes which belong to the flint, dent or Lancaster group, and were characterized as moderately resistant were classified separately as the same susceptible one. This research has demonstrated that currently grown Polish inbred lines, as well the ones used in the past are a valid source of resistance to *Fusarium* ear rot. A strong association was observed between

visible *Fusarium* symptoms with fumonisin concentration in grain samples, suggesting that selection in maize for reduced visible molds should reduce the risk of mycotoxin contamination. NGS techniques provide new tools for overcoming the long selection process and increase the breeding efficiency.

Keywords: maize inbred lines, *Fusarium* ear rot, fumonisin accumulation, genetic distance assessment, ddRADseq

INTRODUCTION

Maize has become one of the most important crops for food and feed production worldwide–both as silage and crop residue. It is also used industrially for starch and oil extraction. The production area in Poland has reached 1200 thousand ha. Fungal diseases are among the most important factors limiting the yield and grain quality of maize, with *Fusarium* ear rots (FER) caused by *Fusarium* at the top of the list. *Fusaria* has the ability to produce toxins which are harmful to both humans and animals alike. The environment has a huge impact on these processes and this is also being studied. In Europe the most common ear rotting fungal species are: *F. verticillioides* (Sacc.) Nirenberg, causing pink ear rot, and *F. graminearum* Schwabe, causing red ear rot. However, a number of minor species are also present: *F. temperatum*, *F. poae*, *F. proliferatum*, *F. avenaceum, F. culmorum F. subglutinans,* and *F. sporotrichioides*. Maize grain is mostly contaminated with fumonisins produced by *F. verticillioides* and *F. proliferatum*, and/or by deoxynivalenol and other trichothecenes along with zearalenone produced by *F. graminearum*, which affect the health of human and animals (Desjardins and Plattner, 2000; Logrieco et al., 2002; Bennett and Klich, 2003; Munkvold, 2003b; Oldenburg and Ellner, 2005; Voss et al., 2006; Dorn et al., 2009; Czembor et al., 2014, 2015; Gallo et al., 2015; Stoycho, 2015; Miedaner et al., 2017). The maximum acceptable levels of mycotoxin content have been established for both maize and maize products. The guidance has been placed for foodstuffs (EC, 2007) and for animal feed in the European Union (EC, 2006). Contamination of maize grain or feed product is influenced by environmental conditions, agricultural practices, genotype resistance and the interaction between all of these factors (Maiorano et al., 2009a,b; Vasileiadis et al., 2011; Zijlstra et al., 2011; Mesterhazy et al., 2012; Cao et al., 2014b; Miedaner et al., 2017). *Fusarium verticillioides* can cause disease, at all developmental stages of the plant, in some cases without displaying any symptoms and, consequently, fumonisins are present in symptomless infected kernels (Desjardins and Plattner, 2000; Desjardins et al., 2002; Miedaner et al., 2010).

Ear rot caused by *F. verticillioides* favored warm and dry conditions, however, warm and wet conditions following silking have been reported to be conducive for disease development (Munkvold, 2003b). Weather conditions during flowering are critical for primary infection, as well as for toxin accumulation during flowering and then before harvesting (De La Campa et al., 2005; Maiorano et al., 2009a,b; Cao et al., 2014b). Low rainfall and a high number of days with maximum temperatures around 30-35°C during flowering favor disease development. Additionally, precipitation stimulates mycotoxin accumulation before the maturity stage because of the extended harvest period.

Appropriate agronomic practice is one of the most effective approaches to reduce mycotoxin contamination of maize grain (Munkvold, 2003a; Ariño et al., 2009; Mesterhazy et al., 2012; de Galarreta et al., 2015) along with the use of less susceptible hybrids, which can be developed either by traditional breeding methods or by transgenic technology (Munkvold, 2003a; Smith et al., 2004; Presello et al., 2005, 2011; Butrón et al., 2006; Smith, 2007; Toldi et al., 2008; Eller et al., 2010; Lanubile et al., 2011; Mesterhazy et al., 2012; Czembor et al., 2015). Genetic resistance is needed in currently used cultivars and it can be deployed from available intra-specific variability. The understanding of the mechanisms underlying maize resistance to ear rot is still limited. Their nature is polygenic and mapped resistance quantitative trait loci (QTL) have relatively small effects and are not consistent between populations (Pérez-Brito et al., 2001; Robertson-Hoyt et al., 2006; Ding et al., 2008; Xiang et al., 2010; Ali and Yan, 2012; Chen et al., 2012; Yuan et al., 2013; Zila et al., 2013, 2014; Mideros et al., 2014; Butrón et al., 2015; Lanubile et al., 2017). The accumulation of mycotoxins can also be affected by the plant genotype. Pedigree breeding has caused maize inbreeds to become not only more-elite but also genetically more uniform. Older generations of inbred lines are still used in inbred line development and genetic studies or as testers in many breeding programs (Presello et al., 2005, 2011; Mesterhazy et al., 2012). The most utilized inbreds belong into the heterotic groups such as Reid Yellow Dent, Iowa Stiff Stalk Synthetic (SSS), Lancaster, Iodent (IDT) and have not been subjected to phenotypic selection for FER resistance. Flint and popcorn hybrids tend to exhibit less FER severity and grain mycotoxin contamination than dent ones, though resistant dent hybrids are also available (Presello et al., 2007). The stability of the earlier germplasms from Argentina was evaluated in Argentinian and Canadian environments (Presello et al., 2004, 2005, 2011). German conditions were evaluated by Bolduan et al. (2009) and Löffler et al. (2010) who concluded that the sources of resistance are effective in different locations. South African conditions were evaluated by Small et al. (2012), Italian by Balconi et al. (2014) Central European (Poland) by Czembor and Frasinski (2018) and Czembor et al. (2013a,b, 2015).

The breeding programs intensified the development of more resistant genotypes and the identification of new resistance sources, the plant selection procedures and QTL mapping. The resistance mechanism is also being studied. Recently, next-generation sequencing (NGS) technology has emerged as a cutting-edge approach for high-throughput sequence determination. It has improved the efficiency and speed of gene discovery, reducing the time, labor, and cost (Robertson et al.,

2006; Elshire et al., 2011; Mesterhazy et al., 2012; Peterson et al., 2012; Zila et al., 2014).

In summary the objectives of this study were: (i) to evaluate the variation of FER resistance and mycotoxin contamination caused by *F. verticilliides* among a broad base of early, mid-early and late groups of maize elite inbred lines belonging to currently used flint and dent groups as well as historical heterotic groups such as Lancaster, IDT, SSS, and (ii) to estimate the level of genetic diversity among and within these groups using NGS technology. Inbreds possessing resistance to FER and fumonisin accumulation would be valuable materials for future breeding programs.

MATERIALS AND METHODS

Plant Materials

Ninety-eight inbred lines were evaluated, belonging to currently used flint ($n = 23$) and dent ($n = 39$) inbred groups, as well as historically used heterotic groups such as Lancaster ($n = 4$), Iodent Reid (IDT, $n = 9$), Stiff Stalk Synthetic (SSS, $n = 8$) and SSS/IDT (S/I, $n = 5$).A heterotic group of 10 lines was unknown. Based on phenotypic FER assessment, genotypes were divided into 4 groups: highly resistant, moderately resistant, moderately susceptible and very susceptible. Moderately resistant and very susceptible genotypes, representing each heterotic group (30 inbreds: 10 dents, 8 flints, 3 IDT, 2 Lancaster, 3 SSS, 2 SSS/IDT, 2 of the unknown heterotic group), were selected for further research aimed at determining the content of fumonisins in grain and cob fractions (**Figure 1**).

FIGURE 1 | Ears morphology of inbred lines belonging to different heterotic groups: flint, dent, Lancaster, Iodent (IDT), Stiff Stalk Synthetic (SSS), SSS/IDT and unknown groups and symptoms of the *Fusarium* ear rot (FER) disease after kernel inoculation with *F. verticillioides*.

Field Experiment and Phenotypic Ear Rot Resistance Assessment

Two-year field experiments were conducted in Radzików, Central Poland (N: 52.21929, 20.63137, sea level: 87 m), across 2011-2012 seasons, as was suggested by Bolduan et al. (2009). They recommended a two-stage selection: an online personal contribution by artificial infection at one place and the next between test hybrids in several (2–3) locations. An RCBD (randomized complete block design) model was used for the field experiment. About 25 plants of maize inbred lines were grown in one row, in three replications (0.75 m between rows and 0.25 m between plants in the row).

To produce inoculum, a well-characterized fumonisin-producing *F. verticillioides* strain was used. This isolate was selected from the collection carried out by Plant Breeding and Acclimatization Institute-NRI based on the results of a 2-year experiment as the most aggressive in relation to two hybrids of maize. A PDA (Potato dextrose agar) plug with 7-day-old culture was transferred to a 10-mL vial containing 12 autoclaved toothpicks and 8-mL SNA (Synthetic low-Nutrient Agar) and incubated for 2 weeks at 25°C. Prior to autoclaving, the toothpicks were washed and boiled in excess water for 1 h to remove any toxic substances that might inhibit fungal growth (Jardine and Leslie, 1992). After incubation the toothpicks were removed from the vials and air-dried on a sterile bench overnight.

Inoculation of individual ears was conducted 10–12 days after silking time. At least 20 plants were inoculated for each genotype (6–7 plants in three replicates). Control plants were inoculated using toothpicks without the pathogen. At maturity, ears from each plot were dehusked and harvested manually, dried to approximately 15% grain moisture content and individually rated for FER symptoms using a seven-point scale: 1 = no visible disease symptoms, 2 = 1–3%, 3 = 4-10%, 4 = 11–25%, 5 = 26–50%, 6 = 51–75%, and 7 = 76–100% of kernels exhibiting visual symptoms of infection, such as brown, pink, or reddish discoloration of kernels and pinkish or white mycelial growth (Clements et al., 2003a,b; **Supplementary Figure 1**). Ear rot severity scores were converted to percentages of the ear exhibiting symptoms replacing each score with the mid-point of the interval.

Fumonisins Analysis

Fumonisin B_1, B_2, B_3 standards were purchased with a standard grade certificate from Sigma-Aldrich (Steinheim, Germany). Sodium dihydrophosphate, potassium chloride, acetic acid and *o*-phosphoric acid were purchased from POCh (Gliwice, Poland). Organic solvents (HPLC grade), disodium tetraborate, 2-mercaptoethanol and all the other chemicals were also purchased from Sigma-Aldrich (Steinheim, Germany). Water for the HPLC mobile phase was purified using a Milli-Q system (Millipore, Bedford, MA, USA).

Extraction and purification procedure: 10 g of homogenized ground samples of maize kernels were prepared for analysis. Mycotoxins (FBs) were extracted and purified according to the detailed procedure described earlier (Waśkiewicz et al., 2013a,b). The eluates were evaporated to dryness at 40°C under a

stream of nitrogen. The dry residue was stored at −20°C until the HPLC analyses. The chromatographic system consisted of Waters 2695 high-performance liquid chromatography (Waters, Milford, USA) with Waters 2475 Multi λ Fluorescence Detector (λex = 335 nm, λem = 440 nm) with an XBridge column (3.0 × 100 mm). Quantification of mycotoxins was performed by measuring the peak areas at the retention time according to a relevant calibration curve. The limit of detection was 0.01 $\mu g\, g^{-1}$.

Genetic Distance Assessment

The level of genetic diversity among 17 distinct maize genotypes was analyzed using NGS technology. They were selected as moderately resistant and susceptible to ear rot, based on the evaluation under field conditions after inoculation and fumonisin content.

For different combinations of restriction enzymes, it is possible to perform sequencing from 0.01 to 1.99% of maize genome size due to the ddRAD *in silico* pipeline (Yang et al., 2016). That fraction selected by the ddRADseq pipeline is enough for a broad spectrum of research. The ddRADseq method is used in phylogeny analysis and establishing a genetic relationship among different genotypes. Different restriction enzymes and broad or narrow size selection make the library proper to MiSeq capacity. DdRADseq does not need a reference sequence (Peterson et al., 2012).

Genomic DNA was extracted from 200 mg of 14-day-old single plant leaf tissue by CTAB method (Waśkiewicz et al., 2013b) with RNase A (Qiagen) treatment before precipitation (30 min at 37°C). DNA quality was evaluated on 1% agarose gel and quantity was measured by NanoDrop 1000 (NanoDrop Technologies Inc., USA).

Double-digest restriction-associated DNA sequencing (ddRADseq) protocol described previously by Peterson et al. (2012) was used to detected molecular data. The library was prepared using 200 ng genomic DNA of each sample. DNA was digested at 37°C for 3 h using the 8U HindIII and 8U FspBI restriction enzymes. In the next step, digested DNA was ligated to adapters using T4 Ligase for 2 h at 16°C. Adapters included Illumina primer sequences and unique barcodes. Purification of ligation products was prepared by AMPure (Beckman Coulter, USA) with beads: sample ratio 1:1. Cleaned DNA was re-suspended in 150 μl of water. Fifteen microlite of ligation products were amplified with NeBNext Ultra II Q5 Master Mix (New England Biolabs, UK) using primers with Illumina index sequences due to the single-indexing method. PCR programme: preliminary denaturation 98°C/30 s., 16 cycles of denaturation at 98°C/10 s. and combined annealing and elongation 65°C/75 s., final elongation 65°C/5 min., hold at 4°C. All PCR products were pooled and cleaned-up with AMPure (Beckman Coulter, USA) with bead: sample ratio 1:1 and next 0.6: 1 to size selection of 400-600 bp. A library was quantified on fluorimeter Qubit (ThermoFisher Scientific, USA) by Quant-iT™ High-Sensitivity dsDNA Assay Kit. A library was diluted to 4 nM and denatured with 0.2N NaOH for 5 min. A denatured library was diluted to 20 pM. 600 μl of a prepared library was sequenced using Illumina MiSeq with Miseq Reagent Kit v3 and final PhiX concentration of 12.5 pM and pair reading protocol for 151 cycles.

Quality control of reads was checked in FastQC software (https://www.bioinformatics.babraham.ac.uk/projects/fastqc/; FastQC A Quality Control tool for High Throughput Sequence Data by: S. Andrews). Reads-analysis were prepared with Geneious 11.0 software (https://www.geneious.com, Kearse et al., 2012). The parameters of the substitution model define a rate matrix that can be used to calculate the probability of evolving from one base to another in a given period of time. Most models are variations of two sets of parameters–the equilibrium frequencies and relative substitution rates. Genetic Distance Model: Tamura-Nei. This model also assumes different equilibrium base frequencies. In addition to distinguishing between transitions and transversions, it also allows the two types of transitions (A ↔ G and C ↔ T) to have different rates (Tamura and Nei, 1993). Before analyzing, the reads were split by barcode data. Then, the ends were trimmed, paired reads merged and duplicate reads removed (**Supplementary Figure 2**). The reads were *de novo* assembled using original data by the Geneious *de novo* overlap assembler to a high accuracy level (**Supplementary Figure 3**). A genotype tree was made using the neighbor-joining method with a genetic distance model. The tree was constructed with standard software settings. In this method, neighbors are defined as a pair of leaves with one node connecting them, minimizing the total branch length at each stage of clustering, starting with a star-like tree. The branch lengths and an unrooted tree topology can quickly be obtained by using this method without assuming a molecular clock (Saitou and Nei, 1987).

Meteorological Data

Field trials were conducted in Radzików, Central Poland. The generative stages of hybrids belonging to the middle-early group were as follows: silking (R1)–I decade of July, blister (R2)–II decade of July, milk (R3)–III decade of July, dough (R4)–I decade of August, dent (R5)–from the II decade of August until the end of I decade of September. Physiological maturity (R6) stage and harvesting time were in the II decade of September. The generative stages of hybrids belonging to the middle-late group started 7 days later (II decade of July) and lasted until the half of the III decade of September. The average temperatures and rainfalls during this time are presented in **Figure 2**.

Statistical Analyses

Comparison between inbred lines was done using Fisher's least significant difference test using InfoStat software. In addition to the mold-covered surface proportion of the maize grain, fumonisin content in the infected maize grain meal and the content of the infected maize grain meal, the so-called Toxin-Mold-Index (TMI), was also calculated according to the method described by Arpad et al. (1997), by multiplying the sum of mycotoxin contents, expressed in mg per kg, by the proportion of mold-covered surfaces of maize ear expressed as percentage of the total surface where: $TMI = (FB_1+FB_2+FB_3)^*A$; FB_1, FB_2, FB_3 content in maize meal obtained from grain and corn cobs; A - proportion of the mold-covered area of ears in % of the total areas of ears.

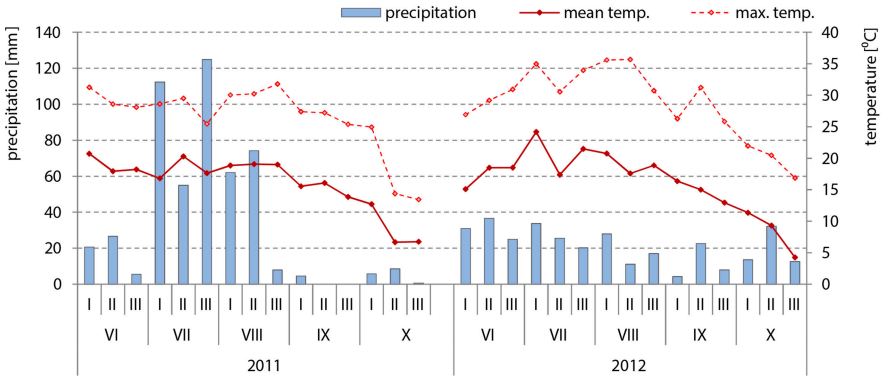

FIGURE 2 | Weather conditions in the years 2011 and 2012 when the FER resistance assessment of 98 maize inbred lines was carried out under field conditions with a natural infection and after inoculation with *F. verticillioides*: mean temperature and precipitation data from sowing time (April) till harvesting time (October) were shown.

Differences between inbred lines within years were determined with Fisher's protected least significant difference (LSD) test. Linear correlation coefficients were determined for the relationship between FER severity and fumonisin concentration in grain and cobs sampled from non-inoculated and inoculated plants in 2012 using InfoStat software.

RESULTS

Fusarium Ear Rot Severity and Fumonisin Contamination

All inoculations resulted in visible disease symptoms (DI = 100%). A summary of statistical data such as mean, SD, minimum and maximum of ear rot ratings of flint (n = 23), dent (n = 39), IDT (n = 9), Lancaster (n = 4), SSS (n = 8), SSS/IDT (n = 5), and unknown (n = 10) heterotic groups under natural infection (non-inoculated) and inoculated with *F. verticillioides* in 2011 and 2012 are shown in **Table 1**. The Variability of ear rot incidence was observed between, and within, heterotic groups. **Figure 1** shows ears representing individual origin groups and symptoms of the disease after inoculation.

In July, when the primary infection usually takes place, maximum temperatures were higher in 2012 than in 2011 by ca. 5°C and favored the development of *F. verticillioides*, used for artificial infection (**Figure 2**). In 2011, high precipitation in July (112 mm, 55 mm and 127 mm in the first, second and third decades, respectively) and August (62 mm and 74 mm in the first and second decades, respectively) did not stimulate disease development. The effects of maize heterotic groups and inbred lines on disease severity differed between years.

Significant differences in FER severity were observed among inbred lines and heterotic groups evaluated under natural infection and after inoculation in both years. *Fusarium* ear rot severity was significantly higher in 2012 than in 2011 with means of 4.9 and 1.8% of the ear exhibiting disease symptoms under natural conditions, respectively, and 15.2 and 8.07% after inoculation with *F. verticillioides*. Under natural infection, FER severity for all 98 inbred lines ranged from 1.6 to 45.5% of the ear exhibiting disease symptoms in 2012 and from 0.0 to 7.0% of the ear in 2011. After inoculation, FER severity ranged from 3.0 to 63.0% of the ear exhibiting disease symptoms in 2012 and from 1.4 to 50.5% of the ear in 2011. In 2012 the means of ear rot severity of evaluated groups ranged from 10.9 to 30.99% of ears covered by disease symptoms. The most susceptible group was SSS/IDT (**Table 1**). The most resistant inbred lines belonged, mostly, to the unknown heterotic group. The SD in all heterotic groups ranged from 1.13 to 2.2 and from 2.10 to 6.76 under natural infection in 2011 and 2012, respectively. They were much higher after artificial inoculation; ranging from 2.32 to 17.89 in 2011 and 2012, respectively.

On average, for more than 91% of all evaluated inbred lines, the symptoms of the disease did not exceed 10% of the total ear area under natural infection (**Figure 3**). In 2011, for 73% of all evaluated inbred lines, the symptoms of the disease covered <10% of the ear area, and in 2012 the same applied to 43.9% of lines tested. In 2012, for 10.2% of evaluated inbred lines, the disease symptoms were observed within a range of 26–50% of ear area.

A simple correlation analysis and a principal component analysis (PCA, **Figure 4**) were performed to decipher the relationships between FER severity under natural infection and after inoculation. Using Pearson's correlation coefficients it was shown that the FER severity under natural infection in 2012 was significantly correlated with FER after the *F. verticillioides* kernel inoculation (r = 0.48*, p < 0.005). Furthermore, the results of FER scored in 2011 after inoculation was positively correlated with the results obtained in 2012 (0.46*, p < 0.005). The purpose of the PCA was to group individual parameters in a more comprehensive manner. Two principal components (PC) explained 69.2% of the variability. The length of the vectors represents the PCA loadings of the variables on the first two principal components, PC1 (44.5%) had strong positive loading from FER after inoculation in 2011 and 2012 and FER under natural infection in 2012. PC2 (24.7%) had positive loading from FER under natural infection in 2011. The highest diversity among inbreds was

TABLE 1 | Summary statistics of ear rot ratings of $n = 98$ inbred lines that belong to flint, dent, Lancaster, SSS, IDT, SSS/IDT and "unknown" heterotic groups under natural infection and inoculated with *F. verticillioides* in 2011 and 2012 years.

No.	Heterotic group	n	*Fusarium* ear rot (%)							
			non-inoculated				inoculated			
			2011		2012		2011		2012	
			mean[a]	range	mean[a]	range	mean[a]	range	mean[a]	range
1	dent	39	2.2 ± 0.62	0.0–7.0	5.4 ± 6.76	1.2–48.0	6.8 ± 4.35	1.2–22.0	14.9 ± 11.75	2.0–63.0
2	flint	23	1.4 ± 0.56	0.0–4.5	4.3 ± 3.47	1.6–45.5	9.1 ± 6.85	2.0–45.5	16.4 ± 9.35	3.0–58.0
3	IDT	9	1.8 ± 0.80	0.0–4.5	3.4 ± 2.23	1.6–18.0	6.3 ± 4.27	1.2–18.0	11.3 ± 8.06	4.0–34.0
4	lancaster	4	1.9 ± 0.75	0.0–7.0	8.6 ± 7.53	1.2–22.0	16.3 ± 17.89	2.0–50.5	10.9 ± 7.54	5.0–22.0
5	SSS	8	1.8 ± 0.78	0.0–7.0	4.5 ± 5.54	1.6–26.0	6.8 ± 5.20	1.4–15.8	14.7 ± 12.89	3.0–43.0
6	SSS / IDT	5	1.3 ± 0.60	0.0–2.0	7.5 ± 6.50	1.6–22.0	21.7 ± 8.47	7.0–45.5	31.0 ± 16.55	11.4–63.0
7	unknown	10	1.8 ± 0.97	0.0–7.0	3.5 ± 2.10	1.6–18.0	4.2 ± 2.32	1.3–9.2	11.2 ± 5.01	3.0–26.0
Mean		98	4.93 ± 6.13	1.6–45.5	1.82 ± 1.13	0.0–7.0	8.07 ± 7.77	1.4–50.5	15.15 ± 11.55	3.0–63.0
LSD Fisher $_{p < 0.05}$		98	5.941		1.709		7.845		6.319	

[a]*Mean ear rot severity is reported as the average of the entry least square means (back-transformed to the original 0-100% disease severity scale).*

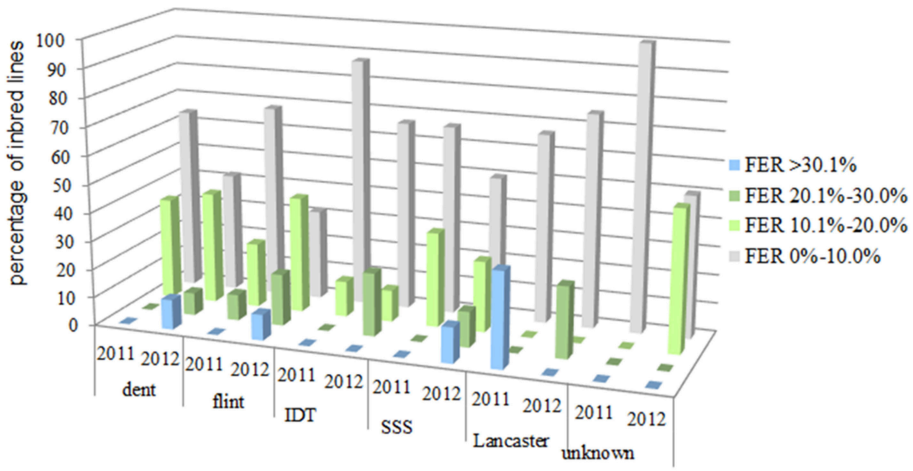

FIGURE 3 | Distribution for percentage data of inbred lines for which the disease symptoms covering: 0.0–10.0%, 10.1–20.0%, 20.1–30.0% and above 30.1% of the total ear area after kernel inoculation with *F. verticillioides* in 2011 and 2012 belonging to different heterotic groups: 23 flint, 39 dent, 4 Lancaster, 9 Iodent (IDT), 8 Stiff Stalk Synthetic (SSS) 5 SSS/IDT and 10 unknown heterogenic group.

associated with FER, evaluated after inoculation in 2012. The most susceptible and moderately resistant inbred lines from each group of origin were selected for fumonisin content analysis.

Ear rot severity of these genotypes in 2011 and 2012, fumonisin contamination in grain and cobs sampled from inoculated and non-inoculated plants in 2012 and TMI index are shown in **Table 2**. Under natural infection, cobs were more contaminated with fumonisin B_1 than grain samples. The frequency of cob samples contaminated with FB_1 was 66.7% and for grain samples contaminated with FB_1 it was 29.6%. Maize inbred lines accumulated different levels of fumonisins in grain and in cobs. In grains sampled from inbred lines of dent, flint, SSS, IDT, SSS/IDT and Lancaster heterotic groups after kernel inoculation with *F. verticillioides*, the FB_1 contamination ranged from 0.99 to 99.04 mg/kg, FB_2 contamination ranged from 0.05 to 21.44 mg/kg and FB_3 from 0.0 to 2.21 mg/kg. In cob samples FB_1 contamination ranged from 0.02 to 23.05 mg/kg, FB_2 from 0.0 to 4.5 mg/kg and FB_3 from 0.0 to 1.82 mg/kg. Based on the TMI index it was possible to identify highly resistant and susceptible genotypes. A hierarchical clustering of the inbred lines representing resistant and very susceptible genotypes belonging to each heterotic group was created based on the TMI index (**Figure 5**). Inbreds with low fumonisin content belonged to two separate clusters with low distance between them. Susceptible inbreds belonged to the very inconsistent group with large distances from each other.

In 2012, ear rot severity positively correlated with fumonisin content in grain samples (FB_1, FB_2, and FB_3), with r factor ranging from $r = 0.82^{***}$ to 0.91^{***}. The correlations between

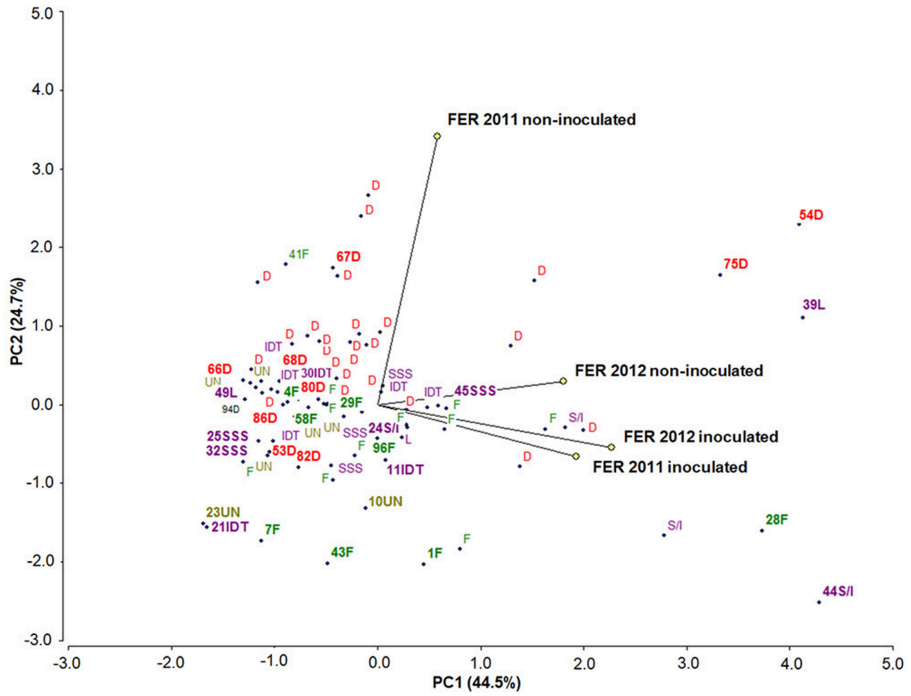

FIGURE 4 | Scatter plot of the first principal component scores derived from rating the FER severity, showing the dispersion of 98 inbred lines belonging to different heterotic groups: 23 flint (F), 39 dent (D), 4 Lancaster (L), 9 Iodent (IDT), 8 Stiff Stalk Synthetic (SSS), 5 SSS/IDT and 10 unknown (UN). Colored dots represent individual subjects with a subject identification group. Colored dots represent individual subjects with a subject identification number were selected for fumonisin content analysis as a moderate resistant (negatively correlated with FER) and susceptible one (positively correlated with FER). The length of the vectors represents the PCA loadings of the variables on the first two principal components, which explain 69.2% of the variability.

individual fumonisins were also highly significant (in grain samples they ranged from $r = 0.90^{***}$ to $r = 0.93^{***}$ $p < 0.005$ and for cobs they ranged from $r = 0.92^{***}$ to 0.97^{***} $p < 0.005$). No correlations were found between the ear rot severity and toxin content in maize cobs.

Molecular Markers and Population Genotyping

The level of genetic heterogeneity among inbreds with contrasting ear rot resistance was studied using the ddRADseq genome sampling method. They belonged to the following groups: flint, dent, Lancaster, IDT, SSS and SSS/IDT. The range of quality values across all bases at each position for our results in the FastQ file was high and it was conceivable to observe a difference for a number of reads for genotypes, even if they belonged to the same origin group (**Figure 6**; **Supplementary Figures 2, 3**). The genotype tree was made using the neighbor-joining method with a genetic distance model. Branch length expressed nucleotide differences. The relative genetic distances between haplotypes were high. One haplotype contained moderately resistant inbred lines belonging to the IDT historical heterotic group (lines 11, 21, 30), SSS / IDT (line 22) and SSS (line 32). Susceptible inbreds belonged to the SSS (line 45) and SSS/IDT groups (line 44) and were classified separately. Likewise, lines from the Lancaster group, described as resistant (line 49) and susceptible (line 39) did not belong to the same haplotype. Furthermore, in the dent group, resistant and susceptible lines were separate. Interestingly, resistant lines from the flint heterotic group belonged to the same haplotype and susceptible flint line was classified separately. Haplotypes of the genotype tree corresponded to the data of the co-ancestry heat map (**Figure 7**).

DISCUSSION

The rapid increase of maize cultivation area, the use of inappropriate crop rotation and global warming have resulted in a rise in frequency of diseases including ear rot fusariosis (*Fusarium* spp.). Using highly resistant hybrids is one of the most important methods of integrated plant protection (Vasileiadis et al., 2011; Zijlstra et al., 2011).

Artificial inoculations are necessary for the evaluation of maize FER under field conditions because the disease symptoms under natural infection are not repeatable and largely depend on local environmental factors (Santiago et al., 2015). Different methods of inoculation were developed and described (Drepper and Renfro, 1990; Schaafsma et al., 1993; Munkvold and Carlton, 1997; Munkvold et al., 1997; Reid et al., 2002). These methods correspond with natural disease development processes. Flowering and kernel drying are critical periods for disease development and kernel contamination with fumonisins (Munkvold, 2003b; Bush et al., 2004; De La Campa et al., 2005;

TABLE 2 | *Fusarium* ear rot resistance (FER) of elite inbred lines under natural infection and after *Fusarium verticillioides* inoculation, fumonisin content in grain and cobs sampled in 2012 along with the Toxin-Mold-Index (TMI).

Heterotic group	Inbred line	FER		Toxin content								TMI	
		non-inoculated	inoculated	non-inoculated		inoculated							
				grain	cobs	grain			cobs				
				FB_1	FB_1	FB_1	FB_2	FB_3	FB_1	FB_2	FB_3	non-inoculated	inoculated
dent ($n = 10$)	53D	2.3	8.1	0.00	0.21	5.35	0.93	0.04	4.36	0.26	0.04		
	54D	10.3	56.3	0.00	0.39	99.04	21.44	2.21	6.50	1.65	0.29	4.0	7378.5
	66D	2.9	2.7	0.00	0.00	5.04	0.58	0.04	0.17	0.06	0.01	0.0	15.5
	67D	4.3	7.5	0.00	0.00	5.41	0.33	0.05	3.31	0.16	0.03	0.0	66.3
	68D	2.1	10.7	0.00	0.00	7.70	0.57	0.05	1.60	0.33	0.04	0.0	106.4
	75D	26.5	39.7	1.07	0.88	44.74	8.41	0.67	1.10	0.25	0.03	51.8	2174.3
	80D	2.3	7.0	0.00	0.00	7.57	1.08	0.12	1.71	0.56	0.07	0.0	77.8
	82D	37.3	12.1	0.00	0.00	12.43	1.22	0.07	2.84	0.87	0.14	0.0	211.7
	86D	2.5	11.4	0.00	0.61	10.31	0.98	0.11	0.85	0.22	0.01	1.6	137.5
	90D	2.9	5.2	0.31	0.00	3.69	0.28	0.05	0.08	0.01	0.00	0.9	21.4
	Mean	9.4 ± 7.23	16.1 ± 11.96	0.14 ± 0.33	0.21 ± 0.31	20.13 ± 29.73	3.58 ± 6.57	0.35 ± 0.71	2.25 ± 2.03	0.44 ± 0.49	0.07 ± 0.09	5.9 ± 17.14	1026.0 ± 2275.4
flint ($n = 8$)	1F	3.5	16.5	0.00	0.40	5.67	1.73	0.21	5.39	1.22	0.36	1.4	241.3
	28F	18.8	40.3	0.00	0.19	45.75	9.95	1.03	0.02	0.00	0.00	3.4	2351.2
	29F	4.0	16.3	0.00	0.00	6.46	4.33	0.11	0.14	0.05	0.01	0.0	161.3
	43F	2.5	7.7	0.20	0.20	26.14	3.85	0.40	23.05	4.01	1.82	1.0	454.0
	4F	5.2	8.1	1.06	0.00	7.38	1.10	0.15	2.62	0.61	0.25	5.5	99.3
	58F	2.3	9.9	0.00	0.42	7.03	0.96	0.14	4.46	0.75	0.04	1.0	134.3
	7F	5.0	8.1	0.00	0.00	5.32	0.72	0.11	0.17	0.06	0.01	0.0	52.0
	96F	3.9	17.9	0.00	0.11	14.40	2.15	0.14	5.14	1.32	0.29	0.4	409.5
	Mean	5.7 ± 5.33	15.6 ± 10.19	0.16 ± 0.36	0.17 ± 0.16	14.77 ± 14.47	3.10 ± 3.31	0.29 ± 0.28	5.12 ± 7.33	1.00 ± 1.27	0.35 ± 0.59	1.58 ± 2.21	487.9 ± 792.37
IDT ($nn = 3$)	11IDT	3.2	23.3	0.00	0.00	3.37	0.29	0.05	3.90	0.83	0.30	0.0	207.6
	21IDT	1.7	6.4	0.00	0.00	0.98	0.05	0.00	0.27	0.03	0.00	0.0	9.0
	30IDT	2.6	6.3	0.00	0.00	7.44	1.11	0.11	1.01	0.10	0.02	0.0	61.8
Lancaster ($n = 2$)	39L	17.1	22.0	0.00	0.41	15.41	2.08	0.29	19.76	4.50	1.43	7.0	956.3
	49L	3.3	6.0	0.00	0.00	3.38	0.30	0.03	0.08	0.01	0.00	0.0	22.8
SSS ($n = 3$)	25SSS	2.2	8.9	0.00	0.19	13.09	11.55	0.24	0.48	0.08	0.00	0.4	262.1
	32SSS	2.5	5.4	0.00	0.00	4.28	0.35	0.03	0.05	0.00	0.00	0.0	26.9
	45SSS	4.0	43.0	0.41	0.00	48.23	14.27	0.99	11.37	2.21	0.41	1.7	3331.8
SSS/IDT ($n = 2$)	24 SSS/IDT	2.7	13.6	0.00	0.15	11.08	3.75	0.95	11.53	2.12	0.14	0.4	406.3

(Continued)

TABLE 2 | Continued

Heterotic group	Inbred line	FER		Toxin content								TMI	
		non-inoculated	inoculated	non-inoculated			inoculated					non-inoculated	inoculated
				grain	cobs		grain			cobs			
				FB_1	FB_1	FB_1	FB_2	FB_3	FB_1	FB_2	FB_3		
	44SSS/IDT	18.6	58.0	0.00	0.20	69.15	10.68	1.00	0.21	0.04	0.00	3.8	4726.0
Uknown ($n = 2$)	10UN	4.0	21.9	0.00	0.00	10.51	2.57	0.12	5.78	0.73	0.14	0.0	424.7
	23UN	2.7	4.3	0.00	0.00	0.95	0.06	0.00	0.67	0.14	0.04	0.0	7.9
LSD Fisher ($P<0.05$) ($n = 30$ inbred lines)		9.379	6.924	0.039	0.03	9.90	5.03	0.331	1.771	0.3632	0.103	8.404	15.705

[a]*Mean ear rot severity is reported as the average of the entry least square means (back-transformed to the original 0-100% disease severity scale).*

Maiorano et al., 2009a,b; Venturini et al., 2011; Cao et al., 2014a,b; Czembor and Matusiak, 2014). Weather conditions affect all of these processes. We could not confirm that high rainfall or high temperature just before harvest are conducive for fumonisin contamination, particularly concerning rainfall data for 2011 and 2012.

In our study, the inoculation technique was very effective, both for FER assessment and for the assessment of the fumonisin contamination of the grain. Kernel samples collected from the most resistant inbred line were also not heavily contaminated with FBs after inoculation. The correlation between FB_1, FB_2 and FB_3 contamination of grain samples and FER severity were highly significant. No significant correlations were observed between the content of fumonisins in samples collected from cobs, both under natural infection and after inoculation. Also in other studies the correlation between the concentration of fumonisin and the severity of FER after inoculation is usually found. Desjardins et al. (2002) and Desjardins and Plattner (2000) reported a very high correlation between fumonisin concentration and visible symptoms, with fumonisin levels being higher in symptomatic kernels and lower in symptomless kernels, respectively. However, in some studies the correlations were not present (Clements et al., 2003a,b).

NGS techniques provide new tools for overcoming the long selection process and increase the breeding efficiency. The knowledge of the QTL genomic location is essential to investigate their potential, as well as their effectiveness toward FER and environmental conditions examined locally (Campos-Bermudez et al., 2013). Here, ddRADseq genome sampling method was deployed to distinguish genetic differences between genotypes with contrasting ear rot resistances (selected based on the field evaluation after inoculation and fumonisin quantification) but also belonging to different heterotic groups: flint and dent groups, as well as to the historical heterotic groups, such as Lancaster, IDT, SSS. The genetic distances between haplotypes were large, indicating an ancient gene pool and possible interspecific hybridization events in maize ancestry. However, among the among the lines of the flint group, as well as in the historical groups, it was possible to find relationship between moderately resistant and susceptible genotypes. Lanubile et al. (2012) summarized reports on mapping disease resistance genes in maize. Using SNPs it was found that QTL located on chromosomes 1, 5, and 9 play significant roles in FER resistance (Zila et al., 2013, 2014). Seven SNPs in six genes associated with FER resistance were identified on chromosomes 4, 5, and 9 based on evaluation of the collection of 1,687 maize inbred lines. Maschietto et al. (2017) found eight QTL associated with FER resistance and FB_1 contamination and Lanubile et al. (2014) mapped 24 candidate genes for FER resistance on the same chromosomal regions. Based on these findings, it is possible to conclude that the QTL with the highest effect for FER resistance was located distally on Chromosome 1. Wisser et al. (2006) postulated that known disease resistance QTL covered 89% of the maize genome. This high degree of coverage is unlikely and possibly related to the relatively

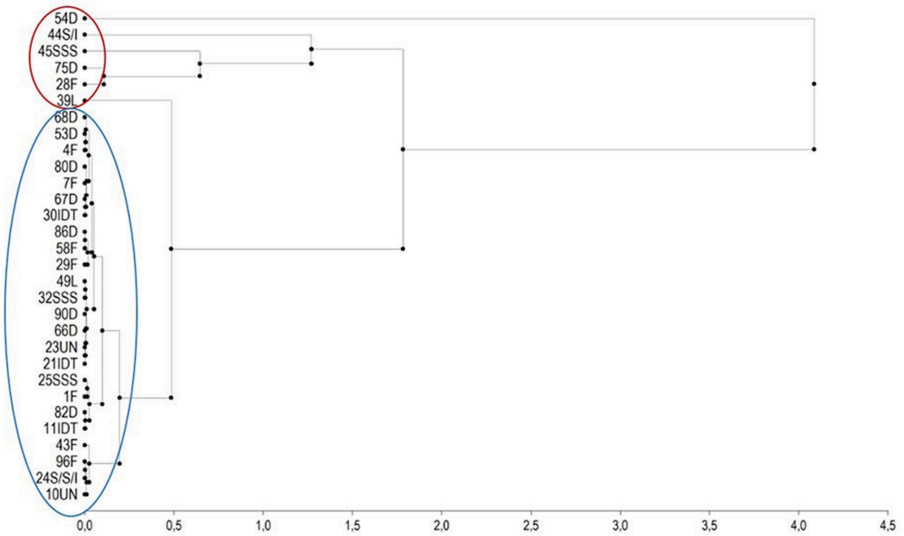

FIGURE 5 | Hierarchical clustering of the inbred lines representing moderately resistant and very susceptible genotypes selected from the collection of 98 inbred based on the disease assessment of non-inoculated and inoculated ears with *F. verticillioides* in 2011 and 2012 years using the Euclidean distance of the elements of relationship matrix A (based on TMI index genotypes in a red cluster represent a very susceptible group). Thirty inbred lines belonging to different heterotic groups 10 dent (D), 8 flint (F), 3 Iodent (IDT), 2 Lancaster (L), 3 Stiff Stalk Synthetic (SSS), 2 SSS/IDT, and 2 unknown (UN). Red color circle: susceptible group, blue color circle: moderate resistant group.

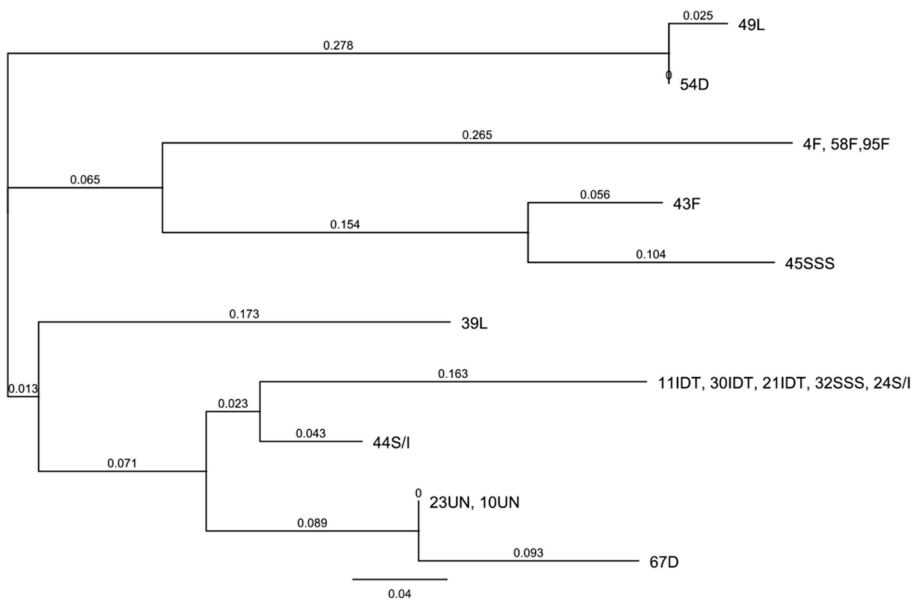

FIGURE 6 | Hierarchical clustering of the inbred lines representing moderate resistant (MR) and susceptible (S) genotypes using Neighbor-joining tree representing phylogenetic distances between objects of relationship matrix.

low precision and accuracy of QTL mapping and not taking into account other relevant factors. Our study stands in line with this hypothesis. It is because of the strong influence of environmental factors, plant phenotype and/or interaction of factors, on the spread of the disease in different locations, where FER resistance studies are conducted. That's why QTL mapping results have often been contradictory and their verification in different genetic backgrounds is necessary (Pérez-Brito et al., 2001; Robertson-Hoyt et al., 2006; Ding et al., 2008; Santiago et al., 2013). A new approach to identify candidate genes and QTL for resistance is represented by plant metabolome investigation after pathogen infection (Lanubile et al., 2017) and differential transcriptomic analyses showing genes potentially involved in resistance processes.

Maize breeding has undergone significant changes through the last four decades and so have the materials used. Facing

	FER	49L	54D	4F; 58F-95F	43F	45SSS	39L
49L	R		13.99	9.78	18.48	17.24	15.02
54D	S	13.99		12.09	18.97	18.06	12.87
4F; 58F; 95F	MR	9.78	12.09		13.22	11.78	7.01
43F	MS	18.48	18.97	13.22		21.85	16.46
45SSS	S	17.24	18.06	11.78	21.85		15.52
39L	S	15.02	12.87	7.01	16.46	15.52	
11IDT; 30 IDT; 21IDT; 32SSS; 24S/I	MR	12.10	12.72	15.69	13.81	14.01	7.55
44S/I	S	5.21	4.22	1.48	5.08	5.35	9.23
23UN; 10UN	MR	12.48	14.73	12.30	18.79	16.07	10.62
67D	MR	16.22	19.17	16.84	24.50	21.29	12.90

FIGURE 7 | Co-ancestry heat map (the color code corresponds to the degrees of similarity-from green means the most similar to red as the least similar). Inbred lines belong to heterotic group: dent (D), flint (F), Iodent (IDT), Lancaster, Stiff Stalk Synthetic (SSS), SSS/IDT and unknown pedigree (un).

the dramatic climate changes it becomes obvious that pathogen populations are being changed as well, along with the maize lines grown. *Fusarium* ear rot resistance remains one of the most important traits in constant selection of materials and sources of this resistance have never been compared until now. This research has demonstrated that currently grown Polish inbreds and also the ones grown in the past may serve as a valid source of resistance to FER. A strong association was observed between visible *Fusarium* symptoms after inoculation with fumonisin concentration in grain samples, suggesting that selection in maize for reduced visible molds should reduce the risk of mycotoxin contamination. Under natural infection, the cobs contained more fumonisin B_1 than grain samples. This finding suggests that *F. verticillioides* contaminates grain more intensively when applied artificially. When found naturally, it tends to overgrow preferably the cobs and not the grain. Moreover, under natural infection one has to take into account the presence of other species like *F. graminearum*, *F. poae*, *F. temperatum* or *F. proliferatum*, which may compete for nutrients and it has been shown that mycotoxin biosynthesis is one of the strategies used by the pathogen to get the advantage over a competitor. To validate this hypothesis a different experimental approach will be established in the future research. Resistance to FER and to fumonisin accumulation is determined by many factors, such as: environmental conditions, infection timing, presence of other competitive species, ear morphology, the kernel's structure and nutrient components, as well as by the interaction between all these factors, which makes drawing conclusions from a single experimental approach challenging. The use of NGS technique in combination with disease symptom screening and mycotoxin contamination allows for fast analysis which genotypes will be most valuable in incorporating the resistance into current breeding programs.

DATA AVAILABILITY

This manuscript contains previously unpublished data. The name of the repository and accession number are not available.

AUTHOR CONTRIBUTIONS

EC designed and conducted field experiments. AW conducted toxins analyses. MP, UP, and JC performed the molecular studies. EC, AW, MP, and UP interpreted the data. EC, AW, MP, UP, JC, and LS drafted the manuscript, designed figures and tables. All authors read and approved the final manuscript.

FUNDING

This work was funded by Polish Ministry of Agriculture and Rural Development.

ACKNOWLEDGMENTS

This work was funded by The Polish Ministry of Agriculture and Rural Development.

SUPPLEMENTARY MATERIAL

The Supplementary Material for this article can be found online at: https://www.frontiersin.org/articles/10.3389/fmicb.2019.00449/full#supplementary-material

Supplementary Figure 1 | Seven-point scale used to score FER: 1 = no visible disease symptoms, 2 = 1–3%, 3 = 4–10%, 4 = 11–25%, 5 = 26–50%, 6 = 51–75%, and 7 = 76–100% of kernels exhibiting visual symptoms of infection, such as brown, pink, or reddish discolouration of kernels and pinkish or white mycelial growth (Clements et al., 2003a,b).

Supplementary Figure 2 | Number of reads before (blue) and after (red) removing duplicates from data to reduce the impact of a heterogenous PCR step prior to sequencing.

Supplementary Figure 3 | The range of quality values across all bases at each position in the FastQ file. The y-axis shows the quality scores. The higher the score, the better the base call. The background of the graph divides the y axis into very good quality calls (green), calls of reasonable quality (orange), and calls of poor quality (red). The elements of the plot are as follows: the yellow box represents the inter-quartile range (25–75%), the upper and lower whiskers represent the 10 and 90% points. The blue line represents the mean quality.

Supplementary Table 1 | 1. Table of relevant maize accession numbers with indexes and barcodes used, which allow to de-multiplexing NGS resultant sequences. 2. Link to the cloud with raw resultant sequencing data, which is available for everyone after logging to BaseSpace Cloud.

REFERENCES

Ali, F., and Yan, J. (2012). Disease resistance in maize and the role of molecular breeding in defending against global threat. *J. Integr. Plant Biol.* 54, 134–151. doi: 10.1111/j.1744-7909.2012.01105.x

Ariño, A., Herrera, M., Juan, T., Estopañan, G., Carramiñana, J. J., and Rota, C. (2009). Influence of agricultural practices on the contamination of maize by fumonisin mycotoxins. *J. Food Prot.* 72, 898–902. doi: 10.4315/0362-028X-72.4.898

Arpad, B., Rafai, P., Kovacs, G., and Halasz, A. (1997). A new method for evaluation of the resistance of maize hybrids for fusarial ear rot

– the Toxin –Mould-Index (TMI). *Period. Politech. Ser. Chem. Eng.* 41,3–10.

Balconi, C., Berardo, N., Locatelli, S., Lanzanova, C., Torri, A., and Redaelli, R. (2014). Evaluation of ear rot (*Fusarium verticillioides*) resistance and fumonisin accumulation in Italian maize inbred lines. *Phytopathol. Mediterr.* 53, 14–26. doi: 10.14601/Phytopathol_Mediterr/11776

Bennett, J. W., and Klich, M. (2003). Mycotoxins. *Clin. Microbiol. Rev.* 16, 497–516. doi: 10.1128/CMR.16.3.497-516.2003

Bolduan, C., Miedaner, T., Schipprack, W., Dhillon, B. S., and Melchinger, A. E. (2009). Genetic variation for resistance to ear rots and mycotoxins contamination in early European maize inbred lines. *Crop Sci. Soc. Am.* 49, 2019–2028. doi: 10.2135/cropsci2008.12.0701

Bush, B. J., Carson, M. L., Cubeta, M. A., Hagler, W. M., and Payne, G. A. (2004). Infection and fumonisin production by *Fusarium verticillioides* in developing maize kernels. *Phytopathology* 94, 88–93. doi: 10.1094/PHYTO.2004.94.1.88

Butrón, A., Reid, L. M., Santiago, R., Cao, A., and Malvar, R. A. (2015). Inheritance of maize resistance to *Gibberella* and *Fusarium* ear rots and kernel contamination with deoxynivalenol and fumonisins. *Plant Pathol.* 64, 1053–1060. doi: 10.1111/ppa.12351

Butrón, A., Santiago, R., Mansilla, P., Pintos-Varela, C., Ordás, A., and Malvar, R. A. (2006). Maize (*Zea mays* L.) genetic factors for preventing fumonisin contamination. *J. Agric. Food Chem.* 54, 6113–6117. doi: 10.1021/jf0611163

Campos-Bermudez, V. A., Fauguel, C. M., Tronconi, M. A., Casati, P., Presello, D. A., and Andreo, C. S. (2013). Transcriptional and metabolic changes associated to the infection by *Fusarium verticillioides* in maize inbreds with contrasting ear rot resistance. *PLoS ONE* 8:e61580. doi: 10.1371/journal.pone.0061580

Cao, A., Butrón, A., Ramos, A. J., Marín, S., Souto, C., and Santiago, R. (2014a). Assessing white maize resistance to fumonisin contamination. *Eur. J. Plant Pathol.* 138, 283–292. doi: 10.1007/s10658-013-0328-y

Cao, A., Santiago, R., Ramos, A. J., Souto, X. C., Aguín, O., Malvar, R. A., et al. (2014b). Critical environmental and genotypic factors for *Fusarium verticillioides* infection, fungal growth and fumonisin contamination in maize grown in northwestern Spain. *Int. J. Food Microbiol.* 177, 63–71. doi: 10.1016/j.ijfoodmicro.2014.02.004

Chen, J., Ding, J., Li, H., Li, Z., Sun, X., Li, J., et al. (2012). Detection and verification of quantitative trait loci for resistance to *Fusarium* ear rot in maize. *Mol. Breed.* 30, 1649–1656. doi: 10.1007/s11032-012-9748-1

Clements, M. J., Campbell, K. W., Maragos, C. M., Pilcher, C., Headrick, J. M., Pataky, J. K., et al. (2003a). Influence of cry1ab protein and hybrid genotype on fumonisin contamination and *Fusarium* ear rot of corn. *Crop Sci.* 43, 1283–1293. doi: 10.2135/cropsci2003.1283

Clements, M. J., Kleinschmidt, C. E., Pataky, J. K., and White, D. G. (2003b). Evaluation of inoculation techniques for *Fusarium* ear Rot and fumonisin contamination of corn. *Plant Dis.* 147–153. doi: 10.1094/PDIS.2003.87.2.147

Czembor, E., and Frasinski, S. (2018). Polish maize elite inbred lines as a source of resistance for ear rot (*Fusarium* spp.) and common smut (*Ustilago maydis*). *J. Plant Prot.* 58, 22–27. doi: 10.14199/ppp-2018-002

Czembor, E., and Matusiak, M. (2014). Kinetics of red ear rot of maize caused by *Fusarium graminearum* and deoxynivalenol accumulation in the grain [Dynamika rozwoju fuzariozy kolb kukurydzy powodowanej przez *Fusarium graminearum* oraz akumulacji deoksyniwalenolu w ziarnie. *Biul. IHAR.* 274, 27–39.

Czembor, E., Matusiak, M., and Ochodzki, P. (2013b). Resistance of maize hybrids to ear rot caused by *Fusarium graminearum* and *F. verticillioides* in Poland in years 2008–2009 [Odporność mieszanców kukurydzy na fuzarioze kolb powodowana przez *Fusarium graminearum* i *F. verticillioides* w Polsce w latach 2008-2009]. *Biul. IHAR.* 270, 55–74.

Czembor, E., Matusiak, M., and Warzecha, R. (2013a). Looking for sources of resistance to ear rot and stalk rot on the basis of the pedigree selection [Poszukiwanie zródeł odporności kukurydzy na fuzarioze kolb i zgorzel podstawy łodyg metoda rodowodowa]. *Biul. IHAR.* 269, 123–140.

Czembor, E., Stepie,n, Ł., and Waśkiewicz, A. (2014). *Fusarium temperatum* as a new species causing ear rot in Poland. *Plant Dis.* 98:1001. doi: 10.1094/PDIS-11-13-1184-PDN

Czembor, E., Stepien, Ł., and Waśkiewicz, A. (2015). Effect of environmental factors on *Fusarium* species and associated mycotoxins in maize grain grown in Poland. *PLoS ONE* 10:e0133644. doi: 10.1371/journal.pone.0133644

de Galarreta, J. I. R., Butrón, A., Ortiz-Barredo, A., Malvar, R. A., Ordás, A., Landa, A., et al. (2015). Mycotoxins in maize grains grown in organic and conventional agriculture. *Food Control* 52, 98–102. doi: 10.1016/j.foodcont.2014.12.016

De La Campa, R., Hooker, D. C., Miller, J. D., Schaafsma, A. W., and Hammond, B. G. (2005). Modeling effects of environment, insect damage, and Bt genotypes on fumonisin accumulation in maize in Argentina and the Philippines. *Mycopathologia* 159, 539–552. doi: 10.1007/s11046-005-2150-3

Desjardins, A. E., Munkvold, G. P., Plattner, R. D., and Proctor, R. H. (2002). *FUM1* - a gene required for fumonisin biosynthesis but not for maize ear rot and ear infection by *Gibberella moniliformis* in field tests. *Mol. Plant Microbe Interact.* 15, 1157–1164. doi: 10.1094/MPMI.2002.15.11.1157

Desjardins, A. E., and Plattner, R. D. (2000). Fumonisin B_1-sonproducing strains of *Fusarium verticillioides* cause maize (*Zea mays*) ear infection and ear rot. *J. Agric. Food Chem.* 48, 5773–5780. doi: 10.1021/jf000619k

Ding, J. Q., Wang, X. M., Chander, S., Yan, J. B., and Li, J. S. (2008). QTL mapping of resistance to *Fusarium* ear rot using a RIL population in maize. *Mol. Breed.* 22, 395–403. doi: 10.1007/s11032-008-9184-4

Dorn, B., Forrer, H. R., Schurch, S., and Vogelgsang, S. (2009). *Fusarium* species complex on maize in Switzerland: occurrence, prevalence, impact and mycotoxins in commercial hybrids under natural infection. *Eur. J. Plant Pathol.* 125, 51–61. doi: 10.1007/s10658-009-9457-8

Drepper, W. J., and Renfro, B. L. (1990). Comparison of methods for inoculation of ears and stalks of maize with *Fusarium moniliforme*. *Plant Dis.* 74, 952–956. doi: 10.1094/PD-74-0952

EC (2006). *Commission Recommendation of 17 August 2006 on the Presence of Deoxynivalenol, Zearalenone, Ochratoxin A, T-2 and HT-2 and Fumonisins in Products Intended for Animal Feeding.*

EC (2007). *Commission Regulation (EC) No 1126/2007 of 28 September 2007 Amending Regulation (EC) No 1881/2006 Setting Maximum Levels for Certain Contaminants in Foodstuffs As Regards Fusarium toxins in Maize and Maize Products.*

Eller, M. S., Payne, G. A., and Holland, J. B. (2010). Selection for reduced *Fusarium* ear rot and fumonisin content in advanced backcross maize lines and their topcross hybrids. *Crop Sci.* 50, 2249–2260. doi: 10.2135/cropsci2009.11.0683

Elshire, R. J., Glaubitz, J. C., Sun, Q., Poland, J. A., Kawamoto, K., Buckler, E. S., et al. (2011). A robust, simple genotyping-by-sequencing (GBS) approach for high diversity species. *PLoS ONE* 6:e19379. doi: 10.1371/journal.pone.0019379

Gallo, A., Giuberti, G., Frisvad, J. C., Bertuzzi, T., and Nielsen, K. F. (2015). Review on mycotoxin issues in ruminants: occurrence in forages, effects of mycotoxin ingestion on health status and animal performance and practical strategies to counteract their negative effects. *Toxins (Basel).* 7, 3057–3111. doi: 10.3390/toxins7083057

Jardine, D. J., and Leslie, J. F. (1992). Aggressiveness of *Gibberella fujikuroi* (*Fusarium moniliforme*) isolates to grain-sorghum under greenhouse conditions. *Plant Dis.* 76, 897–900. doi: 10.1094/PD-76-0897

Kearse, M., Moir, R., Wilson, A., Stones-Havas, S., Cheung, M., Sturrock, S., et al. (2012). Geneious basic: an integrated and extendable desktop software platform for the organization and analysis of sequence data. *Bioinformatics* 28, 1647–1649. doi: 10.1093/bioinformatics/bts199

Lanubile, A., Bernardi, J., Battilani, P., Logrieco, A., and Marocco, A. (2012). Resistant and susceptible maize genotypes activate different transcriptional responses against *Fusarium verticillioides*. *Physiol. Mol. Plant Pathol.* 77, 52–59. doi: 10.1016/j.pmpp.2011.12.002

Lanubile, A., Ferrarini, A., Maschietto, V., Delledonne, M., Marocco, A., and Bellin, D. (2014). Functional genomic analysis of constitutive and inducible defense responses to *Fusarium verticillioides* infection in maize genotypes with contrasting ear rot resistance. *BMC Genomics* 15:710. doi: 10.1186/1471-2164-15-710

Lanubile, A., Maschietto, V., Borrelli, V., Stagnati, L., Logrieco, A. F., and Marocco, A. (2017). Molecular basis of resistance to *Fusarium* ear rot in maize. *Front. Plant Sci.* 8:1774. doi: 10.3389/fpls.2017.01774

Lanubile, A., Pasini, L., Lo Pinto, M., Battilani, P., Prandini, A., and Marocco, A. (2011). Evaluation of broad spectrum sources of resistance to *Fusarium verticillioides* and advanced maize breeding lines. *World Mycotoxin J.* 4, 43–51. doi: 10.3920/WMJ2010.1206

Löffler, M., Kessel, B., Ouzunova, M., and Miedaner, T. (2010). Population parameters for resistance to *Fusarium graminearum* and *Fusarium verticillioides* ear rot among large sets of early, mid-late and late maturing European maize (*Zea mays* L.) inbred lines. *Theor. Appl. Genet.* 120, 1053–1062. doi: 10.1007/s00122-009-1233-9

Logrieco, A., Mule, G., Moretti, A., and Bottalico, A. (2002). Toxigenic *Fusarium* species and mycotoxins associated with maize ear rot in Europe. *Eur. J. Plant Pathol.* 108, 597–609. doi: 10.1023/A:1020679029993

Maiorano, A., Reyneri, A., Magni, A., and Ramponi, C. A. (2009a). Decision tool for evaluating the agronomic risk of exposure to fumonisins of different maize crop management systems in Italy. *Agric. Syst.* 102, 17–23. doi: 10.1016/j.agsy.2009.06.003

Maiorano, A., Reyneri, A., Sacco, D., Magni, A., and Ramponi, C. (2009b). A dynamic risk assessment model (FUMAgrain) of fumonisin synthesis by *Fusarium verticillioides* in maize grain in Italy. *Crop Prot.* 28, 243–256. doi: 10.1016/j.cropro.2008.10.012

Maschietto, V., Colombi, C., Pirona, R., Pea, G., Strozzi, F., Marocco, A., et al. (2017). QTL mapping and candidate genes for resistance to *Fusarium* ear rot and fumonisin contamination in maize. *BMC Plant Biol.* 17, 1–21. doi: 10.1186/s12870-017-0970-1

Mesterhazy, A., Lemmens, M., and Reid, L. M. (2012). Breeding for resistance to ear rots caused by *Fusarium* spp. in maize - a review. *Plant Breed.* 131, 1–19. doi: 10.1111/j.1439-0523.2011.01936.x

Mideros, S. X., Warburton, M. L., Jamann, T. M., Windham, G. L., Williams, W. P., and Nelson, R. J. (2014). Quantitative trait loci influencing mycotoxin contamination of maize: analysis by linkage mapping, characterization of near-isogenic lines, and meta-analysis. *Crop Sci.* 54, 127–142. doi: 10.2135/cropsci2013.04.0249

Miedaner, T., Bolduan, C., and Melchinger, A. E. (2010). Aggressiveness and mycotoxin production of eight isolates each of *Fusarium graminearum* and *Fusarium verticillioides* for ear rot on susceptible and resistant early maize inbred lines. *Eur. J. Plant Pathol.* 127, 113–123. doi: 10.1007/s10658-009-9576-2

Miedaner, T., Gwiazdowska, D., and Waśkiewicz, A. (2017). Editorial: management of *Fusarium* species and their mycotoxins in cereal food and feed. *Front. Microbiol.* 8:1543. doi: 10.3389/fmicb.2017.01543

Munkvold, G. P. (2003a). Cultural and genetic approaches to managing mycotoxins in maize. *Ann. Rev. Phytopathol.* 41, 99–116. doi: 10.1146/annurev.phyto.41.052002.095510

Munkvold, G. P. (2003b). Epidemiology of *Fusarium* diseases and their mycotoxins in maize ears. *Eur. J. Plant Pathol.* 109, 705–713. doi: 10.1023/A:1026078324268

Munkvold, G. P., and Carlton, W. M. (1997). Influence of inoculation method on systemic *Fusarium moniliforme* infection of maize plants grown from infected seeds. *Plant Dis.* 81, 211–216.

Munkvold, G. P., McGee, D. C., and Carlton, W. M. (1997). Importance of different pathways for maize kernel infection by *Fusarium moniliforme*. *Phytopathology* 87, 209–217.

Oldenburg,. E., and Ellner, F. (2005). *Fusarium* mycotoxins in forage maize - detection and evaluation. *Mycotoxin Res.* 21, 105–107. doi: 10.1007/BF02954430

Pérez-Brito, D., Jeffers, D., González-de-León, D., Khairallah, M., Cortés-Cruz, M., Velázquez-Cardelas, G., et al. (2001). QTL mapping of *Fusarium moniliforme* ear rot resistance in highland maize, Mexico. *Agrociencia* 35, 181–196.

Peterson, B. K., Weber, J. N., Kay, E. H., Fisher, H. S., and Hoekstra, H. E. (2012). Double Digest RADseq: an inexpensive method for *de novo* SNP discovery and genotyping in model and non-model species. *PLoS ONE.* 7:e37135. doi: 10.1371/journal.pone.0037135

Presello, D. A., Iglesias, J., Botta, G., and Eyhérabide, G. H. (2007). Severity of *Fusarium* ear rot and concentration of fumonisin in grain of Argentinian maize hybrids. *Crop Prot.* 26, 852–855. doi: 10.1016/j.cropro.2006.08.004

Presello, D. A., Pereyra, A. O., Iglesias, J., Fauguel, C. M., Sampietro, D. A., and Eyherabide, G. H. (2011). Responses to selection of S_5 inbreds for broad-based resistance to ear rots and grain mycotoxin contamination caused by *Fusarium* spp. in maize. *Euphytica* 178, 23–29. doi: 10.1007/s10681-010-0255-3

Presello, D. A., Reid, L. M., Butler, G., and Mather, D. E. (2005). Pedigree selection for *Gibberella* ear rot resistance in maize populations. *Euphytica* 143, 1–8. doi: 10.1007/s10681-005-6149-0

Presello, D. A., Reid, L. M., and Mather, D. E. (2004). Resistance of Argentine maize germplasm to *Gibberella* and *Fusarium* ear rots. *Maydica* 49, 73–81.

Reid, L. M., Woldemariam, T., Zhu, X., Stewart, D. W., and Schaafsma, A. W. (2002). Effect of inoculation time and point of entry on disease severity in *Fusarium graminearum*, *Fusarium verticillioides*, or *Fusarium subglutinans* inoculated maize ears. *Can. J. Plant Pathol.* 24, 162–167. doi: 10.1080/07060660309506991

Robertson, L. A., Kleinschmidt, C. E., White, D. G., Payne, G. A., Maragos, C. M., and Holland, J. B. (2006). Heritabilities and correlations of *Fusarium* ear rot resistance and fumonisin contamination resistance in two maize populations. *Crop Sci.* 46, 353–361. doi: 10.2135/cropsci2005.0139

Robertson-Hoyt, L. A., Jines, M. P., Balint-Kurti, P. J., Kleinschmidt, C. E., White, D. G., Payne, G. A., et al. (2006). QTL Mapping for *Fusarium* ear rot and fumonisin contamination resistance in two maize populations. *Crop Sci.* 46, 1734–1743. doi: 10.2135/cropsci2005.12-0450

Saitou, N., and Nei, M. (1987). The neighbor-joining method: a new method for reconstructing phylogenetic trees. *Mol. Biol. Evol.* 4, 406–425

Santiago, R., Cao, A., and Butrón, A. (2015). Genetic factors involved in fumonisin accumulation in maize kernels and their implications in maize agronomic management and breeding. *Toxins (Basel).* 7, 3267–3296. doi: 10.3390/toxins7083267

Santiago, R., Cao, A., Malvar, R. A., and Butron, A. (2013). Is it possible to control fumonisin contamination in maize kernels by using genotypes resistant to the mediterranean corn borer? *J. Econ. Entomol.* 106, 2241–2246. doi: 10.1603/EC13084

Schaafsma, A. W., Miller, J. D., Savard, M., and Ewing, R. J. (1993). Ear rot development and mycotoxin production in corn in relation to inoculation method, corn hybrid, and species of *Fusarium*. *Can. J. Plant Pathol.* 15, 185–192. doi: 10.1080/07060669309500821

Small, I. M., Flett, B. C., Marasas, W. F. O., McLeod, A., Stander, M. A., and Viljoen, A. (2012). Resistance in maize inbred lines to *Fusarium verticillioides* and fumonisin accumulation in South Africa. *Plant Dis.* 96, 881–888. doi: 10.1094/PDIS-08-11-0695

Smith, J. S. C., Duvick, D. N., Smith, O. S., Cooper, M., and Feng, L. (2004). Changes in pedigree backgrounds of pioneer brand maize hybrids widely grown from 1930 to 1999. *Crop Sci.* 44, 1935–1946. doi: 10.2135/cropsci2004.1935

Smith, S. (2007). Pedigree background changes in U.S. hybrid maize between 1980 and 2004. *Crop Sci. Soc. Am.* 47, 1914–1926. doi: 10.2135/cropsci2006.12.0763

Stoycho, D. S. (2015). Foodborne mycotoxicoses, risk assessment and underestimated hazard of masked mycotoxins and joint mycotoxin effects or interaction. *Environ. Toxicol. Pharmacol.* 39, 794–809. doi: 10.1016/j.etap.2015.01.022

Tamura, K., and Nei, M. (1993). Estimation of the number of nucleotide substitutions in the control region of mitochondrial DNA in humans and chimpanzees. *Mol. Biol. Evol.*10, 512–526.

Toldi, E., Bartok, T., Varga, M., Szekeres, A., Toth, B., and Mesterhazy, A. (2008). The role of breeding in reducing mycotoxin contamination in maize. *Cereal Res. Commun.* 36, 83–191.

Vasileiadis, V. P., Otto, S., Sattin, M., Palinkás, Z., Veres, A., Bán, R., et al. (2011). Crop protection in European maize-based cropping systems: current practices and recommendations for innovative integrated pest management. *Agric. Syst.* 104, 533–540. doi: 10.1016/j.agsy.2011.04.002

Venturini, G., Assante, G., and Vercesi, A. (2011). *Fusarium verticillioides* contamination patterns in northern Italian maize during the growing season. *Phytopathol. Mediterr.* 50, 110–120. doi: 10.14601/Phytopathol_Mediterr-8680

Voss, K. A., Gelineau-van Waes, J. B., and Riley, R. T. (2006). Fumonisins: current research trends in developmental toxicology. *Mycotoxin Res.* 22, 61–69. doi: 10.1007/BF02954559

Waśkiewicz, A., Irzykowska, L., Bocianowski, J., Karolewski, Z., Weber, Z., and Golinski, P. (2013a). Fusariotoxins in asparagus – their biosynthesis and migration. *Food Add. Contam.* 30, 1332–1338. doi: 10.1080/19440049.2013.796095

Waśkiewicz, A., Stepien, Ł., Wilman, K., and Kachlicki, P. (2013b). Diversity of pea-associated *F. proliferatum* and *F. verticillioides* populations revealed by *FUM1* sequence analysis and fumonisin biosynthesis. *Toxins* 5, 488–503. doi: 10.3390/toxins5030488

Wisser, R. J., Balint-Kurti, P. J., and Nelson, R. J. (2006). The genetic architecture of disease resistance in maize: a synthesis of published studies. *Phytopathology* 96, 120–129. doi: 10.1094/PHYTO-96-0120

Xiang, K., Zhang, Z. M., Reid, L. M., Zhu, X. Y., Yuan, G. S., and Pan, G. T. (2010). A meta-analysis of QTL associated with ear rot resistance in maize. *Maydica* 55, 281–290.

Yang, G. Q., Chen, Y.-M., Wang, J.-P., Guo, C., Zhao, L., Wang, X.-Y., et al. (2016). Development of a universal and simplified ddRAD library preparation approach for SNP discovery and genotyping in angiosperm plants. *Plant Meth.* 12:39. doi: 10.1186/s13007-016-0139-1

Yuan, G., Zhang, Z., Xiang, K., Shen, Y., Du, J., Lin, H., et al. (2013). Different gene expressions of resistant and susceptible maize inbreds in response to *Fusarium verticillioides* infection. *Plant Mol. Biol. Rep*. 31, 925–935. doi: 10.1007/s11105-013-0567-2

Zijlstra, C., Lund, I., Justesen, A., Nicolaisen, M., Bianciotto, V., Posta, K., et al. (2011). Combining novel monitoring tools and precision application technologies for integrated high-tech crop protection in the future (a discussion document). *Pest Manag. Sci.* 67, 616–625. doi: 10.1002/ps.2134

Zila, C. T., Ogut, F., Romay, M. C., Gardner, C. A., Buckler, E. S., and Holland, J. B. (2014). Genome-wide association study of *Fusarium* ear rot disease in the U.S.A. maize inbred line collection. *BMC Plant Biol*. 14:372. doi: 10.1186/s12870-014-0372-6

Zila, C. T., Samayoa, L. F., Santiago, R., Butrón, A., and Holland, J. B. (2013). A genome-wide association study reveals genes associated with *Fusarium* ear rot resistance in a maize core diversity panel. *G3 Genes Genomes Genet*. 3, 2095–2104. doi: 10.1534/g3.113.007328

Conflict of Interest Statement: The authors declare that the research was conducted in the absence of any commercial or financial relationships that could be construed as a potential conflict of interest.

frontiers in Microbiology

ORIGINAL RESEARCH
published: 09 April 2019
doi: 10.3389/fmicb.2019.00685

Cytoprotective Co-chaperone BcBAG1 Is a Component for Fungal Development, Virulence, and Unfolded Protein Response (UPR) of *Botrytis cinerea*

Honghong Zhang[1,2,3], Yurong Li[2,3†], Martin B. Dickman[2,3] and Zonghua Wang[1,4]*

[1] *Fujian University Key Laboratory for Plant-Microbe Interaction, College of Plant Protection, Fujian Agriculture and Forestry University, Fuzhou, China,* [2] *Institute for Plant Genomics and Biotechnology, College of Agriculture and Life Sciences, Texas A&M University, College Station, TX, United States,* [3] *Department of Plant Pathology and Microbiology, College of Agriculture and Life Sciences, Texas A&M University, College Station, TX, United States,* [4] *Institute of Oceanography, Minjiang University, Fuzhou, China*

OPEN ACCESS

Edited by:
Marco Catoni, University of Birmingham, United Kingdom

Reviewed by:
Mehdi Kabbage, University of Wisconsin-Madison, United States
Chang Ho Kang, Gyeongsang National University, South Korea

***Correspondence:**
Zonghua Wang
wangzh@fafu.edu.cn

†Present address:
Yurong Li, Corteva Agriscience™, Johnston, IA, United States

Specialty section:
This article was submitted to Plant Microbe Interactions, a section of the journal Frontiers in Microbiology

Received: *07 December 2018*
Accepted: *19 March 2019*
Published: *09 April 2019*

Citation:
Zhang H, Li Y, Dickman MB and Wang Z (2019) Cytoprotective Co-chaperone BcBAG1 Is a Component for Fungal Development, Virulence, and Unfolded Protein Response (UPR) of Botrytis cinerea. Front. Microbiol. 10:685. doi: 10.3389/fmicb.2019.00685

The Bcl-2 associated athanogene (BAG) family is an evolutionarily conserved group of co-chaperones that confers stress protection against a variety of cellular insults extending from yeasts, plants to humans. Little is known, however, regarding the biological role of BAG proteins in phytopathogenic fungi. Here, we identified the unique BAG gene (*BcBAG1*) from the necrotrophic fungal pathogen, *Botrytis cinerea*. BcBAG1 is the homolog of *Arabidopsis thaliana* AtBAG4, and ectopic expression of *BcBAG1* in *atbag4* knock-out mutants restores salt tolerance. *BcBAG1* deletion mutants (Δ*Bcbag1*) exhibited decreased conidiation, enhanced melanin accumulation and lost the ability to develop sclerotia. Also, *BcBAG1* disruption blocked fungal conidial germination and successful penetration, leading to a reduced virulence in host plants. BcBAG1 contains BAG (BD) domain at C-terminus and ubiquitin-like (UBL) domain at N-terminus. Complementation assays indicated that BD can largely restored pathogenicity of Δ*Bcbag1*. Abiotic stress assays showed Δ*Bcbag1* was more sensitive than the wild-type strain to NaCl, calcofluor white, SDS, tunicamycin, dithiothreitol (DTT), heat and cold stress, suggesting BcBAG1 plays a cytoprotective role during salt stress, cell wall stress, and ER stress. BcBAG1 negatively regulated the expression of *BcBIP1*, *BcIRE1* and the splicing of *BcHAC1* mRNA, which are core regulators of unfolded protein response (UPR) during ER stress. Moreover, BcBAG1 interacted with HSP70-type chaperones, BcBIP1 and BcSKS2. In summary, this work demonstrates that BcBAG1 is pleiotropic and not only essential for fungal development, hyphal melanization, and virulence, but also required for response to multiple abiotic stresses and UPR pathway of *B. cinerea*.

Keywords: BAG protein, co-chaperone, *Botrytis cinerea*, pathogenicity/virulence, unfolded protein response

INTRODUCTION

Co-chaperones are proteins that assist chaperones in protein folding, oligomeric assembly, and protein transportation and degradation (Hartl, 1996). The Bcl-2-associated athanogene (BAG) family is a group of broadly conserved co-chaperones of 70-kilodalton heat shock protein (HSP70) (Bracher and Verghese, 2015). In mammals, the BAG family was initially identified by screening mouse cDNA library for Bcl-2 interaction proteins (Takayama et al., 1995). Using the ATPase domain of HSC70/HSP70 as molecular bait in yeast two-hybrid screening, additional BAG family members were identified from human, *Caenorhabditis elegans* and the fission yeast *Schizosaccharomyces pombe* (Takayama et al., 1999). The human BAGs contain six members, BAG1 to BAG6, and share a conserved BAG domain (BD) of approximately 45 amino acids, located near the C terminus (Takayama and Reed, 2001). As nucleotide exchange factors (NEFs) of HSP70, BAG proteins play a major role in both positively and negatively modulating HSP70 ATP activity via the BAG domain (Gassler et al., 2001). Moreover, BAGs act as scaffolds between HSP70 and target transcription factors or proteins, thus affecting diverse physiological events (Townsend et al., 2003; Kabbage and Dickman, 2008).

The identification and preliminary characterization of plant BAG proteins is still underway. Using a combination of bioinformatics and structural algorithms, seven BAGs have been identified from *Arabidopsis thaliana* (AtBAG1–AtBAG7) (Doukhanina et al., 2006), several of which have been selected for functional characterization. The structural and biochemical data of AtBAGs demonstrate that the AtBAGs function as NEFs for HSP70/HSC70 and the regulation mechanism of HSP70/HSC7 is conserved in plants (Fang et al., 2013). Our previous work has uncovered that AtBAG4, 6, and 7 exhibit different cytoprotective specificities. Briefly, AtBAG4 appears to protect plants from various abiotic stress stimuli, e.g., salt and drought (Doukhanina et al., 2006). AtBAG6 is activated via proteolytic cleavage by a specific plant aspartyl protease that is required for autophagic cell death *in planta* and subsequent resistance to the necrotrophic fungus *Botrytis cinerea* (Kabbage et al., 2016; Li and Dickman, 2016; Li et al., 2016). Consistently, overexpression of AtBAG6 induced programmed cell death (PCD) in both yeast and plants (Kang et al., 2006). The ER-localized AtBAG7 is an essential component of the unfolded protein response (UPR) and directly interacts with UPR regulator AtBIP2 (Williams et al., 2010). Under heat stress, AtBAG7 is also proteolytically processed in the ER lumen and translocate from the ER to the nucleus, where it interacts with the transcriptional factor WRKY29 for heat tolerance (Li et al., 2017). A number of BAGs have also been reported in other plant species. For example, OsBAG4 from rice interacts with an E3 ubiquitin ligase EBR1 and regulates PCD, which controls plant immunity and broad-spectrum disease resistance (You et al., 2016). Taken together, plant BAGs are multifunctional and modulate numerous physiological and biological processes.

Although the functions of human and plants BAG family members are extensively studied, there is limited knowledge on the roles of the BAGs in fungi. Previous studies showed that SNL1, a mammalian homolog of BAG1 in *Saccharomyces cerevisiae*, is functionally linked to the nuclear pore complex and plays a role in promoting both protein biogenesis and translation by recruiting ribosomes and HSP70 to the ER membrane (Ho et al., 1998; Verghese and Morano, 2012). Two other BAG1 homologs from *Schizosaccharomyces pombe*, *BAG101* and *BAG102*, are co-factors of 26S proteasomes, and play as HSP70 chaperones (Kriegenburg et al., 2014). Overexpression of *BAG101* and *BAG102* inhibit cell growth by triggering HSP70 to release and activate HSF1 (heat shock factor 1) (Poulsen et al., 2017). To date, the only example in filamentous fungi is BAGA from *Aspergillus nidulans*, which impacts fungal sexual development and modulates secondary metabolism (Jain et al., 2018).

The endoplasmic reticulum (ER) is the central intracellular organelle for protein translocation, protein folding, and protein post-translational modifications, allowing further transport of proteins to the Golgi apparatus and ultimately to vesicles for secretion or display on the plasma surface. Perturbations in ER function, named "ER-stress," unfolded or misfolded proteins accumulate within the ER and disrupt ER homeostasis to activate an intracellular signaling pathway, known as the UPR eventually culminating in cell death (Malhotra and Kaufman, 2007). As a conserved survival pathway to counteract the lethal effects caused by ER stress, UPR can mitigate accumulation of unfolded proteins and restore ER homeostasis by reducing protein translation and while increasing and misfolded proteins degradation aided by molecular chaperones (e.g., binding immunoglobulin proteins, BiPs) (Sitia and Braakman, 2003; Ron and Walter, 2007). BiPs work as HSP70 chaperones and carry aberrant proteins from the ER to the cytoplasm for degradation by the proteasome (Gething, 1999). The IRE1-HAC1/XBP-1 pathway (HAC1 mRNA in yeast and XBP1 mRNA in metazoans) is a major branch of UPR that is remarkably conserved from yeast to human (Back et al., 2005). UPR is initiated by the activation of the ER stress sensor IRE1, which transmits the signal by removing a non-conventional intron from a transcription factor HAC1/XBP-1 mRNA to produce potent transcriptional activator of UPR targets (Ron and Walter, 2007). Comparing to the extensive studies of UPR in human and plant systems, UPR has only been delineated in small number of fungal pathogens, including *Aspergillus fumigatus* (Feng et al., 2011), *Alternaria brassicicola* (Joubert et al., 2011), *Ustilago maydis* (Heimel et al., 2013; Lo Presti et al., 2016), and all of which demonstrate that UPR regulation is correlated with fungal pathogenicity.

In this study, we identified a unique *BAG* gene in the necrotrophic fungal pathogen *Botrytis cinerea*, the causal agent of gray mold diseases to over 1,400 species of cultivated plants worldwide (Elad, 2016). Target gene replacement of *BcBAG1* resulted to defect in vegetative growth, conidiation, sclerotial formation, penetration and attenuated virulence in *B. cinerea*, Δ*Bcbag1* mutants were more sensitive to various stress conditions indicating that BcBAG1 regulates stress tolerance in *B. cinerea*. In particular, *BcBAG1* deletion mutants significantly increased susceptibility to diverse ER stress-inducer including heat, cold, tunicamycin (Tm), and dithiothreitol (DTT). We demonstrated that BcBAG1 binds to the ER chaperone BcBIP1 and negatively regulate UPR components, including

the expression of *BcBIP1*, *BcIRE1* and the splicing of *BcHAC1* mRNA, suggesting BcBAG1 is necessary for the maintenance of the UPR in *B. cinerea*. Collectively, we present the evidence of identification and functional characterization for BcBAG1 a member of BAG family in *B. cinerea*, which is vital for fungal virulence on host plants and is required for ER stress response with regards to maintenance of UPR.

MATERIALS AND METHODS

Strains and Culture Conditions

BcBAG1 deletion mutant, Δ*Bcbag1*, was generated from the *B. cinerea* WT strain B05.10 (Quidde et al., 1999). All strains (**Supplementary Table S1**) were maintained on potato dextrose agar (PDA) medium at 22°C. Mycelia used for protoplast preparation, genomic DNA and total RNA extraction were grown in YEPD (1% peptone, 0.3% yeast extract, 2% glucose, pH 6.7) at 150 rpm, 22°C for 36 h. *B. cinerea* protoplast was recovered on SH medium (20% sucrose, 0.5 mM hepes, 1 mM $NH_4H_2PO_4$, pH 7.0) at 22°C for 12–16 h. The selectable marker, 100 μg/ml hygromycin B (VWR) or 100 μg/ml nourseothricin sulfate (Research Products International) was supplemented to PDA containing 1% agar.

Bioinformatic Analysis

Preliminary BAG protein search and DNA sequence downloading were conducted in *B. cinerea* B05.10 genome database[1]. The phylogenetic tree was generated through MEGA v7.0 based on the neighbor-joining method (Kumar et al., 2016). Domain is predicted by Pfam[2] and InterPro programs[3]. The multiple alignment of BAG domain sequence were constructed using Clustal X (Larkin et al., 2007).

BcBAG1 Gene Deletion and Complementation

Primers used in this study are listed in **Supplementary Table S2**. The replacement constructs for *BcBAG1* were generated through the split-marker approach as described before (Goswami, 2012). Briefly, the 800-bp upstream and 855-bp downstream fragments of *BcBAG1* were amplified with primer pairs AF/AR and BF/BR (**Supplementary Table S2**), respectively. The resulting amplicons ligated with the hygromycin phosphotransferase (*hph*) fragments by using Splicing Overlap Extension (SOE)-PCR. The resulting PCR products (20 μg) were transformed into protoplasts of *B. cinerea*. Protoplast preparation and PEG-mediated transformation of *B. cinerea* were performed as the established protocol (Gronover et al., 2001). After transformation, hygromycin-resistant transformants were picked individually and PCR analyses with designated primer pairs OF/OR, UF/UR, and AF/BR were performed to identify transformants that carried the insertion of *hph* at the *BcBAG1* locus. Then all positive transformants were confirmed by subsequent RT-PCR and Southern blotting.

The full length of *BcBAG1* was amplified from B05.10 genomic DNA, then ligated into pNAH-OGG with *NcoI* to create *BcBAG1-GFP*. GFP-fusion constructs were transformed into B05.10 for subcellular localization analysis. For complementation, the CDS of *BcBAG1* with native promoter sequence were amplified with relative primer pairs (CF/CR) and cloned into pNAH-OMG harboring nourseothricin acetyltransferase gene (*NAT1*) with *SpeI*/*NcoI* to make *BcBAG1-Com*, conferring resistance to antibiotics nourseothricin sulfate. Similar method was used to create the truncated $BcBAG1A^{1-141}$ and $BcBAG1B^{142-298}$ constructs. These constructs were transformed into Δ*Bcbag1* mutants. Transformants with resistance to both nourseothricin and hygromycin were selected and confirmed by PCR and RT-PCR.

Southern Blotting and Real-Time PCR

Fungal genomic DNA was extracted as described (Raeder and Broda, 1985). For Southern blotting, the genomic DNAs were digested with *PvuI* (NEB) for 24 h at 37°C. Probe labeling, hybridization and detection were performed in accordance with the manufacturer's instructions for the Digoxigenin High Prime DNA Labeling and Detection Starter Kit I (Roche Applied Science).

Total RNA was isolated using Eastep™ Total RNA extraction Kit, following the manufacturer recommendation (Corp). The first-strand cDNA was synthesized with the M-MLV (Moloney Murine Leukemia Virus) reverse transcriptase (Life Technologies). Quantitative RT-PCR (qRT-PCR) was performed with SYBR Green PCR master mix (Applied Biosystems). The fungal actin gene was used as an internal reference. The relative expression levels were calculated by the $2^{-\Delta\Delta Ct}$ method (Livak and Schmittgen, 2001).

Mycelial Growth, Conidiation, and Sclerotial Formation Tests

For vegetative growth assays, 5 mm diameter mycelial plugs were cultured on fresh PDA in the dark at 22°C. Radial growth was measured by colony diameters after 3 days. Determination of the sensitivity of Δ*Bcbag1* to environmental stresses were performed on modified PDA plates with: 1 M NaCl, 1.2 M D-sorbitol, 2 μg/ml Tm, 2.5 mM DTT, 20 mM H_2O_2, 0.5 mM tert-butyl hydroperoxide (TBHP), 15 μM bortezomib (Bort), 200 μM MG132, 600 μg/ml calcofluor white (CFW), 0.02% SDS, 1 μg/ml iprodione (Ipro), 0.1 μg/ml fludioxonil (Flud). The percentage of mycelial radial growth inhibition (RGI) was calculated using the formula RGI% = $[(C - N)/C * 100]$, where C is colony diameter of the control, and N is colony diameter of the experimental treatment.

For conidiation assays, conidia of WT and mutants were collected from a 10-day-old PDA plate with 5 ml sterile water and spores were counted microscopically with a hemocytometer. For sclerotial formation, 5 mm diameter mycelial plugs were inoculated to PDA and incubated in the dark at 22°C, the number of mature (melanized) sclerotia were counted after 4 weeks.

[1]http://fungi.ensembl.org/Botrytis_cinerea/Info/Index

[2]https://pfam.xfam.org/

[3]https://www.ebi.ac.uk/interpro/

Conidial Germination and Fungal Penetration Assays

Conidial germination was conducted as described by Doehlemann et al. (2006). Briefly, conidial suspensions were adjusted to 1.0–1.5 × 10^5 spores/ml in 10 mM KH_2PO_4 and 10 mM glucose solution and placed in the center of a glass slide. Incubation was kept in a moist chamber at 22°C for 12 h, 24 h, and 48 h. For the onion infection assay, 20 μl droplets (5.0 × 10^4 spores/ml) were deposited on the hydrophobic epidermis layers of onion and incubated for 48 h in the dark and moist chamber at 22°C (Viefhues et al., 2014).

Pathogenicity Assay

Three-day-old mycelial plugs with 5 mm diameter or 10-day-old conidial suspensions (1.0–1.5 × 10^5 spores/ml) were inoculated on 4-week-old detached tomato leaves and grape. Inoculated plant materials were incubated in 16 h daylight humid chamber at 22°C. Results were recorded after 4 days and 7 days. The experiment was repeated at least three times.

Yeast Two-Hybrid (Y2H) Assay

The Y2H assay was conducted according to the manufacturer's standard instructions (Clontech). The cDNA of *BcBAG1* was cloned into pGBKT7 as the bait vector and the cDNAs of HSP70-type chaperones were cloned into pGADT7 as the prey constructs, respectively. The pGBKT7-*BcBAG1* and each prey vector were co-transformed into the AH109 yeast strain to evaluate interactions. The positive and negative controls were from the Kit (Clontech).

Arabidopsis Complementation Assays

Arabidopsis thaliana Col-0 and *atbag4* T-DNA knock out mutants were obtained from *Arabidopsis* Stock Center[4]. *Atbag4* homozygous mutants (SALK_027577C) were confirmed by PCR. The *BcBAG1* full-length cDNA was cloned into pCB302ES containing the 35S promoter and the HA-epitope tag (Hwang and Sheen, 2002). This construct was transferred into the *atbag4* knockout mutants by the floral dipping method (Zhang et al., 2006).

For salt stress assays, seeds were surface sterilized in 70% ethanol for 10 min and in 5% bleach solution for 5 min, and germinated on 1/2 Murashige and Skoog (MS) medium (Invitrogen) at 23°C for 5 days. The seedlings were transferred to fresh 1/2 MS medium containing 100 mM NaCl and grown at 23°C for 2 weeks to 5 weeks.

RESULTS

Identification and Characterization of *BcBAG1*

To identify BAG proteins in *B. cinerea*, we searched *B. cinerea* B05.10 genome database with "BAG" as a query, and obtained one hit (Bcin10g01250.1/BC1G_05107). Additionally, based on Pfam and SMART programs, we search for all gene with BAG domain (BD domain) in genome database. Results indicated that there is only one gene with a single copy (Bcin10g01250.1/BC1G_05107) containing BAG domain, designated BcBAG1 hereafter. Phylogenetic analysis revealed that BcBAG1 shares low similarity with BAGs in yeast, plants and animals while it is closely related to BAG homologs from other filamentous fungi, e.g., *Sclerotinia sclerotiorum* (86.53%), *Magnaporthe oryzae* (57.04%), *Fusarium oxysporum* (52.01%), and *Aspergillus nidulans* (45.30%) (**Supplementary Figure S1A** and **Supplementary Table S3**). BcBAG1 contains a ubiquitin-like domain (UBL) at the N-terminus and a BAG domain at the C-terminus, encoding a 35 kD protein with 298 amino acids (**Supplementary Figure S1B**). The alignment also showed that most of the key interaction residues for BAG-HSC70/HSP70 binding are conserved in BAG proteins across filamentous fungi, yeast, Arabidopsis, and human (**Supplementary Figure S1C**).

To address the function of *BcBAG1*, we generated knockout mutants of *BcBAG1* (Δ*Bcbag1*), in the wild-type (WT) strain B05.10 (**Supplementary Figure S2A**). Two individual Δ*Bcbag1* lines, K3-7 and K8-6, were validated and selected for later use (**Supplementary Figures S2B,C**). We obtained three complemented strains by transforming the full-length *BcBAG1* under its native promoter into mutants and all strains equally restored the defects of Δ*Bcbag1*. Thus one complemented strain (*BcBAG1-Com*) was used in the following studies.

BcBAG1 Is Required for Vegetative Growth, Conidiation, and Sclerotial Formation

To evaluate the role of BcBAG1 during vegetative growth of *B. cinerea*, we examined hyphal growth on PDA. As shown in **Figures 1A,C**, the diameters of the Δ*Bcbag1* colonies were similar to WT strain B05.10 and the complementation strain *BcBAG1-Com*. However, Δ*Bcbag1* formed a thick hyphal layer on the surface of plates and the amount of aerial hypha drastically increased in comparison with B05.10 and *BcBAG1-Com* (**Figure 1B**). These results indicate that BcBAG1 influences on vegetative growth of *B. cinerea*.

Given that wind-dispersal of conidia determines the severity of gray mold disease in the field (Leroch et al., 2013), we assessed the role of BcBAG1 in conidial production. Conidiation of B05.10, Δ*Bcbag1* and *BcBAG1-Com* from 10-day-old PDA culture was measured using microscopic examination. Although Δ*Bcbag1* still produced aerial mycelia (**Figure 1B**), conidiogenesis of Δ*Bcbag1* is significantly reduced (**Figure 2A**), in detail, the mutants produced approximately 2.1 × 10^7 conidia/PDA plate, while the WT produced approximately 2.0 × 10^8 conidia/PDA plate ($P < 0.01$) (**Figure 2D**). However, the conidia exhibited normal morphology between Δ*Bcbag1* and WT (**Figure 2B**). These results indicate that BcBAG1 involved in conidial production but do not affect conidial morphology in *B. cinerea*.

Melanization of sclerotia is considered as a survival strategy of various fungi when encountering harsh environments like over-wintering (Williamson et al., 2007). Here, we examined sclerotial formation following *BcBAG1* deletion in *B. cinerea*.

[4]https://www.arabidopsis.org/

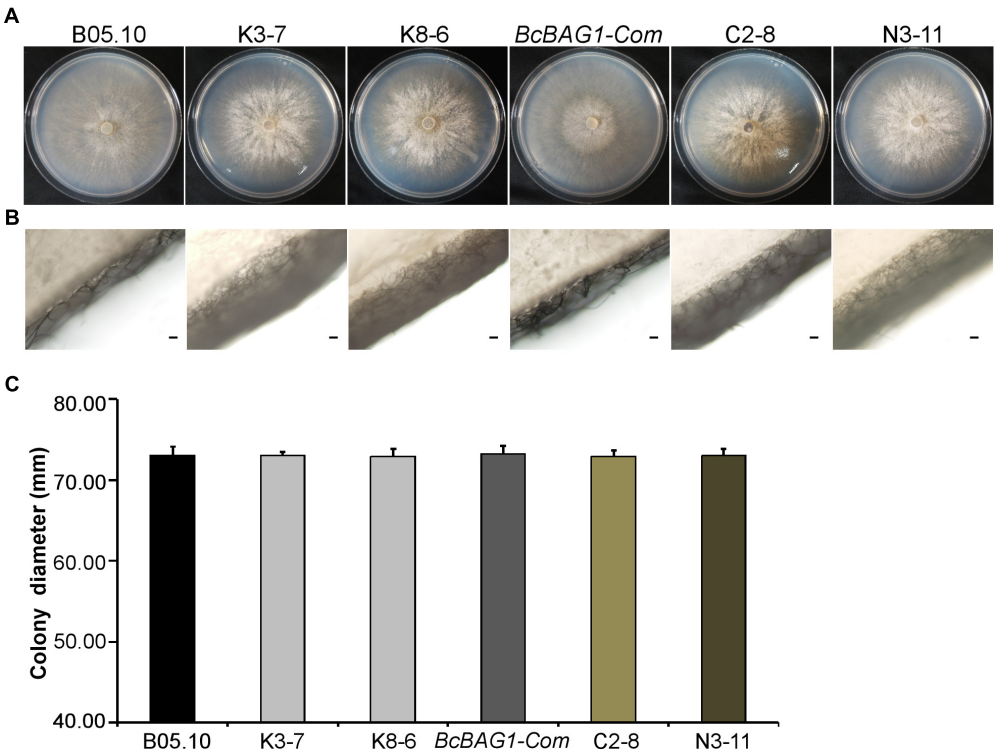

FIGURE 1 | BcBAG1 is required for normal mycelial growth. Colonies **(A)** and aerial hyphae **(B)** of all strains were photographed after 3 days growth on PDA medium at 22°C. Scale bar: 100 μm. **(C)** Statistical analysis of the colony diameters of above strains. B05.10: the wild-type strain; K-3 and K8-6: Δ*Bcbag1* mutant lines; *BcBAG1-Com* (full-length *BcBAG1*), C2-8 (C-terminus of *BcBAG1*) and N3-11 (N-terminus of *BcBAG1*): complemented strains. Error bars represent the standard deviations from three independent experiments.

After 4-week incubation on PDA in the dark, we observed that Δ*Bcbag1* mutants were unable to produce sclerotia, while B05.10 and *BcBAG1-Com* produced abundant sclerotia on PDA (**Figures 2C,E**), suggesting BcBAG1 is essential for sclerotial formation. Taken together, we reasoned that BcBAG1 plays a crucial role in regulating vegetative growth, conidiation and sclerotial formation in *B. cinerea*.

BcBAG1 Is Involved in the Regulation of Hyphal Melanization

After incubating on PDA for 7 days, we noticed that Δ*Bcbag1* displayed increased generation of black pigment when compared to WT (**Figure 3A**). It has been reported that the dark pigmentation in fungi is due to the accumulation of 1,8 dihydroxynaphthalene (DHN) melanin (Henson et al., 1999). Melanin is a dark durable pigment that protects fungi against diverse environmental stresses, such as UV irradiation and temperature extremes (Bell and Wheeler, 1986; Butler and Day, 1998). We therefore examined whether BcBAG1 participates in melanin biosynthesis. The Δ*Bcbag1*, *BcBAG1-Com* and the WT strains were cultured on PDA supplemented with 50 μg/ml tricyclazole, a fungicide that specifically inhibits DHN-melanin biosynthesis (Thompson et al., 2000). The result showed tricyclazole was able to repress the massive melanin synthesis in Δ*Bcbag1* mutants caused by *BcBAG1* deletion (**Figure 3A**). Additionally, we instituted RT-PCR assays to monitor the expression level of *THR1* (1,3,8-trihydroxynaphthalene reductase gene), a key component in melanin biosynthesis pathway (Perpetua et al., 1996). Corresponding results obtained from RT-PCR analysis revealed a significantly up-regulation (about 10-folds) in the expression pattern of *THR1* in Δ*Bcbag1* compared to WT (**Figure 3B**). These data indicate that BcBAG1 negatively regulates melanin biosynthesis pathway to suppress melanin production in *B. cinerea*.

BcBAG1 Is Required for Virulence of *B. cinerea*

To determine the role of BcBAG1 in pathogenicity and virulence of *B. cinerea*, we conducted infection assays by inoculating mycelial plugs containing the WT, Δ*Bcbag1* and *BcBAG1-Com*, on detached tomato leaves and grapes, respectively. Four days post-inoculation (dpi), Δ*Bcbag1* only initiated a small localized lesions, whereas the WT and the complemented strains have produced fully expanded lesions that were already at the soft rot stage (**Figure 4A**). We also performed infection assays on tomato leaves, with conidial suspensions (1.0×10^5 spores/ml). Consistently, Δ*Bcbag1* showed apparently attenuated virulence compared to the WT and *BcBAG1-Com* (**Figures 4A,B**). These results indicate that BcBAG1 functions as a virulence factor by enhancing colonization on the hosts.

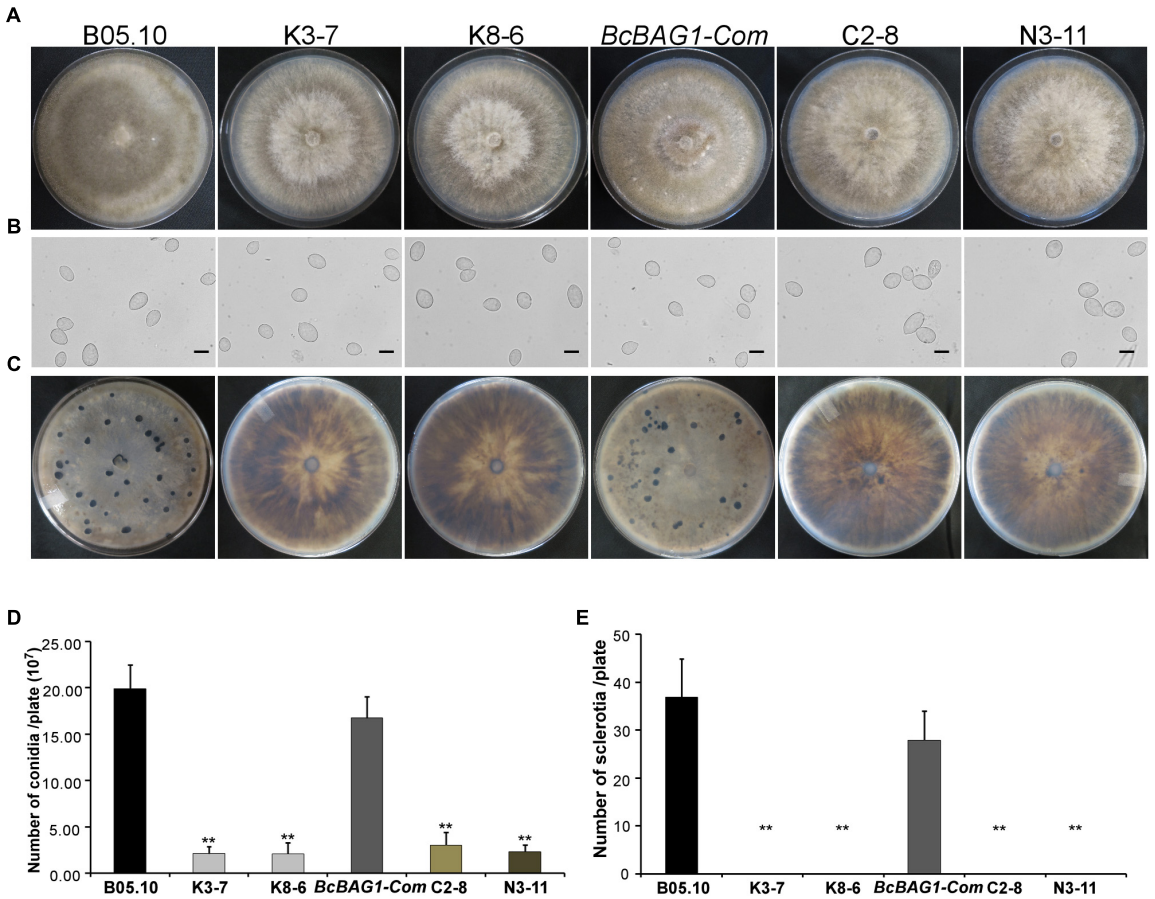

FIGURE 2 | BcBAG1 is essential to conidiation and sclerotial formation. **(A)** Conidiation is affected by *BcBAG1* disruption. Strains grown on PDA for 10 days were examined by light microscopy. **(B)** Conidia shape comparison. Conidia were collected from 10 days colonies of strains on PDA. Scale bar: 10 μm. **(C)** Sclerotial formation is abolished in the Δ*Bcbag1* mutants. Strains were incubated PDA for 10 days in the dark. **(D)** Quantification of conidia production on PDA plates. **(E)** Quantification of sclerotia formation on PDA plates. Wild-type strain (B05.10), Δ*Bcbag1* mutant lines (K3-7 and K8-6), and complemented strains (*BcBAG1-Com*, C2-8 and N3-11). Error bars represent the standard deviations from three independent experiments and asterisks denote statistical significance ($P < 0.01$).

During infection, *B. cinerea* produces three types of penetration structures, including germ tube apices (GA), appressoria (HA) and infection cushions (IC) (Vandenheuvel and Waterreus, 1983). To investigate whether the weak virulence of Δ*Bcbag1* resulted from penetration defects, we evaluated conidial germination using hydrophobic coverslips and the penetration on onion epidermis cells for microscopic observation (**Figure 5A**). Although all strains initiated germination 12 h post-incubation (hpi), the germination rate of Δ*Bcbag1* was significantly reduced (by 50%) compared to the germination recorded for the WT and *BcBAG1-Com* (**Figure 5C**). Moreover, deletion of *BcBAG1* delayed the onset of appressoria formation at 24 hpi and the development of infection cushions (IC) at 48 hpi (**Figure 5A**). Cotton blue was used to stain the appressorium-like structure, the infection cushion and the hyphae of *B. cinerea* on onion epidermal cells. As shown in **Figure 5B**, the conidia of WT and *BcBAG1-Com* germinated, and the infection cushions surrounded by abundant invasive hyphae were typically developed for penetration on the onion epidermis 48 hpi. In contrast, Δ*Bcbag1* attenuated the ability to form infection cushions and only few germ tubes and invasive hyphae appeared on onion cells. These results suggest that the reduced virulence of Δ*Bcbag1* is correlated with the developmental defects of infection and penetration structures.

Both UBL and BAG Domains Contribute to BcBAG1 Function

BcBAG1 possesses an N-terminal ubiquitin-like (UBL) domain and a conserved C-terminal BAG domain (BD) (**Supplementary Figure S1B**). Human BAG-1 interacts with HSP70 via its BAG domain and utilizes the UBL domain in targeting the chaperone cofactor to the 26S proteasome for degradation (Demand et al., 2001). The UBL/BAG domain proteins in *S. pombe,* SpBAG101 and SpBAG102, display similar interaction pattern to human BAG-1 (Kriegenburg et al., 2014; Poulsen et al., 2017). To validate the functionality of the UBL and the BAG domain of BcBAG1, we generated two truncated forms of BcBAG1; BcBAG1A$^{1-141}$ and BcBAG1B$^{142-298}$ (**Supplementary Figure S1B**), containing UBL and BAG domain, respectively. The BcBAG1A$^{1-141}$ and

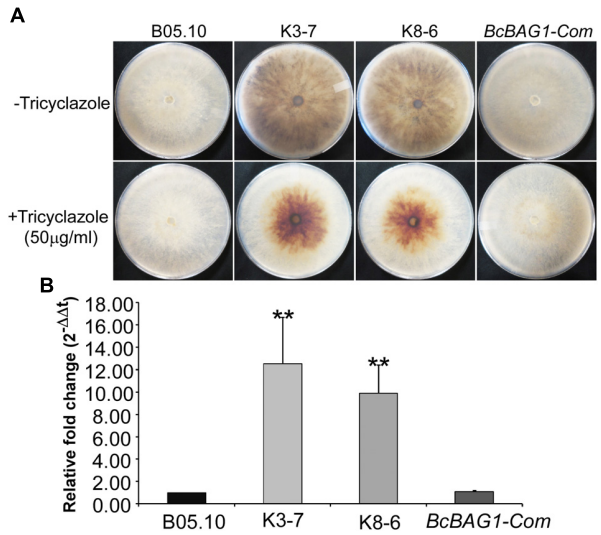

FIGURE 3 | BcBAG1 negatively regulates hypal melanization. **(A)** Mycelial pigmentation were monitored on PDA for 7 days in darkness without (upper panel) and with (lower panel) tricyclazole (an inhibitor of DHN-melanin biosynthesis) in the wild-type (B05.10), Δ*Bcbag1* mutants (K-3 and K8-6) and complemented strain (*BcBAG1-Com*). **(B)** Transcription analysis of *THR1* (1,3,8-trihydroxynaphthalene reductase gene) by RT-PCR. Total RNAs of corresponding strains grown on PDB medium were extracted and conducted for RT-PCR, asterisks denote statistical significance ($P < 0.01$).

BcBAG1B$^{142-298}$ constructs were subsequently transformed into Δ*Bcbag1* for complementation, designated as N3-11 and C2-8, respectively. Both N3-11 and C2-8 could not effectively rescue defects in conidia production and sclerotia formation (**Figure 2**). Interestingly, C2-8 could partially restored conidial germination, infection structure formation and pathogenicity to WT levels (**Figures 4**, **5**). These data suggest that both UBL and BAG domains are necessary for integral BcBAG1 function and we further inferred that the BAG domain plays an indispensable role for pathogenicity of *B. cinerea*.

BcBAG1 Modulates Multiple Stress Responses in *B. cinerea*

BAG family members are involved in cell protection during variable biotic and abiotic stress responses (Doukhanina et al., 2006; Behl, 2016). To investigate the function of BcBAG1 in response to environmental stress, we examined the sensitivity of Δ*Bcbag1* to various abiotic stress stimuli. As shown in **Figure 6**, Δ*Bcbag1* was more sensitive to salt stress (1 M NaCl) than WT, but no different with WT to another osmotic stress inducer 1.2 M D-sorbitol. Mycelial growth in response to cell wall stress inducers (0.6 mg/ml CFW; and 0.02% SDS) was measured. Δ*Bcbag1* showed dramatically increased sensitivity to both CFW and SDS compared to WT (**Figure 6**). In contrast, when exposing to oxidative stimuli, 20 mM H_2O_2 and 0.5 mM TBHP, Δ*Bcbag1* led to an average ∼7% (20 mM H_2O_2) and ∼8% (0.5 mM TBHP) lower growth inhibition rate than the WT strain (**Figure 6**), indicating that disruption of *BcBAG1* is more resistance to oxidative stress.

Human BAG-1 is a coupling factor between HSP70 and 26S proteasome (Luders et al., 2000). BAG3, as a co-chaperone, forms a complex with HSP70 to facilitate the degradation of ubiquitinated proteins via the proteasome or autophagy pathways (Gamerdinger et al., 2011; Minoia et al., 2014). Thus, we examined the role of BcBAG1 in proteasome degradation by testing the sensitivity of Δ*Bcbag1* to proteasome inhibitors, MG132 and Bort (Huang and Chen, 2009). Unexpectedly, results showed that the growth rate of Δ*Bcbag1* is not statistically different from WT and *BcBAG1-Com* (**Figure 6**), implying that BcBAG1 is not involved in response to proteasome inhibitors, MG132 and Bort. Although human BAG3 mediate the responses to Bort and MG132 (Judge et al., 2017), BcBAG1 does not share the same role in this perspective as the human counterpart.

BcBAG1 Negatively Regulates Unfolded Protein Response (UPR)

Previous work revealed that Arabidopsis BAG7 (AtBAG7) functions as an ER stress co-chaperone to maintain the UPR and protect plants from ER stress-induced cell death (Williams et al., 2010). Except AtBAG4, BcBAG1 shares relative higher identity to AtBAG7 in comparison to other Arabidopsis BAGs (**Supplementary Table S3**), we therefore examined whether BcBAG1 plays a role in ER stress signaling pathway. ER stress can be induced by chemical compounds, e.g., Tm or DTT (Oslowski and Urano, 2011). Besides, environmental/abiotic stress including excessive heat and cold also trigger ER stress (Williams et al., 2010). Accordingly, we cultured the WT, Δ*Bcbag1* and *BcBAG1-Com* on media supplemented with 2 μg/ml Tm and 2.5 mM DTT for 3 days at 22°C. The results showed that the growth of Δ*Bcbag1* was strongly inhibited by Tm and DTT with a much higher inhibition rate comparing to WT and *BcBAG1-Com* (**Figure 6**). In addition, after incubating on PDA under heat (30°C) and cold (4°C) conditions for 7 days, Δ*Bcbag1* was more sensitive than the WT and *BcBAG1-Com* to both heat and cold treatments (**Figures 7A–C**). Quantitative real-time (qRT-PCR) analysis demonstrated that the transcription of *BcBAG1* was highly induced upon above ER stress conditions, including heat treatment (50°C for 30 min), Tm (2 μg/ml for 1 h), or DTT (20 mM for 1 h) (**Figure 7C**), indicating that *BcBAG1* is responsible for ER stress tolerance.

To cope with ER stress, eukaryotes utilize UPR to alleviate the detrimental effects (Schroder and Kaufman, 2005). In *S. cerevisiae*, UPR is sensed by transmembrane protein kinase and ribonuclease (RNase) IRE1 and initiated with IRE1-mediated splicing of an unconventional intron (252-nucleotide) from the *HAC1* transcript (Cox and Walter, 1996; Ruegsegger et al., 2001). HAC1 encodes a basic leucine zipper-type (bZIP) transcription factor, and the splicing of *HAC1* regulates the expression of UPR target genes thus to mitigate ER stress (Mori et al., 1996). To explore the underlying mechanism within the sensitivity of Δ*Bcbag1* to ER stress, we detected the presence of the spliced and unspliced form of *BcHAC1* mRNA by RT-PCR. Spliced form of *BcHAC1* (*BcHAC1*^{S}) in B05.10 was significantly increased upon ER stress, suggesting *B. cinerea* shares the similar *HAC1* splicing process with other organisms during UPR (**Figure 8A**). Notably,

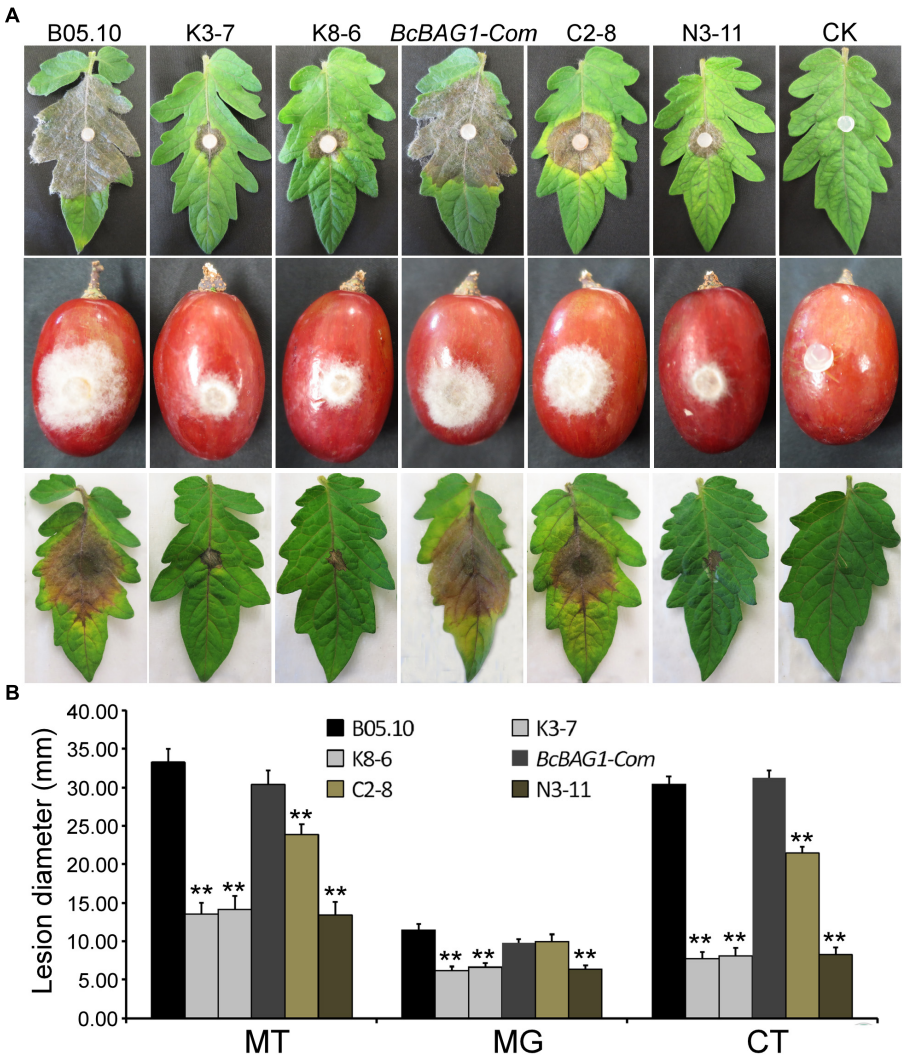

FIGURE 4 | *BcBAG1* deletion mutants attenuated pathogenicity. **(A)** Inoculation assays were implemented on different host plants. Mycelial plugs from PDA after 3 days growth were inoculated on detached tomato leaves (Moneymaker) (upper panel) and wounded grapes (middle panel). The disease phenotype was recorded 4 days post inoculation. Conidial suspensions (1.0–1.5 × 10^5 spores/ml) were inoculated on detached tomato leaves (Moneymaker) (lower panel) and the disease symptom was recorded 7 days post inoculation. **(B)** Quantification of lesion diameters of above inoculation. MT, mycelial plugs were inoculated on tomato leaves; MG, mycelial plugs were inoculated on grapes; CT, conidial suspensions were inoculated on tomato leaves. Wild-type strain (B05.10), Δ*Bcbag1* mutant lines (K3-7 and K8-6), and complemented strains (*BcBAG1-Com*, C2-8 and N3-11); CK, negative control. Error bars represent the standard deviations from three independent experiments and asterisks indicate statistical significance ($P < 0.01$).

under normal conditions, the amount of $BcHAC1^S$ was drastically more abundant in Δ*Bcbag1* than the WT (**Figure 8A**, upper panel). More interestingly, *BcHAC1* was constitutively spliced in Δ*Bcbag1* under both conditions that are with/with-out stress (**Figure 8A**). DNA sequencing confirmed that a 20 nucleotide of the fragment was absent in the spliced form compared to the unspliced form (**Figure 8A**, lower panel). Meanwhile, we examined the expression of UPR-related genes in *B. cinerea*, BcBIP1 and BcIRE1, homologs of ER chaperone KAR2/BIP1 and ER stress sensor/transducer IRE1 in *S. cerevisiae*, respectively (Pincus et al., 2010). Both *BcBIP1* and *BcIRE1* were induced following ER stress in the WT (**Figure 8B**). Without stress, the expression levels of *BcIRE1* and *BcBIP1* were increased by threefold and fivefold, respectively, in Δ*Bcbag1* (**Figure 8B**). All these results indicates that, *BcBAG1* deletion causes constitutive activation of UPR through negatively regulating the expression of *BcBIP1*, *BcIRE1* and the splicing of *BcHAC1* mRNA. We speculate that BcBAG1 effectively repress the harmful and excessive constitutive activation of UPR, thus to maintain the proper UPR level during ER stress signaling pathway.

BcBAG1 Binds HSP70-Type Chaperones

The heat shock proteins HSP70 family play crucial roles in assisting a variety of protein folding processes (Mayer and Bukau, 2005). Human BAG-1 binds the ATPase domain of Hsc70 to stimulates Hsc70 ATP hydrolysis which results in the

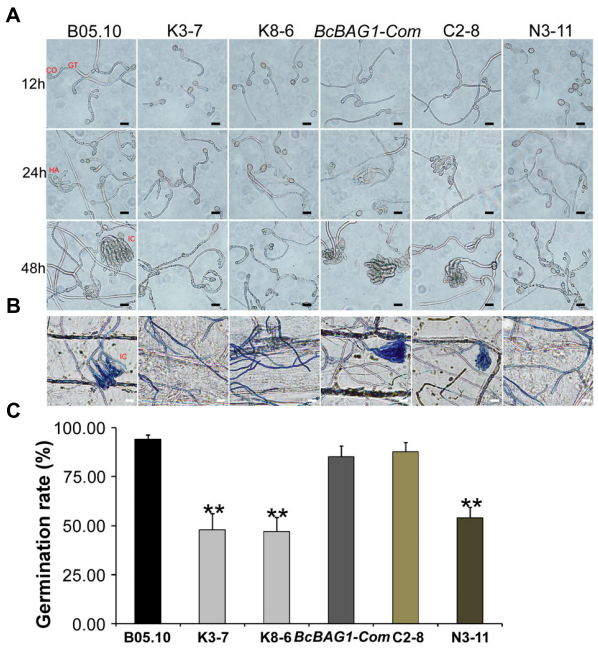

FIGURE 5 | BcBAG1 is required for conidial germination and penetration. **(A)** Time course of conidial germination on glass slides when conidia were suspended in 10 mM KH_2PO_4 and glucose solution (pH 6.0). CO, conidia; GT, germ tubes; HA, appressoria; IC, infection cushions. Scale bar: 20 μm. **(B)** Penetration assay on onion epidermal cells. Onion epidermal cells were inoculated with conidial suspension (5.0×10^4 spores/ml) and the penetration was observed 48 h post incubation (hpi). External fungal structures are stained blue with cotton blue, whereas penetrated hyphae remain unstained. Scale bar: 20 μm. **(C)** Quantification of conidial germination rates after 12 hpi on hydrophobic glass slide. Error bars represent the standard deviations from three independent experiments (more than 100 conidia per strain). Asterisks denote statistical significance ($P < 0.01$).

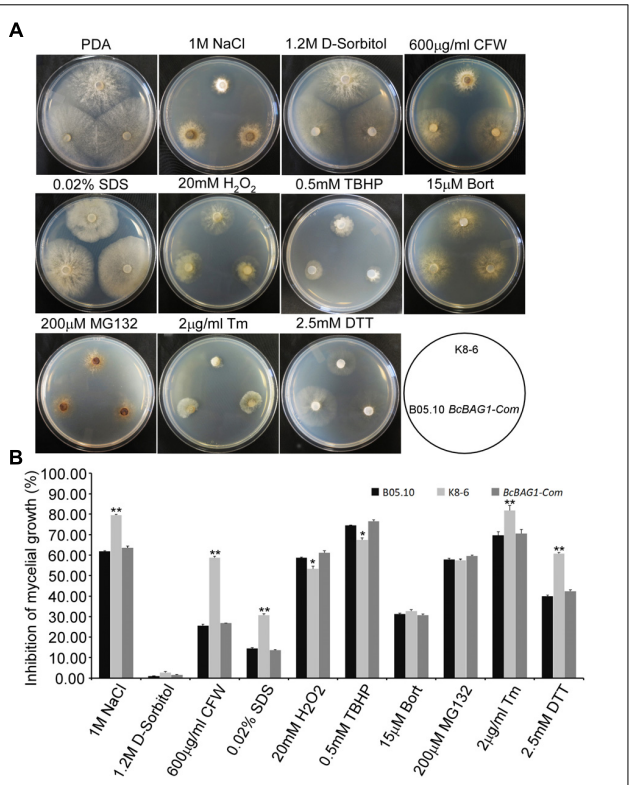

FIGURE 6 | BcBAG1 responses to various stress conditions. **(A)** Wild-type B05.10, Δ*Bcbag1* (K8-6) and *BcBAG1-Com* strains were cultured on PDA medium supplemented with various stresses inducers and photographed after 3 days. **(B)** Statistical analyses of the inhibition rates of all strains under different stresses. Error bars indicate the standard deviations from three independent experiments and asterisks indicate statistical significance ($P < 0.05$; $P < 0.01$).

release of ADP from Hsc70, thereby regulates specific protein folding and maturation pathways (Hohfeld and Jentsch, 1997). To ascertain whether BcBAG1 bind HSP70-type chaperone in *B. cinerea*, we performed the yeast two-hybrid assay to establish possible interaction between BcBAG1 and the HSP70 family members, including BcBIP1, BcSSC1, BcSKS2, BcSSA1, BcPSS1, and BcLHS1, which are homologs of HSP70 family in the fission yeast. Results showed that BcBAG1 only interacted with BcBIP1 and BcSKS2 (**Figure 8C**), demonstrating BcBAG1 does function as a co-chaperone of HSP70 proteins, in accordance with that has been reported in other systems (Gassler et al., 2001; Sondermann et al., 2002; Poulsen et al., 2017).

BcBAG1 Restores Salt Stress Tolerance to *atbag4*

Using NCBI blastp and blastn programs, we found BcBAG1 is predicted to be the closest homolog of Arabidopsis BAG protein AtBAG4, in light of the amino acid sequences of the BAG domains between BcBAG1 and AtBAG4 share 33% identity and 50% similarity (**Supplementary Figures S1A,C** and **Supplementary Table S3**). To determine whether BcBAG1 is able to functionally complement the AtBAG4 T-DNA mutants, full-length *BcBAG1* was overexpressed using the cauliflower mosaic virus 35S promoter in the *atbag4* T-DNA mutants (*atbag4::BcBAG1*). Expression levels of *BcBAG1* in *atbag4* was confirmed by RT-PCR (**Figure 9A**). Previous studies indicated that *atbag4* mutants were more susceptible to salt stress (100 mM NaCl) compared to the WT Col-0 (Doukhanina et al., 2006). Here, we performed the salt tolerance assay for *atbag4::BcBAG1*, taking Col-0 and *atbag4* as the positive and negative controls, respectively. Arabidopsis seedlings were cultured on 1/2 MS medium supplemented with 100 mM NaCl. After 2 weeks treatment, no difference was observed from seedlings. However, 5 weeks later, *atbag4* mutants displayed massive chlorosis and bleaching of leaves, while Col-0 and *atbag4::BcBAG1* plants grew well and exhibited nearly the same growth tendency under salt conditions (**Figure 9B**). These observations demonstrate that BcBAG1 can be ectopically expressed in Arabidopsis and fully restore salt tolerance in *atbag4*.

DISCUSSION

As an evolutionarily conserved group, BAG proteins from yeast to plants and mammals have been associated with

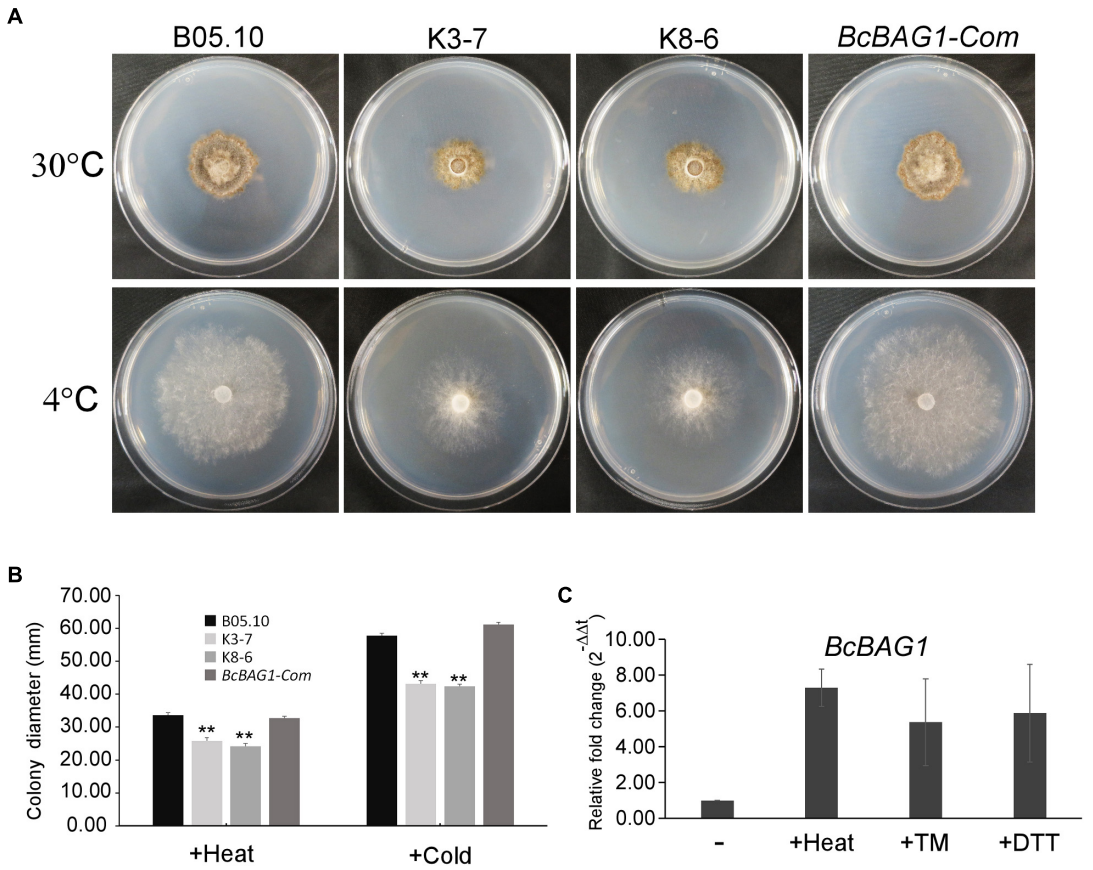

FIGURE 7 | *BcBAG1* knock-out mutants are susceptible to ER stress conditions. **(A)** Wild-type B05.10, Δ*Bcbag1* (K3-7 and K8-6) and *BcBAG1-Com* strains were grown on PDA medium at 30°C and 4°C, respectively, for 7 days. **(B)** Statistical analysis of the colony diameters of above strains. **(C)** The expression of *BcBAG1* is induced by heat, Tm, and DTT treatments. Quantitative RT-PCR was used to evaluate the *BcBAG1* transcript levels in the wild-type B05.10 following heat treatment (50°C for 30 min), tunicamycin (Tm, 15 μg/ml for 1 h) and DTT (20 mM for 1 h). Error bars represent the standard deviations from three independent experiments. Asterisks denote statistical significance ($P < 0.01$).

regulation of PCD and cell protection. Recently, they have also been found to play an important role in autophagy, UPR and ubiquitin-proteasome system (Kabbage et al., 2017). However, the identification and characterization of BAG proteins in phytopathogenic fungi is rare. In this study, we explored the *B. cinerea* genome and identified a unique *BAG* gene, *BcBAG1*. Targeted deletion of *BcBAG1* exerted strong adverse effects on vegetative growth, conidiation, sclerotia formation, hyphal melanization, stress response, conidial germination, penetration and virulence, suggesting that the pleiotropic function of BAGs delineated in mammals and plants appears to be maintained in *B. cinerea*. The BAG domain of BcBAG1 shares highest similarity with AtBAG4 in Arabidopsis, also an ectopic expression of BcBAG1 fully restored salt tolerance of *atbag4* mutants (**Figure 9**). In addition, deletion of *BcBAG1* resulted in increased sensitivity to salt, cell wall stressors, ER stress inducers, and heat or cold treatments. These results parallel plant AtBAG4 studies in which AtBAG4-overexpressing transgenic tobacco plants confer tolerance to a wide range of stresses such as UV light, cold, salt treatments (Doukhanina et al., 2006). From this perspective, the cytoprotective function of BAGs in response to diverse stresses is relatively conserved between the fungi and plants.

Our previous studies have addressed the importance of AtBAG7 in the maintenance of the UPR and the mechanisms of ER-localized co-chaperone AtBAG7 in stress protection (Williams et al., 2010; Li et al., 2017). Interestingly, BcBAG1 showed a close evolutionary relationship with AtBAG7 among plant BAGs (**Supplementary Figure S1A** and **Supplementary Table S3**). Moreover, Δ*Bcbag1* were more sensitive to ER stress stimuli (**Figure 6**) and expression of *BcBAG1* was induced under ER stress (**Figure 7B**), suggesting that both BcBAG1 and AtBAG7 are functionally associated with the ER stress. Of note, we found that the deletion of *BcBAG1* gives rise to the constitutive activation of UPR with high levels even without stress (**Figures 8A,B**), indicating that BcBAG1 is necessary for the inhibition of excess UPR under normal condition. Given the defects in fungal development and differentiation caused by deletion of *BcBAG1*, we speculate that under normal conditions, the abnormal activated UPR is actually harmful to the fungus. It has been reported that

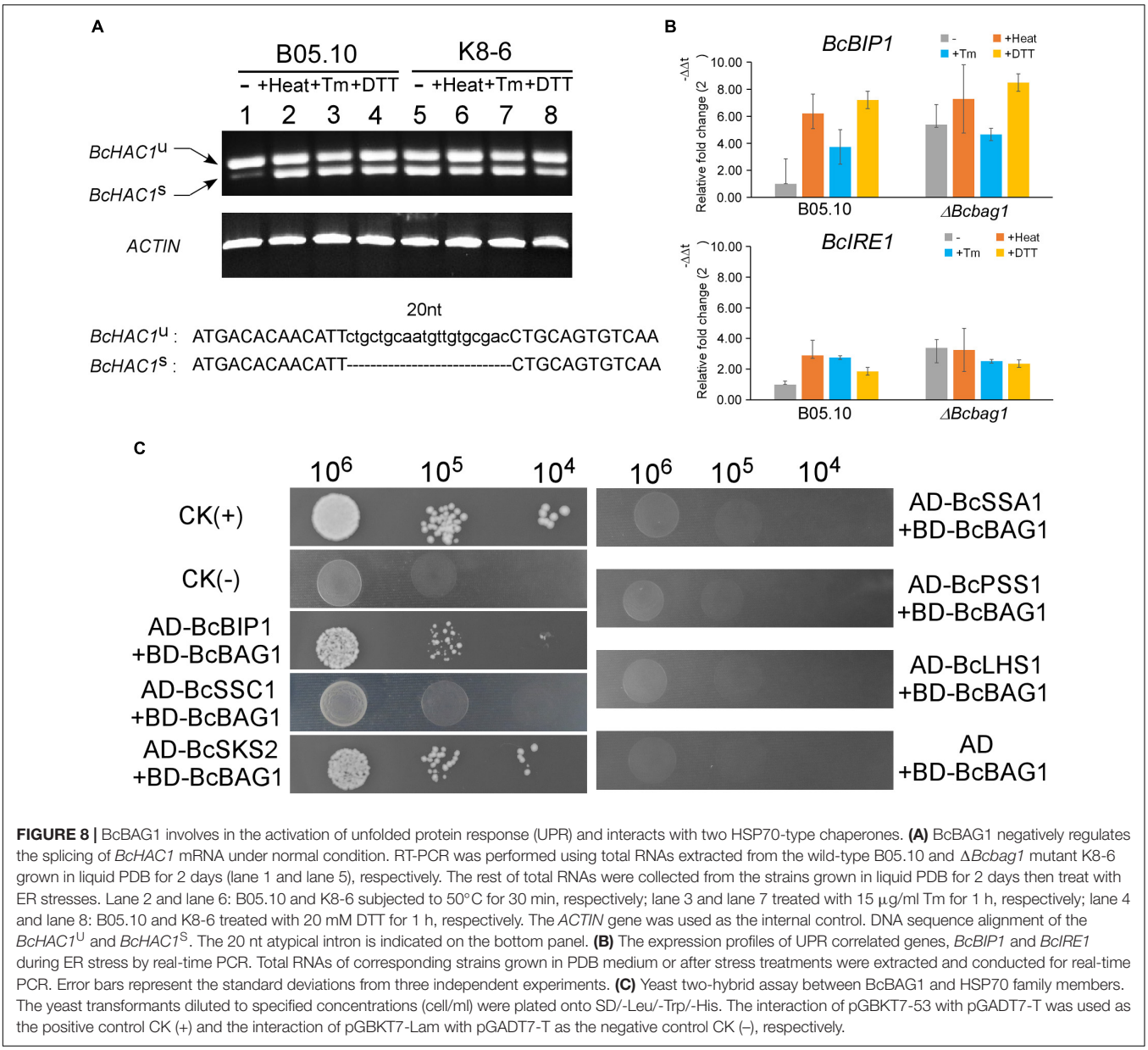

FIGURE 8 | BcBAG1 involves in the activation of unfolded protein response (UPR) and interacts with two HSP70-type chaperones. **(A)** BcBAG1 negatively regulates the splicing of *BcHAC1* mRNA under normal condition. RT-PCR was performed using total RNAs extracted from the wild-type B05.10 and Δ*Bcbag1* mutant K8-6 grown in liquid PDB for 2 days (lane 1 and lane 5), respectively. The rest of total RNAs were collected from the strains grown in liquid PDB for 2 days then treat with ER stresses. Lane 2 and lane 6: B05.10 and K8-6 subjected to 50°C for 30 min, respectively; lane 3 and lane 7 treated with 15 μg/ml Tm for 1 h, respectively; lane 4 and lane 8: B05.10 and K8-6 treated with 20 mM DTT for 1 h, respectively. The *ACTIN* gene was used as the internal control. DNA sequence alignment of the *BcHAC1*^{U} and *BcHAC1*^{S}. The 20 nt atypical intron is indicated on the bottom panel. **(B)** The expression profiles of UPR correlated genes, *BcBIP1* and *BcIRE1* during ER stress by real-time PCR. Total RNAs of corresponding strains grown in PDB medium or after stress treatments were extracted and conducted for real-time PCR. Error bars represent the standard deviations from three independent experiments. **(C)** Yeast two-hybrid assay between BcBAG1 and HSP70 family members. The yeast transformants diluted to specified concentrations (cell/ml) were plated onto SD/-Leu/-Trp/-His. The interaction of pGBKT7-53 with pGADT7-T was used as the positive control CK (+) and the interaction of pGBKT7-Lam with pGADT7-T as the negative control CK (–), respectively.

moderate activation of UPR is necessary for ER recovery when responding to stress in *S. cerevisiae* (Chawla et al., 2011). Thus, we suggest that constitutive activation of UPR in Δ*BcBag1* results in loss of normal ER protein-folding capacity, which impinges upon the ability to sustain resistance to ER stress. Thus, Δ*Bcbag1* displayed growth defects during ER stress. In addition, as a multifaceted HSP70 molecular chaperone, BIP ensures an appropriate response to restore protein folding homeostasis to the ER by providing a buffer for inactive IRE1 (Pincus et al., 2010). Our result revealed that disruption of *BcBAG1* increases the expression of *BcBIP1* and *BcIRE1* (**Figure 8B**) and BcBAG1 interacts with BcBIP1 (**Figure 8C**). We conclude that the regulation of UPR by BcBAG1 correlates to BcBIP1. The relationship between BcBAG1/BcBIP1/BcIRE1 and how BcBAG1 modulates the ER machinery require further studies.

Previous studies of human BAG-1/HSC70 complex revealed that BAG-1 exploits Glu^{212}, Asp^{222}, Arg^{237}, and Gln^{245} residues in the BAG domain to bind with Hsc70 ATPase domain (Sondermann et al., 2001). Multiple alignment showed that these residues, with the exception of Glu^{212}, are highly conserved in BcBAG1 BD (**Supplementary Figure S1C**), implying that BcBAG1 interacts with HSP70 in a similar manner as with human BAG-1. We did examine the interaction between BcBAG1 and HSP70 proteins by Y2H and found that BcBAG1 exclusively interacts with BcBIP1 and BcSKS2 in the HSP70 family, but fails to bind to BcSSC1, BcSSA1, BcPSS1, and BcLHS1 (**Figure 8C**). Previous studies demonstrated that the *S. cerevisiae* BAG protein SNL1 interacts with HSP70

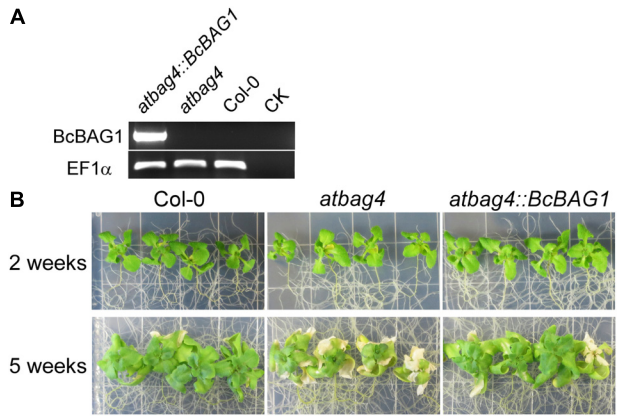

FIGURE 9 | BcBAG1 restores the salt stress tolerance of AtBAG4 T-DNA knock-out mutant. **(A)** BcBAG1 ectopically expressed in Arabidopsis plants. BcBAG1 driven by 35S promoter was transformed in to *atbag4* mutant (*atbag4::BcBAG1*) and the expression of BcBAG1 was confirmed by RT-PCR. Taking *atbag4* and the wild-type plant Col-0 as controls. CK, negative control. The *EF1a* gene was used as the internal control. **(B)** Col-0, *atbag4* and *atbag4::BcBAG1* were subjected to salt stress. Plants were grown on half-strength Murashige and Skoog (MS) medium with 2% sucrose and subjected to 100 mM NaCl treatment. Plants growth was recorded after 2 weeks and 5 weeks.

family members including SSA1, SSB1, SSB2, SEE1, and SEE2 (Sondermann et al., 2002; Verghese and Morano, 2012; Abrams et al., 2014). While the *S. pombe* BAG proteins SpBAG101 and SpBAG102 exclusively interact with SSA1, SSA2, and SKS2 (Poulsen et al., 2017). These data suggest BAGs from different origins show different affinity and specificity to HSP70s members. Notably, the interaction between BcBAG1 and BcSKS2 is conserved from that in yeast studies. BcSKS2 is the homolog of fission yeast ribosome-associated chaperone SKS2, and the *S. cerevisiae* orthologs of fission yeast SKS2, called SSB1 and SSB2. SSB1/2 chaperones play a dual role in *de novo* protein folding and ribosome biogenesis (Mudholkar et al., 2017). We conjectured that the binding to primary HSP70 chaperone might be responsible for the functional pleiotropy of BcBAG1.

Apart from the BAG domain, BcBAG1 also contains a UBL domain. Human BAG-1 function as a link between HSC/HSP70 and 26S proteasome degradation system via its UBL domain, chaperone-bound substrates are released and degraded (Luders et al., 2000; Alberti et al., 2002). Co-precipitation experiments in fission yeast provide direct evidence that both SpBAG101 and SpBAG102 interact with 26S proteasomes depend on the UBL domain (Poulsen et al., 2017). However, we found that response to proteasome inhibitors, e.g., Bort and MG132, by *BcBAG1* deletion was unaffected in fungus (**Figure 6**). Besides, the result of ubiquitination assay confirmed that deletion of *BcBAG1* does not alter the levels of ubiquitination (**Supplementary Figure S3**). Therefore, we inferred that BcBAG1 is not a key player in the proteasome degradation. However, we cannot exclude the possibility that other proteasome inhibitors may work on BcBAG1 or BcBAG1 can be targeting some proteasome substrate for degradation.

Botrytis cinerea, however, integrates a number of hurdles that must be traversed for successful colonization and defense against the plethora of plant hosts that are encountered (Elad et al., 2007). Therefore, it is relatively difficult to present a precise mechanism for the alteration of pathogenicity and virulence in the host. Based on our data, we supposed that the attenuated pathogenicity of Δ*Bcbag1* is directly or indirectly related to the following reasons. First, Δ*BcBag1* showed a decrease of conidial germination, and delayed the formation of appressoria and infection cushions on an artificial surface and onion epidermis (**Figure 6**). At the same time, we observed that BcBAG1 resides in the cytoplasm throughout growth stages, but the localization is altered and most likely concentrated at the infection spots during invasion (**Supplementary Figure S4**), suggesting the expression of *BcBAG1* contributes to the formation of penetration structures. Therefore, the impairment of penetration structures in Δ*BcBag1* weakens the ability of breaching the host tissues to effectively cause disease. Second, it is reported that cell wall integrity is crucial for *B. cinerea* virulence and pathogenicity (Soulie et al., 2003, 2006; Cui et al., 2013). Δ*BcBag1* increased sensitivity to cell wall stressors, CFW and SDS (**Figure 6**), indicating BcBAG1 involves in cell wall integrity pathway. Therefore, defect in cell wall integrity is one key to the reduction of virulence. Third, melanin is a factor affecting the virulence of *B. cinerea*. BcPKS13 and BcBRN1, encoding polyketide synthase and tetrahydroxynaphthalene (THN) reductases, respectively, both are involving in fungal DHN melanin biosynthesis (Zhang et al., 2015). Loss of *BcPKS13* and *BcBRN1* blocks melanization resulting in enhanced virulence. Conversely, overexpression of *BcBRN1* enhances melanization, decreases secretion for virulence factors such as several hydrolytic enzymes and oxalic acid, and attenuated virulence (Zhang et al., 2015). From this perspective, an increment of melanin biosynthesis negatively affects the pathogenesis of *B. cinerea*. Consistently, our results showed that BcBAG1 negatively regulates melanin biosynthesis (**Figure 3**), thus the increased mycelial melanin biosynthesis suppress fungal virulence for Δ*BcBag1*. Fourth, previous studies indicated UPR plays as a central regulator of fungal pathogenesis (Heimel et al., 2013; Guillemette et al., 2014; Krishnan and Askew, 2014a,b). Our study found that BcBAG1 is responsible for proper maintenance of UPR, as a result, abnormal activation of UPR in Δ*Bcbag1* could cause the attenuated virulence.

In summary, this paper details the biological functions of BcBAG1. We have shown that BcBAG1 exhibits functional versatility and is involved in fungal development, differentiation, stress response, and pathogenicity. BcBAG1 acts as a co-chaperone of HSP70 and is a key regulator required for maintenance of the UPR. In light of these findings, future studies involving translocation of BcBAG1 during infection and identification of other targets are of interest. Taken together, these results demonstrate the importance of the BAG family in filamentous fungus cell death pathways and cytoprotection.

AUTHOR CONTRIBUTIONS

HZ and MD designed the research. HZ performed the experiments. HZ, YL, and MD analyzed the data. HZ, YL, MD, and ZW wrote the article. MD and ZW revised and approved the manuscript.

FUNDING

This work was partially supported by NSFC (Grant No. 31471739).

ACKNOWLEDGMENTS

We thank Professor Matthias Hahn (Kaiserslautern University, Germany) for providing vector pNAH-OGG and pNAH-OMG. We also thank the Chinese CSC Scholarship Program for the grant of HZ.

SUPPLEMENTARY MATERIAL

The Supplementary Material for this article can be found online at: https://www.frontiersin.org/articles/10.3389/fmicb.2019.00685/full#supplementary-material

FIGURE S1 | Phylogenetic and sequence analysis of BAG1 in *Botrytis cinerea* (BcBAG1). **(A)** The phylogenetic tree of BAG proteins. Evolutionary analyses were conducted in MEGA7.0. The evolutionary history was inferred by using a neighbor-joining method based on the amino acid sequences. The numbers at nodes inferred the percentage of their occurrence in 10,000 bootstrap replicates. Species names and GenBank accession numbers of each sequence are represented as follows: SsBAG1 (*Sclerotinia sclerotiorum*, XP_001591798.1); MoBAG1 (*Magnaporthe oryzae*, XP_003710309.1); FoBAG1 (*Fusarium oxysporum f. sp. Lycopersici*, XP_018239181.1); NcBAG1 (*Neurospora crassa*, XP_961586.1); AnBAG1 (*Aspergillus nidulans*, XP_661815.1); UmBAG1 (*Ustilago maydis*, KIS67500.1); SpBAG101 (*Schizosaccharomyces pombe*, NP_596760.1); SpBAG102 (*Schizosaccharomyces pombe*, NP_595316.1); ScSNL1 (*Saccharomyces cerevisiae*, KZV10602.1); HsBAG-1M (*Homo sapiens*, NP_001336215.1); HsBAG2 (*Homo sapiens*, NP_004273.1); HsBAG3 (*Homo sapiens*, NP_004272.2); HsBAG4 (*Homo sapiens*, NP_004865.1); HsBAG5 (*Homo sapiens*, NP_001015049.1); HsBAG6 (*Homo sapiens*, P46379.2); AtBAG1 (*Arabidopsis thaliana*, NP_200019.2); AtBAG2 (*Arabidopsis thaliana*, NP_568950.2); AtBAG3 (*Arabidopsis thaliana*, NP_196339.1); AtBAG4 (*Arabidopsis thaliana*, NP_190746.2); AtBAG5 (*Arabidopsis thaliana*, NP_172670.2); AtBAG6 (*Arabidopsis thaliana*, AEC10664.1); AtBAG7 (*Arabidopsis thaliana*, NP_201045.1). **(B)** Schematic diagram of BcBAG1. Purple red and green boxes indicate the UBL and BAG domain of BcBAG1, respectively. **(C)** Sequence alignment of the conserved BAG domain from different organisms. Three predicted helixes labeled on the top. Conserved residues which involving in binding of BAG protein to Hsc70 ATPase domain in human HsBAG-1M are indicated by red arrow, and residues critical to packing interactions are highlighted by blue arrow.

FIGURE S2 | Sketch of gene deletion and identification of deletion mutants and complemented transformants. **(A)** Diagram of targeted gene replacement. **(B)** RT-PCR confirmation. Lane 1:100 bp DNA Ladder (NEB); lanes 2 and 3: K3-7 and K8-6, respectively; lane 4: B05.10; lanes 5 and 6: complemented transformants; lane 7: PCR negative control. **(C)** Southern blotting confirmation. Total genomic DNAs were digested by *PvuI*, and a DNA fragment in the upstream of 5′ terminus of BcBAG1 was selected and labeled as the probe shown in panel **(A)**. M: 1 kb DNA Ladder (NEB).

FIGURE S3 | Disruption of *BcBAG1* does not affect protein ubiquitination. Total protein extracts from corresponding strains was western blotted with (upper panel) an anti-Ub antibody (P4D1) and stained with Coomassie brilliant blue (lower panel) as the loading control. B05.10: the wild-type strain; K8-6: Δ*Bcbag1* mutant lines; C2-8 (C-terminus of *BcBAG1*) and N3-11 (N-terminus of *BcBAG1*).

FIGURE S4 | Subcellular localization of BcBAG1. GFP-BcBAG1 was overexpressed in the Δ*Bcbag1* mutant (OG2-7) and the fluorescence for BcBAG1 localization at different stages was visualized by confocal microscopy. **(A)** Vegetative hyphae; **(B)** conidia; **(C,D)** conidia on hydrophobic glass slides for 12 and 24 h, respectively. **(E,F)** Both are conidia on onion epidermal cells for 24 h and 48 h, respectively. Scale bars: 20 μm.

TABLE S1 | Wild-type and mutant strains of *Botrytis cinerea* used in this study.

TABLE S2 | Oligonucleotide primers used in this study.

TABLE S3 | Similarity of full length and BAG domain amino acid sequence between BcBAG1 and other BAGs.

REFERENCES

Abrams, J. L., Verghese, J., Gibney, P. A., and Morano, K. A. (2014). Hierarchical functional specificity of cytosolic heat shock protein 70 (Hsp70) nucleotide exchange factors in yeast. *J. Biol. Chem.* 289, 13155–13167. doi: 10.1074/jbc.M113.530014

Alberti, S., Demand, J., Esser, C., Emmerich, N., Schild, H., and Hohfeld, J. (2002). Ubiquitylation of BAG-1 suggests a novel regulatory mechanism during the sorting of chaperone substrates to the proteasome. *J. Biol. Chem.* 277, 45920–45927. doi: 10.1074/jbc.M204196200

Back, S. H., Schroder, M., Lee, K., Zhang, K., and Kaufman, R. J. (2005). ER stress signaling by regulated splicing: IRE1/HAC1/XBP1. *Methods* 35, 395–416. doi: 10.1016/j.ymeth.2005.03.001

Behl, C. (2016). Breaking BAG: the Co-Chaperone BAG3 in health and disease. *Trends Pharmacol. Sci.* 37, 672–688. doi: 10.1016/j.tips.2016.04.007

Bell, A. A., and Wheeler, M. H. (1986). Biosynthesis and functions of fungal melanins. *Annu. Rev. Phytopathol.* 24, 411–451. doi: 10.1146/annurev.py.24.090186.002211

Bracher, A., and Verghese, J. (2015). GrpE, Hsp110/Grp170, HspBP1/Sil1 and BAG domain proteins: nucleotide exchange factors for Hsp70 molecular chaperones. *Subcell Biochem.* 78, 1–33. doi: 10.1007/978-3-319-11731-7_1

Butler, M. J., and Day, A. W. (1998). Fungal melanins: a review. *Can. J. Microbiol.* 44, 1115–1136. doi: 10.1139/cjm-44-12-1115

Chawla, A., Chakrabarti, S., Ghosh, G., and Niwa, M. (2011). Attenuation of yeast UPR is essential for survival and is mediated by IRE1 kinase. *J. Cell Biol.* 193, 41–50. doi: 10.1083/jcb.201008071

Cox, J. S., and Walter, P. (1996). A novel mechanism for regulating activity of a transcription factor that controls the unfolded protein response. *Cell* 87, 391–404. doi: 10.1016/S0092-8674(00)81360-4

Cui, Z. F., Wang, Y. H., Lei, N., Wang, K., and Zhu, T. H. (2013). Botrytis cinerea chitin synthase BcChsVI is required for normal growth and pathogenicity. *Curr. Genet.* 59, 119–128. doi: 10.1007/s00294-013-0393-y

Demand, J., Alberti, S., Patterson, C., and Hohfeld, J. (2001). Cooperation of a ubiquitin domain protein and an E3 ubiquitin ligase during chaperone/proteasome coupling. *Curr. Biol.* 11, 1569–1577. doi: 10.1016/S0960-9822(01)00487-0

Doehlemann, G., Berndt, P., and Hahn, M. (2006). Different signalling pathways involving a G alpha protein, cAMP and a MAP kinase control germination of Botrytis cinerea conidia. *Mol. Microbiol.* 59, 821–835. doi: 10.1111/j.1365-2958.2005.04991.x

Doukhanina, E. V., Chen, S., van der Zalm, E., Godzik, A., Reed, J., and Dickman, M. B. (2006). Identification and functional characterization of the BAG protein family in *Arabidopsis thaliana*. *J. Biol. Chem.* 281, 18793–18801. doi: 10.1074/jbc.M511794200

Elad, S. F. Y. (2016). *Botrytis - the Fungus, the Pathogen and its Management in Agricultural Systems*. Berlin: springer.

Elad, Y., Williamson, B., Tudzynski, P., and Delen, N. (2007). *Botrytis: Biology, Pathology and Control*. Berlin: SpringerLink. doi: 10.1007/978-1-4020-2626-3

Fang, S., Li, L., Cui, B., Men, S., Shen, Y., and Yang, X. (2013). Structural insight into plant programmed cell death mediated by BAG proteins in *Arabidopsis thaliana*. *Acta Crystallogr. D Biol. Crystallogr.* 69(Pt 6), 934–945. doi: 10.1107/S0907444913003624

Feng, X., Krishnan, K., Richie, D. L., Aimanianda, V., Hartl, L., Grahl, N., et al. (2011). HacA-independent functions of the ER stress sensor IreA synergize with the canonical UPR to influence virulence traits in *Aspergillus fumigatus*. *PLoS Pathog.* 7:e1002330. doi: 10.1371/journal.ppat.1002330

Gamerdinger, M., Kaya, A. M., Wolfrum, U., Clement, A. M., and Behl, C. (2011). BAG3 mediates chaperone-based aggresome-targeting and selective autophagy of misfolded proteins. *Embo Rep.* 12, 149–156. doi: 10.1038/embor.2010.203

Gassler, C. S., Wiederkehr, T., Brehmer, D., Bukau, B., and Mayer, M. P. (2001). Bag-1M accelerates nucleotide release for human Hsc70 and Hsp70 and can act concentration-dependent as positive and negative cofactor. *J. Biol. Chem.* 276, 32538–32544. doi: 10.1074/jbc.M105328200

Gething, M. J. (1999). Role and regulation of the ER chaperone BiP. *Semin. Cell Dev. Biol.* 10, 465–472. doi: 10.1006/scdb.1999.0318

Goswami, R. S. (2012). Targeted gene replacement in fungi using a split-marker approach. *Methods Mol. Biol.* 835, 255–269. doi: 10.1007/978-1-61779-501-5_16

Gronover, C. S., Kasulke, D., Tudzynski, P., and Tudzynski, B. (2001). The role of G protein alpha subunits in the infection process of the gray mold fungus *Botrytis cinerea*. *Mol. Plant. Microbe Interact.* 14, 1293–1302. doi: 10.1094/MPMI.2001.14.11.1293

Guillemette, T., Calmes, B., and Simoneau, P. (2014). Impact of the UPR on the virulence of the plant fungal pathogen A-brassicicola. *Virulence* 5, 357–364. doi: 10.4161/viru.26772

Hartl, F. U. (1996). Molecular chaperones in cellular protein folding. *Nature* 381, 571–579. doi: 10.1038/381571a0

Heimel, K., Freitag, J., Hampel, M., Ast, J., Bolker, M., and Kamper, J. (2013). Crosstalk between the unfolded protein response and pathways that regulate pathogenic development in *Ustilago maydis*. *Plant Cell* 25, 4262–4277. doi: 10.1105/tpc.113.115899

Henson, J. M., Butler, M. J., and Day, A. W. (1999). The dark side of the mycelium: melanins of phytopathogenic fungi. *Annu. Rev. Phytopathol.* 37, 447–471. doi: 10.1146/annurev.phyto.37.1.447

Ho, A. K., Raczniak, G. A., Ives, E. B., and Wente, S. R. (1998). The integral membrane protein snl1p is genetically linked to yeast nuclear pore complex function. *Mol. Biol. Cell* 9, 355–373. doi: 10.1091/mbc.9.2.355

Hohfeld, J., and Jentsch, S. (1997). GrpE-like regulation of the hsc70 chaperone by the anti-apoptotic protein BAG-1. *EMBO J.* 16, 6209–6216. doi: 10.1093/emboj/16.20.6209

Huang, L., and Chen, C. H. (2009). Proteasome regulators: activators and inhibitors. *Curr Med Chem* 16, 931–939. doi: 10.2174/092986709787581860

Hwang, I., and Sheen, J. (2002). Two-component circuitry in Arabidopsis cytokinin signal transduction. *Dev. Biol.* 247, 484–484.

Jain, S., Wiemann, P., Thill, E., Williams, B., Keller, N. P., and Kabbage, M. (2018). A Bcl-2 Associated Athanogene (bagA) modulates sexual development and secondary metabolism in the filamentous fungus *Aspergillus nidulans*. *Front. Microbiol.* 9:1316. doi: 10.3389/fmicb.2018.01316

Joubert, A., Simoneau, P., Campion, C., Bataille-Simoneau, N., Iacomi-Vasilescu, B., Poupard, P., et al. (2011). Impact of the unfolded protein response on the pathogenicity of the necrotrophic fungus *Alternaria brassicicola*. *Mol. Microbiol.* 79, 1305–1324. doi: 10.1111/j.1365-2958.2010.07522.x

Judge, L. M., Perez-Bermejo, J. A., Truong, A., Ribeiro, A. J., Yoo, J. C., Jensen, C. L., et al. (2017). A BAG3 chaperone complex maintains cardiomyocyte function during proteotoxic stress. *JCI Insight* 2:94623. doi: 10.1172/jci.insight.94623

Kabbage, M., and Dickman, M. B. (2008). The BAG proteins: a ubiquitous family of chaperone regulators. *Cell Mol. Life Sci.* 65, 1390–1402. doi: 10.1007/s00018-008-7535-2

Kabbage, M., Kessens, R., Bartholomay, L. C., and Williams, B. (2017). The life and death of a plant cell. *Annu. Rev. Plant Biol.* 68, 375–404. doi: 10.1146/annurev-arplant-043015-111655

Kabbage, M., Kessens, R., and Dickman, M. B. (2016). A plant Bcl-2-associated athanogene is proteolytically activated to confer fungal resistance. *Microb. Cell* 3, 224–226. doi: 10.15698/mic2016.05.501

Kang, C. H., Jung, W. Y., Kang, Y. H., Kim, J. Y., Kim, D. G., Jeong, J. C., et al. (2006). AtBAG6, a novel calmodulin-binding protein, induces programmed cell death in yeast and plants. *Cell Death Differ.* 13, 84–95. doi: 10.1038/sj.cdd.4401712

Kriegenburg, F., Jakopec, V., Poulsen, E. G., Nielsen, S. V., Roguev, A., Krogan, N., et al. (2014). A chaperone-assisted degradation pathway targets kinetochore proteins to ensure genome stability. *PLoS Genet.* 10:e1004140. doi: 10.1371/journal.pgen.1004140

Krishnan, K., and Askew, D. S. (2014a). Endoplasmic reticulum stress and fungal pathogenesis. *Fungal Biol. Rev.* 28, 29–35. doi: 10.1016/j.fbr.2014.07.001

Krishnan, K., and Askew, D. S. (2014b). The fungal UPR A regulatory hub for virulence traits in the mold pathogen Aspergillus fumigatus. *Virulence* 5, 334–340. doi: 10.4161/viru.26571

Kumar, S., Stecher, G., and Tamura, K. (2016). MEGA7: molecular evolutionary genetics analysis version 7.0 for bigger datasets. *Mol. Biol. Evol.* 33, 1870–1874. doi: 10.1093/molbev/msw054

Larkin, M. A., Blackshields, G., Brown, N. P., Chenna, R., McGettigan, P. A., McWilliam, H., et al. (2007). Clustal W and Clustal X version 2.0. *Bioinformatics* 23, 2947–2948. doi: 10.1093/bioinformatics/btm404

Leroch, M., Kleber, A., Silva, E., Coenen, T., Koppenhofer, D., Shmaryahu, A., et al. (2013). Transcriptome profiling of Botrytis cinerea conidial germination reveals upregulation of infection-related genes during the prepenetration stage. *Eukaryot. Cell* 12, 614–626. doi: 10.1128/EC.00295-12

Li, Y., and Dickman, M. (2016). Processing of AtBAG6 triggers autophagy and fungal resistance. *Plant Signal. Behav.* 11:e1175699. doi: 10.1080/15592324.2016.1175699

Li, Y., Kabbage, M., Liu, W., and Dickman, M. B. (2016). Aspartyl protease-mediated cleavage of BAG6 is necessary for autophagy and fungal resistance in plants. *Plant Cell* 28, 233–247. doi: 10.1105/tpc.15.00626

Li, Y., Williams, B., and Dickman, M. (2017). Arabidopsis B-cell lymphoma2 (Bcl-2)-associated athanogene 7 (BAG7)-mediated heat tolerance requires translocation, sumoylation and binding to WRKY29. *New Phytol.* 214, 695–705. doi: 10.1111/nph.14388

Livak, K. J., and Schmittgen, T. D. (2001). Analysis of relative gene expression data using real-time quantitative PCR and the 2(-Delta Delta C(T)) Method. *Methods* 25, 402–408. doi: 10.1006/meth.2001.1262

Lo Presti, L., Lopez Diaz, C., Turra, D., Di Pietro, A., Hampel, M., Heimel, K., et al. (2016). A conserved co-chaperone is required for virulence in fungal plant pathogens. *New Phytol.* 209, 1135–1148. doi: 10.1111/nph.13703

Luders, J., Demand, J., and Hohfeld, J. (2000). The ubiquitin-related BAG-1 provides a link between the molecular chaperones Hsc70/Hsp70 and the proteasome. *J. Biol. Chem.* 275, 4613–4617. doi: 10.1074/jbc.275.7.4613

Malhotra, J. D., and Kaufman, R. J. (2007). The endoplasmic reticulum and the unfolded protein response. *Semin. Cell Dev. Biol.* 18, 716–731. doi: 10.1016/j.semcdb.2007.09.003

Mayer, M. P., and Bukau, B. (2005). Hsp70 chaperones: cellular functions and molecular mechanism. *Cell Mol. Life Sci.* 62, 670–684. doi: 10.1007/s00018-004-4464-6

Minoia, M., Boncoraglio, A., Vinet, J., Morelli, F. F., Brunsting, J. F., Poletti, A., et al. (2014). BAG3 induces the sequestration of proteasomal clients into cytoplasmic puncta Implications for a proteasome-to-autophagy switch. *Autophagy* 10, 1603–1621. doi: 10.4161/auto.29409

Mori, K., Kawahara, T., Yoshida, H., Yanagi, H., and Yura, T. (1996). Signalling from endoplasmic reticulum to nucleus: transcription factor with a basic-leucine zipper motif is required for the unfolded protein-response pathway. *Genes Cells* 1, 803–817. doi: 10.1046/j.1365-2443.1996.d01-274.x

Mudholkar, K., Fitzke, E., Prinz, C., Mayer, M. P., and Rospert, S. (2017). The Hsp70 homolog Ssb affects ribosome biogenesis via the TORC1-Sch9 signaling pathway. *Nat. Commun.* 8:937. doi: 10.1038/s41467-017-00635-z

Oslowski, C. M., and Urano, F. (2011). Measuring er stress and the unfolded protein response using mammalian tissue culture system. *Methods Enzymol.* 490(Pt B), 71–92. doi: 10.1016/B978-0-12-385114-7.00004-0

Perpetua, N. S., Kubo, Y., Yasuda, N., Takano, Y., and Furusawa, I. (1996). Cloning and characterization of a melanin biosynthetic THR1 reductase gene essential for appressorial penetration of Colletotrichum lagenarium. *Mol. Plant Microbe Interact.* 9, 323–329. doi: 10.1094/MPMI-9-0323

Pincus, D., Chevalier, M. W., Aragon, T., van Anken, E., Vidal, S. E., El-Samad, H., et al. (2010). BiP binding to the ER-stress sensor Ire1 tunes the homeostatic

behavior of the unfolded protein response. *PLoS Biol.* 8:e1000415. doi: 10.1371/journal.pbio.1000415

Poulsen, E. G., Kampmeyer, C., Kriegenburg, F., Johansen, J. V., Hofmann, K., Holmberg, C., et al. (2017). UBL/BAG-domain co-chaperones cause cellular stress upon overexpression through constitutive activation of Hsf1. *Cell Stress Chaperones* 22, 143–154. doi: 10.1007/s12192-016-0751-z

Quidde, T., Buttner, P., and Tudzynski, P. (1999). Evidence for three different specific saponin-detoxifying activities in Botrytis cinerea and cloning and functional analysis of a gene coding for a putative avenacinase. *Eur. J. Plant Pathol.* 105, 273–283. doi: 10.1023/A:1008796006051

Raeder, U., and Broda, P. (1985). Rapid preparation Of DNA from filamentous fungi. *Lett. Appl. Microbiol.* 1, 17–20. doi: 10.1111/j.1472-765X.1985.tb01479.x

Ron, D., and Walter, P. (2007). Signal integration in the endoplasmic reticulum unfolded protein response. *Nat. Rev. Mol. Cell Biol.* 8, 519–529. doi: 10.1038/nrm2199

Ruegsegger, U., Leber, J. H., and Walter, P. (2001). Block of HAC1 mRNA translation by long-range base pairing is released by cytoplasmic splicing upon induction of the unfolded protein response. *Cell* 107, 103–114. doi: 10.1016/S0092-8674(01)00505-0

Schroder, M., and Kaufman, R. J. (2005). ER stress and the unfolded protein response. *Mutat. Res.* 569, 29–63. doi: 10.1016/j.mrfmmm.2004.06.056

Sitia, R., and Braakman, I. (2003). Quality control in the endoplasmic reticulum protein factory. *Nature* 426, 891–894. doi: 10.1038/nature02262

Sondermann, H., Ho, A. K., Listenberger, L. L., Siegers, K., Moarefi, I., Wente, S. R., et al. (2002). Prediction of novel Bag-1 homologs based on structure/function analysis identifies Snl1p as an Hsp70 co-chaperone in Saccharomyces cerevisiae. *J. Biol. Chem.* 277, 33220–33227. doi: 10.1074/jbc.M204624200

Sondermann, H., Scheufler, C., Schneider, C., Hohfeld, J., Hartl, F. U., and Moarefi, I. (2001). Structure of a Bag/Hsc70 complex: convergent functional evolution of Hsp70 nucleotide exchange factors. *Science* 291, 1553–1557. doi: 10.1126/science.291.5508.1553

Soulie, M. C., Perino, C., Piffeteau, A., Choquer, M., Malfatti, P., Cimerman, A., et al. (2006). Botrytis cinerea virulence is drastically reduced after disruption of chitin synthase class III gene (Bcchs3a). *Cell. Microbiol.* 8, 1310–1321. doi: 10.1111/j.1462-5822.2006.00711.x

Soulie, M. C., Piffeteau, A., Choquer, M., Boccara, M., and Vidal-Cros, A. (2003). Disruption of Botrytis cinerea class I chitin synthase gene Bcchs1 results in cell wall weakening and reduced virulence. *Fungal Genet. Biol.* 40, 38–46. doi: 10.1016/S1087-1845(03)0005-3

Takayama, S., and Reed, J. C. (2001). Molecular chaperone targeting and regulation by BAG family proteins. *Nat. Cell Biol.* 3, E237–E241. doi: 10.1038/ncb1001-e237

Takayama, S., Sato, T., Krajewski, S., Kochel, K., Irie, S., Millan, J. A., et al. (1995). Cloning and functional analysis of BAG-1: a novel Bcl-2-binding protein with anti-cell death activity. *Cell* 80, 279–284. doi: 10.1016/0092-8674(95)90410-7

Takayama, S., Xie, Z. H., and Reed, J. C. (1999). An evolutionarily conserved family of Hsp70/Hsc70 molecular chaperone regulators. *J. Biol. Chem.* 274, 781–786. doi: 10.1074/jbc.274.2.781

Thompson, J. E., Fahnestock, S., Farrall, L., Liao, D. I., Valent, B., and Jordan, D. B. (2000). The second naphthol reductase of fungal melanin biosynthesis in *Magnaporthe grisea*: tetrahydroxynaphthalene reductase. *J. Biol. Chem.* 275, 34867–34872. doi: 10.1074/jbc.M006659200

Townsend, P. A., Cutress, R. I., Sharp, A., Brimmell, M., and Packham, G. (2003). BAG-1: a multifunctional regulator of cell growth and survival. *Biochim. Biophys. Acta* 1603, 83–98. doi: 10.1016/S0304-419X(03)00002-7

Vandenheuvel, J., and Waterreus, L. P. (1983). Conidial concentration as an important factor determining the type of pre-penetration structures formed by botrytis-cinerea on leaves of french bean (Phaseolus-Vulgaris). *Plant Pathol.* 32, 263–272. doi: 10.1111/j.1365-3059.1983.tb02833.x

Verghese, J., and Morano, K. A. (2012). A lysine-rich region within fungal BAG domain-containing proteins mediates a novel association with ribosomes. *Eukaryot. Cell* 11, 1003–1011. doi: 10.1128/EC.00146-12

Viefhues, A., Heller, J., Temme, N., and Tudzynski, P. (2014). Redox systems in botrytis cinerea: impact on development and virulence. *Mol. Plant Microbe Interact.* 27, 858–874. doi: 10.1094/Mpmi-01-14-0012-R

Williams, B., Kabbage, M., Britt, R., and Dickman, M. B. (2010). AtBAG7, an Arabidopsis Bcl-2-associated athanogene, resides in the endoplasmic reticulum and is involved in the unfolded protein response. *Proc. Natl. Acad. Sci. U.S.A.* 107, 6088–6093. doi: 10.1073/pnas.0912670107

Williamson, B., Tudzynski, B., Tudzynski, P., and van Kan, J. A. (2007). Botrytis cinerea: the cause of grey mould disease. *Mol. Plant Pathol.* 8, 561–580. doi: 10.1111/j.1364-3703.2007.00417.x

You, Q., Zhai, K., Yang, D., Yang, W., Wu, J., Liu, J., et al. (2016). An E3 Ubiquitin Ligase-BAG protein module controls plant innate immunity and broad-spectrum disease resistance. *Cell Host Microbe* 20, 758–769. doi: 10.1016/j.chom.2016.10.023

Zhang, C. H., He, Y. F., Zhu, P. K., Chen, L., Wang, Y. W., Ni, B., et al. (2015). Loss of bcbrn1 and bcpks13 in Botrytis cinerea not only blocks melanization but also increases vegetative growth and virulence. *Mol. Plant Microbe Interact.* 28, 1091–1101. doi: 10.1094/Mpmi-04-15-0085-R

Zhang, X. R., Henriques, R., Lin, S. S., Niu, Q. W., and Chua, N. H. (2006). Agrobacterium-mediated transformation of *Arabidopsis thaliana* using the floral dip method. *Nat. Protoc.* 1, 641–646. doi: 10.1038/nprot.2006.97

Conflict of Interest Statement: The authors declare that the research was conducted in the absence of any commercial or financial relationships that could be construed as a potential conflict of interest.

frontiers in Plant Science

ORIGINAL RESEARCH
published: 17 May 2019
doi: 10.3389/fpls.2019.00633

Spatial Effects and GWA Mapping of Root Colonization Assessed in the Interaction Between the Rice Diversity Panel 1 and an Arbuscular Mycorrhizal Fungus

*Hazel Davidson, Roshi Shrestha, Thomas Cornulier, Alex Douglas, Tony Travis, David Johnson† and Adam H. Price**

Institute of Biological and Environmental Sciences, University of Aberdeen, Aberdeen, United Kingdom

OPEN ACCESS

Edited by:
Marco Catoni, University of Birmingham, United Kingdom

Reviewed by:
Katsuharu Saito, Shinshu University, Japan
Vanesa Silvani, University of Buenos Aires, Argentina
Cristiana Sbrana, Istituto di Biologia e Biotecnologia Agraria (IBBA), Italy

***Correspondence:**
Adam H. Price
a.price@abdn.ac.uk

†Present address:
David Johnson, School of Earth and Environmental Sciences, The University of Manchester, Manchester, United Kingdom

Specialty section:
This article was submitted to Plant Microbe Interactions, a section of the journal Frontiers in Plant Science

Received: *31 January 2019*
Accepted: *26 April 2019*
Published: *17 May 2019*

Citation:
Davidson H, Shrestha R, Cornulier T, Douglas A, Travis T, Johnson D and Price AH (2019) Spatial Effects and GWA Mapping of Root Colonization Assessed in the Interaction Between the Rice Diversity Panel 1 and an Arbuscular Mycorrhizal Fungus. Front. Plant Sci. 10:633. doi: 10.3389/fpls.2019.00633

If water saving methods of rice management are to be adopted, the interaction between rice plants and arbuscular mycorrhizal (AM) fungi will grow in agronomic significance. As yet there are very few studies on the interaction between rice and AM fungi and none on host genetics. A subset 334 cultivars from the Rice Diversity Panel 1 were grown in 250 L boxes filled with phosphorus (P) deficient aerobic soil without addition, with added rock phosphate and with rock phosphate and the AM fungus *Rhizophagus irregularis*. Statistical analysis of position of plants revealed a positive effect of their neighbors on their dry weight which was stronger in the presence of rock phosphate and even stronger with rock phosphate and AM fungi. A weak but significant difference in the response of cultivars to AM fungus treatment in terms of shoot dry weight (SDW) was revealed. Neighbor hyphal colonization was positively related to a plant's hyphal colonization, providing insights into the way a network of AM fungi interact with multiple hosts. Hyphal colonization ranged from 21 to 89%, and 42% of the variation was explained by rice genotype. Colonization was slightly lower in *aus* cultivars than other rice subgroups and high in cultivars from the Philippines. Genome wide association (GWA) mapping for hyphal colonization revealed 23 putative quantitative trait loci (QTLs) indicating there is an opportunity to investigate the impact of allelic variation in rice on AM fungal colonization. Using published transcriptomics data for AM response in rice, some promising candidate genes are revealed under these QTLs being a calcium/calmodulin serine/threonine protein kinase at 4.9 Mbp on chromosome 1, two ammonium transporters genes at 24.6 Mbp on chromosome 2 and a cluster of subtilisin genes at 1.2 Mbp on chromosome 4. Future studies should concentrate on the biological significance of genetic variation in rice for AM colonization.

Keywords: *Oryza sativa*, *Rhizophagus irregularis*, *Glomus intraradices*, common mycorrhizal network, GWA mapping, QTL

INTRODUCTION

The symbiotic interaction between land plants and mycorrhizal fungi is ancient and is thought to be driven by the provision of nutrients (particularly P and N) to the plant in exchange for carbon (Smith and Read, 2008) in the form of sugar and lipids (Keymer and Gutjahr, 2018). Most grasses, including major crop plants, form symbioses with arbuscular mycorrhizal (AM) fungi that can affect agricultural plant productivity (Van Der Heijden et al., 2015), but research on the interaction between the grass crop rice and AM fungi has been very limited. This is probably because in flooded soil, in which most rice is grown, this association is traditionally considered unimportant. It has, for example, been shown that in flooded conditions AM fungi are very scarce on rice (Ilag et al., 1987) while it has been demonstrated that flooding of aerobically-grown rice roots decreases AM fungal colonization within 7 days- although it does not eliminate AM fungi completely (Vallino et al., 2014). Fieldwork has begun to provide evidence for an impact of AM fungi on rice productivity in upland (aerobic) soils (Maiti et al., 2011) but not for flooded rice. Yet as water availability and sustainability of crop production grow as drivers for crop management decisions [see for example page 8–9 in Bouman et al. (2007)], it can be predicted that increasing amounts of the world's rice production will adopt one of a number of water saving techniques including aerobic rice, alternate wetting and drying or the system of rice intensification (SRI) (Bouman et al., 2007, p. 19–28). Under these growing conditions, rice-AM fungi interactions are more likely to be important. Indeed it has recently been shown that AM fungi colonization and AM fungal species richness were substantially higher under SRI (which includes a more aerobic soil condition) than conventional flooding (Watanarojanaporn et al., 2013). So it is timely to investigate the interaction more closely in order to consider the possibility that future rice breeding might need to incorporate the knowledge gained.

Molecular characterization of the AM fungi-rice interactions has provided insight into the biology of the interaction (Güimil et al., 2005; Campos-Soriano et al., 2012; Gutjahr et al., 2015). However, there has been almost no studies investigating if there are differences between rice cultivars in their interaction with AM fungi and no studies on the host genetics of the interaction. In a comparison of six upland cultivars from China, one was found to have much lower colonization when infected by either of two AM fungi (Gao et al., 2007), while Li et al. (2016) found differences in colonization of six cultivars with *Rhizophagus intraradices*. In the field in Italy no differences in colonization between 12 cultivars was detected (Vallino et al., 2009). Suzuki et al. (2015) assessed the growth response of 64 cultivars of rice to *Funneliformis mosseae* and found wide differences (from −4 to +119%). The authors assessed colonization in 12 cultivars (names not specified) and although this did differ between cultivar it did not related to the degree of growth response. We are not aware of any other studies that assessed differences in colonization between rice cultivars.

While there have been no studies on genetic mapping AM fungal interaction in rice, there have been on other crops. Leiser et al. (2016) found very little evidence of QTLs for AM colonization in sorghum probably because of weak repeatability between replicates. In contrast, Lehnert et al. (2017) examining wheat found strong genetic variation but still rather weak evidence of quantitative trait loci (QTLs) suggesting AM colonization is controlled by small effect genes, meaning QTLs and potential candidate genes reported are speculative. Finally, De Vita et al. (2018) screened 108 durum wheat cultivars for colonization by *R. irregularis* and *F. mosseae*, detecting substantial variation and seven putative QTLs by genome wide association (GWA) mapping.

In this study, the well characterized global collection of rice cultivars, the Rice Diversity Panel 1 (Zhao et al., 2011) was screened for growth and colonization in response to inoculation with the 'model' AM fungus *R. irregularis* (formerly known as *Glomus intraradices*). This species has been found colonizing aerobically-grown rice roots in India (Bhattacharjee and Sharma, 2011) and dominating them in Italy (Vallino et al., 2009), and was the first AM fungus sequenced (Tisserant et al., 2013; Van Der Heijden et al., 2015).

The main aim of this study was to test the hypothesis that there is genetic variation within rice for the colonization and the impact of AM fungus *R. irregularis*, and that these are correlated. Further, we test the hypothesis that genetic variation for AM fungal colonization can be genetic mapped. This was done using 334 accessions of the Rice Diversity Panel 1, allowing GWA mapping since there are 5.2 million SNP markers available for this population (Wang et al., 2018). To provide phenotype data that are relevant, discriminating and achievable required that a time-efficient screening system be developed. The design of the boxes used, specifically the competitive nature of the arrangement of plants, allowed three further hypotheses to be tested; (1) that spatial relationships between the rice plants affect the growth of the rice plant, (2) that the degree of neighbor interactions is different if an AM fungus is present, and (3) that AM fungal colonization rates are affected by the size and AM fungal colonization of neighboring plants.

MATERIALS AND METHODS

Rice Genotypes

A random set of 334 accessions of the Rice Diversity Panel 1 (RDP1) (Zhao et al., 2011) was used for this study (see **Supplementary Table S1**). RDP1 represents 372 cultivars which come from the five subpopulations of rice (indica, aus, tropical japonica, temperate japonica, and aromatic). The cultivars have been genotyped using the High-Density Rice Array (HDRA) of 700,00 SNPs, with ∼1 informative SNP per kb (McCouch et al., 2016) and this data base has recently been extended to 5.2 million SNPs by imputation (Wang et al., 2018). In addition to the RDP1, cultivars Azucena and Bala which have been continuously grown in Aberdeen from seed originally obtained from the International Rice Research Institute were used as local check cultivars. These are distinguished from the Azucena and Bala in the RDP1 population by referring to them as "Own Azucena" and "Own Bala."

AM Inoculum

Rhizophagus irregularis inoculum was purchased from INVAM, United States and amplified in maize by growing three plants per pot in four pots of 2.5 L capacity filled with fine sand, each pot receiving 60 g of inoculum. These were fed weekly with zero P Yoshida's nutrient solution (Yoshida et al., 1976) and on two occasions 1/4 P was included in the nutrient solution. After 3 months growth, when 100% hyphal colonization was confirmed in subsampled roots, the maize plants were dried by withholding water, the roots cut into fine pieces and the roots and sand used as inoculum.

Soil

Throughout, the soil used was a mixture of 1 part subsoil from Insch Field Farm [previously described in MacMillan et al., 2006 (available P 12.24 $\mu g\ g^{-1}$, total P 814 $\mu g\ g^{-1}$)] and 3 parts fine sand (Sibelco UK; available P 1.95 $\mu g\ g^{-1}$, total P 12.2 $\mu g\ g^{-1}$). This was chosen as previous research had shown it suitable for experiments on P response (Al-Ogaidi, 2013).

Greenhouse Conditions

All experiments were conducted in the Cruickshank Greenhouse of the University of Aberdeen where the temperature is set to 25°C and plants received ambient light plus 12 h a day of supplementary light of approximately 150 $\mu M\ m^{-2}\ s^{-1}$ PAR.

AM Colonization Measurement

The proportion of roots containing hyphae, arbuscules or vesicles of the AM fungus was assessed using the magnified intersections method of McGonigle et al. (1990) and slight modifications of the staining method of Vierheilig et al. (1998). Roots were washed to be free of soil and stored in 60% ethanol. Approximately 8–12 fine root sections of 3–4 cm in length were selected at random from the central portion of the root. After washing out the ethanol, they were bathed in 10 ml of 10% KOH at 90°C for 10 min. After clearing, samples were rinsed in cold water and acidified by dipping in 1% HCl for 30 s and then transferred to test tubes containing 8 ml of 1% ink (Parker's Quink Black) in 1% HCl at 85°C for 4 min. This was followed by degassing under vacuum (while still in the stain) for 2 min. Samples were then washed in water to remove excess stain. Finally, they were transferred into sample storage jars containing lactic acid and glycerol (1:1:14 glycerol:water:lactic acid) de-stain for at least 24 h. These were mounted on microscope slides in glycerol. The proportion of approximately 100 root-graticule intersections observed for each plant containing a visible fungal hyphae, or an arbuscle or a vesicle was recorded. Hyphal colonization was calculated as the sum of all three of those since an arbuscle and a vesicle must be accompanied by a hyphae.

Optimizing the Screening Method

Four preliminary experiments were conducted in order to optimize the screening methodology.

Dose Response

A dose experiment was conducted in the greenhouse using 1 L pots where 200 ml of soil/sand mix was placed at the bottom, 500 ml was placed in the middle and 100 ml on top. Different concentrations of inoculum were incorporated into the middle portion to give seven treatments being of 0, 1, 2, 5, 10, and 20% with an addition 10% autoclaved inoculum. Four replicates were used. Surface sterilized seeds of Azucena were placed in each pot and grown for 8 weeks with 200 ml of Yoshida's nutrient minus P being given twice a week. SDW and colonization were assessed. This revealed no impact of the autoclaved inoculum on plant growth, AM fungi substantially reduced growth, 1% inoculum had a smaller effect, while the other treatments were identical. Hyphal colonization were not different between 2, 5, and 20% inoculum. No more than 2% was therefore considered an appropriate rate of inoculation. Importantly, no hyphae were observed in the 0 and 10% autoclaved treatments (in 12–14 roots of 4 replicate plants of both treatments) indicating the subsoil used is not a source of AM inoculum.

Time Course

A time course was conducted in which 1 and 10% inoculation (using the same pots, soil, filling methods, rice genotype and growth conditions as described above) were harvested at 21, 36, and 51 days. Arbuscles, vesicles, and hyphal colonization was assessed (**Figure 1**). The colonization rate increased with time (from 19–65%) but while 1% inoculum consistently showed a lower colonization rate than 10% inoculum, there was no interaction between dose and time (based on two way ANOVA $P > 0.05$). It was considered that a dose of 1% or more and a 4 weeks growth period should be suitable for studying the genetics of AM fungus-rice interactions.

AM Fungi and Rock Phosphate

A third preliminary experiment was conducted to examine the interaction between AM fungus and rock phosphate using pots, soils, soil filling, rice genotype and plant growth conditions as above. Treatments with 0, 50, 100, 200, and 300 mg of rock phosphate per pot were applied with and without AM fungi at 2% with four replicates. At 4 weeks, SDW and leaf P uptake were assessed while the AM colonization was assessed on the AM fungus treatment. AM treatment reduced SDW by 25% but rock phosphate did not affect it. AM fungus reduced leaf P concentration (from 1.47 to 1.08 mg g^{-1}: $P < 0.001$) while rock phosphate increased it (from 1.08 to 1.46 mg g^{-1}: $P = 0.022$) and there was no interaction. Rock phosphate increased hyphal colonization in a linear fashion (0 = 27%, 50 = 36%, 100 = 42%, 200 = 49%, and 300 = 61%; $P = 0.035$). This experiment suggested adding rock phosphate did not affect growth of these plants at this young age but did increase AM colonization.

Genetic Variation in Two Cultivars

A final preliminary experiment determined if there were genetic differences in colonization rates by testing cultivars Azucena and Bala [parents of the mapping population described in Price et al. (2000)]. Zero and 300 mg rock phosphate and zero and 2% AM fungus inoculation were used in a fully factorial design with four replicates. Other conditions were as above. Root and shoot fresh weight (not dry weight) were recorded. The AM fungus reduced the root weight of both cultivars ($P = 0.010$) but it did not

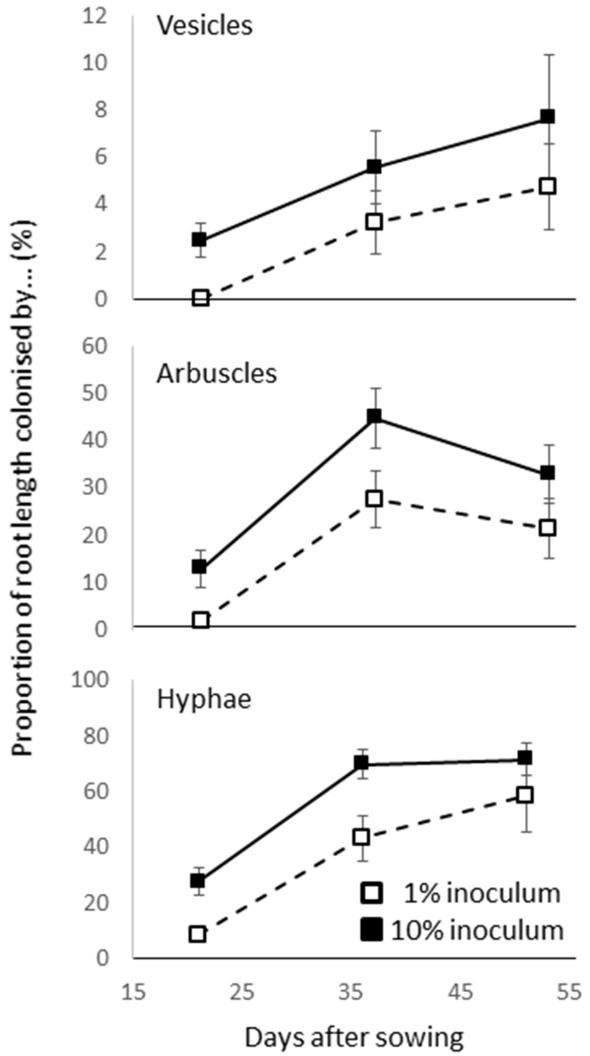

FIGURE 1 | Arbuscular mycorrhizal (AM) colonization of roots in preliminary time course experiment in which cultivar Azucena was inoculated with 1 and 10% inoculum and the presence of vesicles, arbuscles, and hyphae were assessed on three occasions. Bar is standard error (n = 4).

affect shoot weight while rock phosphate increased shoot weight (P = 0.013) but did not affect root weight. There was a highly significant genotype by rock phosphate by AM fungus interaction for % root mass (root fresh weight/total fresh weight × 100) (P = 0.004) which was high in both cultivars in the absence of rock P (65–67%) but was lowest for Azucena with rock phosphate and AM fungus (61%) and lowest in Bala with rock phosphate but without AM fungus (58%). There was a highly significant difference in hyphal colonization rate between Bala and Azucena (P < 0.001) (Azucena 55.1%, Bala 30.4%), and a significant interaction between rock phosphate and cultivar (P = 0.010) where colonization was halved in Bala by rock phosphate (from 40.7 to 20.1%) but Azucena was not affected. It was concluded that treatment with rock phosphate may increase the ability to discriminate between cultivars.

Screening the Rice Diversity Panel 1

Boxes were built from plywood 3 m long, 0.85 m wide and approximately 0.35 m deep and lined with plastic sheet. They were then divided into three 1 m long sections orientated north to south using stiff plastic and each section filled with subsoil/sand mix according to three treatments to a depth of 0.3 m (approximately 250 L of subsoil/sand in each) (**Figure 2**). A control treatment had no additions, a rock phosphate treatment (RP) had 100 mg per plant placed in a band in the top 10 cm and a rock phosphate and AM fungus treatment (RP + AM) had 100 mg per plant rock phosphate and 1% AM fungal inoculum placed in a band in the top 10 cm. Two surface-sterilized seeds of 334 cultivars of the Rice Diversity Panel 1 were sown completely randomized in a grid pattern of 17 × 20 with a spacing of 5 cm between plants. The same randomization was used for each of the three treatments within a replicate run. After germination, plants were thinned to one. Plants were watered daily while every other day they received Yoshida's nutrient solution without P so that they received approximately 0.125 L each (equivalent to 5 mg of N which would produce a plant of approximately 0.25 g shoot dry weight (SDW) if not restricted by P). After 4 weeks growth, shoots were harvested for dry weight measurement while for the AM treatment alone the roots were harvested for colonization assessment. The experiment was repeated in four replicate runs starting on 15th May, 29th May, 9th July, and 23rd July 2013 each with a different randomization of the 334 genotypes. The order of the treatments was also randomized between runs and consisted of, from south to north run 1 Control:RP + AM:RP; run 2 AM + RP:RP:Control; run 3 RP + AM:RP:Control; run 4 RP:Control:RP + AM. Note AM hyphal colonization were assessed on 4–6 plants from the control and RP treatment in every run. On one occasion, 12% colonization was found, but the vast majority of samples contained no evidence of colonization.

Spatial Statistics

Spatial and genetic variation in SDW was modeled using generalized additive mixed models, assuming a Gaussian error after log transformation, in order to stabilize the variance. Hyphal colonization (%) was modeled using generalized additive mixed models, assuming a Gaussian error. The models included a combination of fixed, smooth and random effects listed in **Table 1**, as well as second-order interactions between the fixed effects. The models were fitted by REML with the gamm and gamm4 functions of the R packages 'mgcv' and 'gamm4,' respectively (Wood et al., 2013). For the SDW analysis, the 'Variety' random intercept was nested in 'Subgroup,' and a genotype by treatment interaction was evaluated by fitting the corresponding random effect (see **Table 1**). We tested if separate spatial trends (smoothing splines) were required for each block, box or run, or if all 4 runs could be suitably described by a common spatial trend, using the Bayesian Information Criterion as an indication of most parsimonious model. For the hyphal colonization analysis, we used a 'Variety' random intercept nested in 'Subgroup.' Spatial dependence of hyphal colonization of the focal plant on the colonization of its immediate neighbors was

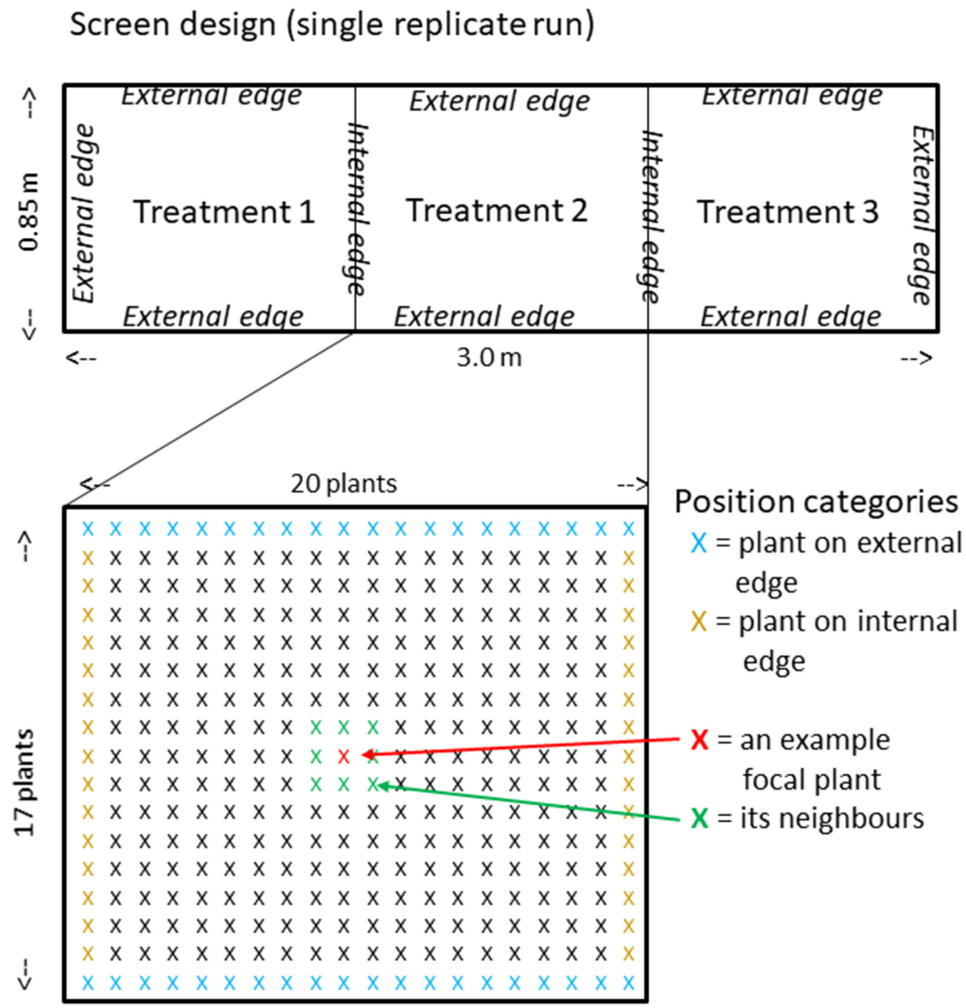

FIGURE 2 | RDP1 screen design. Above, plan of the three treatments (randomly allocated) of each replicate run showing internal and external edges. Below, expanded plan of single central treatment showing individual plants (marked with X) highlighting plants on external and internal edges, plus a graphic explanation of the meaning of neighbors in relation to a focal plant.

modeled using a Markov random field (MRF) smoother within each block. For both analyses, fixed effects were selected or discarded based on the significance of the p-values of their coefficients (Null hypothesis: coefficient value is zero).

A Pot Experiment on 16 Cultivars

Using 16 cultivars selected to have a range of colonization in the screen of the RDP1, colonization rate was assessed in plants grown in 500 ml pots as described in the optimization steps above using a complete randomized block design with four replicate blocks. They were inoculated with 2% AM fungus inoculum, sown on the August 6th, 2015 and grown in the greenhouse as described earlier. After 32 days they were harvested and colonization assessed as described above.

Genome Wide Association Mapping

Genome wide association mapping was performed with the 5.2 m SNP database (Wang et al., 2018) using a mixed model approach on all the cultivars implemented using EMMA (Efficient Mixed Model Analysis) (Yu et al., 2006), as described in Norton et al. (2014) (a SNP was selected as worth reporting if the *P*-value was <0.0001 and if the minor allele frequency (MAF) was $>5\%$). The false discovery rate (FDR) of detected associations was estimated using the R-language Bioconductor "multtest" library to calculate Benjamini–Hochberg adjusted probabilities (Benjamini and Hochberg, 1995). A significance threshold of 10% FDR is normally used to identify putative SNP associations (McCouch et al., 2016) but it is not uncommon for no SNPs to reach this conservative threshold.

Significant SNPs within 200 kb of each other (based on consideration of linkage disequilibrium decay reported in this population as suggested by Zhao et al., 2011) were considered to represent SNP clusters of the same QTL and singleton SNPs were not considered QTLs (there must be at least 1 other SNP with $P < 0.001$ within 200 kb). Gene annotation was examined 200 kb either side of the most significant SNP of a QTL.

TABLE 1 | Predictors used in the spatial statistical models.

Variable name	Type	Fixed/random	Levels	Definition
Run*§	Categorical	Fixed	1, 2, 3, 4	Time block over which experiment was run
Treatment*	Categorical	Fixed	RP, AM + RP, Control	Experimental treatment
Treatment by Variety*	Categorical	Random (by Variety)	RP, AM + RP, Control	Genotype by treatment interaction
Edge*§	Categorical	Fixed	0 (Away from edge), 1 (Along edge)	Location of plant with respect to box edge
Exterior*§	Categorical	Fixed	0 (Away from edge), 1 (Along external edge of box)	Is plant on an external box edge (as opposed to internal box edge separating treatment blocks)?
Neigh.SDW*§	Numeric	Fixed		Mean SDW of 1st-order neighbors
X, Y*	Numeric	Bivariate smoothing spline		Describes smooth spatial trends in response variable
MRF§	Categorical	Markov random field	One per observation	Describes the dependence of focal plant hyphal colonization (HC) on neighbors HC (spatial autocorrelation)
Run*	Categorical	Indicator for the smoothing spline	1, 2, 3, 4	When used, a separate smooth spatial trend was estimated for each run
Box*	Categorical	Indicator for the smoothing spline	1, 2	When used, one smooth spatial trend was estimated for each breeding box (holding 3 treatments each)
Block*§	Categorical	Indicator for the smoothing spline	12 levels (3 treatments × 4 runs)	When used, one smooth spatial trend was estimated for each treatment block within a breeding box
Subgroup*§	Categorical	Random	7 levels: (n = 132), "ADMIX" (n = 417), "AROMATIC" (n = 144), "AUS" (n = 648), "IND" (n = 759), "TEJ" (n = 984), "TRJ" (n = 996)	Rice genotypic ensemble
AP.Variety*§	Categorical	Random	(334 levels)	Rice variety

*Predictors used in shoot dry weight model are denoted by * and those in the hyphal colonization model are denoted with §.*

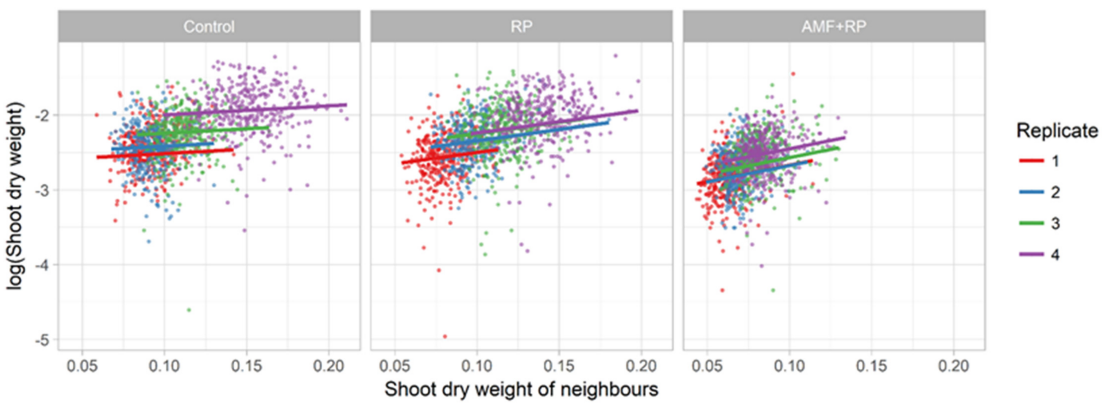

FIGURE 3 | Plot of log shoot dry weight (SDW) of focal plant against the SDW of its neighbors, for each treatment. The positive effect is significant in all treatments ($P < 0.005$), with a slope increasing from Control to RP + AMF. For RP + AMF slope (effect) = 4.40 ± 0.53 (SE); for RP slope = 3.03 ± 0.39; for Control slope = 1.21 ± 0.40. Comparison of slopes between treatments are different as follows; Control to RP $P = 0.0006$; RP to RP + AMF $P = 0.033$.

RESULTS

Shoot Dry Weight

The mean values for SDW and AM colonization rate are provided in **Supplementary Table S1**. SDW was affected by treatment such that the RP + AM plants were smaller while the other two treatments were only marginally different. Replicate runs, neighbor's size, position within the box and cultivar all had an effect on SDW at least as large as treatment. With replicate run, there was a gradual increase in SDW with number such that the averages were 78, 87, 102, and 125 mg per plant for runs 1–4, respectively. The spatial statistical analysis showed that plants on an external edge were slightly bigger than those that were not (103 mg vs. 98). More strikingly, plants on an internal edge were bigger than those that were not (110 mg vs. 97). The focal plant was larger when its neighbors were larger, and this positive effect of the neighbors' average size was greater in the AM + RP than in the RP treatments, and least in the control treatment (**Figure 3**).

The most parsimonious description of the spatial trends in plant SDW involved a significant spatial trend, common across all replicates ($P = 1.28 \times 10^{-12}$, Bayesian Information Criterion difference with models involving different spatial trends per box or block was greater than 15), which suggested an effect of the general orientation of the experimental setup in the greenhouse (see spatial trend in **Supplementary Figure S1**), independent of the position of the treatment in the box.

Once variation due to position and neighbors was removed from the data by subtracting their estimated effect from the observations, a two way analysis of variance (factors; treatment and genotype) on the SDW of the controls and rock phosphate treatment demonstrated a weakly significant effect of the rock phosphate treatment ($P = 0.045$) explaining less than 1% of the variation with rock phosphate stimulating growth (84.6 vs. 83.6 mg) and no cultivar by treatment interaction, while cultivar explained 68% of the non-spatial variation. This contrasts to ANOVA performed before the spatial analysis was conducted in which treatment and cultivar together only explained 30% of the total variation. When comparing rock phosphate to rock phosphate and AM fungus, the proportion of variation explained by treatment, cultivar and their interaction was 67% where it was only 49% before spatial correction. In this comparison, cultivar explained 50.1% of the variation, treatment 15.8% and the interaction 3.9%, the latter being small but highly significant ($P < 0.001$). Thus there is no evidence that cultivar relative performance differed between the control and rock phosphate treatment but it did when AM fungus was introduced. Ranking cultivars by their responsiveness to AM treatment (SDW ratio RP + AM:RP treatment) did not reveal any discernible pattern (between subpopulations or country/region of origin for example).

Scatter plots of SDW for control vs. rock phosphate and for rock phosphate vs. rock phosphate plus AM fungus are shown in **Figures 4A,B**, respectively. These show the regression line and the 1:1 line (dashed). It clearly demonstrates the lack of effect of rock phosphate (**Figure 4A**), and the negative effect of AM fungus on SDW (**Figure 4B**). The correlation is better for the upper graph indicating that cultivar performance is more divergent in the comparison between rock phosphate and rock phosphate plus AM fungus.

There was a difference in the SDW between subpopulations of the Rice Diversity Panel 1 which was consistent between treatments ($P < 0.001$, $R^2 = 14.7$–18.2%), where aus ($n = 54$) and indica ($n = 63$) were high, tropical japonica ($n = 83$) were lower and temperate japonica ($n = 82$) were lowest (**Figure 5**).

Hyphal Colonization

Hyphal colonization was roughly normally distributed in each run (**Supplementary Figure S1**) while both proportion of roots with arbuscles and vesicles were skewed toward low numbers and many zeros (**Supplementary Figure S1**). One way ANOVA on the raw data indicated heritability for proportion of roots with hyphae, arbuscles, and vesicles were 39, 29, and 35%, respectively. Mean hyphae colonization was highly correlated with mean arbuscles ($r = 0.554$, **Supplementary Figure S1**), and mean vesicles ($r = 0.700$, **Supplementary Figure S2C**). Based on these observations, it was decided that further analysis would be conducted on the hyphal colonization data alone.

Spatial analysis indicated hyphal colonization of a particular plant increased with its SDW ($P = 0.026$) and the mean SDW of its nearest (8) neighbors ($P = 0.0012$). The interaction between the effects of focal plant and neighbors' SDWs was close to significant ($P = 0.066$) (**Figure 6B**) so the data did not provide clear support for one model over the other. In other words, the difference in the predictions of the simple additive model and of the interactive model was small (**Figures 6A,B**). Both models agreed that large SDW of either the focal plant or its neighbors increased hyphal colonization of focal plant in similar ways.

The model indicated significant and idiosyncratic spatial trends in each of the four replicates (Markov Random Field component: $P < 2 \times 10^{-16}$; see **Supplementary Figure S3**). This spatial analysis allowed for a correction of estimation of the colonization of the plants such that the proportion of variation in colonization explained by cultivar (from one way ANOVA) increased from 35 to 42% with heritability increased from 39 to 54%. The mean colonization rates for each cultivar are presented in **Supplementary Table S1** while **Figure 7** shows a histogram of the distribution. The average coefficient of variation for the trait was 0.25 (it was 0.30 before spatial analysis). The range in colonization was considerable, from the Bangladesh aus cultivar DZ 193 at 22.9 ± 8.3% (±standard deviation) to the Chinese indica cultivar Kun Min Tsieh Hunan at 89.8 ± 9.3%. Colonization rates differed between subgroup ($P < 0.001$) where indica, temperate japonica and tropical japonica were similar (58.0, 54.5, and 55.0%, respectively) while aus were lower (50.0%) (**Figure 5**). Within each subgroup there were large variations but it is considered noteworthy that while there were several aus cultivars in the top 30 cultivars, there were no indicas in the lowest 30 cultivars. Differences were also detected between countries or regions (country groups when individual countries had less than 10 cultivars) ($P < 0.001$, $R^2 = 12.7\%$) where the Philippines and China were high and Bangladesh and United States were low (**Supplementary Figure S4**). These differences are probably partly driven by different subgroup compositions for countries (e.g., Bangladesh is dominated by aus cultivars) but in the tropical japonica subgroup there is still a detectable country/region difference ($P = 0.006$, $R^2 = 26.3\%$) where the six Philippine cultivars had higher colonization (71.9%) than 13 South American (55.7%), 15 West African (55.0%), 10 SE Asian (55.0%), and 15 United States (49.5%) cultivars.

Pot Experiment on 16 Cultivars

The colonization of 16 cultivars grown in pots differed significantly ($P = 0.002$) and cultivar explained 50% of the variation. Conducting a two way ANOVA on colonization data from both the full RDP1 screen and the pot experiment with factors cultivar and method (pot or RDP screen) found the model explained 62% of the variation and indicated all factors were significant at $P < 0.001$, including the cultivar by method interaction ($F = 27.8$, 5.6, and 3.1 for cultivar, method and interaction, respectively). Colonization in pots is plotted against the results obtained in the RDP1 screen in **Figure 8**.

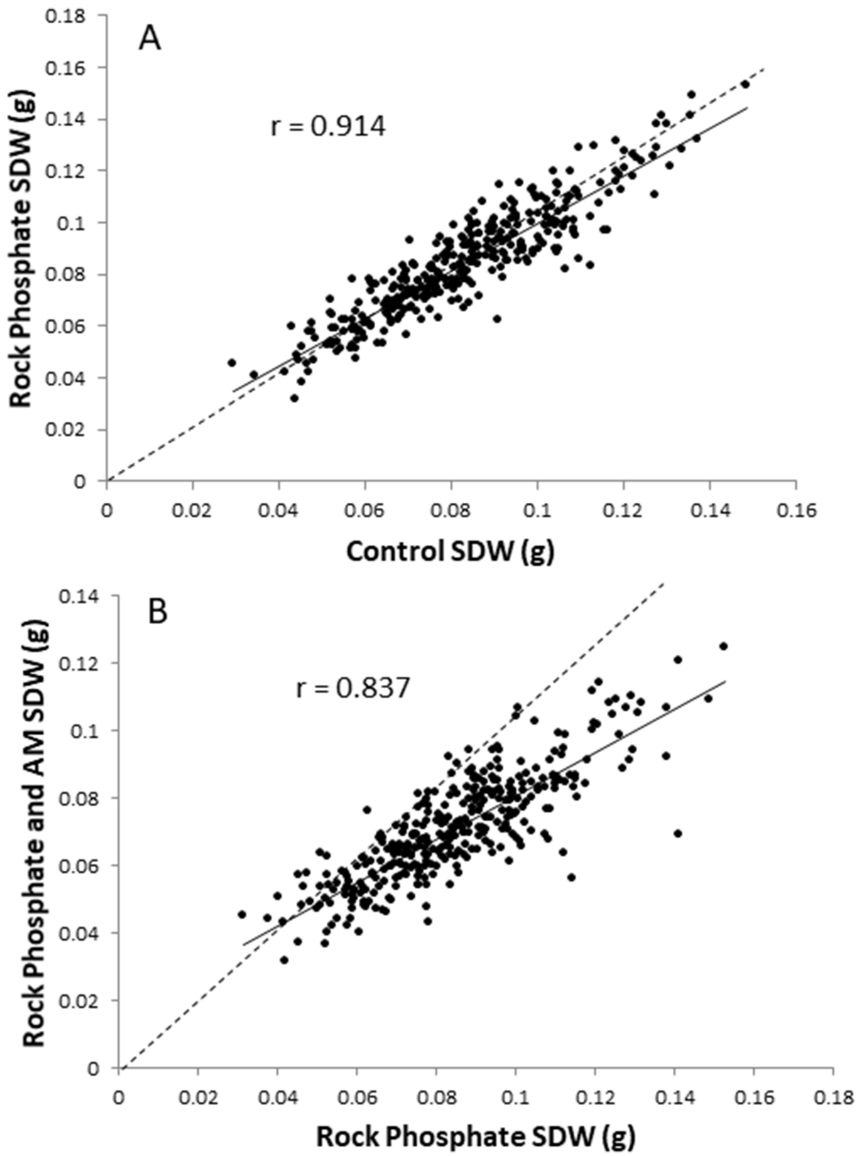

FIGURE 4 | Plots of RDP1 cultivar mean SDW using spatially corrected data; **(A)** control vs. rock phosphate treatment; **(B)** rock phosphate vs. rock phosphate + AM fungus treatment. Solid line is regression, dotted line is 1:1 line.

There is no correlation between the colonization rates obtained in the two experiments. However, it is remarkable how close most of the cultivars are to the 1 to 1 line indicating most performed very similarly in both experiments. Three cultivars (Ta Mao Tsao, Lusitano and Agostano) appear to have very substantially different colonization rates in the pot. Indeed, if these three are removed, the remaining 13 cultivars correlate with $r = 0.806$.

GWA Mapping

The results of GWA mapping for the hyphal colonization with all subgroups is presented in **Supplementary Figure S5** and summarized in **Table 2** while the results of analysis with the All analysis (all cultivars) is graphed for more clarity in **Figure 9**. No SNPs were considered significant using the FDR of 10%. In total 23 putative QTLs were revealed in the analysis of all cultivars using the criteria that for at least 1 SNP $P < 0.0001$ and MAF $> 5\%$ and there is at least one other SNP with $P < 0.001$ within 200 kb. A further two putative QTLs were identified either in the aus subpopulation or both the aus and tropical subpopulation. No putative QTLs were detected in the indica or temperate japonica subpopulations. Genes within 200 kb of the most significant SNPs were listed and their responsiveness to AM colonization as reported by Fiorilli et al. (2015) and Gutjahr et al. (2015) is given in **Supplementary Table S2**. The number of genes in the lists ranges from 50 to 99 and they had an average of 8.8% of genes being differentially expressed in either Fiorilli et al. (2015) or Gutjahr et al. (2015) or both.

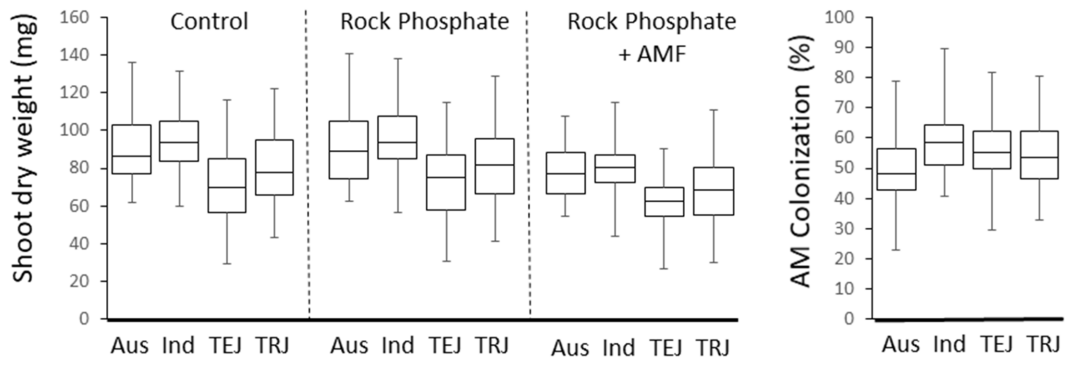

FIGURE 5 | Boxplots of SDWs of each treatment, and hyphal colonization in the four main rice subgroups.

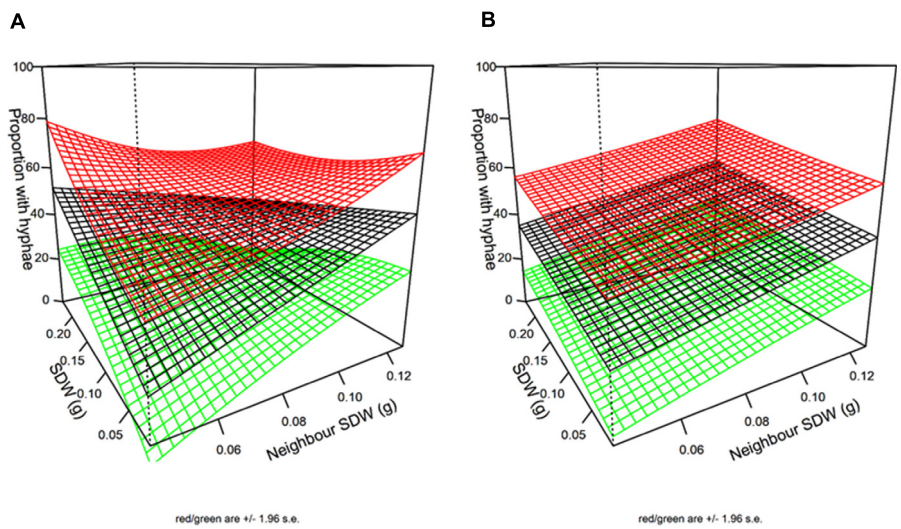

FIGURE 6 | 3D plots of the impact of neighbor and first order neighbor SDW (SDW) on hyphal colonization. The additive model **(A)** and the interactive model **(B)** are equally well supported by the data (AIC difference < 2). The black surface is the fitted model while the green and red surfaces are the 95% confidence intervals. Units are g for SWD and % colonization for hyphae.

DISCUSSION

Cultivars Differ in Colonization by *R. irregularis* and the Impact of the AM Fungus on Plant Growth

The main aim of this study was to test the hypothesis that there is genetic variation within rice for colonization and the impact of the AM fungus on rice growth. The study clearly showed there is. Firstly, there was highly significant differences between cultivars in colonization with a very wide range from 23–90% (**Figure 7**). Secondly, it shows that impact of AM fungus on shoot growth, all be it almost entirely negative, is different between cultivars (**Figure 4B**). There are few studies showing cultivar differences in rice. A meta-analysis of the impact of AM fungi on annual crop plants has been conducted on 39 papers containing 320 species by Lehmann et al. (2012) which concluded that cultivars differed in colonization rates, and interestingly old and new cultivars had less colonization that ancestral ones, and that colonization rate was quite strongly correlated to responsiveness (of host growth) to AM fungi. However, the analysis included only one study specific to rice (Gao et al., 2007). Gao et al. (2007) pot experiments found one of six aerobic rice cultivars had lower root colonization. Differences between an upland and a lowland cultivar were found to depend on the species of AM fungus used and the amount of arsenic applied as a treatment (Li et al., 2011). Suzuki et al. (2015) assess 64 rice cultivars for growth response to a different AM fungus and measured colonization in 12 of them. Only two cultivars are in common between that study and the current one (Nipponbare and Kasalath) and while they appeared to differ in growth response in Suzuki et al. (2015), here they do not. Considering examples of studies within other grass species, differences in five Canadian durum wheats have been reported including an interaction between soil fertility and cultivar (Singh et al., 2012). Amongst six winter wheats and maize accessions, Zhu et al. (2001) found cultivar differences,

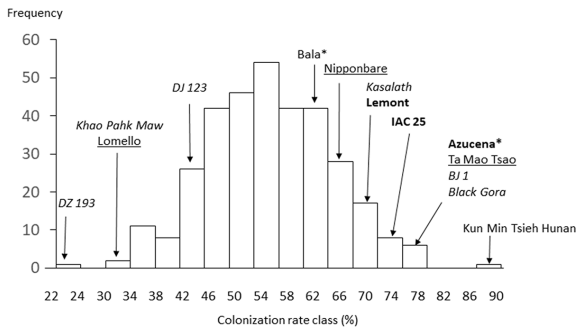

FIGURE 7 | Frequency distribution of mean hyphal colonization in the Rice Diversity Panel 1 cultivars highlighting values of some notable cultivars. * for Azucena and Bala indicates these are the Aberdeen "own" genotypes for these cultivars. The font used for cultivars indicate subpopulation; normal = indica, underlined = temperate japonica, italic = aus, bold = tropical japonica.

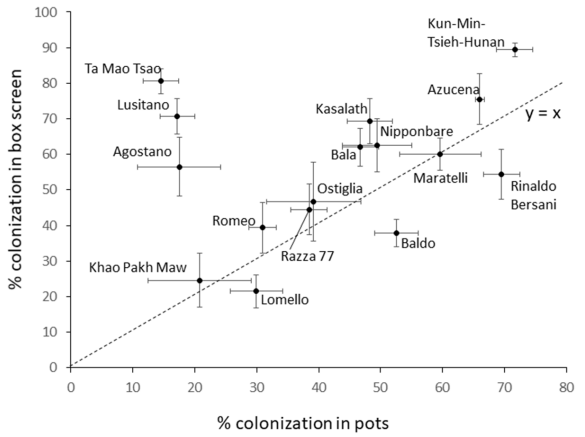

FIGURE 8 | Mean hyphal colonization for 16 cultivars tested in both the large box screen, and individual pots. Bars are standard error. Dotted line is the 1:1 line.

while Chu et al. (2013) found differences in four maize cultivars but not at the lowest P addition. Recently three studies have examined a wide range of either sorghum (Leiser et al., 2016), or wheat (Lehnert et al., 2017) or durum wheat (De Vita et al., 2018). Leiser et al. (2016) tested 187 sorghum cultivars grown in pots 38 days and found only limited variation in AM fungal colonization rates in terms of range (38.5–72.9%) or heritability (15%). Lehnert et al. (2017) tested 94 wheat cultivars grown in pots until mature. They showed very strong genotypic differences but a lower range of colonization (24–56%). De Vita et al. (2018) found large differences in colonization of durum wheat roots with both AM fungi *R. irregularis* and *F. mosseae*, and discovered seven QTLs apparently common between the species suggestive of common genetic regulation within the host.

The differential cultivar response of shoot growth to AM fungal plus rock phosphate treatment relative to the rock phosphate treatment alone detected in this experiment was highly significant but small and did not fall into any discernible pattern (e.g., between subgroups or country of origin). This implies the host genetics of rice-AMF interaction are influential in determining plant growth, but much more research is needed to determine its biological significance. Despite the high statistical difference and big range of variation in colonization detected here, there is no particularly striking pattern that provides conclusive evidence of the biological implications. While aus cultivars are generally lower than other subpopulations (**Figure 5**), and there are differences related to the country of origin of the cultivars, these do not explain a large proportions of the variation or provide clear reasons for such differences. Aus cultivars, which are revealed to have a low colonization on average, are notable as the donors of a number of important abiotic resistance traits [e.g., submergence tolerance from FR 13A (Xu et al., 2006); phosphorus starvation tolerance from Kasalath (Gamuyao et al., 2012); drought resistance from N22 and Dular (Gowda et al., 2011)] and might be expected to be adapted to poor soils and might therefore be expected to have strong associations with AM fungi. It is perhaps notable then that Kasalath does have a high colonization rate (ranked 19th) while the other three cultivars mentioned above are not remarkable. Kasalath was identified as having high phosphorus uptake efficiency of 30 rice genotypes in a study which also identified the Brazilian tropical japonica IAC 25 as high for P uptake efficiency and the United States tropical japonica Lemont as low (Wissuwa and Ae, 2001). IAC 25 is ranked 9th here so is high for AM colonization, but Lemont ranked 33rd for colonization which is definitely not low.

The fact that cultivars from the Philippines and China have high root colonization and those from Bangladesh are low (**Supplementary Figure S2**) is not currently explicable. One hypothesis that could be forwarded would be that upland cultivars adapted to aerobic soils would have a greater need of, and therefore stronger association with AM fungi than flooded cultivars. Unfortunately information on the hydrological environment of the cultivars in the RDP1 is lacking.

The repeated test of 16 cultivars in a pot experiment produced an interesting result (**Figure 9**), being a remarkably strong agreement in colonization rates between the large box screen and pots for 13 of the cultivars, but for three cultivars their colonization in pots was much lower than in the box screen. It can be hypothesized that this reflects cultivar differences in the impact of soil properties on colonization. The preliminary experiments reported here demonstrate that colonization of Bala was sensitive to rock phosphate while in Azucena it was not. Since Bala was included amongst the 16 tested in pots, and its colonization was very similar to the box screen colonization rate, it seems unlikely the same edaphic factor is acting in the pot experiment reported in **Figure 8** and the preliminary experiments. The cultivar difference in the impact of edaphic factors on root colonization by AM fungi merits further study.

Impact of *R. irregularis* on the Rice Plants

The optimization experiments do not provide convincing evidence that P uptake efficiency and root colonization

TABLE 2 | The most significant SNP at each of the 23 identified GWA putative QTLs for hyphal colonization across all populations plus three from subpopulation analysis.

QTL	Analysis	Most significant SNP id	Chromosome	Position (bp)	*P*-value	MAF (%)	Effect
1.1	All	mlid0092747457	1	5069003	4.60E-05	7.3	4.6
1.2	All	mlid0001644797	1	8119524	7.58E-05	20	4.0
1.3	All	mlid0002847008	1	13328067	3.37E-05	21	−4.6
1.4	All	mlid0004161541	1	18083827	2.15E-05	39	−5.0
2.1a	Aus	mlid0014401085	2	22623115	7.49E-06	44	−12.7
2.2	All	mlid0014856649	2	24494645	6.07E-05	31	2.7
3.1	All	mlid0017818601	3	4455505	7.02E-05	31	−5.1
3.2	All	mlid0020494652	3	17569164	6.83E-06	45	5.4
3.3	All	mlid0023902122	3	32806262	8.53E-05	11	−7.0
4.1	All	mlid0024944825	4	1252233	3.92E-05	14	8.6
4.2	All	mlid0029088874	4	16530764	6.25E-06	10	5.3
4.3	All	mlid0031764657	4	29353046	2.87E-06	42	3.7
5.1	All	mlid0033051374	5	774066	6.90E-05	19	−4.8
6.1	All	mlid0043758793	6	17006825	7.81E-05	11	6.2
6.2	All	mlid0046376100	6	28107199	5.11E-05	24	−4.8
7.1	All	mlid0048451088	7	7182668	3.04E-05	31	−4.8
7.2	All	mlid0052022846	7	20886439	4.41E-05	14	9.1
8.1	All	mlid0056191014	8	9715485	4.38E-05	22	3.6
9.1	All	mlid0062250420	9	5765734	4.16E-05	41	5.7
10.1	All	mlid0067485302	10	4753692	4.47E-05	7.3	−5.1
11.1	All	mlid0076234181	11	17686395	1.29E-05	20	−5.1
11.2tr	Trj	mlid0077311363	11	21793808	1.81E-05	12	−8.1
11.2a	Aus	mlid0094185850	11	22027960	6.21E-05	10	−10.8
12.1	All	mlid0081838150	12	10779534	5.12E-05	19	4.3
12.2	All	mlid0082869441	12	14246478	6.38E-05	23	5.2
12.3	All	mlid0083460931	12	16261109	9.29E-05	38	4.5

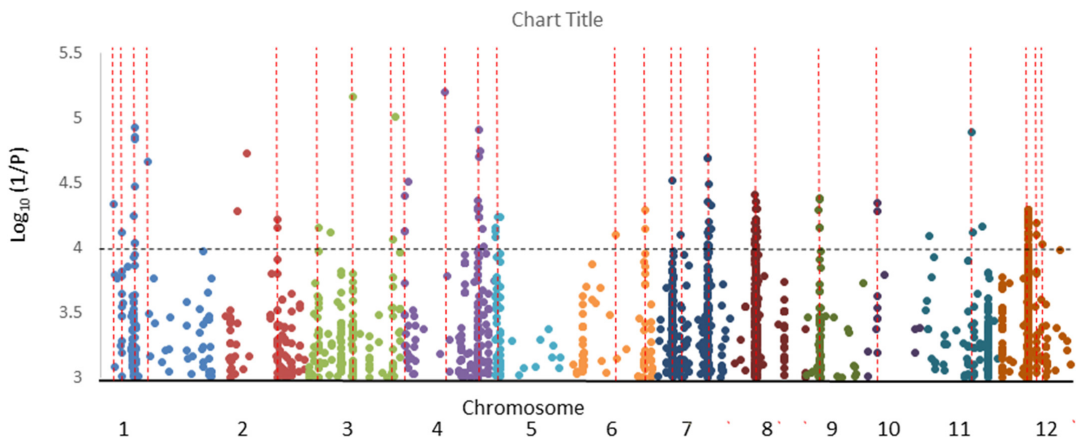

FIGURE 9 | Genome wide association mapping of the All analysis showing only SNPs where $P < 0.001$. Lines indicate where there is at least one other marker within 200 kb. Each color represents a different chromosome.

by AM fungi are linked, which may occur because P uptake is more likely to be related to proliferation of extra-radical mycelium (Sawers et al., 2017), or that under these conditions, *R. irregularis* is behaving toward the parasitic end of the plant-mycorrhiza continuum (Johnson, 2010). It will be important to test if different root colonization rates detected here reflect colonization obtained with other species of AM fungi and colonization in the field environment.

In the preliminary experiments and the main screen described in this report, the AM treatment invariably reduced plant growth, which is not a unique observation (Van Der Heijden and Horton, 2009). We would suggest that this is a feature of the soil medium used here since other experiments in Aberdeen with

the same rice genotypes and the same AM fungal inoculum, but with different growing medium, do not always have a negative effect. What is highly remarkable from study is the strong positive neighbor effects detected on both plant growth and root colonization in the presence of *R. irregularis*. The positive nature of these effects of neighbors suggest *R. irregularis* has formed a common mycorrhizal network (CMN) inter-connecting roots of individual plants (Selosse et al., 2006). Recent work has shown that CMNs can affect growth and nutrition of neighbors grown in pairs (Walder et al., 2012). This should be tested on rice to determine the repeatability, extent and mechanism of this apparent facilitation. If proven more than just specific to the conductions used in this experiment, the result has major implications for consideration of mycorrhizal crop plants and their productivity since it demonstrates that when connected by a CMN, one plant can have a positive impact on its neighbors. This phenomenon merits further study, especially at the field level.

Putative QTLs for Root Colonization by AM Fungi by GWA Mapping

In this study, 23 putative QTLs for root colonization by AMF were detected, mostly in the analysis of the whole population. Two important observations need to be made. First, no association was above the 10% FDR; this does not mean they are not real, but they must be treated with caution, hence they are termed putative QTLs. Second, the number is high. If these QTLs are to be believed, the implication is that there are many genes involved in determining the degree of colonization in rice–AM fungal symbiosis and the trait is truly quantitative. In the study of sorghum (Leiser et al., 2016) the GWA mapping revealed no SNP associated with colonization with a *P*-value below $P = 0.0001$ which they considered reflected the low heritability (15%). In contrast, the wheat study of Lehnert et al. (2017), which had a heritability of 54% for root colonization (the same as reported here for rice), found six QTLs. More studies are needed before we can determine if root colonization in grasses is generally regulated by multiple, small effect genes as implied in the studies to date.

It is worth noting that none of the QTLs reported here match the 97 and 16 loci found associated with either controlled environment or field resistance to the fungal pathogen blast in this population [as reported by Kang et al. (2016) and Zhu et al. (2016), respectively]. This implies that the loci reported for AM colonization are not associated with genes affecting the basic plant/fungus interaction process.

Candidate Genes for Putative QTLs

Identifying the most promising functional candidate genes from the gene lists for the 23 putative QTLs reported here (**Table 2** and **Supplementary Table S2**) will depend on individual and community understanding of the molecular mechanisms involved in the AM fungus-rice interaction which will improve with time. However, some notable observations on examination of these lists are given below.

In QTL 1.1 is LOC_Os01g09580, a calcium/calmodulin serine/threonine protein kinase which is massively downregulated in AMF in both the Fiorilli et al. (2015) and Gutjahr et al. (2015) study. Over expression in rice of *Medicago* DMI3 (a Ca+/calmodulin-dependent serine/threonine protein kinase that is known to be a component of the common symbiotic pathway between AM fungi and *rhizobium*) supported elevated AM fungal colonization (Ortiz-Berrocal et al., 2017).

In QTL 2.2 is a pair of excellent candidate genes. The genes LOC_Os02g40710 and LOC_Os02g40730 are annotated as ammonium transporters. These genes are *OsAMT1.2* and *OsAMT1.3*, respectively. The transport of ammonia from AM fungi to plant host within the arbuscule is considered a central process in AM symbiosis (Guether et al., 2009). Transcriptomics studies on rice exposed to *R. irregularis* identified ammonium transporters (although not these two) as responsive (Güimil et al., 2005; Gutjahr et al., 2015), while the expression of ammonium transporter *OsAMT3.1* has been used as a marker for rice-AM interaction (Vallino et al., 2014). Furthermore, AMT2:3 appears to be important in influencing the life span of *Medicago*-associated AM fungi (Breuillin-Sessoms et al., 2015). Fiorilli et al. (2015) revealed that LOC_Os02g40730 is strongly upregulated by *R. irregularis* inoculation (2.2-fold in large laterals, 9-fold in fine laterals). Both *OsAMT1.2* and *OsAMT1.3* have a highly root-specific expression pattern in rice (Sato et al., 2013).

In QTL 4.1 is a cluster of seven subtilisin or subtilisin-like proteases including LOC_Os04g02980 annotated as OsSub33 which is upregulated in both root types in the Fiorilli et al. (2015) study. Subtilisins are a class of serine proteases also known as subtilases. A review on subtilases (Schaller et al., 2017) highlights studies that suggests some subtilases are linked to AM colonization, having a role in arbuscule development. Further, a subtilase was identified by Kistner et al. (2005) as one of seven host genes required for mycorrhiza and symbiotic bacteria to enter root epidermal or cortical cells based on the study of a mutant of *Lotus japonicus* that are impaired for nodulation. While this makes these genes good candidates for rice-AM fungal interaction, it must be noted that there are 71 genes in rice annotated as subtilisin-like or Subtilisin homologs.

Recently a 53 kbp deletion at 29 Mbp on chromosome 1 regulating strigolactone production and strongly associated with resistance to the parasitic plant *Striga* was reported (Cardoso et al., 2014). This deletion was tested by PCR on the RDP1 and used as a marker in the GWA mapping conducted here. It is surprising perhaps that there is no association detected at this locus since the production of strigolactone is considered to be an evolutionary adaptation critical to the signaling by plants to mycorrhiza (Akiyama et al., 2005).

CONCLUSION

These experiments clearly demonstrate that rice cultivars differ very widely for colonization by *R. irregularis* and reports putative QTLs which appear to contribute to that variation. While the pattern of variation in colonization in rice offers little insight into the evolution or biological significance, it lays a foundation for further research. This may be determining if variation detected here matches variation in the field and if it impacts nutrient uptake in low nutrient, aerobic environments.

Some of the genes under the QTLs shown here should be further investigated. A supplementary finding is strong evidence of positive interactions between neighboring rice plants facilitated by a common mycorrhizal network.

AUTHOR CONTRIBUTIONS

AP conceived and designed the experiments and largely wrote the manuscript. HD conducted preliminary experiments and the screen of RDP1. RS conducted the study of 16 cultivars in pots. TC did the spatial statistical analysis. AD and TT conducted the GWA mapping. DJ advised on the role of mycorrhiza in common mycorrhizal networks. All authors contributed to editing the manuscript.

FUNDING

The majority of the research reported here is an output of EU project "EURoot" (FP7-KBBE-2011-5 Grant Agreement No. 289300) project. RS's contribution was funded by FACCE-JPI NET project "GreenRice" (Sustainable and environmental friendly rice cultivation systems in Europe) and was funded by the BBSRC award BB/M018415/1.

SUPPLEMENTARY MATERIAL

The Supplementary Material for this article can be found online at: https://www.frontiersin.org/articles/10.3389/fpls.2019.00633/full#supplementary-material

FIGURE S1 | Spatial trend in shoot dry weight (SDW), shared between all four replicate runs (showing deviations from predicted value, on the log-scale in grams). Values increase from red to white.

FIGURE S2 | Raw AM colonization data showing; **(A)** frequency distribution of hyphal colonization in each run; **(B)** scatter plot of mean hyphal colonization vs. mean arbuscle colonization and; **(C)** hyphal colonization vs. mean vesicle colonization.

FIGURE S3 | Spatial trends in hyphal colonization in each of the four replicate runs (deviation from predicted value). Units are % colonization.

FIGURE S4 | Boxplots of hyphal colonization in Rice Diversity Panel 1 according to country of origin (with *n* in brackets). Letters above bars represent results of Tukey's test of difference between groups.

FIGURE S5 | Manhattan and QQ plots for hyphal colonization for all cultivars, aus (AUS), indica (IND), tropical japonica (TRJ), and temperate japonica (TEJ) cultivars. Red dotted lines indicate putative QTLs from the all analysis, green in subgroups.

TABLE S1 | List of rice accession and phenotype data.

TABLE S2 | List of genes observed in each of the putative QTLs with information on available transcriptomics data for response to AM treatment [using data from Fiorilli et al. (2015) or Gutjahr et al. (2015)].

REFERENCES

Akiyama, K., Matsuzaki, K., and Hayashi, H. (2005). Plant sesquiterpenes induce hyphal branching in arbuscular mycorrhizal fungi. *Nature* 435, 824–827. doi: 10.1038/nature03608

Al-Ogaidi, F. (2013). *Understanding Rice and Soil Phosphorus Interactions with an Emphasis on Rice Genetics and Soil Microbes*. Ph.D. thesis, University of Aberdeen, Aberdeen.

Benjamini, Y., and Hochberg, Y. (1995). Controlling the false discovery rate: a practical and powerful approach to multiple testing. *J. R. Stat. Soc.* 57, 289–300.

Bhattacharjee, S., and Sharma, G. D. (2011). The vesicular arbuscular mycorrhiza associated with three cultivars of rice (*Oryza sativa* L.). *Indian J. Microbiol.* 51, 377–383. doi: 10.1007/s12088-011-0090-9

Bouman, B. A. M., Lampayan, R. M., and Tuong, T. T. (2007). *Water Management in Irrigated Rice: Coping with Water Scarcity*. Philippines: International Rice Research Institute.

Breuillin-Sessoms, F., Floss, D. S., Gomez, S. K., Pumplin, N., Ding, Y., Levesque-Tremblay, V., et al. (2015). Suppression of arbuscule degeneration in *Medicago truncatula* phosphate transporter4 mutants is dependent on the ammonium transporter 2 family protein AMT2;3. *Plant Cell* 27, 1352–1366. doi: 10.1105/tpc.114.131144

Campos-Soriano, L., Garcia-Martinez, J., and Segundo, B. S. (2012). The arbuscular mycorrhizal symbiosis promotes the systemic induction of regulatory defence-related genes in rice leaves and confers resistance to pathogen infection. *Mol. Plant Pathol.* 13, 579–592. doi: 10.1111/j.1364-3703.2011.00773.x

Cardoso, C., Zhang, Y., Jamil, M., Hepworth, J., Charnikhova, T., Dimkpa, S. O. N., et al. (2014). Natural variation of rice strigolactone biosynthesis is associated with the deletion of two MAX1 orthologs. *PNAS* 111, 2379–2384. doi: 10.1073/pnas.1317360111

Chu, Q., Wang, X., Yang, Y., Chen, F., Zhang, F., and Feng, G. (2013). Mycorrhizal responsiveness of maize (*Zea mays* L.) genotypes as related to releasing date and available P content in soil. *Mycorrhiza* 23, 497–505. doi: 10.1007/s00572-013-0492-0

De Vita, P., Avio, L., Sbrana, C., Laidò, G., Marone, D., Mastrangelo, A. M., et al. (2018). Genetic markers associated to arbuscular mycorrhizal colonization in durum wheat. *Sci. Rep.* 8:10612. doi: 10.1038/s41598-018-29020-6

Fiorilli, V., Vallino, M., Biselli, C., Faccio, A., Bagnaresi, P., and Bonfante, P. (2015). Host and non-host roots in rice: cellular and molecular approaches reveal differential responses to arbuscular mycorrhizal fungi. *Front. Plant Sci.* 6:636. doi: 10.3389/fpls.2015.00636

Gamuyao, R., Chin, J. H., Pariasca-Tanaka, J., Pesaresi, P., Catausan, S., Dalid, C., et al. (2012). The protein kinase pstol1 from traditional rice confers tolerance of phosphorus deficiency. *Nature* 488, 535–539. doi: 10.1038/nature11346

Gao, X., Kuyper, T. W., Zou, C., Zhang, F., and Hoffland, E. (2007). Mycorrhizal responsiveness of aerobic rice genotypes is negatively correlated with their zinc uptake when nonmycorrhizal. *Plant Soil* 290, 283–291. doi: 10.1007/s11104-006-9160-x

Gowda, V. R. P., Henry, A., Yamauchi, A., Shashidhar, H. E., and Serraj, R. (2011). Root biology and genetic improvement for drought avoidance in rice. *Field Crop Res.* 122, 1–13. doi: 10.1016/j.fcr.2011.03.001

Guether, M., Neuhäuser, B., Balestrini, R., Dynowski, M., Ludewig, U., and Bonfante, P. (2009). A mycorrhizal-specific ammonium transporter from lotus japonicus acquires nitrogen released by arbuscular mycorrhizal fungi. *Plant Physiol.* 150, 73–83. doi: 10.1104/pp.109.136390

Güimil, S., Chang, H. S., Zhu, T., Sesma, A., Osbourn, A., Roux, C., et al. (2005). Comparative transcriptomics of rice reveals an ancient pattern of response to microbial colonisation. *PNAS* 102, 8066–8070. doi: 10.1073/pnas.0502999102

Gutjahr, C., Sawers, R. J. H., Marti, G., Andrés-Hernández, L., Yang, S.-Y., and Casieri, L. (2015). Transcriptome diversity among rice root types during asymbiosis and interaction with arbuscular mycorrhizal fungi. *PNAS* 112, 6754–6759. doi: 10.1073/pnas.1504142112

Ilag, L. L., Rosales, A. M., Elazegui, F. A., and Mew, T. W. (1987). Changes in the population of infective endomycorrhizal fungi in a rice-based cropping system. *Plant Soil* 103, 67–73. doi: 10.1007/BF02370669

Johnson, N. C. (2010). Tansley review: resource stoichiometry elucidates the structure and function of arbuscular mycorrhizas across scales. *New Phytol.* 185, 631–647.

Kang, H. X., Wang, Y., Peng, S. S., Zhang, Y. L., Xiao, Y. H., Wang, D., et al. (2016). Dissection of the genetic architecture of rice resistance to the blast fungus *Magnaporthe oryzae*. *Mol. Plant Pathol.* 10, 959–972. doi: 10.1111/mpp.12340

Keymer, A., and Gutjahr, C. (2018). Cross-kingdom lipid transfer in arbuscular mycorrhiza symbiosis and beyond. *Curr. Opin. Plant Biol.* 44, 137–144. doi: 10.1016/j.pbi.2018.04.005

Kistner, C., Winzer, T., Pitzschke, A., Mulder, L., Sato, S., Kaneko, T., et al. (2005). Seven *Lotus japonicus* genes required for transcriptional reprogramming of the root during fungal and bacterial symbiosis. *Plant Cell* 17, 2217–2229.

Lehmann, A., Barto, E. K., Powell, J. R., and Rillig, M. C. (2012). Mycorrhizal responsiveness trends in annual crop plants and their wild relatives-a meta-analysis on studies from 1981 to 2010. *Plant Soil* 355, 231–250. doi: 10.1007/s11104-011-1095-1

Lehnert, H., Serfling, A., Enders, M., Friedt, W., and Ordon, F. (2017). Genetics of mycorrhizal symbiosis in winter wheat (*Triticum aestivum*). *New Phytol.* 215, 779–791. doi: 10.1111/nph.14595

Leiser, W. L., Olatoye, M. O., Rattunde, H. F. W., Neumann, G., Weltzien, E., and Haussmann, B. I. G. (2016). No need to breed for enhanced colonisation by arbuscular mycorrhizal fungi to improve low-P adaptation of West African sorghums. *Plant Soil* 401, 51–64. doi: 10.1007/s11104-015-2437-1

Li, H., Chen, X. W., and Wong, M. H. (2016). Arbuscular mycorrhizal fungi reduced the ratios of inorganic/organic arsenic in rice grains. *Chemosphere* 145, 224–230. doi: 10.1016/j.chemosphere.2015.10.067

Li, H., Ye, Z. H., Chan, W. F., Chen, X. W., Wu, F. Y., Wu, S. C., et al. (2011). Can arbuscular mycorrhizal fungi improve grain yield, as uptake and tolerance of rice grown under aerobic conditions? *Environ. Pollut.* 159, 2537–2545. doi: 10.1016/j.envpol.2011.06.017

MacMillan, K., Emrich, K., Piepho, H. P., Mullins, C. E., and Price, A. H. (2006). Assessing the importance of genotype x environment interaction for root traits in rice using a mapping population I: a soil-filled box screen. *Theor. Appl. Genet.* 113, 977–986. doi: 10.1007/s00122-006-0357-4

Maiti, D., Variar, M., and Singh, R. K. (2011). Optimizing tillage schedule for maintaining activity of the arbuscular mycorrhizal fungal population in a rainfed upland rice (*Oryza sativa* L.) agro-ecosystem. *Mycorrhiza* 21, 167–171. doi: 10.1007/s00572-010-0324-4

McCouch, S. R., Wright, M. H., Tung, C. W., Maron, L. G., McNally, K. L., Fitzgerald, M., et al. (2016). Open access resources for genome-wide association mapping in rice. *Nat. Commun.* 7:10532.

McGonigle, T. P., Miller, M. H., Evans, D. G., Fairchild, G. L., and Swan, J. A. (1990). A new method which gives an objective measure of colonisation of roots by vesicular-arbuscular mycorrhizal fungi. *New Phytol.* 115, 495–501. doi: 10.1111/j.1469-8137.1990.tb00476.x

Norton, G. J., Douglas, A., Lahner, B., Yakubova, E., Guerinot, M. L., Pinson, S. R. M., et al. (2014).). Genome wide association mapping of grain arsenic, copper, molybdenum and zinc in rice (*Oryza sativa* L.) grown at four international field sites. *PLoS One* 9:e89685. doi: 10.1371/journal.pone.0089685

Ortiz-Berrocal, M., Lozano, L., Sanchez-Flores, A., Nava, N., Hernandez, G., and Reddy, P. M. (2017). Expression in rice of an autoactive variant of *Medicago truncatula* DMI3, the Ca+2/calmodulin-dependent protein kinase from the common symbiotic pathway modifies root transcriptome and improves mycorrhizal colonisation. *Plant Biotech. Rep.* 11, 271–287. doi: 10.1007/s11816-017-0449-4

Price, A. H., Steele, K. A., Moore, B. J., Barraclough, P. P., and Clark, L. J. (2000). A combined RFLP and AFLP linkage map of upland rice (*Oryza sativa* L.) used to identify QTLs for root-penetration ability. *Theor. Appl. Genet.* 100, 49–56. doi: 10.1007/s001220050007

Sato, Y., Takehisa, H., Kamatsuki, K., Minami, H., Namiki, N., and Ikawa, H. (2013). RiceXPro version 3.0: expanding the informatics resource for rice transcriptome. *Nucleic Acids Res.* 41, 1206–1213. doi: 10.1093/nar/gks1125

Sawers, R. J. H., Svane, S. F., Quan, C., Grønlund, M., Wozniak, B., Gebreselassie, M. N., et al. (2017). Phosphorus acquisition efficiency in arbuscular mycorrhizal maize is correlated with the abundance of root-external hyphae and the accumulation of transcripts encoding PHT1 phosphate transporters. *New Phytol.* 214, 632–643. doi: 10.1111/nph.14403

Schaller, A., Stintzi, A., Rivas, S., Serrano, I., Chichkova, N. V., Vartapetian, A. B., et al. (2017). From structure to function – a family portrait of plant subtilases. *New Phytol.* 218, 901–915. doi: 10.1111/nph.14582

Selosse, M. A., Richard, F., He, X., and Simard, S. W. (2006). Mycorrhizal networks: des liaisons dangereuses? *Trends Ecol. Evol.* 21, 621–628. doi: 10.1016/j.tree.2006.07.003

Singh, A. K., Hamel, C., DePauw, R. M., and Knox, R. E. (2012). Genetic variability in arbuscular mycorrhizal fungi compatibility supports the selection of durum wheat genotypes for enhancing soil ecological services and cropping systems in Canada. *Can. J. Microbiol.* 58, 293–302. doi: 10.1139/w11-140

Smith, S. E., and Read, D. (2008). *Mycorrhizal Symbiosis*, 3rd Edn. Amsterdam: Elsevier Ltd.

Suzuki, S., Kobae, Y., Sisaphaithong, T., Tomioka, R., Takenaka, C., and Hata, S. (2015). Differential Growth responses of rice cultivars to an arbuscular mycorrhizal fungus, funneliformis mosseae. *J. Hort.* 2:3. doi: 10.4172/2376-0354.1000142

Tisserant, E., Malbreil, M., Kuo, A., Kohler, A., Symeonidi, A., Balestrini, R., et al. (2013). Genome of an arbuscular mycorrhizal fungus provides insight into the oldest plant symbiosis. *PNAS* 110, 20117–20122. doi: 10.1073/pnas.1313452110

Vallino, M., Fiorilli, V., and Bonfante, P. (2014). Rice flooding negatively impacts root branching and arbuscular mycorrhizal colonisation, but not fungal viability. *Plant Cell Environ.* 37, 557–572. doi: 10.1111/pce.12177

Vallino, M., Greppi, D., Novero, M., Bonfante, P., and Lupotto, E. (2009). Rice root colonisation by mycorrhizal and endophytic fungi in aerobic soil. *Ann. Appl. Biol.* 154, 195–204. doi: 10.1111/j.1744-7348.2008.00286.x

Van Der Heijden, M. G. A., and Horton, T. R. (2009). Socialism in soil? The importance of mycorrhizal fungal networks for facilitation in natural ecosystems. *J. Ecol.* 97, 1139–1150. doi: 10.1111/j.1365-2745.2009.01570.x

Van Der Heijden, M. G. A., Martin, F. M., Selosse, M. A., and Sanders, I. R. (2015). Mycorrhizal ecology and evolution: the past, the present, and the future. *New Phytol.* 205, 1406–1423. doi: 10.1111/nph.13288

Vierheilig, H., Coughlan, A. P., Wyss, U., and Piché, Y. (1998). Ink and vinegar, a simple staining technique for arbuscular-mycorrhizal fungi. *Appl. Environ. Microbiol.* 64, 5004–5007.

Walder, F., Niemann, H., Natarajan, M., Lehmann, M. F., Boller, T., and Wiemken, A. (2012). Mycorrhizal networks: common goods of plants shared under unequal terms of trade. *Plant Physiol.* 159, 789–797. doi: 10.1104/pp.112.195727

Wang, D. R., Agosto-Pérez, F. J., Chebotarov, D., Shi, Y., Marchini, J., Fitzgerald, M., et al. (2018). An imputation platform to enhance integration of rice genetic resources. *Nat. Genet.* 9:3519. doi: 10.1038/s41467-018-05538-1

Watanarojanaporn, N., Boonkerd, N., Tittabutr, P., Longtonglang, A., Young, J. P. W., and Teaumroong, N. (2013). Effect of rice cultivation systems on indigenous arbuscular mycorrhizal fungal community structure. *Microbes Environ.* 28, 316–324. doi: 10.1264/jsme2.ME13011

Wissuwa, M., and Ae, N. (2001). Genotypic variation for tolerance to phosphorus deficiency in rice and the potential for its exploitation in rice improvement. *Plant Breed.* 120, 43–48. doi: 10.1046/j.1439-0523.2001.00561.x

Wood, S. N., Scheipl, F., and Faraway, J. J. (2013). Straightforward intermediate rank tensor product smoothing in mixed models. *Stat. Comput.* 23, 341–360.

Xu, K., Xu, X., Fukao, T., Canlas, P., Maghirang-Rodriguez, R., and Heuer, S. (2006). Sub1A is an ethylene-response-factor-like gene that confers submergence tolerance to rice. *Nature* 442, 705–708. doi: 10.1038/nature04920

Yoshida, S., Forno, D. A., Cock, J. H., and Gomez, K. A. (1976). *Laboratory Manual for the Physiological Studies of Rice*. Manila: International Rice Research Institute.

Yu, J., Pressoir, G., Briggs, W. H., Vroh, B. I, Yamasaki, M., and Doebley, J. F. (2006). A unified mixed-model method for association mapping that accounts for multiple levels of relatedness. *Nat. Genet.* 38, 203–208. doi: 10.1038/ng1702

Zhao, K., Tung, C. W., Eizenga, G. C., Wright, M. H., Ali, M. L., Price, A. H., et al. (2011). Genome-wide association mapping reveals a rich genetic architecture of complex traits in *Oryza sativa*. *Nat. Commun.* 2:467. doi: 10.1038/ncomms1467

Zhu, D., Kang, H. X., Li, Z. Q., Liu, M. H., Zhu, X. L., Wang, Y., et al. (2016). A genome-wide association study of field resistance to *Magnaporthe oryzae* in rice. *Rice* 9:44. doi: 10.1186/s12284-016-0116-3

Zhu, Y. G., Smith, S. E., Barritt, A. R., and Smith, F. A. (2001). Phosphorus (P) efficiencies and mycorrhizal responsiveness of old and modern wheat cultivars. *Plant Soil* 237, 249–255. doi: 10.1023/A:1013343811110

Conflict of Interest Statement: The authors declare that the research was conducted in the absence of any commercial or financial relationships that could be construed as a potential conflict of interest.

frontiers in Plant Science

REVIEW
published: 28 May 2019
doi: 10.3389/fpls.2019.00632

Plant Aquaporins in Infection by and Immunity Against Pathogens – A Critical Review

*Liyuan Zhang[1], Lei Chen[1] and Hansong Dong[1,2]**

[1] Plant Immunity Research Group, National Key Laboratory of Crop Science, Department of Plant Pathology, Shandong Agricultural University, Tai'an, China, [2] Plant Immunity Laboratory, Department of Plant Pathology, Nanjing Agricultural University, Nanjing, China

Plant aquaporins (AQPs) of the plasma membrane intrinsic protein (PIP) family face constant risk of hijack by pathogens aiming to infect plants. PIPs can also be involved in plant immunity against infection. This review will utilize two case studies to discuss biochemical and structural mechanisms that govern the functions of PIPs in the regulation of plant infection and immunity. The first example concerns the interaction between rice *Oryza sativa* and the bacterial blight pathogen *Xanthomonas oryzae* pv. *oryzae* (Xoo). To infect rice, Xoo uses the type III (T3) secretion system to secrete the proteic translocator Hpa1, and Hpa1 subsequently mediates the translocation of T3 effectors secreted by this system. Once shifted from bacteria into rice cells, effectors exert virulent or avirulent effects depending on the susceptibility of the rice varieties. The translocator function of Hpa1 requires cooperation with OsPIP1;3, the rice interactor of Hpa1. This role of OsPIP1;3 is related to regulatory models of effector translocation. The regulatory models have been proposed as, translocon-dependent delivery, translocon-independent pore formation, and effector endocytosis with membrane protein/lipid trafficking. The second case study includes the interaction of Hpa1 with the H_2O_2 transport channel AtPIP1;4, and the associated consequence for H_2O_2 signal transduction of immunity pathways in *Arabidopsis thaliana*, a non-host of Xoo. H_2O_2 is generated in the apoplast upon induction by a pathogen or microbial pattern. H_2O_2 from this source translocates quickly into Arabidopsis cells, where it interacts with pathways of intracellular immunity to confer plant resistance against diseases. To expedite H_2O_2 transport, AtPIP1;4 must adopt a specific conformation in a number of ways, including channel width extension through amino acid interactions and selectivity for H_2O_2 through amino acid protonation and tautomeric reactions. Both topics will reference relevant studies, conducted on other organisms and AQPs, to highlight possible mechanisms of T3 effector translocation currently under debate, and highlight the structural basis of AtPIP1;4 in H_2O_2 transport facilitated by gating and trafficking regulation.

Keywords: aquaporin, plasma membrane intrinsic protein, H_2O_2 transport, immunity signaling, translocon, type III effectors

OPEN ACCESS

Edited by:
Valentina Fiorilli, University of Turin, Italy

Reviewed by:
Raffaella Balestrini, Italian National Research Council (IPSP-CNR), Italy
Kalyan K. Mondal, Indian Agricultural Research Institute (ICAR), India

***Correspondence:**
Hansong Dong
hsdong@njau.edu.cn

Specialty section:
This article was submitted to Plant Microbe Interactions, a section of the journal Frontiers in Plant Science

Received: *08 January 2019*
Accepted: *26 April 2019*
Published: *28 May 2019*

Citation:
Zhang L, Chen L and Dong H (2019) Plant Aquaporins in Infection by and Immunity Against Pathogens – A Critical Review. Front. Plant Sci. 10:632. doi: 10.3389/fpls.2019.00632

INTRODUCTION

Aquaporins (AQPs) are membrane-intrinsic proteins initially defined as water (H_2O) transporting channels in all organisms and subsequently found to have many other substrate specificities (de Groot and Grubmuller, 2001; Maurel et al., 2008, 2015; Sutka et al., 2017), such as hydrogen peroxide (H_2O_2; Tian et al., 2016). In plants, AQPs are classified into five major families (Chaumont et al., 2001; Maurel, 2007), including the plasma membrane intrinsic proteins (PIPs), tonoplast intrinsic proteins (TIPs), nodulin 26 like intrinsic proteins (NIPs), small basic intrinsic proteins (SIPs), and X intrinsic proteins (XIPs). The PIP family is further divided into the PIP1 subfamily made of PIP1;1 to PIP1;5 and the PIP2 subfamily consisting of PIP2;1 to PIP2;8 in most plant species (Maurel, 2007; Gomes et al., 2009; Laloux et al., 2018). While AQPs of the other four families function in substrate trafficking between organelles, PIPs are responsible for substrate transportation between the exterior and interior of cells (Maurel, 2007; Gomes et al., 2009; Kaldenhoff et al., 2014; Li et al., 2015; Bao, 2017).

Recently discovered functions of AQPs surpass the original "water channel" concept (Preston et al., 1992; Wudick et al., 2009; Heckwolf et al., 2011; Brown, 2017), and suggest implications in infection and immunity in both animals (Hara-Chikuma et al., 2015; Yang, 2017) and plants (Maurel et al., 2015; Wang F. et al., 2014; Zhang et al., 2018; Li et al., 2019). The functions of animal AQPs are no longer confined to substrate-transport-based processes such as urinary concentration and body fluid homeostasis (Brown, 2017), and are now known to include roles in various disease conditions and pathological states (Yang, 2017). Similarly, functional diversity – redundancy, overlapping, and extension beyond substrate transport – is a property of plant AQPs, especially PIPs (Ji and Dong, 2015b; Li et al., 2015; Zhang et al., 2018, 2019; Li et al., 2019). The functional scope of PIPs goes far beyond water relations or drought tolerance, extending to the subcellular transport of reactive oxygen species (ROS), including H_2O_2 (Tian et al., 2016; Smirnoff and Arnaud, 2019). H_2O_2 transport connects with signaling between the cell exterior and interior and between organelles, resulting in plant resistance to pathogen infection (Tian et al., 2016).

PIPs possess extracellular regions exposed to the outside environment (Maurel et al., 2015), and have potential to partake in plant responses to biotic and abiotic stresses. Here are several examples. Previous uses of induced resistance in crop protection (for example: Chen et al., 2008a,b; Fu et al., 2014; Wang F. et al., 2014) confirm the practical value of PIP-mediated immunity signal transduction (Tian et al., 2016). The correlation of PIP function in water transport with stress response results in promising strategies for improvement of plant tolerance to abiotic stresses, including drought (Balestrini et al., 2018). Drought tolerance in a variety of plant species is related to arbuscular mycorrhizal (AM) symbiosis, in which AM fungi (*Rhizophagus* spp.) show enhanced expression of AQP-encoding genes (Bárzana et al., 2014, 2015; Calvo-Polanco et al., 2016; Ruiz-Lozano et al., 2016; Sánchez-Romera et al., 2016; Ruiz-Lozano and Aroca, 2017). Surprisingly, the AM fungus *R. clarus* contributes its aquaglyceroporin (glycerol/water-transporting AQP) RcAQP3 to the mediation of long-distant polyphosphate translocation from the fungal vacuoles into cells of plant roots and leaves (Kikuchi et al., 2016). Genetic resources of plants, including the AQP transcriptome, can be used in responses to environmental cues, symbiotic microbes (AM fungi and rhizobia), and microbial pathogens (Desaki et al., 2018; Rey and Jacquet, 2018; Wang R. et al., 2018).

Due to their direct contact with the extracellular environment, PIPs risk being appropriated by plant pathogens to expedite infection (Zhang et al., 2018; Li et al., 2019). When infection is imminent, the real-time function of PIPs may switch from substrate transport to the regulation of plant responses to pathogens (Zhang et al., 2018; Li et al., 2019). This is either favorable or unfavorable to plant growth and development, depending on plant responses to pathogenicity determinants, called effectors, whose functions are subject to regulation of PIPs (Tian et al., 2016; Wang X. et al., 2018; Li et al., 2019; Zhang et al., 2019).

This review will summarize recent studies on the roles of PIPs in plant infection and immunity, and discuss the molecular, biochemical, and structural mechanisms involved. Discussion of infection will focus on type III (T3) effector translocation (T3ET) from *Xanthomonas oryzae* pv. *oryzae* (Xoo) into rice cells. Discussion of immunity will focus on the response of Arabidopsis to pathogens or pathogen-associated molecular patterns (PAMPs), also termed microbial patterns. This review will reference studies investigating AQPs in animals, microbes, and other plants to highlight the broad importance of PIP function, from substrate transport to infection and immunity in plants.

THE CIRCUMSTANTIAL FUNCTION OF A PIP IN T3ET

PIPs possess three extracellular regions that are exposed to the outside environment (Maurel et al., 2015). As a result, they are at a constant risk of being hijacked by pathogens attempting to infect plants, and inevitably partake in immunity against infection. Therefore, PIPs are required to extend their function from substrate transport to plant infection and immunity when the circumstances demand it. Emerging evidence suggests the implication of OsPIP1;3 in rice infection by Xoo (Zhang et al., 2018; Bian et al., 2019; Li et al., 2019). In this case, OsPIP1;3 functions with the bacterial hydrophilic protein Hpa1, which belongs to the harpin-group proteins secreted by the T3 secretion pathway of Gram-negative plant-pathogenic bacteria (Wei et al., 1992; Tejeda-Dominguez et al., 2017; Zhang et al., 2018; Li et al., 2019). Hpa1 produced by *X. oryzae* (Zhu et al., 2000; Chen et al., 2008a) is involved in the virulence of bacterial pathogens (Wang X. et al., 2018). Hpa1 modulates physiological and pathological processes in plants in association with PIPs (Sang et al., 2012; Li et al., 2013, 2014, 2015, 2019; Ji and Dong, 2015b; Zhang et al., 2018). The virulence role of Hpa1 is determined by its biochemical properties. Hpa1 is a one-domain harpin, which share a unitary hydrophilic "harpin" domain distinct from the enzymatic domain

present in two-domain harpins (Kvitko et al., 2007; Choi et al., 2013; Ji and Dong, 2015b). Two-domain harpins have potential to associate with the bacterial periplasm or plant cell walls to facilitate assembly of the T3 secretion machinery (Mushegian et al., 1996; Koraimann, 2003; Zhang et al., 2008; Dik et al., 2017; Hausner et al., 2017). One-domain harpins, including Hpa1, target plasma membranes (PMs), where they serve as T3 translocators to mediate T3ET (Kvitko et al., 2007; Bocsanczy et al., 2008; Wang X. et al., 2018; Bian et al., 2019; Li et al., 2019).

In Xoo-infected rice plants, secreted Hpa1 translocates at least two transcription activator-like (TAL) effectors – AvrXa10 and PthXo1, which are also produced via the pathway (Wang X. et al., 2018). Translocated effectors exert virulent or avirulent effects depending on the susceptibility of the plant variety (Yang et al., 2006; Büttner, 2016; Schreiber et al., 2016; Schwartz et al., 2017; Zhang et al., 2018). The rice variety Nipponbare is susceptible to the TAL effector PthXo1 secreted by PXO99^{A}, a well-studied Xoo strain (Yang et al., 2006; Wang X. et al., 2018; Zhang et al., 2018). To infect Nipponbare plants, PXO99^{A} secretes Hpa1 and delivers it to the cell surface, where Hpa1 interacts with OsPIP1;3 to facilitate the translocation of subsequently secreted PthXo1 into Nipponbare cells (Wang X. et al., 2018; Li et al., 2019). PthXo1 then induces virulence by activating its regulatory target – the host susceptibility gene *OsSWEET11* (Yang et al., 2006) in an OsPIP1;3-dependent manner (Zhang et al., 2018; Li et al., 2019). If the *OsPIP1;3* gene is silenced by hairpin or knocked out by TALEN^{14}, both PthXo1 translocation and *OsSWEET11* expression incur concomitant impairments up to 70%, highly alleviating virulence as a consequence (Zhang et al., 2018; Li et al., 2019). In contrast, both events acquire >2-fold enhancements if *OsPIP1;3* is overexpressed, causing marked aggravations in virulence (Li et al., 2019).

AvrXa10 is an avirulent effector secreted by the Xoo strain PXO86, and induces immune responses in the resistant rice variety IRBB10 (Tian et al., 2014). The plant immunity is determined by the disease-resistant gene *Xa10*, which is the target of AvrXa10 (Tian et al., 2014). *Xa10* has two homologs in the Nipponbare genome – *Xa10-Ni* and *Xa23-Ni*, both of which function similarly to confer immune responses in Nipponbare plants inoculated with recombinant PXO99^{A} strains that deliver the matching artificially designed TAL effectors (Wang et al., 2017). When *avrXa10* is transferred from PXO86 into the PXO99^{A} genome, the resulting PXO99^{A}/*avrXa10* recombinant delivers AvrXa10 in IRBB10 cells (Wang X. et al., 2018). Thereafter, AvrXa10 activates the disease resistant gene *Xa10-Ni* to confer the plant resistance against the blight disease (Wang X. et al., 2018). The AvrXa10 translocation and *Xa10-Ni* activation incur concomitant impairments in plants inoculated with the *hpa1*-deleted mutant; the absence of *hpa1* markedly reduces the quantity of AvrXa10 translocation, decreasing the expression level of *Xa10-Ni* (Wang X. et al., 2018). The AvrXa10 translocation and *Xa10-Ni* activation requires *OsPIP1;3*, and both events are enhanced by *OsPIP1;3* overexpression but inhibited by *OsPIP1;3* silencing (Bian et al., 2019).

These findings demonstrate the important role of OsPIP1;3 in the translocation of T3 effectors, at least the TAL effectors PthXo1 and AvrXa10, from bacterial cells into the cytosol of rice cells. OsPIP1;3 functions either as a disease-susceptibility or -resistance factor, depending on a virulent or avirulent function of the translocated effector.

POTENTIAL MECHANISMS OF T3ET REGULATION

Passages of proteic T3 effectors are 1.2–5.0 nanometers in width (Ji and Dong, 2015b; Guignot and Tran Van Nhieu, 2016), in contrast to PIP/AQP channels with an aperture around 3 Å, which is permeable to small substrates (Heckwolf et al., 2011; Li et al., 2015; Tian et al., 2016) but impossible for proteins to pass (Li et al., 2019). Presumably, the role of OsPIP1;3 in T3ET complies with one of regulation models currently in debate (Domingues et al., 2016; Prasad et al., 2016; Santi-Rocca and Blanchard, 2017; Scheibner et al., 2017; Tejeda-Dominguez et al., 2017; Gaytán et al., 2018; Wagner et al., 2018; Shanmugam and Dalbey, 2019). Three models have been proposed as the canonical translocon-dependent delivery (Büttner, 2012; **Figure 1** middle purple route) and the translocon-independent pore formation (Rüter et al., 2010; **Figure 1** left black route) and endocytosis (Santi-Rocca and Blanchard, 2017; **Figure 1** right red route). To date, studies on the three models have obtained empirical genetic evidence (Finsel and Hilbi, 2015; Domingues et al., 2016; Dong et al., 2016; Chakravarthy et al., 2017; Scheibner et al., 2017), but the structural basis of each model remains to be analyzed.

The first model of T3ET (**Figure 1** middle purple route) was proposed to emphasize molecular interactions between T3 translocators and molecular interactions of T3 translocators with PM receptors (Büttner and Bonas, 2002; Büttner et al., 2008; Büttner, 2012; Ji and Dong, 2015b), either lipids (Haapalainen et al., 2011; Li et al., 2011), or proteins (Oh and Beer, 2007; Li et al., 2015; Adam et al., 2017). T3 translocators include one hydrophilic protein, such as Hpa1 from xanthomonads – bacteria in the *Xanthomonas* genus (Zhu et al., 2000; Chen et al., 2008a; Wang X. et al., 2018), and two hydrophobic proteins (Büttner et al., 2008; Ji and Dong, 2015b), such as HrpF from the same bacteria (Büttner et al., 2002; Li et al., 2011; Hausner et al., 2017). Recognition of the hydrophilic translocator by a component of the PM composition is the first step towards translocon assembly (Goure et al., 2004; Mueller et al., 2008; Sawa et al., 2014). Then, the translocon is finalized by the binding of lipids to hydrophobic translocators (Büttner et al., 2008; Büttner, 2012; Ji and Dong, 2015b). A completed translocon possesses an inner conduit that opens into a target cell and accommodates bacterial effector translocation (Büttner et al., 2008; Chatterjee et al., 2013; Ji and Dong, 2015b; Büttner, 2016).

Although there is no evidence so far to verify the T3 translocon assembly, many studies suggest the involvement of T3 translocators in effector translocation from animal- and plant-pathogenic bacteria into cells of their corresponding eukaryotic hosts (summarized in Scheibner et al., 2017). Mounting evidence indicates the engagement of PM phospholipids in T3ET, especially phosphatidylinositol phosphates PI(n)Pn (Lee et al., 2001a,b; Büttner et al., 2002; Weber et al., 2006; Hubber and Roy, 2010; Li et al., 2011; Finsel and Hilbi, 2015; Dong et al., 2016). For T3ET

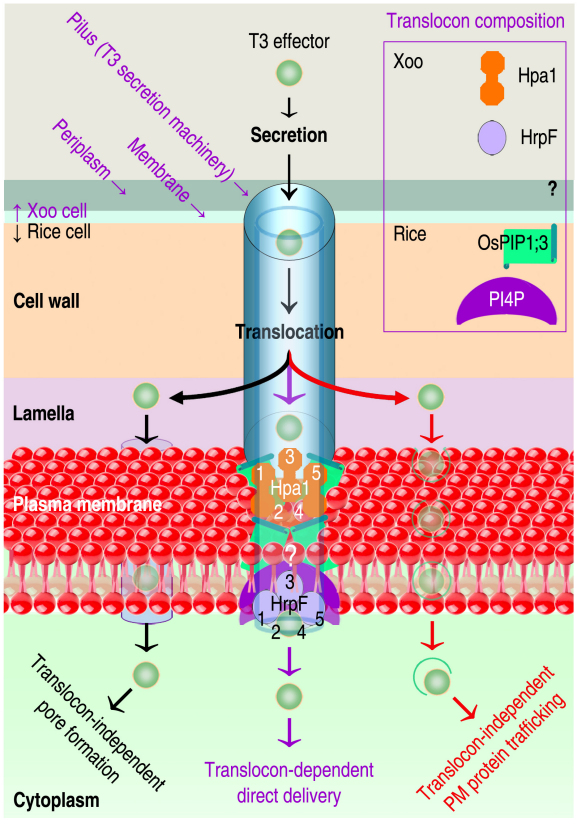

FIGURE 1 | Hypothetic routes of T3ET using Xoo as an example. Effector translocation may use the left black route (Rüter et al., 2010; Scheibner et al., 2017) or the right red pathway (Lu et al., 2007; Santi-Rocca and Blanchard, 2017) according to recently proposed models. In a previously proposed model, T3ET occurs via the translocon (the middle purple route) hypothetically assembled by interactions between translocators, and their receptors in eukaryotic PMs (Büttner, 2012; Ji and Dong, 2015b). Three translocators have been identified in animal-pathogenic bacteria, but the number of T3 translocator remains unknown in plant-pathogenic bacteria including Xoo. In Xoo, the hydrophilic protein Hpa1 (Wang X. et al., 2018) and the hydrophobic protein HrpF (Büttner et al., 2002; Li et al., 2011) were determined to function as T3 translocators, but whether the third translocator exists is unclear (question marks). Regarding molecular interactions during the translocon assembly, OsPIP1;3 has been verified to interact with Hpa1 at rice PMs to expedite the translocation of TAL effectors AvrXa10 and PthXo1 (Zhang et al., 2018; Li et al., 2019). In the cartoon, numbers 1 through 5 refer to the order of the translocator in self oligomerization to form the homogenous complex, which is assumed to be consisting of 5 or 8 monomers (Mueller et al., 2008). *In vitro* assays indicated HrpF binding to lipids (Büttner et al., 2002; Li et al., 2011), such as PI4P, but no evidence was available to demonstrate the lipid binding at plant PMs and the subsequent effect on T3 effector translocation.

from xanthomonads, lipids in the plant PM associates with the bacterial hydrophobic T3 translocator HrpF (Büttner et al., 2002; Li et al., 2011). HrpF was the first reported T3 translocator and is regarded as a marker of T3 translocon in xanthomonads (Büttner et al., 2002; Scheibner et al., 2017). HrpF is highly conserved in xanthomonads (Sugio et al., 2005) and has been shown to mediate the translocation of AvrBs3 from *X. campestris* pv. *vesicatoria* (*Xcv*) – the bacterial spot pathogen of pepper (Büttner et al., 2002; Noël et al., 2002), and from *X. oryzae* pv. *oryzicola* — the pathogen that causes bacterial leaf streak in rice (Li et al., 2011). Evidence is further provided by our demonstrations that the hydrophilic T3 translocator Hpa1 of Xoo interacts with OsPIP1;3 at rice PMs to expedite translocation of TAL effectors PthXo1 and AvrXa10 from Xoo cells into the cytosol of rice cells (Zhang et al., 2018; Bian et al., 2019; Li et al., 2019).

The second model of T3ET (**Figure 1** left black pathway) is the translocon-independent pore formation by bacterial effectors characteristic of cell-penetrating peptide (RPP; Scharnert et al., 2013; Rüter and Schmidt, 2017). Pore forming in eukaryotic PMs is momentary, occurs quickly upon recognition of bacterial effectors, and is regulated by membrane repair mechanisms (Scharnert et al., 2013). RPPs are either autonomously transported across the membrane or delivered by endocytosis (Wang F. et al., 2014). Autonomous translocation was found with the T3 effector YopM from *Yersinia enterocolitica* (Rüter et al., 2010). The YopM sequence contains two N-terminal α-helices, which determines the interaction with eukaryotic PMs (Li et al., 2019), and two putative nuclear localization signals at the C-terminus (Benabdillah et al., 2004). Therefore, YopM can be translocated directly into the cytosol of target cells and further transported into the nucleus via vesicle trafficking (Skrzypek et al., 1998).

Little is known about the translocon-independent translocation of T3 effectors from plant-pathogenic bacteria except for the TAL effector AvrBs3 from *Xcv*. Preliminary infection experiments with *Xcv* translocon mutants and endocytosis inhibitors deny a contribution of endocytosis to the delivery of AvrBs3 (Scheibner et al., 2017). A possible route for AvrBs3 translocation from the translocon mutants is a direct transportation through pore formation. The pore could be proteolipidic (Gilbert et al., 2014) and could be generated by means of proteic and lipidic constituents, which are required for the translocation of T3 effectors from xanthomonads (Büttner et al., 2002; Li et al., 2011, 2019). However, the efficiency of AvrBs3 translocation from the translocon mutants is much lower than that from the WT strain, indicating that the translocon-independent route is used in the absence of alternative.

The third model of T3ET (**Figure 1** left black pathway) was recently proposed to emphasize the effector endocytosis through direct interaction with receptors situated in eukaryotic PMs (Domingues et al., 2016). The molecular interaction may trigger the membrane trafficking mechanism (Allgood and Neunuebel, 2018) either by endoplasmic reticulum (ER) or vesicles (Wudick et al., 2015), providing a potential scheme for bacterial effector endocytosis (**Figure 2**). Protein and lipid trafficking via ER is universal (Cybulsky, 2017; Obacz et al., 2017), and vesicle-mediated PIP trafficking has been elucidated in roots of Arabidopsis following treatment with H_2O_2 (Wudick et al., 2015). The treatment induces AtPIP2;1 accumulation in the late endosomal compartments, and increases stability of the PIP and its homologs in the cytoplasm (Wudick et al., 2015). Like AtPIP1;4 (Li et al., 2015, 2019), AtPIP2;1 also is an $H_2O/H_2O_2/CO_2$ triple channel (Heckwolf et al., 2011; Rodrigues et al., 2017), but no study shows whether or not AtPIP2;1 resembles AtPIP1;4 to regulate bacterial effector translocation.

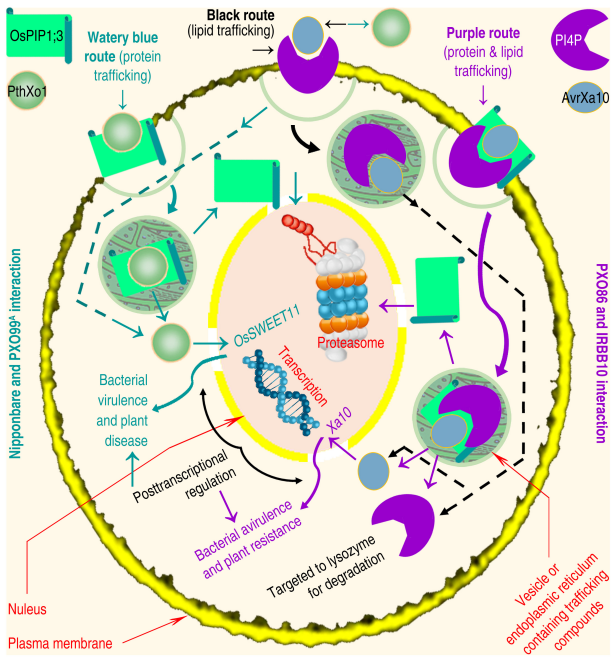

FIGURE 2 | Diagram of hypothesized PM protein and lipid trafficking that is going through ER (Obacz et al., 2017) or vesicles (Wudick et al., 2015) and drives T3 effector endocytosis (Domingues et al., 2016). The OsPIP1;3-dependent and/or PI4P-involved PthXo1 and AvrXa10 translocation is used as a study paradigm. The protein and lipid trafficking pathways are annotated as a motivation for both effectors to be internalized and then both effectors execute the transcriptional regulation on their target genes. Both pathways may involve unannotated response, that is the recognition of Hpa1 by OsPIP1;3 and HrpF by PI4P (Büttner et al., 2002; Büttner, 2012; Ji and Dong, 2015b). The protein and lipid trafficking may be concurrent, cooperative or independent, making responses on PMs more intricate than the regular remodeling in the absence of bacterial proteins (Hubber and Roy, 2010; Piscatelli et al., 2016; Santi-Rocca and Blanchard, 2017).

It is deserved of studying whether multiple substrate specificities of a PIP enable it to accommodate bacterial effectors.

There are two examples indicating the possibility that T3 effectors of plant-pathogenic bacteria are translocated along with membrane trafficking. One is the T3 effector HopZ1a of *Pseudomonas syringae* pv. *syringae*, bacterial pathogen of many plants. HopZ1a, HopZ1b, and HopZ1c are allelic forms, constitute the HopZ1 family of *P. syringae* T3 secretion system, and share a consensus myristoylation site required for membrane localization (Zhou et al., 2009). HopZ1a is an acetyltransferase, is activated by the eukaryotic co-factor phytic acid, and turns to acetylate itself and tubulin. Tubulin acetylation causes a decrease in microtubule networks, disrupts the secretory pathway, and suppresses cell wall-associated defense in plants (Lee et al., 2012). The defense is subject to complex regulatory networks, which involve vesicle trafficking linked to microtubules (Lehman et al., 2017). The other example is the T3 effector HopM1 of *P. syringae* pv. *tomato*. To infect tomato plants, the bacteria secrets HopM1, and delivers it into the plant PM-derived trans-Golgi network/early endosome (Nomura et al., 2011), suggesting a role of vesicle trafficking in HopM1 translocation.

The involvement of AQPs in T3 effector endocytosis can be speculated from independent studies summarized below. The trafficking of animal AQPs towards the cell interior is triggered by the AQP binding to a different protein (Zelazny et al., 2009; Ji and Dong, 2015a), such as vasopressin (Kamsteeg et al., 2006), or heat shock protein HSP70 (Lu et al., 2007). Nevertheless, molecular interactions at the PM transiently affect PM integrity (Laliberté and Sanfaçon, 2010; Guignot and Tran Van Nhieu, 2016; Santi-Rocca and Blanchard, 2017), which may extricate and internalize PM-associated proteins to accommodate foreign molecules like T3 effectors. It is possible that AvrBs3 and PthXo1 use this mechanism to enter rice cells together with OsPIP1;3 trafficking (**Figure 2**). Both effectors may be internalized through trafficking of OsPIP1;3 en route to degradation by the proteasome (Hirano et al., 2003; Centrone et al., 2017) or the autophagosome (Khositseth et al., 2017). This mode of trafficking and degradation has been shown to regulate animal AQP turnover (Khositseth et al., 2017; Shen et al., 2019) and may also apply to plant AQPs. It is necessary to verify whether OsPIP1;3, or any other PIPs, can interact with any of the bacterial effectors, in the absence of Hpa1, to cause the PIP and effector internalization.

How could PM binding lead to endocytosis of bacterial effectors? The binding of effectors or translocators to the PM induces transient damage to the integrity and function of PM compositions, providing an abnormal pathway for bacterial effector translocation (Guignot and Tran Van Nhieu, 2016). In addition to T3, other secretion systems, such as T4, may be involved also (Domingues et al., 2016). *Salmonella enterica* serovars are intracellular facultative pathogens with a wide host range, and cause serious diseases including typhoid fever and cholera in humans (Domingues et al., 2016; Piscatelli et al., 2016). About 40 different T3 effectors confer differential virulence to different serovars. For infection, *Salmonella* bacteria establish a bacteria-containing vacuole (BVC), induce tubules, and then deliver the T3 effector SteA onto the BCV and tubules. In both structures, SteA specifically interacts with PI4P to move into host cells (Domingues et al., 2016). *Legionella pneumophila*, the pathogen responsible for Legionnaire' disease, creates BCV through effectors secreted by the Dot/Icm T4 system (Finsel and Hilbi, 2015). In BCV, the pathogen hijacks host PM trafficking to induce BCV maturation (Hubber and Roy, 2010). The BCV membrane mainly contains PI4P (Weber et al., 2006; Finsel and Hilbi, 2015), which is important for anchoring many Dot/Icm effectors onto BCV (Dong et al., 2016). The T4 effector LepBd of *L. pneumophila* is a phosphatase (PP), and specifically converts PI3P into $PI(3,4)P_2$. $PI(3,4)P_2$ is efficiently hydrolyzed into PI4P (Dong et al., 2016), which may be used to replenish the PI4P stock of BCV. This mechanism is also employed by the T3 effector SopB of cholera pathogen *S. enterica* serovar Typhimurium. Like the T4 effector LepBd of *L. pneumophila*, the T3 effector SopB of Typhimurium is also a PP, but possesses both 4-PP and 5-PP activities. This dual enzymatic function is essential for the formation of BCV membrane ruffles and subsequent bacterial invasion. The 5-PP activity of SopB is assumed to generate $PI(3,4)P_2$, which is then recruited by sorting nexin 9 (SNX9), an actin-modulating protein. The 4-PP activity converts $PI(3,4)P_2$ to PI3P. Alone, neither activity is sufficient for

membrane ruffling. Instead, combined 4-PP and 5-PP activities induce SNX9-mediated membrane ruffling and bacterial invasion (Dong et al., 2016).

The three models of T3ET may be chosen to use circumstantially by bacteria with genetic variations in the T3 repertoire. For example, the translocon-dependent mechanism guarantees efficient translocation of AvrBs3 from the wild-type *Xcv* strain (Büttner et al., 2002), in contrast to insufficient translocation from the bacterial translocon mutants in a translocon-independent manner (Scheibner et al., 2017). An early report stated that the carboxy (C)-terminal region of HrpF is essential for the entry of *Xcv* AvrBs3 into plant cells, whereas the nitrogen (N)-terminal contains a secretion signal and has no effect on effector translocation (Büttner et al., 2002). This suggests that xanthomonads T3ET occurs in a translocon-dependent manner. By contrast, a recent report proposed a translocon-independent pathway (Scheibner et al., 2017). The N-terminal 10 and 50 amino acids are required for T3 secretion and AvrBs3 translocation, respectively. Additional signals in the N-terminal 30 amino acids and the region between amino acids 64 and 152 promote AvrBs3 translocation. AvrBs3 translocation occurs in the absence of the T3 secretion chaperon HpaB, and in the absence of HrpF, which is a predicted component of the T3 translocon assembly. The authors suggested that the delivery of AvrBs3 begins during the early stages of infection, before the activation of HpaB or translocon integration into the plant PM (Scheibner et al., 2017). It is more likely that a different translocator, present in reserve and lacking function when the bacteria possesses a workable HrpF, is employed when HrpF loses function or is removed from the bacterial proteome.

A CYTOLOGICAL GAP BETWEEN H_2O_2 SIGNALING AND IMMUNITY PATHWAYS

H_2O_2 is stable compared with other ROS molecules such as the superoxide anion O_2^- and hydroxyl radical OH^-. In plants, H_2O_2 is produced by the enzymatic activities via multiple biochemical mechanisms (Smirnoff and Arnaud, 2019). These mechanisms include electron leakage from the electron transport chain in chloroplasts and mitochondria, the activity of peroxisomal oxidases and peroxidases in cytoplasm or plant cell walls, as well as the activity of NADPH oxidases (NOXs) in the PM (Smirnoff and Arnaud, 2019). The rapid production of ROS, especially H_2O_2, indicates the successful recognition of pathogen infection and molecular patterns (Alvarez et al., 1998; Torres, 2009). Well-known examples of pathogenic patterns include invariant microbial epitopes, such as fungal chitin (Kaku et al., 2006) and bacterial flagellin (Zipfel et al., 2004) and harpin proteins (Sang et al., 2012; Choi et al., 2013). These pattern molecules can be recognized by pattern receptors within the PM, which induce immune responses, including H_2O_2 production, in plants (Levine et al., 1994; Ausubel, 2005; Galletti et al., 2011).

The production of H_2O_2 is typically apoplastic, resulting mainly from the enzymatic activity of NOXs located in PMs (Sagi and Fluhr, 2006; Kärkönen and Kuchitsu, 2015; Smirnoff and Arnaud, 2019). Then, there is crosstalk between H_2O_2 and immunity pathways, such as systemic acquired resistance (SAR) and pattern-triggered immunity (PTI) to regulate plant disease resistance (Torres, 2009). SAR is characteristic of the induced expression of pathogenesis-related (PR) genes, typically *PR-1* and *PR-2*, under the regulation of non-inducer of *PR* genes-1 (NPR1) (Cao et al., 1997; Kim et al., 2011). NPR1 functions through conformational changes under cytoplasmic redox conditions (Tada et al., 2008) and through proteasome-mediated turnover in the nucleus (Spoel et al., 2009). The PTI pathway activates a cytoplasmic MAPK cascade (Asai et al., 2002), including a branch in which MPK3 and MPK6 phosphorylate different substrates (Bigeard et al., 2015; Pitzschke, 2015) to activate immune responses, including H_2O_2 and callose production (Bethke et al., 2012; Daudi et al., 2012). Callose is a β-1,3-glucan synthesized by glucan synthase-like (GSL) enzymes, with GSL5 playing a critical role in cellular immune responses (Lü et al., 2011). Therefore, both the SAR and PTI pathways comprise pivotal tiers of intracellular responses in the crosstalk with H_2O_2 produced in the apoplast (Sagi and Fluhr, 2006). It is clear that a cytological gap exists between H_2O_2 generation and functional performance. In fact, it remains unclear for a long time how apoplastic H_2O_2 penetrates plant PMs to enter the cytoplasm and regulate immunity.

PIP-MEDIATED H_2O_2 TRANSPORT AND ITS IMMUNOLOGICAL IMPORTANCE

Hpa1, applied to plants or produced in transgenic plants, functions as a bacterial pattern to activate the PTI and SAR pathways (Tian et al., 2016). Both pathways are activated by the generation of ROS, especially H_2O_2, in plant apoplasts. In Arabidopsis, inoculation with the bacterial pathogen *Pseudomonas syringae* pv. *tomato* or treatment with bacterial patterns, including Hpa1 and the flagellin functional fragment flg22, induce H_2O_2 generation in the apoplast. This H_2O_2 moves quickly into the cytoplasm, where H_2O_2 associates with PTI and SAR signal transduction. AtPIP1;4 serves as a H_2O_2 transport channel to facilitate apoplastic H_2O_2 import into the cytoplasm (**Figure 3A**), bridging the cytological gap in immunity signaling cascades (Tian et al., 2016).

This finding validates the hypothesis that H_2O_2 transport across a biomembrane is mediated by particular AQP isoforms in addition to certain membrane lipids (Bienert et al., 2006, 2007; Bienert and Chaumont, 2014; Aguayo et al., 2015). AQPs are transmembrane channels essential for the transport of H_2O, H_2O_2, and other small substrates in all living cells (Maurel, 2007; Gomes et al., 2009). In this way, AQPs can modulate many physiological and/or pathological processes (Maurel, 2007; Ji and Dong, 2015a,b; Li et al., 2019; Pawłowicz and Masajada, 2019; Zhang et al., 2019). In most plant species, five major families of AQPs exist. The PIP family has 11 members, PIP1;1–5 and PIP2;1–8 (Gomes et al., 2009; Abascal et al., 2014; Maurel et al., 2015). These are believed to mediate the transport of different substrates across plant PMs in an overlapping or redundant substrate-specific manner (Maurel, 2007; Péret et al., 2012, 2013; Prado et al., 2013). To date, five AtPIP isoforms (2;1, 2;2, 2;4, 2;5,

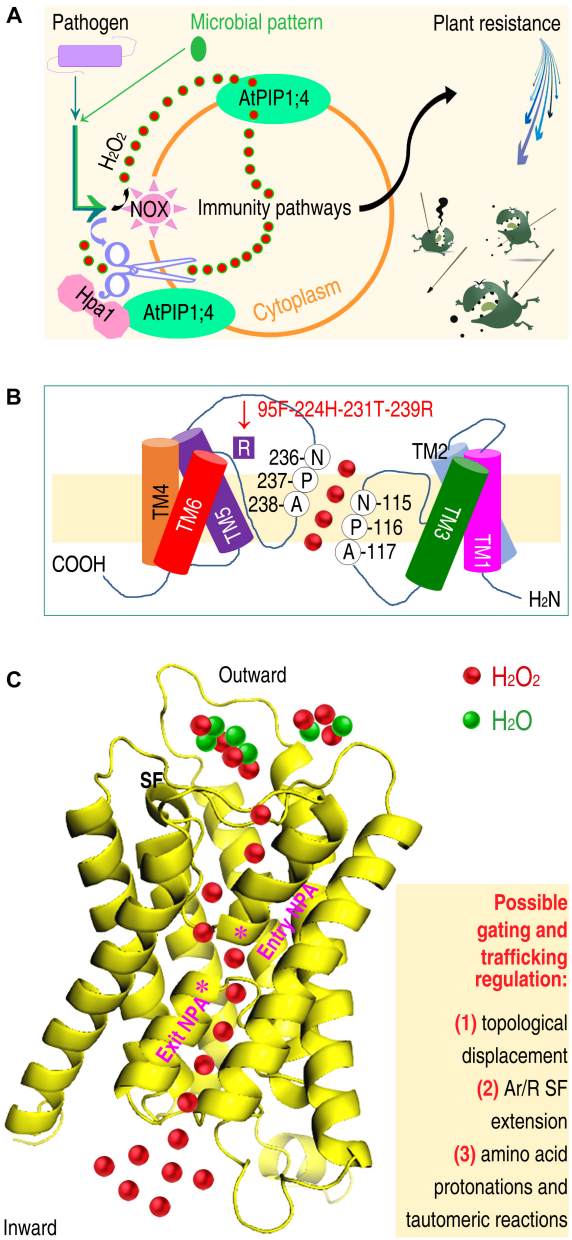

FIGURE 3 | Crosstalk of AtPIP1;4-mediated H_2O_2 transport with the intracellular immunity pathways and predicted mechanisms by which AtPIP1;4 fulfills the substrate transport function. **(A)** Plant sensing of a pathogen or microbial pattern not only is an essential step of apoplastic generation and cytoplasmic import of H_2O_2, but also induces damages to the PM integrity (Guignot and Tran Van Nhieu, 2016). Impairment of the PM integrity is likely to provide an abnormal channel, which is wider than the normal conduit, and capable of accommodating substrates larger than H_2O. **(B)** Hypothetic determinants of AtPIP1;4 conformation for H_2O_2 transport include amino acid compositions and locations in the NPA and SF regions. **(C)** Gating and trafficking regulation of the AtPIP1;4 channel for H_2O_2 transport across plant PMs (left) may be subject to the annotated factors (right). The 3D-structure of AtPIP1;4 was predicted by using the PHYRE2 (Protein Homology/analogy Recognition Engine V 2.0) program (http://www.sbg.bio.ic.ac.uk/phyre2/html/page.cgi?id~=~index). The diagrammatic transport of H_2O_2 over H_2O is a surmise, predicted to occur by the combined mechanisms indicated on right.

and 2;7) are assumed to mediate H_2O_2 transport in engineered yeast cells (Bienert and Chaumont, 2014). The *de novo* expression of these PIPs can increase H_2O_2 sensitivity and decrease the viability of yeast (Dynowski et al., 2008; Hooijmaijers et al., 2012). Based on incomplete literature search, not all PIPs whose expression increases H_2O_2 sensitivity and decreases the viability of yeast have been verified for the H_2O_2 transporting function. AtPIP2;1 was determined to increase H_2O_2 uptake by yeast cells (Dynowski et al., 2008; Bienert and Chaumont, 2014) and by Arabidopsis guard cells (Rodrigues et al., 2017). AtPIP1;4 has been shown to function in H_2O_2 transport from the apoplast into the cytoplasm of Arabidopsis (Tian et al., 2016). Many works are required to test *in planta* function of the AQP candidates in H_2O_2 translocation.

CONSERVATIVE AQP FUNCTION FOR H_2O_2 TRANSPORT

AtPIP1;4 was determined to have triple substrate specificities (Li et al., 2015; Tian et al., 2016). In addition to transporting H_2O_2 (Tian et al., 2016), AtPIP1;4 partakes in the cellular hydraulic conductance (P_f) of roots, and in mesophyll conductance of CO_2 (g_m); however, it does not affect stomatal CO_2 conductance (g_s) or P_f in leaves (Li et al., 2015). The interaction of AtPIP1;4 with Hpa1 at Arabidopsis PMs promotes substrate transport, increasing the net photosynthesis rate (A_N), while P_f is also increased in leaves and roots (Li et al., 2015). Therefore, a PIP can alter its physiological functions or effect extents in response to plant pathogens or bacterial patterns.

The function of AtPIP1;4 in immunity is an extension of its primary roles in substrate transport, which was initially assigned to AQPs in mammals (Preston and Agre, 1991) and subsequently in plants (Maurel et al., 1993). The functional extension of AtPIP1;4 has biological importance for at least two reasons. First, AtPIP1;4-dependent SAR responses induced by bacterial pathogens effectively repress pathogen virulence (Tian et al., 2016; **Figure 3A**). In this case, pathogen-associated repressors of plant immunity (Oh and Collmer, 2005; Zhang et al., 2007; Guo et al., 2009) may be inhibited, or their immunity-repressing functions may be counteracted by the role of AtPIP1;4 in H_2O_2 translocation, which is linked to the immunity pathway. Second, AtPIP1;4 is an integral component of PTI in response to typical patterns, with conserved microbial cell-surface composition, i.e., flagellin (Zipfel et al., 2004) and chitin (Kaku et al., 2006). Despite their different biochemical nature, both patterns require AtPIP1;4 to induce PTI responses, except in the absence of induced *MPK6* expression (Tian et al., 2016). This is consistent with previous findings that the MAPK cascade diverges at MPK3 and MPK6 (Asai et al., 2002; Bigeard et al., 2015) to regulate distinct substrates in response to different patterns (Galletti et al., 2011; Pitzschke, 2015). Moreover, the induction of *MPK3* expression represents a circuit of the MAPK cascade in response to H_2O_2 (Gudesblat et al., 2007). These sets of information suggest that AtPIP1;4 plays a prominent role in immunity signaling by mediating apoplastic H_2O_2 translocation into plant cells.

AQP-mediated H_2O_2 transport in immune signaling also occurs in mammals. Among 13 AQPs, AQP3 is a H_2O_2 transport channel (Miller et al., 2010). AQP3-mediated H_2O_2 transport is associated with necrosis factor-κB (NF-κB) signaling in keratinocytes, and in the pathogenesis of psoriasis in response to cytokine regulation (Hara-Chikuma et al., 2015). The induction of psoriasis by cytokines, NF-κB activation, and intracellular H_2O_2 accumulation are concomitantly reduced in AQP3-knockout mice. In primary keratinocyte cultures, H_2O_2 is generated by membrane-associated NOX2 in response to TNF-α, and moves into intracellular spaces. Cellular import of H_2O_2 is facilitated by AQP3 and is required for NF-κB activation under PP2A regulation. Since AQP3 associates with NOX2 at PMs, this interplay may constitute H_2O_2-mediated signaling in response to TNF-α stimulation (Hara-Chikuma et al., 2015). Moreover, under oxidative stress, AQP3-mediated H_2O_2 transport attenuates apoptosis by regulating the P38 MAPK pathway (Xu et al., 2018; He and Yang, 2019). Based on these findings, and those regarding PIPs, cytoplasmic import across the PM can reduce the cytological distance for H_2O_2 generation, and functional performance (Bienert et al., 2006; Sang et al., 2012; Tian et al., 2016). Apocytoplastic signaling is conserved in plants and animals.

AQP STRUCTURE FOR H_2O TRANSPORT

It is unclear how different AQPs function in the transport of corresponding substrates, and how an AQP, such as AtPIP1;4 (Li et al., 2015; Tian et al., 2016), can function as a triple substrate transport conduit. One hypothesis is that structural details allow for differences in selectivity and modes of regulation (Kreida and Törnroth-Horsefield, 2015). Regarding H_2O_2 transport, the structures of AQP/PIP channels have not been studied, but can be inferred from information on structures of AQPs that function as water channels.

Plant aquaporins are predominant channels of H_2O transport between the outside and inside of the cell, and between intracellular organelles (Huang et al., 2017). Although cotransporters and uniporters have been implicated in water homeostasis, AQPs have been accepted as intramolecular channels for the transmembrane movement of H_2O down an osmotic gradient (Maurel et al., 2015; Huang et al., 2017; Yang, 2017; Pawłowicz et al., 2018). H_2O transport by AQPs is determined by their three-dimensional structure.

Structural studies have characterized AQPs as homotetramers, which are integrated into the membrane with conserved configurations (Fu et al., 2000; Sui et al., 2001; Törnroth-Horsefield et al., 2006; Horsefield et al., 2008; Eriksson et al., 2013; Kirscht et al., 2016). Each monomer has a functional pore formed by six α-helical TM domains (TM1–TM6), five connecting loops (LA–LE), and two shorter helices (HB and HE). The outward end of HB and inward end of LE contain a pair of asparagine (N), proline (P), and alamine (A) tandem (NPA) motifs, which constitute the central channel through the membrane (Kirscht et al., 2016). Two NPAs form a conical funnel or traditional hourglass, which are linked at the tip and open outward from LE and inward from TM5 (Törnroth-Horsefield et al., 2010), and are essential for AQP function (Wree et al., 2011; Chen et al., 2018). Within LE, TM2 and TM5, the aromatic/arginine (Ar/R) selective filter (SF) is formed by four residues including aromatic amino acids and an arginine (R) residue; hence its name (de Groot et al., 2003). The SF is located in the outward opening of the channel and allows H_2O to pass while repelling protons and cations (Eriksson et al., 2013). Multiple physical factors, such as hydrophilic and hydrophobic interactions, electrostatic repulsion, and dipole alignment between amino acid residues within or around the NPA and SF, influence substrate selectivity (Törnroth-Horsefield et al., 2006).

A pivotal step toward the substrate-transporting function of AQPs is the regulation of gating (opening and closing) and trafficking (substrate transport). This has been elucidated for water channels at angstrom (Å) or sub-Å resolution (Daniels et al., 1999; Fotiadis et al., 2001; Kukulski et al., 2005; Kreida and Törnroth-Horsefield, 2015). Considering spinach *Spinacia oleracea* SoPIP2;1, channel opening is triggered by the phosphorylation of conserved serine (S) 197 (Johansson et al., 1996; Kukulski et al., 2005), and is expedited by hydrogen bond networks in LD (Törnroth-Horsefield et al., 2010). Channel closure results from the dephosphorylation of S115 in LB and S274 in the C-terminal region of the AQP sequence under conditions of drought stress, or from the protonation of a conserved histidine (H) residue following a decrease in cytoplasmic pH due to anoxia during flooding. Dissection of SoPIP2;1 crystal structures, both the closed conformation at 2.1 Å and the open conformation at 3.9 Å, reveals the importance of LD displacement for gating and trafficking. The dephosphorylation of S115 and S274 prevents outward NPA entry from LB, and inward NPA exit in TM5. In the open conformation of SoPIP2;1, S197 is phosphorylated at LD, LD is displaced up to 16 Å, the nitrogen terminus of TM5 extends a further half-turn into the cytoplasm, and NPA entry and exit are promoted. In addition, H193 protonation and interactions between amino acids, including hydrogen bond networks and electrostatic repulsion, also influence the switch between opening and closing of the channel (Törnroth-Horsefield et al., 2010).

Crystal structure analysis of Aqγ1, the only AQP in yeast *Pichia pastoris*, at a sub-Å (0.88 Å) resolution, provides evidence for tautomeric reactions to expedite H_2O transport (Eriksson et al., 2013). Hydrophilic amino acids in NPA and SF interact to bind H_2O molecules, which are then navigated through the channel. With polar hydrogen bond configurations, four H_2O molecules per group pass the SF, and then divide into two pairs to pass through the inward NPA region. There are two types of tautomerism between hydrophilic amino acids in the SF. One is proton transfer – the atom Nδ, but not Nε, of H212 is protonated to provide a proton for L208, with the role of guiding H_2O movement. The other one is covalent binding – atoms Cζ and Nη2 of R227 maximally bind to each other, Nη2 is closest to the central conduit, and its positive

charge repels cations, creating favorable conditions for H_2O to travel through the SF. With this advantage, four compact H_2O molecules are located within the full space of the SF, where they synchronize to move within and across the SF passage. Due to high impacts of atom tautomerism and hydrogen-bond interactions restricted to the H_2O molecules in transport, other H_2O molecules must wait for the next round of the channel opening and trafficking, and proton or cations are unable to enter the SF.

In addition to the structural configuration, biochemical regulation is also indispensable to the function of AQPs. In this aspect, channel gating and trafficking regulation by phosphorylation are ubiquitous for all AQPs (Li and Wang, 2017; Kapilan et al., 2018; Laloux et al., 2018; Nesverova and Törnroth-Horsefield, 2019). Additionally critical mechanisms underlying the functional regulation of different AQPs include biotic and abiotic signals. They induce the transport of different substrates (Tian et al., 2016; Ruiz-Lozano and Aroca, 2017; Balestrini et al., 2018; Smirnoff and Arnaud, 2019) by stimulating AQPs themselves with gradients over membranes and by interacting with other proteins (Ji and Dong, 2015a; Roche and Törnroth-Horsefield, 2017). These have been topics of many literatures (for example: Maurel and Plassard, 2011; Hara-Chikuma et al., 2015; Ji and Dong, 2015a; Maurel et al., 2015; Yang, 2017; Roche and Törnroth-Horsefield, 2017) and will not been discussed in this article.

CONTROL OF SUBSTRATE SPECIFICITIES

This is a question for AQPs capable of transporting substrates other than H_2O, especially those that have multiple permeation properties. In addition to H_2O, approximately 20 other substrates require AQPs to move between the exterior and interior of cells, and between organelles (Laloux et al., 2018). A fifth pore created by four AQP monomers of a homotetramer in the lipid bilayer (Wang et al., 2007) or yeast membrane (Otto et al., 2010) has been proposed for gas (CO_2 and O_2) and ion transport (Kaldenhoff et al., 2014). Moreover, many AQPs have more than one substrate (Kreida and Törnroth-Horsefield, 2015; Maurel et al., 2015; Fox et al., 2017; Laloux et al., 2018). Examples include AtPIP2;1 for H_2O/H_2O_2 (Dynowski et al., 2008; Verdoucq et al., 2008), AtPIP1;4 for $H_2O/H_2O_2/CO_2$ (Li et al., 2015; Tian et al., 2016), and TIPs for H_2O, H_2O_2 and/or ammonia (NH_3; Maurel et al., 1993; Loque et al., 2005; Bárzana et al., 2014) transport. Regulation of gating and trafficking must differ considerably between specialist channels, different generalist channels, and channels for H_2O and a different substrate. Variation in NPA diameter, the composition and width of SF, neighboring residues, and their interactions with each other and with the substrate might explain multiple functions of AQPs/PIPs in the transport of different substrates, and the multiple substrate transport capacities of a single AQP/PIP (Fox et al., 2017).

Recently, a smart solution was proposed in a study on the 1.18 Å crystal structure of AtTIP2;1 (Kirscht et al., 2016). That study characterized AtTIP2;1 as an NH_3 transport channel, which functions with an extended SF. The channel diameter in the NPA region is smaller than that of other AQPs, but remains constant at ∼3Å along the channel; this is in contrast to the narrowing of SF in other AQPs. The topological positions of four SF residues in TM2, TM5, LE, and HE are thought to determine substrate selectivity (de Groot et al., 2001). Consistent with this model, TIP2s deviate from other AQPs in terms of the wider SF, which is mainly caused by an isoleucine (I185) in TM5, replacing a histidine that is conserved in water-specific AQPs (Kirscht et al., 2016). The most striking feature of the SF in AtTIP2;1 is the R200 located in HE, while the arginine in HE is conserved in most AQPs. In AtTIP2;1, the R200 side chain is located at the edge of the channel due to the H131 situated in LC, making histidine the fifth residue of the extended SF. The position of this arginine is further stabilized by a hydrogen bond with histidine (H63) in TM2, which occupies the same space as the corresponding aromatic residues of water and glycerol channels without direct effects on the channel opening (Kirscht et al., 2016). Moreover, H131 in LC interacts directly with the substrate in the selectivity region. These structural features define the extended SF at five positions: I185, R200, H131, and H63, which have properties and configurations that establish the novel SF, plus G191 in LE, which is conserved in the canonical and extended SF. The concept of extended SF is instructive to conceiving study schemes before initiating analysis of APQ/PIP channels for transport of H_2O_2 and more substrates other than H_2O and NH_3.

STRUCTURAL BASIS OF PIPS FOR MEDIATION OF H_2O_2 TRANSPORT

Until the structural basis of PIP/AQP functions in H_2O_2 transport is dissected, no more than inspiration can be deduced from referencing the crystal structures of SoPIP2;1 for NH_3 transport (Kirscht et al., 2016) and both Aqy1 (Eriksson et al., 2013) and AtTIP2;1 (Törnroth-Horsefield et al., 2010) for H_2O transport. The topological displacement of the connecting loop (Törnroth-Horsefield et al., 2010) may have a broad importance for AQPs. Tautomeric reactions (Eriksson et al., 2013) and the SF extension (Kirscht et al., 2016) might be used by certain PIPs/AQPs to expedite H_2O_2 transport. However, these features are likely to be insufficient to support H_2O_2 transport, due to the difference in diameter/molecular mass of H_2O_2 (3.70 Å/34), H_2O (2.96 Å/33) and NH_3 (<2.96 Å/17), and in the Ar/R SF features. The location and composition of the SF is identical (F87, H126, T225, R231) in the H_2O_2 channel AtPIP2;1 (Rodrigues et al., 2017) and the water channel SoPIP2;1 (Kirscht et al., 2016). However, the SF composition shared by AtPIP2;1 and SoPIP2;1 is distinct from that in the corresponding positions (G87, I126, L225, and T231) of the H_2O_2 channel AtPIP1;4 (Tian et al., 2016). AtPIP1;4 is the same length as OsPIP2;1, but possesses six more residues than SoPIP2;1, with a predicted Ar/R SF comprising F95, H224, T231, and R239 (**Figure 3B**). If the SF extension permits AQPs to mediate H_2O_2 transport, the degree of the SF extension must be considerably higher than that in the NH_3 transport channel (Kirscht et al., 2016).

Three issues are considered to infer the structural basis of the function of PIPs in H_2O_2 transport between the outside and inside of plant cells. First, the apocytoplastic transport of H_2O_2 is more intricate as compared to the signal shift ways by the cell-to-cell traveling via plasmodesmata (Wang et al., 2009) and via vesicle-aided trafficking between organelles through the ER system within the cell interior (Ashtamker et al., 2007; Melo et al., 2017). Second, H_2O_2 transport in and out of plant cells is not constant throughout the life circle of plants (Dynowski et al., 2008; Tian et al., 2016). Third, H_2O_2 trafficking across the PM is induced but is not constitutive, and occurs only when apoplastic H_2O_2 is generated in response to pathogens, microbial patterns, or environmental signals (Levine et al., 1994; Xin et al., 2015; Liu and He, 2016; Tian et al., 2016).

Plasma membrane sensing of these distinct signals will promote H_2O_2 generation in apoplasts and its immediate translocation into the cytoplasm (Ausubel, 2005; Ashtamker et al., 2007; Tian et al., 2016) by three possible mechanisms. One is inductivity (**Figure 3A**). When plants are infected by a pathogen or respond to a microbial pattern, such as Hpa1 or flg22, the enzymatic activity of NOX is induced to catalyze the generation of H_2O_2 by peroxidation and superoxidation in PMs (Tian et al., 2016; Smirnoff and Arnaud, 2019). The generated H_2O_2 accumulates, and the concentration increases temporarily in the apoplast. This creates a gradient from the outside to the inside of the cell (Tian et al., 2016), and induces the PIP channel to function (Tian et al., 2016).

The second mechanism is speculated to be the combination of factors (**Figure 3C**) found in SoPIP2;1 (Törnroth-Horsefield et al., 2010), Aqy1 (Eriksson et al., 2013), and AtTIP2;1 (Kirscht et al., 2016). Combined factors facilitate the passage of H_2O_2 through the PIP channel, which could be established by SF extension (Kirscht et al., 2016), and optimized by amino acid protonation (Eriksson et al., 2013). H_2O_2 generation ($2O_2^- + 2H^+ = H_2O_2$) requires protons, and may reduce the likelihood that amino acid residues near the SF and NPA regions are protonated. As the protonation navigates H_2O movement along the channel (Eriksson et al., 2013), decreased protonation will disturb H_2O transport. This might promotes the transport of H_2O_2 over H_2O through a PIP channel once a sufficient diameter is reached (>3.70 Å).

The third mechanism is supposed to be biochemical responses (**Figure 3C**) associated with the regulation of PM remodeling – injury and repair (Laliberté and Sanfaçon, 2010; Santi-Rocca and Blanchard, 2017). PM remodeling is triggered by the binding of an active extrinsic protein, including microbial patterns such as Hpa1 (Li et al., 2015; Tian et al., 2016), bacterial T3 translocators such as HrpF (Büttner et al., 2002; Li et al., 2011), and bacterial effectors (Hubber and Roy, 2010; Domingues et al., 2016; Dong et al., 2016). Binding of these bioactive proteins affects the PM integrity (Ji and Dong, 2015a; Guignot and Tran Van Nhieu, 2016). Reduced PM integrity is advantageous for solute influx, which, however, is strictly regulated by proteins and lipids that recognize microbial patterns, T3 effectors, or translocators (Gilbert et al., 2014).

The former two mechanisms may synergize in the gating and trafficking regulation, requiring AtPIP1;4 to transport H_2O_2 in plants grown under regular conditions without any input signal, except for externally applied H_2O_2 or H_2O_2 induced by a pathogen or a microbial pattern (Tian et al., 2016). The third mechanism may occur in the presence of Hpa1 following application to plants or production in transgenic plants, in which AtPIP1;4 interacts with Hpa1 (Li et al., 2015) to increase the substrate transport function. Studies should aim to verify this hypothesis in order to elucidate the structures of PIP orthologs as transport channels for H_2O_2 or different substrates.

CONCLUSION AND PERSPECTIVES

Finite research performed on these case studies is based on a solid foundation obtained through extensive studies; research on the structural regulation of PIP function in plant infection and immunity is invited. The first case study on Hpa1-mediated, OsPIP1;3-associated, and virulence-relevant PthXo1 translocation offers multiple experimental avenues to characterize interactions between T3 translocators and their receptors at target PMs, as well as the associated implications for effector translocation and virulence. The two subjects discussed here are yet to be thoroughly studied. First, which of the assumed delivery lanes is used by different effectors is a long-standing question for all plant-pathogenic bacteria. Xoo possesses more than 30 effectors secreted by the T3 system (White et al., 2009), similar to the number in other bacteria. Further study is needed to identify all T3 effectors in the three proposed mechanisms: translocon-independent pore formation (**Figure 1**), endocytosis with PM protein or lipid trafficking (**Figures 1**, **2**), and translocon-dependent delivery (**Figure 1**). The second subject includes the contribution of PM lipids and proteins to T3 effector translocation. T3 translocon assembly or pore formation must recruit both lipids and proteins situated in plant PMs (Büttner et al., 2008; Gilbert et al., 2014; Heilmann and Heilmann, 2015; Ji and Dong, 2015b; Guignot and Tran Van Nhieu, 2016). It would be of great interest to determine how effectors are internalized with PM protein or lipid trafficking, and how protein and lipid receptors of T3 translocators coordinate their actions to generate pores or translocons in plant PMs.

The second case study discusses AtPIP1;4-regulated, Hpa1-promoted, and immunity-linked H_2O_2 transport, and establishes a cytological connection between the generation and function of H_2O_2 in the apoplast and cytoplasm, respectively (Tian et al., 2016). The cytoplasmic import of H_2O_2 bridges a physical gap, which was unknown for at least 20 years since the biphasic H_2O_2 accumulation following induction was awarded biological significance (Levine et al., 1994). AtPIP1;4-mediated H_2O_2 translocation is a pivotal step in apocytoplastic signal transduction for intracellular immunity pathways, which regulate SAR and PTI responses, leading to plant resistance against diseases (Dong et al., 1999; Chen et al., 2008a,b; Choi et al., 2013; Zhao et al., 2014). The future focus of studies will be difficult, highlighting the regulation of gating and trafficking of the AtPIP1;4 channel for H_2O_2 transport. To date, the structures of AQP channels have only been determined for the transport of NH_3 (Kirscht et al., 2016)

and H_2O (Daniels et al., 1999; Fotiadis et al., 2001; Kukulski et al., 2005; Kreida and Törnroth-Horsefield, 2015), and almost 20 substrates remain to be understood (Laloux et al., 2018). Rational hypotheses on structural themes in both gating and trafficking (Kreida and Törnroth-Horsefield, 2015) requires the efforts of researchers to explore structural mechanisms that govern diverse AQP channels. It is necessary to dissect the conformation of AtPIP1;4 (**Figures 3B,C**) involved in H_2O_2 transport in response pathogens or patterns (**Figure 3A**). It is especially necessary to study whether the H_2O_2 transport is facilitated by combined impetuses, including the SF extension, amino acid residue interactions (**Figure 3C**), and PM protein trafficking (**Figure 2**).

The two case studies have been designed to converge at the intersection Hpa1-PIP cooperation and branch into two directions. One targets plant immunity, for which Hpa1 functions as a bacterial pattern in a pathogen-independent manner. The other contributes to plant infection, in which Hpa1 acts as a T3 translocator after secretion by the bacteria, and mediates the translocation of virulent effectors that lead to disease. These findings provide insight into disease control either through induced immunity, or the prevention of bacteria from usurping the substrate transport gate. Practical application of both strategies to strengthen crop protection (Krinke et al., 2007; Chen et al., 2008b; Fu et al., 2014; Wang D. et al., 2014; Li et al., 2019) will integrate with crop involvement by using AQPs from plants themselves (Ruiz-Lozano and Aroca, 2017; Balestrini et al., 2018) and from symbiotic microbes as well (Kikuchi et al., 2016; Desaki et al., 2018).

AUTHOR CONTRIBUTIONS

LZ, LC, and HD drafted the manuscript. LZ predicted the 3D structure of AtPIP1;4. HD finalized the manuscript.

FUNDING

This study was supported by Natural Science Foundation of China (Grant No. 31772247) and China National Key Research and Development Plan (Grant No. 2017YFD0200901) to HD and Talent Recruitment Funding of Shandong Agricultural University (Grant No. 20171226) to HD, LC, and LZ.

ACKNOWLEDGMENTS

We thank Mr. Hao Wang (doctoral student in the laboratory) for his advice in the structural analysis.

REFERENCES

Abascal, F., Irisarri, I., and Zardoya, R. (2014). Diversity and evolution of membrane intrinsic proteins. *Biochim. Biophys. Acta* 1840, 1468–1481. doi: 10.1016/j.bbagen.2013.12.001

Adam, P. R., Barta, M. L., and Dickenson, N. E. (2017). "Characterization of type three secretion system translocator interactions with phospholipid membranes," in *Type 3 Secretion Systems: Methods and Protocols, Methods in Molecular Biology*, Vol. 1531, eds M. L. Nilles and D. L. J. Condry (New York, NY: Springer Science + Business Media), 81–91. doi: 10.1007/978-1-4939-6649-3_7

Aguayo, D., Pacheco, N., Morales, E. H., Collao, B., Luraschi, R., Cabezas, C., et al. (2015). Hydrogen peroxide and hypochlorous acid influx through the major *S. typhimurium* porin OmpD is affected by substitution of key residues of the channel. *Arch. Biochem. Biophys.* 568, 38–45. doi: 10.1016/j.abb.2015.01.005

Allgood, S. C., and Neunuebel, M. R. (2018). The recycling endosome and bacterial pathogens. *Cell. Microbiol.* 20:e12857. doi: 10.3389/fimmu.2016.00084

Alvarez, M. E., Pennell, R. L., Meijer, R.-J., Ishikawa, A., Dixon, R. A., and Lamb, C. (1998). Reactive oxygen intermediates mediate a systemic signal network in the establishment of plant immunity. *Cell* 92, 773–784. doi: 10.1016/s0092-8674(00)81405-1

Asai, T., Tena, G., Plotnikova, J., Willmann, M. R., Chiu, W. L., Gomez-Gomez, L., et al. (2002). MAP kinase signalling cascade in *Arabidopsis* innate immunity. *Nature* 415, 977–983. doi: 10.1038/415977a

Ashtamker, C., Kiss, V., Sagi, M., Davydov, O., and Fluhr, R. (2007). Diverse subcellular locations of cryptogein-induced reactive oxygen species production in tobacco Bright Yellow-2 cells. *Plant Physiol.* 143, 1817–1826. doi: 10.1104/pp.106.090902

Ausubel, F. M. (2005). Are innate immune signaling pathways in plants and animals conserved? *Nat. Immunol.* 6, 973–979. doi: 10.1038/ni1253

Balestrini, R., Chitarra, W., Antoniou, C., Ruocco, M., and Fotopoulos, V. (2018). Improvement of plant performance under water deficit with the employment of biological and chemical priming agents. *J. Agric. Sci.* 156, 680–688. doi: 10.1017/s0021859618000126

Bao, Y. (2017). *Advances in Experimental Medicine and Biology 969 Aquaporins*. Dordrecht: Springer Science + Business Media B.V, 279.

Bárzana, G., Aroca, R., Bienert, G. P., Chaumont, F., and Ruiz-Lozano, J. M. (2014). New insights into the regulation of aquaporins by the arbuscular mycorrhizal symbiosis in maize plants under drought stress and possible implications for plant performance. *Mol. Plant Microbe Interact.* 27, 349–363. doi: 10.1094/MPMI-09-13-0268-R

Bárzana, G., Aroca, R., and Ruiz-Lozano, J. M. (2015). Localized and non-localized effects of arbuscular mycorrhizal symbiosis on accumulation of osmolytes and aquaporins and on antioxidant systems in maize plants subjected to total or partial root drying. *Plant Cell Environ.* 38, 1613–1627. doi: 10.1111/pce.12507

Benabdillah, R., Mota, L. J., Lützelschwab, S., Demoinet, E., and Cornelis, G. R. (2004). Identification of a nuclear targeting signal in YopM from *Yersinia* spp. *Microb. Pathog.* 36, 247–261. doi: 10.1016/j.micpath.2003.12.006

Bethke, G., Pecher, P., Eschen-Lippold, L., Tsuda, K., Katagiri, F., Glazebrook, J., et al. (2012). Activation of the *Arabidopsis thaliana* mitogen-activated protein kinase MPK11 by the flagellin-derived elicitor peptide, flg22. *Mol. Plant Microbe Interact.* 25, 471–480. doi: 10.1094/MPMI-11-11-0281

Bian, H., Zhang, L., Chen, L., Wang, W., Ji, H., and Dan, S. (2019). Real-time monitoring of translocation of selected type III effectors from *Xanthomonas oryzae* pv. *oryzae* into rice cells. *J. Biosci.* (in press).

Bienert, G. P., and Chaumont, F. (2014). Aquaporin-facilitated transmembrane diffusion of hydrogen peroxide. *Biochim. Biophys. Acta* 1840, 1596–1604. doi: 10.1016/j.bbagen.2013.09.017

Bienert, G. P., Moller, A. L., Kristiansen, K. A., Schulz, A., Moller, I. M., Schjoerring, J. K., et al. (2007). Specific aquaporins facilitate the diffusion of hydrogen peroxide across membranes. *J. Biol. Chem.* 282, 1183–1192. doi: 10.1074/jbc.M603761200

Bienert, G. P., Schjoerring, J. K., and Jahn, T. P. (2006). Membrane transport of hydrogen peroxide. *Biochim. Biophys. Acta* 1758, 994–1003. doi: 10.1016/j.bbamem.2006.02.015

Bigeard, J., Colcombet, J., and Hirt, H. (2015). Signaling mechanisms in pattern-triggered immunity (PTI). *Mol. Plant* 8, 521–539. doi: 10.1016/j.molp.2014.12.022

Bocsanczy, A. M., Nissinen, R. M., Oh, C. S., and Beer, S. V. (2008). HrpN of *Erwinia amylovora* functions in the translocation of DspA/E into plant cells. *Mol. Plant Pathol.* 9, 425–434. doi: 10.1111/j.1364-3703.2008.00471.x

Brown, D. (2017). The discovery of water channels (aquaporins). *Ann. Nutr. Metab.* 70(Suppl. 1), 37–42. doi: 10.1159/000463061

Büttner, C. R., Sorg, I., Cornelis, G. R., Heinz, D. W., and Niemann, H. H. (2008). Structure of the *Yersinia enterocolitica* type III secretion translocator chaperone SycD. *J. Mol. Biol.* 375, 997–1012. doi: 10.1016/j.jmb.2007.11.009

Büttner, D. (2012). Protein export according to schedule: architecture, assembly, and regulation of type III secretion systems from plant- and animal-pathogenic bacteria. *Microbiol. Mol. Biol. Rev.* 76, 262–310. doi: 10.1128/MMBR.05017-11

Büttner, D. (2016). Behind the lines-actions of bacterial type III effector proteins in plant cells. *FEMS Microbiol. Rev.* 40, 894–937. doi: 10.1093/femsre/fuw026

Büttner, D., and Bonas, U. (2002). Port of entry – the type III secretion translocon. *Trends Microbiol.* 10, 186–192. doi: 10.1016/s0966-842x(02)02331-4

Büttner, D., Nennstiel, D., Klüsener, B., and Bonas, U. (2002). Functional analysis of HrpF, a putative type III translocon protein from *Xanthomonas campestris* pv. *vesicatoria*. *J. Bacteriol.* 184, 2389–2398. doi: 10.1128/jb.184.9.2389-2398.2002

Calvo-Polanco, M., Sánchez-Castro, I., Cantos, M., García, J. L., Azcón, R., Ruiz-Lozano, J. M., et al. (2016). Effects of different arbuscular mycorrhizal fungal backgrounds and soils on olive plants growth and water relation properties under well-watered and drought conditions. *Plant Cell Environ.* 39, 2498–2514. doi: 10.1111/pce.12807

Cao, H., Glazebrook, J., Clarke, J. D., Volko, S., and Dong, X. (1997). The *Arabidopsis NPR1* gene that controls systemic acquired resistance encodes a novel protein containing ankyrin repeats. *Cell* 88, 57–63. doi: 10.1016/s0092-8674(00)81858-9

Centrone, M., Ranieri, M., Di Mise, A., Berlingerio, S. P., Russo, A., Deen, P. M. T., et al. (2017). AQP2 abundance is regulated by the E3-ligase CHIP via HSP70. *Cell. Physiol. Biochem.* 44, 515–531. doi: 10.1159/000485088

Chakravarthy, S., Huot, B., and Kvitko, B. H. (2017). Effector translocation: Cya reporter assay. *Methods Mol. Biol.* 1615, 473–487. doi: 10.1007/978-1-4939-7033-9_33

Chatterjee, S., Chaudhury, S., McShan, A. C., Kaur, K., and De Guzman, R. N. (2013). Structure and biophysics of type III secretion in bacteria. *Biochemistry* 52, 2508–2517. doi: 10.1021/bi400160a

Chaumont, F., Barrieu, F., Wojcik, E., Chrispeels, M. J., and Jung, R. (2001). Aquaporins constitute a large and highly divergent protein family in maize. *Plant Physiol.* 125, 1206–1215. doi: 10.1104/pp.125.3.1206

Chen, G., Wang, W., Chen, H., Dai, W., Peng, X., Li, X., et al. (2018). In vitro expression and functional characterization of NPA motifs in aquaporins of *Nosema bombycis*. *Parasitol. Res.* 117, 3473–3479. doi: 10.1007/s00436-018-6044-y

Chen, L., Qian, J., Long, J., Yin, Q., Zhang, C., Wu, X., et al. (2008a). Identification of specific fragments of $HpaG_{Xooc}$, a harpin protein from *Xanthomonas oryzae* pv. *oryzicola*, that induces disease resistance and enhanced growth in rice. *Phtopathology* 98, 781–791. doi: 10.1094/PHYTO-98-7-0781

Chen, L., Zhang, S. J., Zhang, S. S., Qu, S., Long, J., Ren, H., et al. (2008b). A fragment of the *Xanthomonas oryzae* pv. *oryzicola* harpin $HpaG_{Xooc}$ reduces disease and increases yield of rice in extensive grower plantings. *Phytopathology* 98, 792–802. doi: 10.1094/PHYTO-98-7-0792

Choi, M. S., Kim, W., Lee, C., and Oh, C. S. (2013). Harpins, multifunctional proteins secreted by Gram-negative plant-pathogenic bacteria. *Mol. Plant Microbe Interact.* 26, 1115–1122. doi: 10.1094/MPMI-02-13-0050-CR

Cybulsky, A. V. (2017). Endoplasmic reticulum stress, the unfolded protein response and autophagy in kidney diseases. *Nat. Rev. Nephrol.* 13, 681–696. doi: 10.1038/nrneph.2017.129

Daniels, M. J., Chrispeels, M. J., and Yeager, M. (1999). Projection structure of a plant vacuole membrane aquaporin by electron cryo-crystallography. *J. Mol. Biol.* 294, 1337–1349. doi: 10.1006/jmbi.1999.3293

Daudi, A., Cheng, Z., O'Brien, J. A., Mammarella, N., Khan, S., Ausubel, F. M., et al. (2012). The apoplastic oxidative burst peroxidase in *Arabidopsis* is a major component of pattern-triggered immunity. *Plant Cell* 24, 275–287. doi: 10.1105/tpc.111.093039

de Groot, B. L., Engel, A., and Grubmüller, H. (2001). A refined structure of human aquaporin-1. *FEBS Lett.* 504, 201–211. doi: 10.1016/S0014-5793(01)02743-0

de Groot, B. L., Frigato, T., Helms, V., and Grubmuller, H. (2003). The mechanism of proton exclusion in the aquaporin-1 water channel. *J. Mol. Biol.* 333, 279–293. doi: 10.1016/j.jmb.2003.08.003

de Groot, B. L., and Grubmuller, H. (2001). Water permeation across biological membranes: mechanism and dynamics of aquaporin-1 and GlpF. *Science* 294, 2353–2357. doi: 10.1126/science.1062459

Desaki, Y., Miyata, K., Suzuki, M., Shibuya, N., and Kaku, H. (2018). Plant immunity and symbiosis signaling mediated by LysM receptors. *Innate Immun.* 24, 92–100. doi: 10.1177/1753425917738885

Dik, D. A., Marous, D. R., Fisher, J. F., and Mobashery, S. (2017). Lytic transglycosylases: concinnity in concision of the bacterial cell wall. *Crit. Rev. Biochem. Mol. Biol.* 52, 503–542. doi: 10.1080/10409238.2017.1337705

Domingues, L., Ismail, A., Charro, N., Rodríguez-Escudero, I., Holden, D. W., Molina, M., et al. (2016). The *Salmonella* effector SteA binds phosphatidylinositol 4-phosphate for subcellular targeting within host cells. *Cell. Microbiol.* 18, 949–969. doi: 10.1111/cmi.12558

Dong, H., Delaney, T. P., Bauer, D. W., and Beer, S. V. (1999). Harpin induces disease resistance in *Arabidopsis* through the systemic acquired resistance pathway mediated by salicylic acid and the *NIM1* gene. *Plant J.* 20, 207–215. doi: 10.1046/j.1365-313x.1999.00595.x

Dong, N., Niu, M., Hu, L., Yao, Q. I., Zou, R., and Shao, F. (2016). Modulation of membrane phosphoinositide dynamics by the phosphatidylinositide 4-kinase activity of the *Legionella* LepB effector. *Nat. Microbiol.* 2:16236. doi: 10.1038/nmicrobiol.2016.236

Dynowski, M., Schaaf, G., Loque, D., Moran, O., and Ludewig, U. (2008). Plant plasma membrane water channels conduct the signalling molecule H_2O_2. *Biochem. J.* 414, 53–61. doi: 10.1042/BJ20080287

Eriksson, U. K., Fischer, G., Friemann, R., Enkavi, G., Tajkhorshid, E., and Neutze, R. (2013). Subangstrom resolution X-ray structure details aquaporin-water interactions. *Science* 340, 1346–1349. doi: 10.1126/science.1234306

Finsel, I., and Hilbi, H. (2015). Formation of a pathogen vacuole according to *Legionella pneumophila*: how to kill one bird with many stones. *Cell. Microbiol.* 17, 935–950. doi: 10.1111/cmi.12450

Fotiadis, D., Jeno, P., Mini, T., Wirtz, S., Muller, S. A., Fraysse, L., et al. (2001). Structural characterization of two aquaporins isolated from native spinach leaf plasma membranes. *J. Biol. Chem.* 276, 1707–1714. doi: 10.1074/jbc.M009383200

Fox, A. R., Maistriaux, L. C., and Chaumont, F. (2017). Toward understanding of the high number of plant aquaporin isoforms and multiple regulation mechanisms. *Plant Sci.* 264, 179–187. doi: 10.1016/j.plantsci.2017.07.021

Fu, D., Libson, A., Miercke, L. J., Weitzman, C., Nollert, P., Krucinski, J., et al. (2000). Structure of a glycerol-conducting channel and the basis for its selectivity. *Science* 290, 481–486. doi: 10.1126/science.290.5491.481

Fu, M., Xu, M., Zhou, T., Wang, D., Tian, S., Zhang, C., et al. (2014). Transgenic expression of a functional fragment of harpin protein Hpa1 in wheat induces the phloem-based defence against English grain aphid. *J. Exp. Bot.* 65, 1439–1453. doi: 10.1093/jxb/ert488

Galletti, R., Ferrari, S., and De Lorenzo, G. (2011). *Arabidopsis* MPK3 and MPK6 play different roles in basal and oligogalacturonide- or flagellin-induced resistance against *Botrytis cinerea*. *Plant Physiol.* 157, 804–814. doi: 10.1104/pp.111.174003

Gaytán, M. O., Monjarás Feria, J., Soto, E., Espinosa, N., Benítez, M., and Georgellis, D. (2018). Novel insights into the mechanism of SepL-mediated control of effector secretion in enteropathogenic *Escherichia coli*. *Microbiologyopen* 7:e00571. doi: 10.1002/mbo3.571

Gilbert, R. J., Dalla Serra, M., Froelich, C. J., Wallace, M. I., and Anderluh, G. (2014). Membrane pore formation at protein-lipid interfaces. *Trends Biochem. Sci.* 39, 510–516. doi: 10.1016/j.tibs.2014.09.002

Gomes, D., Agasse, A., Thiébaud, P., Delrot, S., Gerós, H., and Chaumont, F. (2009). Aquaporins are multifunctional water and solute transporters highly divergent in living organisms. *Biochim. Biophys. Acta* 1788, 1213–1228. doi: 10.1016/j.bbamem.2009.03.009

Goure, J., Pastor, A., Faudry, E., Chabert, J., Dessen, A., and Attree, I. (2004). The V antigen of *Pseudomonas aeruginosa* is required for assembly of the functional PopB/PopD translocation pore in host cell membranes. *Infect. Immun.* 72, 4741–4750. doi: 10.1128/IAI.72.8.4741-4750.2004

Gudesblat, G. E., Iusem, N. D., and Morris, P. C. (2007). Guard cell-specific inhibition of *Arabidopsis MPK3* expression causes abnormal stomatal responses

to abscisic acid and hydrogen peroxide. *New Phytol.* 173, 713–721. doi: 10.1111/j.1469-8137.2006.01953.x

Guignot, J., and Tran Van Nhieu, G. (2016). Bacterial control of pores induced by the type III secretion system: mind the gap. *Front. Immunol.* 7:84. doi: 10.3389/fimmu.2016.00084

Guo, M., Tian, F., Wamboldt, Y., and Alfano, J. R. (2009). The majority of the type III effector inventory of *Pseudomonas syringae* pv. *tomato* DC3000 can suppress plant immunity. *Mol. Plant Microbe Interact.* 22, 1069–1080. doi: 10.1094/MPMI-22-9-1069

Haapalainen, M., Engelhardt, S., Küfner, I., Li, C. M., Nürnberger, T., Lee, J., et al. (2011). Functional mapping of harpin HrpZ of *Pseudomonas syringae* reveals the sites responsible for protein oligomerization, lipid interactions and plant defence induction. *Mol. Plant Pathol.* 12, 151–166. doi: 10.1111/j.1364-3703.2010.00655.x

Hammond, G. R., Fischer, M. J., Anderson, K. E., Holdich, J., Koteci, A., Balla, T., et al. (2009). PI4P and PI(4,5)P_2 are essential but independent lipid determinants of membrane integrity. *Science* 37, 727–730. doi: 10.1126/science.1222483

Hara-Chikuma, M., Satooka, H., Watanabe, S., Honda, T., Miyachi, Y., Watanabe, T., et al. (2015). Aquaporin-3-mediated hydrogen peroxide transport is required for NF-κB signalling in keratinocytes and development of psoriasis. *Nat. Commun.* 23:7454. doi: 10.1038/ncomms8454

Hausner, J., Hartmann, N., Jordan, M., and Büttner, D. (2017). The predicted lytic transglycosylase HpaH from *Xanthomonas campestris* pv. *vesicatoria* associates with the type III secretion system and promotes effector protein translocation. *Infect. Immun.* 85:e00788-16. doi: 10.1128/IAI.00788-16

He, J., and Yang, B. (2019). Aquaporins in renal diseases. *Intl. J. Mol. Sci.* 20:366. doi: 10.3390/ijms20020366

Heckwolf, M., Pater, D., Hanson, D. T., and Kaldenhoff, R. (2011). The *Arabidopsis thaliana* aquaporin AtPIP1;2 is a physiologically relevant CO_2 transport facilitator. *Plant J.* 67, 795–804. doi: 10.1111/j.1365-313X.2011.04634.x

Heilmann, M., and Heilmann, I. (2015). Plant phosphoinositides-complex networks controlling growth and adaptation. *Biochim. Biophys. Acta* 851, 759–769. doi: 10.1016/j.bbalip.2014.09.018

Hirano, K., Zuber, C., Roth, J., and Ziak, M. (2003). The proteasome is involved in the degradation of different aquaporin-2 mutants causing nephrogenic diabetes insipidus. *Am. J. Pathol.* 163, 111–120. doi: 10.1016/S0002-9440(10)63635-8

Hooijmaijers, C., Rhee, J. Y., Kwak, K. J., Chung, G. C., Horie, T., and Katsuhara, M. (2012). Hydrogen peroxide permeability of plasma membrane aquaporins of *Arabidopsis thaliana*. *J. Plant Res.* 125, 147–153. doi: 10.1007/s10265-011-0413-2

Horsefield, R., Norden, K., Fellert, M., Backmark, A., Törnroth-Horsefield, S., van Scheltinga, A. C., et al. (2008). High-resolution x-ray structure of human aquaporin 5. *Proc. Natl. Acad. Sci. U.S.A.* 105, 13327–13332. doi: 10.1073/pnas.0801466105

Huang, B., Wang, H., and Yang, B. (2017). "Water transport mediated by other membrane proteins," in *Advances in Experimental Medicine and Biology 969 Aquaporins*, ed. B. Yang (Dordrecht: Springer Science + Business Media B.V), 251–261. doi: 10.1007/978-94-024-1057-0_17

Hubber, A., and Roy, C. R. (2010). Modulation of host cell function by *Legionella pneumophila* type IV effectors. *Annu. Rev. Cell Dev. Biol.* 26, 261–283. doi: 10.1146/annurev-cellbio-100109-104034

Ji, H., and Dong, H. (2015a). Biological significance and topological basis of aquaporin-partnering protein-protein interactions. *Plant Signal. Behav.* 10:e1011947. doi: 10.1080/15592324.2015.1011947

Ji, H., and Dong, H. (2015b). Key steps in type III secretion system (T3SS) towards translocon assembly with potential sensor at plant plasma membrane. *Mol. Plant Pathol.* 16, 762–773. doi: 10.1111/mpp.12223

Johansson, I., Larsson, C., Ek, B., and Kjellbom, P. (1996). The major integral proteins of spinach leaf plasma membranes are putative aquaporins and are phosphorylated in response to Ca^{2+} and apoplastic water potential. *Plant Cell* 8, 1181–1191. doi: 10.1105/tpc.8.7.1181

Kaku, H., Nishizawa, Y., Ishii-Minami, N., Akimoto-Tomiyama, C., Dohmae, N., Takio, K., et al. (2006). Plant cells recognize chitin fragments for defense signaling through a plasma membrane receptor. *Proc. Natl. Acad. Sci. U.S.A.* 103, 11086–11091. doi: 10.1073/pnas.0508882103

Kaldenhoff, R., Kai, L., and Uehlein, N. (2014). Aquaporins and membrane diffusion of CO_2 in living organisms. *Biochim. Biophys. Acta* 1840, 1592–1595. doi: 10.1016/j.bbagen.2013.09.037

Kamsteeg, E. J., Hendriks, G., Boone, M., Konings, I. B., Oorschot, V., van der Sluijs, P., et al. (2006). Short-chain ubiquitination mediates the regulated endocytosis of the aquaporin-2 water channel. *Proc. Natl. Acad. Sci. U.S.A.* 103, 18344–18349. doi: 10.1073/pnas.0604073103

Kapilan, R., Vaziri, M., and Zwiazek, J. J. (2018). Regulation of aquaporins in plants under stress. *Biol. Res.* 51:4. doi: 10.1186/s40659-018-0152-0

Kärkönen, A., and Kuchitsu, K. (2015). Reactive oxygen species in cell wall metabolism and development in plants. *Phytochemistry* 112, 22–32. doi: 10.1016/j.phytochem.2014.09.016

Khositseth, S., Charngkaew, K., Boonkrai, C., Somparn, P., Uawithya, P., Chomanee, N., et al. (2017). Hypercalcemia induces targeted autophagic degradation of aquaporin-2 at the onset of nephrogenic diabetes insipidus. *Kidney Int.* 91, 1070–1087. doi: 10.1016/j.kint.2016.12.005

Kikuchi, Y., Hijikata, N., Ohtomo, R., Handa, Y., Kawaguchi, M., Saito, K., et al. (2016). Aquaporin-mediated long-distance polyphosphate translocation directed towards the host in arbuscular mycorrhizal symbiosis: application of virus-induced gene silencing. *New Phytol.* 211, 1202–1208. doi: 10.1111/nph.14016

Kim, S. G., Kim, S. T., Wang, Y., Yu, S., Choi, I. S., Kim, Y. C., et al. (2011). The RNase activity of rice probenazole-induced protein1 (PBZ1) plays a key role in cell death in plants. *Mol. Cells* 31, 25–31. doi: 10.1007/s10059-011-0004-z

Kirscht, A., Kaptan, S. S., Bienert, G. P., Chaumont, F., Nissen, P., de Groot, B. L., et al. (2016). Crystal structure of an ammonia-permeable aquaporin. *PLoS Biol.* 14:e1002411. doi: 10.1371/journal.pbio.1002411

Koraimann, G. (2003). Lytic transglycosylases in macromolecular transport systems of Gram-negative bacteria. *Cell. Mol. Life Sci.* 60, 2371–2388. doi: 10.1007/s00018-003-3056-1

Kreida, S., and Törnroth-Horsefield, S. (2015). Structural insights into aquaporin selectivity and regulation. *Curr. Opin. Struct. Biol.* 33, 126–134. doi: 10.1016/j.sbi.2015.08.004

Krinke, O., Ruelland, E., Valentová, O., Vergnolle, C., Renou, J. P., Taconnat, L., et al. (2007). Phosphatidylinositol 4-kinase activation is an early response to salicylic acid in *Arabidopsis* suspension cells. *Plant Physiol.* 144, 1347–1359. doi: 10.1104/pp.107.100842

Kukulski, W., Schenk, A. D., Johanson, U., Braun, T., de Groot, B. L., Fotiadis, D., et al. (2005). The 5Å structure of heterologously expressed plant aquaporin SoPIP2;1. *J. Mol. Biol.* 350, 611–616. doi: 10.1016/j.jmb.2005.05.001

Kvitko, B. H., Ramos, A. R., Morello, J. E., Oh, H. S., and Collmer, A. (2007). Identification of harpins in *Pseudomonas syringae* pv. *tomato* DC3000, which are functionally similar to HrpK1 in promoting translocation of type III secretion system effectors. *J. Bacteriol.* 189, 8059–8072. doi: 10.1128/JB.01146-07

Laliberté, J. F., and Sanfaçon, H. (2010). Cellular remodeling during plant virus infection. *Annu. Rev. Phytopathol.* 48, 69–91. doi: 10.1146/annurev-phyto-073009-114239

Laloux, T., Junqueira, B., Maistriaux, L. C., Ahmed, J., Jurkiewicz, A., and François Chaumont, F. (2018). Plant and mammal aquaporins: same but different. *Intl. J. Mol. Sci.* 19:E521. doi: 10.3390/ijms19020521

Lee, A. H., Hurley, B., Felsensteiner, C., Yea, C., Ckurshumova, W., Bartetzko, V., et al. (2012). A bacterial acetyltransferase destroys plant microtubule networks and blocks secretion. *PLoS Pathog.* 8:e1002523. doi: 10.1371/journal.ppat.1002523

Lee, J., Klessig, D., and Nurnberger, T. (2001a). A harpin binding site in tobacco plasma membranes mediates activation of the pathogenesis related gene *HIN1* independent of extracellular calcium but dependent on mitogen-activated protein kinase activity. *Plant Cell* 13, 1079–1093. doi: 10.1105/tpc.13.5.1079

Lee, J., Klusener, B., Tsiamis, G., Stevens, C., Neyt, C., Tampakaki, A. P., et al. (2001b). $HrpZ_{Psph}$ from the plant pathogen *Pseudomonas syringae* pv. *phaseolicola* binds to lipid bilayers and forms an ion-conducting pore *in vitro*. *Proc. Natl. Acad. Sci. U.S.A.* 98, 289–294. doi: 10.1073/pnas.011265298

Lehman, T. A., Smertenko, A., and Sanguinet, K. A. (2017). Auxin, microtubules, and vesicle trafficking: conspirators behind the cell wall. *J. Exp. Bot.* 68, 3321–3329. doi: 10.1093/jxb/erx205

Levine, A., Tenhaken, R., Dixon, R., and Lamb, C. (1994). H_2O_2 from the oxidative burst orchestrates the plant hypersensitive disease resistance response. *Cell* 79, 583–593. doi: 10.1016/0092-8674(94)90544-4

Li, C., and Wang, W. (2017). Molecular biology of aquaporins. *Adv. Exp. Med. Biol.* 969, 1–34. doi: 10.1007/978-94-024-1057-0_1

Li, L., Wang, H., Gago, J., Cui, H., Qian, Z., Kodama, N., et al. (2015). Harpin Hpa1 interacts with aquaporin PIP1;4 to promote the substrate transport and photosynthesis in *Arabidopsis*. *Sci. Rep.* 10:1038. doi: 10.1038/srep17207

Li, P., Zhang, L., Mo, X., Ji, H., Bian, H., Hu, Y., et al. (2019). Aquaporin PIP1;3 of rice and harpin Hpa1 of bacterial blight pathogen cooperate in a type III effector translocation. *J. Exp. Bot.* doi: 10.1093/jxb/erz130 [Epub ahead of print].

Li, X., Han, B., Xu, M., Han, L., Zhao, Y., Dong, H., et al. (2014). Plant growth enhancement and associated physiological responses are coregulated by ethylene and gibberellin in response to harpin protein Hpa1. *Planta* 239, 831–846. doi: 10.1007/s00425-013-2013-y

Li, X., Han, L., Zhao, Y., You, Z., Dong, H., and Zhang, C. (2013). Harpin Hpa1 needs nitroxyl terminus to promote vegetative growth and leaf photosynthesis in *Arabidopsis*. *J. Biosci.* 39, 127–137. doi: 10.1007/s12038-013-9408-6

Li, Y. R., Che, Y. Z., Zou, H. S., Cui, Y. P., Guo, W., Zou, L. F., et al. (2011). Hpa2 required by HrpF to translocate *Xanthomonas oryzae* transcriptional activator-like effectors into rice for pathogenicity. *Appl. Environ. Microbiol.* 77, 3809–3818. doi: 10.1128/AEM.02849-10

Liu, Y., and He, C. (2016). Regulation of plant reactive oxygen species (ROS) in stress responses: learning from AtRBOHD. *Plant Cell Rep.* 35, 995–1007. doi: 10.1007/s00299-016-1950-x

Loque, D., Ludewig, U., Yuan, L., and von Wiren, N. (2005). Tonoplast intrinsic proteins AtTIP2;1 and AtTIP2;3 facilitate NH_3 transport into the vacuole. *Plant Physiol.* 137, 671–680. doi: 10.1104/pp.104.051268

Lü, B. B., Sun, W. W., Zhang, S. P., Zhang, C. L., Qian, J., Wang, X. M., et al. (2011). $HrpN_{Ea}$-induced deterrent effect on phloem feeding of the green peach aphid *Myzus persicae* requires *AtGSL5* and *AtMYB44* genes in *Arabidopsis thaliana*. *J. Biosci.* 36, 123–137. doi: 10.1007/s12038-011-9016-2

Lu, H. A., Sun, T. X., Matsuzaki, T., Yi, X. H., Eswara, J., Bouley, R., et al. (2007). Heat shock protein 70 interacts with aquaporin-2 and regulates its trafficking. *J. Biol. Chem.* 282, 28721–28732. doi: 10.1074/jbc.M611101200

Maurel, C. (2007). Plant aquaporins: novel functions and regulation properties. *FEBS Lett.* 581, 2227–2236. doi: 10.1016/j.febslet.2007.03.021

Maurel, C., Boursiac, Y., Luu, D.-T., Santoni, V., Shahzad, Z., and Verdoucq, L. (2015). Aquaporins in plants. *Phsiol. Rev.* 95, 1321–1358. doi: 10.1152/physrev.00008.2015

Maurel, C., and Plassard, C. (2011). Aquaporins: for more than water at the plant-fungus interface? *New Phytol.* 190, 815–817. doi: 10.1111/j.1469-8137.2011.03731.x

Maurel, C., Reizer, J., Schroeder, J. I., and Chrispeels, M. J. (1993). The vacuolar membrane protein γ-TIP creates water specific channels in *Xenopus* oocytes. *EMBO. J.* 12, 2241–2247. doi: 10.1002/j.1460-2075.1993.tb05877.x

Maurel, C., Verdoucqm, L., Luu, D. T., and Santoni, V. (2008). Plant aquaporins: membrane channels with multiple integrated functions. *Annu. Rev. Plant Biol.* 59, 595–624. doi: 10.1146/annurev.arplant.59.032607.092734

Melo, E. P., Lopes, C., Gollwitzer, P., Lortz, S., Lenzen, S., Mehmeti, I., et al. (2017). TriPer, an optical probe tuned to the endoplasmic reticulum tracks changes in luminal H_2O_2. *BMC Plant Biol.* 15:24. doi: 10.1186/s12915-017-0367-5

Miller, E. W., Dickinson, B. C., and Chang, C. J. (2010). Aquaporin-3 mediates hydrogen peroxide uptake to regulate downstream intracellular signaling. *Proc. Natl. Acad. Sci. U.S.A.* 107, 1568–15686. doi: 10.1073/pnas.1005776107

Mueller, C. A., Broz, P., and Cornelis, G. R. (2008). The type III secretion system tip complex and translocon. *Mol. Microbiol.* 68, 1085–1095. doi: 10.1111/j.1365-2958.2008.06237.x

Mushegian, A. R., Fullner, K. J., Koonin, E. V., and Nester, E. W. (1996). A family of lysozyme-like virulence factors in bacterial pathogens of plants and animals. *Proc. Natl. Acad. Sci. U.S.A.* 93, 7321–7326. doi: 10.1073/pnas.93.14.7321

Nesverova, V., and Törnroth-Horsefield, S. (2019). Phosphorylation-dependent regulation of mammalian aquaporins. *Cells* 8:E82. doi: 10.3390/cells8020082

Noël, L., Thieme, F., Nennstiel, D., and Bonas, U. (2002). Two novel type III-secreted proteins of *Xanthomonas campestris* pv. *vesicatoria* are encoded within the Hrp pathogenicity island. *J. Bacteriol.* 184, 1340–1348. doi: 10.1128/jb.184.5.1340-1348.2002

Nomura, K., Mecey, C., Lee, Y. N., Imboden, L. A., Chang, J. H., and He, S. Y. (2011). Effector-triggered immunity blocks pathogen degradation of an immunity-associated vesicle traffic regulator in *Arabidopsis*. *Proc. Natl. Acad. Sci. U.S.A.* 108, 10774–10779. doi: 10.1073/pnas.1103338108

Obacz, J., Avril, T., Le Reste, P. J., Urra, H., Quillien, V., Hetz, C., et al. (2017). Endoplasmic reticulum proteostasis in glioblastoma-From molecular mechanisms to therapeutic perspectives. *Sci. Signal.* 10:eaal2323. doi: 10.1126/scisignal.aal2323

Oh, C., and Beer, S. (2007). AtHIPM, an ortholog of the apple HrpN-interacting protein, is a negative regulator of plant growth and mediates the growth-enhancing effect of HrpN in *Arabidopsis*. *Plant Physiol.* 145, 426–436. doi: 10.1104/pp.107.103432

Oh, H. S., and Collmer, A. (2005). Basal resistance against bacteria in *Nicotiana benthamiana* leaves is accompanied by reduced vascular staining and suppressed by multiple *Pseudomonas syringae* type III secretion system effector proteins. *Plant J.* 42, 348–359. doi: 10.1111/j.1365-313X.2005.02529.x

Otto, B., Uehlein, N., Sdorra, S., Fischer, M., Ayaz, M., Belastegui-Macadam, X., et al. (2010). Aquaporin tetramer composition modifies the function of tobacco aquaporins. *J. Biol. Chem.* 285, 31253–31260. doi: 10.1074/jbc.M110.115881

Pawłowicz, I., and Masajada, K. (2019). Aquaporins as a link between water relations and photosynthetic pathway in abiotic stress tolerance in plants. *Gene* 687, 166–172. doi: 10.1016/j.gene.2018.11.031

Pawłowicz, I., Waśkiewicz, A., Perlikowski, D., Rapacz, M., Ratajczak, D., Kosmala, A. (2018). Remodeling of chloroplast proteome under salinity affects salt tolerance of *Festuca arundinacea*. *Photosynth. Res.* 137, 475–492. doi: 10.1007/s11120-018-0527-7

Péret, B., Li, G., Zhao, J., Band, L. R., Voß, U., Postaire, O., et al. (2012). Auxin regulates aquaporin function to facilitate lateral root emergence. *Nat. Cell Biol.* 4, 991–998. doi: 10.1038/ncb2573

Péret, B., Middleton, A. M., French, A. P., Larrieu, A., Bishopp, A., Njo, M., et al. (2013). Sequential induction of auxin efflux and influx carriers regulates lateral root emergence. *Mol. Syst. Biol.* 9:699. doi: 10.1038/msb.2013.43

Piscatelli, H. L., Li, M., and Zhou, D. (2016). Dual 4- and 5-phosphatase activities regulate SopB-dependent phosphoinositide dynamics to promote bacterial entry. *Cell. Microbiol.* 18, 705–719. doi: 10.1111/cmi.12542

Pitzschke, A. (2015). Modes of MAPK substrate recognition and control. *Trends Plant Sci.* 20, 49–55. doi: 10.1016/j.tplants.2014.09.006

Prado, K., Boursiac, Y., Tournaire-Roux, C., Monneuse, J. M., Postair, O., Da Ines, O., et al. (2013). Regulation of *Arabidopsis* leaf hydraulics involves light-dependent phosphorylation of aquaporins in veins. *Plant Cell* 25, 1029–1039. doi: 10.1105/tpc.112.108456

Prasad, S., Xu, J., Zhang, Y., and Wang, N. (2016). SEC-translocon dependent extracytoplasmic proteins of *Candidatus Liberibacter* asiaticus. *Front. Microbiol.* 7:1989. doi: 10.3389/fmicb.2016.01989

Preston, G. M., and Agre, P. (1991). Isolation of the cDNA for erythrocyte integral membrane protein of 28 kilodaltons: member of an ancient channel family. *Proc. Natl. Acad. Sci. U.S.A.* 88, 11110–11114. doi: 10.1073/pnas.88.24.11110

Preston, G. M., Carroll, T. P., Guggino, W. B., and Agre, P. (1992). Appearance of water channels in *Xenopus* oocytes expressing red cell CHIP28 protein. *Science* 256, 385–387. doi: 10.1126/science.256.5055.385

Rey, T., and Jacquet, C. (2018). Symbiosis genes for immunity and vice versa. *Curr. Opin. Plant Biol.* 44, 64–71. doi: 10.1016/j.pbi.2018.02.010

Roche, J. V., and Törnroth-Horsefield, S. (2017). Aquaporin protein-protein interactions. *Int. J. Mol. Sci.* 18:E2255. doi: 10.3390/ijms18112255

Rodrigues, O., Reshetnyak, G., Grondin, A., Saijo, Y., Leonhardt, N., Maurel, C., et al. (2017). Aquaporins facilitate hydrogen peroxide entry into guard cells to mediate ABA- and pathogen-triggered stomatal closure. *Proc. Natl. Acad. Sci. U.S.A.* 114, 9200–9205. doi: 10.1073/pnas.1704754114

Ruiz-Lozano, J. M., and Aroca, R. (2017). "Plant aquaporins and mycorrhizae: their regulation and involvement in plant physiology and performance," in *Plant Aquaporins: From Transport to Signaling*, eds F. Chaumont and S. D. Tyerman (Cham: Springer International Publishing), 333–353. doi: 10.1007/978-3-319-49395-4_15

Ruiz-Lozano, J. M., Aroca, R., Zamarreño, A. M., Molina, S., Andreo-Jiménez, B., Porcel, R., et al. (2016). Arbuscular mycorrhizal symbiosis induces strigolactone biosynthesis under drought and improves drought tolerance in lettuce and *tomato*. *Plant Cell Environ.* 39, 441–452. doi: 10.1111/pce.12631

Rüter, C., Buss, C., Scharnert, J., Heusipp, G., and Schmidt, M. A. (2010). A newly identified bacterial cell-penetrating peptide that reduces the transcription of pro-inflammatory cytokines. *J. Cell Sci.* 123, 2190–2198. doi: 10.1242/jcs.063016

Rüter, C., and Schmidt, M. A. (2017). Cell-penetrating bacterial effector proteins: better tools than targets. *Trends Biotechnol.* 35, 109–120. doi: 10.1016/j.tibtech.2016.08.002

Sagi, M., and Fluhr, R. (2006). Production of reactive oxygen species by plant NADPH oxidases. *Plant Physiol.* 141, 336–340. doi: 10.1104/pp.106.078089

Sánchez-Romera, B., Ruiz-Lozano, J. M., Zamarreño, Á. M., García-Mina, J. M., and Aroca, R. (2016). Arbuscular mycorrhizal symbiosis and methyl jasmonate avoid the inhibition of root hydraulic conductivity caused by drought. *Mycorrhiza* 26, 111–122. doi: 10.1007/s00572-015-0650-7

Sang, S., Li, X., Gao, R., You, Z., Lü, B., Liu, P., et al. (2012). Apoplastic and cytoplasmic location of harpin protein $Hpa1_{Xoo}$ plays different roles in H_2O_2 generation and pathogen resistance in *Arabidopsis*. *Plant Mol. Biol.* 79, 375–391. doi: 10.1007/s11103-012-9918-x

Santi-Rocca, J., and Blanchard, N. (2017). Membrane trafficking and remodeling at the host-parasite interface. *Curr. Opin. Microbiol.* 40, 145–151. doi: 10.1016/j.mib.2017.11.013

Sawa, T., Katoh, H., and Yasumoto, H. (2014). V-antigen homologs in pathogenic gram-negative bacteria. *Microbiol. Immunol.* 58, 267–285. doi: 10.1111/1348-0421.12147

Scharnert, J., Greune, L., Zeuschner, D., Lubos, M. L., Alexander Schmidt, M., and Rüter, C. (2013). Autonomous translocation and intracellular trafficking of the cell-penetrating and immune-suppressive effector protein YopM. *Cell. Mol. Life Sci.* 70, 4809–4823. doi: 10.1007/s00018-013-1413-2

Scheibner, F., Marillonnet, S., and Büttner, D. (2017). The TAL effector AvrBs3 from *Xanthomonas campestris* pv. *vesicatoria* contains multiple export signals and can enter plant cells in the absence of the type III secretion translocon. *Front. Microbiol.* 8:2180. doi: 10.3389/fmicb.2017.02180

Schreiber, K. J., Baudin, M., Hassan, J. A., and Lewis, J. D. (2016). Die another day: molecular mechanisms of effector-triggered immunity elicited by type III secreted effector proteins. *Semin. Cell Dev. Biol.* 56, 124–133. doi: 10.1016/j.semcdb.2016.05.001

Schwartz, A. R., Morbitzer, R., Lahaye, T., and Staskawicz, B. J. (2017). TALE-induced bHLH transcription factors that activate a pectate lyase contribute to water soaking in bacterial spot of *tomato*. *Proc. Natl. Acad. Sci. U.S.A.* 114, E897–E903. doi: 10.1073/pnas.1620407114

Shanmugam, S. K., and Dalbey, R. E. (2019). The conserved role of YidC in membrane protein biogenesis. *Microbiol. Spectr.* 7:PSIB-0014-2018. doi: 10.1128/microbiolspec.PSIB-0014-2018

Shen, M., Bao, L. Z., Zheng, X., Zhao, X. X., and Guo, Z. F. (2019). Obestatin downregulating aquaporin 2 plasma membrane distribution through a short-term regulatory effect. *Am. J. Med. Sci.* 357, 247–254. doi: 10.1016/j.amjms.2018.12.010

Skrzypek, E., Cowan, C., and Straley, S. C. (1998). Targeting of the *Yersinia pestis* YopM protein into HeLa cells and intracellular trafficking to the nucleus. *Mol. Microbiol.* 30, 1051–1065. doi: 10.1046/j.1365-2958.1998.01135.x

Smirnoff, N., and Arnaud, D. (2019). Hydrogen peroxide metabolism and functions in plants. *New Phytol.* 221, 1197–1214. doi: 10.1111/nph.15488

Spoel, S. H., Mou, Z., Tada, Y., Spivey, N. W., Genschik, P., and Dong, X. (2009). Proteasome-mediated turnover of the transcription coactivator NPR1 plays dual roles in regulating plant immunity. *Cell* 137, 860–872. doi: 10.1016/j.cell.2009.03.038

Sugio, A., Yang, B., and White, F. F. (2005). Characterization of the *hrpF* pathogenicity peninsula of *Xanthomonas oryzae* pv. *oryzae*. *Mol. Plant Microbe Interact.* 18, 546–554. doi: 10.1094/MPMI-18-0546

Sui, H., Han, B. G., Lee, J. K., Walian, P., and Jap, B. K. (2001). Structural basis of water-specific transport through the AQP1 water channel. *Nature* 414, 872–878. doi: 10.1038/414872a

Sutka, M., Amodeo, G., and Ozu, M. (2017). Plant and animal aquaporins crosstalk: what can be revealed from distinct perspectives. *Biophys. Rev.* 9, 545–562. doi: 10.1007/s12551-017-0313-3

Tada, Y., Spoel, S. H., Pajerowska-Mukhtar, K., Mou, Z., Song, J., Wang, C., et al. (2008). Plant immunity requires conformational charges of NPR1 via S-nitrosylation and thioredoxins. *Science* 321, 952–956. doi: 10.1126/science.1156970

Tejeda-Dominguez, F., Huerta-Cantillo, J., Chavez-Dueñas, L., and Navarro-Garcia, F. (2017). A novel mechanism for protein delivery by the type 3 secretion system for extracellularly secreted proteins. *mBio* 8:e00184-17. doi: 10.1128/mBio.00184-17

Tian, D., Wang, J., Zeng, X., Gu, K., Qiu, C., Yang, X., et al. (2014). The rice TAL effector–dependent resistance protein Xa10 triggers cell death and calcium depletion in the endoplasmic reticulum. *Plant Cell* 26, 497–515. doi: 10.1105/tpc.113.119255

Tian, S., Wang, X., Li, P., Wang, H., Ji, H., Xie, J., et al. (2016). Plant aquaporin AtPIP1;4 links apoplastic H_2O_2 induction to disease immunity pathways. *Plant Physiol.* 171, 1635–1650. doi: 10.1104/pp.15.01237

Törnroth-Horsefield, S., Hedfalk, K., Fischer, G., Lindkvist-Petersson, K., and Neutze, R. (2010). Structural insights into eukaryotic aquaporin regulation. *FEBS Lett.* 584, 2580–2588. doi: 10.1016/j.febslet.2010.04.037

Törnroth-Horsefield, S., Wang, Y., Hedfalk, K., Johanson, U., Karlsson, M., Tajkhorshid, E., et al. (2006). Structural mechanism of plant aquaporin gating. *Nature* 439, 688–694. doi: 10.1038/nature04316

Torres, M. A. (2009). ROS in biotic interactions. *Physiol. Plant* 139, 414–429. doi: 10.1111/j.1399-3054.2009.01326.x

Verdoucq, L., Grondin, A., and Maurel, C. (2008). Structure-function analysis of plant aquaporin AtPIP2;1 gating by divalent cations and protons. *Biochem. J.* 415, 409–416. doi: 10.1042/BJ20080275

Wagner, S., Grin, I., Malmsheimer, S., Singh, N., Torres-Vargas, C. E., and Westerhausen, S. (2018). Bacterial type III secretion systems: a complex device for the delivery of bacterial effector proteins into eukaryotic host cells. *FEMS Microbiol. Lett.* 365:fny201. doi: 10.1093/femsle/fny201

Wang, D., Wang, Y., Fu, M., Mu, S., Han, B., Ji, H., et al. (2014). Transgenic expression of the functional fragment $Hpa1_{10-42}$ of the harpin protein Hpa1 imparts enhanced resistance to powdery mildew in wheat. *Plant Dis.* 98, 448–455. doi: 10.1094/PDIS-07-13-0687-RE

Wang, F., Wang, Y., Zhang, X., Zhang, W., Guo, S., and Jin, F. (2014). Recent progress of cell-penetrating peptides as new carriers for intracellular cargo delivery. *J. Control. Release* 174, 126–136. doi: 10.1016/j.jconrel.2013.11.020

Wang, J., Tian, D., Gu, K., Yang, X., Wang, L., Zeng, X., et al. (2017). Induction of Xa10-like genes in rice cultivar Nipponbare confers disease resistance to rice bacterial blight. *Mol. Plant Microbe Interact.* 30, 466–477. doi: 10.1094/MPMI-11-16-0229-R

Wang, R., Wang, M., Chen, K., Wang, S., Mur, L. A. J., and Guo, S. (2018). Exploring the roles of aquaporins in plant-microbe interactions. *Cells* 7:E267. doi: 10.3390/cells7120267

Wang, X., Zhang, L., Ji, H., Mo, X., Li, P., Wang, J., et al. (2018). Hpa1 is a type III translocator in *Xanthomonas oryzae* pv. *oryzae*. *BMC Microbiol.* 18:105. doi: 10.1186/s12866-018-1251-3

Wang, Y., Cohen, J., Boron, W. F., Schulten, K., and Tajkhorshid, E. (2007). Exploring gas permeability of cellular membranes and membrane channels with molecular dynamics. *J. Struct. Biol.* 157, 534–544. doi: 10.1016/j.jsb.2006.11.008

Wang, Y., Liu, R., Wang, Y. C., Liang, Y. C., Wu, X., Li, B., et al. (2009). *Nicotiana tabacum* TTG1 contributes to ParA1-induced signalling and cell death in leaf trichomes. *J. Cell Sci.* 122, 2673–2685. doi: 10.1242/jcs.049023

Weber, S. S., Ragaz, C., Reus, K., Nyfeler, Y., and Hilbi, H. (2006). *Legionella pneumophila* exploits PI(4)P to anchor secreted effector proteins to the replicative vacuole. *PLoS Pathog.* 2:e46. doi: 10.1371/journal.ppat.0020046

Wei, Z.-M., Lacy, R. J., Zumoff, C. H., Bauer, D. W., He, S. Y., Collmer, A., et al. (1992). Harpin, elicitor of the hypersensitive response produced by the plant pathogen *Erwinia amylovora*. *Science* 257, 85–88. doi: 10.1126/science.1621099

White, F. F., Potnis, N., Jones, J. B., and Koebnik, R. (2009). The type III effectors of *Xanthomonas*. *Mol. Plant Pathol.* 10, 749–766. doi: 10.1111/j.1364-3703.2009.00590.x

Wree, D., Wu, B., Zeuthen, T., and Beitz, E. (2011). Requirement for asparagine in the aquaporin NPA sequence signature motifs for cation exclusion. *FEBS J.* 278, 740–748. doi: 10.1111/j.1742-4658.2010.07993.x

Wudick, M. M., Li, X., Valentini, V., Geldner, N., Chory, J., Lin, J., et al. (2015). Subcellular redistribution of root aquaporins induced by hydrogen peroxide. *Mol. Plant* 8, 1103–1114. doi: 10.1016/j.molp.2015.02.017

Wudick, M. M., Luu, D. T., and Maurel, C. (2009). A look inside: localization patterns and functions of intracellular plant aquaporins. *New Phytol.* 184, 289–302. doi: 10.1111/j.1469-8137.2009.02985.x

Xin, X. F., Nomura, K., Aung, K., Velásquez, A. C., Yao, J., Boutrot, F., et al. (2015). Bacteria establish an aqueous living space in plants crucial for virulence. *Nature* 539, 524–529. doi: 10.1038/nature20166

Xu, Y., Yao, H., Wang, Q., Xu, W., Liu, K., Zhang, J., et al. (2018). Aquaporin-3 attenuates oxidative stress-induced nucleus pulposus cell apoptosis through regulating the p38 MAPK pathway. *Cell. Physiol. Biochem.* 50, 1687–1697. doi: 10.1159/000494788

Yang, B. (2017). *Advances in Experimental Medicine and Biology 969 Aquaporins*. Dordrecht: Springer Science + Business Media B.V.

Yang, B., Sugio, A., and White, F. F. (2006). *Os8N3* is a host disease-susceptibility gene for bacterial blight of rice. *Proc. Natl. Acad. Sci. U.S.A.* 103, 10503–10508. doi: 10.1073/pnas.0604088103

Zelazny, E., Miecielica, U., Borst, J. W., Hemminga, M. A., and Chaumont, F. (2009). An N-terminal diacidic motif is required for the trafficking of maize aquaporins ZmPIP2;4 and ZmPIP2;5 to the plasma membrane. *Plant J.* 57, 346–355. doi: 10.1111/j.1365-313X.2008.03691.x

Zhang, J., Shao, F., Li, Y., Cui, H., Chen, L., Li, H., et al. (2007). A *Pseudomonas syringae* effector inactivates MAPKs to suppress PAMP-induced immunity in plants. *Cell Host Microbe* 17, 175–185. doi: 10.1016/j.chom.2007.03.006

Zhang, J., Wang, X., Zhang, Y., Zhang, G., and Wang, J. (2008). A conserved Hpa2 protein has lytic activity against the bacterial cell wall in phytopathogenic *Xanthomonas oryzae*. *Appl. Microbiol. Biotechnol.* 79, 605–616. doi: 10.1007/s00253-008-1457-7

Zhang, L., Hu, Y., Li, P., Wang, X., and Dong, H. (2018). Silencing of an aquaporin gene diminishes bacterial blight disease in rice. *Aust. Plant Pathol.* 48, 143–158. doi: 10.1007/s13313-018-0609-1

Zhang, S., Feng, M., Chen, W., Zhou, X., Lu, J., Wang, Y., et al. (2019). In rose, transcription factor PTM balances growth and drought survival via PIP2;1 aquaporin. *Nat. Plants* 5, 290–299. doi: 10.1038/s41477-019-0376-1

Zhao, Y. Y., Li, C., Ge, J., Xu, M. Y., Zhu, Q., Wu, T. Q., et al. (2014). Recessive mutation identifies auxin-repressed protein ARP1 that regulates growth and disease resistance in tobacco. *Mol. Plant Microbe Interact.* 27, 638–654. doi: 10.1094/MPMI-08-13-0250-R

Zhou, H., Morgan, R. L., Guttman, D. S., and Ma, W. (2009). Allelic variants of the *Pseudomonas syringae* type III effector HopZ1 are differentially recognized by plant resistance systems. *Mol. Plant Microbe Interact.* 22, 176–189. doi: 10.1094/MPMI-22-2-0176

Zhu, W., MaGbanua, M. M., and White, F. F. (2000). Identification of two novel *Hrp*-associated genes in the *Hrp* gene cluster of *Xanthomonas oryzae* pv. *oryzae*. *J. Bacteriol.* 182, 1844–1853. doi: 10.1128/jb.182.7.1844-1853.2000

Zipfel, C., Robatzek, S., Navarro, L., Oakeley, E. J., Jones, J. D., Felix, G., et al. (2004). Bacterial disease resistance in *Arabidopsis* through flagellin perception. *Nature* 428, 764–767. doi: 10.1038/nature02485

Conflict of Interest Statement: The authors declare that the research was conducted in the absence of any commercial or financial relationships that could be construed as a potential conflict of interest.

frontiers in Microbiology

ORIGINAL RESEARCH
published: 28 May 2019
doi: 10.3389/fmicb.2019.01208

Comparative Transcriptomics and Proteomics of *Atractylodes lancea* in Response to Endophytic Fungus *Gilmaniella* sp. AL12 Reveals Regulation in Plant Metabolism

Jie Yuan[1], Wei Zhang[1], Kai Sun[1], Meng-Jun Tang[1], Piao-Xue Chen[1], Xia Li[2] and Chuan-Chao Dai[1]**

[1] Jiangsu Key Laboratory for Microbes and Functional Genomics, Jiangsu Engineering and Technology Research Center for Industrialization of Microbial Resources, College of Life Sciences, Nanjing Normal University, Nanjing, China, [2] Jiangsu High Quality Rice Research and Development Center, Nanjing Branch of Chinese National Center Rice Improvement, Institute of Food Crops, Jiangsu Academy of Agricultural Sciences, Nanjing, China

OPEN ACCESS

Edited by:
Marco Catoni, University of Birmingham, United Kingdom

Reviewed by:
Khondoker M. G. Dastogeer, Tokyo University of Agriculture and Technology, Japan
Stefania Daghino, University of Turin, Italy

***Correspondence:**
Chuan-Chao Dai
daichuanchao@njnu.edu.cn
Xia Li
jspplx@jaas.ac.cn

Specialty section:
This article was submitted to Plant Microbe Interactions, a section of the journal Frontiers in Microbiology

Received: *14 March 2019*
Accepted: *13 May 2019*
Published: *28 May 2019*

Citation:
Yuan J, Zhang W, Sun K, Tang M-J, Chen P-X, Li X and Dai C-C (2019) Comparative Transcriptomics and Proteomics of Atractylodes lancea in Response to Endophytic Fungus Gilmaniella sp. AL12 Reveals Regulation in Plant Metabolism. Front. Microbiol. 10:1208. doi: 10.3389/fmicb.2019.01208

The fungal endophyte *Gilmaniella* sp. AL12 can establish a beneficial association with the medicinal herb *Atractylodes lancea*, and improve plant growth and sesquiterpenoids accumulation, which is termed "double promotion." Our previous studies have uncovered the underling primary mechanism based on some physiological evidences. However, a global understanding of gene or protein expression regulation in primary and secondary metabolism and related regulatory processes is still lacking. In this study, we employed transcriptomics and proteomics of *Gilmaniella* sp. AL12-inoculated and *Gilmaniella* sp. AL12-free plants to study the impact of endophyte inoculation at the transcriptional and translational levels. The results showed that plant genes involved in plant immunity and signaling were suppressed, similar to the plant response caused by some endophytic fungi and biotroph pathogen. The downregulated plant immunity may contribute to plant-endophyte beneficial interaction. Additionally, genes and proteins related to primary metabolism (carbon fixation, carbohydrate metabolism, and energy metabolism) tended to be upregulated after *Gilmaniella* sp. AL12 inoculation, which was consistent with our previous physiological evidences. And, *Gilmaniella* sp. AL12 upregulated genes involved in terpene skeleton biosynthesis, and upregulated genes annotated as β-farnesene synthase and β-caryophyllene synthase. Based on the above results, we proposed that endophyte-plant associations may improve production (biomass and sesquiterpenoids accumulation) by increasing the source (photosynthesis), expanding the sink (glycolysis and tricarboxylic acid cycle), and enhancing the metabolic flux (sesquiterpenoids biosynthesis pathway) in *A. lancea*. And, this study will help to further clarify plant-endophyte interactions.

Keywords: *Atractylodes lancea*, endophytic fungi, beneficial interaction, plant immunity, metabolism, terpenoid biosynthesis

INTRODUCTION

Medicinal plants are rich in active compounds such as artemisinin (Sharma and Agrawal, 2013) and ginseng saponin (Wei et al., 2018), which are important sources of modern drugs. Within the increasing population pressure, costs and side effects of drugs, demands for the uses of medicines from plants for treatment of various human ailments are increasing. Compared with synthetic medicines, compounds from plants are thought to be safe to human beings and the ecosystem (Nema et al., 2013). To meet the market demand for these medicinal materials, artificial cultivation technology has been employed for planting medicinal herbs in some Asian countries (Zhou et al., 2005; Sharma et al., 2010; Oh et al., 2014; Lv et al., 2017). However, it is difficult to guarantee the quality and quantity of artificially cultivated medicinal plants because they are more vulnerable to infections by pests and pathogens. Thus, it is imperative to seek effective methods for medicinal plant cultivation. In the past few years, endophytic fungi possessing plant growth promoting properties have been an effective tool for medicinal plant cultivation (Mandal et al., 2013; Ming et al., 2013; Sharma and Agrawal, 2013; Zheng et al., 2016; Zhai et al., 2018).

Atractylodes lancea (Thunb.) DC., belonging to the Asteraceae family, is an endangered traditional Chinese medicinal herb (Wang et al., 2008). Its bioactive component, the sesquiterpenoids, possesses various pharmacology properties such as antibacterial, antitumour, and immunomodulation abilities (Wang et al., 2008; Koonrungsesomboon et al., 2014; Na-Bangchang et al., 2017). Over the past few years, natural sources of *A. lancea* have been in short supply because of the excessive exploitation and slow growth rate of the herb (Zhou et al., 2016). The medicinal source of *A. lancea* mainly derives from artificial cultivation, but the yield and quality of this herb are relatively low (Zhou et al., 2016). At present, it is urgent to improve the quality and quantity of the herb as the market demand for *A. lancea* is increasing on a daily basis. The endophytic fungus *Gilmaniella* sp. AL12 isolated from stem of *A. lancea* can establish a beneficial interaction with the host plant (Wang et al., 2012) and promote plant growth and sesquiterpenoid accumulation of tissue culture seedings, which is termed the "double promotion" effect of the endophyte on *A. lancea* (Yuan et al., 2016b). Consistent with this phenomenon, the endophytic fungi AL12 promotes plant growth and sesquiterpenoid accumulation within two years of growth in field experiments. Therefore, a beneficial interaction of *Gilmaniella* sp. AL12 with *A. lancea* is considered suitable for cultivation of *A. lancea* and will provide a theoretical reference for endophytic fungi-medicinal herb interactions.

In view of the limited carbon and energy source in plants, the accumulation of secondary metabolites occurs at the cost of primary metabolism, representing a discrepancy with the "double promotion" effect of *Gilmaniella* sp. AL12 on *A. lancea*. The plant growth promotion effect of the endophyte on *A. lancea* has been preliminarily ascribed to nutrient assimilation, photosynthesis, and phytohormone content regulation (Yuan et al., 2016b). Moreover, the enhanced sesquiterpenoids accumulation of *A. lancea* has been shown to be mediated by multiple defense related signals of the host induced by the endophyte (Wang et al., 2011; Ren and Dai, 2012, 2013; Yuan et al., 2016a). Given that primary metabolism-dependent terpenoid precursor biosynthesis and secondary metabolism-related terpenoid skeleton biosynthesis and transformation are simultaneously involved in sesquiterpenoid synthesis (Dudareva et al., 2006; Chen W. et al., 2017; Sharma et al., 2017; Vattekkatte et al., 2018), the molecular and biochemical regulation of the plants relevant to primary and secondary metabolism should be considered. However, thus far, a global understanding of the -regulated expression of genes or proteins in primary and secondary metabolism and related regulatory processes is still lacking.

In this study, we employed transcriptomics and proteomics on endophyte-inoculated and endophyte free plants to better understand the impact of *Gilmaniella* sp. AL12 on plant metabolism and related regulatory processes of *A. lancea* at the transcriptional and translational level. The following four essential questions were addressed in this study: (1) Which plant metabolic or regulatory processes of *A. lancea* are affected by *Gilmaniella* sp. AL12? (2) What is the effect of the fungal endophyte on the regulation of primary metabolism-dependent terpenoid precursor biosynthesis in *A. lancea*? (3) What is the effect of the fungal endophyte on the regulation of secondary metabolism-related terpenoid skeleton biosynthesis and transformation in *A. lancea*? (4) Are other potential signals involved in the fungal endophyte-induced sesquiterpenoids biosynthesis of *A. lancea*?

MATERIALS AND METHODS

Plantlet Material and Fungal Inoculation

Atractylodes lancea meristem cultures were established using sterilized plantlets according to our previous studies (Wang et al., 2012). Firstly, meristem cultures were established using mature *A. lancea* planted in Maoshan, Jiangsu Province, China (Wang et al., 2012). Sterile adventitious buds (approximately 2–3 cm long) of young stems were collected and carefully washed under running tap water. They were surface sterilized by immersing in ethanol (75%) for 30 s, followed by soaking in mercury chloride solution (1%) for 10 min and rinsing in sterile distilled water five times (Wang et al., 2012). Subsequent procedures were conducted aseptically (Wang et al., 2012). The explants were transferred in 50 mL Murashige and Skoog medium containing sucrose (30 g L^{-1}), agar (10 g L^{-1}),

Abbreviations: *A. lancea*, *Atractylodes lancea*; AL12, *Gilmaniella* sp. AL12; AMF, arbuscular mycorrhizal fungi; ATP, triphosadenine; BAK1, brassinosteroid insensitive 1-associated receptor kinase 1; DEGs, differentially expressed genes; DPI, days post-AL12 inoculation; EFR, LRR receptor-like serine/threonine-protein kinase EFR; ETI, effector triggered immunity; FPKM, the fragments per kilobase of transcript per million mapped reads; GC, gas chromatography; GO, gene ontology database; KEGG, Kyoto Encyclopedia of Genes and Genomes database; LRR, leucine-rich repeat; MDH, malate dehydrogenase; NCBI, National Center for Biotechnology Information; OAA, oxaloacetate; PAMPs, pathogen-associated molecular patterns; Pi, orthophosphate; PLD, phospholipase D; PS II, photosystem II; PTI, PAMP triggered immunity; RT-qPCR, real-time quantitative PCR; TCA cycle, tricarboxylic acid cycle; 2-DE, two-dimensional gel electrophoresis.

naphthaleneacetic acid (0.3 mg L^{-1}), and 6-benzyladenine (2.0 mg L^{-1}) in 150-mL sealed Erlenmeyer flask to emerge adventitious buds for 4 weeks (Wang et al., 2012). Then, newborn adventitious buds were separated and grown in 50 mL Murashige and Skoog medium containing sucrose (30 g L^{-1}), agar (10 g L^{-1}), naphthaleneacetic acid (0.3 mg L^{-1}) and 6-benzyladenine (2.0 mg L^{-1}) in 150-mL sealed Erlenmeyer flask for further differentiation until newborn adventitious buds were suficient for transplantation. After separation, newborn axillary buds were transplanted into 50 mL Murashige and Skoog medium containing sucrose (30 g L^{-1}), agar (10 g L^{-1}), and naphthaleneacetic acid (0.25 mg L^{-1}) in a 150-mL sealed Erlenmeyer flask to develop into rooting plantlets. Each bud was cultured in an Erlenmeyer flask. All plantlets were grown in growth chamber (PGX-600A-12H, Ningbo Lifewww Technology Co., China) with a photoperiod of 12 h, a light density of 3,400 lm m^{-2}, and a temperature cycle of 25/18°C day/night. Thirty-day-old rooting plantlets were chosen for the endophytic fungus inoculation experiments. The endophytic fungus *Gilmaniella* sp. AL12 isolated from the stem of *A. lancea* was grown on potato dextrose agar medium (Chen et al., 2008; Wang et al., 2012). After five days of culture at 28°C, 5-mm *Gilmaniella* sp. AL12 mycelial disks were placed near the plant caudexes on the medium for inoculation. Additionally, equal-sized potato dextrose agar disks were used as the control (Yuan et al., 2016a). All plantlets were grown in growth chamber and performed in triplicate.

Plant Growth and Sesquiterpenoid Content Analysis

Plantlets were harvested at 15 DPI for the shoot dry weight and sesquiterpenoid content analysis. Briefly, harvested plants were dried at 30°C until the weight was constant, and then 1 g of the ground powder was extracted with 4 mL cyclohexane at room temperature for 10 h. After 15 min of sonication (60 Hz), the mixture was centrifuged for 5 min at 5,000 *g* at 4°C. After filtering through 0.22-μm-diameter microporous membranes, the total cyclohexane extract was dried over anhydrous sodium sulfate and stored in a dark glass bottle at 4°C before gas chromatography (GC) analysis (Yuan et al., 2016b).

A GC system (Agilent 7890A, United States) equipped with a fame ionization detector was used for sesquiterpenoid analysis (Yuan et al., 2016b). The GC column was DB-1ms (30 m × 0.32 mm × 0.10 μm) with high-purity nitrogen as a carrier gas at a flow rate of 0.8 mL min^{-1}. For sesquiterpenoid analysis, 1 μl of cyclohexane was directly injected onto the GC column with the following temperature program: injection at 240°C, an initial temperature of 100°C (4 min hold) raised to 140°C at a rate of 10°C min^{-1} (10-min hold), followed by an increase to 220°C at a rate of 10°C min^{-1} (10-min hold), raised to 260°C at a rate of 10°C min^{-1} (2-min hold). The detector temperature was then set at 350°C. As previously described, qualitative and quantitative analyses of seven sesquiterpenoids were performed according to authentic standards (Yuan et al., 2016b).

Determination of Photosynthetic Parameters

Plantlets were harvested at 10: 00 AM at 15 DPI for Chlorophyll a fluorescence measurement using a Handy-PEA instrument (Handy PEA, Hansatech, United Kingdom) (Wang et al., 2017). Prior to measurement, *A. lances* leaves were dark-adapted for 30 min at room temperature to relax the reaction centers. The leaves were exposed to red light of 650 nm at an excitation irradiance of 3,000 μmol m^{-2} s^{-1} for 800 ms. Then, fluorescence parameters were calculated according to **Supplementary Table S1**.

RNA Sequencing and Functional Annotation of Differentially Expressed Genes

Plantlets were harvested at 15 DPI. Shoot tissue of endophyte-inoculated or endophyte-free plants were harvested for RNA extraction using TRIzol reagent (Invitrogen, CA, United States) (Chen F. et al., 2017). After quality and purity checking, equal amounts of RNA samples from three biological replicates of CK (endophyte-free plants for control) and AL12 (endophyte-inoculated plants) were used for construction of six mRNA-Seq libraries. Libraries were indexed, pooled and then sequenced on an Illumina HiSeq™ 4000 sequencing platform (Vazyme Biotech Co., Nanjing, China). After filtering, the remaining high-quality reads were assembled *de novo* by using the Trinity program. Certain short reads with overlapping regions were assembled into longer clusters (contigs). Paired-end reads were used to fill scaffolds gaps to obtain unigenes. Based on a BLASTX search (E value $< 10^{-5}$), functional annotation of these unigenes was performed with the following public databases, including the National Center for Biotechnology Information (NCBI) non-redundant protein (NR) and nucleotide (NT) database, Swiss-Prot protein database, Gene Ontology (GO) database, Cluster of Orthologous Groups (COGs) database, and Kyoto Encyclopedia of Genes and Genomes (KEGG) database. The fragments per kilobase of transcript per million mapped reads (FPKM) method was used to determine the unigene expression. Differentially expressed genes (DEGs) between CK and AL12 samples were identified with $\log_{10}(AL12_{FPKM}/CK_{FPKM}) \geq 1$ and a false discovery rate (FDR) ≤ 0.05. Subsequently, upregulated and downregulated DEGs were conducted by GO and KEGG enrichment analysis, respectively. The RNA sequencing data for this article were submitted to the NCBI Sequence Read Archive (SRA) under accession number SRP132616.

Real-Time Quantitative PCR Validation

Real-time quantitative PCR (RT-qPCR) was performed to determine the expression levels of differentially expressed genes of *A. lancea* cultured *in vitro*. Elongation factor 1 alpha gene (*EF1a*) was used as an internal reference (Yuan et al., 2016b). Primers for the selected DEGs are listed in **Supplementary Table S2**. One microgram of total RNA was transcribed into cDNA using HisCRIPT® II Q RT SuperMix for qPCR (+gDNA wiper) (Vazyme Biotech Co., Nanjing, China) according to the manufacturer's instruction. Subsequently, RT-qPCR was

conducted using the DNA Engine Opticon 2 Real-time PCR Detection System (Bio-Rad, Hercules, CA, United States). The reaction system consisted of a volume of 20 μL, which included 10 μL of 2 × AceQ qPCR SYBR® Green Master Mix (High ROX Premixed) (Vazyme Biotech Co., Nanjing, China), 2 μL of the cDNA template, 0.4 μL of each primer, and 7.6 μL ddH_2O. The reaction conditions were 95°C for 5 min, followed by 40 cycles of 95°C for 30 s, 60°C for 30 s, 95°C for 15 s, 60°C for 60 s, and 95°C for 15 s. All assays were performed in triplicate. Relative expression levels for each cDNA sample were calculated by the $2^{-\Delta\Delta Ct}$ method (Wang et al., 2015; Liu et al., 2018).

Total Protein Extraction, Two-Dimensional Gel Electrophoresis (2-DE) Separation, Image Analysis, In-Gel Digestion, Protein Identification and Functional Analysis

Plant shoots were harvested at 15 DPI for protein extraction. Protein was extracted using the trichloroacetic acid/acetone precipitation method (Wang et al., 2016). For this purpose, 2 g of shoot material was frozen in liquid nitrogen, ground into a fine powder, mixed with 10 mL cold trichloroacetic acid/acetone buffer (13% (w/v) trichloroacetic acid, 0.07% (v/v) 2-mercaptoethanol in acetone, and kept overnight at −20°C. After shaking for 1 h, the proteins were separated by centrifugation (10,000 *g*, 15 min, 4°C), and washed twice with cold acetone and once with 80% (v/v) acetone. The proteins were then air-dried and dissolved in protein lysis buffer (7 M urea, 2 M thiourea, 4% (w/v) 3-[(3-cholamidopropyl) dimethylam-monio]-1-propanesulphonate (CHAPS), 2% (v/v) IPG buffer, 1% (v/v) phenylmethanesulphonyl fluoride (PMSF), 10 mM Na_3VO_4, 10 mM NaF, 50 mM glycerophosphate, 5 μg mL^{-1} antiprotease, 5 μg mL^{-1} trasylol and 5 μg mL^{-1} leupeptin). After sonication and centrifugation, the resulting protein extraction was quantified using a commercial dye reagent (Bio-Rad Laboratories, Hercules, CA, United States).

Proteins (900 μg) were separated using immobilized pH gradient (IPG) strips (pH 3–10, nonlinear gradient, 24 cm) and rehydrated for 12 h. First-dimension isoelectric focusing was performed at 20°C for 1 h at 250 V, 2 h at 1,000 V, 5 h at 10,000 V, and 12 h at 500 V (Chen et al., 2016). The strips were then equilibrated with a buffer containing 6 M urea, 2% (w/v) sodium dodecyl sulphate (SDS), 75 mM Tris-HCl (pH 8.8), 30% (v/v) glycerol, and 1% (w/v) dithiothreitol (DTT). In the second dimension, 12% (w/v) sodium dodecyl sulfate polyacrylamide gel electrophoresis (SDS-PAGE) was used, and then coomassie brilliant blue stained (GE Healthcare). Gel images were scanned using an Image Scanner III (GE Healthcare) and analyzed using the Image Mater 2D Platinum 7.0 (GE Healthcare). Each spot was normalized to a relative volume. Quantitative analysis sets were created between each control and AL12-inoculated plants, and each treatment was performed in triplicate.

Differentially expressed spots were selected, manually excised, digested with trypsin (Tatli et al., 2017), and analyzed by UltrafleXtreme TOF/TOF (Bruker Daltonics, Germany). Reflector positive mode was used, with a wavelength of 355 nm and acceleration voltage of 2 kV. MS and MS/MS data were analyzed, and peak lists were generated using FlexAnalysis 3.1 (Bruker Daltonics, Germany). MS and MS/MS analyses were compared to the NCBI green plant protein database using the MASCOT 2.4 search engine (Matrix Science, London, United Kingdom) (Chen et al., 2016; Tatli et al., 2017). Search parameters were as follows: trypsin digestion with one missed cleavage, variable modifications (oxidation of methionine and carbamidomethylation of cysteine), and mass tolerance of a precursor ion and fragment ion at 0.2 Da for +1 charged ions. For all proteins successfully identified by a Peptide Mass Fingerprint and/or MS/MS, a Mascot score greater than 50 (the default MASCOT threshold for such searches) was accepted as significant ($P < 0.05$) (Tatli et al., 2017).

Statistical Analysis

The mean values and standard deviations were calculated using SPSS Statistics 17.0 software (SPSS Inc., Chicago, United States), and the statistical evaluation between two treatments was compared using the independent-samples *t*-test. Values are the means of three independent experiments. Bars represent standard deviations. Asterisks denote significant differences from the control (*t*-test; $^*P < 0.05$; $^{**}P < 0.01$).

RESULTS

Gilmaniella sp. AL12 Improved Shoot Growth and Sesquiterpenoid Accumulation in *A. lancea*

The content of β-caryophyllene, zingiberene, β-sesquiphellandrene, caryophyllene oxide, and atractylone in shoots of *A. lancea* all significantly increased after fungal endophyte inoculation (**Figure 1A**). The shoot dry weight of endophyte-inoculated plants was higher than that of endophyte-free *A. lancea* (**Figure 1B**). And, we analyzed chlorophyll fluorescence parameter of endophyte-inoculated and endophyte-free *A. lancea* (**Figures 1C,D**). The active photosynthesis II (PSII) reaction center captures of light energy to transform into excitation energy, then converts part of excitation energy into chemical energy, thus promotes carbon assimilation reaction, and the rest of excitation energy dissipates (Li et al., 2005). Although the maximum quantum yield of primary photochemistry (F_v/F_m) of *A. lancea* was unchanged after endophyte inoculation (**Figure 1C**), the endophyte increased phenomenological fluxes per cross section including absorption flux of photons (ABS/CS_m), phenomenological fluxes for trapping (TR_o/CS_m), and potential electron transport (ET_o/CS_m) of *A. lancea* (**Figure 1D**), indicating that the fungal endophyte improved PS II reaction center performance in *A. lancea.*

Gilmaniella sp. AL12 Induced Shoot Transcriptional Changes in *A. lancea*

We analyzed the transcriptome of *A. lancea* shoots inoculated or not inoculated with endophytic fungi AL12. A total of 1956 upregulated and 2063 downregulated genes were identified

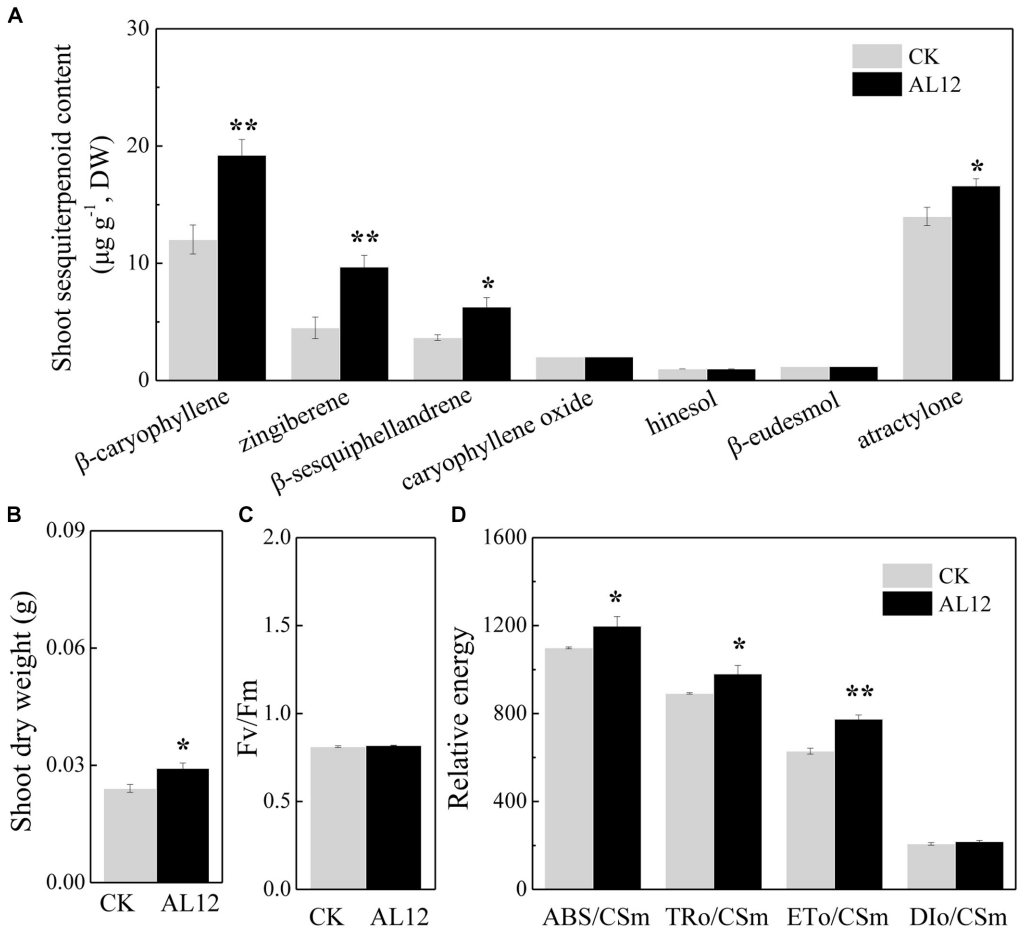

FIGURE 1 | The effect of the fungal endophyte *Gilmaniella* sp. AL12 inoculation on shoot sesquiterpenoid content **(A)**, shoot dry weight **(B)**, chlorophyll fluorescence relative value **(C)**, and phenomenological fluxes per cross section **(D)** of *A. lancea*. Thirty-day-old plantlets treated with 5-mm AL12 mycelial disks were harvested at 15 DPI. Controls were established using equal sized potato dextrose agar disks. Values are the means of three independent experiments. Bars represent standard deviations. Asterisks denote significant differences from the control (*t*-test; $^{*}P < 0.05$; $^{**}P < 0.01$).

(**Supplementary Figure S1**). To further elaborate the function of the DEGs, we first conducted GO enrichment analysis (**Supplementary Figure S2**). The most upregulated DEGs belonged to oxidation-reduction-related GO terms. Among the downregulated DEGs, stress response-related GO terms were the most enriched. We further performed KEGG pathway enrichment analysis for the upregulated and downregulated DEGs (**Figure 2**). For the upregulated DEGs, "metabolic pathway" and "biosynthesis of secondary metabolism" were the most enriched KEGG pathways (**Figure 2A**), while "plant-pathogen interaction" and "plant hormone signal transduction" were significantly enriched pathways for the downregulated DEGs (**Figure 2B**).

The DEGs were functionally related to known metabolic pathways, secondary metabolic pathways, and regulatory processes using the online software iPath2: interactive Pathways Explorer. And, pathways including transcription, translation, replication and repair, protein folding, and transport tend to be upregulated, while protein degradation pathway tend to be downregulated in shoots of *A. lancea* after the fungal endophyte inoculation (**Supplementary Table S3**). Compared with non-inoculated plants, in endophyte-inoculated plants, nucleotide metabolism, glycan biosynthesis and metabolism, and lipid metabolism pathways tends to be downregulated (**Supplementary Table S4**). Additionally, the endophytic fungus AL12 upregulated the energy, carbohydrate, amino acid, cofactor and vitamin, and secondary metabolism pathways in shoots of *A. lancea* (**Supplementary Tables S5–S7**).

Gilmaniella sp. AL12 Upregulated Genes Involved in Primary Metabolism

Our results revealed that most DEGs annotated as functioning in photosynthesis and oxidative phosphorylation were globally upregulated after AL12 inoculation (**Supplementary Table S5** and **Figure 3**), including genes annotated as ferredoxin-NADP^{+} reductase (FNR), photosystem II oxygen-evolving enhancer protein 2 (OEE), ribulose-1,5-bisphosphate

http://pathways.embl.de/iPath2.cgi#

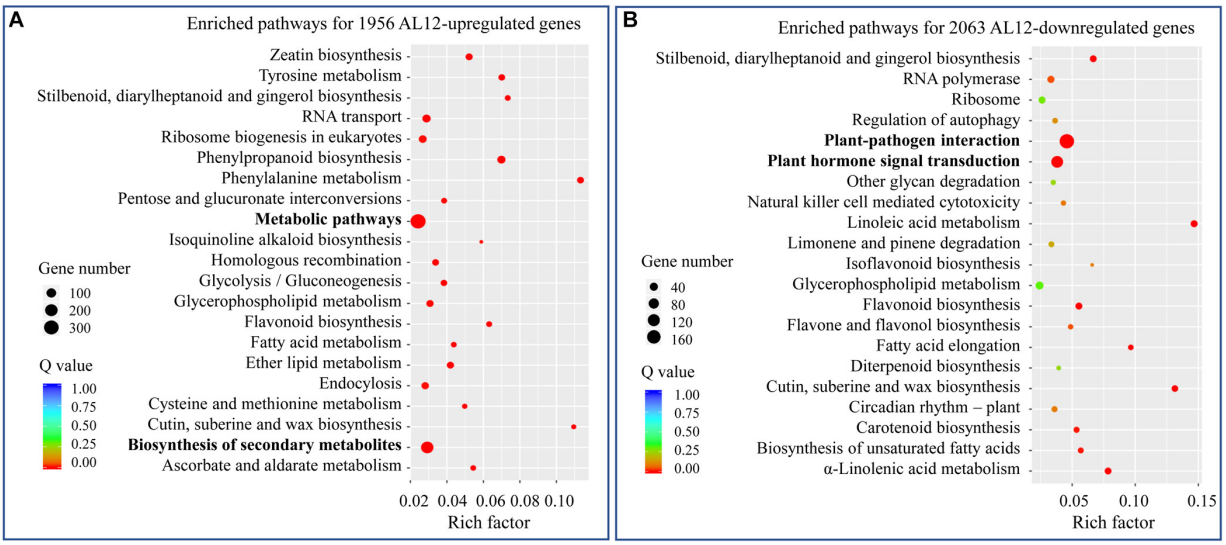

FIGURE 2 | KEGG analysis of differentially expressed genes in shoots of *A. lancea* after the fungal endophyte *Gilmaniella* sp. AL12 inoculation. **(A)** The top 21 enriched KEGG pathways of AL12 upregulated and **(B)** AL12 downregulated genes in shoots of *A. lancea*.

carboxylase/oxygenase activase (RCA), NADH dehydrogenase, and V-type H^+-transporting ATPase, among others. However, three genes encoding chlorophyll A/B binding protein (LHCP) were down-regulated.

Endophyte inoculation enhanced plant carbon metabolism, with an upregulation of genes involved in carbohydrate metabolism and transport (**Figure 3**). For instance, most DEGs annotated as phosphate transporter (TPT), amylase, invertase, β-glucosidase (GlcCerase), fructokinase (FRK), glyceraldehyde 3-phosphate dehydrogenase (GAPDH), phosphopyruvate hydratase (enolase), and phosphoenolpyruvate carboxykinase (PEPCK) were upregulated. Interestingly, genes that function in controlling pyruvate and acetyl-CoA biosynthesis were upregulated. For example, AL12 upregulated genes encoding lactate dehydrogenase (LDHD), pyruvate decarboxylase (PDC), and aldehyde dehydrogenase (ALDH), suggesting that it promotes the conversion of lactate into pyruvate and the biosynthesis of acetic acid. Similarly, the expression of genes encoding alcohol dehydrogenase (ADH) and malate dehydrogenase (MDH) was increased after AL12 inoculation, indicating that oxaloacetate (OAA) and acetic acid biosynthesis were improved. Moreover, the endophytic fungus *Gilmaniella* sp. AL12 upregulated genes encoding MDH and pyruvate dehydrogenase (PDHE), thus contributing to acetyl-CoA biosynthesis and OAA regeneration. Consistent with the improved tricarboxylic acid cycle (TCA cycle), seven genes annotated as malate transporter were up-regulated.

The balance of carbon and nitrogen metabolism is very important for plant metabolism. Most DEGs annotated as functioning in nitrogen metabolism were upregulated after AL12 inoculation (**Figure 3**). These included genes encoding high affinity nitrate transporter (NRT2), glutamate dehydrogenase (GDH), and others. In particular, one gene encoding glutamine synthetase (GS) exhibited a 10-fold increase in expression in response AL12 inoculation. Additionally, most DEGs annotated as functioning in amino acid metabolism were upregulated (**Supplementary Table S6**).

Most DEGs annotated as functioning in lipid metabolism were downregulated after AL12 treatment (**Supplementary Table S4**). These DEGs compass fatty acid elongation, the biosynthesis of unsaturated fatty acids, wax biosynthesis, linoleic acid metabolism, alpha-linolenic acid metabolism, and others. In contrast, most genes involved in fatty acid metabolism, steroid biosynthesis, glycerophospholipid metabolism, ether lipid metabolism, and sphingolipid metabolism were upregulated. Among the upregulated genes, it is worth noting that 32 DEGs encoding phospholipase D (PLD) were upregulated after AL12 inoculation, and eight showed a greater than 10-fold increase in expression (**Supplementary Table S8**).

Gilmaniella sp. AL12 Upregulated Genes Involved in Secondary Metabolism

A total of 299 DEGs involved in 18 biosynthesis pathways of secondary metabolites were regulated in *A. lancea* after AL12 inoculation (**Figure 4**). Among these pathways, DEGs involved in eight biosynthesis pathways of secondary metabolites were significantly regulated in *A. lancea* after AL12 inoculation (**Supplementary Table S9**). The eight pathways include Phenylpropanoid biosynthesis, Zeatin biosynthesis, Flavonoid biosynthesis, Stilbenoid, diarylheptanoid and gingerol biosynthesis, Limonene and pinene degradation, Flavone and flavonol biosynthesis, Carotenoid biosynthesis, and Diterpenoid biosynthesis. The largest subcategory was phenylpropanoid biosynthesis, followed by zeatin biosynthesis. The upregulated DEGs involved in phenylpropanoid biosynthesis were associated with lignin biosynthesis. Additionally, most of the DEGs involved in zeatin biosynthesis were upregulated,

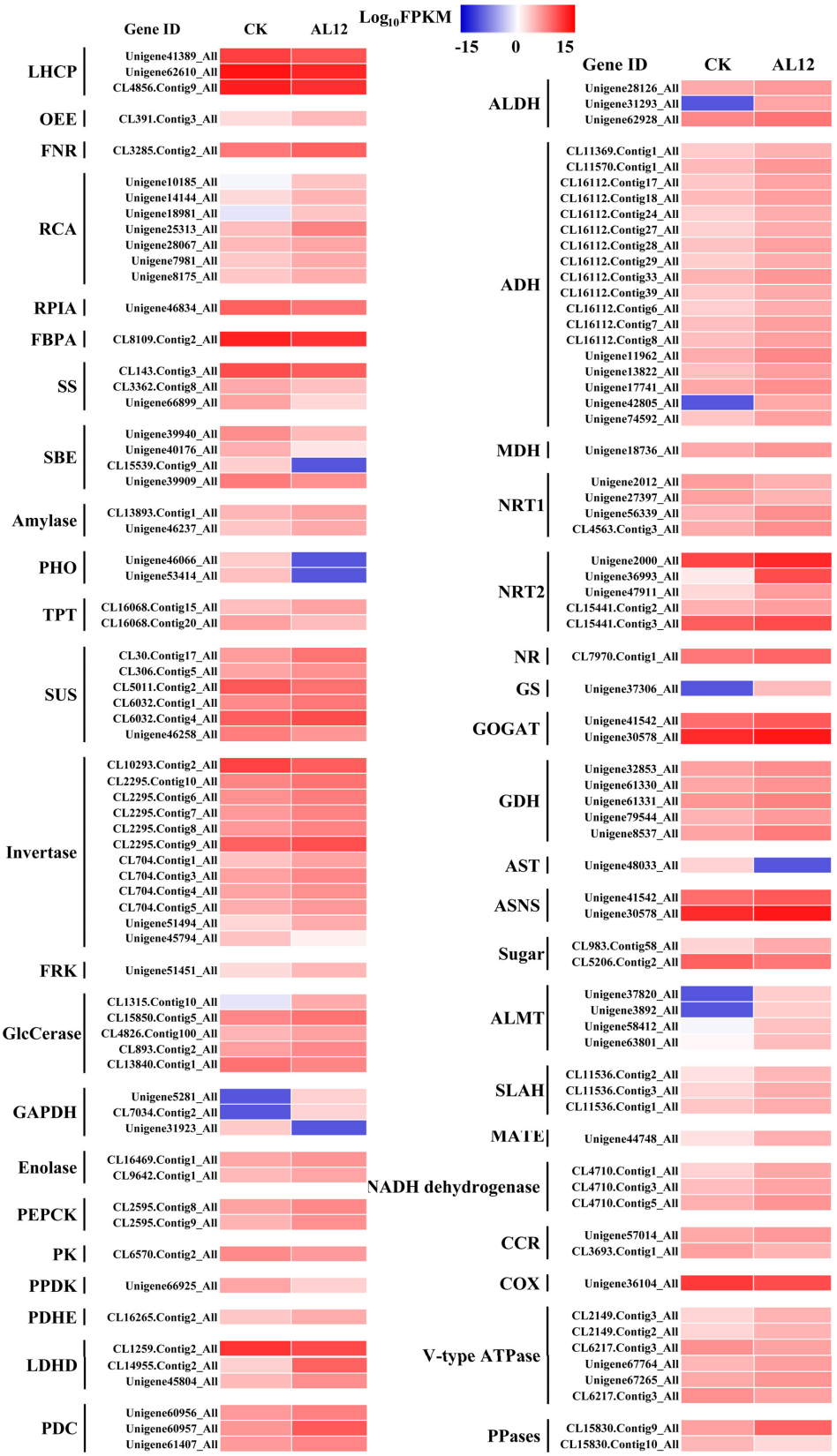

FIGURE 3 | Continued

FIGURE 3 | Differentially expression genes involved in photosynthesis, carbon/nitrogen metabolism, and oxidative phosphorylation in shoots of *A. lancea* after the fungal endophyte *Gilmaniella* sp. AL12 inoculation. LHCP, light-harvesting chlorophyll a/b-binding protein; OEE, PSII oxygen-evolving enhancer protein; FNR, Ferredoxin-NADP reductase; RCA, ribulose bisphosphate carboxylase/oxygenase activase; RPLA, Ribose 5-phosphate isomerase; FBPA, fructose-bisphosphate aldolase; SS, starch synthase; SBE, 1,4-alpha-glucan branching enzyme; amylase, PHO, starch phosphorylase; TPT, Glucose-6-phosphate/phosphate-translocator; SUS, sucrose synthase; invertase, β-fructosidases; FRK, fructokinase; GlcCerase, Beta-glucosidase-related glycosidases; GAPDH, glyceraldehyde 3-phosphate dehydrogenase; PEPCK, phosphoenolpyruvate carboxykinase (ATP); PK, pyruvate kinase; PPDK, Pyruvate orthophosphate dikinase; PDHE, pyruvate dehydrogenase; LDHD, lactate dehydrogenase; PDC, pyruvate decarboxylase; ALDH, aldehyde dehydrogenase (NAD^+); ADH, alcohol dehydrogenase; MDH, malate dehydrogenase; NRT1, low-affinity nitrate transporter; NRT2, high-affinity nitrate transporter; NR, nitrate reductase; GS, glutamine synthetase; GOGAT, glutamate synthase; GDH, glutamate dehydrogenase; AST, asparagine transaminase; ASNS, asparagine synthetase; sugar, bidirectional sugar transporter; ALMT, aluminum-activated malate transporter; SLAH, S-type anion channel; MATE, MATE efflux family protein; CCR, cytochrome-c reductase; COX, Cytochrome c oxidase; PPases, Inorganic pyrophosphatase.

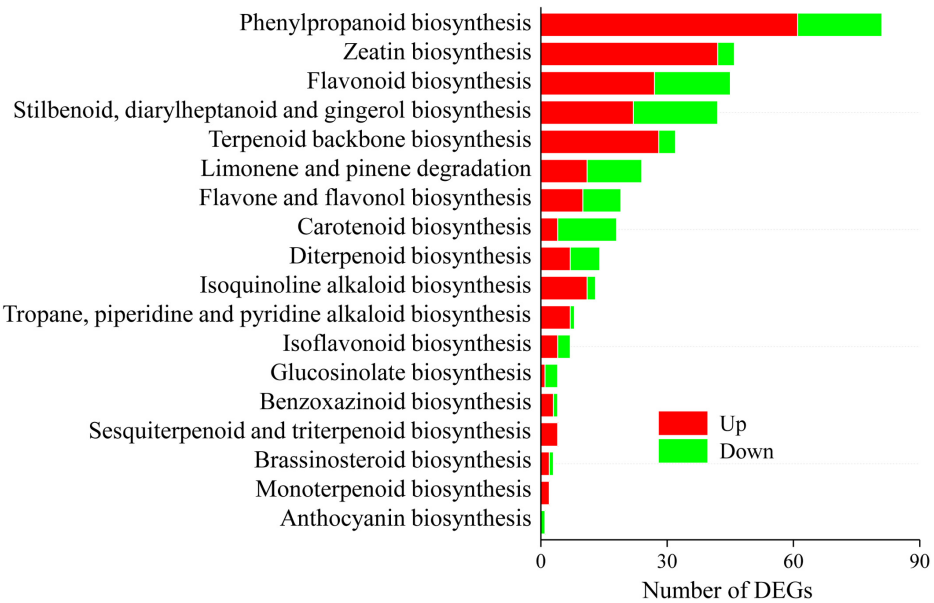

FIGURE 4 | Distribution of differentially expression genes involved in secondary metabolism in shoots of *A. lancea* after the fungal endophyte *Gilmaniella* sp. AL12 inoculation. The *x* axis indicates the KEGG pathway. The *y* axis presents the number of DEGs. Numbers in red block or green blocks represent the number of upregulated or downregulated DEGs, respectively.

particularly adenylate dimethylallyl transferase (IPT). Consistent with the increased sesquiterpenoids content in *A. lancea* shoots (**Figure 1A**), the expression of genes associated with terpenoid backbone biosynthesis and sesquiterpene biosynthesis was increased (**Figure 4** and **Supplementary Figure S3**). Genes encoding farnesyl diphosphate synthase (FDPS) and β-farnesene synthase were increased after AL12 treatment (**Supplementary Figures S3, S4**).

Gilmaniella sp. AL12 Downregulated Genes Involved in Plant-Pathogen Interactions

Most DEGs associated with plant-pathogen interaction were downregulated after AL12 inoculation (**Figure 5**). Among the genes related to pathogen-associated molecular pattern (PAMP)-triggered immunity (PTI), DEGs annotated as leucine-rich repeat (LRR) receptor-like kinase FLS2, brassinosteroid insensitive 1-associated receptor kinase 1 (BAK1), LRR receptor-like serine/threonine-protein kinase EFR, calcium-dependent protein kinase (CDPK), calmodulin/calcium-binding protein (CaM/CML), mitogen-activated protein kinase kinase kinase 1 (MEKK1), and WRKY29 tended to be downregulated. However, DEGs encoding NADPHox (Rboh) and mitogen-activated protein kinase kinase 1 (MKK1/2) tended to be upregulated in inoculated compared with control plants. Regarding effector-triggered immunity (ETI), the endophytic inoculation particularly decreased the expression of genes encoding the disease resistance proteins RPM1, RPS2, and RPS5. Additionally, defense genes such as WRKY and pathogenesis-related protein1 (PR1) also tended to be repressed after AL12 inoculation.

Gilmaniella sp. AL12-Regulated Genes Involved in Signaling

Our result shows that DEGs involved in auxin, cytokinin, and ethylene biosynthesis tended to be upregulated (**Figure 6**), and DEGs involved in cytokinin and ethylene signal transduction also tended to be upregulated (**Figure 6**). In total, 99 TF-coding genes were differentially expressed between CK and AL12 samples (**Supplementary Figure S5**). These DEGs were

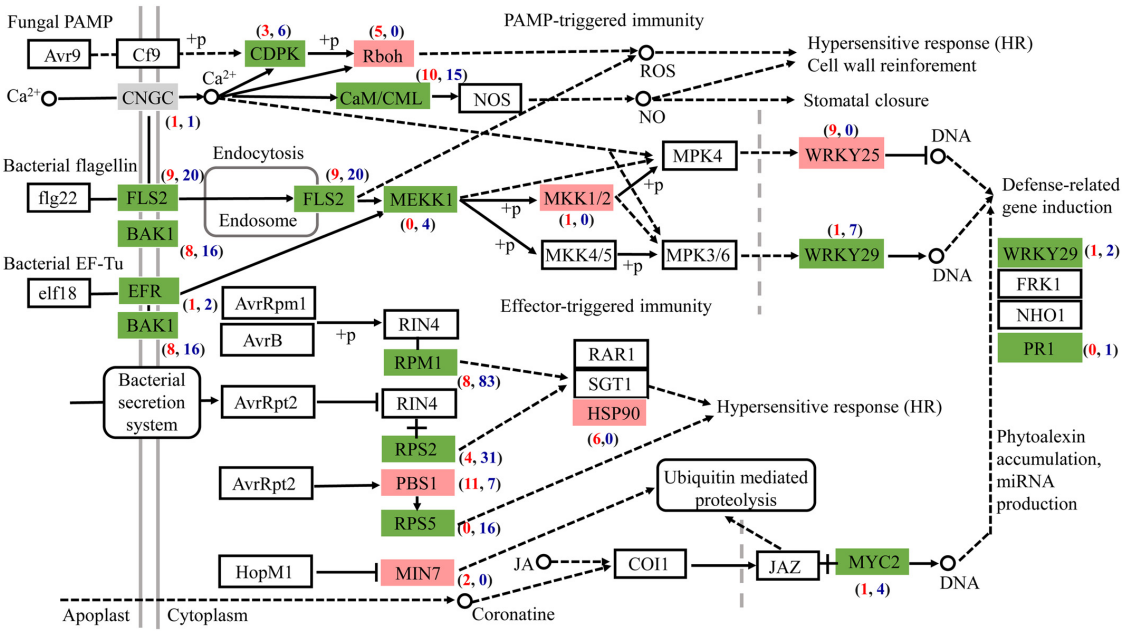

FIGURE 5 | The fungal endophyte *Gilmaniella* sp. AL12 affects the expression of genes involved in plant-pathogen interactions in shoots of *A. lancea*. Red boxes indicate most upregulated genes. Green boxes indicate most downregulated genes. Gray boxes indicate equally upregulated and downregulated genes. CNGC, cyclic nucleotide gated channel; FLS2, LRR receptor-like serine/threonine-protein kinase FLS2; BAK1, brassinosteroid insensitive 1-associated receptor kinase 1; EFR, LRR receptor-like serine/threonine-protein kinase EFR; CDPK, calcium-dependent protein kinase; Rboh, respiratory burst oxidase; CaM/CML, calmodulin/calcium-binding protein CML MEKK1, mitogen-activated protein kinase kinase kinase 1; MKK1/2, mitogen-activated protein kinase kinase 1; WRKY 25, transcription factor WRKY25; WRKY 29, transcription factor WRKY29; RPM1, disease resistance protein RPM1; RPS2, disease resistance protein RPS2; RPS5, disease resistance protein RPS5; PBS1, serine/threonine-protein kinase; MIN7, guanine nucleotide-exchange factor; HSP90, heat shock protein 90; MYC2, transcription factor MYC2.

divided into 17 families, including *WRKY*, *APETALA2/Ethylene-Response Factors* (*AP2/ERF*), *MYB*, *basic Helix-Loop-Helix* (*bHLH*), *DELLA*, *Heat stress*, *Trilelix*, *GATA*, and *NAC*, among others. Of these families, DEGs encoding *MYB*, *Trilelix*, *and NAC* transcription factor tended to be upregulated, while many genes encoding *AP2/ERF*, *WRKY*, *DELLA*, *Heat stress* and *GATA* were downregulated.

RT-qPCR Validation of Gene Expression

To further validate the transcriptomic results, 15 transcripts related to primary metabolism, secondary metabolism, and defense were selected for RT-qPCR analysis (**Supplementary Table S2** and **Figure 7**). As shown in **Figure 7**, the results of the RT-qPCR analysis were largely consistent with the RNA sequencing analysis, supporting the high quality of the RNA sequencing datasets. In particular, the expression of genes annotated as GAPDH, GS, and β-caryophyllene synthase CPS1 markedly increased after endophytic fungus inoculation (**Figure 7**).

Shoot Proteome Changes by *Gilmaniella* sp. AL12 Inoculation Involved Diverse Biological Processes

To identify proteins that responded to the endophyte inoculation, we employed 2-DE to compare the shoot protein profiles of the CK and AL12 samples. A total of approximately 2136 protein spots were separated (**Supplementary Figure S6**). After optimization of the 2-DE gels, approximately 129 differentially expressed proteins with at least a two-fold change were identified (**Supplementary Figure S6**). Finally, 125 proteins were successfully identified via MALDI-TOF MS/MS (**Supplementary Figure S7** and **Supplementary Table S10**). These proteins were classified into nine functional categories (**Supplementary Figure S7**), including "energy metabolism," "carbohydrate metabolism," "amino acid metabolism," "lipid metabolism," "defense/stress," "plant secondary metabolism," "signal transduction," "transcription and translation," and "cell growth/division."

The expression of energy metabolism-related proteins, including ribulose bisphosphate carboxylase, ferredoxin-nitrite reductase, chloroplast oxygen-evolving enhancer protein, and phosphoenolpyruvate carboxylase, were upregulated (**Table 1**). Regarding carbohydrate metabolism, glyceraldehyde-3-phosphate dehydrogenase and NAD-dependent glyceraldehyde-3-phosphate dehydrogenase were up-regulated, whereas carbon catabolite repressor protein was down-regulated (**Table 1**). Four plant secondary metabolism-associated proteins were upregulated, including tropinone reductase, Type III polyketide synthase and cytochrome P450 CYP76F12 (**Table 1**).

Among the 30 proteins involved in signal transduction, 17 were upregulated. These proteins included membrane-associated

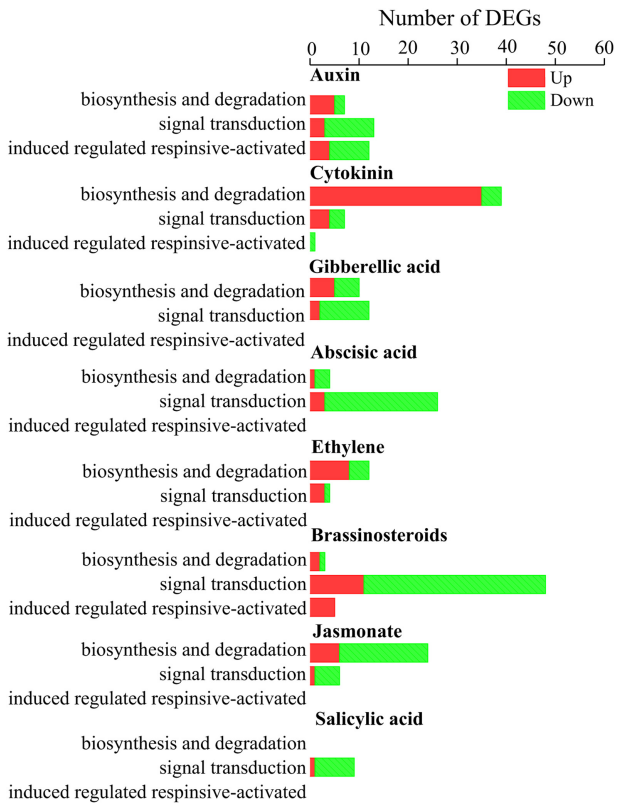

FIGURE 6 | Distribution of differentially expression genes involved in hormone biosynthesis and signal transduction in shoots of *A. lancea* after the fungal endophyte *Gilmaniella* sp. AL12 inoculation. The *x* axis presents number of DEGs. The *y* axis indicates different hormone signals.

protein, protein kinase, protein phosphatase, abscisic acid (ABA) responsive protein, gibberellin (GA) biosynthesis related proteins, indoleacetic acid (IAA) biosynthesis related proteins, and a few transcription factors (**Supplementary Table S10**). The other 13 downregulated proteins incorporated pentapeptide, ethylene biosynthesis-related protein, and ubiquitin conjugate factors, among others (**Supplementary Table S10**). Additionally, AL12-regulated proteins involved in defense/stress response, amino acid and lipid metabolism, transcription and translation, cell growth, and other function were differentially regulated (**Supplementary Table S10**).

DISCUSSION

The pharmaceutical value of medicinal plants relies on the accumulation of active pharmaceutical ingredient, and guaranteeing the yield and quality of these herbs is the main challenge (Yang et al., 2012). Endophytes have been proven to exert multiple effects on their host plants, including plant growth promotion, secondary metabolite biosynthesis promotion, stress resistance enhancement (Ludwig-Müller, 2015; Yang et al., 2016; Dastogeer et al., 2018). The advantages provided by the endophyte fungus AL12 on the host plant *A. lancea* were an improved plant biomass and increased sesquiterpenoids content (Yuan et al., 2016b). In this study, transcriptomics and proteomics were employed to analyze how endophytic fungi affect the regulation of transcription and translation in *A. lancea*. Compared to the reported endophyte associations (Doehlemann et al., 2008; Kawahara et al., 2012; Morán-Diez et al., 2012; Perazzolli et al., 2012; De Cremer et al., 2013; Zouari et al., 2014; Adolfsson et al., 2017; Chen W. et al., 2017; Dinkins et al., 2017; Hao et al., 2017; Bajaj et al., 2018), the endophyte *Gilmaniella* sp. AL12 resulted in 2.7% differential gene expression, thus demonstrating a greater impact on their host than most other endophytes (**Supplementary Table S11**). During the plant life cycle, a dynamic trade-off between growth and defense is necessary for plant resource assignment in response to multiple developmental cues and environmental stimuli (Hou et al., 2013). In contrast to the common downregulated plant-pathogen interactions and most phytohormone signaling events, *Gilmaniella* sp. AL12 upregulated genes involved in primary and secondary metabolism (**Figures 2–4**, **8**). Consistent with the improved cytokinin content of *A. lancea* after AL12 inoculation (Yuan et al., 2016b), DEGs involved in cytokinin biosynthesis and signal transduction both tended to be upregulated (**Figure 6**), which may induce cell division, accelerate chlorophyll biosynthesis, and delay leaf senescence (Cortleven and Schmülling, 2015). In addition, ethylene induced by the endophyte mediates sesquiterpenoid biosynthesis in *A. lancea* (Yuan et al., 2016a). Based on these results, we propose that colonization by the endophytic fungus *Gilmaniella* sp. AL12 will shift plant metabolism from defense to growth, allowing the host plant to utilize limited energy for carbon assimilation and, thus, to achieve an increased biomass and sesquiterpenoid content in *A. lancea*.

It is acknowledged that plant primary metabolism and secondary metabolism required large amounts of energy. One way to support the increased energy demands is to enhance the carbon assimilation efficiency (Rozpądek et al., 2015, 2019). We have previously observed that the net photosynthesis rate and contents of chlorophyll, rubisco, and soluble carbohydrate in *A. lancea* increase after AL12 inoculation (Yuan et al., 2016b). In the present study, phenomenological fluxes per cross section of the host plant was improved after AL12 inoculation (**Figure 1D**), indicating the improvement of PS II reaction center performance in *A. lancea*. As shown by the transcriptome and proteome results, endophyte inoculation would enhance NADPH production and CO_2 assimilation (**Table 1**, **Figures 3**, **8** and **Supplementary Figure S8**), thus explaining the positive effects of endophyte inoculation on plant photosynthesis. Similarly, *Dactylis glomerate* inoculated with *Epichloë typhina*, *Medicago truncatula*, and *Populus alba* inoculated with AMF all displayed a similar photosynthesis performance with improved plant light-driven energy production efficiency, Rubisco content, CO_2 assimilation and PS II photochemistry efficiency (Lingua et al., 2008; Aloui et al., 2009; Cicatelli et al., 2010, 2012; Rozpądek et al., 2015, 2019). Although *Gilmaniella* sp. AL12, *Epichloë typhina* and AMF belong to distinct fungal species, they all provide a benefit, such as improving similar photosynthesis apparatuses of their host plant. Plant photosynthesis and

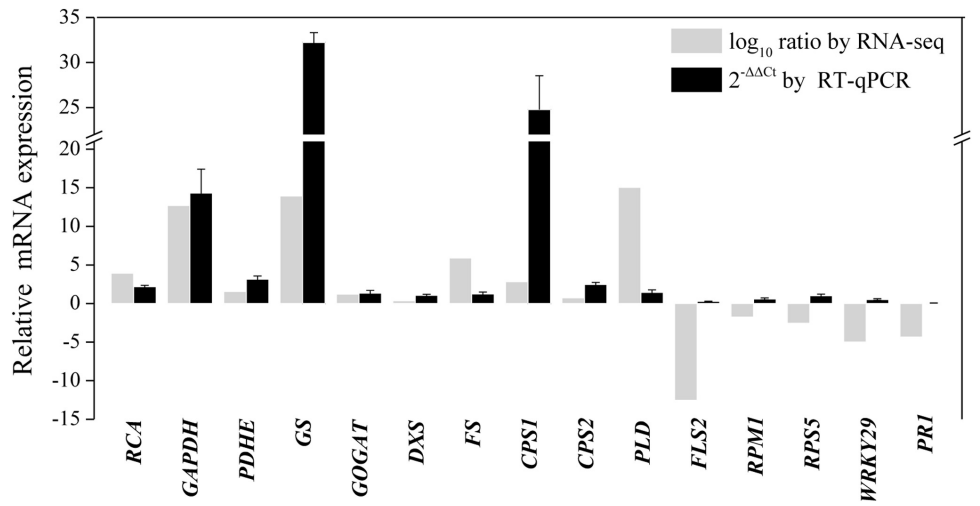

FIGURE 7 | RT-qPCR validation of differentially expressed genes involved in primary metabolism, secondary metabolism, and the defense response in shoots of *A. lancea* after the fungal endophyte *Gilmaniella* sp. AL12 inoculation. Elongation factor 1 alpha gene (*EF1a*) was used as an internal reference, and the $2^{-\Delta\Delta Ct}$ method was used to analyze the relative mRNA expression. Values are the means of three independent experiments. Bars represent standard deviations. RCA, ribulose-1,5-bisphosphate carboxylase/oxygenase activase; GAPDH, glyceraldehyde 3-phosphate dehydrogenase; PDHE, pyruvate dehydrogenase; GS, glutamine synthetase; GOGAT, glutamate synthase; DXS, 1-deoxy-d-xylulose 5-phosphate synthase; FS, β-farnesene synthase; CPS1, β-caryophyllene synthase 1; CPS2, β-caryophyllene synthase 2; PLD, Phospholipase D; FLS2, LRR receptor-like kinase FLS2; RPM1, disease resistance protein RPM1; RPS5, disease resistance protein RPS5; WRKY29, transcription factor WRKY29; PR1, pathogenesis-related protein1.

respiration processes exist with each other interdependently and share adenosine diphosphate (ADP) and $NADP^+$ or NAD^+. Additionally, O_2 produced by photosynthesis can be utilized by the respiration process, and CO_2 produced by respiration can also be assimilated by photosynthesis. As speculated based on the results of this study (**Table 1** and **Figure 3**), NADPH and O_2 production by chloroplasts, as well as NADH dehydrogenation and triphosadenine (ATP) production by mitochondria, were improved after AL12 inoculation, supporting energy storage for plant metabolism. The TCA cycle mainly converts pyruvate to malate to produce ATP, incorporating citric acid biosynthesis, oxidation and decarboxylation, and OAA regeneration (Fernie et al., 2004). *Epichloë typhina* has been shown to markably strengthen NADPH-MDH enzyme activity in its host *Dactylis glomerate* (Rozpądek et al., 2015). Likewise, the endophytic fungus *Gilmaniella* sp. AL12 upregulated genes encoding MDH and pyruvate dehydrogenase (PDHE) (**Figure 3**), thus contributing to acetyl-CoA biosynthesis and OAA regeneration (**Figure 8**). Acetyl-CoA and pyruvate biosynthesis were improved in *A. lancea* after endophyte inoculation (**Figure 8**), indicating that more precursor substances and energy were available for plant secondary metabolite biosynthesis (Nema et al., 2013). As the precursor substances of terpenoid biosynthesis (Chen F. et al., 2017), pyruvate and acetyl-CoA content increased after AL12 inoculation (Yuan et al., 2016b). Additionally, in contrast to the general downregulation of fatty acid biosynthesis (**Supplementary Table S4**), genes associated with terpenoid biosynthesis were upregulated after AL12 inoculation (**Supplementary Figure S3**), indicating that a greater amount of acetyl-CoA would be diverted into terpene biosynthesis.

Plant terpenoids are derived from isopentenyl diphosphate (IPP) and dimethylallyl diphosphate (DMAPP) synthesized through the mevalonic acid (MVA) and the 2-C-methyl-D-erythritol-4-phosphate (MEP) pathway (Vattekkatte et al., 2018). The different molecular rates of isopentenyl diphosphate and dimethylallyl diphosphate condensation lead to geranyl diphosphate (GPP) for monoterpene, farnesyl diphosphate (FPP) for sesquiterpene and geranylgeranyl diphosphate (GGPP) for triterpene biosynthesis (Dudareva et al., 2013; Vattekkatte et al., 2018). Consistent with the increased sesquiterpenoids content in *A. lance*a shoots (**Figure 1A**), DEGs associated with terpenoid backbone biosynthesis and sesquiterpene biosynthesis were increased (**Supplementary Figure S3**). Unfortunately, we did not detect any spot identified associated with terpene backbone biosynthesis or sesquiterpenoids biosynthesis in proteome (**Table 1**). Considering that there is no database of *A. lancea* or related genus in NCBI, we identified proteins using NCBI green plant database. Thus, we considered that maybe some proteins related to secondary metabolism may not identified exactly. Yet despite that, comparative transcriptomics showed that genes related to terpene backbone biosynthesis and sesquiterpenoids biosynthesis tended to be upregulated in shoots of *A. lancea* after the endophyte inoculation (**Supplementary Figure S3**). In this study, high-quality reads were assembled *de novo* by using the Trinity program. The results showed that genes annotated as β-farnesene synthase and β-caryophyllene synthase were upregulated after AL12 inoculation, as shown by the transcriptome (**Supplementary Figure S4**) and RT-qPCR results (**Figure 7**). It is known that one terpene synthase can catalyze formation more than one terpene (Dudareva et al., 2013). For example, TPS21 and TPS11 from *Arabidopsis*

TABLE 1 | Identification of differentially expressed proteins related to energy, carbohydrate, and secondary metabolism in shoots of *A. lancea* after endophyte inoculation.

Spot	Accession no.	Protein name	MS	SC	Mr (KDa)/pI	FC
Energy metabolism						
11	AIN35032.1	AtpB (chloroplast) [*Atractylodes lancea*]	124	0.62	53.475/5.07	1.57
12	AIN35032.1	AtpB (chloroplast) [*Atractylodes lancea*]	122	0.62	53.475/5.07	1.00
13	XP_020108762.1	acetylornithine aminotransferase, chloroplastic/mitochondrial-like [Ananas comosus]	66	0.36	50.817/6.61	2.34
14	AFV93500.1	chloroplast ribulose bisphosphate carboxylase/oxygenase activase beta2, partial [Gossypium barbadense]	68	0.53	27.983/5.48	1.60
18	P28426.1	RecName: Full = Ribulose bisphosphate carboxylase large chain; Short = RuBisCO large subunit	85	0.46	51.982/6.10	2.25
19	AKG48845.1	ribulose-1,5-bisphosphate carboxylase/oxygenase large subunit, partial (chloroplast) [Desmodium triflorum]	81	0.36	49.071/6.08	4.50
20	AHW52074.1	ribulose-1,5-bisphosphate carboxylase/oxygenase large subunit, partial (chloroplast) [Cuscuta glomerata]	93	0.49	39.449/8.12	2.74
42	CAA46941.1	ferredoxin-nitrite reductase, partial [Nicotiana tabacum]	72	0.66	39.410/6.22	2.50
51	KQL23007.1	hypothetical protein SETIT_029918mg [Setaria italica](maturation RBCL)	75	0.55	49.921/7.56	2.20
59	AEO21912.1	chloroplast oxygen-evolving enhancer protein 1 [Dimocarpus longan]	77	0.51	35.386/5.85	2.08
63	XP_021983238.1	oxygen-evolving enhancer protein 1, chloroplastic [Helianthus annuus]	92	0.51	34.483/5.40	1.22
70	CAX65710.1	phosphoenolpyruvate carboxylase, partial [Stipagrostis plumosa]	61	0.57	57.090/6.62	1.31
73	CAX65709.1	phosphoenolpyruvate carboxylase, partial [Stipagrostis plumosa]	63	0.51	56.953/6.62	2.20
85	XP_017235881.1	PREDICTED: 4-hydroxy-3-methylbut-2-en-1-yl diphosphate synthase (ferredoxin), chloroplastic [Daucus carota subsp. sativus]	63	0.34	82.658/5.88	2.29
86	XP_019702089.1	PREDICTED: ATP-dependent Clp protease ATP-binding subunit CLPT1, chloroplastic-like [Elaeis guineensis]	69	0.58	26,047/9.52	1.88
87	XP_010066998.2	PREDICTED: ATP-dependent Clp protease proteolytic subunit 2, mitochondrial [Eucalyptus grandis]	64	0.48	27.713/8.48	2.16
21	AKG49084.1	ribulose-1,5-bisphosphate carboxylase/oxygenase large subunit, partial (chloroplast) [Mikania scandens]	85	0.55	48.515/5.90	0.13
22	AAV65407.1	ribulose-1,5-bisphosphate carboxylase/oxygenase large subunit, partial (chloroplast) [Baccaurea javanica]	69	0.32	52.288/6.20	0.41
25	BAJ16757.1	ribulose-1,5-bisphosphate carboxylase/oxygenase large subunit, partial (chloroplast) [Porana sp. SH-2010]	88	0.51	47.096/6.69	0.26
27	AAY16675.1	ribulose-1,5-bisphosphate carboxylase/oxygenase large subunit, partial (chloroplast) [Sclerocroton cornutus]	79	0.46	52.129/6.23	0.30
28	CAA60835.1	ribulose-1,5-bisphosphate carboxylase, partial (chloroplast) [Coopernookia strophiolata]	67	0.39	52.117/6.09	0.27
79	ASP44102.1	ribosomal protein subunit 4, partial (chloroplast) [Pohlia leucostoma]	90	0.58	22.957/10.33	0.20
92	XP_013456760.1	rubisco large subunit N-methyltransferase [Medicago truncatula]	74	0.35	39.912/9.23	0.38
94	EMT15451.1	Protochlorophyllide reductase A, chloroplastic [Aegilops tauschii]	59	0.37	36.226/9.57	0.26
Carbohydrate metabolism						
15	O04016.1	RecName: Full = Pyrroline-5-carboxylate reductase; Short = P5C reductase; Short = P5CR	68	0.42	28.986/9.04	2.74
44	AFD54987.1	beta-galactosidase [Momordica charantia]	59	0.31	81.056/8.34	1.55
52	BAJ10716.1	glyceraldehyde-3-phosphate dehydrogenase [Cladopus doianus]	72	0.41	23.904/6.12	2.69
58	EMS64835.1	putative alpha,alpha-trehalose-phosphate synthase [UDP-forming] 7 [Triticum urartu]	70	0.35	90.131/5.53	2.94
83	AIF74649.1	NAD-dependent glyceraldehyde-3-phosphate dehydrogenase short paralog, partial [Cystopteris bulbifera]	69	0.57	24.075/8.97	1.88
32	XP_020208539.1	carbon catabolite repressor protein 4 homolog 3-like [Cajanus cajan]	62	0.39	20.682/9.49	0.32
49	AAK97663.1	At1g66700/F4N21_16 [Arabidopsis thaliana] (SAM dependent carboxyl methyltransferase)	78	0.56	36.507/6.61	0.34
104	XP_013688170.1	PREDICTED: pectinesterase/pectinesterase inhibitor-like [Brassica napus]	51	0.47	10.386/6.45	0.63
125	XP_002445591.1	pectinesterase isoform X2 [Sorghum bicolor]	58	0.18	68.257/8.98	0.32
Secondary metabolism						
34	XP_016571991.1	PREDICTED: tropinone reductase-like 3 isoform X2 [Capsicum annuum]	69	0.41	23.370/8.81	4.99
56	BAF26158.2	Os10g0177300 [Oryza sativa Japonica Group] (Type III polyketide synthase family protein)	77	0.42	44.280/6.08	2.09
84	XP_013752435.1	PREDICTED: caffeic acid 3-O-methyltransferase-like [Brassica napus]	63	0.35	43.001/5.30	2.70
103	AOE22893.1	cytochrome P450 CYP76F12 [Vitis vinifera]	62	0.24	57.215/6.55	2.60

The spot number corresponds to the number shown in ***Supplementary Figure S6****. MS, mascot score; SC, sequences coverage; MW, molecular weight; pI, isoelectric points; FC, fold change.*

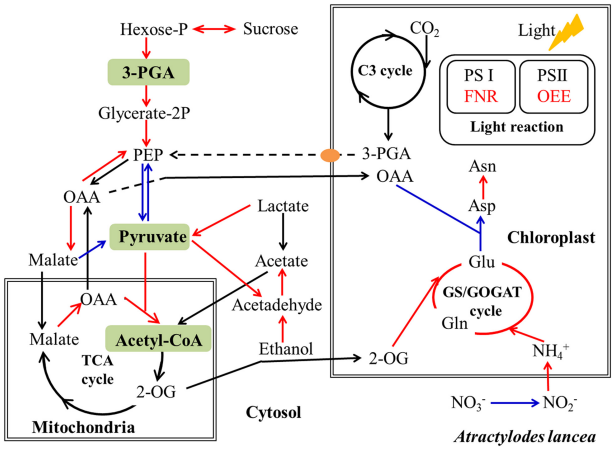

FIGURE 8 | Simplified schematic summary of metabolic changes in shoots of *A. lancea* after the fungal endophyte *Gilmaniella* sp. AL12 inoculation. DEGs with significant differences in endophyte inoculated plants are shown as colored arrows (upregulated DEGs in red and downregulated DEGs in blue). The yellow ellipse indicates the phosphate translocator (TPT). Letters in green blocks represent precursor substances of terpenoid biosynthesis. C3 cycle, Benson-Calvin cycle; GS/GOGAT, glutamine synthetase (GS)/glutamate synthase (GOGAT); TCA cycle, tricarboxylic acid cycle; PS I, photosystem I; PS II, photosystem II; 3-PGA, glycerate-3-phosphate; OAA, oxaloacetate; 2-OG, 2-oxoglutarate; FNR, ferredoxin-NADP reductase; OEE, photosystem II oxygen-evolving enhancer protein.

thaliana are responsible for the biosynthesis of more than 20 sesquiterpenoids in flower fragrance (Tholl et al., 2005). Additionally, OkBCS of *Ocimum* can catalyze the production of β-caryophyllene and α-humulene (Jayaramaiah et al., 2016). The main sesquiterpenoids of *A. lancea* incorporate β-caryophyllene, zingiberene, β-sesquiphellandrene, caryophyllene oxide, hinesol, β-eudesmol and atractylone (Yuan et al., 2016b). Considering the multifunction of sesquiterpene synthase, we propose that β-farnesene synthase and β-caryophyllene synthase are crucial terpene synthases induced by AL12 to supply higher sesquiterpenoid contents in *A. lancea*. Further experiments will include the functional characterization of these sesquiterpene synthases, and how the fungal endophyte regulate genes coding for these sesquiterpene synthases.

The accumulation of secondary metabolites is regulated by cross-talking signaling cascades. Our previous studies have demonstrated that the endophyte AL12 activates multiple signals to induce plant sesquiterpenoids accumulation (Wang et al., 2011; Ren and Dai, 2012, 2013; Yuan et al., 2016a). In addition, mannan-binding lectin has been proposed to recognize mannan of *Gilmaniella* sp. AL12, thus causing signal transduction (Chen et al., 2016). It is worth noting that 32 DEGs encoding PLD tended to be upregulated after AL12 inoculation in the present study (**Supplementary Table S8**). PLD can hydrolyse phospholipids into phospholipid acid, which acts as an important molecular signal mediating heat stress-induced triterpene ganoderic acid biosynthesis in *Ganoderma lucidum* (Liu et al., 2017). These results indicate that phospholipid acid may be an essential signaling molecule in *A. lancea* after AL12 inoculation. Additionally, metabolomics and transcriptomics are required to study whether PLD or phospholipid signaling in *A. lancea* are activated and whether they mediate sesquiterpenoid biosynthesis after AL12 inoculation, which will help to understand their roles in inducing the biosynthesis of the secondary metabolites.

In contrast to the enhanced primary and secondary metabolism most genes involved in the plant-pathogen interaction were downregulated (**Figures 2**, **5**). Plants evolve pattern recognition receptors (PRRs) to recognize evolutionarily conservative PAMPs, triggering the host MAPK cascade (**Figure 5**). Then, MAPK activates plant hormone signal transduction to integrate diverse aspects of PTI (Cui et al., 2015; Pandey et al., 2016). These optional signaling events will give rise to various immune responses (Akira and Hemmi, 2003). Furthermore, effectors produced by the fungus are also known to inhibit MAPK cascade signaling or block plant-resistant protein expression, thus suppressing plant basic immune response PTI (Zhang et al., 2012; Meng and Zhang, 2013). Fungi deploy these co-evolved effectors to modify host plant cell processes or to establish biotrophic or other types of symbiotic relationship with the host (Le Fevre et al., 2015). In turn, fungal effectors can be recognized by plant disease resistance proteins (R proteins) and thus trigger plant ETI, which usually causes the plant hypersensitive response (HR) (Jones and Dangl, 2006; Liu et al., 2007). With endophytic fungal AL12 inoculation, genes annotated as plant PRRs, including LRR receptor-like kinase FLS2, BAK1 and EFR, tended to be downregulated (**Figure 5**), indicating a weakened PAMP recognition ability of the host plant. Furthermore, genes involved in the response of PAMPs or effectors were also repressed (**Figure 5**), suggesting that endophyte inoculation suppressed host immune reactions. As shown in our previous study (Yang and Dai, 2013), AL12 could successfully colonize the leaves of *A. lancea*, resulting in an altered hyphal morphology such as smooth and unbranched hyphae. In addition, slightly pointed hyphal tips of the endophyte also appears similar as the ends of a nematode (Yang and Dai, 2013). Considering that genes related to PTI and ETI of *A. lancea* were downregulated after AL12 inoculation (**Figure 5**) and that the hyphae of the endophyte were altered morphologically (Yang and Dai, 2013), we deduced that either masked fungal PAMPs were not detected by the host plant, or that the plant defense response was suppressed by the host or the endophyte (Dupont et al., 2015), potentially contributing to the compatible association of *Gilmaniella* sp. AL12 with *A. lancea*.

Given the apparent downregulation of genes involved in the plant-pathogen interaction, endophyte inoculation would enhance the pathogen susceptibility of the host plant. However, this is not the actual fact. Although plant defense-related genes of *Perennial ryegrass* were down-regulated after *Epichloë festucae* var. *lolii* infection, its resistance to fungal pathogens was enhanced due to the production of phenolic compounds (Tian et al., 2008; Pańka et al., 2013; Dupont et al., 2015). Similarly, *Gilmaniella* sp. AL12 upregulated genes involved in the biosynthesis of phenylpropanoids and terpenes (**Figure 4**). Terpenoids are frequently used as phytoalexins, the accumulation of which are enhanced by biotic or abiotic stress (Schmelz et al., 2014; Vaughan et al., 2015). The sesquiterpenoid

phytoalexins such as gossypol, hemigossypolone and heliocides can provide defense mechanisms against pathogens and herbivores of cotton (Yang C. Q. et al., 2013). Additionally, β-caryophyllene can defend against *Helicoverpa armigera* and *Pseudomonas syringae* pv. *tomato* DC3000 (Huang et al., 2012; Singh et al., 2014). Similarly, the monoterpene S-limonene and triterpene momilactones or oryzalexins function as defensive metabolites against *Magnaporthe oryzae* or *Magnaporthe grisea* (Toyomasu et al., 2008; Chen et al., 2018). Therefore, although defense-related genes of *A. lancea* were downregulated after *Gilmaniella* sp. AL12 inoculation, the enhanced synthesis of phenylpropanoids and terpenoids may function as defensive strategy against other microbial pathogens or herbivores, functioning as a possible competitive exclusion tactic of the endophyte.

In this study, shoots of *A. lancea* were sterile, and were appropriate for investigating the effect of the fungal endophyte on plantlets without the distraction of other biotic or abiotic factors, thus helping to understand plant-endophyte interactions. The above results showed that the fungal endophyte *Gilmaniella* sp. AL12 weakened the plant immune response, which might contribute to its successful and stable colonization of the host plant (**Figure 9**). The decreased plant immunity resulted in large amounts of energy for plant primary or secondary metabolism. Moreover, the fungal endophyte improved photosynthesis, carbon fixation, carbohydrate transformation, and the conversion from pyruvate to acetyl-CoA in the host plant, indicating that the endophyte promoted the accumulation of precursors for terpenoid biosynthesis. In addition, the fungal endophyte specifically induced sesquiterpenoid biosynthesis by regulating genes involved in sesquiterpenoid biosynthesis and related signaling events in *A. lancea*. Thus, we propose that the fungal endophyte-plant association increased production (biomass and sesquiterpenoid content) by increasing the source (photosynthesis), expanding the sink (glycolysis and the TCA cycle), and enhancing metabolic flux (sesquiterpenoids biosynthesis-related genes) in *A. lancea* (**Figure 9**). Consistent with the "double promotion" in this study, the endophytic fungi AL12 promotes plant growth and sesquiterpenoid accumulation within two years of growth in field experiments. Further studies will be conducted to investigate whether pre-inoculation with the fungal endophyte *Gilmaniella* sp. AL12 regulate metabolism and immunity of *A. lancea* in the field experiments, which will help to understand plant-endophyte interactions, and will contribute to the application of the fungal endophyte in cultivating of *A. lancea*.

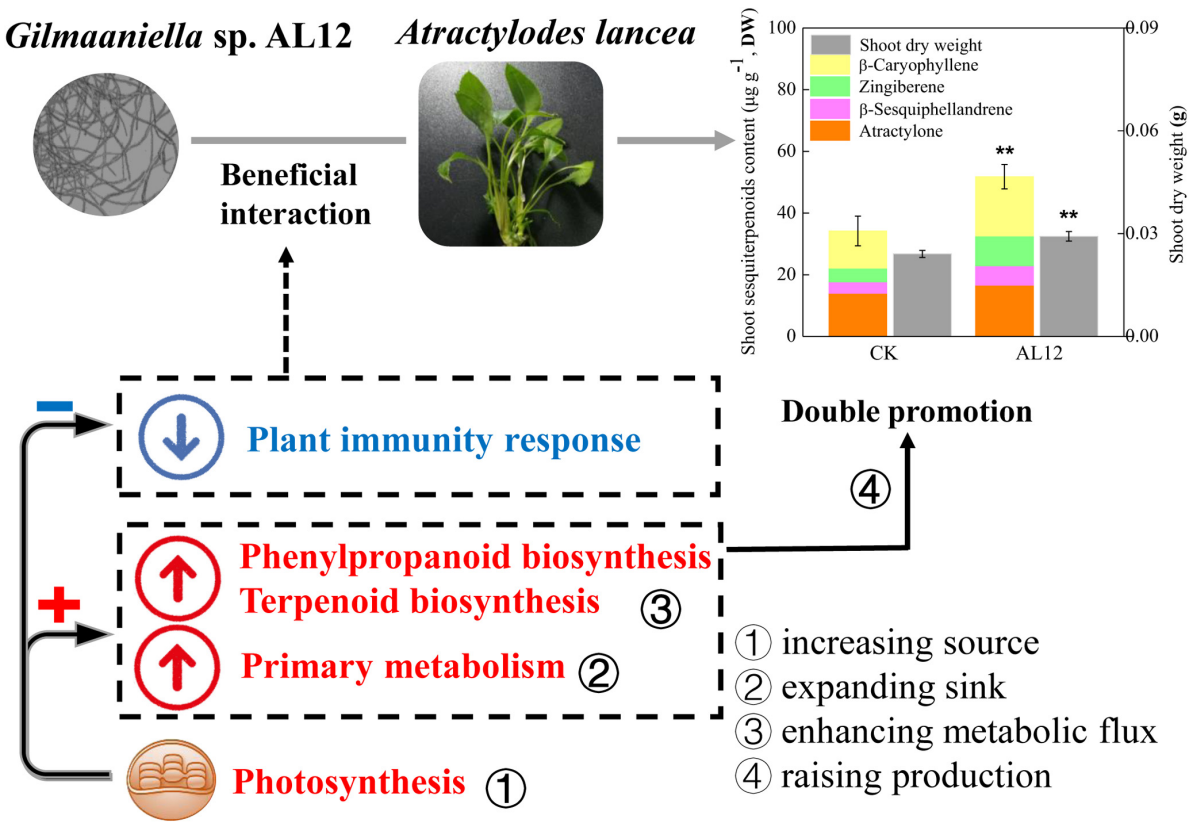

FIGURE 9 | Simplified schematic summary of the "double-promotion" effect on *A. lancea* bring by the fungal endophyte *Gilmaniella* sp. AL12. The fungal endophyte *Gilmaniella* sp. AL12 weakened the plant immune response of *A. lancea*, thus may contributing to plant-endophyte beneficial interaction. Additionally, endophyte-plant association increased production (biomass and sesquiterpenoid content) by increasing the source (photosynthesis), expanding the sink (glycolysis and the TCA cycle), and enhancing metabolic flux (sesquiterpenoids biosynthesis-related genes) in *A. lancea*.

Medicinal plants are rich in active compounds such as artemisinin (Sharma and Agrawal, 2013) and ginseng saponin (Wei et al., 2018), which are important sources of modern drugs. You-You Tu, the mother of artemisinin, was awarded Nobel Prize in medicine in 2015. The development of the medicinal plants gradually becomes a focused issue, and medicinal plants-endophytes interactions have received much attentions. A review of the medicinal plant microbiome has shown that the secondary metabolite content of medicinal herbs depends on where they are cultivated, which can be partly ascribed to different rhizospheric or endophytic microbes associated with their cultivation location (Köberl et al., 2013; Huang et al., 2018). Plantlets of *A. lancea* grown in the Maoshan area of southeast China represent the geo–authentic medicinal plant, with a much greater sesquiterpenoid content and diversity than *A. lancea* in other cultivation area (Zhou et al., 2018). The endophytic fungus *Gilmaniella* sp. AL12 was isolated from the stem of the geo–authentic *A. lancea*, and the compatible association contributes some benefits to the host plant, including the promotion of plant growth and sesquiterpenoid content, and the prevention of root rot (Wang et al., 2011; Ren and Dai, 2012, 2013; Wang et al., 2012; Yuan et al., 2016a,b; Ren et al., 2017). Whether *Gilmaniella* sp. AL12 is a key member of the core microbiome of geo–authentic *A. lancea* remain unanswered. In this regard, our previous studies have shown that prioritizing endophytic *Gilmaniella* sp. AL12 inoculation enhances the diversity and size of phyllospheric microbial communities of *A. lancea* by increasing the soluble sugar content in the rhizosphere (Yang T. et al., 2013). Given that the endophyte provided physiological and biochemical benefits to the host and affected host phyllospheric microbial communities, we more broadly propose a beneficial association of endophytic *Gilmaniella* sp. AL12 with *A. lancea* as a potential model for endophytic fungi-medicinal herb interaction. The endophyte-*A. lancea* association contributes to medicinal herb cultivation and helps to further clarify plant-endophyte interactions.

CONCLUSION

In summary, this study showed that the fungal endophyte *Gilmaniella* sp. AL12 weakened the plant immune response of *A. lancea*, thus may contributing to the beneficial plant-endophyte interaction. Additionally, endophyte-plant association increased production (biomass and sesquiterpenoid content) by increasing the source (photosynthesis), expanding the sink (glycolysis and the TCA cycle), and enhancing metabolic flux (sesquiterpenoids biosynthesis-related genes) in *A. lancea*. This study revealed the regulation of *Gilmaniella* sp. AL12 on plant metabolism and related regulatory processes in shoots of *A. lancea* at the transcriptional and translational level. This study provides a theoretical basis for medicinal herb cultivation and helps to further clarify plant-endophyte interactions.

DATA AVAILABILITY

The raw data supporting the conclusions of this manuscript will be made available by the authors, without undue reservation, to any qualified researcher.

AUTHOR CONTRIBUTIONS

C-CD and JY designed the experiments, analyzed the data, and wrote the manuscript. P-XC and M-JT helped extract plant RNA and protein. WZ, KS, and XL helped supervise the manuscript writing. All the authors read and approved the final manuscript.

FUNDING

This work was supported by the National Key Research and Development Program of China (Grant No. 2017YFD0800705).

SUPPLEMENTARY MATERIAL

The Supplementary Material for this article can be found online at: https://www.frontiersin.org/articles/10.3389/fmicb.2019.01208/full#supplementary-material

REFERENCES

Adolfsson, L., Nziengui, H., Abreu, I. N., Šimura, J., Beebo, A., Herdean, A., et al. (2017). Enhanced secondary- and hormone metabolism in leaves of arbuscular mycorrhizal *Medicago truncatula*. *Plant Physiol.* 175, 392–411. doi: 10.1104/pp.16.01509

Akira, S., and Hemmi, H. (2003). Recognition of pathogen-associated molecular patterns by TLR family. *Immunol. Lett.* 85, 85–95. doi: 10.1016/S0165-2478(02)00228-6

Aloui, A., Recorbet, G., Gollotte, A., Robert, F., Valot, B., Gianinazzi-Pearson, V., et al. (2009). On the mechanisms of cadmium stress alleviation in *Medicago truncatula* by arbuscular mycorrhizal symbiosis: a root proteomic study. *Proteomics* 9, 420–433. doi: 10.1002/pmic.200800336

Bajaj, R., Huang, Y., Gebrechristos, S., Mikolajczyk, B., Brown, H., Prasad, R., et al. (2018). Transcriptional responses of soybean roots to colonization with the root endophytic fungus *Piriformospora indica* reveals altered phenylpropanoid and secondary metabolism. *Sci. Rep.* 8:10227. doi: 10.1038/s41598-018-26809-3

Chen, F., Ren, C. G., Zhou, T., Wei, Y. J., and Dai, C. C. (2016). A novel exopolysaccharide elicitor from endophytic fungus *Gilmaniella* sp. AL12 on volatile oils accumulation in *Atractylodes lancea*. *Sci. Rep.* 6:34735. doi: 10.1038/srep34735

Chen, F., Wei, Y. X., Zhang, J. M., Sang, X. M., and Dai, C. C. (2017). Transcriptomics analysis investigates sesquiterpenoids accumulation pattern in different tissues of *Atractylodes lancea* (Thunb.) DC. plantlet. *Plant Cell Tiss. Org.* 130, 73–90. doi: 10.1007/s11240-017-1205-8

Chen, W., Li, J., Zhu, H., Xu, P., Chen, J., and Yao, Q. (2017). Arbuscular mycorrhizal fungus enhances lateral root formation in *Poncirus trifoliata* (L.) as revealed by RNA-seq analysis. *Front. Plant Sci.* 8:2039. doi: 10.3389/fpls.2017.02039

Chen, X., Chen, H., Yuan, J. S., Köllner, T. G., Chen, Y., Guo, Y., et al. (2018). The rice terpene synthase gene OsTPS19 functions as an (S)-limonene synthase in planta, and its overexpression leads to enhanced resistance to the blast fungus *Magnaporthe oryzae*. *Plant Biotechnol. J.* 16, 1778–1787. doi: 10.1111/pbi.12914

Chen, J. X., Dai, C. C., Li, X., Tian, L. S., and Xie, H. (2008). Endophytic fungi screening from *Atractylodes lancea* and inoculating into the host plantlet. *Guihaia* 28, 256–260.

Cicatelli, A., Lingua, G., Todeschini, V., Biondi, S., Torrigiani, P., and Castiglione, S. (2010). Arbuscular mycorrhizal fungi restore normal growth in a white poplar clone grown on heavy metal-contaminated soil, and this is associated with upregulation of foliar metallothionein and polyamine biosynthetic gene expression. *Ann. Bot.* 106, 791–802. doi: 10.1093/aob/mcq170

Cicatelli, A., Lingua, G., Todeschini, V., Biondi, S., Torrigiani, P., and Castiglione, S. (2012). Arbuscular mycorrhizal fungi modulate the leaf transcriptome of a *Populus alba* L. clone grown on a zinc and copper-contaminated soil. *Environ. Exp. Bot.* 75, 25–35. doi: 10.1016/j.envexpbot.2011.08.012

Cortleven, A., and Schmülling, T. (2015). Regulation of chloroplast development and function by cytokinin. *J. Exp. Bot.* 66, 4999–5013. doi: 10.1093/jxb/erv132

Cui, H. T., Tsuda, K., and Parker, J. E. (2015). Effector-triggered immunity: from pathogen perception to robust defense. *Annu. Rev. Plant Biol.* 66, 487–511. doi: 10.1146/annurev-arplant-050213-040012

Dastogeer, K. M. G., Li, H., Sivasithamparam, K., Jones, M. G. K., and Wylie, S. J. (2018). Fungal endophytes and a virus confer drought tolerance to *Nicotiana benthamiana* plants through modulating osmolytes, antioxidant enzymes and expression of host drought responsive genes. *Env. Exp. Bot.* 149, 95–108. doi: 10.1016/j.envexpbot.2018.02.009

De Cremer, K., Mathys, J., Vos, C., Froenicke, L., Michelmore, R. W., Cammue, B. P., et al. (2013). RNAseq-based transcriptome analysis of *Lactuca sativa* infected by the fungal necrotroph *Botrytis cinereal*. *Plant Cell Environ.* 36, 1992–2007. doi: 10.1111/pce.12106

Dinkins, R. D., Nagabhyru, P., Graham, M. A., Boykin, D., and Schardl, C. L. (2017). Transcriptome response of *Lolium arundinaceum* to its fungal endophyte *Epichloë coenophiala*. *New Phytol.* 213, 324–337. doi: 10.1111/nph.14103

Doehlemann, G., Wahl, R., Horst, R. J., Voll, L. M., Usadel, B., Poree, F., et al. (2008). Reprogramming a maize plant: transcriptional and metabolic changes induced by the fungal biotroph *Ustilago maydis*. *Plant J.* 2008, 181–195. doi: 10.1111/j.1365-313X.2008.03590.x

Dudareva, N., Klempien, A., Muhlemann, J. K., and Kaplan, I. (2013). Biosynthesis, function and metabolic engineering of plant volatile organic compounds. *New Phytol.* 198, 16–32. doi: 10.1111/nph.12145

Dudareva, N., Negre, F., Nagegowda, D. A., and Orlova, I. (2006). Plant volatiles: recent advances and future perspectives. *Crit. Rev. Plant Sci.* 25, 417–440. doi: 10.1080/07352680600899973

Dupont, P. Y., Eaton, C. J., Wargent, J. J., Fechtner, S., Solomon, P., Schmid, J., et al. (2015). Fungal endophyte infection of ryegrass reprograms host metabolism and alters development. *New Phytol.* 208, 1227–1240. doi: 10.1111/nph.13614

Fernie, A. R., Carrari, F., and Sweetlove, L. J. (2004). Respiratory metabolism: glycolysis, the TCA cycle and mitochondrial electron transport. *Curr. Opin. Plant Biol.* 7, 254–261. doi: 10.1016/j.pbi.2004.03.007

Hao, K., Wang, F., Nong, X., McNeill, M. R., Liu, S., Wang, G., et al. (2017). Response of peanut *Arachis hypogaea* roots to the presence of beneficial and pathogenic fungi by transcriptome analysis. *Sci. Rep.* 7:964. doi: 10.1038/s41598-017-01029-3

Hou, X. L., Ding, L. H., and Yu, H. (2013). Crosstalk between GA and JA signaling mediates plant growth and defense. *Plant Cell Rep.* 32, 1067–1074. doi: 10.1007/s00299-013-1423-4

Huang, M., Sanchez-Moreiras, A. M., Abel, C., Sohrabi, R., Lee, S., Gershenzon, J., et al. (2012). The major volatile organic compound emitted from *Arabidopsis thaliana* flowers, the sesquiterpene (E)-beta-caryophyllene, is a defense against a bacterial pathogen. *New Phytol.* 193, 997–1008. doi: 10.1111/j.1469-8137.2011.04001.x

Huang, W., Long, C., and Lam, E. (2018). Roles of plant-associated microbiota in traditional herbal medicine. *Trends Plant Sci.* 23, 559–562. doi: 10.1016/j.tplants.2018.05.003

Jayaramaiah, R. H., Anand, A., Beedkar, S. D., Dholakia, B. B., Punekar, S. A., Kalunke, R. M., et al. (2016). Functional characterization and transient expression manipulation of a new sesquiterpene synthase involved in beta-caryophyllene accumulation in *Ocimum*. *Biochem Bioph Res. Co.* 473, 265–271. doi: 10.1016/j.bbrc.2016.03.090

Jones, J. D., and Dangl, J. L. (2006). The plant immune system. *Nature* 444, 323–329. doi: 10.1038/nature05286

Kawahara, Y., Oono, Y., Kanamori, H., Matsumoto, T., Itoh, T., and Minami, E. (2012). Simultaneous RNA-seq analysis of a mixed transcriptome of rice and blast fungus interaction. *PLoS One* 7:e49423. doi: 10.1371/journal.pone.0049423

Köberl, M., Schmidt, R., Ramadan, E. M., Bauer, R., and Berg, G. (2013). The microbiome of medicinal plants: diversity and importance for plant growth, quality and health. *Front. Microbiol.* 4:400. doi: 10.3389/fmicb.2013.00400

Koonrungsesomboon, N., Na-Bangchang, K., and Karbwang, J. (2014). Therapeutic potential and pharmacological activities of *Atractylodes lancea* (Thunb.) DC. *Asian Pac. J. Trop. Med.* 7, 421–428. doi: 10.1016/S1995-7645(14)60069-9

Le Fevre, R., Evangelisti, E., Rey, T., and Schornack, S. (2015). Modulation of host cell biology by plant pathogenic microbes. *Annu. Rev. Cell Dev. Biol.* 31, 201–229. doi: 10.1146/annurev-cellbio-102314-112502

Li, P. M., Gao, H. Y., and Reto, J. S. (2005). Application of the fast chlorophyll fluorescence induction dynamics analysis in photosynthesis study. *J. Plant Physiol. Mol. Biol.* 31, 559–566. doi: 10.3321/j.issn:1671-3877.2005.06.001

Lingua, G., Franchin, C., Todeschini, V., Castiglione, S., Biondi, S., Burlando, B., et al. (2008). Arbuscular mycorrhizal fungi differentially affect the response to high zinc concentrations of two registered poplar clones. *Environ. Pollut.* 153, 137–147. doi: 10.1016/j.envpol.2007.07.012

Liu, G., Liu, J., Zhang, C., You, X., Zhao, T., Jiang, J., et al. (2018). Physiological and RNA-seq analyses provide insights into the response mechanism of the Cf-10-mediated resistance to *Cladosporium fulvum* infection in tomato. *Plant Mol. Biol.* 96, 403–416. doi: 10.1007/s11103-018-0706-0

Liu, Y., Ren, D., Pike, S., Pallardy, S., Gassmann, W., and Zhang, S. (2007). Chloroplast-generated reactive oxygen species are involved in hypersensitive response-like cell death mediated by a mitogen-activated protein kinase cascade. *Plant J.* 51, 941–954. doi: 10.1111/j.1365-313X.2007.03191.x

Liu, Y. N., Lu, X. X., Chen, D., Lu, Y. P., Ren, A., Shi, L., et al. (2017). Phospholipase D and phosphatidic acid mediate heat stress induced secondary metabolism in *Ganoderma lucidum*. *Environ. Microbiol.* 19, 4657–4669. doi: 10.1111/1462-2920.13928

Ludwig-Müller, J. (2015). Plants and endophytes: equal partners in secondary metabolite production? *Biotech Lett.* 37, 1325–1334. doi: 10.1007/s10529-015-1814-s1814

Lv, Z. Y., Zhang, L., and Tang, K. X. (2017). New insights into artemisinin regulation. *Plant Signal Behav.* 12:10. doi: 10.1080/15592324.2017.1366398

Mandal, S., Evelin, H., Girl, B., Singh, V. P., and Kapoor, R. (2013). Arbuscular mycorrhiza enhances the production of stevioside and rebaudioside-A in *Stevia rebaudiana* via nutritional and non-nutritional mechanisms. *Appl. Soil Ecol.* 72, 187–194. doi: 10.1016/j.apsoil.2013.07.003

Meng, X. Z., and Zhang, S. Q. (2013). MAPK Cascades in plant disease resistance signaling. *Annu. Rev. Phytopathol.* 51, 245–266. doi: 10.1146/annurev-phyto-082712-102314

Ming, Q., Su, C., Zheng, C., Jia, M., Zhang, Q., Zhang, H., et al. (2013). Elicitors from the endophytic fungus *Trichoderma atroviride* promote *Salvia miltiorrhiza* hairy root growth and tanshinone biosynthesis. *J. Exp. Bot.* 64, 5687–5694. doi: 10.1093/jxb/ert342

Morán-Diez, E., Rubio, B., Domínguez, S., Hermosa, R., Monte, E., and Nicolás, C. (2012). Transcriptomic response of *Arabidopsis thaliana* after 24 h incubation with the biocontrol fungus *Trichoderma harzianum*. *J. Plant Physiol.* 169, 614–620. doi: 10.1016/j.jplph.2011.12.016

Na-Bangchang, K., Plengsuriyakarn, T., and Karbwang, J. (2017). Research and Development of *Atractylodes lancea* (Thunb) DC. as a Promising Candidate for *Cholangiocarcinoma* chemotherapeutics. *Evid-based Compl. Alt.* 2017:5929234. doi: 10.1155/2017/5929234

Nema, R., Khare, S., Jain, P., Pradhan, A., Gupta, A., and Singh, D. (2013). Natural Products Potential and Scope for Modern Cancer Research. *Am. J. Plant Sci.* 4, 1270–1277. doi: 10.4236/ajps.2013.46157

Oh, H. J., Park, J. E., Park, Y. G., and Jeong, B. R. (2014). Growth and quality of plug seedlings of three indigenous medicinal plants as affected by ionic strength of the nutrient solution. *Hort. Environ. Biotechnol.* 55, 63–69. doi: 10.1007/s13580-014-0074-x

Pandey, D., Rajendran, S. R. C. K., Gaur, M., Sajeesh, P. K., and Kumar, A. (2016). Plant defense signaling and responses against necrotrophic fungal pathogens. *J. Plant Growth Reg.* 35, 1159–1174. doi: 10.1007/s00344-016-9600-7

Pańka, D., Piesik, D., Jeske, M., and Baturo-Cieśniewska, A. (2013). Production of phenolics and the emission of volatile organic compounds by perennial ryegrass (*Lolium perenne* L.)/Neotyphodium lolii association as a response to infection by Fusarium poae. *J. Plant Physiol.* 170, 1010–1019. doi: 10.1016/j.jplph.2013.02.009

Perazzolli, M., Moretto, M., Fontana, P., Ferrarini, A., Velasco, R., Moser, C., et al. (2012). Downy mildew resistance induced by *Trichoderma harzianum* T39 in susceptible grapevines partially mimics transcriptional changes of resistant genotypes. *BMC Genomics* 13:660. doi: 10.1186/1471-2164-13-660

Ren, C. G., Chen, F., and Dai, C. C. (2017). Fungal endophyte protects *Atractylodes lancea* from root rot caused by *Fusarium oxysporum*. *Plant Pathol.* 66, 223–229. doi: 10.1111/ppa.12567

Ren, C. G., and Dai, C. C. (2012). Jasmonic acid is involved in the signaling pathway for fungal endophyte-induced volatile oil accumulation of *Atractylodes lancea* plantlets. *BMC Plant Biol.* 12:128. doi: 10.1186/1471-2229-12-128

Ren, C. G., and Dai, C. C. (2013). Nitric oxide and brassinosteroids mediated fungal endophyte-induced volatile oil production through protein phosphorylation pathways in *Atractylodes lancea* plantlets. *J. Integr. Plant Biol.* 55, 1136–1146. doi: 10.1111/jipb.12087

Rozpądek, P., Nosek, M., Domka, A., Ważny, R., Jędrzejczyk, R. J., Tokarz, K., et al. (2019). Acclimation of the photosynthetic apparatus and alterations in sugar metabolism in response to inoculation with endophytic fungi. *Plant Cell Environ.* 42, 1408–1423. doi: 10.1111/pce.13485

Rozpądek, P., Wezowicz, K., Nosek, M., Ważny, R., Tokarz, K., Lembicz, M., et al. (2015). The fungal endophyte *Epichloë typhina* improves photosynthesis efficiency of its host orchard grass (*Dactylis glomerata*). *Planta* 242, 1025–1035. doi: 10.1007/s00425-015-2337-x

Schmelz, E. A., Huffaker, A., Sims, J. W., Christensen, S. A., Lu, X., Okada, K., et al. (2014). Biosynthesis, elicitation and roles of monocot terpenoid phytoalexins. *Plant J.* 79, 659–678. doi: 10.1111/tpj.12436

Sharma, E., Anand, G., and Kapoor, R. (2017). Terpenoids in plant and arbuscular mycorrhiza-reinforced defence against herbivorous insects. *Ann. Bot.* 119, 791–801. doi: 10.1093/aob/mcw263

Sharma, G., and Agrawal, V. (2013). Marked enhancement in the artemisinin content and biomass productivity in *Artemisia annua* L. shoots co-cultivated with Piriformospora indica. *World J. Microb. Biot.* 29, 1133–1138. doi: 10.1007/s11274-013-1263-y

Sharma, S., Rathi, N., Kamal, B., Pundir, D., Kaur, B., and Arya, S. (2010). Conservation of biodiversity of highly important medicinal plants of India through tissue culture technology- a review. *Agric. Biol. J. N. Am.* 1, 827–833. doi: 10.5251/abjna.2010.1.5.827.833

Singh, P., Jayaramaiah, R. H., Sarate, P., Thulasiram, H. V., Kulkarni, M. J., and Giri, A. P. (2014). Insecticidal potential of defense metabolites from *Ocimum kilimandscharicum* against *Helicoverpa armigera*. *PLoS One* 9:e104377. doi: 10.1016/j.compbiolchem.2016.06.004

Tatli, O., Sogutmaz Ozdemir, B., and Dinler Doganay, G. (2017). Time-dependent leaf proteome alterations of *Brachypodium distachyon* in response to drought stress. *Plant Mol. Biol.* 94, 609–623. doi: 10.1007/s11103-017-0628-2

Tholl, D., Chen, F., Petri, J., Gershenzon, J., and Pichersky, E. (2005). Two sesquiterpene synthases are responsible for the complex mixture of sesquiterpenes emitted from *Arabidopsis* flowers. *Plant J.* 42, 757–771. doi: 10.1111/j.1365-313X.2005.02417.x

Tian, P., Nan, Z. B., Li, C. J., and Spangenberg, G. (2008). Effect of the endophyte *Neotyphodium lolii* on susceptibility and host physiological response of perennial ryegrass to fungal pathogens. *Eur. J. Plant Pathol.* 122, 593–602. doi: 10.1007/s10658-008-9329-7

Toyomasu, T., Kagahara, T., Okada, K., Koga, J., Hasegawa, M., Mitsuhashi, W., et al. (2008). Diterpene phytoalexins are biosynthesized in and exuded from the roots of rice seedlings. *Biosci. Biotech. Bioch.* 72, 562–567. doi: 10.1271/bbb.70677

Vattekkatte, A., Garms, S., Brandt, W., and Boland, W. (2018). Enhanced structural diversity in terpenoid biosynthesis: enzymes, substrates and cofactors. *Org. Biomol. Chem.* 16, 348–362. doi: 10.1039/c7ob02040f

Vaughan, M. M., Christensen, S., Schmelz, E. A., Huffaker, A., McAuslane, H. J., Alborn, H. T., et al. (2015). Accumulation of terpenoid phytoalexins in maize roots is associated with drought tolerance. *Plant Cell Environ.* 38, 2195–2207. doi: 10.1111/pce.12482

Wang, H. X., Liu, C. M., Liu, Q., and Gao, K. (2008). Three types of sesquiterpenes from rhizomes of *Atractylodes lancea*. *Phytochemistry* 69, 2088–2094. doi: 10.1016/j.phytochem.2008.04.008

Wang, N., Wu, X. L., Ku, L. X., Chen, Y. H., and Wang, W. (2016). evaluation of three protein-extraction methods for proteome analysis of maize leaf midrib, a compound tissue rich in sclerenchyma cells. *Front. Plant Sci.* 7:856. doi: 10.3389/fpls.2016.00856

Wang, X. M., Yang, B., Ren, C. G., Wang, H. W., Wang, J. Y., and Dai, C. C. (2015). Involvement of abscisic acid and salicylic acid in signal cascade regulating bacterial endophyte-induced volatile oil biosynthesis in plantlets of *Atractylodes lancea*. *Physiol. Plantarum* 153, 30–42. doi: 10.1111/ppl.12236

Wang, Y., Dai, C. C., Cao, J. L., and Xu, D. S. (2012). Comparison of the effects of fungal endophyte *Gilmaniella* sp. and its elicitor on *Atractylodes lancea* plantlets. *World J. Microb. Biot.* 28, 575–584. doi: 10.1007/s11274-011-0850-z

Wang, Y., Dai, C. C., Zhao, Y. W., and Peng, Y. (2011). Fungal endophyte-induced volatile oil accumulation in *Atractylodes lancea* plantlets is mediated by nitric oxide, salicylic acid and hydrogen peroxide. *Process Biochem.* 46, 730–735. doi: 10.1016/j.procbio.2010.11.020

Wang, Y. W., Xu, C., Li, K., Cai, X. J., Wu, M., and Chen, G. X. (2017). Fe deficiency induced changes in rice (*Oryza sativa* L.) thylakoids. *Environ. Sci. Pollut. R.* 24, 1380–1388. doi: 10.1007/s11356-016-7900-x

Wei, G. F., Dong, L. L., Yang, J., Zhang, L. J., Xu, J., Yang, F., et al. (2018). Integrated metabolomic and transcriptomic analyses revealed the distribution of saponins in *Panax notoginseng*. *Acta Pharm. Sin. B* 8, 458–465. doi: 10.1016/j.apsb.2017.12.010

Yang, C. Q., Fang, X., Wu, X. M., Mao, Y. B., Wang, L. J., and Chen, X. Y. (2012). Transcriptional regulation of plant secondary metabolism. *J. Integr. Plant Biol.* 54, 703–712. doi: 10.1111/j.1744-7909.2012.01161.x

Yang, C. Q., Wu, X. M., Ruan, J. X., Hu, W. L., Mao, Y. B., Chen, X. Y., et al. (2013). Isolation and characterization of terpene synthases in cotton (*Gossypium hirsutum*). *Phytochemistry* 96, 46–56. doi: 10.1016/j.phytochem.2013.09.009

Yang, M. Z., Ma, M. D., Yuan, M. Q., Huang, Z. Y., Yang, W. X., Zhang, H. B., et al. (2016). Fungal endophytes as a metabolic fine-tuning regulator for wine grape. *PLoS One* 11:e0163186. doi: 10.1371/journal.pone.0163186

Yang, T., and Dai, C. C. (2013). Interactions of two endophytic fungi colonizing *Atractylodes lancea* and effects on the host's essential oils. *Acta Ecol. Sinica* 33, 87–93. doi: 10.1016/j.chnaes.2013.01.004

Yang, T., Du, W., Zhou, J. Y., Wang, X. M., and Dai, C. C. (2013). Effects of the symbiosis between fungal endophytes and *Atractylodes lancea* on rhizosphere and phyllosphere microbial communities. *Symbiosis* 61, 23–36. doi: 10.1007/s13199-013-0254-y

Yuan, J., Sun, K., Deng-Wang, M. Y., and Dai, C. C. (2016a). The Mechanism of ethylene signaling induced by endophytic fungus *Gilmaniella* sp. AL12 mediating sesquiterpenoids biosynthesis in *Atractylodes lancea*. *Front. Plant Sci.* 7:361. doi: 10.3389/fpls.2016.00361

Yuan, J., Zhou, J. Y., Li, X., and Dai, C. C. (2016b). The primary mechanism of endophytic fungus *Gilmaniella* sp AL12 promotion of plant growth and sesquiterpenoid accumulation in *Atractylodes lancea*. *Plant Cell Tiss. Org.* 125, 571–584. doi: 10.1007/s11240-016-0971-z

Zhai, X., Luo, D., Li, X. Q., Han, T., Jia, M., Kong, Z. Y., et al. (2018). Endophyte *Chaetomium globosum* D38 promotes bioactive constituents accumulation and root production in *Salvia miltiorrhiza*. *Front. Microbiol.* 8:2694. doi: 10.1080/1040841X.2016.1201041

Zhang, Z. B., Wu, Y. L., Gao, M. H., Zhang, J., Kong, Q., Liu, Y. A., et al. (2012). Disruption of PAMP-induced map kinase cascade by a *Pseudomonas syringae* effector activates plant immunity mediated by the NB-LRR protein SUMM2. *Cell Host Microbe* 11, 253–263. doi: 10.1016/j.chom.2012.01.015

Zheng, L. P., Tian, H., Yuan, Y. F., and Wang, J. W. (2016). The influence of endophytic *Penicillium oxalicum* B4 on growth and artemisinin biosynthesis of in vitro propagated plantlets of *Artemisia annua* L. *Plant Growth Regul.* 80, 93–102. doi: 10.1007/s10725-016-0162-2

Zhou, J. Y., Li, X., Zhao, D., Deng-Wang, M. Y., and Dai, C. C. (2016). Reactive oxygen species and hormone signaling cascades in endophytic bacterium induced essential oil accumulation in *Atractylodes lancea*. *Planta* 244, 699–712. doi: 10.1007/s00425-016-2536-0

Zhou, J. Y., Sun, K., Chen, F., Yuan, J., Li, X., and Dai, C. C. (2018). Endophytic *Pseudomonas* induces metabolic flux changes that enhance medicinal

sesquiterpenoid accumulation in *Atractylodes lancea*. *Plant Physiol. Bioch.* 130, 473–481. doi: 10.1016/j.plaphy.2018.07.016

Zhou, L., Zuo, Z., and Chow, M. S. (2005). Danshen: an overview of its chemistry, pharmacology, pharmacokinetics, and clinical use. *J. Clin. Pharmacol.* 45, 1345–1359. doi: 10.1002/jcph.96

Zouari, I., Salvioli, A., Chialva, M., Novero, M., Miozzi, L., Tenore, G. C., et al. (2014). From root to fruit: RNA-Seq analysis shows that arbuscular mycorrhizal symbiosis may affect tomato fruit metabolism. *BMC Genomics* 15:221. doi: 10.1186/1471-2164-15-221

Conflict of Interest Statement: The authors declare that the research was conducted in the absence of any commercial or financial relationships that could be construed as a potential conflict of interest.

frontiers in Microbiology

ORIGINAL RESEARCH
published: 29 May 2019
doi: 10.3389/fmicb.2019.01119

Diazotrophic *Paenibacillus beijingensis* BJ-18 Provides Nitrogen for Plant and Promotes Plant Growth, Nitrogen Uptake and Metabolism

*Yongbin Li, Yunlong Li, Haowei Zhang, Minyang Wang and Sanfeng Chen**

State Key Laboratory for Agrobiotechnology and College of Biological Sciences, China Agricultural University, Beijing, China

OPEN ACCESS

Edited by:
Marco Catoni, University of Birmingham, United Kingdom

Reviewed by:
Hassan Etesami, University of Tehran, Iran
Christopher Peter Chanway, University of British Columbia, Canada
Akshit Puri, University of British Columbia, Canada, in collaboration with reviewer CC

****Correspondence:***
Sanfeng Chen
chensf@cau.edu.cn

Specialty section:
This article was submitted to Plant Microbe Interactions, a section of the journal Frontiers in Microbiology

Received: *21 January 2019*
Accepted: *03 May 2019*
Published: *29 May 2019*

Citation:
Li Y, Li Y, Zhang H, Wang M and Chen S (2019) Diazotrophic Paenibacillus beijingensis BJ-18 Provides Nitrogen for Plant and Promotes Plant Growth, Nitrogen Uptake and Metabolism. Front. Microbiol. 10:1119. doi: 10.3389/fmicb.2019.01119

Diazotrophic bacteria can reduce N_2 into plant-available ammonium (NH_4^+), promoting plant growth and reducing nitrogen (N) fertilizer requirements. However, there are few systematic studies on the effects of diazotrophic bacteria on biological N_2 fixation (BNF) contribution rate and host plant N uptake and metabolism. In this study, the interactions of the diazotrophic *Paenibacillus beijingensis* BJ-18 with wheat, maize, and cucumber were investigated when it was inoculated to these plant seedlings grown in both low N and high N soils, with un-inoculated plants as controls. This study showed that GFP-tagged *P. beijingensis* BJ-18 colonized inside and outside seedlings, forming rhizospheric and endophytic colonies in roots, stems, and leaves. The numbers of this bacterium in the inoculated plants depended on soil N levels. Under low N, inoculation significantly increased shoot dry weight (wheat 86.1%, maize 46.6%, and cucumber 103.6%) and root dry weight (wheat 46.0%, maize 47.5%, and cucumber 20.3%). The ^{15}N-isotope-enrichment experiment indicated that plant seedlings derived 12.9–36.4% N from BNF. The transcript levels of *nifH* in the inoculated plants were 0.75–1.61 folds higher in low N soil than those in high N soil. Inoculation enhanced NH_4^+ and nitrate (NO_3^-) uptake from soil especially under low N. The total N in the inoculated plants were increased by 49.1–92.3% under low N and by 13–15.5% under high N. Inoculation enhanced activities of glutamine synthetase (GS) and nitrate reductase (NR) in plants, especially under low N. The expression levels of N uptake and N metabolism genes: *AMT* (ammonium transporter), *NRT* (nitrate transporter), *NiR* (nitrite reductase), *NR*, *GS* and *GOGAT* (glutamate synthase) in the inoculated plants grown under low N were up-regulated 1.5–91.9 folds, but they were not obviously changed under high N. Taken together, *P. beijingensis* BJ-18 was an effective, endophytic and diazotrophic bacterium. This bacterium contributed to plants with fixed N_2, promoted plant growth and N uptake, and enhanced gene expression and enzyme activities involved in N uptake and assimilation in plants. However, these positive effects on plants were regulated by soil N status. This study might provide insight into the interactions of plants with beneficial associative and endophytic diazotrophic bacteria.

Keywords: diazotroph, ^{15}N isotope enrichment, biological N_2 fixation, colonization, GFP, wheat, maize, cucumber

INTRODUCTION

Biological nitrogen (N) fixation (BNF) is the major natural process through which atmospheric N_2 is reduced to bioavailable NH_4^+, providing a large amount of natural N into cultivated agricultural systems (Galloway et al., 2008). In addition to symbiotic N_2-fixing *Rhizobia* associated with legumes, the non-symbiotic diazotrophic bacteria are also important contributors to the N nutrition of non-legumes (Gupta et al., 2006). It is estimated that the microbial N accounts for roughly 30–50% of the total N in crop fields (Liu et al., 2017). The non-symbiotic diazotrophic bacteria are highly diverse and associated with plants in different ways. Some bacteria live in the rhizosphere and are designated rhizobacteria (Kloepper and Beauchamp, 1992). *Herbaspirilla seropedicae* strain Z67 mainly colonize on the riceroot surface and are usually called associative diazotrophic bacteria (Monteiro et al., 2012). *Paenibacillus polymyxa* WLY78 live inside the plant without causing damage and are classified as endophytic diazotrophic bacteria (Hao and Chen, 2017). Endophytic diazotrophic bacteria may have an advantage over associative diazotrophic bacteria and rhizobacteria, since they live within plant tissues where better niches are established for N_2 fixation and assimilation of fixed N_2 by the plant (Reinhold-Hurek and Hurek, 1998, 2011).

The well-known associative and endophytic diazotrophic bacteria include *Azospirillum* (Boddey et al., 1986), *Azoarcus* (Hurek et al., 2002), *Burkholderia* (Baldani et al., 2000), *Enterobacter* (Magnani et al., 2010), *Gluconacetobacter* (James et al., 2001), *Herbaspirillum* (Boddey et al., 1995). BNF quantification experiments show that associative and endophytic bacteria can fix N_2 in plant tissues with higher efficiency (Carvalho et al., 2014). *G. diazotrophicus* inoculation enhanced sugarcane yield by providing 50–80% N from BNF (Boddey et al., 1995). It is estimated that an 18–28% of plant N derives from BNF of endophytic *Enterobacter* sp. strain (Mirza et al., 2001). Diazotrophic bacteria present in the mucilage of aerial roots contribute 29–82% of the N nutrition of Sierra Mixe maize (Van Deynze et al., 2018).

Although the positive effects of diazotrophic bacteria on plants are observed, little is known about plant response to inoculation with diazotrophic bacteria. Plant N metabolism is a complex process requiring some key enzymes. The plant genes *NR* (nitrate reductase), *NiR* (nitrite reductase), *GS* (glutamine synthetase) and *GOGAT* (glutamate synthase) play very important roles in N metabolism (Bloom et al., 1992; Lea and Miflin, 2003). The plant genes *AMT* (ammonium transporter) (Bloom et al., 1992) and *NRT* (nitrate transporter) (Sugiura et al., 2007) are involved in N uptake. It is shown that some endophytic fungi affect expression of N metabolism of plants (Yang et al., 2014).

Paenibacillus beijingensis BJ-18, isolated from wheat rhizosphere, was a N_2-fixer (Wang et al., 2013). Inoculation with *P. beijingensis* BJ-18 promoted the growth of tomato seedlings (Xie et al., 2016) and increased wheat yield by 26.9% in field experiment (Shi et al., 2016), suggesting that this bacterium promotes plant growth. It was generally recognized that plant growth-promoting bacteria (PGPB) promoted plant growth by direct mechanisms (e.g., N fixation, phosphate solubilization, sequestering iron) and indirect mechanisms [e.g., indole-3-acetic acid (IAA), cytokinins, gibberellins] (Glick, 2012). However, the mechanisms utilized by *P. beijingensis* BJ-18 to promote plant growth were not clear. In this study, we investigated the colonization pattern and contributions of N_2 fixation by *P. beijingensis* BJ-18 to plants, and the plant responses (N uptake and metabolism processes) to the infection.

MATERIALS AND METHODS

Bacteria Strains and Growth Conditions

Paenibacillus beijingensis BJ-18 (accession number: JN873136), isolated from wheat rhizosphere, is a novel species with N_2-fixing ability [1043 ± 12.9 nmol C_2H_4 (mg protein h)$^{-1}$] (Wang et al., 2013). This bacterium has multiple antagonistic activities against plant pathogens and produces IAA (24.95 μg mL^{-1}) (Xie et al., 2016). The bacterial suspension of *P. beijingensis* BJ-18 used in inoculation was prepared as follows. The *P. beijingensis* 1–18 cells were cultured overnight in Luria-Bertani (LB) broth at 30°C and 180 rpm, and then cells in the logarithmic growth phase were harvested by centrifugation and finally the pellet was suspended with sterile normal saline (0.89% w/v NaCl in double distilled water) to the final concentration at 10^8 cells mL^{-1}.

Colonization of GFP-Tagged *P. beijingensis* BJ-18 in Wheat, Maize, and Cucumber Tissues

The recombinant plasmid pGFP300 carrying *gfp* gene (Hao and Chen, 2017) was introduced into *P. beijingensis* BJ-18 by electrotransformation (Zhang et al., 2013), yielding GFP-tagged *P. beijingensis* BJ-18. And the physiological ability of GFP-tagged *P. beijingensis* BJ-18 was not changed, compared with wild-type *P. beijingensis* BJ-18 (data not published). The GFP-tagged *P. beijingensis* BJ-18 suspension was obtained as described above. Plump seeds of wheat "Jimai 22" (Shandong Runfeng Seed Industry Co., Ltd), maize "Zhengdan 958" (Henan Shangke Seed Co., Ltd.) and cucumber "Zhongnong 8" (Beijing Shengfeng Garden Agricultural Technology Co., Ltd) were surface-disinfected with 10% sodium hypochlorite for 10 min, followed by rinsing with sterilized water three times, and grown on the sterile petri dishes containing moist filter papers in darkness at room temperature (25°C) for 3–5 days, respectively. These plant seedlings had two treatments: inoculation with GFP-tagged *P. beijingensis* BJ-18 (E+) and mock inoculation (E-). For inoculation, the plant seedlings were soaked in bacterial suspension (10^8 cells mL^{-1}) of GFP-tagged *P. beijingensis* BJ-18 for 30 min to facilitate colonization. For mock inoculation, the plant seedlings were soaked in sterilized deionized water for 30 min. The germinated wheat, maize and cucumber seeds were, respectively, sown in sterile flask (3 seeds per flask, 6 cm in diameter and 10 cm in height) containing 100 mL 1/2 × Murashige and Skoog semisolid agar medium (Prod

No: M519, PhytoTechnology Laboratories, Shawnee Mission, United States) (Murashige and Skoog, 1962). Then these seedlings were grown in the light growth chamber (27°C, 70% humidity and 16 h day/8 h night, with light at 250 μmol m^{-2} s^{-1}). The GFP-tagged *P. beijingensis* BJ-18 in plant tissues was observed at 2 weeks after inoculation by confocal laser scanning microscopy (CLSM, Olympus FluoView^{TM} FV1000 confocal microscope, Olympus Corporation, Tokyo, Japan). These images were collected using FV10-ASW software (03.01.02.02, Olympus Europa Holding GmbH, Hamburg Germany) and processed in Adobe Photoshop CC 2015 and Adobe Illustrator CS6 (Adobe, San Jose, CA, United States).

Plant Culture and Collection

Seedling growth assays were performed in plastic pots (diameter of 35 cm; height of 25 cm) filled with 5 kg non-sterile soil which was top soil (0–20 cm depth) taken from the Shangzhuang Experimental Station of China Agricultural University, Beijing, China (40°08′12.15″ N, 116°10′44.83″ E, 50.21 m above sea level). The soil was low N-content sandy loam (N_{min}, 7.8 mg kg^{-1}; Olsen-P, 7.3 mg kg^{-1}; NH_4OAc-K, 115.8 mg kg^{-1}; O.M., 7.2 g kg^{-1}; pH 7.7; E.C., 0.4 dS m^{-1}). The soil was air-dried, crushed, and screened by a 2 mm sieve to remove debris and reduce heterogeneity for cultivating plants: wheat, maize and cucumber. Before planting, P (Na_2HPO_4) and K (KCl) fertilizer were applied to soil as base fertilizers at amounts of 50 mg P and 17 mg K per kg soil, respectively, based on the recommendation by Ke et al. (2018). The microelements were not applied to soil during plant growth.

The experimental design was randomized with factorial arrangement (a 2 × 2 factorial design) in three replications with bacterial factor at two levels and N factor at two levels. Three different plants (wheat, maize, and cucumber) were chosen to obtain an objective conclusion. Therefore, the experiments had twelve treatments.

The seeds (wheat, maize, and cucumber) were germinated as described above. After germination, vigorous and homogenous seedlings were chosen for transplanting into plastic pots. These plant seedlings had two treatments: inoculation with *P. beijingensis* BJ-18 (E+) and mock inoculation (E-). For inoculation, the plant seedlings were soaked in bacterial suspension (10^8 cells mL^{-1}) of *P. beijingensis* BJ-18 for 30 min to facilitate colonization. For mock inoculation, the plant seedlings were soaked in sterilized deionized water. Then the inoculated seedlings and un-inoculated seedlings were, respectively, transplanted into pots (cucumber: 4 seedlings per pot; maize: 2 seedlings per pot; wheat: 4 hills per pot and 10 seedlings per hill). On day 7, 80 ml of the bacterial suspension was applied to pot containing inoculated seedlings and 80 mL of sterile water was applied to pot containing non-inoculated seedlings. Each of inoculation and mock inoculation treatments had three replicates.

There were two levels of N treatments: high N level (250 mg N kg^{-1} soil) and low N level (83 mg N kg^{-1} soil). The ^{15}N-labeled $(NH_4)_2SO_4$ (10.16% ^{15}N atom, Shanghai Research Institute of Chemical Industry, China) was applied to soils in all pots. The N fertilizer was added in three separate applications: the first application was done before planting as base fertilizer (approximately 33.3% of total N), and successive two applications (approximately 33.3% of total N per time) were made on day 7 and 14 after transplanting, respectively. Pots were placed in the greenhouse under optimum conditions (15 h light/9 h dark cycle, 25–30/15–20°C day/night temperature and 40% day/60% humidity). The seedlings were regularly watered (tap water) to 40% relative soil moisture by weighing method every 5 days.

The samples of wheat, maize, and cucumber were harvested from each treatment on day 35 after transplanting, respectively.

Firstly, the whole seedling was uprooted, and then shoot and root samples were separated and washed with deionized water to remove the adhering soil. Shoot and root samples were oven-died at 105°C for 30 min to inactivate the enzyme, respectively, followed by 65°C until constant weight for dry weight analysis. Then, the oven-dried samples were grinded, screened by a 1 mm sieve, and stored in zip-lock bag for plant N content and ^{15}N enrichment determination. Afterward, the remaining samples were immediately frozen in liquid N and then maintained at −80°C until further analysis.

Bacterial Cell Concentration Within Plant Tissues

The cell densities of diazotrophic *P. beijingensis* BJ-18 within the inoculated plant tissues were estimated by qPCR according to the method described by Rasmussen et al. (2007). Primers for qPCR of the *nifB* from *P. beijingensis* BJ-18 included *nifB* F (5′-GAAGGTGAGAGTGAGGATGG-3′) and *nifB* R (5′-TTGCTTCAGGCTCATCTCC-3′). qPCR was performed with plant genomic DNA as template which was extracted form plant seedlings using DNA Kit [TianGen Biotech (Beijing) Co., Ltd.]. The 129 bp PCR product was ligated to the PMD 19-T vector (Takara, Otsu, Japan) and then introduced into *Escherichia coli* JM109. The introduced *E. coli* JM109 was grown in liquid LB medium, and the recombinant plasmids carrying *nifB* fragment were extracted and purified using TIANprep Mini Plasmid Kit [TianGen Biotech (Beijing) Co., Ltd.]. A standard curve was generated for each run 10-fold dilution series from 2 × 10^1 to 2 × 10^7 copies. The plant genomic DNA isolated from each of the different treatments was mixed with SYBR® Premix Ex TaqTM (Takara, Kyoto, Japan), primer pairs and ddH_2O in a total volume of 20 uL for qPCR on a 7500 Real-Time PCR System (Applied Biosystems, Foster City, CA, United States). Ct values were measured to quantify initial amounts of target DNA.

Quantification of Biological N_2 Fixation Contribution

In this study, BNF contribution of *P. beijingensis* BJ-18 to plants was quantified by the method of ^{15}N isotope dilution technique. N content and ^{15}N enrichment in plant tissues were determined by DELTA V Advantage isotope ratio mass spectrometer (Thermo Fisher Scientific, Inc., United States). The plants without *P. beijingensis* BJ-18 inoculation were used as references to calculate the BNF contribution. The BNF

contribution was calculated according to formula 1 described by Boddey and Knowles (1987):

$$\%\text{Ndfa} = \left(1 - \frac{\%^{15}\text{Na.e.}_{\text{I}}}{\%^{15}\text{Na.e.}_{\text{UI}}}\right) \times 100 \quad (1)$$

Where, %Ndfa is the percentage of N derived from air and percent ^{15}Na.e. ($\%^{15}$N atom excess) is the enrichment of the inoculated (I) and un-inoculated (UI) plants, respectively.

Determination of the Concentration of Free NH_4^+, NO_3^-, and Activities of GS and NR

In order to determine the concentrations of the free ammonium (NH_4^+) and nitrate (NO_3^-), fresh plant tissues were ground with a mortar on ice in extraction buffer. The buffer consisted of 10 mM imidazole, 50 mM Tris-HCl (pH 8.0), and 0.5% (w/v) β-mercaptoethanol. After grinding, the samples were centrifuged at 12,000 × *g* for 20 min at 4°C and the supernatant was collected for free NH_4^+ and NO_3^- determination (Oliveira et al., 2002; Yang et al., 2014). Free NH_4^+ concentration [$\mu g\ g^{-1}$ fresh weight (FW)] in the supernatant was assayed using the Berthelot color reaction method (Gordon et al., 1978), and free NO_3^- concentration ($\mu g\ g^{-1}$ FW) in the supernatant was determined using the Griess method (Eckhardt et al., 1999).

For analysis of GS activity, fresh plant tissues were ground with a mortar in pre-cold extraction buffer (containing10 mM $MgSO_4$, 2 mM dithiothreitol, 70 mM 3 (n-morpholino) propane-sulfonic acid (pH 6.8), 5 mM glutamate, 10% (v/v) ethanediol, 0.1% (v/v) TritonX-100). The extracts were centrifuged at 12,000 × *g* for 30 min at 4°C and the supernatant was collected for plant GS activity determination using NH_2OH as a substrate, and the amount of γ-glutamyl hydroxamate (GHA, ug^{-1} FW min^{-1}) released was determined spectrophotometrically at 540 nm according to the method of Yang et al. (2014).

To measure NR activity, fresh plant tissues were ground on ice in extraction buffer consisting of 25 mM phosphate buffer (pH 7.5, a mixture of K_2HPO_4 and KH_2PO_4), 5 mM cysteine and 5 mM EDTA-Na_2. The mixture was centrifuged at 4,000 × *g* and 4°C for 10 min and the supernatant was collected. NR activity was measured spectrophotometrically at 540 nm according to Yu and Zhang (2012). NR activity was expressed as $\mu g\ NO_2^-\ g^{-1}$ FW h^{-1}.

Quantitative Real-Time PCR Analysis of Plant Genes and *nifH* in Plant Roots and Shoots

Total RNA was extracted from plant tissues using RNAiso Plus reagent (RaKaRa, Kyoto, Japan). Then, RNA was digested with DNase I and reversely transcribed into cDNA using PrimeScript^{TM} RT reagent kit (RaKaRa, Kyoto, Japan). Gene expression levels were determined by quantitative real-time PCR (qRT-PCR) analysis. The specific primers for qRT-PCR were shown in **Table 1**. The plant housekeeping gene *actin* was used as plant internal control, and the bacterial 16S rRNA was used as bacterium internal control. The relative expression of the target genes were calculated according to the standard comparative C(t) method (Livak and Schmittgen, 2001). Each treatment had three biological replicates, with three technical replicates for each biological replicate.

Statistical Analysis

Statistical tests were performed using SPSS software version 20 (SPSS Inc., Chicago, IL, United States). Two-way analysis of variance (ANOVA) was employed to check the significant differences between treatments. Means of different treatments were compared using the least significant difference (LSD) at 0.05 or 0.01 level of probability. Graphs were prepared using SigmaPlot software version 12.5 (Systat Software, Inc., CA, United States).

RESULTS

Colonization of GFP-Tagged *P. beijingensis* BJ-18 in Wheat, Maize, and Cucumber Tissues

The CLSM observation showed that the GFP-tagged *P. beijingensis* BJ-18 cells emitted bright green fluorescence (**Figure 1a**). The GFP-tagged *P. beijingensis* cells were found to colonize on the surface of the primary roots and the root hair zone of wheat (**Figures 1b,c**). The bacterial cells were found to be distributed within cortex of wheat primary roots (**Figure 1d**) and colonized in the wheat vascular bundle (**Figure 1e**). Moreover, bacterial cells were observed in the vascular bundle of wheat stem (**Figures 1f,g**) and in wheat leaf vein (**Figure 1h**). In the maize seedlings, the *P. beijingensis* cells were found to colonize the surface of the primary roots (**Figure 2a**), and on the junction of the primary and lateral roots (**Figure 2b**). The bacteria cells were found within the intercellular spaces and xylem vessels of maize roots and stems (**Figures 2c–e**) and leaves (**Figure 2f**). The colonization pattern in cucumber was similar to those obtained in wheat and maize seedlings. The bacterial cells were found to colonize the surface of the primary roots and the root hair zone (**Figure 3a**). The *P. beijingensis* cells were in cortex (**Figure 3b**) and vascular bundle (**Figure 3c**) of cucumber roots. As shown in **Figures 3d,e**, bacterial cells invaded the xylem vessels of cucumber stem. Moreover, the bacterial cells were found within the cucumber leaves (**Figure 3f**).

Taken together, *P. beijingensis* cells colonized on the surface of roots and within roots, stems and leaves of wheat, maize, and cucumber, indicating that the colonization patterns in the three plants were similar.

Concentration of Diazotrophic *P. beijingensis* BJ-18 in Wheat, Maize, and Cucumber Tissues

The concentration of *P. beijingensis* BJ-18 in the inoculated plants at 35 day after inoculation was assessed using qPCR and was expressed as the number of copies of the specific *nifB* genes per total (plant seedlings + bacteria) genomic DNA. As shown in **Figure 4**, copy numbers of *nifB* gene in the

TABLE 1 | Primers sequence and accession number in NCBI.

Primer	Primer sequence 5′-3′	Size (bp)	NCBI Accession No.	References
CsAMT1	TTCTCTATCAGTGGGCTTTCG AGAACCAATGGGACACAACC	141	AY642427	This study
CsAMT3	AAGGTAGACGACACAATGG CGTAGAAGATGTTGTTGAGG	109	XM_004138819	This study
CsNRT 1.3	CACAAGCCTTCAGAGAATTGG TCAACCAGAAAGCACTTATACG	131	JX206800	This study
CsNR1	GCACAACTCAGACCAATCC GATGAGAATGCTGTCCATACC	103	HM755943	This study
CsNR2	TGTGCGTGTATTCAGATTCG GTGCTAGAGGGCGTATAGG	132	HM755944	This study
CsNiR	AGGATTGGTAGCTTGCACTGG ACTGTGACTCGCCGTTGC	105	EF397679	This study
CsGS1	ATGAGGGAAGAAGGAGGTTACG AGAGAAGGTGTGGATGTCAGC	147	JQ277263	This study
CsGOGAT	GGCTGCTCAAGGAAAGGAACC TGCTGGATTTGTCACCTGTGC	127	DQ641082	This study
TaAMT1.1	ACAGCTTCTTCCTCTTCC CCGAGTAGATGAGGTAGG	105	AY525637	This study
TaNRT1.1	ATGCCAGGTTGTCATTGC CCGAGTCCAGTTGTATGC	135	AY587265	This study
TaNRT2.1	TGGACTCCGAGCACAAGG GACGAAGCAGGTGAAGAAGG	104	AF288688	This study
TaNRT2.3	TGGTCAGAGGAGGAGAAGG GTGGCGAGGATAACATTGC	101	AY053452	This study
TaNR	ATACACCATGAAAGGATACG TACTTGTTCGGCTTCTCC	126	KY244026	This study
TaNiR	CTACACCAACCTCCTCTCC GCCAGGTCGTTGATATGC	138	FJ527909	This study
TaGS1	CCTTGTCATGTGCGATTGC GTGTACTCCTGCTCGATACC	135	DQ124211	This study
Ta GOGAT	AAACCAAGGGACCTCAGTATTC AATGACCACCACCTTCTTACC	150	DW986179	This study
ZmAMT1;1a	CATCGTCGGAAGGTGTGG TTGGATGATGAGCAGTGACC	109	GRMZM2G175140	This study
ZmAMT1;1b	CTACGACTTCTTCCTATACC CGGAGTAGATGAGGTAGG	111	GRMZM2G118950	This study
ZmNrt2.1	TGGACTCAGAGCACAAGG CGAAGCAGGTGAAGAAGG	102	AY129953	This study
ZmNR	GCCAGCATTGAAGGGAAG GCTCGTTCTTGAAGTAGACC	106	M77792	This study
ZmGS1-3	CTTGTGATGTGCGATTGC CTCCTGCTCAATACCATACC	129	X65928	This study
ZmGS1-4	AGGCATCAACATCAGTGG AGAATGTAGCGAGCAACC	117	X65929	This study
Zm GOGAT	*CGCTCTTCTGGCAACTGG* *CACCTTCCTGTAGTCTGATTCG*	133	M59190	This study
CsACTIN	AGAGATGGCTGGAATAGAAC CTGGTGATGGTGTGAGTC	333	DQ641117	Wei et al. (2015)
ZmACTIN	CATGGAGAACTGGCATCACACCTT CTGCGTCATTTTCTCTCTGTTGGC	118	J01238.1	Galli et al. (2013)
TaACTIN	GTCGGTGAAGGGGACTTACA TTCATACAGCAGGCAAGCAC	187	AB181991.1	Moloudi et al. (2013)

(Continued)

TABLE 1 | Continued

Primer	Primer sequence 5′-3′	Size (bp)	NCBI Accession No.	References
nifB	GAAGGTGAGAGTGAGGATGG TTGCTTCAGGCTCATCTCC	88	MH202771	This study
nifH	GCAACAGTCGGAATACGG TTGGGTCACGGTCATACG	136	MH555146	This study

inoculated plant tissues under low N level were much higher than under high N level. Wheat had the highest copy numbers of *P. beijingensis nifB* gene, followed by cucumber and then maize under both low N and high N levels. Copy numbers of *nifB* gene in roots of the three plants were much higher (62.5–185.3%) than in shoots under both low N and high N levels. These data suggested that the concentrations of the bacterial cells in plant tissues were related to soil N levels, plant species and plant tissues.

Plant Growth Promotion

To assess the impacts of *P. beijingensis* inoculation on plant growth, the biomass (dry weight) was analyzed in inoculated and un-inoculated plants under low N and high N levels. Dry weights of wheat shoots and in roots under low N were increased by 86.1 and 46.0%, respectively. Dry weights of maize shoots and in roots under low N were increased by 46.6 and 47.5%, respectively. Dry weights of cucumber shoots and in roots under low N were increased by 103.6 and 20.3%, respectively. The data suggested that *P. beijingensis* BJ-18 could efficiently promote the growth of the three plants (**Figure 5**). The increased shoot and root biomass by *P. beijingensis* BJ-18 inoculation under low N condition were significantly higher than those under high N condition, consistent with the concentration of *P. beijingensis* BJ-18 in these plant tissues under different N conditions.

Quantification of BNF in the *P. beijingensis*-Inoculated Wheat, Maize, and Cucumber

To estimate the contribution of BNF, ^{15}N isotope enrichment analysis was conducted to analyze inoculated seedling of wheat, maize and cucumber grown in soil contain ^{15}N-labeled $(NH_4)_2SO_4$ as N fertilizer in greenhouse conditions, in comparison with un-inoculated plants. As shown in **Table 2**, the roots and shoots of seedlings inoculated with *P. beijingensis* BJ-18 had significantly lower $\delta^{15}N$ value than un-inoculated seedlings under both low and high N conditions, suggesting that these plants derived a portion of N from atmospheric N_2. The plant N derived from the atmosphere (%Ndfa) ranged from 18 to 36.4% under low N level and from 12.9 to 30.5% under high N level. Among the three plants, wheat showed maximum %Ndfa (30.5 and 36.4%) under both high N and low N levels, followed by cucumber (25.4 and 27.8%) and then maize (12.9 and 20.9%). These data suggest that the contribution of BNF was closely related to soil N levels and to plant species. These results were in agreement with the concentration of *P. beijingensis* BJ-18 within plants and the plant biomass under different N levels.

Transcript Levels of *nifH* Gene

To investigate whether *nif* genes coding nitrogenase of *P. beijingensis* BJ-18 were expressed within plant tissues, the transcript levels of *nifH* gene, one of *nif* genes coding Fe protein of nitrogenase, were quantified. As shown in **Figure 6**, transcripts of *nifH* under low N were up-regulated in wheat shoots and roots by 1.09 and 1.61 folds, respectively, in maize shoots and roots by 0.77 and 1.0 folds, respectively, and in cucumber shoots and roots by 0.75 and 1.61 folds, respectively, compared to those under high N. The results suggested that soil N status affected transcript level of *P. beijingensis nifH*. The data were consistent with BNF rate and the concentration of *P. beijingensis* BJ-18 in plants grown in soils containing different N levels.

Promotion of N Uptake and Total N Content in Plants by Inoculation With *P. beijingensis* BJ-18

Compared to un-inoculated shoots and roots under low N level, a significant increase of free NH_4^+ concentration was observed in shoots of wheat (26.6%), maize (21.9%) and cucumber (22.2%) and in roots of wheat (24.9%), maize (52.7%) and cucumber (32.2%) (**Figure 7A**). In contrast, inoculation did not significantly enhance free NH_4^+ concentration in plant tissues under high N (**Figure 7B**).

Similarly, *P. beijingensis* inoculation significantly increased the free NO_3^- concentration in shoots of wheat (26.3%), maize (23.4%) and cucumber (43.7%) and in roots of wheat (60.7%), maize (62.6%) and cucumber (67.4%) under low N (**Figure 7C**). In contrast, inoculation did not significantly enhance free NO_3^- concentration in plant tissues under high N (**Figure 7D**).

Compared to un-inoculated shoots under low N level, a significant increase of total N content was observed in inoculated shoots of wheat (76.3%), maize (49.1%) and cucumber (88.8%) (**Figure 7E**). Similarly, inoculation greatly enhanced total N content in inoculated roots of wheat (61.6%), maize (68.9%) and cucumber (92.3%) (**Figure 7F**). In contrast, the increased levels of total N content in root and shoots were lower under high N (**Figures 7E,F**). The data were consistent with the change of the concentrations of the free NH_4^+, and free NO_3^- under low N and high N.

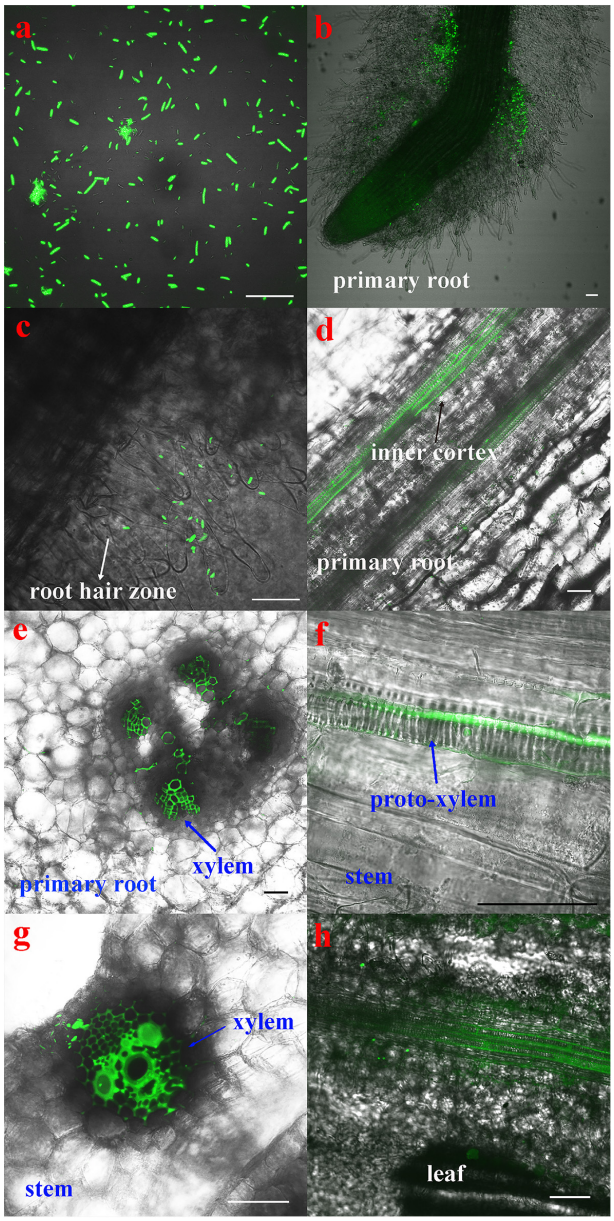

FIGURE 1 | Colonization of the GFP-tagged *P. beijingensis* BJ-18 in the seedlings of wheat. Wheat seedlings were grown in the presence of GFP-tagged *P. beijingensis* BJ-18 for 2 weeks. Images were taken with a fluorescent microscope. Excitation was at 488 nm. **(a)** Confocal image of the GFP-tagged *P. beijingensis* BJ-18 cells; **(b–e)** Colonization patterns in the root; **(f,g)** Colonization patterns in the stem; **(h)** Colonization patterns in the leaf. Bars represent 50 μm.

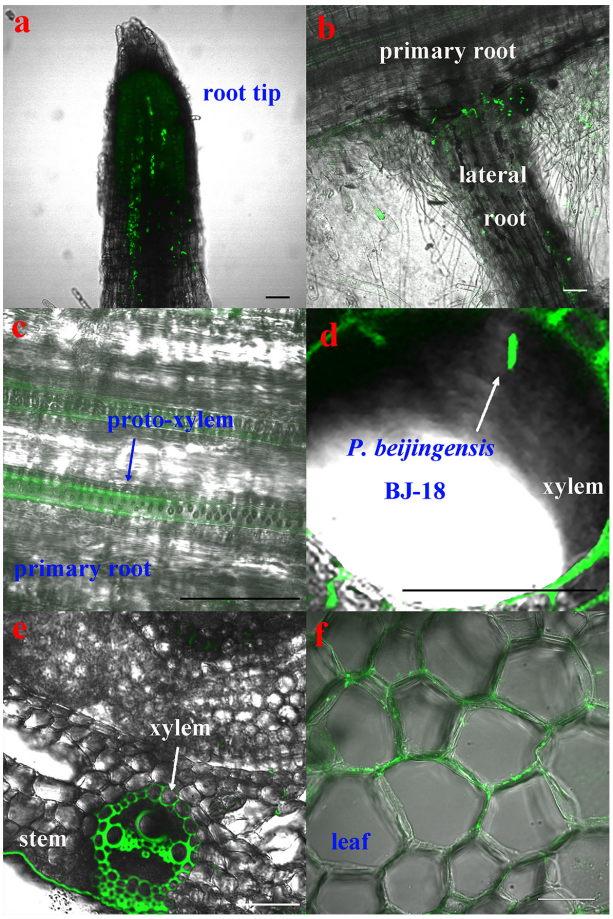

FIGURE 2 | Colonization of the GFP-tagged *P. beijingensis* BJ-18 in the seedlings of maize. Maize seedlings were grown in the presence of GFP-tagged *P. beijingensis* BJ-18 for 2 weeks. Images were taken with a fluorescent microscope. **(a–c)** Colonization patterns in the root; **(d,e)** Colonization patterns in the stem; **(f)** Colonization patterns in the leaf. Bars represent 50 μm.

Enhancement of GS and NR Activities of Plants by Inoculation With *P. beijingensis* 1-18

Compared to un-inoculated plant shoots and roots under low N (**Figures 8A,B**), GS activities were significantly increased in inoculated shoots of wheat (89.7%), maize (19.0%) and cucumber (46.9%) and in inoculated roots of wheat (45.0%), maize (85.5%) and cucumber (40.4%), but inoculation did not obviously enhance the GS activities of plants grown in high N soil.

As shown in **Figures 8C,D**, compared to un-inoculated plant shoots and roots grown in low N soil, NR activities were significantly enhanced in inoculated shoots of wheat (20.9%), maize (42.0%) and cucumber (28.9%) and in inoculated roots of wheat (28.9%), maize (66.2%) and cucumber (44.3%). In contrast, inoculation did not obviously enhance the NR activities of plants grown in high N soil.

Up-Regulation of Expression of N Uptake and N Assimilation Genes in Plants by Inoculation With *P. beijingensis*

In maize, the transcript levels of three genes (*ZmAMT1,1a*, *ZmAMT1,1b*, and *ZmNRT2.1*) involved in N uptake and five genes (*ZmNR*, *ZmNiR*, *ZmGS1-3*, *ZmGS1-4*, and *Zm CsGOGAT*) involved N metabolism were analyzed (**Figure 9**). Under low

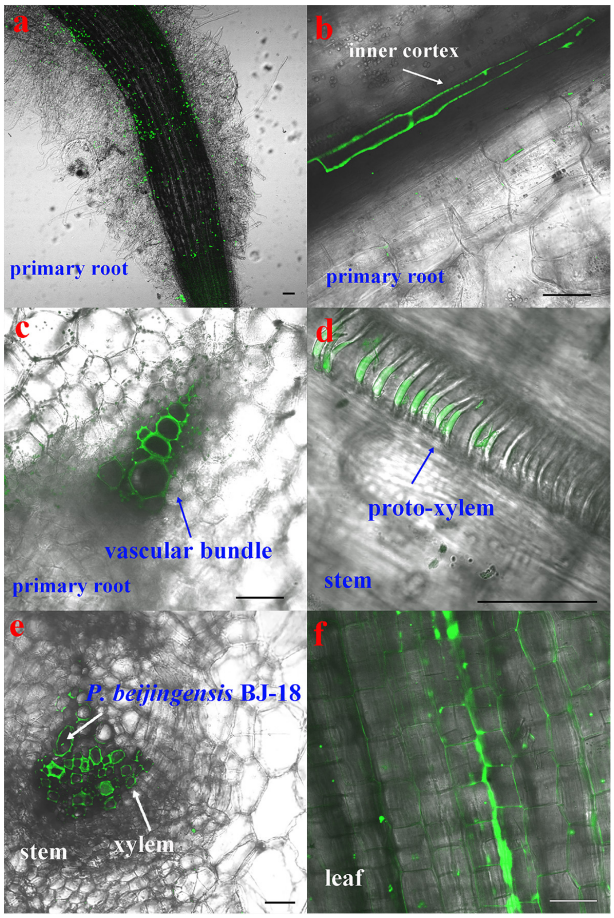

FIGURE 3 | Colonization of the GFP-tagged *P. beijingensis* BJ-18 in the seedlings of cucumber. Cucumber seedlings were grown in the presence of GFP-tagged *P. beijingensis* BJ-18 for 2 weeks. Images were taken with a fluorescent microscope. **(a–d)** Colonization patterns in the root; **(e)** Colonization patterns in the stem; **(f)** Colonization patterns in the leaf. Bars represent 50 μm.

N level, the transcript levels of *ZmAMT1,1a*, *ZmAMT1,1b*, and *ZmNRT2.1* were up-regulated by 1.83–3.93 folds in the inoculated shoots, while in inoculated roots, they were up-regulated 2.97–14.17 folds (**Figures 9A–C**), suggesting that inoculation promoted expression of plant N uptake genes. Similarly, inoculation significantly enhanced the transcript levels of *ZmNR*, *ZmGS1-3*, and *ZmGS1-4* in shoots by 18.46, 7.44, and 11.79 folds, respectively, and in roots by 5.63, 6.64, and 6.59 folds, respectively (**Figures 9D,F,G**). In contrast, inoculation did not obviously affect the transcript levels of these genes in maize shoots and roots under high N condition. However, inoculation did not affect the transcript levels of *ZmNiR* and *ZmGOGAT* under both low N and high N conditions (**Figures 9E,H**).

In wheat, the transcript levels of four genes (*TaAMT1.1*, *TaNRT1.1*, *TaNRT2.1*, and *TaNRT2.3)* involved in N uptake and four genes (*TaNR*, *TaNiR*, *TaGS1*, and *TaGOGAT)* involved N metabolism were analyzed. Similar to maize, the eight genes in the inoculated shoots of wheat in low N were up-regulated by 1.56–46.49 folds, while they were up-regulated 1.98–91.93 folds in inoculated roots (**Figure 10**). In contrast, inoculation did not obviously affect the transcript levels of these genes under high N condition.

In cucumber, the transcript levels of four genes (*CsAMT1*, *CsAMT3*, *CsNRT1.3*, and *CsNRT2.2*) involved in N uptake and five genes (*CsNR1*, *CsNR2*, *CsNiR*, *CsGS1*, and *CsGOGAT*) involved N metabolism were also analyzed. Similar to wheat and maize, the nine genes in the inoculated shoots of cucumber in low N soil were up-regulated 1.60–5.82 folds, while they were up-regulated 1.47–11.85 folds in inoculated roots (**Figure 11**). However, these effects of inoculated were weak when cucumber was grown in high N soil.

DISCUSSION

The N_2-fixing *Paenibacillus* strains have gained much attention due to their capacity of forming endospore to survive for long periods of time under adverse conditions (Grady et al., 2016). In this study, *P. beijingensis* BJ-18 was tagged by GFP and observation by laser confocal microscopy revealed that in seedlings of wheat, maize, and cucumber, bacterial cells could be found in the inner cortex and vascular bundle of roots and stems as well as within the leaves, suggesting *P. beijingensis* BJ-18 has similar invasion patterns in both monocotyledons and dicotyledons. The data indicated that *P. beijingensis* BJ-18 spread systemically from roots to stems and leaves of wheat, maize, and cucumber via xylem vessels. Therefore, *P. beijingensis* BJ-18 could be defined as a plant endophytic diazotrophic bacterium and it had a broad range of host plants. Similar colonization patterns were observed in the association of *P. polymyxa* WLY78 with wheat, maize, and cucumber (Hao and Chen, 2017) and in the association of *P. polymyxa* P2b-2R with lodgepole pine (a gymnosperm tree species) (Anand and Chanway, 2013). The colonization pattern of *P. beijingensis* BJ-18 was a little different form that of the associated diazotrophic *A. brasilense* Yu62 which colonized mainly on the surface of maize roots and only small part entered into maize tissues (Liu et al., 2003). These results indicated that on one side the diazotrophic *Paenibacillus* species/strains may fix N_2 inside plants and rapidly transfer the fixed product to plants, and on the other side they fix N_2 on the root surfaces and part of the fixed product may be remain in the soil.

In this study, the concentrations of *P. beijingensis* cells in inoculated plant tissues under high N and low N levels were determined by qPCR, with un-inoculated plant tissues as control. The results showed that the bacterial cell numbers were significantly higher in inoculated plant tissues grown under low N condition than those under high N condition, suggesting that soil N status controlled the concentration of bacterial cells in plants. Similar reports were found in sugarcane where high dose of N (ammonium nitrate) resulted in reduction of endophytic *Acetobacter diazotrophicus* concentration (Fuentes-Ramirez et al., 1999) and a higher number of endophytic diazotrophs were isolated from sugarcane plants under low N than under high N (de Oliveira et al., 2003). Moreover,

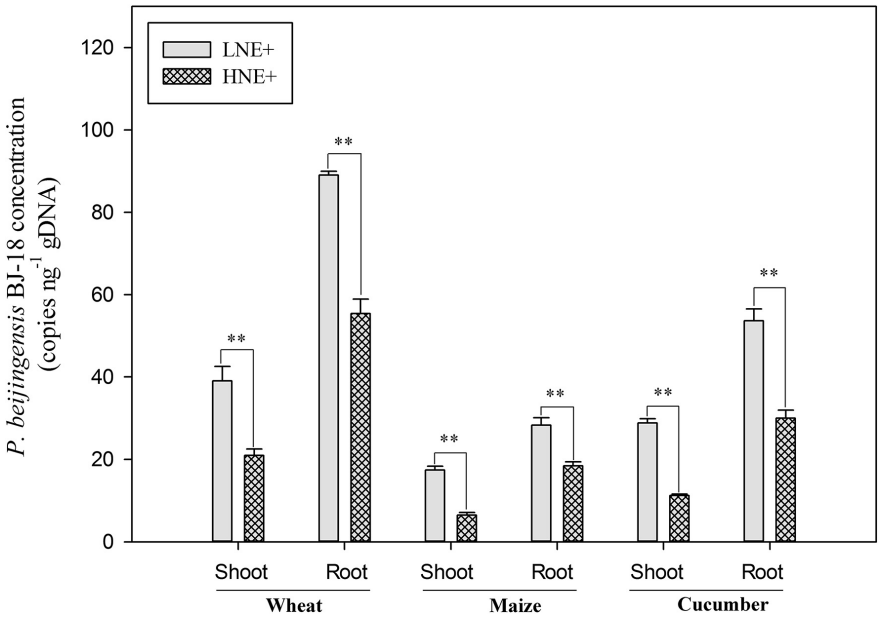

FIGURE 4 | The cell concentrations of *P. beijingensis* BJ-18 in the inoculated shoots and roots of wheat, maize, and cucumber seedlings in high N (HN) and low N (LN) levels. The concentrations of *P. beijingensis* BJ-18 are represented by *nifB* gene copies ng^{-1} total genomic DNA. Values are given as mean of three independent biological replicates, and single asterisks or double asterisks (* or **) indicate significant differences between HNE+ and LNE+ treatments determined by LSD at $P < 0.05$ or $P < 0.01$. The bars represent the standard error. LNE+ indicates plants grown in low N level of soils and inoculated with *P. beijingensis* BJ-18; HNE+ indicates plants grown in high N level of soils and inoculated with *P. beijingensis* BJ-18.

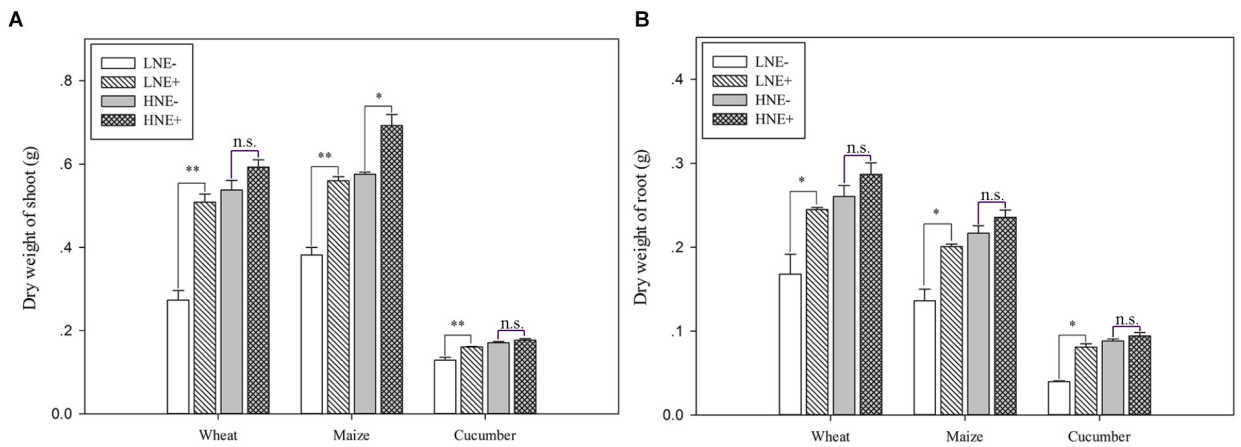

FIGURE 5 | Dry weight (DW) in shoots **(A)** and roots **(B)** of wheat, maize, and cucumber seedlings inoculated with *P. beijingensis* BJ-18 under high N (HN) and low N (LN) levels. Values are given as mean of three independent biological replicates, and single asterisks or double asterisks (* or **) indicate significant differences between inoculated (E+) and un-inoculated (E-) plants determined by LSD at $P < 0.05$ or $P < 0.01$. The bars represent the standard error. The wheat dry weight represents five seedlings per pot, and the dry weight of maize and cucumber represents one seedling per pot. LNE- indicates plants grown in low N level of soil and un-inoculated with *P. beijingensis* BJ-18; LNE+ indicates plants grown in low N level of soils and inoculated with *P. beijingensis* BJ-18; HNE- indicates plants grown in high N level of soil and un-inoculated with *P. beijingensis* BJ-18; HNE+ indicates plants grown in high N level of soils and inoculated with *P. beijingensis* BJ-18.

it was reported that the plant endogenous N status could also induce plant defense responses to regulate bacterial colonization (Carvalho et al., 2014). The increase in N compounds and amino acids (such as phenylalanine and hydroxyproline) was necessary to activate plant defense responses (Snoeijers et al., 2000). Amino acid transporters regulated by N status also have regulatory function in plant defense responses (Liu et al., 2010; Seifi et al., 2013). This study also showed that total N content and concentrations of NH_4^+ and NO_3^- in un-inoculated plants under high N were much higher than those under low N. This finding may explain why high N caused a decrease in the numbers of *P. beijingensis* cells in plants tissues.

Furthermore, this study investigated whether *nifH* gene was expressed in the inoculated plants. The expression levels of *nifH*

TABLE 2 | ^{15}N isotope enrichment determination of biological N_2 fixation rate in inoculated plants grown in soils containing high N and low N.

Treatments			δ15N value (versus at-air)		%Ndfa	
			High N	Low N	High N	Low N
Cucumber	Shoot	E-		10952 ± 1251a	3680 ± 261a	
		E+	7641 ± 727a	2656 ± 176b	25.4 ± 0.4b	27.8 ± 0.4a
	Root	E-	12926 ± 443a	4282 ± 738a	—	—
		E+	9457 ± 197b	2935 ± 503b	26.8 ± 1.1b	31.4 ± 0.9a
Wheat	Shoot	E-	6662 ± 1076a	3056 ± 299a	—	—
		E+	4596 ± 631a	1940 ± 171b	30.5 ± 1.8b	36.4 ± 0.6a
	Root	E-	6123 ± 316a	3573 ± 234a	—	—
		E+	4758 ± 274b	2614 ± 172b	22.3 ± 0.9b	26.9 ± 0.4a
Maize	Shoot	E-	5383 ± 434a	2222 ± 137a	—	—
		E+	4677 ± 296a	1756 ± 88b	12.9 ± 1.5b	20.9 ± 1.0a
	Root	E-	4523 ± 174a	2357 ± 292a	—	—
		E+	3885 ± 160a	1932 ± 235b	14.1 ± 0.4b	18.0 ± 0.3a

Values are given as mean ± SE of three independent biological replicates. Different letters indicates indicate significantly differences in δ15N value inoculated (E+) and un-inoculated (E-) plants according to the LSD test ($P < 0.05$); Different letters indicate significantly differences in %Ndfa between high N and low N according to the LSD test ($P < 0.05$); $\delta^{15}N$ value: percent atom excess ^{15}N; %Ndfa: percent N derived from atmosphere.

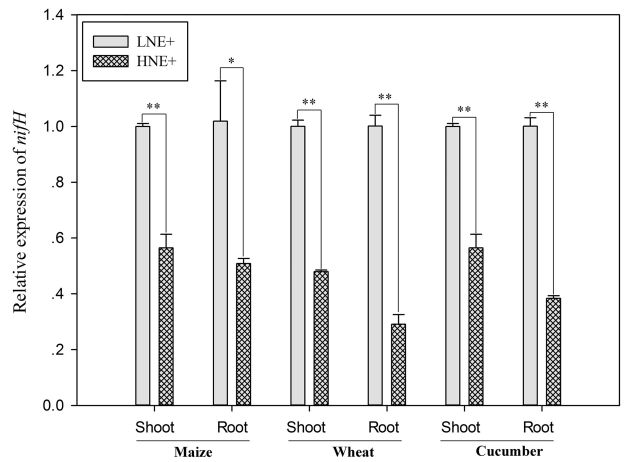

FIGURE 6 | The *nifH* transcript levels of *P. beijingensis* BJ-18 in shoots and roots of wheat, maize and cucumber seedlings inoculated with *P. beijingensis* BJ-18 under high N (HN) and low N (LN) levels. Values are given as mean of three independent biological replicates, and single asterisks or double asterisks (* or **) indicate significant differences between HNE+ and LNE+ treatments determined by LSD at $P < 0.05$ or $P < 0.01$. The bars represent the standard error. LNE+ indicates plants grown in low N level of soils and inoculated with *P. beijingensis* BJ-18; HNE+ indicates plants grown in high N level of soils and inoculated with *P. beijingensis* BJ-18.

in the inoculated plant shoots and roots under low N were significantly higher than those under high N, consistent with the concentrations of *P. beijingensis* cells. It was well known that *nif* gene expression was inhibited by high concentrations of NH_4^+ (Dixon and Kahn, 2004). GlnR mediated positive and negative regulation of *nif* gene expression in *P. polymyxa* WLY78 according to N availably (Wang et al., 2018). As mentioned above, there were high concentrations of NH_4^+ in plants under high N. Thus, *P. beijingensis* cells in plant tissues sensed the N signal and then regulated *nifH* expression according to change of N levels. The expression of *nif* gene of *Herbaspirillum seropedicae* in maize, sorghum, wheat, and rice plants was reported (Roncato-Maccari et al., 2003). Similar report was found that N fertilizer application inhibited *nifH* gene expression of the endophytic diazotroph in sugarcane leaves (Jia Hui et al., 2017).

An important metric to evaluate the role of diazotrophic bacteria is whether they can provide fixed N_2 to the host plant. The ^{15}N isotope dilution analysis has been widely applied to quantify BNF in non-legume plant species such as rice inoculated with *Herbaspirillum seropedicae* Z67 (James et al., 2002), wheat with *Azospirillum brasilense* Wa5 (Christiansenweniger and Vanveen, 1991), Kallar grass with *Azoarcus* sp. BH72 (Hurek et al., 2002) and maize with *P. polymyxa* P2b-2R (Puri et al., 2015). Here, ^{15}N isotope enrichment analysis method was used to estimate the contribution of BNF by *P. beijingensis* BJ-18 inoculation to plants. The BNF rates in the three different plants were higher under low N level than under high N level, indicating that BNF was affected by N levels. The data were consistent with the *nif* gene expression and the concentrations of *P. beijingensis* BJ-18 within the plant tissues under different N levels. Similar results were reported that sugarcane plants inoculated with diazotrophic strains gained higher N from BNF in the N-deficient soil (de Oliveira et al., 2003). This study also revealed that wheat gained the highest N from BNF under both low N and high N levels, followed by cucumber and then by maize, suggesting that BNF rate was related to host plant species. The shoots and roots of palm inoculated with *Bacillus sphaericus* UPMB-10 gained 13.2–13.4% N from BNF (Zakry et al., 2012), which was lower than that gained by inoculation with *P. beijingensis* BJ-18.

In this study, the effects of *P. beijingensis* BJ-18 inoculation on plant N uptake and metabolism were investigated. The

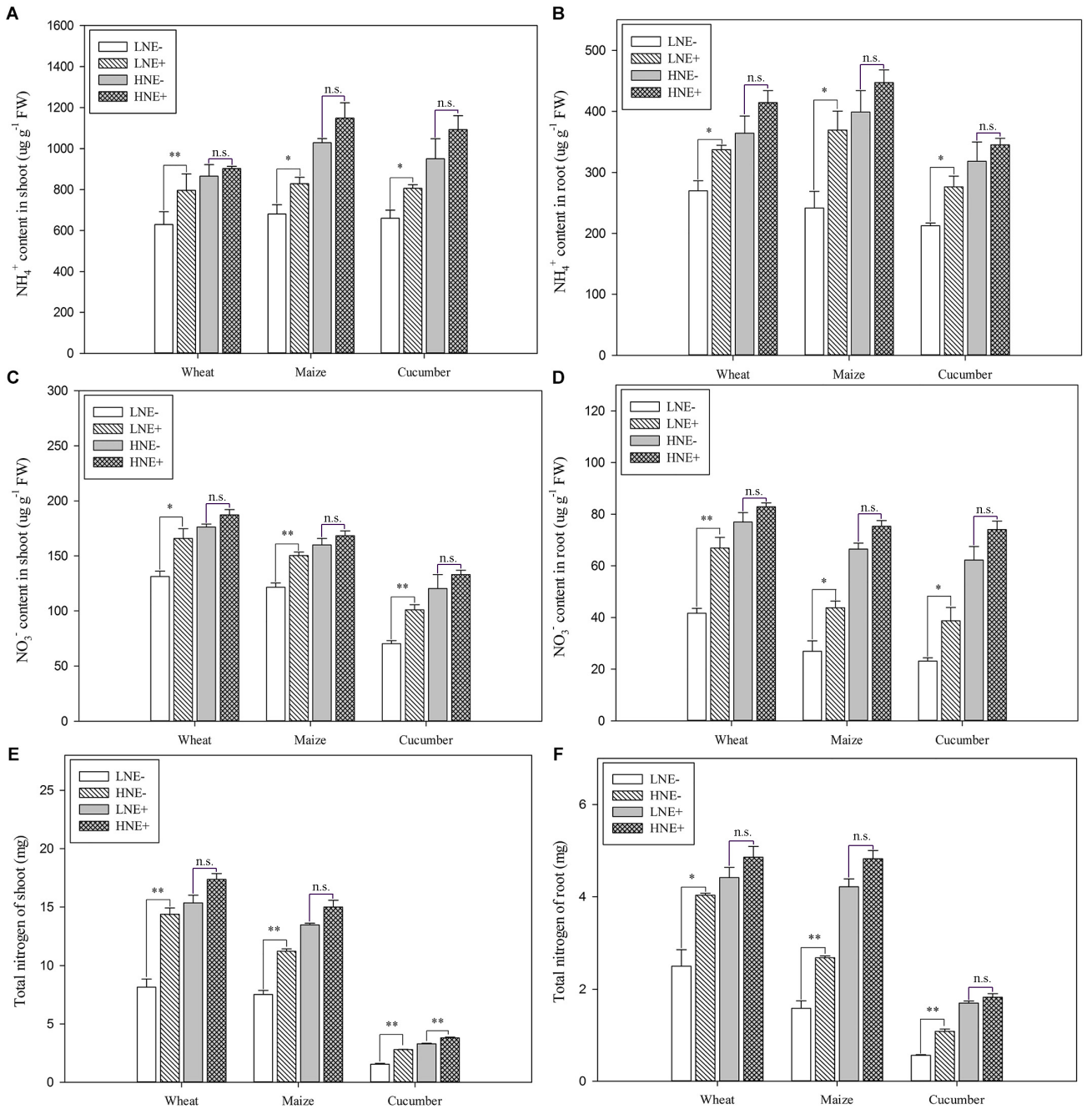

FIGURE 7 | Ammonium (NH_4^+) (**A**: shoot; **B**: root), nitrate (NO_3^-) (**C**: shoot; **D**: root) and total N (**E**: shoot; **F**: root) content in shoots and roots of wheat, maize and cucumber seedlings inoculated with *P. beijingensis* BJ-18 under high N (HN) and low N (LN) levels. Values are given as mean of three independent biological replicates, and single asterisks or double asterisks (* or **) indicate significant differences between inoculated (E+) and un-inoculated (E-) plants determined by LSD at $P < 0.05$ or $P < 0.01$. The bars represent the standard error. LNE- indicates plants grown in low N level of soil and un-inoculated with *P. beijingensis* BJ-18; LNE+ indicates plants grown in low N level of soils and inoculated with *P. beijingensis* BJ-18; HNE- indicates plants grown in high N level of soil and un-inoculated with *P. beijingensis* BJ-18; HNE+ indicates plants grown in high N level of soils and inoculated with *P. beijingensis* BJ-18.

concentrations of NO_3^-, NH_4^+ and total N were higher in roots and shoots of inoculated plants than in un-inoculated plants, and were higher in roots than in shoots. The positive effects were also controlled by soil N status. The results indicated that inoculation with *P. beijingensis* BJ-18 promoted plants to uptake NO_3^- and NH_4^+ from soil. The increased concentrations of NH_4^+ and total N in inoculated plants were at least partially resulted from BNF. Studies on the effects of diazotrophs on plant N uptake and metabolism were rare. However, inoculations with some endophytic fungi significantly

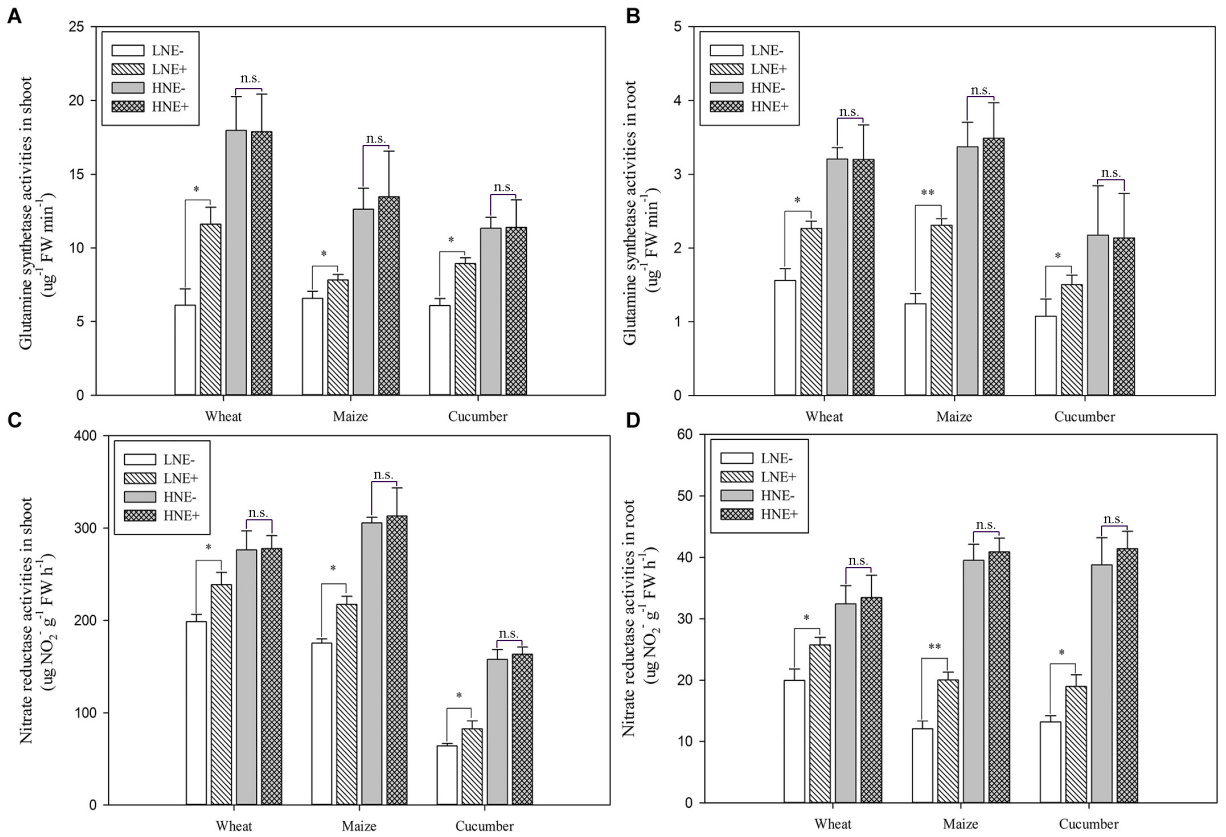

FIGURE 8 | Glutamine synthetase (GS) (**A**: shoot; **B**: root) and Nitrate reductase (NR) (**C**: shoot; **D**: root) activities in shoots and roots of wheat, maize, and cucumber seedling inoculated with *P. beijingensis* BJ-18 under high N (HN) and low (LN) levels. Values are given as mean of three independent biological replicates, and single asterisks or double asterisks (* or **) indicate significant differences between inoculated (E+) and un-inoculated (E-) plants determined by LSD at $P < 0.05$ or $P < 0.01$. The bars represent the standard error. LNE- indicates plants grown in low N level of soil and un-inoculated with *P. beijingensis* BJ-18; LNE+ indicates plants grown in low N level of soils and inoculated with *P. beijingensis* BJ-18; HNE- indicates plants grown in high N level of soil and un-inoculated with *P. beijingensis* BJ-18; HNE+ indicates plants grown in high N level of soils and inoculated with *P. beijingensis* BJ-18.

improved N accumulation and metabolism were observed in rice (Yang et al., 2014), sugar beet (Shi et al., 2009), and tall fescue (Lyons et al., 1990).

NO_3^- was mainly absorbed via NRT protein family members, and then transformed into NH_4^+ by NR. In this study, *P. beijingensis* BJ-18-inoculated plants showed significantly higher expression levels of *NRT* genes (*CsNRT1.3* and *CsNRT2.2* in cucumber; *TaNRT1.1*, *TaNRT2.1*, and *TaNRT2.3* in wheat; *ZmNRT2.1* in maize) in both shoots and roots under low N condition. Similar reports were found that under low N condition *NRT* genes were significantly up-regulated in rice inoculated with endophytic fungus *Phomopsis liquidambari* (Yang et al., 2014) and in tomato inoculated with diazotrophic *Enterobacter radicincitans* (Berger et al., 2013).

Higher NR activities were observed in the *P. beijingensis* BJ-18-inoculated plants. It was reported that inoculation with endophytic fungus *Plectosphaerella cucumerina* F11 greatly increased the activity of NR in sugar beet (Shi et al., 2009). To investigate whether the changes of NR activities in the *P. beijingensis* BJ-18- inoculated plants were closely related to differential expression of plant *NR* genes, the expression levels of *NR* genes were quantified. qRT-PCR analysis indicated that the expression levels of *NR* genes (*CsNR2* in cucumber, *TaNR* in wheat and *ZmNR* in maize) were significantly higher in inoculated plants than in un-inoculated plants under low N. It was reported that the endophytic fungus *Piriformospora indica* inoculation promoted N accumulation in *Arabidopsis* and tobacco seedlings by inducing the expression of *NR* (Sherameti et al., 2005). In contrast, endophytic fungus *Phomopsis liquidambari* inoculation significantly reduced NO_3^- concentration in rice shoots under low N condition, since the higher NR activity made more NO_3^- to be transformed into NH_4^+ (Yang et al., 2014).

This study demonstrated that *P. beijingensis* BJ-18-inoculated plants showed higher NH_4^+ concentration in roots and shoots, compared with those in un-inoculated plants. NH_4^+ was absorbed via AMT protein family members mainly, and then transformed into organic molecules by GS and GOGAT. GS is an important rate-limiting enzyme in NH_4^+ assimilation. The higher GS activities were observed in the *P. beijingensis* BJ-18-inoculated plants than those in un-inoculated plants. GS activities were closely related to soil N status. Transcript levels of

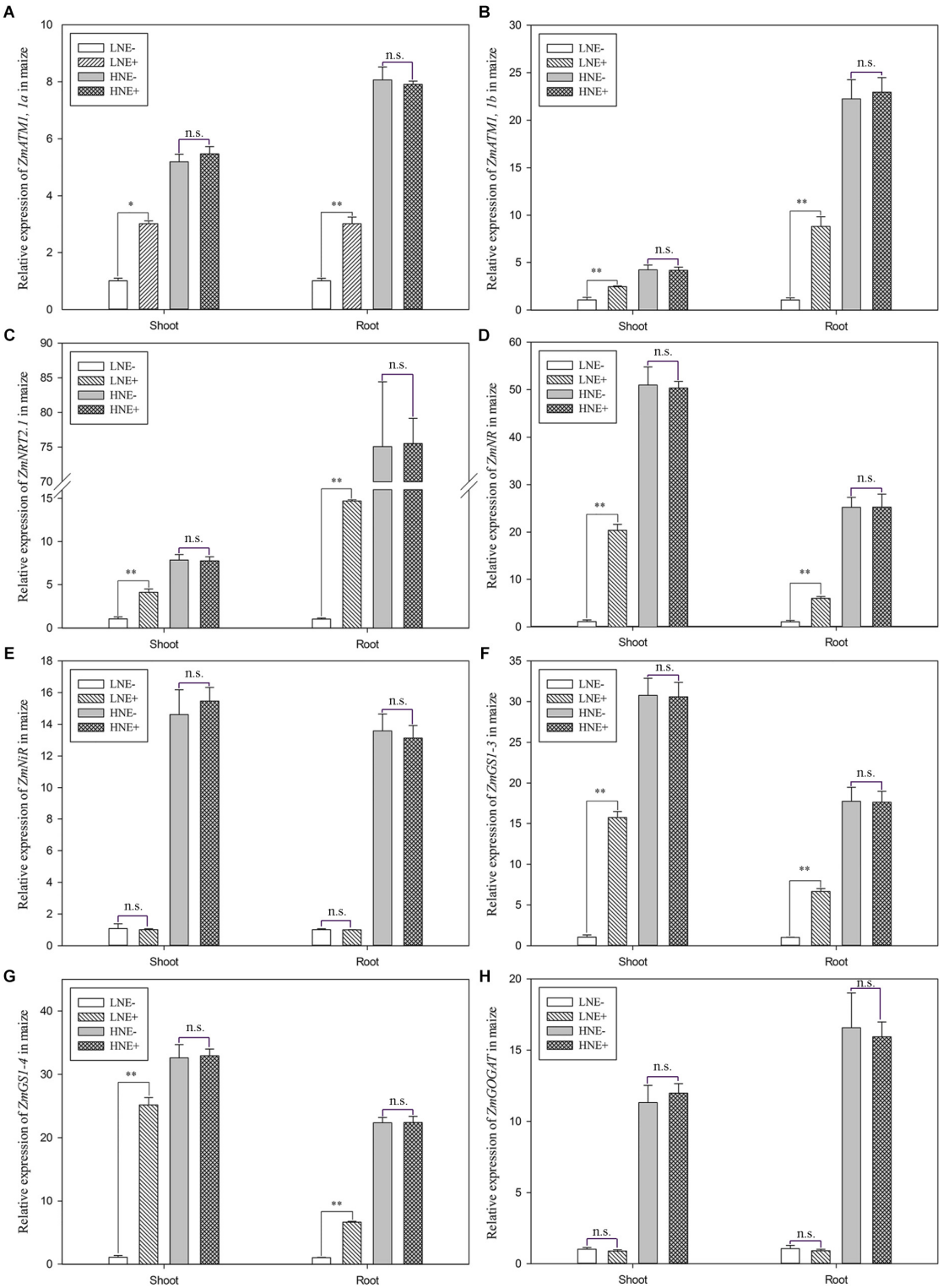

FIGURE 9 | The transcript levels of genes involved N uptake (**A**: *ZmAMT1, 1a*; **B**: *ZmAMT1, 1b*; **C**: *Zm NRT2.1*) and assimilation (**D**: *ZmNR*; **E**: *ZmNiR*; **F**: *ZmGS1-3*; **G**: *ZmGS-4*; **H**: *ZmGOGAT*) in shoots and roots of maize seedlings inoculated with *P. beijingensis* BJ-18 under high N (HN) and low N (LN) levels. Values are given as mean of three independent biological replicates, and single asterisks or double asterisks (* or **) indicate significant differences between inoculated (E+) and un-inoculated (E-) plants determined by LSD at $P < 0.05$ or $P < 0.01$. The bars represent the standard error. LNE- indicates plants grown in low N level of soil and un-inoculated with *P. beijingensis* BJ-18; LNE+ indicates plants grown in low N level of soils and inoculated with *P. beijingensis* BJ-18; HNE- indicates plants grown in high N level of soil and un-inoculated with *P. beijingensis* BJ-18; HNE+ indicates plants grown in high N level of soils and inoculated with *P. beijingensis* BJ-18.

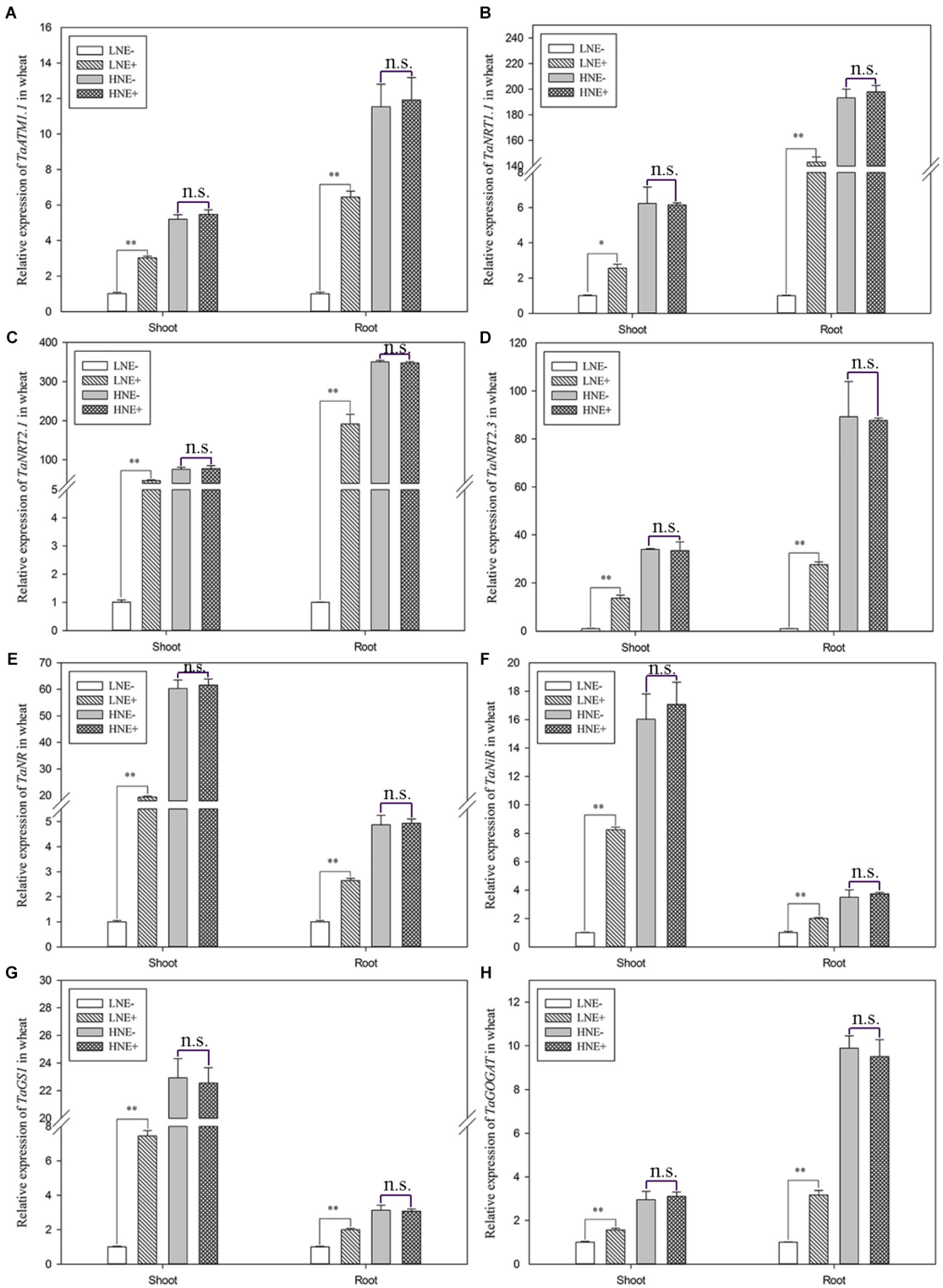

FIGURE 10 | Transcript levels of genes involved N uptake (**A**: *TaAMT1.1*; **B**: *TaNRT1.1*; **C**: *TaNRT2.1*; **D**: *TaNRT2.3*) and assimilation (**E**: *TaNR*; **F**: *TaNiR*; **G**: *TaGS1*; **H**: *TaGOGAT*) in shoots and roots of wheat seedlings inoculated with *P. beijingensis* BJ-18 under high N (HN) and low N (LN) levels. Values are given as mean of three independent biological replicates, and single asterisks or double asterisks (* or **) indicate significant differences between inoculated (E+) and un-inoculated (E-) plants determined by LSD at $P < 0.05$ or $P < 0.01$. The bars represent the standard error. LNE- indicates plants grown in low N level of soil and un-inoculated with *P. beijingensis* BJ-18; LNE+ indicates plants grown in low N level of soils and inoculated with *P. beijingensis* BJ-18; HNE- indicates plants grown in high N level of soil and un-inoculated with *P. beijingensis* BJ-18; HNE+ indicates plants grown in high N level of soils and inoculated with *P. beijingensis* BJ-18.

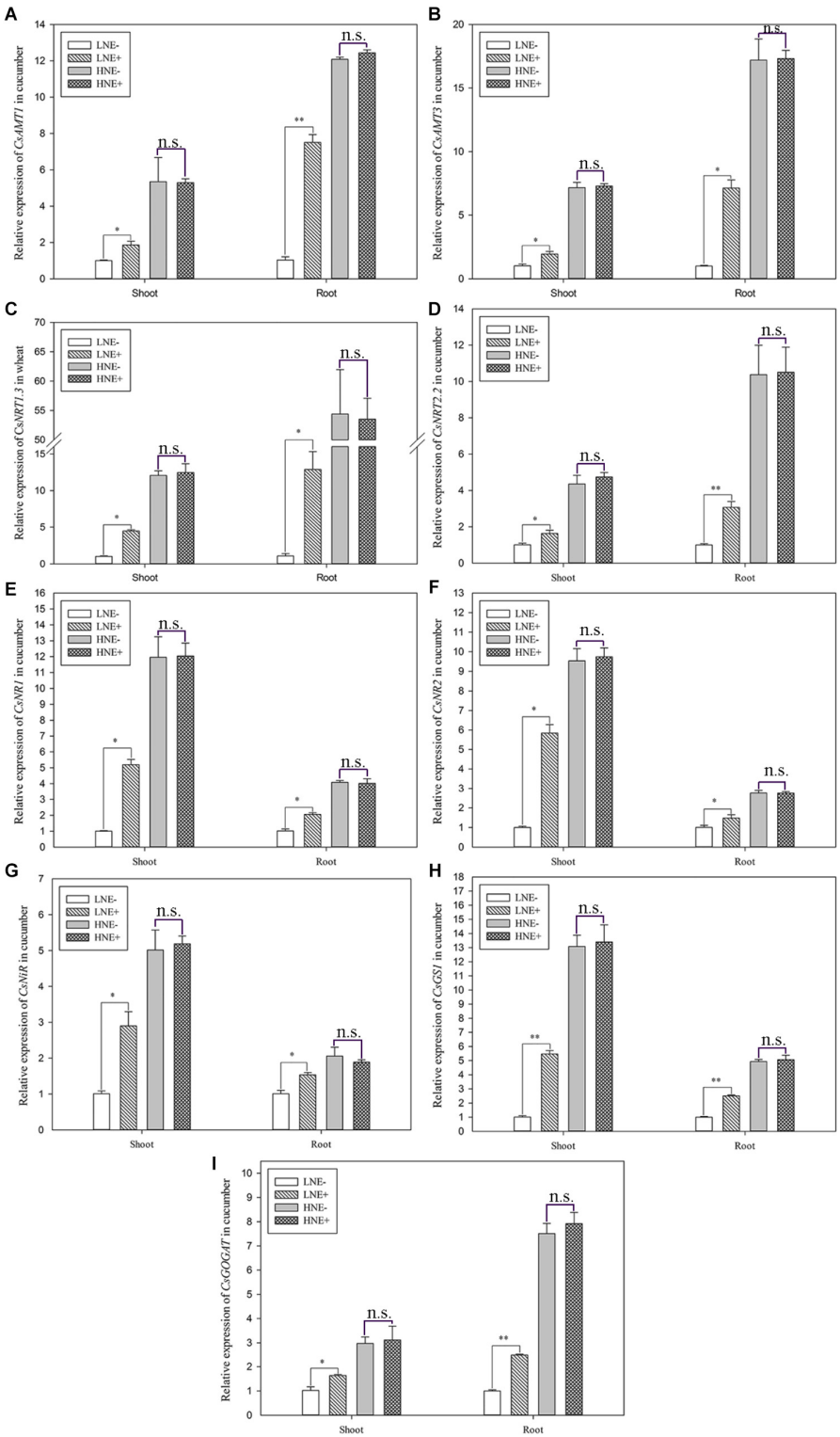

FIGURE 11 | The transcript levels of genes involved N uptake (**A**: *CsAMT1*; **B**: *CsAMT3*; **C**: *CsNRT1.3*; **D**: *CsNRT2.2*) and assimilation (**E**: *CsNR1*; **F**: *CsNR2*; **G**: *CsNiR*; **H**: *CsGS1*; **I**: *CsGOGAT*) in shoots and roots of cucumber seedlings inoculated with *P. beijingensis* BJ-18 under high N (HN) and low N (LN) levels. Values are given as mean of three independent biological replicates, and single asterisks or double asterisks (* or **) indicate significant differences between inoculated (E+) and un-inoculated (E-) plants determined by LSD at $P < 0.05$ or $P < 0.01$. The bars represent the standard error. LNE- indicates plants grown in low N level of soil and un-inoculated with *P. beijingensis* BJ-18; LNE+ indicates plants grown in low N level of soils and inoculated with *P. beijingensis* BJ-18; HNE- indicates plants grown in high N level of soil and un-inoculated with *P. beijingensis* BJ-18; HNE+ indicates plants grown in high N level of soils and inoculated with *P. beijingensis* BJ-18.

GS genes were also measured to confirm whether the changes of GS activities in plants caused by *P. beijingensis* BJ-18 inoculation were related to *GS* genes transcription. qRT-PCR indicated that the higher expression levels of *GS* genes (*CsGS1*, *TaGS1*, *ZmGS1-3*, and *ZmGS1-4*) in inoculated plant tissues than in un-inoculated ones under low N. Similarly, it was also reported that the expression levels of *GS* genes were also significantly higher in inoculated plants with the endophytic fungus *P. liquidambari* than in un-inoculated plants under low N (Yang et al., 2014).

This study demonstrated that inoculation with *P. beijingensis* BJ-18 promoted dry weight of plant roots and shoots grown under low N to be increased by 20.3–103.6%. The current results were in agreement with previous reports that inoculation with *P. beijingensis* BJ-18 increased wheat yield by 26.9% in field experiment (Shi et al., 2016) and increased tomato shoot length, fresh weight, and dry weight in the pot experiments (Xie et al., 2016).

The plant-growth-promoting rhizobacteria facilitate plant growth by several direct and indirect mechanisms. Direct mechanisms include P solubilization, N fixation and hormone (e.g., IAA, cytokinins and gibberellins) production. Indirect mechanisms include controlling phytopathogens by producing antibiotics or lytic enzymes (Glick, 2012). As mentioned above, *P. beijingensis* BJ-18 provided N for plants by BNF and thus promoted plant growth. Also, this bacterium may promote plant growth by producing IAA and antimicrobial compounds (Xie et al., 2016). Compared to *A. brasilense* Yu62 which produced high amount of IAA, *P. beijingensis* BJ-18 produced a little amount of IAA. Thus, IAA produced by *P. beijingensis* BJ-18 might be not the major factor promoting plant growth. Since the soil used in greenhouse study was not sterile, the BNF/plant growth promotion observed in this study could have been in part due to one or several indigenous microbes present in that soil. This study for the first time revealed that *P. beijingensis* BJ-18 promoted plants to uptake N from soil and enhanced gene expression and enzyme activities involved in N uptake and assimilation in plants. In addition to BNF, these endogenous changes in plants induced by *P. beijingensis* BJ-18 might be another major factor promoting plant growth.

CONCLUSION

This study demonstrated that *P. beijingensis* BJ-18 was an effective and endophytic diazotrophic bacterium which has similar colonization patterns in monocotylous and dicotyledonous plants. This bacterium promoted plant growth by direct mechanisms through BNF. Also, this bacterium might promote plant growth by indirect mechanisms through inducing endogenous changes in plants, including enhancement of N uptake and enzyme activities, and expression of N uptake and assimilation genes. The bacterial density within plant was closely related to the BNF efficiency and the endogenous changes in plants. However, the bacterial density, the BNF efficiency and the endogenous changes in plants during the association with *P. beijingensis* BJ-18 were controlled by the soil N status. These data suggested that successful colonization of *P. beijingensis* BJ-18 on plant was the first key step for this bacterium to promote plant growth by BNF and by inducing endogenous changes in plants. How soil N level affects bacterial colonization deserves further study.

AUTHOR CONTRIBUTIONS

YbL and SC designed and wrote the manuscript. YbL, YlL, HZ, and MW conducted the experiments.

FUNDING

This work was funded by the National Key Research and Development Program of China (No. 2017YFD0200807) and by National Nature Science Foundation of China (Grant No. 31770083).

ACKNOWLEDGMENTS

We would like to thank Caixia Wang for helping in writing early manuscript.

REFERENCES

Anand, R., and Chanway, C. P. (2013). Detection of GFP-labeled *Paenibacillus polymyxa* in autofluorescing pine seedling tissues. *Biol. Fert. Soils* 49, 111–118. doi: 10.1007/s00374-012-0727-9

Baldani, V. L. D., Baldani, J. I., and Dobereiner, J. (2000). Inoculation of rice plants with the endophytic diazotrophs *Herbaspirillum seropedicae* and *Burkholderia* spp. *Biol. Fert. Soils* 30, 485–491. doi: 10.1007/s003740050027

Berger, B., Brock, A. K., and Ruppel, S. (2013). Nitrogen supply influences plant growth and transcriptional responses induced by *Enterobacter radicincitans* in *Solanum lycopersicum*. *Plant Soil* 370, 641–652. doi: 10.1007/s11104-013-1633-0

Bloom, A. J., Sukrapanna, S. S., and Warner, R. L. (1992). Root respiration associated with ammonium and nitrate absorption and assimilation by barley. *Plant Physiol.* 99, 1294–1301. doi: 10.1104/pp.99.4.1294

Boddey, R. M., Baldani, V. L., Baldani, J. I., and Dobereiner, J. (1986). Effect of inoculation of *Azospirillum* spp. on nitrogen accumulation by field-grown wheat. *Plant Soil* 95, 109–121. doi: 10.1007/bf02378857

Boddey, R. M., and Knowles, R. (1987). Methods for quantification of nitrogen fixation associated with gramineae. *Crit. Rev. Plant Sci.* 6, 209–266. doi: 10.1080/07352688709382251

Boddey, R. M., Oliveira, O. C. D., Urquiaga, S., Reis, V. M., Olivares, F. L. D., Baldani, V. L. D., et al. (1995). Biological nitrogen fixation associated with sugar cane and rice: contributions and prospects for improvement. *Plant Soil* 174, 195–209. doi: 10.1007/BF00032247

Carvalho, T. L., Balsemao-Pires, E., Saraiva, R. M., Ferreira, P. C., and Hemerly, A. S. (2014). Nitrogen signalling in plant interactions with associative and endophytic diazotrophic bacteria. *J. Exp. Bot.* 65, 5631–5642. doi: 10.1093/jxb/eru319

Christiansenweniger, C., and Vanveen, J. A. (1991). NH4+-excreting *Azospirillum brasilense* mutants enhance the nitrogen supply of a wheat host. *Appl. Environ. Microb.* 57, 3006–3012.

de Oliveira, A. L. M., Canuto, E. D., Reis, V. M., and Baldani, J. I. (2003). Response of micropropagated sugarcane varieties to inoculation with endophytic diazotrophic bacteria. *Braz. J. Microbiol.* 34, 59–61. doi: 10.1590/s1517-83822003000500020

Dixon, R., and Kahn, D. (2004). Genetic regulation of biological nitrogen fixation. *Nat. Rev. Microbiol.* 2, 621–631. doi: 10.1038/nrmicro954

Eckhardt, W., Bellmann, K., and Kolb, H. (1999). Regulation of inducible nitric oxide synthase expression in β cells by environmental factors: heavy metals. *Biochem. J.* 338(Pt 3), 695-700. doi: 10.1042/bj3400871u

Fuentes-Ramirez, L. E., Caballero-Mellado, J., Sepulveda, J., and Martinez-Romero, E. (1999). Colonization of sugarcane by *Acetobacter diazotrophicus* is inhibited by high N-fertilization. *FEMS Microbiol. Ecol.* 29, 117–128. doi: 10.1111/j.1574-6941.1999.tb00603.x

Galli, V., Messias, R. D., Silva, S., and Rombaldi, C. V. (2013). Selection of reliable reference genes for quantitative real-time polymerase chain reaction studies in maize grains. *Plant Cell Rep.* 32, 1869–1877. doi: 10.1007/s00299-013-1499-x

Galloway, J. N., Townsend, A. R., Erisman, J. W., Bekunda, M., Cai, Z., Freney, J. R., et al. (2008). Transformation of the nitrogen cycle: recent trends, questions, and potential solutions. *Science* 320, 889–892. doi: 10.1126/science.1136674

Glick, B. R. (2012). Plant growth-promoting bacteria: mechanisms and applications. *Scientifica* 2012:963401. doi: 10.6064/2012/963401

Gordon, S. A., Fleck, A., and Bell, J. (1978). Optimal conditions for the estimation of ammonium by the berthelot reaction. *Ann. Clin.Biochem.* 15, 270–275.

Grady, E. N., Macdonald, J., Liu, L., Richman, A., and Yuan, Z. C. (2016). Current knowledge and perspectives of *Paenibacillus:* a review. *Microb. Cell Fact.* 15:203. doi: 10.1186/s12934-016-0603-7

Gupta, V., Roper, M. M., and Roget, D. K. (2006). Potential for non-symbiotic N2-fixation in different agroecological zones of southern Australia. *Aust. J. Soil Res.* 44, 343–354. doi: 10.1071/sr05122

Hao, T., and Chen, S. (2017). Colonization of wheat, maize and cucumber by *Paenibacillus polymyxa* WLY78. *PLoS One* 12:e0169980. doi: 10.1371/journal.pone.0169980

Hurek, T., Handley, L. L., Reinhold-Hurek, B., and Piche, Y. (2002). *Azoarcus* grass endophytes contribute fixed nitrogen to the plant in an unculturable state. *Mol. Plant Microbe Interact.* 15, 233–242. doi: 10.1094/mpmi.2002.15.3.233

James, E. K., Gyaneshwar, P., Mathan, N., Barraquio, Q. L., Reddy, P. M., Iannetta, P. P. M., et al. (2002). Infection and colonization of rice seedlings by the plant growth-promoting bacterium *Herbaspirillum seropedicae* Z67. *Mol. Plant Microbe Interact.* 15, 894–906. doi: 10.1094/mpmi.2002.15.9.894

James, E. K., Olivares, F. L., De Oliveira, A. L. M., Dos Reis, F. B., Da Silva, L. G., and Reis, V. M. (2001). Further observations on the interaction between sugar cane and *Gluconacetobacter diazotrophicus* under laboratory and greenhouse conditions. *J. Exp. Bot.* 52, 747–760. doi: 10.1093/jexbot/52.357.747

Jia Hui, L. I., Yuan, D., Jian Ming, L. U., Yang, L. T., Yang Rui, L. I., Xing, Y. X., et al. (2017). Effects of nitrogen fertilizer on the expression of nifH gene of endophytic azotobacter in sugarcane leaves. *Biotechnol. Bull.* 33, 100–106. doi: 10.13560/j.cnki.biotech.bull.1985.20170002

Ke, X., Feng, S., Wang, J., Lu, W., Zhang, W., Chen, M., et al. (2018). Effect of inoculation with nitrogen-fixing bacterium *Pseudomonas stutzeri* A1501 on maize plant growth and the microbiome indigenous to the rhizosphere. *Sys. Appl. Microbiol.* 42, 248–260. doi: 10.1016/j.syapm.2018.10.010

Kloepper, J. W., and Beauchamp, C. J. (1992). A review of issues related to measuring colonization of plant-roots by bacteria. *Can. J. Microbiol.* 38, 1219–1232. doi: 10.1139/m92-202

Lea, P. J., and Miflin, B. J. (2003). Glutamate synthase and the synthesis of glutamate in plants. *Plant Physiol. Bioch.* 41, 555–564. doi: 10.1016/s0981-9428(03)00060-3

Liu, G. S., Ji, Y. Y., Bhuiyan, N. H., Pilot, G., Selvaraj, G., Zou, J. T., et al. (2010). Amino acid homeostasis modulates salicylic acid-associated redox status and defense responses in *Arabidopsis*. *Plant Cell* 22, 3845–3863. doi: 10.1105/tpc.110.079392

Liu, H., Carvalhais, L. C., Crawford, M., Singh, E., Dennis, P. G., Pieterse, C. M. J., et al. (2017). Inner Plant values: diversity, colonization and benefits from endophytic bacteria. *Front. Microbiol.* 8:2552. doi: 10.3389/fmicb.2017.02552

Liu, Y., Chen, S. F., and Li, J. L. (2003). Colonization pattern of *Azospirillum brasilense* Yu62 on maize roots. *Acta Bot. Sin.* 45, 748–752.

Livak, K. J., and Schmittgen, T. D. (2001). Analysis of relative gene expression data using real-time quantitative PCR and the 2(-Delta Delta C(T)) Method. *Methods* 25, 402–408. doi: 10.1006/meth.2001.1262

Lyons, P. C., Evans, J. J., and Bacon, C. W. (1990). Effects of the fungal endophyte *Acremonium coenophialum* on nitrogen accumulation and metabolism in tall fescue. *Plant Physiol.* 92, 726–732. doi: 10.1104/pp.92.3.726

Magnani, G. S., Didonet, C. M., Cruz, L. M., Picheth, C. F., Pedrosa, F. O., and Souza, E. M. (2010). Diversity of endophytic bacteria in Brazilian sugarcane. *Genet. Mol. Res.* 9, 250–258. doi: 10.4238/vol9-1gmr703

Mirza, M. S., Ahmad, W., Latif, F., Haurat, J., Bally, R., Normand, P., et al. (2001). Isolation, partial characterization, and the effect of plant growth-promoting bacteria (PGPB) on micro-propagated sugarcane in vitro. *Plant Soil* 237, 47–54.

Moloudi, F., Navabpour, S., Soltanloo, H., Ramazanpour, S. S., and Sadeghipour, H. (2013). Catalase and metallothionein genes expression analysis in wheat cultivars under drought stress condition. *J. Plant Mol. Breed.* 1, 54–68.

Monteiro, R. A., Balsanelli, E., Wassem, R., Marin, A. M., Brusamarello-Santos, L. C. C., Schmidt, M. A., et al. (2012). *Herbaspirillum*-plant interactions: microscopical, histological and molecular aspects. *Plant Soil* 356, 175–196. doi: 10.1007/s11104-012-1125-7

Murashige, T., and Skoog, F. (1962). A revised medium for rapid growth and bio assays with tobacco tissue cultures. *Physiol. Plant.* 15, 473–497.

Oliveira, I. C., Brears, T., Knight, T. J., Clark, A., and Coruzzi, G. M. (2002). Overexpression of cytosolic glutamine synthetase. Relation to nitrogen, light, and photorespiration. *Plant Physiol* 129, 1170–1180. doi: 10.1104/pp.020013

Puri, A., Padda, K. P., and Chanway, C. P. (2015). Can a diazotrophic endophyte originally isolated from lodgepole pine colonize an agricultural crop (corn) and promote its growth? *Soil Biol. Biochem.* 89, 210–216. doi: 10.1016/j.soilbio.2015.07.012

Rasmussen, S., Parsons, A. J., Bassett, S., Christensen, M. J., Hume, D. E., Johnson, L. J., et al. (2007). High nitrogen supply and carbohydrate content reduce fungal endophyte and alkaloid concentration in *Lolium perenne*. *New Phytol.* 173, 787–797. doi: 10.1111/j.1469-8137.2006.01960.x

Reinhold-Hurek, B., and Hurek, T. (1998). Life in grasses: diazotrophic endophytes. *Trends Microbiol.* 6, 202–202. doi: 10.1016/s0966-842x(98)01277-3

Reinhold-Hurek, B., and Hurek, T. (2011). Living inside plants: bacterial endophytes. *Curr. Opin. Plant Biol.* 14, 435–443. doi: 10.1016/j.pbi.2011.04.004

Roncato-Maccari, L. D. B., Ramos, H. J. O., Pedrosa, F. O., Alquini, Y., Chubatsu, L. S., Yates, M. G., et al. (2003). Endophytic *Herbaspirillum seropedicae* expresses nif genes in gramineous plants. *FEMS Microbiol. Ecol.* 45, 39–47. doi: 10.1016/s0168-6496(03)00108-9

Seifi, H. S., Van Bockhaven, J., Angenon, G., and Hofte, M. (2013). Glutamate metabolism in plant disease and defense: friend or foe? *Mol. Plant Microbe Interact.* 26, 475–485. doi: 10.1094/mpmi-07-12-0176-cr

Sherameti, I., Shahollari, B., Venus, Y., Altschmied, L., Varma, A., and Oelmuller, R. (2005). The endophytic fungus *Piriformospora indica* stimulates the expression of nitrate reductase and the starch-degrading enzyme glucan-water dikinase in tobacco and *Arabidopsis* roots through a homeodomain transcription factor that binds to a conserved motif in their promoters. *J. Biol. Chem.* 280, 26241–26247. doi: 10.1074/jbc.M500447200

Shi, H., Li, Y., Li, P., Wang, Z., and Chen, S. (2016). Effect of nitrogen-fixing *Paenibacillus* spp. on wheat yield. *J. China Agric. Univ.* 21, 52–55.

Shi, Y., Lou, K., and Li, C. (2009). Effects of endophytic fungus on sugar content and key enzymes activity in nitrogen and sugar metabolism of sugar beet (*Beta vulgaris* L.). *Acta Agronomica Sinica* 35, 946–951.

Snoeijers, S. S., Perez-Garcia, A., Joosten, M., and De Wit, P. (2000). The effect of nitrogen on disease development and gene expression in bacterial and fungal plant pathogens. *Eur. J. Plant Pathol.* 106, 493–506. doi: 10.1023/a:1008720704105

Sugiura, M., Georgescu, M. N., and Takahashi, M. (2007). A nitrite transporter associated with nitrite uptake by higher plant chloroplasts. *Plant Cell Physiol.* 48, 1022–1035. doi: 10.1093/pcp/pcm073

Van Deynze, A., Zamora, P., Delaux, P.-M., Heitmann, C., Jayaraman, D., Rajasekar, S., et al. (2018). Nitrogen fixation in a landrace of maize is supported by a mucilage-associated diazotrophic microbiota. *PLoS Biol.* 16:e2006352. doi: 10.1371/journal.pbio.2006352

Wang, L. Y., Li, J., Li, Q. X., and Chen, S. F. (2013). *Paenibacillus beijingensis* sp nov., a nitrogen-fixing species isolated from wheat rhizosphere soil. *Antonie Van Leeuwenhoke* 104, 675–683. doi: 10.1007/s10482-013-9974-5

Wang, T. S., Zhao, X. Y., Shi, H. W., Sun, L., Li, Y. B., Li, Q., et al. (2018). Positive and negative regulation of transferred nif genes mediated by indigenous GlnR in Gram-positive *Paenibacillus* polymyxa. *PLoS Genet.* 14:24. doi: 10.1371/journal.pgen.1007629

Wei, L., Deng, X.-G., Zhu, T., Zheng, T., Li, P.-X., Wu, J.-Q., et al. (2015). Ethylene is involved in brassinosteroids induced alternative respiratory pathway

in cucumber (*Cucumis sativus* L.) seedlings response to abiotic stress. *Front. Plant Sci.* 6:982. doi: 10.3389/fpls.2015.00982

Xie, J., Shi, H., Du, Z., Wang, T., Liu, X., and Chen, S. (2016). Comparative genomic and functional analysis reveal conservation of plant growth promoting traits in *Paenibacillus polymyxa* and its closely related species. *Sci. Rep.* 6:21329. doi: 10.1038/srep21329

Yang, B., Wang, X. M., Ma, H. Y., Jia, Y., Li, X., and Dai, C. C. (2014). Effects of the fungal endophyte *Phomopsis liquidambari* on nitrogen uptake and metabolism in rice. *Plant Growth Regul.* 73, 165–179. doi: 10.1007/s10725-013-9878-4

Yu, X. Z., and Zhang, F. Z. (2012). Activities of nitrate reductase and glutamine synthetase in rice seedlings during cyanide metabolism. *J. Hazard. Mater.* 22, 190–194. doi: 10.1016/j.jhazmat.2012.05.027

Zakry, F. A. A., Shamsuddin, Z. H., Abdul Rahim, K., Zawawi Zakaria, Z., and Abdul Rahim, A. (2012). Inoculation of *Bacillus sphaericus* UPMB-10 to young oil palm and measurement of its uptake of fixed nitrogen using the 15N isotope dilution technique. *Microbes Environ.* 27, 257–262. doi: 10.1264/jsme2.ME11309

Zhang, W., Ding, Y., Yao, L., Liu, K., and Du, B. (2013). Construction of gene knock-out system for *Paenibacillus* polymyxa SC2. *Wei Sheng Wu Xue Bao* 53, 1258–1266.

Conflict of Interest Statement: The authors declare that the research was conducted in the absence of any commercial or financial relationships that could be construed as a potential conflict of interest.

frontiers in Microbiology

MINI REVIEW
published: 04 June 2019
doi: 10.3389/fmicb.2019.01238

Arbuscular Mycorrhizal Symbiosis: Plant Friend or Foe in the Fight Against Viruses?

Laura Miozzi[1], Anna Maria Vaira[1], Marco Catoni[2], Valentina Fiorilli[3], Gian Paolo Accotto[1] and Luisa Lanfranco[3]*

[1] Institute for Sustainable Plant Protection, National Research Council of Italy (IPSP-CNR), Turin, Italy, [2] School of Biosciences, University of Birmingham, Birmingham, United Kingdom, [3] Department of Life Sciences and Systems Biology, University of Turin, Turin, Italy

Plant roots establish interactions with several beneficial soil microorganisms including arbuscular mycorrhizal fungi (AMF). In addition to promoting plant nutrition and growth, AMF colonization can prime systemic plant defense and enhance tolerance to a wide range of environmental stresses and below-ground pathogens. A protective effect of the AMF against above-ground pathogens has also been described in different plant species, but it seems to largely rely on the type of attacker. Viruses are obligate biotrophic pathogens able to infect a large number of plant species, causing massive losses in crop yield worldwide. Despite their economic importance, information on the effect of the AM symbiosis on viral infection is limited and not conclusive. However, several experimental evidences, obtained under controlled conditions, show that AMF colonization may enhance viral infection, affecting susceptibility, symptomatology and viral replication, possibly related to the improved nutritional status and to the delayed induction of pathogenesis-related proteins in the mycorrhizal plants. In this review, we give an overview of the impact of the AMF colonization on plant infection by pathogenic viruses and summarize the current knowledge of the underlying mechanisms. For the cases where AMF colonization increases the susceptibility of plants to viruses, the term "mycorrhiza-induced susceptibility" (MIS) is proposed.

Keywords: arbuscular mycorrhiza, plant virus, mycorrhiza-induced resistance, plant-AMF-pathogen interaction, priming

OPEN ACCESS

Edited by:
Didier Reinhardt, Université de Fribourg, Switzerland

Reviewed by:
Manuela Giovannetti, University of Pisa, Italy
Sergio Saia, Council for Agricultural Research and Economics, Italy

****Correspondence:***
Laura Miozzi
laura.miozzi@ipsp.cnr.it

Specialty section:
This article was submitted to Plant Microbe Interactions, a section of the journal Frontiers in Microbiology

Received: *26 February 2019*
Accepted: *17 May 2019*
Published: *04 June 2019*

Citation:
Miozzi L, Vaira AM, Catoni M, Fiorilli V, Accotto GP and Lanfranco L (2019) Arbuscular Mycorrhizal Symbiosis: Plant Friend or Foe in the Fight Against Viruses? Front. Microbiol. 10:1238. doi: 10.3389/fmicb.2019.01238

INTRODUCTION

Effect of Mycorrhizal Colonization on Plant Responses to Biotic Stress

In natural environments, plants interact with pathogenic and beneficial microorganisms that might affect their growth, performance and survival. Arbuscular mycorrhizal fungi (AMF) (subphylum Glomeromycotina) (Spatafora et al., 2016) establish a mutualistic association with c. 85% of land plants, providing substantial benefits to plant growth and fitness (Jung et al., 2012; Auge et al., 2015). As a consequence of the improved mineral nutrition, AMF colonized plants often display

increased biomass and productivity (Bona et al., 2016; Fiorilli et al., 2018). AMF root colonization induces a systemic effect also evident on epigeous portions of the plant (Fiorilli et al., 2009; Zouari et al., 2014) and exerts beneficial impacts beyond the nutritional status improvement, i.e., an enhanced ability to cope with biotic and abiotic stresses. This advantage relies on physiological and metabolic changes that take place in the plant upon AMF colonization (Fritz et al., 2006; Auge et al., 2015; Fiorilli et al., 2018) and proposes AM symbiosis as a biocontrol agent, impacting on the outcome of below- and above-ground interactions with other organisms.

Enhanced resistance of mycorrhizal plants against soilborne pathogens was often observed (Whipps, 2004), while contrasting results have been obtained for above-ground attackers (Pozo and Azcón-Aguilar, 2007). In roots, the bio-protective effect exerted by AMF seems to rely on several biotic factors such as fungal/host genotypes, mycorrhization degree and soil microbiota alteration, including development of pathogen antagonism and accumulation of defensive compounds (Pozo et al., 2002; Vierheilig et al., 2008; Cameron et al., 2013). The effects on above-ground pathogens seems to greatly depend on the pathogen lifestyle (Shaul et al., 1999; Fiorilli et al., 2011; Miozzi et al., 2011; Campos-Soriano et al., 2012; Jung et al., 2012; Song et al., 2013, 2015; Sanchez-Bel et al., 2016).

The boost of basal defenses in mycorrhizal plants was defined mycorrhiza-induced resistance (MIR) and several studies pointed to priming (Martinez-Medina et al., 2016) as a main mechanism operating in MIR (Pozo and Azcón-Aguilar, 2007; Cameron et al., 2013). Cameron et al. (2013) proposed that MIR is a cumulative effect of plant responses to mycorrhizal colonization, able to confer protection against a wide range of challengers, including biotrophic and necrotrophic pathogens, nematodes and insects. MIR, at least in shoots, seems to be a two-step process with a preliminary induction of a broad range of defense genes (including chitinases, glucanases and Pathogenesis Related (PR) proteins) (Spanu et al., 1989; Liu et al., 2007; Fiorilli et al., 2009) during AMF colonization, followed by a faster and stronger activation of pathogen-specific defense genes upon pathogen challenge (Campos-Soriano et al., 2012; Fiorilli et al., 2018). The main actors proposed to be involved in this process are plant hormones, i.e., salicylic acid (SA), jasmonic acid (JA) and its derivates oxylipins, ethylene and probably abscisic acid (ABA), whose level changes during the different steps of mycorrhizal symbiosis (Foo et al., 2013; Pozo et al., 2015; see section "Conclusion and Perspectives"). It is tempting to speculate that, beside the genetic, molecular and physiological mechanisms, other factors could affect MIR such as AMF associated endobacteria and virome (Bonfante and Desirò, 2017; Turina et al., 2018). Pioneering studies indicate that AMF endobacteria may improve the fungal ecological fitness (Salvioli et al., 2016) and promote antioxidative responses in both fungal and plant hosts (Vannini et al., 2016). However, data on the impact of endobacteria and mycoviruses (Ezawa et al., 2015) on AMF phenotypic expression and higher order biological interactions are scarce and deserve further investigations.

Virus Infection, Damage in Agriculture and Management at Various Scales

Viruses are obligate pathogens able to infect virtually all organisms, including plants. Their infection process depends on the host machinery, allowing the virus to multiply and spread in the host. In plants, virus infections generally induce a disease syndrome, with symptoms such as developmental abnormalities, necrosis and chlorosis. For all major agronomical crops, viral diseases cause huge losses in production and quality, representing a serious threat to global food security (Varma and Malathi, 2003). Virus infection has been often associated to a general reduction of plant performance, i.e., inhibition of photosynthesis (Rahoutei et al., 2000), decrease of biomass (van Mölken and Stuefer, 2011) and pollen production (Harth et al., 2016), although recent evidences suggest that virus infection may improve drought tolerance (Xu et al., 2008; Pantaleo et al., 2016). Majority of viruses spread among plants very efficiently exploiting as vectors other organisms (mostly insects) characterized by a high level of mobility. Since climate changes can favor insect colonization of new habitats (Pureswaran et al., 2018), many viral diseases are representing an emerging problem in agriculture (Varma and Malathi, 2003; Rojas and Gilbertson, 2008; Ghini et al., 2011).

Sustainable and effective approaches to limit viral diseases include the development of viral-resistant/tolerant crop, the integration of crop management strategies to reduce the disease spreading (Nicaise, 2014), the introgression of resistance genes (e.g., NBS-LRR) from wild accessions, the use of transgenic plants expressing viral components, able to interfere with viral infection mechanisms at RNA or protein level. Unfortunately, these strategies are not immediately applicable to uncharacterized emerging viral pathogens.

AMF inoculation has been proposed as a cost-effective and sustainable solution for plant virus control. However, despite some information were available from the early 70's, the studies on the effects of AMF on plant-virus interactions are surprisingly low and contradictory. The aim of this review is to summarize the actual knowledge on the effect of AMF on virus infection and the underlying mechanisms. We propose the term "mycorrhiza-induced susceptibility" (MIS) for the cases where a better performance of the virus, defined by replication efficiency and induced symptomatology, is observed in mycorrhizal plants. Furthermore, the state of the art on the effect of virus infection on mycorrhization will be reported; finally, we suggest different aspects that deserve further investigations.

PLANT PROTECTIVE EFFECT OF THE AMF COLONIZATION AGAINST VIRAL INFECTION

Up to now, three studies highlighted a plant protective effect of the AMF colonization against viral infection. All of them

considered *Solanaceae* or *Cucurbitaceae* plant species and positive single stranded RNA viruses, with the exception of Maffei et al. (2014) that focused on a single-stranded circular DNA geminivirus (**Table 1**). In Maffei et al. (2014), previously AMF-colonized tomato plants displayed attenuated symptoms and reduced virus titre when infected by *Tomato yellow leaf curl Sardinia virus* (TYLCSV) although AMF colonization could not contrast the reduction of root biomass induced by the virus. Since, TYLCSV encodes proteins able to interact with the plant hormone pathways (Lozano-Durán et al., 2011) and particularly with JA, a key hormone in MIR (Cameron et al., 2013), the authors hypothesized that the high JA level in mycorrhizal plants creates an unfavorable environment for TYLCSV, limiting its replication and reducing symptoms severity. This hypothesis is in agreement with the priming effect induced by JA exogenous application during geminivirus infection, which was sufficient to reduce symptoms and viral titre in *Beet curly top virus*-infected plants (Lozano-Durán et al., 2011).

Differently from Maffei et al. (2014), Thiem et al. (2014) investigated the effect of mycorrhizal colonization on potato plants already infected by *Potato virus Y* (PVY): milder symptoms and a significant stimulation of shoot growth were observed in PVY-infected plants inoculated with *Rhizophagus irregularis*.

Finally, tobacco and cucumber plants colonized by *R. irregularis* and infected by *Tobacco mosaic virus* (TMV) and *Cucumber green mottle mosaic virus* (CGMMV), respectively, showed reduced disease symptoms and virus titre if compared to non-mycorrhizal plants (Stolyarchuk et al., 2009); the same authors, in the TMV-tomato system, observed that the content of viral antigens in mycorrhizal plants in respect to non-mycorrhizal ones changed overtime, being equal at 14 days post viral inoculation (dpi), then increasing and subsequently decreasing from 21 to 49 dpi and 56 dpi, respectively.

NEGATIVE IMPACT OF AMF COLONIZATION ON PLANT RESPONSE TO VIRUS INFECTION

Several studies report increased virus multiplication and/or symptom severity in infected mycorrhizal plants. They considered plants belonging to the *Solanaceae*, *Rosaceae* and *Poaceae* families and mostly dealt with single stranded RNA viruses (**Table 1**). Results indicate that mycorrhizal colonization facilitates or enhances virus multiplication, suggesting a prevailing detrimental effect of AMF on plant virus infection, for which we propose the term "mycorrhiza-induced susceptibility" (MIS). Even if, in the first days after inoculation by *Tomato aucuba mosaic virus* (now a TMV strain), the virus titre in tomato plants colonized by *Funneliformis macrocarpa* (formerly *Endogone macrocarpa*) was lower in respect to the control ones, at 8–12 dpi, it became higher in mycorrhizal plants and increased over time (Daft and Okusanya, 1973). Similar results were obtained in leaves and roots of both tomato and strawberry plants inoculated with *Potato virus X* (PVX) (Daft and Okusanya, 1973). No data on plant biomass or performance were reported. These authors observed a similar virus titre increment in infected non-mycorrhizal plants grown with increased concentration of soluble phosphate, and suggested that enhanced viral multiplication could be a general consequence of increased phosphorus availability provided by the symbiosis. This hypothesis relies on the established correlation between phosphate nutrition and TMV infection in tobacco plants (Bawden and Kassanis, 1950; Kassanis, 1953) and was also suggested by Sipahioglu et al. (2009) to explain the increase in PVY titre and symptomatology in potato plants colonized by *R. irregularis*. It is interesting to note that the results of Sipahioglu et al. (2009) were in contrast with those of Thiem et al. (2014) even if the authors considered a similar biological system (potato, *R. irregularis*, PVY) and experimental design (mycorrhization of already PVY-infected plants). Sipahioglu et al. (2009), also observed a reduction in the length, fresh and dry weight of shoots, and in tubers weight, as well as a slight reduction in leaves chlorophyll content in virus-infected mycorrhizal plants.

The MIS outcome, consisting in viral titre increase and worsening of symptoms, was confirmed by Jabaji-Hare and Stobbs (1984) and Shaul et al. (1999) respectively in TMV-infected tomato and tobacco plants colonized by *Glomus* sp. Jabaji-Hare and Stobbs (1984) also observed an increase of roots fresh weight in the virus-infected mycorrhizal plants when compared to non-infected mycorrhizal ones. The results of Shaul et al. (1999) suggest that MIS is not entirely dependent by the improved plant nutritional status; his study excluded any effect of improved phosphorus nutrition and linked the increased plant susceptibility to viral infection with the delay in PR proteins induction in mycorrhizal plants.

More recently, Miozzi et al. (2011) observed increased *Tomato spotted wilt virus* (TSWV) titre in infected mycorrhizal tomato plants at 34 and 56 dpi, but not at 14 dpi, compared to non-mycorrhizal controls. A delay in recovery (symptoms disappearance/reduction in plants initially showing severe disease; Pennazio, 2010) was observed in TSWV-infected mycorrhizal plants at 34 dpi, but disappeared later (56 dpi). Similarly to Shaul et al. (1999), these authors observed a reduction in the number and fold-change of PR proteins coding genes in TSWV-infected mycorrhizal plants when compared with TSWV-infected non-mycorrhizal plants. Since the MIR-related JA-dependent defense priming is hypothesized to be linked to the partial suppression of the salicylic acid (SA)-dependent response (Pozo and Azcón-Aguilar, 2007), it was proposed that the SA level increase induced by TSWV infection may prevent the MIR-mediated response. Within the TSWV-AMF-plant interaction an involvement of ABA and a more complex cross-talk among phytohormones, not limited to SA and JA, were also postulated (Miozzi et al., 2011). Indeed, the pretreatment with ABA can suppress the non-pathogenesis related protein 1 (NPR1) gene, an important regulatory component of SA signaling involved in PR genes activation (Dong, 2004; Yasuda et al., 2008). The long-term changes in virus titre and symptomatology observed by Miozzi et al. (2011) are in agreement with the observation that the protective or

TABLE 1 | AMF-plant-virus biological systems investigated; in the upper section are listed the case studies reporting a protective effect of AMF against viral infection while in the lower section are listed those reporting a detrimental effect.

Plant (family)	Fungus	Virus (genus, family)	Virus type (baltimore classification)	Effect of AMF on virus infection	Plant tissues considered	Effect of virus infection on AMF-colonized plant	References
Tomato (Solanaceae)	*Funneliformis mosseae* (formerly *Glomus mosseae*)	*Tomato yellow leaf curl Sardinia virus* (*Begomovirus*, *geminiviridae*)	ssDNA (Group II)	Decreased virus titre, milder symptoms	Leaves, roots	Reduction of roots fresh weight	Maffei et al., 2014
Potato (Solanaceae)	*Rhizophagus irregularis* (formerly *Glomus intraradices*)	*Potato virus Y* (*Potyvirus*, *potyviridae*)	Positive ssRNA (Gruppo IV)	Milder symptoms	Leaves, stems, roots	Increase of leaves and stems dry weight	Thiem et al., 2014
Tobacco (Solanaceae)	*Rhizophagus irregularis* (formerly *Glomus intraradices*)	*Tobacco mosaic virus* (*Tobamovirus*, *virgaviridae*)	Positive ssRNA (Gruppo IV)	No symptoms, decreased virus titre	Leaves	Not reported	Stolyarchuk et al., 2009
Cucumber (Cucurbitaceae)	*Rhizophagus irregularis* (formerly *Glomus intraradices*)	*Cucumber green mottle mosaic* virus (*Tobamovirus*, *virgaviridae*)	Positive ssRNA (Gruppo IV)	Milder symptoms, reduced virus titre	Leaves	Not reported	Stolyarchuk et al., 2009
Tomato (Solanaceae)	*Funneliformis macrocarpa* (formerly *Endogone macrocarpa*)	*Tomato aucuba mosaic virus** (*Tobamovirus*, *Virgaviridae*)	Positive ssRNA (Gruppo IV)	Increased virus titre	Leaves, roots	Not reported	Daft and Okusanya, 1973
Tomato (Solanaceae)	*Funneliformis macrocarpa* (formerly *Endogone macrocarpa*)	*Potato virus X* (*Potexvirus*, *Alphaflexiviridae*)	Positive ssRNA (Gruppo IV)	Increased virus titre	Leaves, roots	Not reported	Daft and Okusanya, 1973
Petunia (Solanaceae)	*Funneliformis macrocarpa* (formerly *Endogone macrocarpa*)	*Arabis mosaic virus* (*Nepovirus*, *secoviridae*)	Positive ssRNA (Gruppo IV)	Increased virus titre	leaves, roots	Not reported	Daft and Okusanya, 1973
Strawberry (Rosaceae)	*Funneliformis macrocarpa* (formerly *Endogone macrocarpa*)	*Arabis mosaic virus* (*Nepovirus*, *secoviridae*)	Positive ssRNA (Gruppo IV)	Increased virus titre	Leaves, roots	Not reported	Daft and Okusanya, 1973
Tomato (Solanaceae)	*Glomus* sp.	*Tobacco mosaic virus* (*Tobamovirus*, *virgaviridae*)	Positive ssRNA (Gruppo IV)	Increased virus titre, more severe symptoms	Roots, whole plant (for symptoms evaluation)	Increase of roots fresh weight	Jabaji-Hare and Stobbs, 1984
Sour orange (Rutaceae)	*Claroideoglomus etunicatum* (formerly *Glomus etunicatum*)	*Citrus tristeza virus* (*Closterovirus, closteroviridae*)	Positive ssRNA (Gruppo IV)	No difference	whole plant	Reduction of roots fresh weight and plant growth	Nemec and Myhre, 1984
Duncan grapefruit (Rutaceae)	*Claroideoglomus etunicatum* (formerly *Glomus etunicatum*)	*Citrus leaf rugose virus* (*Ilarvirus, bromoviridae*)	Positive ssRNA (Gruppo IV)	No difference	whole plant	Reduction of roots fresh weight and plant growth	Nemec and Myhre, 1984

(Continued)

TABLE 1 | Continued

Plant (family)	Fungus	Virus (genus, family)	Virus type (baltimore classification)	Effect of AMF on virus infection	Plant tissues considered	Effect of virus infection on AMF-colonized plant	References
Tobacco (Solanaceae)	*Rhizophagus irregularis* (formerly *Glomus intraradices*)	*Tobacco mosaic virus* (*Tobamovirus*, *virgaviridae*)	Positive ssRNA (Gruppo IV)	more severe symptoms	leaves	Not reported	Shaul et al., 1999
Potato (Solanaceae)	*Rhizophagus irregularis* (formerly *Glomus intraradices*)	*Potato virus Y* (*Potyvirus*, *potyviridae*)	Positive ssRNA (Gruppo IV)	Increased virus titre, more severe symptoms	leaves,whole plant (for symptoms evaluation)	Reduction of shoots length, fresh and dry weight, and tuber weight. Slight reduction of chlorophyll content	Sipahioglu et al., 2009
Tomato (Solanaceae)	*Rhizophagus irregularis* (formerly *Glomus intraradices*)	*Tobacco mosaic virus* (tobamovirus, *virgaviridae*)	Positive ssRNA (Gruppo IV)	Increased virus titre	Leaves	Not reported	Stolyarchuk et al., 2009
Tomato (Solanaceae)	*Funneliformis mosseae* (formerly *Glomus mosseae*)	*Tomato spotted wilt virus* (*Orthotospovirus*, *tospoviridae*)	Negative ssRNA (Group V)	Increased virus titre, more severe symptoms (lower recovery)	leaves, roots	Reduction of fresh weight of epigean and hypogean parts	Miozzi et al., 2011
Bromus hordeaceus L. (Poaceae)	*Rhizophagus irregularis* (formerly *Glomus intraradices*)	*Barley yellow dwarf virus* (*Luteovirus*, *luteoviridae*)	Positive ssRNA (Gruppo IV)	Increased virus titre (only with elevated CO2 concentration)	leaves	Not reported	Rùa et al., 2013
Bromus hordeaceus L. (Poaceae)	*Rhizophagus irregularis* (formerly *Glomus intraradices*)	*Cereal yellow dwarf virus* (*Polerovirus*, *luteoviridae*)	Positive ssRNA (Gruppo IV)	Increased virus titre (only with elevated CO2 concentration)	leaves	Not reported	Rùa et al., 2013
Avena fatua L. (Poaceae)	*Rhizophagus irregularis* (formerly *Glomus intraradices*)	*Barley yellow dwarf virus* (*Luteovirus*, *luteoviridae*)	Positive ssRNA (Gruppo IV)	Increased virus titre (only with elevated CO2 concentration)	leaves	Not reported	Rùa et al., 2013
Avena fatua L. (Poaceae)	*Rhizophagus irregularis* (formerly *Glomus intraradices*)	*Cereal yellow dwarf virus* (*Polerovirus*, *luteoviridae*)	Positive ssRNA (Gruppo IV)	Increased virus titre (only with elevated CO2 concentration)	leaves	Not reported	Rùa et al., 2013

**a strain of tobacco mosaic virus.*

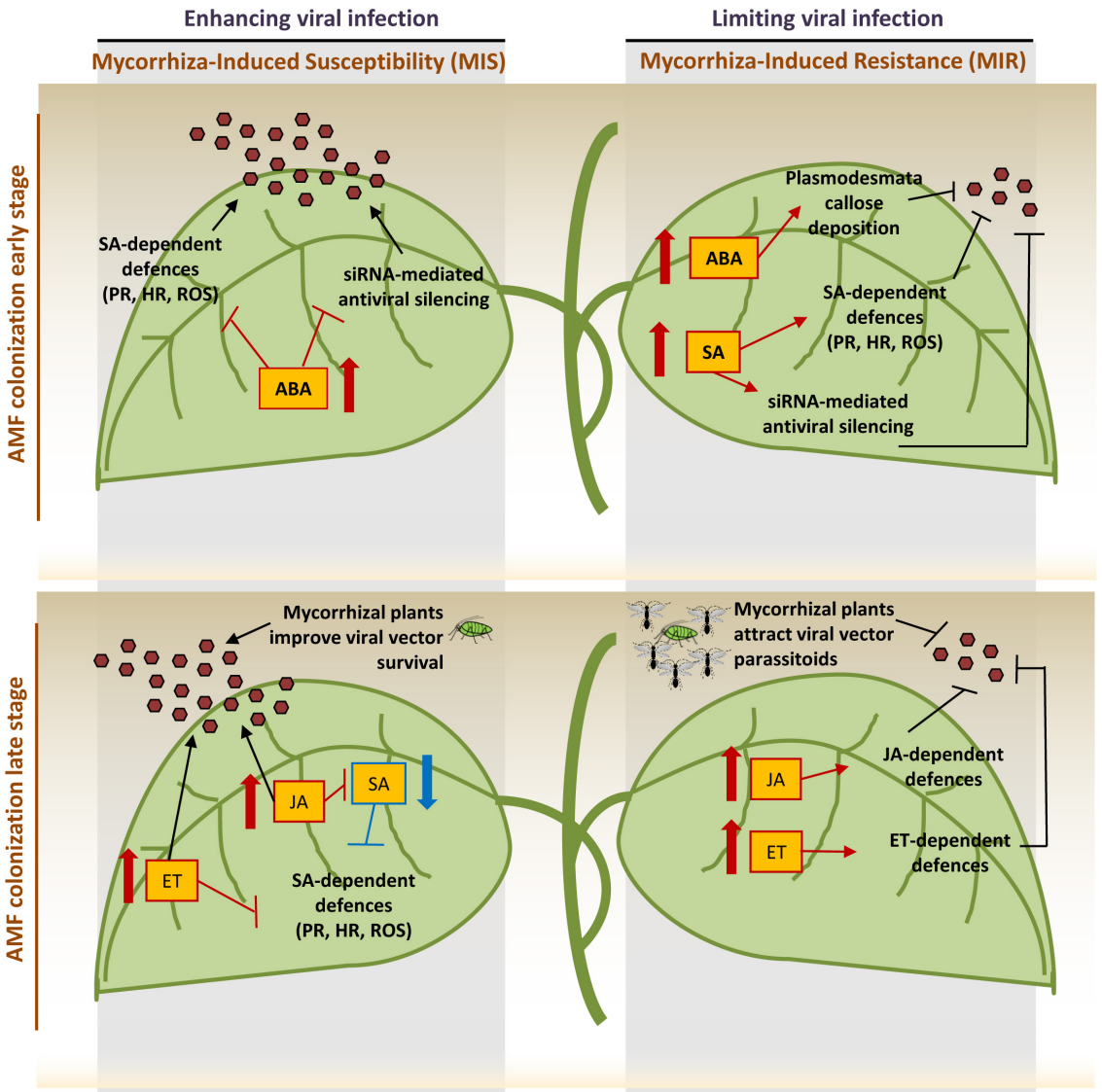

FIGURE 1 | Visual dissection of the events during AMF colonization and virus infection: changes in hormones levels and related processes may enhance (left) or limit (right) viral infection leading to the final outcome of the complex tripartite interaction. In the early stage of mycorrhization, the increase of salicylic acid (SA) induces the priming of SA-dependent defenses, the major defensive pathway against viruses, and enhances the siRNA-mediated antiviral silencing. At the same time, abscisic acid (ABA) increases with both positive and negative consequences on plant defenses: it induces callose deposition on plasmodesmata, limiting cell-to-cell movement, suppresses SA signaling transduction, thus inhibiting defenses controlled by this pathway and weakens siRNA-antiviral system. In the late AMF colonization stage, the increase of jasmonate (JA) and ethylene (ET) induces the priming of JA- and ET-dependent defenses. JA has been shown to reduce viral symptoms at early infection stage but increase susceptibility in late infection stage; on the other hand, JA treatment decreases viral titre during geminivirus infection. ET antagonizes the pathway downstream the SA signaling and may be involved in symptom development, viral systemic movement and formation of necrotic lesions. However, spraying plants with the ET precursor 1-aminocyclopropane-l-carboxylic acid may reduce viral titre. Finally, mycorrhizal plants have been shown to improve aphid survival and increase attractiveness toward aphids parasitoids. PR: pathogenesis-related proteins, HR: hypersensitive response, ROS: reactive oxygen species, brown hexagones indicate viral particles (Lozano-Durán et al., 2011; Cameron et al., 2013; Alazem and Lin, 2015; Volpe et al., 2018).

detrimental effect of mycorrhizal colonization on viral infection can substantially change over time (Daft and Okusanya, 1973; Stolyarchuk et al., 2009) underling that timing is a key parameter in the complex interaction among plant, viruses and AMF. In agreement with other studies here reported, Miozzi and co-authors (2011) observed that the AMF colonization failed to compensate the biomass reduction induced by the virus (**Table 1**).

Rùa et al. (2013), addressing the possible consequences of climate changes and increase of atmospheric CO_2, observed that, under elevated CO_2 concentration, the titre of both *Barley yellow dwarf virus* (BYDV) and *Cereal yellow dwarf virus* (CYDV) increases in the grasses *Bromus hordeaceus* L. and *Avena fatua* L. colonized by *R. irregularis*; no differences were observed under normal CO_2 concentration.

Less investigated is the effect of mycorrhization on fruit trees. Nemec and Myhre (1984), studying the changes induced by *Claroideoglomus etunicatum* (formerly *Glomus etunicatum*) on sour orange and Duncan grapefruit seedlings infected by *Citrus tristeza virus* and *Citrus leaf rugose virus*, respectively, observed that AMF colonization did not significantly reduce the pathogenic effect caused by virus infection. A reduction of roots fresh weight and plant growth in the virus-infected mycorrhizal plants in respect to non-infected mycorrhizal plants was found. Similarly to Thiem et al. (2014) and Sipahioglu et al. (2009), in this work, plants were inoculated with AMF after virus infection.

THE IMPACT OF VIRAL INFECTION ON MYCORRHIZATION

Most studies addressing the plants-viruses-AMF interaction mainly focused on the effect of AMF on virus infection; however, viral infection can impact mycorrhization. In this regard, Nemec and Myhre (1984) observed that the number of fungal spores and the percentage of mycorrhization were generally higher in not-infected plants in respect to infected ones. Maffei et al. (2014) observed that the frequency of mycorrhization moderately but significantly increased in TYLCSV-infected mycorrhizal plants compared to not-infected mycorrhizal ones. However, no differences were observed in intensity of mycorrhization, abundance of arbuscules within colonized areas and percentage of the root system with arbuscules, suggesting that the onset and spread of TYLCSV throughout the whole plant may not significantly interfere with the *F. mosseae* intraradical development. This result is consistent with the up-regulation, in both mycorrhizal and TYLCSV-infected mycorrhizal plants, of five selected plant genes previously described as mycorrhiza-responsive and preferentially expressed in arbuscule-containing cells. Similarly, Sipahioglu et al. (2009) reported equal degree of mycorrhizal colonization in PVY-infected and healthy mycorrhizal potato plants. Finally, Rùa et al. (2013) observed that, only under elevated CO_2 concentration, BYDV and CYDV infection increased the fungal colonization of roots, suggesting that, in this case and condition, AMF and virus interacted to stimulate each other success.

CONCLUSION AND PERSPECTIVES

The picture arising from the reported studies, even if very complex, suggests a prevailing detrimental effect of AMF on plant virus infection, for which we propose the term "mycorrhiza-induced susceptibility" (MIS). Indeed, the interaction among virus, AMF and plant is a complex system where several factors, including viral pathogen lifestyle, plant nutritional status and timing of interaction, can move the dynamic equilibrium toward the final establishment of a MIS or MIR outcome. A key role is probably played by the hormonal crosstalk that finely tunes both plant-AMF and plant-virus interactions (**Figure 1**). In the early stage of AMF colonization, MIR has been associated with SAR (Systemic Acquired Resistance)-like priming of SA-dependent genes, while in the later stage, MIR coincides with priming of JA- and ethylene-dependent defenses. In addition, ABA has been proposed as a new candidate acting as a complementary long-distance signal controlling MIR, and several reports considered JA and its derivates (i.e., oxylipins) as key signals operating in this process (Cordier et al., 1998; Van Wees et al., 2008; Van der Ent et al., 2009; Jung et al., 2012; Song et al., 2013, 2015). In parallel, SA-dependent defenses are the major defensive pathway against viruses while ABA may act either positively and negatively on plant defenses against viruses, respectively, limiting cell-to-cell movement by inducing callose deposition on plasmodesmata, or inhibiting SA-mediated defenses (Alazem and Lin, 2015). Interestingly, SA and ABA may also interact with the plant RNA silencing machinery, respectively inducing dicer-like 1 and 2 and RNA-dependent-RNA polymerase 1 and 2 in virus infected plants (Campos et al., 2015) and regulating the expression of argonaute genes involved in plant antiviral defense (Várallyay et al., 2010; Harvey et al., 2011; Alazem and Lin, 2015). This mechanism could interfere with the siRNA-mediated antiviral plant defense (Alazem and Lin, 2015) and adding further level of complexity to the mechanisms regulating the plant-virus-AMF interaction. Indeed, in this context, the role of siRNAs/miRNAs has not been explored so far, but may be a key element in determining the final interaction outcome. Beyond plant siRNAs, fungal siRNAs have been recently proposed having a functional significance in the *trans*-kingdom communication between the AMF and its host plant (Silvestri et al., 2019), suggesting that their possible role in the final outcome of viral infection in mycorrhizal plants should be addressed.

The complexity of the AMF-plant-virus interaction may further increase if considering that mycorrhiza can impact other trophic levels such as the interaction between plants and insects (Gehring and Bennett, 2009), including those acting as viral vectors. Indeed, AMF *R. irregularis* can improve the survival of the aphid *Macrosiphum euphorbiae*, vector of *Cucumber mosaic virus*, thus possibly improving viral spread, but also activate indirect defenses, attracting the aphid parasitoid *Aphidius ervi* (Volpe et al., 2018).

These observations highlight the intricate network of processes that regulate the plant-virus-AMF interaction, and, far to be conclusive, indicate that several factors able to direct the dynamic equilibrium of the system toward a MIS or MIR outcome remain to be evaluated such as the different changes induced by AMF colonization performed before or after viral infection, and the importance of timing in evaluating the interaction outcome. Moreover, since only few AMF have been analyzed so far, future studies should consider different AMF species and isolates (Sikes, 2010; Turrini et al., 2018) and even AMF consortia for detecting possible synergistic/antagonistic effects. Finally, it must be emphasized that, based on current knowledge, drawing conclusions on the efficacy of AMF to act as biocontrol agents in agricultural environments is extremely difficult, since, in these conditions, many other biotic and abiotic factors have the potential to interfere with the final MIS or MIR outcome.

AUTHOR CONTRIBUTIONS

All authors listed have made a substantial, direct and intellectual contribution to the work, and approved it for publication.

FUNDING

Research in LL's laboratory is supported by the Project Università di Torino – Compagnia di San Paolo Bando ex-post – 2018.

REFERENCES

Alazem, M., and Lin, N. S. (2015). Roles of plant hormones in the regulation of host–virus interactions. *Mol. Plant Pathol.* 16, 529–540. doi: 10.1111/mpp.12204

Auge, R., Toler, H., and Saxton, A. (2015). Arbuscular mycorrhizal symbiosis alters stomatal conductance of host plants more under drought than under amply watered conditions: a meta-analysis. *Mycorrhiza* 25, 13–24. doi: 10.1007/s00572-014-0585-4

Bawden, F. C., and Kassanis, B. (1950). Some effects of host-plant nutrition on the multiplication of viruses. *Ann. Appl. Biol.* 37, 215–228. doi: 10.1111/j.1744-7348.1950.tb01040.x

Bona, E., Scarafoni, A., Marsano, F., Boatti, L., Copetta, A., Massa, N., et al. (2016). Arbuscular mycorrhizal symbiosis affects the grain proteome of *Zea mays*: a field study. *Sci. Rep.* 6:26439. doi: 10.1038/srep26439

Bonfante, P., and Desirò, A. (2017). Who lives in a fungus? The diversity, origins and functions of fungal endobacteria living in Mucoromycota. *ISME J.* 11, 1727–1735. doi: 10.1038/ismej.2017.21

Cameron, D. D., Neal, A. L., van Wees, S. C., and Ton, J. (2013). Mycorrhiza-induced resistance: more than the sum of its parts? *Trends Plant Sci.* 18, 539–545. doi: 10.1016/j.tplants.2013.06.004

Campos, E. V. R., de Oliveira, J. L., Fraceto, L. F., and Singh, B. (2015). Polysaccharides as safer release systems for agrochemicals. *Agron. Sustain. Dev.* 35, 47–66. doi: 10.1016/j.carbpol.2013.10.025

Campos-Soriano, L., García-Martínez, J., and Segundo, B. S. (2012). The arbuscular mycorrhizal symbiosis promotes the systemic induction of regulatory defence-related genes in rice leaves and confers resistance to pathogen infection. *Mol. Plant Pathol.* 13, 579–592. doi: 10.1111/j.1364-3703.2011.00773.x

Cordier, C., Pozo, M. J., Barea, J. M., Gianinazzi, S., and Gianinazzi-Pearson, V. (1998). Cell defense responses associated with localized and systemic resistance to phytophthora parasitica induced in tomato by an arbuscular mycorrhizal fungus. *Mol. Plant Microbe Interact.* 11, 1017–1028. doi: 10.1094/mpmi.1998.11.10.1017

Daft, M. J., and Okusanya, B. O. (1973). Effect of endogone mycorrhiza on plant growth v. Influence of infection on the multiplication of viruses in tomato, petunia and strawberry. *New Phytol.* 72, 975–983. doi: 10.1111/j.1469-8137.1973.tb02074.x

Dong, X. (2004). NPR1, all things considered. *Curr. Opin. Plant Biol.* 7, 547–552. doi: 10.1016/j.pbi.2004.07.005

Ezawa, T., Ikeda, Y., Shimura, H., and Masuta, C. (2015). Detection and characterization of mycoviruses in arbuscular mycorrhizal fungi by deep-sequencing. *Methods Mol. Biol.* 1236, 171–180. doi: 10.1007/978-1-4939-1743-3_13

Fiorilli, V., Catoni, M., Francia, D., Cardinale, F., and Lanfranco, L. (2011). The arbuscular mycorrhizal symbiosis reduces disease severity in tomato plants infected by *Botrytis cinerea*. *J. Plant Pathol.* 93, 237–242.

Fiorilli, V., Catoni, M., Miozzi, L., Novero, M., Accotto, G. P., and Lanfranco, L. (2009). Global and cell-type gene expression profiles in tomato plants colonized by an arbuscular mycorrhizal fungus. *New Phytol.* 184, 975–987. doi: 10.1111/j.1469-8137.2009.03031.x

Fiorilli, V., Vannini, C., Ortolani, F., Garcia-Seco, D., Chiapello, M., Novero, M., et al. (2018). Omics approaches revealed how arbuscular mycorrhizal symbiosis enhances yield and resistance to leaf pathogen in wheat. *Sci. Rep.* 8:9625. doi: 10.1038/s41598-018-27622-8

Foo, E., Ross, J. J., Jones, W. T., and Reid, J. B. (2013). Plant hormones in arbuscular mycorrhizal symbioses: an emerging role for gibberellins. *Ann. Bot.* 111, 769–779. doi: 10.1093/aob/mct041

Fritz, M., Jakobsen, I., Lyngkjær, M. F., Thordal-Christensen, H., and Pons-Kühnemann, J. (2006). Arbuscular mycorrhiza reduces susceptibility of tomato to *Alternaria solani*. *Mycorrhiza* 16, 413–419. doi: 10.1007/s00572-006-0051-z

Gehring, C., and Bennett, A. (2009). Mycorrhizal fungal–plant–insect interactions: the importance of a community approach. *Environ. Entomol.* 38, 93–102. doi: 10.1603/022.038.0111

Ghini, R., Bettiol, W., and Hamada, E. (2011). Diseases in tropical and plantation crops as affected by climate changes: current knowledge and perspectives. *Plant Pathol.* 60, 122–132. doi: 10.1111/j.1365-3059.2010.02403.x

Harth, J. E., Winsor, J. A., Weakland, D. R., Nowak, K. J., Ferrari, M. J., and Stephenson, A. G. (2016). Effects of virus infection on pollen production and pollen performance: implications for the spread of resistance alleles. *Am. J. Bot. Mar.* 103, 577–583. doi: 10.3732/ajb.1500165

Harvey, J. J., Lewsey, M. G., Patel, K., Westwood, J., Heimstädt, S., Carr, J. P., et al. (2011). An antiviral defense role of AGO2 in plants. *PLoS One* 6:e14639. doi: 10.1371/journal.pone.0014639

Jabaji-Hare, S. H., and Stobbs, W. (1984). Electron microscopic examination of tomato roots coinfected with glomus sp. and tobacco mosaic virus. *Phytopathology* 74, 277–279.

Jung, S., Martinez-Medina, A., Lopez-Raez, J., and Pozo, M. (2012). Mycorrhiza-induced resistance and priming of plant defenses. *J. Chem. Ecol.* 38, 651–664. doi: 10.1007/s10886-012-0134-6

Kassanis, B. (1953). Some effects of sucrose and phosphorus in increasing the multiplication of tobacco mosaic virus in detached tobacco leaves. *Microbiology* 9, 467–474. doi: 10.1099/00221287-9-3-467

Liu, J., Maldonado-Mendoza, I., Lopez-Meyer, M., Cheung, F., Town, C. D., and Harrison, M. J. (2007). Arbuscular mycorrhizal symbiosis is accompanied by local and systemic alterations in gene expression and an increase in disease resistance in the shoots. *Plant J.* 50, 529–544. doi: 10.1111/j.1365-313x.2007.03069.x

Lozano-Durán, R., Rosas-Díaz, T., Gusmaroli, G., Luna, A. P., Taconnat, L., Deng, X. W., et al. (2011). Geminiviruses subvert ubiquitination by altering CSN-mediated derubylation of SCF E3 ligase complexes and inhibit jasmonate signaling in Arabidopsis thaliana. *Plant Cell* 23, 1014–1032. doi: 10.1105/tpc.110.080267

Maffei, G., Miozzi, L., Fiorilli, V., Novero, M., Lanfranco, L., and Accotto, G. P. (2014). The arbuscular mycorrhizal symbiosis attenuates symptom severity and reduces virus concentration in tomato infected by Tomato yellow leaf curl Sardinia virus (TYLCSV). *Mycorrhiza* 24, 179–186. doi: 10.1007/s00572-013-0527-6

Martinez-Medina, A., Flors, V., Heil, M., Mauch-Mani, B., Pieterse, C., Pozo, M., et al. (2016). Recognizing plant defense priming. *Trends Plant Sci.* 21, 818–822. doi: 10.1016/j.tplants.2016.07.009

Miozzi, L., Catoni, M., Fiorilli, V., Mullineaux, P. M., Accotto, G. P., and Lanfranco, L. (2011). Arbuscular mycorrhizal symbiosis limits foliar transcriptional responses to viral infection and favors long-term virus accumulation. *Mol. Plant Microbe Interact.* 24, 1562–1572. doi: 10.1094/MPMI-05-11-0116

Nemec, S., and Myhre, D. (1984). Virus-glomus etunicatum interactions in citrus rootstocks. *Plant Dis.* 68, 311–314.

Nicaise, V. (2014). Crop immunity against viruses: outcomes and future challenges. *Front. Plant Sci.* 5:660. doi: 10.3389/fpls.2014.00660

Pantaleo, V., Vitali, M., Boccacci, P., Miozzi, L., Cuozzo, D., Chitarra, W., et al. (2016). Novel functional microRNAs from virus-free and infected *Vitis vinifera* plants under water stress. *Sci. Rep.* 6:20167. doi: 10.1038/srep20167

Pennazio, S. (2010). Recovery. An enigmatic and neglected form of plant resistance to viruses. *Riv. Biol.* 103, 51–70.

Pozo, M. J., and Azcón-Aguilar, C. (2007). Unraveling mycorrhiza-induced resistance. *Curr. Opin. Plant Biol.* 10, 393–398. doi: 10.1016/j.pbi.2007.05.004

Pozo, M. J., Cordier, C., Dumas-Gaudot, E., Gianinazzi, S., Barea, J. M., and Azcón-Aguilar, C. (2002). Localized versus systemic effect of arbuscular mycorrhizal fungi on defence responses to phytophthora infection in tomato plants. *J. Exp. Bot.* 53, 525–534. doi: 10.1093/jexbot/53.368.525

Pozo, M. J., López-Ráez, J. A., Azcón-Aguilar, C., and García-Garrido, J. M. (2015). Phytohormones as integrators of environmental signals in the regulation of mycorrhizal symbioses. *New Phytol.* 205, 1431–1436. doi: 10.1111/nph.13252

Pureswaran, D. S., Roques, A., and Battisti, A. (2018). Forest insects and climate change. *Curr. For. Rep.* 4, 35–50. doi: 10.1007/s40725-018-0075-6

Rahoutei, J., Garcìa-Luque, I., and Baron, M. (2000). Inhibition of photosynthesis by viral infection: effect on PSII structure and function. *Physiol. Plant.* 110, 286–292. doi: 10.1034/j.1399-3054.2000.110220.x

Rojas, M. R., and Gilbertson, R. L. (2008). "Emerging Plant Viruses: a Diversity of Mechanisms and Opportunities," in *Plant Virus Evolution*, ed. M. J. Roossinck (Heidelberg: Springer), 27–51. doi: 10.1007/978-3-540-75763-4_3

Rùa, M., Umbanhowar, J., Hu, S., Burkey, K., and Mitchell, C. (2013). Elevated CO_2 spurs reciprocal positive effects between a plant virus and an arbuscular mycorrhizal fungus. *New Phytol.* 199, 541–549. doi: 10.1111/nph.12273

Salvioli, A., Ghignone, S., Novero, M., Navazio, L., Venice, F., Bagnaresi, P., et al. (2016). Symbiosis with an endobacterium increases the fitness of a mycorrhizal fungus, raising its bioenergetic potential. *ISME J.* 10, 130–144. doi: 10.1038/ismej.2015.91

Sanchez-Bel, P., Troncho, P., Gamir, J., Pozo, M. J., Camañes, G., Cerezo, M., et al. (2016). The nitrogen availability interferes with mycorrhiza-induced resistance against *Botrytis cinerea* in Tomato. *Front. Microbiol.* 7:1598. doi: 10.3389/fmicb.2016.01598

Shaul, O., Galili, S., Volpin, H., Ginzberg, I., Elad, Y., Chet, I., et al. (1999). Mycorrhiza-induced changes in disease severity and PR protein expression in tobacco leaves. *Mol. Plant Microbe Interact.* 12, 1000–1007. doi: 10.1094/mpmi.1999.12.11.1000

Sikes, B. A. (2010). When do arbuscular mycorrhizal fungi protect plant roots from pathogens? *Plant Signal. Behav.* 5, 763–765. doi: 10.4161/psb.5.6.11776

Silvestri, A., Fiorilli, V., Miozzi, L., Accotto, G. P., Turina, M., and Lanfranco, L. (2019). In silico analysis of fungal small RNA accumulation reveals putative plant mRNA targets in the symbiosis between an arbuscular mycorrhizal fungus and its host plant. *BMC Genomics* 20:169. doi: 10.1186/s12864-019-5561-0

Sipahioglu, M. H., Demir, S., Usta, M., and Akkopru, A. (2009). Biological relationship of potato virus Y and arbuscular mycorrhizal fangus *Glomus intraradices* in potato. *Pest Technol.* 3:4.

Song, Y., Chen, D., Lu, K., Sun, Z., and Zeng, R. (2015). Enhanced tomato disease resistance primed by arbuscular mycorrhizal fungus. *Front. Plant Sci.* 6:786. doi: 10.3389/fpls.2015.00786

Song, Y. Y., Ye, M., Li, C. Y., Wang, R. L., Wei, X. C., Luo, S. M., et al. (2013). Priming of anti-herbivore defense in tomato by arbuscular mycorrhizal fungus and involvement of the jasmonate pathway. *J. Chem. Ecol.* 39, 1036–1044. doi: 10.1007/s10886-013-0312-1

Spanu, P., Boller, T., Ludwig, A., Wiemken, A., Faccio, A., and Bonfante-Fasolo, P. (1989). Chitinase in roots of mycorrhizal Allium porrum: regulation and localization. *Planta* 177, 447–455. doi: 10.1007/BF00392612

Spatafora, J. W., Chang, Y., Benny, G. L., Lazarus, K., Smith, M. E., Berbee, M. L., et al. (2016). A phylum-level phylogenetic classification of zygomycete fungi based on genomescale data. *Mycologia* 108, 1028–1046. doi: 10.3852/16-042

Stolyarchuk, I. M., Shevchenko, T. P., Polischuk, V. P., and Kripka, A. V. (2009). Virus infection course in different plant species under influenceof arbuscular mycorrhiza. *Microbiol. Biotechnol.* 6, 70–75. doi: 10.18524/2307-4663.2009.3(7).103120

Thiem, D., Szmidt-Jaworska, A., Baum, C., Muders, K., Niedojadło, K., and Hrynkiewicz, K. (2014). Interactive physiological response of potato (*Solanum tuberosum* L.) plants to fungal colonization and Potato virus Y (PVY) infection. *Acta Mycol.* 49, 291–303. doi: 10.5586/am.2014.015

Turina, M., Ghignone, S., Astolfi, N., Silvestri, A., Bonfante, P., and Lanfranco, L. (2018). The virome of the arbuscular mycorrhizal fungus *Gigaspora margarita* reveals the first report of DNA fragments corresponding to replicating non-retroviral RNA viruses in fungi. *Environ. Microbiol.* 20, 2012–2025. doi: 10.1111/1462-2920.14060

Turrini, A., Avio, L., Giovannetti, M., and Agnolucci, M. (2018). Functional complementarity of arbuscular mycorrhizal fungi and associated microbiota: the challenge of translational research. *Front. Plant Sci.* 9:1407. doi: 10.3389/fpls.2018.01407

Van der Ent, S., Van Wees, S. C., and Pieterse, C. M. (2009). Jasmonate signaling in plant interactions with resistance-inducing beneficial microbes. *Phytochemistry* 70, 1581–1588. doi: 10.1016/j.phytochem.2009.06.009

van Mölken, T., and Stuefer, J. F. (2011). The potential of plant viruses to promote genotypic diversity via genotype 3 environment interactions. *Ann. Bot.* 107, 1391–1397. doi: 10.1093/aob/mcr078

Van Wees, S. C., Van der Ent, S., and Pieterse, C. M. (2008). Plant immune responses triggered by beneficial microbes. *Curr. Opin. Plant Biol.* 11, 443–448. doi: 10.1016/j.pbi.2008.05.005

Vannini, C., Carpentieri, A., Salvioli, A., Novero, M., Marsoni, M., Testa, L., et al. (2016). An interdomain network: the endobacterium of a mycorrhizal fungus promotes antioxidative responses in both fungal and plant hosts. *New Phytol.* 211, 265–275. doi: 10.1111/nph.13895

Várallyay, E., Válóczi, A., Agyi, A., Burgyán, J., and Havelda, Z. (2010). Plant virus-mediated induction of miR168 is associated with repression of ARGONAUTE1 accumulation. *EMBO J.* 29, 3507–3519. doi: 10.1038/emboj.2010.215

Varma, A., and Malathi, V. G. (2003). Emerging geminivirus problems: a serious threat to crop production. *Ann. Appl. Biol.* 142, 145–164. doi: 10.1111/j.1744-7348.2003.tb00240.x

Vierheilig, H., Steinkellner, S., Khaosaad, T., and Garcia-Garrido, J. M. (2008). "The biocontrol effect of mycorrhization on soilborne fungal pathogens and the autoregulation of the AM symbiosis: one mechanism, Two Effects?," in *Mycorrhiza: State of the Art, Genetics and Molecular Biology, Eco-Function, Biotechnology, Eco-Physiology, Structure and Systematics*, ed. A. Varma (Heidelberg: Springer), 307–320. doi: 10.1007/978-3-540-78826-3_15

Volpe, V., Chitarra, W., Cascone, P., Volpe, M. G., Bartolini, P., Moneti, G., et al. (2018). The association with two different arbuscular mycorrhizal fungi differently affects water stress tolerance in tomato. *Front. Plant Sci.* 9:1480. doi: 10.3389/fpls.2018.01480

Whipps, J. M. (2004). Prospects and limitations for mycorrhizas in biocontrol of root pathogens. *Can. J. Bot.* 82, 1198–1227. doi: 10.1139/b04-082

Xu, P., Chen, F., Mannas, J. P., Feldman, T., Sumner, L. W., and Roossinck, M. J. (2008). Virus infection improves drought tolerance. *New Phytol.* 180, 911–921. doi: 10.1111/j.1469-8137.2008.02627.x

Yasuda, M., Ishikawa, A., Jikumaru, Y., Seki, M., Umezawa, T., Asami, T., et al. (2008). Antagonistic interaction between systemic acquired resistance and the abscisic acid-mediated abiotic stress response in Arabidopsis. *Plant Cell* 20, 1678–1692. doi: 10.1105/tpc.107.054296

Zouari, I., Salvioli, A., Chialva, M., Novero, M., Miozzi, L., Tenore, G. C., et al. (2014). From root to fruit: RNA-Seq analysis shows that arbuscular mycorrhizal symbiosis may affect tomato fruit metabolism. *BMC Genomics* 15:221. doi: 10.1186/1471-2164-15-221

Conflict of Interest Statement: The authors declare that the research was conducted in the absence of any commercial or financial relationships that could be construed as a potential conflict of interest.

frontiers in Microbiology

ORIGINAL RESEARCH
published: 03 July 2019
doi: 10.3389/fmicb.2019.01505

Streptomyces Strains Induce Resistance to *Fusarium oxysporum* f. sp. *lycopersici* Race 3 in Tomato Through Different Molecular Mechanisms

Sakineh Abbasi[1], Naser Safaie[1], Akram Sadeghi[2]* and Masoud Shamsbakhsh[1]*

[1] Department of Plant Pathology, Faculty of Agriculture, Tarbiat Modares University, Tehran, Iran, [2] Department of Microbial Biotechnology, Agricultural Biotechnology Research Institute of Iran (ABRII), Agricultural Research, Education and Extension Organization (AREEO), Karaj, Iran

Plant growth promoting rhizobacteria (PGPR) are potential natural alternatives to chemical fungicides in greenhouse production via inducing plant immune system against biotic stresses. In this research, 126 *Streptomyces* isolates were recovered from rhizosphere soils of 13 different commercial vegetable greenhouses in Iran. *Streptomyces* isolates were screened for *in vitro* Plant growth promoting (PGP) traits and ability to antagonize *Fusarium oxysporum* f. sp. *lycopersici* race 3 (*FOL*), the causal agent of Fusarium wilt of tomato (FWT). Six isolates with the highest antagonistic activity and at least three PGP traits were selected and compared with chemical fungicide Carbendazim® in a greenhouse experiment. All bacterial treatments mitigated FWT disease symptoms like chlorosis, stunting and wilting at the same level or better than Carbendazim®. Strains IC10 and Y28 increased shoot length and shoot fresh and dry weight compared to not inoculated control plants. Phenotypic characterization and 16S rRNA gene sequencing showed, strains IC10 and Y28 were closely related to *S. enissocaesilis* and *S. rochei*, respectively. The ability of the superior biocontrol strains to induce antioxidant enzymes activity and systemic resistance (ISR) was investigated. Increased activity of catalase (CAT) in plant treated with both strains as well as an increase in peroxidase (POX) activity in plants treated with Y28 pointed to a strain specific-induced systemic resistance (ss-ISR) in tomato against *FOL*. The differential induced expression of *WRKY70* and *ERF1* (two transcription factors involved in plant defense) and *LOX* and *TPX* by the analyzed *Streptomyces* strains, especially after inoculation with *FOL*, suggests that ss-ISR is triggered at the molecular level.

Keywords: Fusarium wilt, induced systemic resistance, *Streptomyces*, tomato growth promoting, siderophore production

OPEN ACCESS

Edited by:
Luisa Lanfranco,
University of Turin, Italy

Reviewed by:
Soner Soylu,
Mustafa Kemal University, Turkey
Marta Berrocal-Lobo,
Polytechnic University of Madrid, Spain

****Correspondence:***
Naser Safaie
nsafaie@modares.ac.ir
Akram Sadeghi
aksadeghi@abrii.ac.ir

Specialty section:
This article was submitted to Plant Microbe Interactions, a section of the journal Frontiers in Microbiology

Received: *30 January 2019*
Accepted: *17 June 2019*
Published: *03 July 2019*

Citation:
Abbasi S, Safaie N, Sadeghi A and Shamsbakhsh M (2019) Streptomyces Strains Induce Resistance to Fusarium oxysporum f. sp. lycopersici Race 3 in Tomato Through Different Molecular Mechanisms. Front. Microbiol. 10:1505. doi: 10.3389/fmicb.2019.01505

INTRODUCTION

In recent decades, overuse of chemical fertilizers and fungicides to proliferate and protect greenhouse vegetables has been a threat to human safety. Using biological agents is the best alternative for chemical treatments (Pilkington et al., 2010). Soil-borne fungus *Fusarium oxysporum* Schlecht. f. sp. *lycopersici* (Sacc.) Snyder and Hansen (*FOL*) causing Fusarium wilt of tomato

reduces yield in greenhouses (Fravel et al., 2003; McGovern, 2015). Invading through the vascular tissue and soil- borne feature of the pathogen make it difficult to control this disease. Besides, new races of the mentioned pathogen (e.g., race 3) have emerged that can overcome host resistance (Reis et al., 2005). The symptoms of Fusarium wilt disease caused by race 3 are yellowing the lower leaves, vascular necrosis, epinasty, defoliation, plant stunting and ultimately plant death (Sanchez-Pena et al., 2010). Biological control of this pathogen has been the subject of many studies (Ben Abdallah et al., 2016). Plant growth promoting rhizobacteria (PGPR) colonize rhizosphere or plant root and improve plant health and growth. Some of the most important plant growth promoting (PGP) activity include diazotrophic nitrogen fixation, siderophore production, solubilization of mineral phosphates and production of hormones such as indole-3-acetic acid (IAA) (Sadeghi et al., 2012; Dahal et al., 2017; Gouda et al., 2018). Plant defense strategies including physical barriers, numerous secondary metabolites and antimicrobial agents, which the effective, aggressive pathogens have to overcome them (reviewed by Bruce and Pickett, 2007). Some plant defense strategies are constitutive while others are inducible and only launch in response to a stimulating pathogen and/or beneficial microbes (Pieterse et al., 2012). Plant defense strategies keep damage of specific pests below an economic threshold; however, maintain the beneficial organisms involved in integrated pest management (IPM) (Chellemi et al., 2016). IPM considers available pest control techniques that prevent the development of pest populations and keep pesticides to levels that are economically reasonable and reduces risks to human health and the environment. Developing sustainable biocontrol measures for managing Fusarium wilt disease requires a comprehensive understanding of the molecular basis of plant–pathogen–biocontrol interactions. Hormones, PR proteins, terpenoid synthases, polyketide terpene synthases, peroxidases, lignin synthases, transcription factors, calcium signal transducers, and UDP-glucosyltransferases and ubiquitin-protein ligases are components of the plant defense-related genes (Wang et al., 2015). Generally, the plant responses to microbes are regulated through signaling pathways including salicylic acid (SA), jasmonic acid (JA), and ethylene (ET). Jasmonic acid pathway is required for defense against necrotrophic pathogens and chewing insects, while SA pathway is involved in a wide range of plant defense responses, which ends to systemic acquired resistance (SAR) and occurs following the exposure to many biotrophic and some necrotrophic pathogens. Induced systemic resistance (ISR) is also an activated resistance process elicited by contacting with non-pathogenic microorganisms. This procedure is independent of SA and is synchronized by JA and ET (Walters and Heil, 2007). Activated induced resistance (via ISR or SAR) is a broad-spectrum and long-term resistance, which usually suppresses a disease up to 20–85% (Walters et al., 2013). Thus, inducing plants by direct interaction with rhizobacteria prior to pathogen infection, so-called priming, decreases disease severity (Beckers and Conrath, 2007). *Streptomyces* species, are Gram-positive filamentous bacteria, reported as PGP and biocontrol agent of *Alternaria alternata* (Verma et al., 2011), *Rhizoctonia solani* (Goudjal et al., 2014), *F. oxysporum* (Kim et al., 2011), *Phytophthora drechsleri* (Sadeghi et al., 2017), and *Verticillium dahliae* (Cao et al., 2016). Little is known about bio-suppression of tomato wilt by *Streptomyces* in greenhouse conditions.

The aims of this study were to (1) isolate and characterize *Streptomyces* from vegetable greenhouse soils (2) detect PGP characteristics and antagonistic activity of isolates against *FOL* race (3) evaluate Fusarium wilt biocontrol in tomato by superior isolates in greenhouse condition (4) establish induced systemic resistance (ISR) of tomato through inducing antioxidant enzymes and defense-related genes by inoculation of plants with biocontrol *Streptomyces*.

MATERIALS AND METHODS

Microorganisms

Rhizosphere soil samples (500 g soil with pH = 6.2–7 and EC < 2.5 dS/m) were collected from 18 cucumber and tomato commercial greenhouses in Yazd, Isfahan and Kerman provinces of Iran in 2016. There were no symptoms of wilt and damping off diseases developing in these greenhouses. The samples were placed in plastic bags, taken to the laboratory and then air-dried for 7 days. For isolation of *Streptomyces*, 2 g rhizosphere soil was suspended in 100 mL of sterile saline solution (0.9% NaCl) and shaken for 30 min. Two dilutions (1:100 and 1:1000) were prepared using sterile saline solutions in a final volume of 1 mL. An aliquot of 0.1 mL of each dilution was spread on 1.8% water agar supplemented with 300 mM NaCl. The plates were incubated at 29°C for 7 days. Representative colonies were selected and streaked on plates of "International Streptomyces Project media 2" (ISP2) medium (Kampfer et al., 1991) containing 10 g/L malt extract, 4 g/L yeast extract, 4 g/L glucose, and 18 g/L agar, adjusted to pH 7.2. The plates were incubated at 29°C for 7 days. Then morphologically (color, size, and shape) distinct colonies were stored in 30% glycerol solution at −70°C (**Table 1**).

The fungal pathogen was isolated from tomato plants displaying disease symptoms and pathogenicity test was conducted using root-dipping inoculation method on tomato seedlings. The fungus was re-isolated from the vascular tissue of a symptomatic plant. Fungal DNA extraction was carried out by the methods described by Zhang et al. (2010), Salehi et al. (2018, 2019). Polymerase chain reaction (PCR) was performed with universal pair primers (ITS4-ITS5). Race determination of fungus was done using four specific primer pairs designed by Hirano and Arie (2006) based on the sequence of the exo-polygalacturonase gene (**Table 2**). ITS4-ITS5 nucleotide sequence obtained by DNA amplification of fungal pathogen was deposited in NCBI GenBank with accession number MG670445. Blast analysis showed that this pathogen had 99 % similarity to *F. oxysporum*. The result of the race determination using four specific primer pairs showed that the fungal isolate belongs to *F. oxysporum* f.sp. *lycopersici* race 3 (**Supplementary Figure S1**).

Growth on Nitrogen-Free Medium

Screening of the free-living (non-symbiotic) diazotroph isolates was carried out according to the procedure described by Xu and Zheng (1986). Each colony was spot-inoculated on nitrogen-free

TABLE 1 | PGP properties and enzyme activity of selected isolates.

Isolate	Host crop	Location	PGP properties				Hydrolytic enzymes activity		
			Growth on N free medium	Inorganic P solubilization	Siderophore production	IAA production	Cellulase	Protease	Chitinase
IC6	Cucumber	Isfahan	1	0.1 ± 0.1	0.3 ± 0.1	9.2 ± 0.0	1.0 ± 0.0	0.3 ± 0.0	1.0 ± 0.0
IC10	Cucumber	Isfahan	1	0.2 ± 0.0	0.4 ± 0.0	27.1 ± 0.1	0.0 ± 0.0	1.0 ± 0.0	0.9 ± 0.1
IC13	Cucumber	Isfahan	1	0.3 ± 0.0	0.4 ± 0.0	32.3 ± 2.6	1.0 ± 0.0	0.6 ± 0.0	0.9 ± 0.1
IS8	Cucumber	Isfahan	1	1.9 ± 0.1	0.4 ± 0.0	21.9 ± 0.9	0.0 ± 0.0	0.4 ± 0.0	1.0 ± 0.0
SS12	Cucumber	Isfahan	1	0.1 ± 0.0	0.3 ± 0.0	24.1 ± 1.9	1.0 ± 0.0	0.5 ± 0.0	0.8 ± 0.1
CU122	Cucumber	Isfahan	1	0.2 ± 0.0	0.1 ± 0.0	20.5 ± 0.7	0.0 ± 0.0	0.0 ± 0.0	0.0 ± 0.0
IC15	Cucumber	Isfahan	1	0.3 ± 0.0	0.3 ± 0.0	9.6 ± 1.2	0.0 ± 0.0	0.3 ± 0.0	0.9 ± 0.0
SS14	Cucumber	Isfahan	1	0.0 ± 0.0	0.3 ± 0.0	24.5 ± 0.7	1.0 ± 0.0	0.5 ± 0.0	0.0 ± 0.0
IT20	Tomato	Isfahan	1	0.2 ± 0.0	0.4 ± 0.0	24.0 ± 1.3	1.0 ± 0.0	0.5 ± 0.0	0.0 ± 0.0
IT8	Tomato	Isfahan	1	0.0 ± 0.0	0.4 ± 0.0	25.8 ± 0.5	1.0 ± 0.0	0.2 ± 0.0	0.0 ± 0.0
IT25	Tomato	Isfahan	1	0.2 ± 0.0	0.5 ± 0.0	25.8 ± 1.8	0.0 ± 0.0	0.3 ± 0.0	0.8 ± 0.2
Y7	Cucumber	Yazd	1	0.5 ± 0.1	0.0 ± 0.0	7.7 ± 0.9	0.0 ± 0.0	0.0 ± 0.0	0.0 ± 0.0
Y18	Cucumber	Yazd	1	0.1 ± 0.0	0.0 ± 0.0	12.0 ± 0.6	1.0 ± 0.0	0.9 ± 0.1	0.8 ± 0.2
Y27	Tomato	Yazd	1	0.0 ± 0.0	0.0 ± 0.0	30.8 ± 1.1	1.3 ± 0.4	0.3 ± 0.0	0.0 ± 0.0
TO612	Tomato	Yazd	1	0.0 ± 0.0	0.5 ± 0.0	24.7 ± 0.3	1.0 ± 0.0	0.0 ± 0.0	0.0 ± 0.0
Y17	Tomato	Yazd	1	0.0 ± 0.0	0.4 ± 0.0	13.7 ± 2.8	1.0 ± 0.0	0.4 ± 0.0	0.6 ± 0.3
Y28	Tomato	Yazd	1	0.4 ± 0.0	0.3 ± 0.0	16.8 ± 2.1	0.0 ± 0.0	0.0 ± 0.0	0.9 ± 0.0
Y281	Tomato	Yazd	1	0.3 ± 0.0	0.3 ± 0.0	10.0 ± 0.0	0.0 ± 0.0	0.0 ± 0.0	0.0 ± 0.0
Y16	Tomato	Yazd	1	0.0 ± 0.0	0.4 ± 0.1	11.4 ± 0.5	1.4 ± 0.4	0.0 ± 0.0	0.0 ± 0.0
Y33	Tomato	Yazd	1	0.2 ± 0.0	0.0 ± 0.0	9.3 ± 0.2	1.0 ± 0.0	0.3 ± 0.0	0.8 ± 0.2
Y34	Tomato	Yazd	1	0.3 ± 0.1	0.3 ± 0.0	11.8 ± 0.9	1.2 ± 0.2	0.2 ± 0.0	0.7 ± 0.3
KH12	Cucumber	Kerman	1	0.0 ± 0.0	0.1 ± 0.0	7.5 ± 0.7	0.2 ± 0.1	0.3 ± 0.1	0.0 ± 0.0
K40	Cucumber	Kerman	1	0.0 ± 0.0	0.0 ± 0.0	27.5 ± 2.2	0.2 ± 0.0	0.4 ± 0.0	1.0 ± 0.0
K43	Cucumber	Kerman	1	0.0 ± 0.0	0.0 ± 0.0	22.5 ± 3.5	1.0 ± 0.0	0.0 ± 0.0	0.0 ± 0.0

The means halo zone diameter/ colony diameter of three replications ± standard deviation is represented. 1, growth; 0, no growth. The data indicated for IAA production was in μg/mL.

agar medium incubated at 29°C for 14 days, and then growth or lack of growth was compared to ISP2 medium.

Inorganic Phosphate Solubilization

Pikovskaya's medium (PVK) was used to measure calcium phosphate [Ca_3 $(PO_4)_2$]-solubilizing activity. Sterilized PVK medium with pH 7.2 was poured into petri plates. After solidification of the medium, bacterial isolates were spot-inoculated onto the center of the plates and incubated at 29°C for 7 days. Solubilization index was evaluated according to the ratio of the clear zone diameter to colony diameter (Soltani et al., 2010).

Siderophore Production

Siderophore production was evaluated as described by Alexander and Zuberer (1991) on Chrome Azurol agar (CAS) medium. *Streptomyces* isolates were spot-inoculated onto the center of the plate and incubated at 29°C for 7 days. The formation of orange halo around the colonies were considered as siderophore-producing isolates. After 3 days, the ratio of the halo zone diameter to colony diameter was calculated as siderophore production.

IAA Production

To determine amounts of IAA produced by each isolate, 1 mL of bacterial culture in ISP2 broth was inoculated in Tryptic Soy Broth supplemented with 150 mg/L L-tryptophan. Approximately 1 mL of culture solution was centrifuged at 12000 rpm for 5 min, and 1mL of the supernatant was mixed with 2 mL of Salkowski's reagent (150 mL concentrated H_2SO_4, 250 mL distilled water, 7.5 mL 0.5 M $FeCl_3.6H_2O$) and incubated for 20 min in darkness at room temperature (de Oliveira-Longatti et al., 2014). IAA production was qualitatively assayed as pink color development and quantified by measurement of absorbance at 530 nm using a spectrophotometer infinit M200 (Tecan, Switzerland). The calibration plot was constructed using dilutions of a standard IAA (Fluka, Switzerland) solution and the uninoculated medium with the reagent as a standard curve (0, 5, 10, 20, 50, and 100 μg/mL). The quantity of IAA in the culture was expressed as μg/mL.

Antagonistic Effect of PGPRs

Bacterial suspension of candidate PGPR isolates (**Table 1**) (20 μL of the 10^8 cfu/mL sterile saline solution) was inoculated at 29°C linearly at the two opposite sides (1 cm from the plate edge) of potato dextrose agar (PDA) plates for 48 h. Then, one fungal

TABLE 2 | The list of primers used in the q-RT PCR in this study.

Gene Name	Amplicon size (bp)	Sequence
UniF	670	F-5′ATCATCTTGTGCCAACTTCAG3′ R-5′GTTTGTGATCTTTGAGTTGCCA3′
Sp13	445	F-5′GTCAGTCCATTGGCTCTCTC3′ R-5′TCCTTGACACCATCACAGAG3′
Sp23	518	F-5′CCTCTTGTCTTTGTCTCACGA3′ R-5′GCAACAGGTCGTGGGGAAAA3′
Sprl	947	F-5′GATGGTGGAACGGTATGACC3′ R-5CCATCACACAAGAACACAGGA3′
UDP-G	122	F-5′GATGAACGCCACCTTCTTAG3′ R-5′CTCCTTCCATAACAATCCTCAC3′
WRKY70	131	F-5′TGGTAAAGCATAGTGACTCAAC3′ R-5′AGAGGGAGAAGAAGGCATAA3′
PAL1	148	F-5′CATTGTACAGGTTGGTGAGAG3′ R-5′CATCTCTTGAGACACTCCA3′
LOX E	104	F-5′CTTCGGATACCCTTTACCT3′ R-5′GATCTCACCCAACTTCTTTC3′
TPX	133	F-5′AGCATTGACAACACGTACC3′ R-5′AGCACTCCCTGTCTTAACT3′
PR1	136	F-5′GGTAACTGGAGAGGACAA3′ R-5′GACAATCGATCACTTTATTC3′
ERF1	126	F-5′AGACTTGGGAGTTGAATTA3′ R-5′TACATTGCGATCTTGATTA3′
TUB	146	F-5′CAAGAACTCGTCCTACTTTG3′ R-5′GCTCACTCACCCTTCTAA3′

plug (0.5 cm diameter) was inoculated at the center of PDA plate (Kunova et al., 2016) and then incubated for 4 days. The growth inhibition percentage was calculated using the formula (a − b)/a × 100, where "a" is the fungal growth radius of a control culture (in cm) and "b" is the distance of the pathogen growth in the direction of bacteria (in cm).

Chitinase Activity

Chitinase production was determined according to the method of Hsu and Lockwood (1975). *Streptomyces* isolates were grown on chitin agar containing 0.4% colloidal chitin and 1.5% agar adjusted to pH 7.2. Colloidal chitin was prepared according to Berger and Reynolds (1958). Plates were incubated for 5 days at 29°C. The ability of chitinase production was shown by a clear halo around the colonies. The ratio of the clear zone diameter to colony diameter was calculated as chitinase activity.

Cellulase Activity

Carboxymethyl cellulase (CMCase) activity was determined by Mandels-Reese medium with carboxymethyl cellulose (CMC) as sole carbon source (Majidi et al., 2011). The bacteria were grown on CMC agar containing 0.4 g/L KH_2PO_4, 0.02 g/L $CaCl_2$, 0.02 g/L NaCl, 0.02 g/L $FeSO_4$ $7H_2O$, 2.5 g/L CMC, and 15.0 g/L agar. The pH was adjusted to 7.2 with 1 M NaOH. The CMC agar plates were incubated at 29°C for 7 days to allow the secretion of cellulase. To visualize the hydrolysis zone, agar medium was flooded with an aqueous solution of Congo red (1 mg/mL) for 20 min. Congo red solution was then poured off, and the plates were further treated by flooding with 1 M NaCl for 15 min. To indicate cellulase activity, the diameter of the clear zone around each colony was measured. The ratio of the clear zone diameter to colony diameter was calculated as cellulase activity.

Protease Activity

Extracellular protease activity of *Streptomyces* isolates was assayed by a modification method of Mehrotra et al. (1999). Each bacterial isolate was streaked on skim milk agar containing 15 g/L skim milk powder, 0.5 g/L yeast extract and 10 g/L agar. After incubation at 29°C for 48 h, the ratio of the clear zone around bacterial colony to colony diameter was measured as protease activity.

Phenotypic and Molecular Characterization of the Selected Isolates

The potent PGP and antagonist isolates were further characterized by differential morphological traits on ISP2, ISP3, and ISP4 media (Shirling and Gottlieb, 1966), melanin formation (Suter, 1978), growth in high temperatures (37°C and 42°C), and growth on medium supplemented with 6, 10, and 12% NaCl (Kutzner, 1981).

Molecular characterization of the selected isolates was done using PCR amplification of 16S rRNA gene sequence. DNA was extracted according to the method described by Tripathi and Rawal (1998). PCR amplification was performed using the primers 27F: 5′-AGAGTTTGATCCTGGCTCAG-3′ and 1525R: 5′-AAAGGAGGTGATCCAGCC-3′ as described by Chun and Goodfellow (1995). Almost-complete 16S rRNA gene sequences (1400 nt) were deposited in the GenBank database under the accession numbers of MG722685 (strain IT25), MG786938 (strain TO612), MG786894 (strain Y17), MG786896 (strain Y28), MG654776 (strain IC10), and MG676358 (strain IC13). The sequences were aligned manually with corresponding sequences of available *Streptomyces* species deposited in the GenBank, EMBL and DDBJ databases using BLAST search tool (Altschul et al., 1997). Phylogenetic tree was constructed using the MEGA 6.0 software package (Tamura et al., 2013) based on neighbor-joining method. Bootstrap analysis was used to evaluate the stability of relationships based on 1000 resampling. Strains IC10 and Y28 were preserved and deposited in the Agricultural Biotechnology Research Institute of Iran Culture collection (ABRIICC) under accession numbers of ABRIICC 20108 and ABRIICC 20114, respectively.

Greenhouse Experiments

Tomato (*Solanum lycopersicum* L.) cv. Rio Grande susceptible to *FOL* races 2 and 3 (Barker et al., 2005), was used in greenhouse experiments. Seeds were surface sterilized with 1% sodium hypochlorite (NaOCl) and incubated in a growth chamber at 25°C for 7 days. Germinated seedlings were placed into 84-cell plug tray (50 × 30 × 5 cm deep) filled with sterilized soil and peat moss (1:2), with one seedling occupying each cell. Seedlings were watered every day with tap water and kept at 27°C and 16 h brightness/8 h darkness. After 21 days, the seedlings were transferred to pots (15 × 20 cm) filled with a sterile mixture of field soil and peat moss (2:1). For bacterial treatments, *Streptomyces* cell and spore were centrifuged at

8000 rpm for 15 min and then the pellet re-suspended in 10 mL sterile saline solution. Bacterial suspension was added to autoclaved sand and final cfu/g sand adjusted to 10^6. Seven gram of sand containing bacteria was added to the surface of each cultivated pot immediately after transferring of plant to the pot. Sterilized sand was used as a negative control. The pots were watered every 2 days. For *FOL* inoculation, 10 days after bacterial treats, tomato seedlings were uprooted and inoculated with conidial suspension for 30 min (root-dip method). Seedlings submerged in sterile distilled water (mock inoculation) were used for bacterial treatments and negative control. To prepare *FOL* suspension (pathogen inoculum), fungi was cultivated on PDA for 10 days. Conidia were harvested by scraping in sterile water (10 mL/plate) and final conidia/mL adjusted to 5×10^7 using hemocytometer. The treatments were negative control plants (mock inoculation), positive control (*FOL* inoculated), Carbendazim® (soil drenched with fungicide in a concentration of 1.5 g/L) and six *Streptomyces* treatments inoculated or non-inoculated with *FOL*. The plants were harvested 60 days after transferring to the pots. The growth parameters comprising of shoot length, fresh and dry weight of shoot and root were measured and recorded. Further, disease severity (DS) was assessed on a scale from 0 to 5: 1 = symptoms free = 0%; 2 = slight chlorosis, stunting, or wilting = 25%; 3 = moderate chlorosis, stunting, or wilting = 50%; 4 = severe chlorosis, stunting, or wilting = 75%; 5 = death = 100% (Marlatt et al., 1996). Percentage of control value was calculated using the formula (DC − DT)/DC × 100, where "DC" is disease index of inoculated control (*FOL*) and "DT" is disease index of inoculated treatment (%) (Song et al., 2004).

A greenhouse experiment was conducted separately for the next two tests. The procedure of this experiment was similar to the first one, but the experiment duration was shorter and the plants were harvested 14 days after transfer to the pots, also 1 cm of the root end of the seedlings was cut before *FOL*/mock inoculation. Foliar was sprayed with plant hormones (1 mM SA or 10 mM MeJA) 48 h before *FOL* inoculation. The treatments were negative control plants (mock inoculation), positive control (*FOL* inoculated), Carbendazim® (soil drenched with fungicide in a concentration of 1.5 g/L) and two *Streptomyces* treatments (strains IC10 and Y28) inoculated or non-inoculated with *FOL*. Plants leaves were harvested 2 days after *FOL* inoculation, frozen in liquid nitrogen and kept at −70°C for the following analysis.

Antioxidant Enzymes Activity

Frozen leaf samples (100 mg fresh weight) with 10 mg polyvinyl pyrrolydone (PVP) was transferred to 1.5 mL tube and homogenized in 1 mL Na-Pi buffer (1 mM, pH 7). The homogenate was centrifuged at 15000 × g for 15 min. All operations were performed at 4°C. The supernatant was used as a crude enzyme extract. The activities of antioxidant enzymes including peroxidase (POX: EC 1.11.1.7) and catalase (CAT: EC 1.11.3.6) were measured in a reaction containing 250 μL 0.1 M phosphate buffer (pH 7.0), 250 μL 10 mM guaiacol, 30 μL H_2O_2, and 40 μL crude enzyme extract (Chance and Maehly, 1955). The enzyme activity (U/mL) was measured spectrometrically (Cary 300, United States) by monitoring of the degrading H_2O_2 by the increase in the absorbance at 470 nm and the decrease in the absorbance at 290 nm over 3 min.

Quantitative Real-Time PCR Analysis of the Defense-Related Genes

Total RNA was extracted from shoots using RNeasy plant mini kit (QIAGEN). cDNA was synthesized using 1 μg of each RNA sample after treating with RNase-free DNase I (Invitrogen) using iScript cDNA synthesis kit (BioRad) according to manual description. Quantitative PCR was performed in a 25 μL reaction containing 1 μL of template cDNA, 0.5 μL of 10 pM of each forward and reverse specific primer (**Table 2**) and iQ SYBR Green Supermix kit (BioRad) on BioRad multicolor real-time PCR detection system. The PCR profile included an initial denaturation step at 95°C for 3 min, followed by 40 cycles of denaturation (95°C/30 s), primer annealing (60°C/30 s) and primer elongation (72°C/30 s), by a final elongation step (72°C/5 min) and recording melting curves. Results were expressed as the normalized ratio of mRNA level of target gene to internal control tubulin gene (*TUB*). Changes was estimated by using the Relative Expression Software Tool (REST 2009) (Pfaffl et al., 2002).

Statistical Analysis

Statistical analysis was performed using analysis of variance (ANOVA) by Microsoft Excel (Microsoft Corporation, United States) and SPSS version 16.0 (SPSS Inc. Chicago, IL, United States). All data shown are average value of three (*in vitro* experiments) biological replicates ± SE. The greenhouse experiments were carried out in randomized blocks design with four blocks and there were four biological replications for each treatment. The significance differences of the treatments were evaluated using multivariate generalized linear model (GLM) with Duncan multiple range test *post hoc* analysis at level of $P < 0.05$. The relationship between *in vitro* and *in vivo* data was studied using bivariate Pearson test at $P \leq 0.01$.

RESULTS

Isolation and Selection of *Streptomyces* Bacteria

A total of 126 colonies displaying *Streptomyces* appearance including compact colored heaped and wrinkled, waxy, chalky, powdery or velvety colony, were isolated from tomato and cucumber rhizosphere soil collected from Isfahan, Yazd and Kerman (**Figure 1A**). Totally, 106 isolates (84%) were able to grow on solid nitrogen-free medium (**Figure 1B**) of which thirty-eight isolates were able to solubilize inorganic phosphate. Three isolates comprising of IS8, Y7, and Y28 with the ratio 1.9, 0.5, and 0.4 had the most potential to solubilize tricalcium phosphate, respectively (**Figure 1C**). Further, sixty-six percent of 106 isolates were able to produce siderophore (**Figure 1D**). The maximum orange halo due to iron chelation was recorded for isolate TO612 after 7 days of incubation. All 106 isolates produced IAA in a range of 7.0–40.9 μg/mL

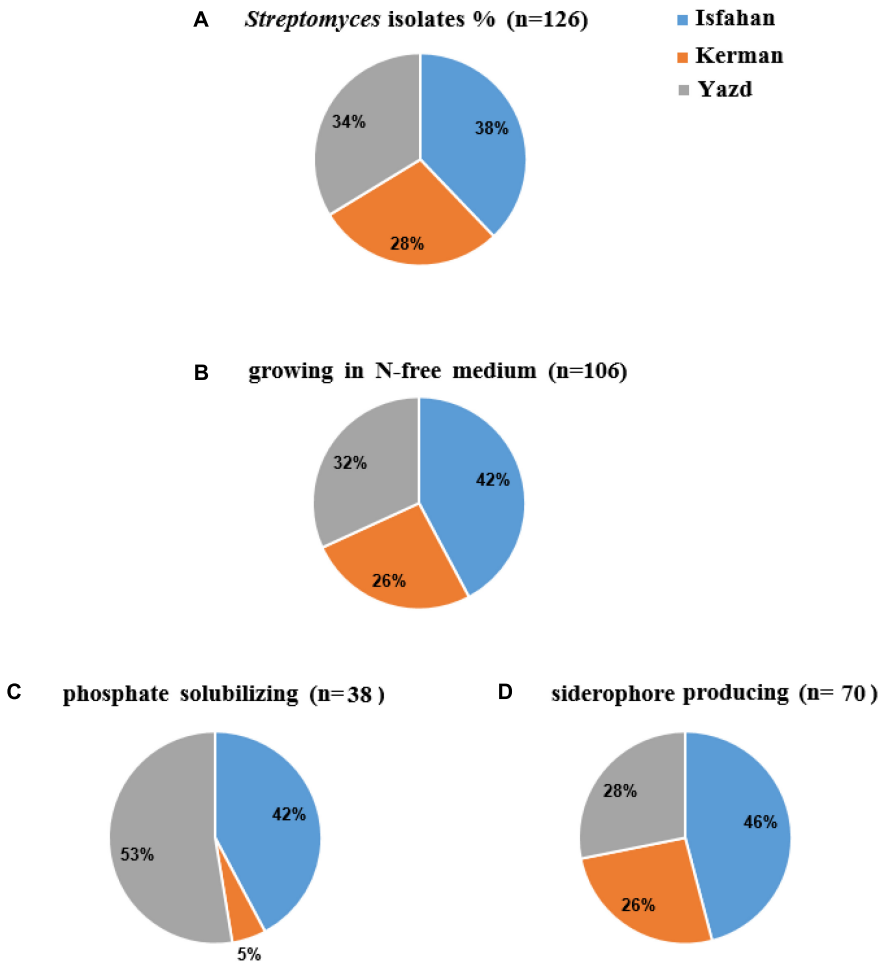

FIGURE 1 | The percent (%) of colonies isolated from Isfahan, Yazd, and Kerman provinces: colonies **(A)** with *Streptomyces* appearance **(B)** growing in N-free medium, **(C)** phosphate solubilizing, and **(D)** siderophore producing.

of which twenty percent produced IAA more than 27 μg/mL. Thirty-two isolates from 106 showed proteolytic enzyme activity. The greatest halo zone/colony diameter ratio for protease activity was 1.0 and recorded for isolate IC10 (**Table 1**). Forty-four isolates were found to produce cellulose. The greatest halo zone/colony diameter ratio for cellulase activity was 1.4 which recorded for Y16. Furthermore, biosynthesis of the chitinolytic enzyme was detectable for 22 isolates. Isolates IC13, K40, SS12, IC6, and Y17 were able to produce all three examined hydrolytic enzymes. Overall, 24 isolates containing at least three PGP traits and hydrolytic enzymes activity were selected for evaluation in the following experiments as shown in **Table 1**.

Growth Inhibition of the Selected Isolates Toward *FOL*

Six isolates (25% of the selected isolates) showed more than 30% inhibitory effect against *FOL* in dual culture test. The highest percentages of growth inhibition were 69, 49, 48, 42, 39, and 38, which were recorded for IC10, IT25, Y17, TO612, Y28, and IC13, respectively (**Table 3**). The biocontrol potential of these isolates (superior PGP antagonistic isolates) was evaluated in a greenhouse experiment.

Phenotypic and Genotypic Characterization of the Superior Isolates

Phenotypical characterization was performed using aerial hyphae and spore chains color of 10-days-old bacterial culture on ISP media. On the medium ISP2, isolates TO612 and Y17 were differentiated from IC10, IC13, IT25, and Y28 according to the color of spore chains. On the medium ISP3, isolates Y28, IT25, and IC10 were distinct from the others based on the color of aerial hyphae. Further, on the medium ISP4, isolate IC13 was differentiated from IC10 by its color of aerial hyphae. Also, these two isolates were recognizable on ISP3 according to the color of their aerial hyphae. Isolates IC10 and Y28 were well distinguished from TO612, Y17 and IC13 using ISP media and from IT25 based on melanin production. Isolates IC10 and Y28 slightly were different from each other on ISP2 medium (**Supplementary Figure S2**). Physiological tests showed only IC13 had potential

TABLE 3 | *In vitro* antagonistic activity against *Fusarium oxysporum* f.sp. *lycopersici* by selected isolates.

Isolates	Growth inhibition (%)	Isolates	Growth inhibition (%)	Isolates	Growth inhibition (%)
IC6	$4.0 \pm 0.1^{j*}$	IT25	49.1 ± 0.8^{b}	IC34	1.7 ± 1.5^{j}
IC10	68.5 ± 1.0^{a}	Y7	0.6 ± 1.1^{j}	KH12	30.0 ± 0.0^{d}
IC13	38.2 ± 0.9^{c}	Y18	1.3 ± 1.1^{j}	K40	4.0 ± 0.0^{j}
IS8	10.6 ± 1.1^{h}	Y27	0.6 ± 1.1^{j}	K43	10.0 ± 2.0^{h}
SS12	0.6 ± 1.1^{j}	TO612	41.5 ± 1.8^{c}		
CU122	0.0 ± 0.0^{k}	Y17	47.5 ± 2.56^{b}		
IC15	17.9 ± 1.4^{g}	Y28	38.7 ± 1.1^{c}		
SS14	1.0 ± 1.1^{j}	Y281	2.3 ± 2.5^{j}		
IT20	$19.3 \pm 0.8^{f,g}$	Y16	2.6 ± 2.5^{j}		
IT8	9.6 ± 0.4^{h}	Y33	1.6 ± 2.8^{j}		

*Values are the means (averaged from three replicates) ± SE. *Same letters within each column represent non-significant difference according to Duncan's Multiple Range Test ($P < 0.05$).*

to grow at 42°C (**Table 4**). All six isolates were able to grow on NaCl 6 % while only isolates Y28 and Y17 were able to grow on medium containing NaCl 10 % (**Table 4**). The preliminary phylogenetic analysis of the 16S rRNA gene sequences showed IC10 and Y28 were closely related to species of the genus *Streptomyces*. The phylogenetic tree constructed from 16S rRNA sequences showed that isolates IC10 and Y28 are two members of *Streptomyces* genus with more than 99.5% sequence similarity to *S. enissocaesilis* NRRL B-16365^{T} and *S. rochei* NBRC 12908^{T}, respectively (**Figure 2**).

Tomato Growth Promotion Activity of the Superior Isolates

Strains TO612, Y28, IC10, and IC13 significantly increased shoot length compared to control plants. Strains Y28 and IC10 increased shoot length up to 20% compared to control (**Figure 3** and **Table 5**). Strains Y17, Y28, IC10 and IC13 significantly ($p < 0.05$) increased fresh shoot weight while only strains IC10 and IC13 increased shoot dry weight. The increases in the shoot fresh and dry weight were in a range 29–36% and 22–37%, respectively (**Table 5**). *Streptomyces* strains did not increase root fresh and dry weight while induced root lateral branching (hairy roots) compared to control (data not shown).

Biocontrol Potential of the Superior Isolates

Biocontrol efficacy of the superior isolates against *FOL* causing wilt disease was evaluated in the greenhouse and compared to the chemical fungicide Carbendazim®. The high level of disease severity (4.3) was observed in positive control. In Carbendazim® treatment, disease severity was 2.1. Disease severity in the plants treated with IC10 and TO612 were 1.6 and 1.9, respectively. Strain IC10 increased control value by 12.5% compared to the chemical fungicide (**Figure 3**). Minimum shoot length, fresh and dry weight were related to positive control and minimum fresh and dry root weight were related to Carbendazim®. All superior isolates significantly increased shoot length, fresh and dry weight of shoot, compared to positive control (**Table 6**). Strains IC13 increased tomato total dry weight by 30 and 51% compared to control and Carbendazim® respectively. Strains Y28 and IC10 with the highest PGP and biocontrol activity were selected to determine their role in the induction of tomato-systemic resistance through antioxidant enzymes and defense-related genes.

Antioxidant Enzymes Activity

Peroxidase activity significantly increased 24 h after inoculation of plants with *FOL*. Further, MeJA individually increased the enzyme activity at the same time interval. Plants inoculated with *FOL* in SA or Y28 treatment increased POX activity after 24 h like positive control (*FOL*). In SA treatment, POX activity increased 48 h after exogenous application. The level of POX activity remained constant in plant treated with *FOL* and MeJA and also SA and Y28 inoculated with *FOL*. In soil treated with strain IC10 and inoculated or non-inoculated with the pathogen, POX activity did not increase during the experiment time (48 h) (**Figure 4**). CAT activity of tomato plants increase 48 h after *FOL* inoculation. Treatments including bacterial strains and plant hormones increased CAT activity after 24 h. Pathogen inoculation slightly suppressed CAT activity in the SA treatment (**Figure 5**).

Quantitative Real-Time PCR Analysis of the Defense-Related Genes

Plant inoculation with *FOL* and MeJA increased UDP-glycosyltransferase (*UDP*) transcripts by 103- and 98-fold,

TABLE 4 | Cultural characteristics of superior PGP antagonistic isolates.

Isolate	Color of aerial hyphae – spore chains on ISP media			Melanin production	Growth (in/on)				GeneBank acc. number
	ISP2	ISP3	ISP4	Tyrosine/no tyrosine media	42°C	NaCl 6%	NaCl 10%	NaCl 13%	
IT25	Yellow – Light purple	Colorless – Light purple	Yellow – purple	–/–	–	++	–	–	MG722685
TO612	Yellow – Light greenish	Yellow – Yellow	Yellow – White	+/+	–	+	–	–	MG786938
Y17	Yellow – Greenish	Yellow – Olive	Dark yellow – White	+/+	–	++	+	–	MG786894
Y28	Yellow – light purple	Colorless – Dark purple	Dark yellow – Purple	–/+	–	++	+	–	MG786896
IC10	Purple –Yellow	Colorless – Purple	Yellow –Purple	–/+	–	+	–	–	MG654776
IC13	Yellow – Light purple	Dark yellow – Purple	Yellow – Dark gray	–/–	+	+	–	–	MG676358

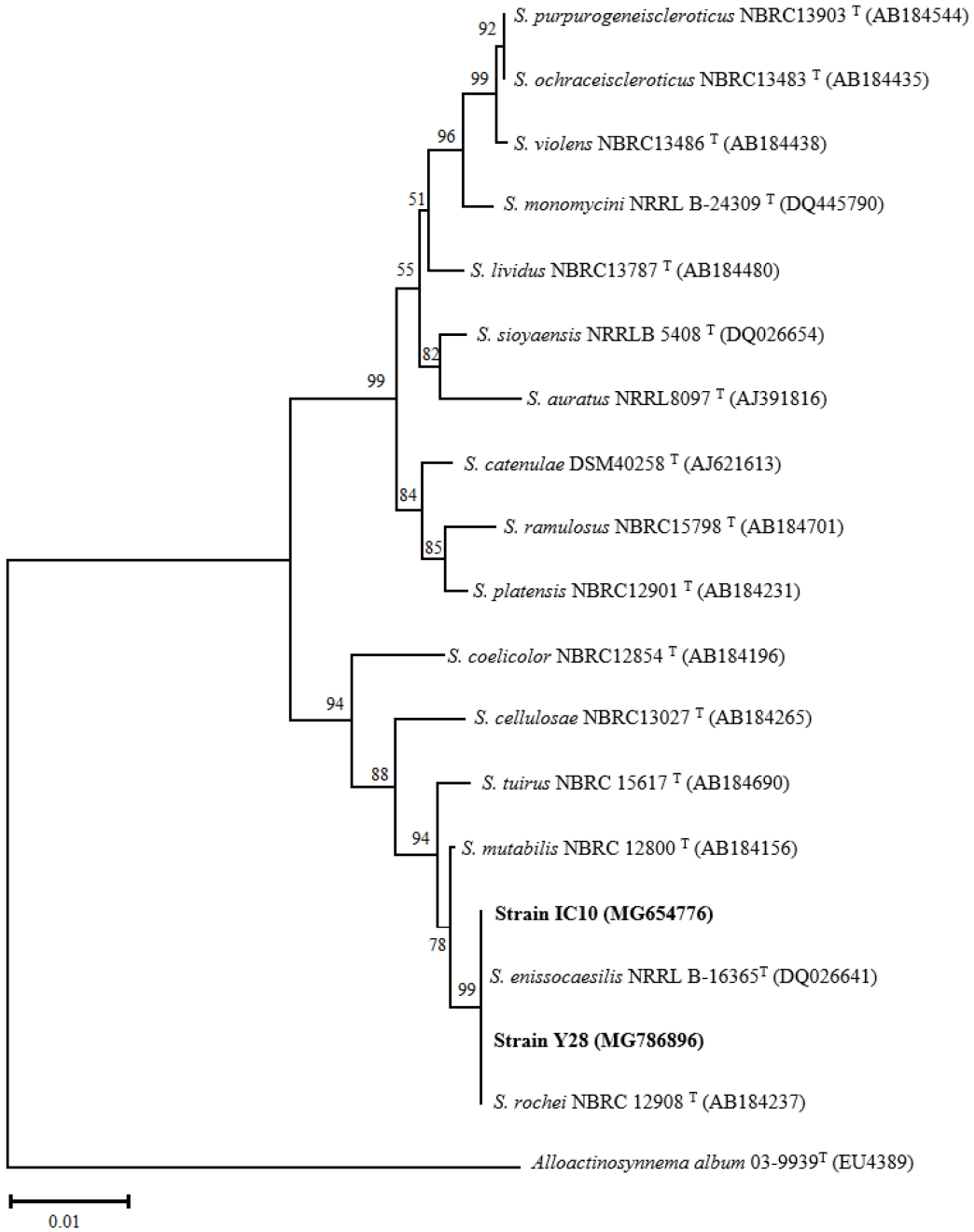

FIGURE 2 | Phylogenetic tree based on almost complete 16S rRNA gene sequences of *S. enissocaesilis* strain IC10 and *S. rochei* strain Y28. Tree was calculated using neighbor-joining method illustrating the taxonomic position of the strains with related species. Accession numbers of the sequences are given in parentheses. The sequences of *Alloactinosynnema album* 03-9939T (EU438907) was used as outgroup. Bootstrap values are based on 1000 resampling and shown at the branching points. Bar indicates 0.01 substitutions per nucleotide position.

respectively, compared to control. Although *Streptomyces* strains induced *UDP* transcription, they significantly suppressed gene expression in the plants inoculated with *FOL* (**Figure 6A**). Treatments including *Streptomyces* strains and plant hormones and not *FOL* significantly increased phenylalanine ammonia-lyase (*PAL*) transcripts compared to control. Salicylic acid and strain IC10 also retained their induction effect in plants inoculated with *FOL* (**Figure 6B**). The results revealed that plants treated with SA, IC10, Y28, SA-*FOL*, and IC10-*FOL* significantly stimulated (up-regulated) *WRKY70* expression. Treatments of *FOL* and MeJA did not increase relative expression of *WRKY70* in tomato plants (**Figure 6C**). Tomato peroxidase (*TPX1*) transcripts was significantly up-regulated in all treatments including *Streptomyces* strains and plant hormones. Salicylic

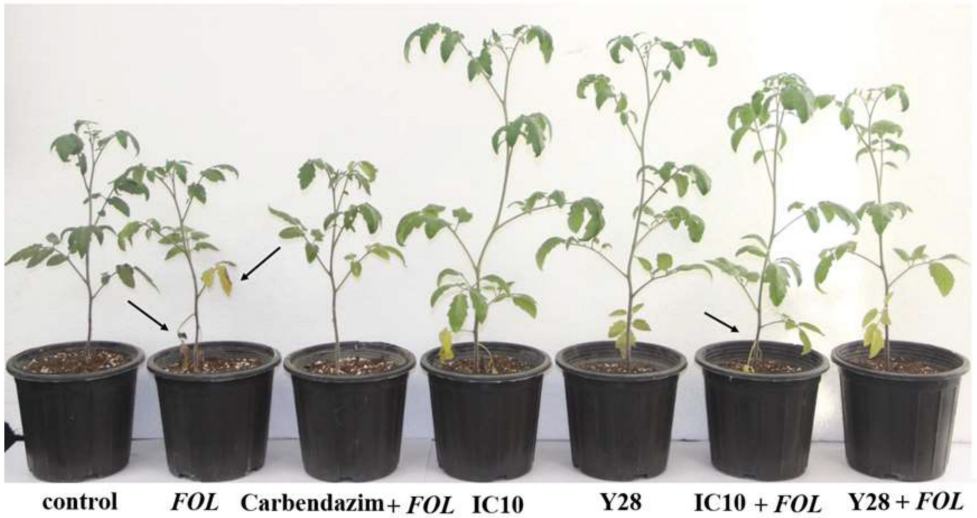

FIGURE 3 | Biocontrol of tomato wilt and stunt caused by *FOL* using *S. enissocaesilis* strain IC10 and *S. rochei* strain Y28 in greenhouse conditions. Data recorded 60 days after bacterial treatment. Stunting is seen in infected plants. Arrows showing wilting symptoms (chlorosis and dried leaves) in *FOL* inoculated plants.

TABLE 5 | Effect of superior PGP antagonistic isolates (IT25, TO612, Y17, Y28, IC10, and IC13) on tomato growth parameters in greenhouse conditions.

Treatment	Shoot length (cm)	Shoot fresh weight (g)/plant	Shoot dry weight (g)/plant	Root fresh weight (g)/plant	Root dry weight (g)/plant
Negative control	$24.18 \pm 0.55^{c*}$	11.36 ± 0.60^{b}	$1.79 \pm 0.14^{b,c}$	3.61 ± 0.14^{a}	1.72 ± 0.10^{a}
IT25	24.87 ± 0.60^{c}	$10.19 \pm 0.35^{b,c}$	1.39 ± 0.16^{c}	$2.36 \pm 0.35^{a,b}$	$0.90 \pm 0.19^{d,e}$
TO612	29.37 ± 0.32^{a}	11.63 ± 0.23^{b}	1.87 ± 0.19^{b}	$2.78 \pm 0.17^{a,b}$	$0.81 \pm 0.16^{d,e}$
Y17	$26.50 \pm 0.20^{b,c}$	15.47 ± 0.30^{a}	$2.18 \pm 0.10^{a,b}$	3.61 ± 0.19^{a}	1.51 ± 0.25^{b}
Y28	$29.00 \pm 0.56^{a,b}$	14.97 ± 0.49^{a}	$2.16 \pm 0.15^{a,b}$	$2.88 \pm 0.12^{a,b}$	1.23 ± 0.18^{c}
IC10	$28.90 \pm 0.25^{a,b}$	15.37 ± 0.38^{a}	2.31 ± 0.39^{a}	1.64 ± 0.32^{b}	$0.92 \pm 0.12^{d,e}$
IC13	$28.62 \pm 0.29^{a,b}$	14.70 ± 0.65^{a}	2.45 ± 0.22^{a}	1.78 ± 0.13^{b}	$0.80 \pm 0.24^{d,e}$

*Data recorded 60 days after bacterial treatment. *Same letters within each column represent non-significant difference at 5%, according to Duncan's tests using the GLM procedure (df = 9, F = 7.16, and $p < 0.05$).*

TABLE 6 | Biocontrol of tomato wilt and stunt caused by *F. oxysporum* f.sp. *lycopersici* race 3 (*FOL*) using superior PGP antagonistic isolates (IT25, TO612, Y17, Y28, IC10, and IC13) in greenhouse conditions.

Treatments	Shoot length (cm)	Shoot fresh weight (g)/plant	Shoot dry weight (g)/plant	Root fresh weight (g)/plant	Root dry weight (g)/plant	Disease severity	Control value (%)
Negative control	$23.62 \pm 0.25^{b*}$	$11.20 \pm 0.63^{a,b}$	$1.35 \pm 0.35^{a,b}$	3.31 ± 0.10^{a}	1.41 ± 0.33^{a}	1.0^{d}	–
Positive control (FOL)	14.00 ± 0.28^{d}	5.56 ± 0.34^{c}	0.78 ± 0.18^{c}	$1.66 \pm 0.33^{a,b}$	$0.37 \pm 0.29^{c,d}$	4.3^{a}	–
Carbendazim®+FOL	15.25 ± 0.22^{d}	$13.00 \pm 0.25^{a,b}$	2.20 ± 0.16^{a}	0.23 ± 0.38^{b}	0.18 ± 0.14^{d}	$2.1^{a,b,c}$	$71.9^{a,b}$
IT25+FOL	20.20 ± 0.43^{c}	$10.23 \pm 0.27^{b,c}$	$1.77 \pm 0.55^{a,b}$	2.48 ± 0.49^{a}	$1.00 \pm 0.37^{a,b}$	$2.3^{a,b}$	$68.8^{b,c}$
TO612+FOL	19.00 ± 0.20^{c}	$12.77 \pm 0.32^{a,b}$	2.40 ± 0.38^{a}	2.90 ± 0.20^{a}	1.40 ± 0.38^{a}	$1.9^{c,d}$	78.1^{a}
Y17+FOL	19.50 ± 0.35^{c}	$13.38 \pm 0.26^{a,b}$	2.09 ± 0.58^{a}	2.76 ± 0.37^{a}	$0.94 \pm 0.29^{a,b}$	$2.0^{b,c}$	$75.0^{b,c}$
Y28+FOL	26.70 ± 0.15^{a}	$11.88 \pm 0.75^{a,b}$	2.02 ± 0.60^{a}	2.94 ± 0.28^{a}	$0.59 \pm 0.33^{b,c}$	$2.0^{b,c}$	$75.0^{b,c}$
IC10+FOL	26.60 ± 0.35^{a}	$12.83 \pm 0.10^{a,b}$	2.07 ± 0.38^{a}	$1.83 \pm 0.18^{a,b}$	$0.96 \pm 0.24^{a,b}$	$1.6^{c,d}$	84.4^{a}
IC13+FOL	21.33 ± 0.39^{c}	15.00 ± 0.29^{a}	2.45 ± 0.41^{a}	2.54 ± 0.30^{a}	$1.15 \pm 0.31^{a,b}$	$2.1^{a,b,c}$	$71.9^{a,b}$

*Data recorded 60 days after bacterial treatment. Disease severity was assessed on a scale of 1 to 5 (1, symptoms free; 5, severe symptoms). *Same letters within each column represent non-significant difference at 5%, according to Duncan's tests using the GLM procedure (df = 11, F = 3.63, and $p < 0.05$).*

acid and strain Y28 also induced *TPX1* gene expression in plants inoculated with *FOL* (**Figure 6D**). The highest lipoxygenase (*LOX*) gene expression level (38- fold) was detected in Y28. There was a significant down-regulation of *LOX* gene in *FOL* and IC10 treatments. On the contrary, MeJA and Y28 stimulated *LOX* expression. Induced *LOX* expression was also observed in plants treated with bacteria and inoculated with *FOL* (**Figure 6E**). In a similar pattern, SA and Y28 significantly increased pathogenesis related protein 1 (*PR1*) and ethylene response factor 1 (*ERF1*) transcripts. Strains IC10 and Y28 also

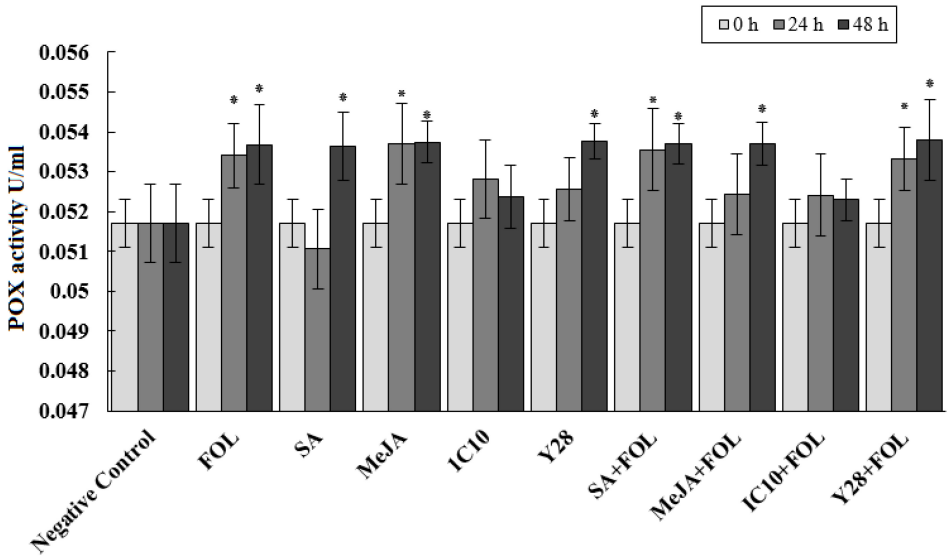

FIGURE 4 | Effect of biological (*S. enissocaesilis* strain IC10 and *S. rochei* strain Y28) and chemical (SA and MeJA) treatments on the induction of peroxidase (POX) activity in tomato leaves non-inoculated (left) and inoculated (right) with *FOL* at different time intervals of inoculation ($df = 29$; $F = 2.90$; $P < 0.01$). Data represent the mean values ± SE of three biological replicates. Negative control: untreated and non-inoculated. In each treatment, the values marked with an asterisk are significantly ($P < 0.05$) different from negative control at time point 0.

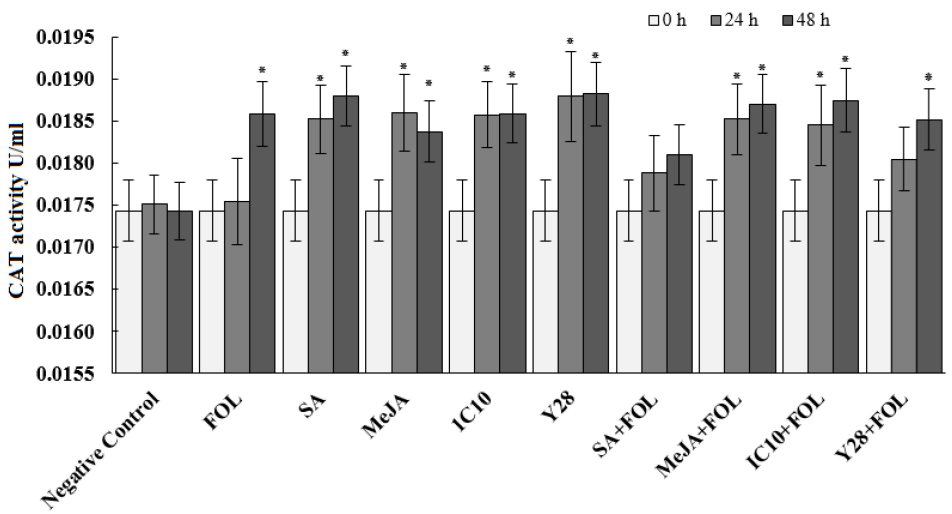

FIGURE 5 | Effect of biological (*S. enissocaesilis* strain IC10 and *S. rochei* strain Y28) and chemical (SA and MeJA) treatments on the induction of catalase (CAT) activity in tomato leaves non-inoculated (left) and inoculated (right) with *FOL* at different time intervals of inoculation ($df = 29$; $F = 30.73$; $P < 0.01$). Data represent the mean values ± SE of three biological replicates. Negative control: untreated and non-inoculated. In each treatment, the values marked with an asterisk are significantly ($P < 0.05$) different from negative control at time point 0.

were able to stimulate the *PR1* expression in the presence of *FOL* (**Figures 6F,G**).

Correlation Analysis

There was a significant relationship between siderophore and IAA production ($r = 0.36$). Besides, a correlation was found between growth inhibition and protease activity ($r = 0.31$). Moreover, growth inhibition of *FOL* in dual culture assay was significantly correlated to siderophore production ($r = 0.64$) (**Table 7**). A significant negative correlation (−0.63) was observed between growth inhibition (*in vitro* assay) and disease severity (*in vivo* assay).

DISCUSSION

Almost half of tomato and cucumber greenhouses in Iran (more than 7000 hectares) is located in Yazd, Isfahan, and Kerman

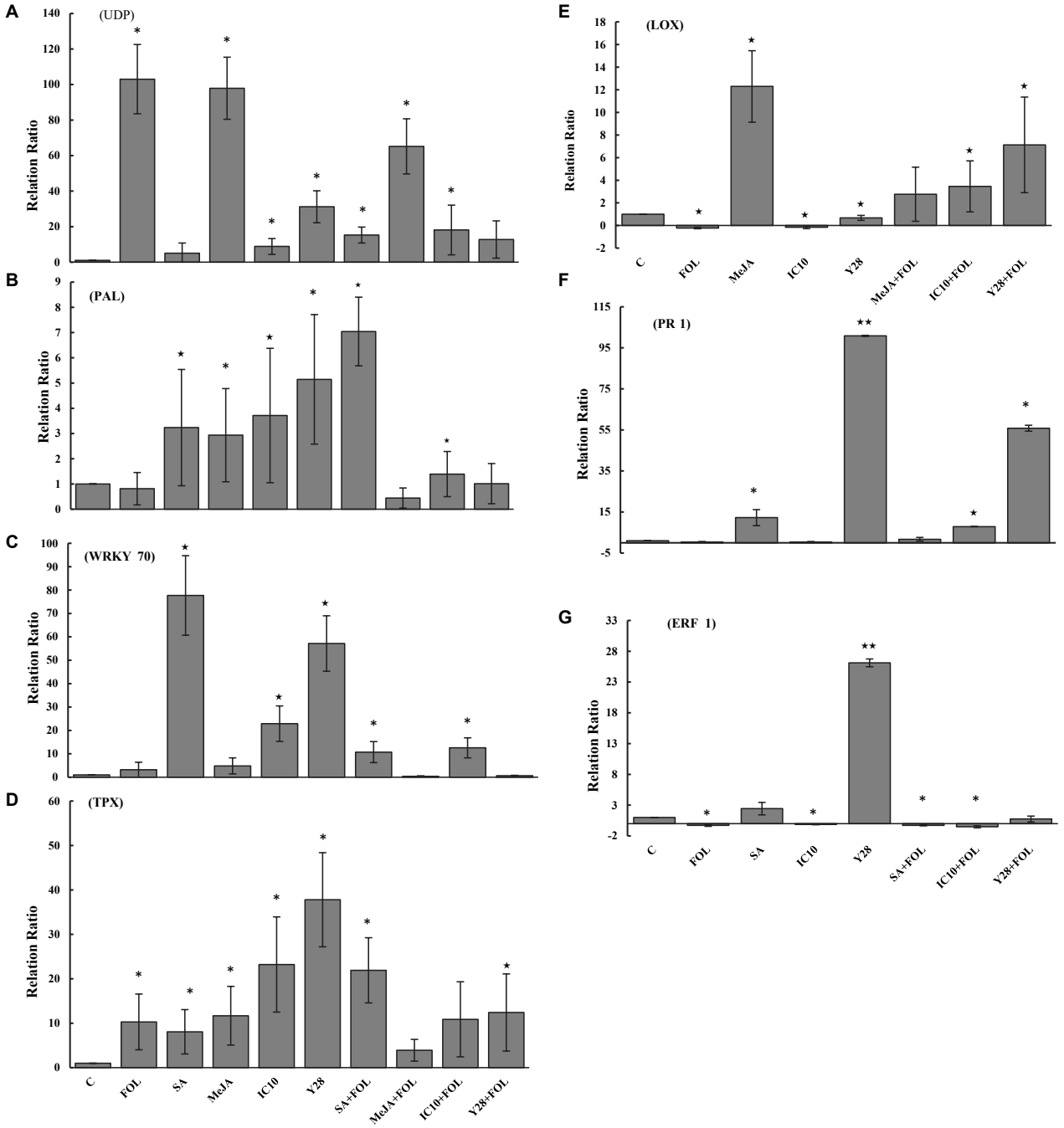

FIGURE 6 | The relative level of gene expression (fold) determined by qRT-PCR of seven target genes including *UDP* **(A)**, *PAL* **(B)**, *WRKY70* **(C)**, *TPX* **(D)**, *LOX* **(E)**, *PR1* **(F)**, and *ERF1* **(G)** versus reference control (*Tubulin* gene) in tomato "Riogrande" treated with chemical (MeJA and SA) or biological agents (*S. enissocaesilis* strain IC10 and *S. rochei* strain Y28) 48 h after inoculation with *FOL*/ distilled water. Untreated and non-inoculated plants were considered as control (C) and as reference sample. Standard error represents for three biological replicates. Positive values of fold change indicate up-regulation while negative values indicate down-regulation. The values marked with one and two asterisk are significantly different from control at $P < 0.05$ and $P < 0.01$, respectively.

provinces. Amount and type of organic fertilizer and soil used to prepare the greenhouse growth bed are different in these provinces. Farmers in Yazd and Kerman use sand from the bed of the nearest rivers to their greenhouse and farmers in Isfahan use soil of the greenhouse floor as a raw material to prepare culture bed (private conversation). Our results showed distribution of the bacterial isolates with the *Streptomyces* appearance in the three provinces is slightly different. Among the isolates

TABLE 7 | Pearson correlation coefficients (r) between PGP traits (*in vitro* assays) and biocontrol activity (*in vivo* assay).

Pearson correlation	*In vitro* assays		*In vivo* assay
Variables	**IAA production**	**Fungal growth inhibition (%)**	**Disease severity**
Protease activity	0.44^{ns}	0.31*	-0.47^{ns}
Siderophore production	0.36*	0.64**	0.24^{ns}
IAA production	1	0.47*	-0.01^{ns}
Fungal growth inhibition			−0.63*

*ns, non-significant; *P < 0.05; and **P < 0.01.*

that showed a PGP trait, a relatively stable share (42–46%) belonged to Isfahan. The contribution of the *Streptomyces* isolated from Yazd or Kerman in each PGP trait was not always constant showing *Streptomyces* with several PGP traits in the field soil is greater than that of rivers sand. A previous study on *Streptomyces* showed that bacterial diversity was more affected by the habitat than the population (Davelos et al., 2004). The restriction of some nutrients in soil may be a major contributor to the change in the microbial diversity due to natural selection.

Growth ability on a nitrogen-free medium and IAA and siderophore production were three dominant characteristics of *Streptomyces* isolated from vegetable rhizosphere soils. A lower percentage (30%) of the isolates had the potential for solubilizing phosphate. Besides, the location of isolation was also effective on this ratio. There was a significant positive correlation between IAA and siderophore production, which may remind a complementary role of the siderophore in plant growth promotion activity (i.e., in addition to its role in antagonistic activity). Such correlation was not observed between other traits involved in antagonist activity and IAA production.

The ability of *FOL* growth inhibition was very different between *Streptomyces* isolates showing PGP properties. Isolate CU122 with four PGP traits, was not able to inhibit *FOL* growth. Failure to inhibit the pathogen growth was correlated to the inability of isolate CU122 to produce chitinase and protease enzymes. On the contrary, isolate IC10 with same *in vitro* PGP features as well as enzymes activity inhibited *FOL* growth very well. The correlation of protease and chitinase activity with inhibition of *FOL* growth was positive and respectively, quantitative and non-quantitative. Only two exceptions did not adhere to this relationship. Isolates TO612 and KH12, which did not show enzyme activity, inhibited *FOL* growth in an acceptable range (equal to or greater than 30%).

This finding revealed that although chitinolytic activity of *Streptomyces* and digestion of the fungal cell wall is an effective mechanism of growth inhibition (Gherbawy et al., 2012), other mechanisms such as antibiosis and even an enzyme like protease (Xu et al., 2016) that is less studied are also involved in antagonism. Interestingly, there was a significant correlation between IAA and siderophore productions and *FOL* growth inhibition, showing relationship between PGP features and antagonistic activities in *Streptomyces*. IAA production is a common characteristic among antagonistic species of *Streptomyces* (Sreevidya et al., 2016). It seems that IAA production alone does not cause plant growth, and other traits, such as siderophore production, also has an important role in increasing plant growth. In this regard, Kunova et al. (2016) showed that the antagonistic isolates producing IAA did not increase growth of different vegetable species. These isolates were not able to produce siderophore. The significant negative correlation that was observed between *FOL* growth inhibition (*in vitro* assay) and disease severity (*in vivo* assay) confirmed a need for *in vitro* tests to select the best biocontrol strains. Recently, Wu et al. (2019) reported that a decreased percentage disease index of rice sheath blight caused by *Rhizoctonia solani* was associated with an increase in *Streptomyces* derived antifungal agent concentration. They concluded that the antifungal agent reduces sheath blight symptoms via exerting a strong antagonistic activity against *R. solani* both *in vivo* and *in vitro* conditions. *S. rochei* ACTA1551 from Greek (Kanini et al., 2013), *S. miharaensis* KPE62302H (Kim et al., 2012), and *S. psammoticus* KP1404 (Kim et al., 2011) from Korea, *S. plicatus* from Egypt (Abd-Allah, 2001) and *S. griseorubens* E44G from Saudi Arabia (Rashad et al., 2017) were reported as successful biocontrol agents to control tomato *Fusarium* wilt. In the previous reports, the pathogen race has not been determined and to our knowledge, this is the first report of biocontrol of Fusarium wilt caused by *F. oxysporum* Schlecht. f. sp. *lycopersici* (Sacc.) race 3 in tomato with *Streptomyces* strains.

Strain Y28 and IC10 were close to *S. rochei* and *S. enissocaesilis*, respectively and are grouped in a clade on the phylogenetic tree. These PGP strains were isolated from the rhizosphere soils of two greenhouses in two different locations with a distance of 300 kilometers. The high similarity in PGP, and biocontrol activity of these two strains revealed that evolutionary process can keep PGP traits and biological control activities together.

All plants treated with SA, MeJA and Y28 or inoculated with *FOL* increased POX activity during 48 h after *FOL* inoculation. The POX activity in hormone or PGPR treated plants was not affected by *FOL* inoculation. Despite the similar biocontrol activity, isolates IC10 and Y28 had a different effect on the induction of plant POX activity. None of the plants treated with IC10, inoculated or non-inoculated with *FOL*, increased POX activity. Peroxidase is considered an important pathogen-related protein (PR-protein) or defense protein involved in many physiological responses of plants to biotic stresses. Contribution to biosynthesis of lignin (Chittoor et al., 1997) and antimicrobial compounds such as phytoalexins and quinones (Mayer, 2006) are two well-known POX roles associated with ISR. Increased peroxidase activity of cucumber was reported in plants showing Fusarium wilt (Zhao et al., 2012) and also plant treated with *Streptomyces* as biocontrol agent (Salla et al., 2016).

Peroxidase, as well as CAT, are involved in plant antioxidant defense system and reduce the harmful effects of stresses by scavenging of ROS (Das and Roychoudhury, 2014). In this study, the effects of *FOL*, plant hormones and PGP strains

to induce CAT activity were the same. Induction of systemic resistance through defense-related enzymes POX and CAT in tomato plants treated with salicylic acid or *Pseudomonas fluorescens* was reported by Nikoo et al. (2014). They showed that pathogen inoculation of plants treated with bacterial or hormonal elicitors increased both POX and CAT activity in higher levels compared to non-inoculated treated plants or plants only inoculated with pathogen. This association was not observed in our experiment.

Relative expression of several candidate genes encoding transcription factors (*WRKY70* and *ERF1*), *PR1*, *TPX1*, *UDP*, *LOX*, and *PAL* was evaluated in this study. The plant-specific transcription factor WRKY70 is an important factor in *Arabidopsis* signaling pathways and its expression is activated by SA and repressed by JA. Ren et al. (2008) showed that overexpression of *WRKY70* reduced JA responses and mutually JA treatment inhibited *WRKY70* expression. On the contrary, WRKY70 is known as a positive regulator of SA-mediated defense because increases *PR1* which is often studied as a marker gene for SA-dependent defense signaling (Li et al., 2004). It is reported that PGP *Bacillus cereus* AR156 stimulated the transcription of *WRKY70* in *Arabidopsis* leaves. According to their study, *WRKY70* modulated *B. cereus*-triggered ISR through activating SA signaling pathway (Wang et al., 2018). Our results are in accordance with the reported studies and showed induction of *WRKY70* transcription upon treatment with SA, and not with MeJA, in *FOL* inoculated and non-inoculated plants. IC10 and Y28 also significantly induced transcription of *WRKY70* and IC10 continued to induce gene expression after *FOL* inoculation. Following increased *WRKY70* transcripts, expression of *PR1* increased in SA and Y28 treatments. Great increase in *PR1* transcript abundance by Y28 and not IC10 indicates that these two PGPRs stimulate different pathways to elicit defense priming in tomato plant.

UDP-glucose dependent hydroquinone: O-glucosyl-transferase (arbutin synthase) is a member of glycosyltransferases catalyze production of arbutin in higher plants (Arend et al., 2000a). Arbutin is a phenolic glycoside that has antimicrobial and antifungal activity (Kundakovic et al., 2014). Arbutin synthase is a multifunctional enzyme converting various natural products, xenobiotics and toxins (Arend et al., 2000b). There is no report about induction of *UDP* in response to *F. oxysporum* or *Streptomyces* PGPRs in tomato plant. A previous report revealed that induction of members of *UDP* family, *UGT73B3* and *UGT73B5* is necessary during the hypersensitive response of *Arabidopsis* to plant pathogen *Pseudomonas syringae* (Langlois-Meurinne et al., 2005). Also treatments of *Arabidopsis* with SA and MeJA induced the expression of another gene family member *UGT73C5* involved in mycotoxin detoxification (Poppenberger et al., 2003). Increased *UDP* transcript in *FOL* inoculated tomato can be attributed to the role of arbutin in detoxification of fungal toxin or its antimicrobial effect (Kuzniak et al., 2015). The increased expression of this gene in treatment of MeJA and not SA represents its role in ISR. Compared to *FOL* inoculation, a significant lower level of *UDP* expression was observed in plants treated with IC10 and Y28 highlighting the potential role of these PGP strains in tomato defense priming.

FOL, SA, MeJA and PGPRs induced expression of *TPX1*. *TPX1*, peroxidase encoding gene, is involved in the synthesis of lignin and suberin (Quiroga et al., 2000). Here, *TPX1* expression induction by Y28 and IC10 revealed their role in ISR. *TPX1* expression at the lower level was observed 48 h after *FOL* inoculation. Different POX activities in plants treated with PGPRs could be related to the *TPX1* transcript abundance.

Phenylalanine ammonia lyase encoded by *PAL* is involved in the biosynthesis of salicylic acid and defense compounds including flavonoids, phenylpropanoids and lignin. Induction of PAL activity in response to various stimulants such as tissue plant pathogens and hormones was reported (Edwards et al., 1985). In this study, induced expression of *PAL* in bacterial and hormonal treatments was observed and there was no difference between the induction effects of bacterial strains. The induction of PAL enzymatic activity and *PAL* gene expression in tomato plants upon pre-treatment with *Bacillus thuringiensis* (Akram et al., 2013) and the mycorrhizal fungus *Funneliformis mosseae* (Song et al., 2015) were also reported.

Members of the ERF protein family are transcription factors involved in ET/JA or SA signaling pathways and cause moderate disease resistance responses in various plant species (Liang et al., 2008). Induced expression of *ERF1* in *Arabidopsis* plants treated with a PGP biocontrol strain of *Paraburkholderia phytofirmans* in response to a model plant pathogen *P. syringae* pv. tomato DC3000 was reported recently (Timmermann et al., 2017). Likewise, induction of *ERF1* by treatment of Y28 tomato was observed in the present study too. On the contrary, plants treated with IC10 decreased *ERF1* expression. Our data supports the hypothesis that studied PGP strains regulate tomato defense responses through different molecular pathways possibly acting at transcriptional level.

LOX is a signaling molecule involved in pathogen plant resistance. Strain Y28 slightly induced *LOX* expression in non-pathogen inoculated plants. *FOL* inoculation and IC10 treatment caused a significant decreased in transcript level of *LOX* compared to the control plants. *FOL* inoculation of both bacterial treatments caused an induction of gene expression. Our finding is consistent with Mariutto et al. (2011) that showed tomato plants treated with PGP *Pseudomonas putida* did not induce *LOX* transcription before inoculation with the pathogen *B. cinerea*. Although transcripts of *LOX* for both strains were higher in *FOL* inoculated plants, gene expression levels in non-inoculated bacterial treatments were different significantly.

CONCLUSION

The superior PGP antagonistic *Streptomyces* strains, show biocontrol activities against Fusarium wilt of tomato caused by *F. oxysporum* Schlecht. f. sp. *lycopersici* (Sacc.) race 3. Significant positive correlation between siderophore and IAA production and siderophore accumulation and growth inhibition showed a relationship between PGP and antagonistic traits. A significant

negative correlation between growth inhibition (*in vitro* assay) and disease severity (*in vivo* assay) confirmed a need for *in vitro* tests to select the best biocontrol strains. The correlation of PGP traits with biocontrol activity in phylogenetically close species isolated from distant habitats refers to the role of the natural selection in preserving traits that give superiority to bacteria in the rhizosphere. Here we showed biocontrol *Streptomyces* stimulate plant defense system through different molecular pathways at the transcriptional level.

AUTHOR CONTRIBUTIONS

NS and AS designed and directed the research. MS gave advice during experiments. SA carried out all experiments. All authors contributed to the interpretation of the results. SA wrote the manuscript with help from NS and AS. All authors read and approved the final manuscript.

FUNDING

This work was supported by the Agricultural Biotechnology Research Institute of Iran (ABRII) (Grant No. 12-05-05-034-09454-950941).

SUPPLEMENTARY MATERIAL

The Supplementary Material for this article can be found online at: https://www.frontiersin.org/articles/10.3389/fmicb.2019.01505/full#supplementary-material

FIGURE S1 | Identification of *Fusarium oxysporum* f. sp. *lycopersici* (*FOL*) physiological race 3 by selective primers. Polymerase chain reactions carried out using unif, sp13, sp23, and sprl primer sets. 1 kb: I kb ladder; C, negative control.

FIGURE S2 | Bacterial colonies, *S. enissocaesilis* strain IC10 and *S. rochei* strain Y28, on ISP2 medium 10 days after cultivation.

REFERENCES

Abd-Allah, E. F. (2001). Streptomyces plicatus as a model biocontrol agent. *Folia. Microbiol.* 46, 309–314. doi: 10.1007/bf02815619

Akram, W., Mahboob, A., and Javed, A. A. (2013). Bacillus thuringiensis strain 199 can induce systemic resistance in tomato against Fusarium wilt. *Eur. J. Microbiol. Immunol.* 3, 275–280. doi: 10.1556/EuJMI.3.2013.4.7

Alexander, D. B., and Zuberer, D. A. (1991). Use of chrome azurol S reagents to evaluate siderophore production by rhizosphere bacteria. *Biol. Fert. Soil* 12, 39–45. doi: 10.1007/bf00369386

Altschul, S. F., Madden, T. L., Schaffer, A. A., Zhang, J., Zhang, Z., Miller, W., et al. (1997). Gapped BLAST and PSI-BLAST: a new generation of protein database search programs. *Nucleic Acids Res.* 25, 3389–3402. doi: 10.1093/nar/25.17.3389

Arend, J., Warzecha, H., and Stockigt, J. (2000a). Hydroquinone:O-glucosyltransferase from cultivated Rauvolfia cells: enrichment and partial amino acid sequences. *Phytochem* 53, 187–193. doi: 10.1016/s0031-9422(99)00539-7

Arend, J., Warzecha, H., Hefner, T., and Stockigt, J. (2000b). Utilizing genetically engineered bacteria to produce plant-specific glucosides. *Biotechnol. Bioengin.* 76, 126–131. doi: 10.1002/bit.1152

Barker, S. J., Edmonds-Tibbett, T. L., Forsyth, L. M., Klingler, J. P., Toussaint, J. P., Smith, F. A., et al. (2005). Root infection of the reduced mycorrhizal colonization (rmc) mutant of tomato reveals genetic interaction between symbiosis and parasitism. *Physiol. Mole. Plant Pathol.* 67, 277–283. doi: 10.1016/j.pmpp.2006.03.003

Beckers, G. J., and Conrath, U. (2007). Priming for stress resistance: from the lab to the field. *Curr. Opin. Plant. Biol.* 10, 425–431. doi: 10.1016/j.pbi.2007.06.002

Ben Abdallah, R. A., Mokni-Tlili, S., Nefzi, A., Jabnoun-Khiareddine, H., and Daami-Remadi, M. (2016). Biocontrol of Fusarium wilt and growth promotion of tomato plants using endophytic bacteria isolated from Nicotiana glauca organs. *Biol. Control* 97, 80–88. doi: 10.1016/j.biocontrol.2016.03.005

Berger, L. R., and Reynolds, D. M. (1958). The chitinase system of a strain of Streptomyces griseus. *Biochim. Biophy. Acta.* 29, 522–534. doi: 10.1016/0006-3002(58)90008-8

Bruce, T. J., and Pickett, J. A. (2007). Plant defence signaling induced by biotic attacks. *Curr.Opin. Plant. Biol.* 10, 387–392. doi: 10.1016/j.pbi.2007.05.002

Cao, P., Liu, C., Sun, P., Fu, X., Wang, S., Wu, F., et al. (2016). An endophytic Streptomyces sp. *strain DHV*3-2 from diseased root as a potential biocontrol agent against Verticillium dahliae and growth elicitor in tomato (Solanum lycopersicum). *Anton. Leeuw.* 109, 1573–1582. doi: 10.1007/s10482-016-0758-6

Chance, B., and Maehly, A. C. (1955). Assay of catalase and peroxidase. *Methods Enzymol.* 2, 764–775.

Chellemi, D. O., Gamliel, A., Katan, J., and Subbarao, K. V. (2016). Development and deployment of systems-based approaches for the management of soilborne plant pathogens. *Phytopathol* 106, 216–225. doi: 10.1094/PHYTO-09-15-0204-RVW

Chittoor, J. M., Leach, J. E., and White, F. F. (1997). Differential Induction of a Peroxidase Gene Family During Infection of Rice by Xanthomonas oryzae pv. *oryzae*. *Mol. Plant. Microbe Interac* 10, 861–871.

Chun, J., and Goodfellow, M. (1995). A phylogenetic analysis of the genus Nocardia with 16S rRNA gene sequences. *Int. J. Sys. Bacteriol* 45, 240–245. doi: 10.1099/00207713-45-2-240

Dahal, B., NandaKafle, G., Perkins, L., and Brozel, V. S. (2017). Diversity of free-Living nitrogen fixing Streptomyces in soils of the badlands of South Dakota. *Microbiol. Res.* 195, 31–39. doi: 10.1016/j.micres.2016.11.004

Das, K., and Roychoudhury, A. (2014). Reactive oxygen species (ROS) and response of antioxidants as ROS-scavengers during environmental stress in plants. *Front. Environ. Sci.* 2:53. doi: 10.3389/fenvs.2014.00053

Davelos, A. L., Xiao, K., Samac, D. A., Martin, A. P., and Kinkel, L. L. (2004). Spatial variation in Streptomyces genetic composition and diversity in a prairie soil. *Microb. Ecol.* 48, 601–612. doi: 10.1007/s00248-004-0031-9

de Oliveira-Longatti, S. M., Marra, L. M., Lima Soares, B., Bomfeti, C. A., da Silva, K., Avelar Ferreira, P. A., et al. (2014). Bacteria isolated from soils of the western Amazon and from rehabilitated bauxite-mining areas have potential as plant growth promoters. *World. J. Microbio.l Biotechnol.* 30, 1239–1250. doi: 10.1007/s11274-013-1547-2

Edwards, K., Cramer, C. L., Bolwell, G. P., Dixon, R. A., Schuch, W., and Lamb, C. J. (1985). Rapid transient induction of phenylalanine ammonia-lyase mRNA in elicitor-treated bean cells. *Proc. Nat. Acad. Sci. U.S.A.* 82, 6731–6735. doi: 10.1073/pnas.82.20.6731

Fravel, D. R., Olivan, C., and Alabouvette, C. (2003). Fusarium oxysporum and its biocontrol. *New Phytol.* 157, 493–502. doi: 10.1046/j.1469-8137.2003.00700.x

Gherbawy, Y., Elhariry, H., Altalhi, A., El-Deeb, B., and Khiralla, G. (2012). Molecular screening of Streptomyces isolates for antifungal activity and family 19 chitinase enzymes. *J. Microbiol.* 50, 459–468. doi: 10.1007/s12275-012-2095-4

Gouda, S., Kerry, G. R., Gitishree, D., Paramithiotis, S., Shin, H.-S., and Patra, J. K. (2018). Revitalization of plant growth promoting rhizobacteria for sustainable development in agriculture. *Microbiol. Res.* 206, 131–140. doi: 10.1016/j.micres.2017.08.016

Goudjal, Y., Toumatia, O., Yekkour, A., Sabaou, N., Mathieu, F., and Zitouni, A. (2014). Biocontrol of Rhizoctonia solani damping-off and promotion of tomato plant growth by endophytic actinomycetes isolated from native plants of Algerian Sahara. *Microbiol. Res* 169, 59–65. doi: 10.1016/j.micres.2013.06.014

Hirano, Y., and Arie, T. (2006). PCR-based differentiation of *Fusarium oxysporum* ff. *sp. lycopersici and radicis-lycopersici and races of F. oxysporum f. sp.*

lycopersici. *J.Gen. Plant Pathol.* 72, 273–283. doi: 10.1007/s10327-006-0287-7

Hsu, S. C., and Lockwood, J. L. (1975). Powdered Chitin Agar as a Selective Medium for Enumeration of Actinomycetes in Water and Soil. *Appl. Microbiol.* 29, 422–426.

Kampfer, P., Kroppenstedt, R. M., and Dott, W. (1991). A numerical classification of the genera Steptomyces and Streptoverticillium using miniaturized physiological tests. *J. Gen. Microbiol.* 137, 1831–1891. doi: 10.1099/00221287-137-8-1831

Kanini, G. S., Katsifas, E. A., Savvides, A. L., and Karagouni, A. D. (2013). Streptomyces rochei ACTA1551, an Indigenous Greek Isolate Studied as a Potential Biocontrol Agent against Fusarium oxysporum f.sp. lycopersici. *BioMed. Res. Int.* 387230, 1–10. doi: 10.1155/2013/387230

Kim, J. D., Han, J. W., Hwang, I. C., Lee, D., and Kim, B. S. (2012). Identification and biocontrol efficacy of "Streptomyces miharaensis producing filipin III against Fusarium wilt. *J. Basic. Microbiol.* 52, 150–159. doi: 10.1002/jobm.201100134

Kim, J. D., Han, J. W., Lee, S. C., Lee, D., Hwang, I. C., and Kim, B. S. (2011). Disease control effect of strevertenes produced by Streptomyces psammoticus against tomato fusarium wilt. *J. Agric. Food Chem.* 59, 1893–1899. doi: 10.1021/jf1038585

Kundakovic, T., Ciric, A., Stanojkovic, T., Sokovic, M., and Kovacevic, N. (2014). Cytotoxicity and antimicrobial activity of Pyrus pyraster Burgsd. *and Pyrus spinosa Forssk. (Rosaceae)*. *Afr. J. Microbiol. Res.* 8, 511–518.

Kunova, A., Bonaldi, M., Saracchi, M., Pizzatti, C., Chen, X., and Cortesi, P. (2016). Selection of Streptomyces against soil borne fungal pathogens by a standardized dual culture assay and evaluation of their effects on seed germination and plant growth. *BMC. Microbiol.* 16:272.

Kutzner, H. J. (1981). "The family Streptomycetaceae," in *The Prokaryotes – A handbook on habitats, isolation and identification of bacteria*, eds M. P. Starr, H. Stolp, H. G. Trüper, A. Balons, and H. G. Schlegel (Berlin: Springer Verlag), 2028–2090.

Kuzniak, E., Wielanek, M., Chwatko, G., Głowacki, R., Libik-Konieczny, M., Piątek, M., et al. (2015). Salicylic acid and cysteine contribute to arbutin-induced alleviation of angular leaf spot disease development in cucumber. *J. Plant Physiol.* 181, 9–13. doi: 10.1016/j.jplph.2015.03.017

Langlois-Meurinne, M., Gachon, C. M., and Saindrenan, P. (2005). Pathogen-responsive expression of glycosyltransferase genes UGT73B3 and UGT73B5 is necessary for resistance to *Pseudomonas* syringae pv tomato in Arabidopsis. *Plant. Physiol.* 139, 1890–1901. doi: 10.1104/pp.105.067223

Li, J., Brader, G., and Palva, E. T. (2004). The WRKY70 transcription factor: a node of convergence for jasmonate-mediated and salicylate-mediated signals in plant defense. *Plant Cell* 16, 319–331. doi: 10.1105/tpc.016980

Liang, H., Lu, Y., Liu, H., Wang, F., Xin, Z., and Zhang, Z. (2008). A novel activator-type ERF of Thinopyrum intermedium, TiERF1, positively regulates defence responses. *J. Exp. Bot.* 59, 3111–3120. doi: 10.1093/jxb/ern165

Majidi, S., Roayaei, M., and Ghezelbash, G. (2011). Carboxymethyl-cellulase and filter-paperase activity of new strains isolated from Persian Gulf. *Microbiol. J.* 1, 8–16. doi: 10.3923/mj.2011.8.16

Mariutto, M., Duby, F., Adam, A., Bureau, C., Fauconnier, M. L., Ongena, M., et al. (2011). The elicitation of a systemic resistance by *Pseudomonas* putida BTP1 in tomato involves the stimulation of two lipoxygenase isoforms. *BMC. Plant. Biol.* 11:29. doi: 10.1186/1471-2229-11-29

Marlatt, M. L., Correll, J. C., Kaufmann, P., and Cooper, P. E. (1996). Two genetically distinct populations of Fusarium oxysporum f. *sp. lycopersici race* 3 in the United States. *Plant Dis.* 80, 1336–1342.

Mayer, A. M. (2006). Polyphenol oxidases in plants and fungi: going places? a review. *Phytochemistry* 67, 2318–31. doi: 10.1016/j.phytochem.2006.08.006

McGovern, R. J. (2015). Management of tomato diseases caused by Fusarium oxysporum. *Crop. Prot.* 73, 78–92. doi: 10.1016/j.cropro.2015.02.021

Mehrotra, S., Pandey, P. K., Gaur, R., and Darmwal, N. S. (1999). The production of alkaline protease by a Bacillus species isolate. *Bioresour. Technol.* 67, 201–203. doi: 10.1016/s0960-8524(98)00107-2

Nikoo, F. S., Sahebani, N., Aminian, H., Mokhtarnejad, L., and Ghaderi, R. (2014). Induction of systemic resistance and defense-related enzymes in tomato plants using *Pseudomonas* fluorescens CHAO and salicylic acid against root-knot nematode Meloidogyne javanica. *J. Plant. Prot. Res.* 4, 383–389. doi: 10.2478/jppr-2014-0057

Pfaffl, M. W., Horgan, G. W., and Dempfle, L. (2002). Relative expression software tool (REST) for group-wise comparison and statistical analysis of relative expression results in real-time PCR. *Nucleic Acids. Res.* 30, e36.

Pieterse, C. M. J., Van der Does, D., Zamioudis, C., Leon-Reyes, A., and Van Wees, S. C. M. (2012). Hormonal modulation of plant immunity. *Annu. Rev. Cell. Dev. Biol.* 28, 489–521. doi: 10.1146/annurev-cellbio-092910-154055

Pilkington, L. J., Messelink, G., van Lenteren, J. C., and Le Mottee, K. (2010). Protected Biological Control" – Biological pest management in the greenhouse industry. *Biol. Control.* 52, 216–220. doi: 10.1002/ps.5270

Poppenberger, B., Berthiller, F., Lucyshyn, D., Sieberer, T., Schuhmacher, R., Krska, R., et al. (2003). Detoxification of the Fusarium mycotoxin deoxynivalenol by a UDP glucosyltransferase from Arabidopsis thaliana. *J. Biol. Chem.* 278, 47905–47914. doi: 10.1074/jbc.m307552200

Quiroga, M., Guerrero, C., Botella, M. A., Barceló, A., Amaya, I., Medina, M. I., et al. (2000). A tomato peroxidase involved in the synthesis of lignin and suberin. *Plant. Physiol.* 122, 1119–1128. doi: 10.1104/pp.122.4.1119

Rashad, Y. M., Al-Askar, A. A., Ghoneem, K. M., Saber, W. I. A., and Hafez, E. E. (2017). Chitinolytic Streptomyces griseorubens E44G enhances the biocontrol efficacy against Fusarium wilt disease of tomato. *Phytoparasit* 45:227. doi: 10.1007/s12600-017-0580-3

Reis, A., Costa, H., Boiteux, L. S., and Lopes, C. A. (2005). First report of Fusarium oxysporum f. *sp. lycopersici race* 3 on tomato in Brazil. *Fitopatol. Bras.* 30, 426–428. doi: 10.1590/s0100-41582005000400017

Ren, C. M., Zhu, Q., Gao, B. D., Ke, S. Y., Yu, W. C., Xie, D. X., et al. (2008). Transcription factor WRKY70 displays important but no indispensable roles in jasmonate and salicylic acid signaling. *J. Integr. Plant. Biol.* 50, 630–637. doi: 10.1111/j.1744-7909.2008.00653.x

Sadeghi, A., Karimi, E., Dahaji, P. A., Javid, M. G., Dalvand, Y., and Askari, H. (2012). Plant growth promoting activity of an auxin and siderophore producing isolate of Streptomyces under saline soil conditions. *World. J. Microbiol. Biotechnol.* 28, 1503–1509. doi: 10.1007/s11274-011-0952-7

Sadeghi, A., Koobaz, P., Azimi, H., Karimi, E., and Akbari, A. R. (2017). Plant growth promotion and suppression of Phytophthora drechsleri damping-off in cucumber by cellulase-producing Streptomyces. *BioControl* 62, 805–819. doi: 10.1007/s10526-017-9838-4

Salehi, M., Moieni, A., and Safaie, N. (2018). Elicitors derived from hazel (Corylus avellana L.) *cell suspension culture enhance growth and paclitaxel production of Epicoccum nigrum*. *Sci. Rep.* 8:12053. doi: 10.1038/s41598-018-29762-3

Salehi, M., Moieni, A., Safaie, N., and Farhadi, S. (2019). Elicitors derived from endophytic fungi *Chaetomium globosum* and *Paraconiothyrium brasiliense* enhance paclitaxel production in *Corylus avellana* cell suspension culture. *Plant Cell Tissue Organ Cult.* 136, 161–171. doi: 10.1007/s11240-018-1503-9

Salla, T. D., Astarita, L. V., and Santarem, E. R. (2016). Defense responses in plants of Eucalyptus elicited by Streptomyces and challenged with Botrytis cinerea. *Planta* 243, 1055–1070. doi: 10.1007/s00425-015-2460-8

Sanchez-Pena, P., Cauich-Pech, S. O., Nunez-Farfan, J., Nunez-Cebreros, R. D., Hernandez-Verdugo, S., Parra-Terraza, S., et al. (2010). Incidence of Fusarium oxysporum f. *sp. lycopersici Races in Tomato in Sinaloa, Mexico*. *Plant Dis.* 94:1376. doi: 10.1094/PDIS-04-10-0255

Shirling, E. B., and Gottlieb, D. (1966). Methods for characterization of Streptomyces species. *Int J. Sys. Bacteriol.* 16, 313–340. doi: 10.1099/00207713-16-3-313

Soltani, A. A., Khavazi, K., Asadi-Rahmani, H., Omidvari, M., Abaszadeh Dahaji, P., and Mirhoseyni, H. (2010). Plant Growth Promoting Characteristics in Some Flavobacterium spp. *isolated from Soils of Iran*. *J. Agri. Sci.* 2, 1–10.

Song, W., Zhou, L., Yang, C., Cao, X., Zhang, L., and Liu, X. (2004). Tomato Fusarium wilt and its chemical control strategies in a hydroponic system. *Crop Prot.* 23, 243–247. doi: 10.1016/j.cropro.2003.08.007

Song, Y., Chen, D., Lu, K., Sun, Z., and Zeng, R. (2015). Enhanced tomato disease resistance primed by arbuscular mycorrhizal fungus. *Front. Plant. Sci.* 6:786. doi: 10.3389/fpls.2015.00786

Sreevidya, M., Gopalakrishnan, S., Kudapa, H., and Varshney, R. K. (2016). Exploring plant growth-promotion actinomycetes from vermicompost and rhizosphere soil for yield enhancement in chickpea. *Braz. J. Microbiol.* 47, 85–95. doi: 10.1016/j.bjm.2015.11.030

Suter, M. A. (1978). *Isolierung von Melanin-negativen Mutanten aus Streptomyces glaucescens. dissesrtation*. Zurich: ETH Zurich, 6276.

Tamura, K., Stecher, G., Peterson, D., Filipski, A., and Kumar, S. (2013). MEGA6: Molecular Evolutionary Genetics Analysis Version 6.0. *Mol. Biol. Evol.* 30, 2725–2729. doi: 10.1093/molbev/mst197

Timmermann, T., Armijo, G., Donoso, R., Seguel, A., Holuigue, L., and Gonzalez, B. (2017). Paraburkholderia phytofirmans PsJN protects Arabidopsis thaliana against a virulent strain of *Pseudomonas* syringae through the Activation of induced resistance. *Mol. Plant. Microbe Interac.* 30, 215–230. doi: 10.1094/MPMI-09-16-0192-R

Tripathi, G., and Rawal, S. K. (1998). A simple and efficient protocol for isolation of high molecular weight DNA from Streptomyces aureofaciens. *Biotechnol. Tech.* 12, 629–631.

Verma, V. C., Singh, S. K., and Prakash, S. (2011). Bio-control and plant growth promotion potential of siderophore producing endophytic Streptomyces from Azadirachta indica A. *Juss. J. Basic Microbiol.* 51:550. doi: 10.1002/jobm.201000155

Walters, D., and Heil, M. (2007). Costs and trade-offs associated with induced resistance. *Physiol. Mol. Plant. Pathol.* 71, 3–17. doi: 10.1016/j.pmpp.2007.09.008

Walters, D. R., Ratsep, J., and Havis, N. D. (2013). Controlling crop diseases using induced resistance: challenges for the future. *J. Exp. Bot*. 64, 1263–1280. doi: 10.1093/jxb/ert026

Wang, P., Liu, X., Guo, J., Liu, C., Fu, N., and Shen, H. (2015). Identification and expression analysis of candidate genes associated with defense responses to *Phytophthora capsici* in pepper line "PI 201234". *Inter. J. Mol. Sci.* 16, 11417–11438. doi: 10.3390/ijms160511417

Wang, S., Zheng, Y., Gu, C., He, C., Yang, M., Zhang, X., et al. (2018). *Bacillus cereus* AR156 activates defense responses to *Pseudomonas syringae* pv. *tomato in Arabidopsis thaliana* similarly to flg22. *Mol. Plant. Microbe Interac.* 31, 311–322. doi: 10.1094/MPMI-10-17-0240-R

Wu, Z., Yang, Y., and Li, K. (2019). Antagonistic activity of a novel antifungalmycin N2 from Streptomyces sp. *N*2 and its biocontrol efficacy against *Rhizoctonia solani*. *FEMS. Microbiol. Lett.* 366:fnz018.

Xu, G. H., and Zheng, H. Y. (1986). *Study Method of Soil Microbiology*. Beijing: Agricultural Press.

Xu, T., Li, Y., Zeng, X., Yang, X., Yang, Y., Yuan, S., et al. (2016). Isolation and evaluation of endophytic Streptomyces endus OsiSh-2 with potential application for biocontrol of rice blast disease. *J. Sci. Food. Ag.* 97, 1149–1157. doi: 10.1002/jsfa.7841

Zhang, Y. J. Zhang, S. Liu, X. Z., Wen, H. A., and Wang, M. (2010). A simple method of genomic DNA extraction suitable for analysis of bulk fungal strains. *Let. Appl. Microbiol.* 51, 114–118. doi: 10.1111/j.1472-765X.2010.02867.x

Zhao, S., Du, C., and Tian, C. (2012). Suppression of Fusarium oxysporum and induced resistance of plants involved in the biocontrol of cucumber Fusarium wilt by Streptomyces bikiniensis HD-087. *World. J. Microbiol. Biotechnol.* 28, 2919–2927. doi: 10.1007/s11274-012-1102-6

Conflict of Interest Statement: The authors declare that the research was conducted in the absence of any commercial or financial relationships that could be construed as a potential conflict of interest.

frontiers in Plant Science

REVIEW
published: 03 July 2019
doi: 10.3389/fpls.2019.00862

Plant Host-Associated Mechanisms for Microbial Selection

Piet Jones[1,2], *Benjamin J. Garcia*[1], *Anna Furches*[1,2], *Gerald A. Tuskan*[1] *and Daniel Jacobson*[1,2]*

[1] Oak Ridge National Laboratory, Biosciences Division, The Center for Bioenergy Innovation, Oak Ridge, TN, United States, [2] The Bredesen Center for Interdisciplinary Research and Graduate Education, University of Tennessee, Knoxville, Knoxville, TN, United States

Plants serve as host to numerous microorganisms. The members of these microbial communities interact among each other and with the plant, and there is increasing evidence to suggest that the microbial community may promote plant growth, improve drought tolerance, facilitate pathogen defense and even assist in environmental remediation. Therefore, it is important to better understand the mechanisms that influence the composition and structure of microbial communities, and what role the host may play in the recruitment and control of its microbiome. In particular, there is a growing body of research to suggest that plant defense systems not only provide a layer of protection against pathogens but may also actively manage the composition of the overall microbiome. In this review, we provide an overview of the current research into mechanisms employed by the plant host to select for and control its microbiome. We specifically review recent research that expands upon the role of keystone microbial species, phytohormones, and abiotic stress, and in how they relate to plant driven dynamic microbial structuring.

Keywords: microbial community, jasmonic acid, salicylic acid, ethylene, keystone species, abiotic stress, biotic stress, microbiota

OPEN ACCESS

Edited by:
Nicolae Radu Zabet,
University of Essex, United Kingdom

Reviewed by:
Laila Pamela Partida-Martinez,
Center for Research and Advanced Studies (CINVESTAV), Mexico
Rong Li,
Nanjing Agricultural University, China

***Correspondence:**
Daniel Jacobson
jacobsonda@ornl.gov

Specialty section:
This article was submitted to Plant Microbe Interactions, a section of the journal Frontiers in Plant Science

Received: *05 February 2019*
Accepted: *14 June 2019*
Published: *03 July 2019*

Citation:
Jones P, Garcia BJ, Furches A, Tuskan GA and Jacobson D (2019) Plant Host-Associated Mechanisms for Microbial Selection. Front. Plant Sci. 10:862. doi: 10.3389/fpls.2019.00862

1. INTRODUCTION

The sessile nature of plants limits their capacity to deal with an immediate and localized disturbance, irrespective of whether the disturbance is caused by biotic or abiotic stress. It therefore stands to reason that plants have evolved systems to manage the impact of these collective and respective stresses. From a biotic microbial view point, plants play host to a number of organisms that reside in the phyllosphere, endosphere, and rhizosphere, influencing how a plant reacts to its environment. If viewed in the context of an ecological unit, the community of organisms is known as the holobiont. Further incorporating the environment results in what is collectively known as the phytobiome, where the possible plant-microbe-stress interactions are given in **Figure 1**.

The holobiont has a much greater evolutionary potential for dealing with biotic and abiotic stress than the plant itself. Therefore, it is potentially more sustainable to manage abiotic/biotic stresses in a holistic and multifaceted manner. The plant employs a combinatorially complex system of receptors and signals to adapt to different stressors (Hacquard et al., 2017). Unraveling the complexity of the system is not a trivial task, with researchers providing different perspectives for elucidating a contextual understanding of the dynamics of plant-microbiome interaction.

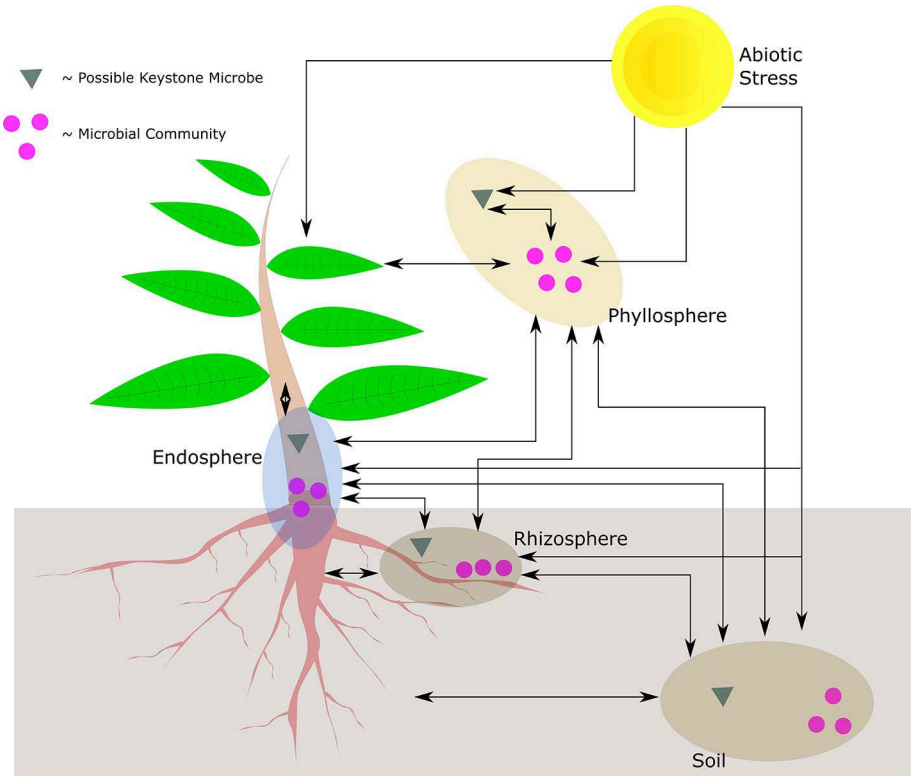

FIGURE 1 | Possible interactions in the phytobiome between the plant, abiotic stress, keystone microbes, and microbial communities. Illustrated are the respective compartments of the holobiont, only the phyllosphere indicates keystone microbial interaction though the other compartments may have the same type of interactions. The phyllosphere may also be epithytic or endophytic. The cross-interaction between different compartments may be mediated at a community level, or by means of individual (keystone) microbes. In addition, the plant may also interact with whole communities or by means of individual microbes.

The improved understanding of the interactions between the plant and its microbiome has broadened our knowledge on the capabilities of the plant to influence its microbiome and vice versa. In interacting with its microbiome, plants have the capacity to release chemical signals into their environment. The signals can either have a positive or negative effect on other plants or members of the microbiome. Root exudates, comprised of allelochemicals, have been associated with signaling in plant-microbe interaction and can also facilitate plant to plant communication (Bais et al., 2004). Exudates with potential allelopathic properties can help the plant both positively and negatively select for members of their phytobiome (Bertin et al., 2003; Sasse et al., 2018), allowing the plant to establish a rhizosphere and soil microbiome that may also be beneficial or detrimental to other plants and microbes. The concept of influencing the plant phytobiome has also been explored in biocontrol strategies, e.g., strategies against nematodes (Stirling, 2017). The ability of the plant, together with individual members of its microbiome, to control and shape the overall microbiome influences a plant's growth and stress response. A better understanding of the resultant interplay between defense and control may allow for an optimized holobiont that can benefit, among others, agricultural and bioremediation efforts (Ojuederie and Babalola, 2017; Pappas et al., 2017; Ab Rahman et al., 2018).

The microbes that a plant hosts are broadly classified as pathogenic or non-pathogenic. The nature of the non-pathogenic interaction may be beneficial, mutualistic, commensal, or neutral and pathogenic interactions may be parasitic or amensal. The plant can play host to biotrophs, who receive nourishment from a living host cell, necrotrophs, who receive nourishment from a dead host cell, and hemitrophs, who switch between the different nourishment states (see **Figure 2**). The nature of plant-microbe relationships and the ability of the plant to influence select neighbors may potentially benefit the plant's own growth or defense (Bulgarelli et al., 2013; Mikiciński et al., 2016). Nutritional deficiencies in the plant can also alter the transcriptional profile of its microbiome and thereby mitigate the impact of nutritional stress (Carvalhais et al., 2013). Additionally, the plant's abiotic stress tolerance and disease resistance may not be a mutually exclusive processes. For example, common mechanisms exist between phytohormone-based pathogen defense responses and the plant's ability to tolerate drought and salt stress (Cho et al., 2013; Huang et al., 2018). At a community level, evidence suggests that the ability of the plant host to shape its microbial community may also serve as an additional layer of defense to disease and stress (Hacquard et al., 2017; Berendsen et al., 2018).

Interaction between plants and microbes has generally been studied with respect to individual (or small collections of) microbes. Additionally, the focus has often been on how the microbe negatively or positively impacts the plant and not how a plant may influence the selection of microbes under biotic or abiotic stress. However, there is dynamic feedback between a plant and a microbe that may impact the plant's microbial community (Bever et al., 2012). The reciprocal nature of the interactions between the plant and its microbial community is poorly understood. It is therefore not only important to determine how individual microbes may impact the plant, but also how the plant may impact its community. There is also evidence to suggest that the plant itself may not be the only determinant in microbial diversity, suggesting the environment and abiotic factors are also important to consider when identifying plant-microbial interactions (Kennedy et al., 2004; Whitaker et al., 2018). There is still much that we can learn about the interplay between the different elements of the phytobiome, including (1) how do the individual microbes influence the plant-mediated structure, (2) how can the plant shape its microbiome through signaling and nutrient availability, and (3) what role does the abiotic stress play in the plant's ability to influence microbial community members and structure? We review recent contributions to the understanding of the impact that keystone members of the microbiome may have on the plant and other community members. We also review the current understanding of the extent to which a plant may shape its microbial community. Finally we look at how abiotic stress on the plant influences the microbial community. Each of the mechanisms that a plant employs to interact with its microbial community and abiotic stresses is part of a complex dynamic system that influences plant growth and stress tolerance.

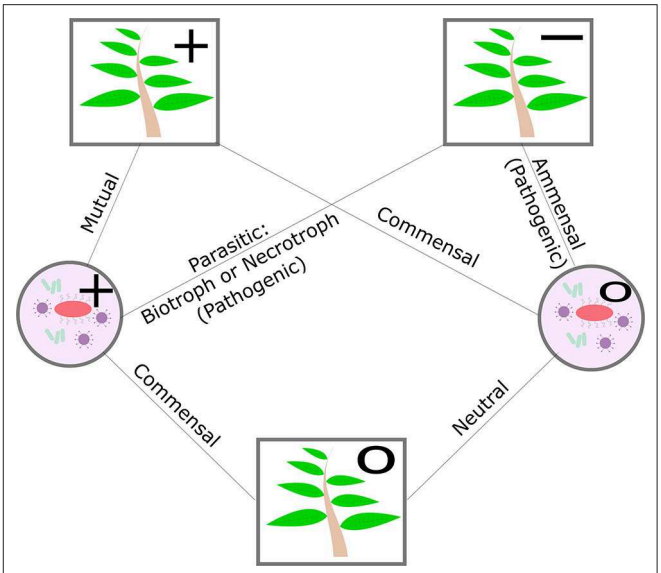

FIGURE 2 | Diagram of plant-microbe symbiosis, excluding negative effects on microbes. Circle nodes in the diagram indicate microbes, square nodes indicate the plant. Positive effects are indicated with "+," negative effects with a "−," and neutral effects by a "o".

2. KEYSTONE MICROBIAL SPECIES

Improving our ability to manipulate plant phenotypes, including growth, is of great interest for agricultural, industrial, and ecological restoration efforts, among others. Understanding the mechanisms that underpin pathogen resistance, abiotic stress tolerance, and range shifts (including the ability to establish crops in marginal agricultural land) is of particular importance in the face of shifting climate conditions. An important mechanism through which a plant shapes its microbiome and larger ecosystem is through interactions with keystone microbial species. The concept of keystone species was developed by ecologist Robert T. Paine (Paine, 1966, 1969) and has since been applied to many different fields and with varied meanings. The classical idea of a keystone is attractive because it represents a top-down mechanism of ecosystem control that humans can potentially understand and manipulate (Busby et al., 2017; Trivedi et al., 2017; Hamonts et al., 2018). A few well-known macroecological examples in which keystones play important roles in stabilizing species diversity and ecosystem function are marine rocky intertidal zones dominated by the top predator starfish *Pisaster ochraceus* (Paine, 1966), riparian habitats dominated by extended *Populus* phenotypes (Whitham et al., 2003), kelp forests that disappear without otters (Estes and Palmisano, 1974), and the very landscape of Yellowstone National Park following the reintroduction of gray wolves (Ripple et al., 2001).

Interest in applying the keystone species concept to microbial communities and the plant microbiome has grown in recent years (Meyer and Leveau, 2012; Ze et al., 2012; Berry and Widder, 2014; Copeland et al., 2015). In the phytobiome, the concept of a keystone is attractive as a means of understanding how the plant controls its microbiome. Several authors have used computational network approaches and experimental methods to identify putative keystones. However, few studies have attempted to validate the role of putative keystones. Moreover, investigation of the mechanisms by which a plant recruits a keystone microbe for the purpose of manipulating its microbiome and larger ecosystem has only recently begun. Early studies show promising results and suggest that further research into keystone species recruitment would contribute significantly to the fields of sustainable agriculture, conservation, and ecological restoration.

2.1. Identification and Validation of Keystone Species

Identifying and validating keystone species is inherently complex. By definition, classical keystones increase alpha and beta diversity and stabilize ecosystem function via top-down mechanisms and are typically described as being rare or low in abundance, having few direct interactions with other community members. In the phytobiome, keystones are theorized to play vital roles in helping establish the core microbiome (Harrison et al., 2018). In contrast to members of the core microbiome, for which low-level taxonomic composition may vary but ensemble

function is conserved (Lemanceau et al., 2017), keystones perform unique functions inherently tied to their identity. While core microbes also perform important functions for the host plant and its community, removal of a core member does not necessarily lead to dissolution of the community. The keystone's status as a community linchpin means its functional role and very presence are often difficult to separate from those of its community members—a "control" community without the keystone simply does not exist or function in any comparable fashion. Furthermore, identifying low abundance and rare microbes that exert top-down control or have an otherwise outsized effect on community structure requires deep or single-cell sequencing of soil and plant samples (Oberholster et al., 2018). However, currently used statistical methods filter out low abundance taxa and those not present in the majority of samples to avoid biasing analyses (Berry and Widder, 2014; Agler et al., 2016; Duhamel et al., 2018; Oberholster et al., 2018), thus rare taxa recovered by deep sequencing are likely to be pruned a priori.

Some studies have taken the approach of focusing on organisms previously theorized to be keystones and then attempting to characterize the putative functional role they fulfill in the community (Agler et al., 2016; Duhamel et al., 2018), while others approach the problem from the opposite direction by seeking out rare organisms that could be candidates for carrying out well-studied functions of interest (Ze et al., 2012). These approaches essentially utilize the classical keystone concept to narrow the hunt for the needle in the haystack. While these studies clearly demonstrate that microbes do fulfill "classical" keystone roles, it is likely that a broader or more flexible definition will become necessary as research in this arena progresses; the "classical" keystone model was developed within the macroecological realm and therefore may not sufficiently encapsulate uniquely microbial keystone characteristics (Meyer and Leveau, 2012). This unexplored frontier means that attempting to find new keystone taxa—particularly in uncharacterized systems—is difficult because the characteristics and roles unique to microbial keystones are largely unknown at this stage. In contrast to description of keystones at the macroecological scale, recent studies have found evidence that microbial keystones may be ephemeral, performing a specific function in a particular environment or developmental stage, but playing a less prominent role in others (Duhamel et al., 2018; Oberholster et al., 2018). For example, many vertically transmitted microbes that are dispersed on seed surfaces (such as *Alternaria fulva* on *Astralagus lentiginosus* seeds) fulfill important roles in early holobiont development that affect the long-term composition of the phytobiome (Harrison et al., 2018).

Interest in using co-occurrence networks to identify putative microbial keystones has been rapidly growing (Berry and Widder, 2014; Copeland et al., 2015; Agler et al., 2016; Banerjee et al., 2018). Such networks are often created by calculating the correlation of pairwise OTU abundances. Several papers have used computational methods to identify network microbial "hubs" (OTUs that have a high number of connections within the community). However, hub taxa are not necessarily keystones (Berry and Widder, 2014; Rottjers and Faust, 2018). Using co-occurrence as a proxy for biologically meaningful interactions is problematic. Understanding microbiome interactions relies upon properly identifying the true sphere and scale in which interactions take place. The lack of directly observed interactions presents an immense challenge because the niches which partition true interaction from mere co-occurrence are an unknown prior and vary greatly, often in ways not understood by researchers. For example, the interior of a single leaf presents a multitude of ecologically distinct microhabitats. Among niches, microbes may have few or zero interactions but still "co-occur" because they are present in the same macrohabitat, i.e., the leaf (Berry and Widder, 2014; Hamonts et al., 2018). Nevertheless, in uncharacterized microbiomes, network methods can offer valuable insight regarding community dynamics and serve as a first step in the process of identifying the keystone taxa that serve as the linchpins in community structure.

2.2. Evidence for Plant-Driven Keystone Interactions

The majority of studies on microbial keystones have not investigated the mechanisms underpinning host interactions, perhaps because methods to explicitly identify and validate the effects of keystone species are still largely under development. However, there appears to be promising evidence that plants are actively recruiting keystone microbes. Using a combination of field experiments and network analyses to investigate the rhizosphere communities of sunflower and sorghum crops, Oberholster et al. (2018) identified 47 hub taxa and putative keystone microbes deemed to be necessary for maintaining network structure, including *Proteobacteria, Rhizoplanes, Flavisolibacter, Povalibacter, Nitrososphaera, Lysobacter,* and *Sphingomonas*. Although investigating plant-keystone-species interactions was outside the scope of the study, Oberholster et al. (2018) found that the abundance of taxa in the rhizosphere varied with soil chemistry and plant developmental stage. Furthermore, changes in soil chemistry were correlated with plant species and plant developmental stage. Phylogenetic diversity of the sorghum rhizosphere was significantly correlated with soil carbon and nitrogen concentrations, whereas sunflower rhizosphere diversity was correlated with potassium, calcium, magnesium, and phosphorus. Together they suggest that differences in plant root exudates likely contributed to the structure of rhizosphere communities, potentially through putative keystone taxa.

Despite the fact that formal investigation of keystone species is still in early days, mycorrhizal fungi have long been recognized as playing an essential role in structuring the microbiome of plant hosts. Both arbuscular mycorrhizal (AM) and ectomycorrhizal (ECM) fungi have been described as keystone species (Gamper et al., 2010; Soka and Ritchie, 2015; Oberholster et al., 2018), and much can be drawn from mycorrhizal fungal host interactions. Duhamel et al. (2018) found a strong association between plant species and rhizosphere communities in greenhouse and field experiments. In greenhouse experiments in which three plant species (*Pinus muricata, Baccharis pilularis,* and *Ceanothus thyrsiflorus*) were planted in media containing a tripartite mix of soils from each plant's native range (and thus each plant's

native microbial community), the final composition of each plant's microbiome most strongly resembled that of each host plant's native range. The significant similarity in community structure between greenhouse and native soils supports the idea that plants can play an active role in selecting their microbiome structure. In agreement with Oberholster et al. (2018), Duhamel et al. (2018) found that community composition and keystone prominence changed over time. For example, members of the genera *Rhizopogon* and *Suillus* (both belonging to Suillineae) are keystone mutualists; these ECM basidiomycetes are abundant during development of *P. muricata* seedlings and under conditions similar to those that occur during range expansion, but are rare during other phases such as in well-established monodominant stands. Although the mechanism by which *P. muricata* recruits keystones such as *Suillus pungens* was not investigated by Duhamel et al. (2018), the obligate relationship of *Pinus* species with ECM has long been of interest. *Suillus* species in particular have been shown to facilitate *Pinus* invasions, as was demonstrated for *S. luteus* and *P. contorta* (Hayward et al., 2015). Kikuchi et al. (2007) found that *S. bovinus* germinated when co-cultured with *P. densiflora*, and could be induced to germinate in the absence of the host by treatment with flavonoids previously reported from root exudates, including hesperidin, morin, rutin, quercitrin, naringenin, genistein, and chrysin. Liao et al. (2016) found that relationships between members of *Pinus* and *Suillus* were species-specific, and that compatible *Pinus* and *Suillus* pairings elicited expression of unique gene sets including genes related to production of fungal small secreted proteins and host leucine-rich repeat-containing R proteins. Moreover, the JA and ET pathways were found to be upregulated during incompatible pairings (but interestingly, SA was not).

In contrast to beneficial keystones that increase microbial alpha and beta diversity (Herren and McMahon, 2018), pathogenic keystones tend to reduce diversity. Agler et al. (2016) found a significant correlation between the obligate biotrophic oomycete *Albugo laibachii* and host genotype in *Arabidopsis thaliana*. The authors found that phyllosphere alpha and beta diversity were dramatically reduced following infection. Similar to the effects of beneficial keystones, community structure was stabilized in infected hosts relative to pathogen-free hosts. Agler et al. (2016) did not investigate the mechanisms involved in susceptibility or resistance to *A. laibachii*; however, closely related *A. candida* has been shown to alter host metabolism in *A. thaliana* (Chou et al., 2000). Ruhe et al. (2016) showed that rather than killing the host or severely decreasing fitness, *A. laibachii* maintains a level of infection that is tolerable to the host. Additionally, there is evidence that *A. laibachii* is largely able to tolerate host defense mechanisms and suppresses only a small portion of host activity. Ruhe et al. (2016) reasoned that the immune tolerance is an adaptation over non-host evolved pathogens that would serve as competitors to *A. laibachii* or kill the host. Even though *A. laibachii* is classified as a pathogen due to predominantly negative effects on the host, leaving the host's defense response intact to compete against more virulent pathogens has a less negative impact on *A. thaliana*. Furthermore, the "keystone" role of *A. laibachii* is in stabilizing the post-infection community composition, which prevents other pathogens from invading while plant immunity is already compromised.

In consideration of the challenges associated with identifying and validating keystone species, it is not a surprise that there is a shortage of studies investigating plant-driven mechanisms for recruiting or maintaining relationships with keystones. However, some inferences can be made based on previous studies that investigated host mechanisms with regards to a single organism or a simple community (many of which will be described in subsequent sections and should influence the future direction of keystone research). Synthetic (constructed) communities offer a promising avenue for isolating host mechanisms (Bodenhausen et al., 2014). Niu et al. (2017) constructed a seven member synthetic community on maize roots and discovered through iterative removal of members that the community collapsed without *Enterobacter cloacae*. In addition, when the community was intact, it functioned to suppress *Fusarium verticillioides*. Niu et al. (2017) did not investigate the host mechanisms involved in these interactions, but we argue doing so is a natural next step that will yield valuable fundamental information. Although simplified communities are likely to miss some important host-microbe dynamics, they are a good place to start for gaining basic understanding. In addition, the use of microfluidics can facilitate the dissection of complex plant-microbe interactions by facilitating the fine-scale manipulation and imaging of real-time plant recruitment of and colonization by microbes (Massalha et al., 2017; Stanley and van der Heijden, 2017). Furthermore, microfluidic methods allow plant exudates, phytohormones, and internal signaling cascades to be characterized using proteomic, transcriptomic, and other techniques to gain new insight into host mechanisms that operate at specific spatial-scales. To date, these methods have largely been used to study culturable microbes. However, the use of ensemble culturing techniques such as those used by Agler et al. (2016) could facilitate study of unculturable and rare taxa, which would provide more nuanced and realistic insights into holobiont dynamics. Furthermore, the use of such techniques in combination with time-series experiments would inform how plant recruitment of keystones varies with developmental stage, which would in turn improve our understanding of the core microbiome changes over time.

3. PLANT DEFENSE MODULATION OF THE MICROBIOME FROM A HOST GENE AND PHYTOHORMONE PERSPECTIVE

Concepts such as evolutionary pressure and dynamical feedback have shaped our understanding of plant-microbe interactions. A recognized hypothesis of the plant immune system, referred to as the zigzag model, characterizes the defense response as a successive pattern-triggered immunity (PTI) and effector-triggered immunity (ETI), set of responses. PTI is viewed as the first line of defense and involves protein recognition receptors (PRRs) on the cell surface. PRRs bind often conserved microbial compounds referred to as microbe (pathogen) associated molecular patterns, or MAMPs (PAMPs). The binding of microbial compounds by PRRs then elicits a signal cascade

of defense responses that inhibit microbial growth. ETI is the second line of defense, comprised of intracellular resistance (R) genes that contain nucleotide binding leucine rich repeat (NB-LRR) domains. Resistance genes code for proteins that bind microbial virulence effector proteins. Binding of the effector proteins then triggers a signal cascade that often results in cell death. PTI can be evaded by the microbe, eliciting successive ETI responses. ETI responses can also be evaded by the microbe, creating an evolution of responses by the plant and evasion by the microbe. However, the model views the PTI and ETI responses as distinct, and implicitly views the PTI responses as more conserved evolutionary than the ETI. The standard PTI-ETI model contradicts observations indicating that PRR may evolve similarly to R genes, and that certain R genes may play a similar role to PRR genes (Cook et al., 2015). The review by Cook et al. (2015) suggests that the plant immune system is an interacting set of co-evolving responses that occur both within and outside the cell, and is a response that involves multiple signal cascades. Phytohormones are a fundamental part of the resultant defense signal.

General defense related phytohormones form part of what is referred to as the plant's systematic acquired resistance (SAR) and induced systemic resistance (ISR) (Pieterse et al., 2012; Fu and Dong, 2013).

Of the various phytohormones, ethylene (ET), jasmonic acid (JA), and salicylic acid (SA) have been classically characterized in some plant defense role (Pieterse et al., 2012) and have been shown to preferentially impact certain bacterial phylla in a community (Carvalhais et al., 2014). There is an emerging interest in the potential of phytohormones to shape the plant's microbial community. Given the importance of the microbial community in plant defense, growth, and sustainability, it is therefore important to understand the hormone-microbial dynamic. We therefore describe recent evidence toward the role of ET, JA, and SA in shaping the microbiome community. Additionally, we look at research into the interplay of the respective hormone biosynthetic pathways and how they may assist in microbial colonization of the plant.

3.1. Ethylene

Originally shown in oats *Avena sativa* and broad bean, *Vicia faba*, the volatile hormone ET influences plant growth (Laan, 1934), with many further studies further characterizing the role of ET on plant growth and development (Burg and Burg, 1966; Smalle et al., 1997; Sukumar, 2010). The role of ET in plant defense was suspected due to a measured increased in ET biosynthesis during early PTI response in *Nicotiana tabacum* (Bailey et al., 1990; Sharon et al., 1993). It later became evident that ET signaling was required for the expression of the receptor kinase (FLS2) which binds bacterial flagelin (flg22) in *A. thaliana* and thereby triggers the defense response (Mersmann et al., 2010). ET has also been shown to be involved with stress tolerance (Thao et al., 2015). There has been emerging interest in characterizing the role that ET may play in not only defense from an individual microbe, but also in how ET influences the community (Nascimento et al., 2018). Mutant *A. thaliana* lines have provided an ideal framework to work toward characterization of ET.

A synthetic community approach was used in *A. thaliana* to determine host genetic factors that may influence phyllospheric bacterial community structure (Bodenhausen et al., 2014). Bodenhausen et al. found that ET-insensitive mutants, which possessed a mutation in the EIN2 gene, displayed a significant shift in the bacterial community structure at the genus level. They identified an increase in the relative abundance of *Variovorax*, a genus consisting of the metabolically diverse gram negative *Variovorax pardoxus* (Han et al., 2011). It is difficult to determine if increased abundance is directly associated with ET, or if it is mediated by pathway cross talk, especially given that Bodenhausen et al. observed a significant decrease in *Variovorax* abundance in the SA-insensitive mutant.

Another experiment involving *ein2* mutants also showed a shift in the rhizosphere bacterial community composition in non-autoclaved soil (Doornbos et al., 2011). However, the result was not observed in autoclaved recolonized soil. The recolonization of the autoclaved soil in particular consisted of either species that survived the autoclave process or those species in the surrounding environment, indicating that the initial microbial community composition may play a role in the capacity of ET to influence microbial structure. While the aforementioned hypothesis was not explored in Doornbos et al. (2011), they did observe supporting evidence in that bacterial community shifts were observed prior to disease symptoms, and no significant differences were observed in the absences of defense signaling. The latter indicates that a potential selective pressure triggering a defense response may be required to observe ET-mediated microbial community shifts. An early shift in community before disease symptoms may be justified in that ET is known as a potential early response signal (Mersmann et al., 2010). Therefore, an existing microbial community may provide the necessary pressure to elicit an ET response that can shape the community structure.

There is evidence to suggest that genotype effect on root microbiome is much weaker than the potential effect on the leaf microbiome (Wagner et al., 2016). While the full genotypic differences were not fully characterized in the Wagner et al. study, it was determined that leaves and roots differ in glucosinolate concentrations. Glucosinolate may be regulated by JA and ET signaling during rhizobacterial colonization (Pangesti et al., 2016). Therefore, glucosinolate secondary metabolites may provide a possible strategy for microbial community selection.

3.2. Jasmonic Acid

The role of JA in plant defense was first described as part of an infection-mediated wound response (Farmer and Ryan, 1992). Other associations to wound healing and herbivory-related defense have since been observed for components of the lipid-derived hormone's biosynthetic pathway (Li et al., 2005; Schilmiller et al., 2007; Koo et al., 2009; Christensen et al., 2013). JA has also been associated with plant necrotroph defense (Plett et al., 2014; Wei et al., 2016).

There is evidence to suggest that the phytohormone JA may have the capacity to shape the root microbial community by means of root exudates (Bertin et al., 2003; Sasse et al., 2018). In particular, evidence of root-associated allelopathic and

chemotactic negative and positive selection for constituents of the microbiome has been discussed in Bais et al. (2004). *Arabidopsis thaliana* knock-out mutants *myc2* and *med25* were shown to have disrupted JA signaling pathways that result in attenuated wounding, herbivory, and defense responses as well as altered root exudate profiles (Carvalhais et al., 2015). Carvalhais et al. found correlations between specific exudate concentrations and the abundances of several bacterial microbes. While the roles of these exudate compounds in shaping the microbial community are not yet fully understood, compounds such as tryptophan and fructose are chemotactic to several bacteria (Ordal et al., 1979; Yang Y. et al., 2015). One way JA might facilitate host-driven selection of the plant microbiome is by fine tuning the concentrations of root exudates that attract various microbes.

Furthermore, a recent root exudate study in maize found benzoxazinoids, which is regulated by JA, exhibited the capacity to alter the composition of the microbial community (Oikawa et al., 2001; Hu et al., 2018). Here, Hu et al. also experimented with the effect of benzoxazinoid inoculation on soil, which identified improved herbivory defense, exhibited genotype dependent growth reduction, and increased levels of JA. It has previously been shown that benzoxazinoids are chemotactic for *Pseudomonas putida* KT2440, which elicit JA priming and thereby resistance to particular fungi (Neal et al., 2012; Neal and Ton, 2013). A differential secondary metabolite analysis of genotype root exudates in Monchgesang et al. identified differential concentration of glucosinolate, SA catabolites, and dihydrohydroxy JA, indicating JA associated genotypic influences on root exudation (Mönchgesang et al., 2016). JA's influence of root exudates may in turn influence the rhizosphere microbiota, given the strong correlation between genotype root exudation and the rhizosphere bacterial community structure (Micallef et al., 2009). However, direct experimentation is needed to test JA's influence and better understand the potential mechanisms involved.

3.3. Salicylic Acid

The role of SA in plant defense was first described in tobacco, against tobacco mosiac virus (White, 1979), where supplementation of diluted aspirin induced a defense response. SA has since been described as an important component in plant defense signaling (Shah, 2003). It is believed that SA forms part of the plant's defense strategy against biotrophes, as opposed to necrotrophes which are more associated with the JA and ET pathways (Glazebrook, 2005).

In its capacity to regulate the microbiome, SA has been shown to modulate the composition of the root microbiome at the family level in *A. thaliana* (Lebeis et al., 2015). *Arabidopsis* knockout mutant lines were used, where essential components of the SA, JA, and ET pathways were targeted. Expectedly, mutants with the three respective pathways knocked out showed a lower survival rate. Apart from the microbial compositional shift, it was shown that certain bacterial endophytic families may actually require SA-related processes to colonize. Exogenous supplementation of SA resulted in an observed altered microbial community profile indicating potential SA-mediated preferential selection for microbial families (Lebeis et al., 2015). Treating ginsing with phenolic acids over a six-year period resulted in rhizosphere fungal community shifts (Li et al., 2018). Li et al. observed dramatic relative abundance changes of taxa at both the genus and phylum levels, with SA-associated changes significantly different from control. However, a study in wheat observed no significant SA-induced root microbial diversity shifts in a 72 h time window (Liu et al., 2018). There is recent evidence examining the heterogeneity of the SA pathway, whereby in wheat the induction of SA may result in various different chemical and even physiological responses (Gondor et al., 2016). It is therefore unclear whether the underlining mechanism is temporal-, genotype-, or community-specific.

3.4. Cross-Talk and the Interplay Between Pathways

Given the potential capacity of ET, JA, and SA to modulate the microbiome, it is often unclear how much cross-talk there is between pathways; however, there is evidence of significant interplay between the respective defense pathways (Koornneef et al., 2008; Diezel et al., 2009; Song et al., 2014; Yang Y.X. et al., 2015). The interplay of phytohormones can be antagonistic, with microbes being able to exploit the antagonism to facilitate colonization and thus evade host defense responses (Jacobs et al., 2011; Plett et al., 2014; Jha et al., 2018). The microbes themselves may utilize effector molecules to actively manipulate the phytohormone pathways and elicit antagonism between the pathways (Kazan and Lyons, 2014). The classical interpretation of the interplay between JA, SA, and ET is reviewed in Yang Y.X. et al. (2015). Unfortunately, little has been done thus far in untangling the potential pathway interaction and their effect on the microbial community. Here we therefore discuss recent evidence that may suggest the capacity of pathway cross-talk to manipulate and shape the microbiome.

As indicated above in the study of Bodenhausen et al. (2014), a statistically significant difference was observed in *Variovorax* abundance in both the ET and SA associated *A. thaliana* knockout mutants. There is the potential that *Variovorax* abundance is actually managed by the interaction between these respective pathways, given that ET and SA generally have a positive interaction and that *Variovorax* has been shown to be positively correlated with SA (Badri et al., 2013; Yang Y.X. et al., 2015).

The phytohormone abscisic acid (ABA) is well-known in its role in drought stress, salinity stress and as a modulator of plant defense signaling. It has been shown to negatively impact the SA-associated defense pathway, both positively and negatively affect JA-associated defense, and has been shown to affect ET-associated pathogen defense (Pieterse et al., 2012; Takatsuji and Jiang, 2014). In potting soil, exogenous application of ABA has resulted in preferential selection for *Cellvibrio*, *Limnobacter*, and *Massilia* microbes at the genus level (Carvalhais et al., 2014). However, cross-talk between ABA and the other phytohormone defenses, in terms of the effect on whole microbial communities, is largely still unexplored. Additionally, the mechanism of ABA's affect on whole microbiomes is poorly understood. Certain microbial species have been shown to leverage ABA cross-interaction

either by producing ABA or effecting ABA biosynthesis, thereby effecting plant-microbe dynamics (Jiang et al., 2010; Ho et al., 2013; Takatsuji and Jiang, 2014).

4. ABIOTIC PLANT STRESS AND THE IMPACT ON MICROBIAL COMMUNITIES

Environmental stressors, including drought stress, temperature stress, and salinity stress, impact plant development, metabolic activity, and the ability for the plant to interact with its phytobiome. The altered phytohormonal signaling and community structure alters the plant's ability to resist stress, resist disease, and alters the capacity for nutrient acquisition (Hawkes and Connor, 2017). While many studies have been performed on the response of the microbiome to abiotic stress and the potential beneficial and deleterious effects on the host, it is less clear how the host influences its microbiome under abiotic stress conditions.

4.1. Drought Stress

Drought stress has a significant impact on plant growth, development, metabolism, and mortality (Allen et al., 2010). Changes in the host in response to drought, in addition to changes in environmental conditions, induce plant-specific (Naylor et al., 2017) and compartment-specific (Santos-Medellín et al., 2017) selection of microbial communities; however, many drought responses, including changes in the microbiome, are conserved across species (Naylor et al., 2017) and soil types (Santos-Medellín et al., 2017).

Actinobacteria is commonly enriched in drought across a wide range of different compartments and plant species (Naylor et al., 2017; Santos-Medellín et al., 2017; Garcia et al., 2018; Timm et al., 2018; Xu et al., 2018). In *Sorghum*, drought causes developmental delays in the root microbiome, selecting for monoderms (Xu et al., 2018). During drought, there was an association between increased carbohydrates in the roots and increased carbohydrate transporters in *Actinobacteria* (Xu et al., 2018), suggesting altered root metabolites may play a role in selecting certain species. Additionally, monoderms are less affected by the increase in ROS by the plant during drought stress, relative to diderms (Shade et al., 2012). Host ROS metabolism genes were shown to be associated with *Streptomyces* (a genus of *Actinobacteria*) in *Populus* leaves (Garcia et al., 2018), potentially showing a more universal drought association between the host and its phytobiome. ROS metabolism has been shown to be a general change across species, omics levels, and compartments in drought (Fang et al., 2015; Abraham et al., 2018; Garcia et al., 2018; Zandalinas et al., 2018) that has impacts beyond that of *Actinobacteria*.

ROS metabolism transcription and defense response transcription are correlated during drought with a variety of taxa including *Rhizophagus* and nematodes (Garcia et al., 2018). ROS have been shown to modulate the host microbiome, including mitigating nematode infection (Nath et al., 2017) in soybeans (Beneventi et al., 2013) and in tomatoes (Vos et al., 2013). ROS have also been show to be beneficial in regulating rhizobial symbiosis in *Medicago truncatula* (Andrio et al., 2013). In addition to ROS, other hormones with defense affecting properties, such as ABA, are able to alter the host microbiome. ABA is upregulated in drought in a variety of plants, including *Populus*, *Arabidopsis*, *Sorghum*, etc. (Daszkowska-Golec, 2016; Sah et al., 2016; Kalladan et al., 2017; Garcia et al., 2018). Upregulation of ABA is associated with increased disease susceptibility in a variety of plants (Xiong and Yang, 2003; Gao et al., 2016; Pye et al., 2018). However, the plant's ability to withstand disease under stress has been shown to be plant- and disease-specific (Sinha et al., 2016). Furthermore, combined drought and disease stress has been shown to have an increased ability to mitigate disease (Pandey et al., 2015).

Metabolite production and exudates of the plant, including carbohydrates, amino acids, and other nutrients, are altered in response to drought stress (Bouskill et al., 2016; Tripathi et al., 2016; Abraham et al., 2018; Timm et al., 2018). Under more mild drought conditions, rhizodeposition is increased, while under more severe drought conditions, rhizodeposition is decreased, causing the exudate profile to be related to the severity of the drought experienced (Preece and Peñuelas, 2016). The change in metabolite profile with the plant also correlates with changes in the bacterial community, with root community composition in *Arabidopsis* shown to be dependent on the exudate profiles of the host plant (Badri et al., 2013). Under drought, an increase in hydrolytic enzymes responsible for breaking down complex carbohydrates such as lignin, cellulose, and other plant metabolites within the microbial communities has been shown (Bouskill et al., 2016). Additionally, bacteria can alter ethylene production within the plant with ACC deaminase (Arshad et al., 2008), which in turn alters plant growth and metabolite profiles to the benefit of plants and microbes (Mayak et al., 2004; Zhang et al., 2018). Not only can the host plant alter its exudate profile to recruit organisms, the microbial community can influence what compounds are being exuded, potentially creating a reciprocal relationship between the community and exudate profile. It is currently unknown how much of the exudate profiles are a plant-driven process and how much the microbial community can influence that process.

4.2. Temperature and Salinity Stress

Temperature stress can often accompany drought stress and has an impact on the fluidity of plant membranes (Sangwan et al., 2002), plant metabolism (Koscielny et al., 2018), ROS activation (Kotak et al., 2007), and protein misfolding (Scharf et al., 2012). Under colder temperatures, root nodulation is decreased in beans, lentils, and peas (Junior et al., 2005), and many organisms that live in the nodules have lower survivability (Singh et al., 2012). Under higher temperatures, a plant is less able to combat pathogens (Mendes et al., 2011), allowing for colonization of disease-causing organisms. However, some of the disease suppression lost during high heat can be associated with the loss of microorganisms that naturally inhibit plant diseases (van der Voort et al., 2016). Conversely, in a wheat high temperature seedling plant, high temperatures induce a WRKY transcription factor that promotes resistance to *Puccinia striiformis* infection (Wang et al., 2017).

In addition to drought and temperature stress, salinity stress also limits the types of plants that can grow in a given area. High salinity can cause ionic and osmotic stress that limits plant growth and damages plant cells (Zhu, 2002). Also, under salinity stress, plants have increased ROS generation, ABA synthesis, and accumulation of carbohydrates within the plant (Gupta and Huang, 2014), resulting in a similar response to water stress. Plants also respond similarly to drought in that ACC deaminase also can confer salinity resistance to the host plant (Qin et al., 2014). Many studies have been performed that have identified potential plant growth promoters under high salinity stress (Yuan et al., 2016; Hussain et al., 2018; Fouda et al., 2019). For example, 14 halotolerant microbes were shown to improve canola root growth under salt stress by decreasing ethelyne production (Siddikee et al., 2010). Additionally, *Piriformospora indica* was correlated with an increase in barley antioxidants under salt stress (Baltruschat et al., 2008). Salt tolerance can also be promoted by fungi, such as *Montagnulaceae* potential improving nitrogen availability in *Suaeda salsa* under salt stress (Yuan et al., 2016). Despite many studies identifying potential plant growth promoters under saline stress, there is limited knowledge of host plants influencing selection of community structure under salinity stress.

5. REMAINING CHALLENGES

It is clear that there are recent efforts toward identifying plant specific modes of action to control its microbiome. However, in a number of cases it is challenging to determine whether any mode of action was plant-mediated, microbial-mediated, or environment-mediated. Furthermore, the complex and potentially reciprocal nature of interaction adds to the challenge of identifying plant control mechanisms, which is evident when identifying and understanding phytohormone-based control mechanisms. Phytohormone pathways are interconnected, and they mediate abiotic stress responses in complex and sometimes antagonistic manners. The multi-layer interplay must then be delineated to understand the plant-microbe dynamic. Apart from the possible plant-associated complexity, there is the dynamic among the microbial community that must also be understood. Individual taxa in a microbiome may have a large effect on the whole microbiome structure, and the plant-based mechanisms may effect influential members.

5.1. Toward Understanding Combinatorial Plant Mechanisms

Diverse plant accession libraries provide a good framework to begin to compartmentalize and understand the dynamic of combinatorial interactions. For example, the *A. thaliana* mutant lines have provided a wealth of information on plant mechanisms that may influence microbial populations; however, they do not address the potential for confounding interactions between pathways. Additionally, the mutant lines on their own do not address the question of whether or not a respective pathway is necessary for the observed microbial shift. Approaches that use the supplementation of plant associated compounds identifying interplay between pathways and microbes need to be further addressed. Mutant lines with a combination of potential pathways effected, or general quantitative trait loci (QTL) studies, may be able to address the interaction confounding factors. Unfortunately, using model organisms such as *Arabidopsis* may not provide generalized results to all species given the variety in hormone pathways and physiological-based mechanisms that plants have for interacting with their microbial communities. There can be significant difference in the phytohormonal pathways between plant species (De Vleesschauwer et al., 2014), with the differences being associated with the biosynthetic pathway itself or the associated function of the pathway (Gondor et al., 2016). Additionally, certain plant species may be more amenable to hormonal amendment than others (De Vleesschauwer et al., 2014). It would therefore be prudent to investigate other, non-model, organisms in a variety of environments with the above mentioned techniques. Furthermore, multiple aspects of a study would need to be manipulated, such as hormone abundance, abiotic stressors, biotic stressors, and presence or absence of a microbial community members (including putative keystone species), to elucidate potential combinatorial effects between genotype, hormones, stress, and microbes.

5.2. Approaches to Unravel Microbial Community Dynamics

Synthetic or constructed communities provide an efficient approach to model microbial diversity. In contrast to axenic controls that allow for the ability to hypothesize about the colonization capacity or pathogenicity of an individual microbe, synthetic communities allow for the discovery of higher level interactions between plants and the microbial community. To therefore begin to understand the complex ecosystem may require an ecosystem point of view, including those based upon constructed communities in controlled environments (http://eco-fab.org/). However, synthetic communities may not be able to capture all of the complex site to site variation observed in natural environments, given that site variation can be a dominant factor in microbial diversity for certain plants (Whitaker et al., 2018). Nevertheless, constructed communities provide a model from which we can begin to reason, hypothesize, and understand the plant's role in dynamic microbial community interactions.

Using computational biology approaches in combination with experimental field and lab methods, including tools such as microfluidics and constructed communities will help advance understanding regarding plant recruitment of keystone microbes. Further understanding of host-mediated recruitment of its microbiome will in turn improve our ability to effectively and efficiently construct or manipulate plant-microbe systems for improved agricultural and ecological restoration efforts.

5.3. The Holobiont

A significant body of literature focuses on the soil or rhizosphere; however, we know that other compartments, including the root microbiota, can also influence above-ground phenotypes (Pangesti et al., 2017). Root exudates have a reciprocal impact on the microbial community and are influenced by the abiotic

stress, biotic stress, and phytohormones. Some drought stresses cause irreversible changes to root exudates (Gargallo-Garriga et al., 2018), which can be important when trying to engineer a community to promote plant growth under a variety of environmental conditions. Therefore, it is important to study plant-mediated effects on other compartments, but determining if effects are compartmental cross-talk, abiotic stress, or direct plant associated is still an open problem.

AUTHOR CONTRIBUTIONS

PJ, AF, and BG wrote the manuscript. DJ and GT edited the manuscript and provided guidance on content.

FUNDING

Funding was provided by The Center for Bioenergy Innovation (CBI). U.S. Department of Energy Bioenergy Research Centers are supported by the Office of Biological and Environmental Research in the DOE Office of Science. Further funding came from the Plant-Microbe Interfaces SFA (https://pmiweb.ornl.gov/), and the Oak Ridge National Laboratory's, Laboratory Directed Research and Development (LDRD) program, project 8321.

ACKNOWLEDGMENTS

We would like to acknowledge the support and guidance of the members of the JAIL CompSysBio team. This manuscript has been authored by UT-Battelle, LLC under Contract No. DE-AC05-00OR22725 with the U.S. Department of Energy. The United States Government retains and the publisher, by accepting the article for publication, acknowledges that the United States Government retains a non-exclusive, paid-up, irrevocable, worldwide license to publish or reproduce the published form of this manuscript, or allow others to do so, for United States Government purposes. The Department of Energy will provide public access to these results of federally sponsored research in accordance with the DOE Public Access Plan (http://energy.gov/downloads/doe-public-access-plan).

REFERENCES

Ab Rahman, S. F. S., Singh, E., Pieterse, C. M., and Schenk, P. M. (2018). Emerging microbial biocontrol strategies for plant pathogens. *Plant Sci.* 267, 102–111. doi: 10.1016/j.plantsci.2017.11.012

Abraham, P. E., Garcia, B. J., Gunter, L. E., Jawdy, S. S., Engle, N., Yang, X., et al. (2018). Quantitative proteome profile of water deficit stress responses in eastern cottonwood (*Populus deltoides*) leaves. *PLoS ONE* 13:e0190019. doi: 10.1371/journal.pone.0190019

Agler, M. T., Ruhe, J., Kroll, S., Morhenn, C., Kim, S. T., Weigel, D., et al. (2016). Microbial hub taxa link host and abiotic factors to plant microbiome variation. *PLoS Biol.* 14:e1002352. doi: 10.1371/journal.pbio.1002352

Allen, C. D., Macalady, A. K., Chenchouni, H., Bachelet, D., McDowell, N., Vennetier, M., et al. (2010). A global overview of drought and heat-induced tree mortality reveals emerging climate change risks for forests. *For. Ecol. Manage.* 259, 660–684. doi: 10.1016/j.foreco.2009.09.001

Andrio, E., Marino, D., Marmeys, A., de Segonzac, M. D., Damiani, I., Genre, A., et al. (2013). Hydrogen peroxide-regulated genes in the *Medicago truncatula–Sinorhizobium meliloti* symbiosis. *New Phytol.* 198, 179–189. doi: 10.1111/nph.12120

Arshad, M., Shaharoona, B., and Mahmood, T. (2008). Inoculation with *Pseudomonas* spp. containing ACC-deaminase partially eliminates the effects of drought stress on growth, yield, and ripening of pea (*Pisum sativum* L.). *Pedosphere* 18, 611–620. doi: 10.1016/S1002-0160(08)60055-7

Badri, D. V., Chaparro, J. M., Zhang, R., Shen, Q., and Vivanco, J. M. (2013). Application of natural blends of phytochemicals derived from the root exudates of *Arabidopsis* to the soil reveal that phenolic related compounds predominantly modulate the soil microbiome. *J. Biol. Chem.* 288, 4502–4512. doi: 10.1074/jbc.M112.433300

Bailey, B. A., Dean, J. F., and Anderson, J. D. (1990). An ethylene biosynthesis-inducing endoxylanase elicits electrolyte leakage and necrosis in *Nicotiana tabacum* cv Xanthi leaves. *Plant Physiol.* 94, 1849–1854. doi: 10.1104/pp.94.4.1849

Bais, H. P., Park, S.-W., Weir, T. L., Callaway, R. M., and Vivanco, J. M. (2004). How plants communicate using the underground information superhighway. *Trends Plant Sci.* 9, 26–32. doi: 10.1016/j.tplants.2003.11.008

Baltruschat, H., Fodor, J., Harrach, B. D., Niemczyk, E., Barna, B., Gullner, G., et al. (2008). Salt tolerance of barley induced by the root endophyte *Piriformospora indica* is associated with a strong increase in antioxidants. *New Phytol.* 180, 501–510. doi: 10.1111/j.1469-8137.2008.02583.x

Banerjee, S., Schlaeppi, K., and van der Heijden, M. G. (2018). Keystone taxa as drivers of microbiome structure and functioning. *Nat. Rev. Microbiol.* 16, 567–576. doi: 10.1038/s41579-018-0024-1

Beneventi, M. A., da Silva, O. B., de Sá, M. E. L., Firmino, A. A. P., de Amorim, R. M. S., Albuquerque, É. V. S., et al. (2013). Transcription profile of soybean-root-knot nematode interaction reveals a key role of phythormones in the resistance reaction. *BMC Genomics* 14:322. doi: 10.1186/1471-2164-14-322

Berendsen, R. L., Vismans, G., Yu, K., Song, Y., Jonge, R., Burgman, W. P., et al. (2018). Disease-induced assemblage of a plant-beneficial bacterial consortium. *ISME J.* 12:1496. doi: 10.1038/s41396-018-0093-1

Berry, D., and Widder, S. (2014). Deciphering microbial interactions and detecting keystone species with co-occurrence networks. *Front. Microbiol.* 5:219. doi: 10.3389/fmicb.2014.00219

Bertin, C., Yang, X., and Weston, L. A. (2003). The role of root exudates and allelochemicals in the rhizosphere. *Plant Soil* 256, 67–83. doi: 10.1023/A:1026290508166

Bever, J. D., Platt, T. G., and Morton, E. R. (2012). Microbial population and community dynamics on plant roots and their feedbacks on plant communities. *Annu. Rev. Microbiol.* 66, 265–283. doi: 10.1146/annurev-micro-092611-150107

Bodenhausen, N., Bortfeld-Miller, M., Ackermann, M., and Vorholt, J. A. (2014). A synthetic community approach reveals plant genotypes affecting the phyllosphere microbiota. *PLoS Genet.* 10:e1004283. doi: 10.1371/journal.pgen.1004283

Bouskill, N. J., Wood, T. E., Baran, R., Ye, Z., Bowen, B. P., Lim, H., et al. (2016). Belowground response to drought in a tropical forest soil. I. Changes in microbial functional potential and metabolism. *Front. Microbiol.* 7:525. doi: 10.3389/fmicb.2016.00525

Bulgarelli, D., Schlaeppi, K., Spaepen, S., van Themaat, E. V. L., and Schulze-Lefert, P. (2013). Structure and functions of the bacterial microbiota of plants. *Annu. Rev. Plant Biol.* 64, 807–838. doi: 10.1146/annurev-arplant-050312-120106

Burg, S. P., and Burg, E. A. (1966). The interaction between auxin and ethylene and its role in plant growth. *Proc. Natl. Acad. Sci. U.S.A.* 55, 262–269. doi: 10.1073/pnas.55.2.262

Busby, P. E., Soman, C., Wagner, M. R., Friesen, M. L., Kremer, J., Bennett, A., et al. (2017). Research priorities for harnessing plant microbiomes in sustainable agriculture. *PLoS Biol.* 15: e2001793. doi: 10.1371/journal.pbio.2001793

Carvalhais, L. C., Dennis, P. G., Badri, D. V., Kidd, B. N., Vivanco, J. M., and Schenk, P. M. (2015). Linking jasmonic acid signaling, root exudates, and rhizosphere microbiomes. *Mol. Plant-Microbe Interact.* 28, 1049–1058. doi: 10.1094/MPMI-01-15-0016-R

Carvalhais, L. C., Dennis, P. G., Fan, B., Fedoseyenko, D., Kierul, K., Becker, A., et al. (2013). Linking plant nutritional status to plant-microbe interactions. *PLoS ONE* 8:e68555. doi: 10.1371/journal.pone.0068555

Carvalhais, L. C., Dennis, P. G., and Schenk, P. M. (2014). Plant defence inducers rapidly influence the diversity of bacterial communities in a potting mix. *Appl. Soil Ecol.* 84, 1–5. doi: 10.1016/j.apsoil.2014.06.011

Cho, S.-M., Kang, B. R., and Kim, Y. C. (2013). Transcriptome analysis of induced systemic drought tolerance elicited by *Pseudomonas chlororaphis* O6 in *Arabidopsis thaliana*. *Plant Pathol. J.* 29, 209–220. doi: 10.5423/PPJ.SI.07.2012.0103

Chou, H. M., Bundock, N., Rolfe, S. A., and Scholes, J. D. (2000). Infection of *Arabidopsis thaliana* leaves with Albugo Candida (white blister rust) causes a reprogramming of host metabolism. *Mol. Plant Pathol.* 1, 99–113. doi: 10.1046/j.1364-3703.2000.00013.x

Christensen, S. A., Nemchenko, A., Borrego, E., Murray, I., Sobhy, I. S., Bosak, L., et al. (2013). The maize lipoxygenase, Zm LOX 10, mediates green leaf volatile, jasmonate and herbivore-induced plant volatile production for defense against insect attack. *Plant J.* 74, 59–73. doi: 10.1111/tpj.12101

Cook, D. E., Mesarich, C. H., and Thomma, B. P. (2015). Understanding plant immunity as a surveillance system to detect invasion. *Annu. Rev. Phytopathol.* 53, 541–563. doi: 10.1146/annurev-phyto-080614-120114

Copeland, J. K., Yuan, L., Layeghifard, M., Wang, P. W., and Guttman, D. S. (2015). Seasonal community succession of the phyllosphere microbiome. *Mol. Plant-Microbe Interact.* 28, 274–285. doi: 10.1094/MPMI-10-14-0331-FI

Daszkowska-Golec, A. (2016). "The role of abscisic acid in drought stress: how ABA helps plants to cope with drought stress," in *Drought Stress Tolerance in Plants, Vol. 2*, eds M. A. Hossain, S. H. Wani, S. Bhattachajee, D. J. Burritt, L. S. P. Tran (Cham: Springer), 123–151.

De Vleesschauwer, D., Xu, J., and Höfte, M. (2014). Making sense of hormone-mediated defense networking: from rice to *Arabidopsis*. *Front. Plant Sci.* 5:611. doi: 10.3389/fpls.2014.00611

Diezel, C., von Dahl, C. C., Gaquerel, E., and Baldwin, I. T. (2009). Different lepidopteran elicitors account for cross-talk in herbivory-induced phytohormone signaling. *Plant Physiol.* 150, 1576–1586. doi: 10.1104/pp.109.139550

Doornbos, R. F., Geraats, B. P., Kuramae, E. E., Van Loon, L., and Bakker, P. A. (2011). Effects of jasmonic acid, ethylene, and salicylic acid signaling on the rhizosphere bacterial community of *Arabidopsis thaliana*. *Mol. Plant-Microbe Interact.* 24, 395–407. doi: 10.1094/MPMI-05-10-0115

Duhamel, A. M., Wan, J., Bogar, L. M., Segnitz, R. M., and J, N. C. D. (2018). Keystone mutualists can facilitate transition between alternative ecosystem states in the soil. *bioRxiv*. doi: 10.1101/392993

Estes, J. A., and Palmisano, J. F. (1974). Sea otters: their role in structuring nearshore communities. *Science* 185, 1058–1060. doi: 10.1126/science.185.4156.1058

Fang, Y., Liao, K., Du, H., Xu, Y., Song, H., Li, X., et al. (2015). A stress-responsive NAC transcription factor SNAC3 confers heat and drought tolerance through modulation of reactive oxygen species in rice. *J. Exp. Bot.* 66, 6803–6817. doi: 10.1093/jxb/erv386

Farmer, E. E., and Ryan, C. A. (1992). Octadecanoid precursors of jasmonic acid activate the synthesis of wound-inducible proteinase inhibitors. *Plant Cell* 4, 129–134. doi: 10.1105/tpc.4.2.129

Fouda, A., Hassan, S. E. D., Eid, A. M., and El-Din Ewais, E. (2019). "The interaction between plants and bacterial endophytes under salinity stress," in *Endophytes and Secondary Metabolites*, ed J. Jha (Cham: Springer), 1–17. doi: 10.1007/978-3-319-76900-4_15-1

Fu, Z. Q., and Dong, X. (2013). Systemic acquired resistance: turning local infection into global defense. *Annu. Rev. Plant Biol.* 64, 839–863. doi: 10.1146/annurev-arplant-042811-105606

Gamper, H. A., van der Heijden, M. G., and Kowalchuk, G. A. (2010). Molecular trait indicators: moving beyond phylogeny in arbuscular mycorrhizal ecology. *New Phytol.* 185, 67–82. doi: 10.1111/j.1469-8137.2009.03058.x

Gao, S., Guo, W., Feng, W., Liu, L., Song, X., Chen, J., et al. (2016). LTP3 contributes to disease susceptibility in *Arabidopsis* by enhancing abscisic acid (ABA) biosynthesis. *Mol. Plant Pathol.* 17, 412–426. doi: 10.1111/mpp.12290

Garcia, B. J., Labbe, J., Jones, P., Abraham, P., Hodge, I., Climer, S., et al. (2018). Phytobiome and transcriptional adaptation of *Populus deltoides* to acute progressive drought and cyclic drought. *Phytobiomes* 2, 2471–2906. doi: 10.1094/PBIOMES-04-18-0021-R

Gargallo-Garriga, A., Preece, C., Sardans, J., Oravec, M., Urban, O., and Peñuelas, J. (2018). Root exudate metabolomes change under drought and show limited capacity for recovery. *Sci. Rep.* 8:12696. doi: 10.1038/s41598-018-30150-0

Glazebrook, J. (2005). Contrasting mechanisms of defense against biotrophic and necrotrophic pathogens. *Annu. Rev. Phytopathol.* 43, 205–227. doi: 10.1146/annurev.phyto.43.040204.135923

Gondor, O. K., Janda, T., Soós, V., Pál, M., Majláth, I., Adak, M. K., et al. (2016). Salicylic acid induction of flavonoid biosynthesis pathways in wheat varies by treatment. *Front. Plant Sci.* 7:1447. doi: 10.3389/fpls.2016.01447

Gupta, B., and Huang, B. (2014). Mechanism of salinity tolerance in plants: physiological, biochemical, and molecular characterization. *Int. J. Genomics* 2014:701596. doi: 10.1155/2014/701596

Hacquard, S., Spaepen, S., Garrido-Oter, R., and Schulze-Lefert, P. (2017). Interplay between innate immunity and the plant microbiota. *Annu. Rev. Phytopathol.* 55, 565–589. doi: 10.1146/annurev-phyto-080516-035623

Hamonts, K., Trivedi, P., Garg, A., Janitz, C., Grinyer, J., Holford, P., et al. (2018). Field study reveals core plant microbiota and relative importance of their drivers. *Environ. Microbiol.* 20, 124–140. doi: 10.1111/1462-2920.14031

Han, J.-I., Choi, H.-K., Lee, S.-W., Orwin, P. M., Kim, J., LaRoe, S. L., et al. (2011). Complete genome sequence of the metabolically versatile plant growth-promoting endophyte *Variovorax paradoxus S110*. *J. Bacteriol.* 193, 1183–1190. doi: 10.1128/JB.00925-10

Harrison, J. G., Parchman, T. L., Cook, D., Gardner, D. R., and Forister, M. L. (2018). A heritable symbiont and host-associated factors shape fungal endophyte communities across spatial scales. *J. Ecol.* 106, 2274–2286. doi: 10.1111/1365-2745.12967

Hawkes, C. V., and Connor, E. W. (2017). Translating phytobiomes from theory to practice: ecological and evolutionary considerations. *Phytobiomes* 1, 57–69. doi: 10.1094/PBIOMES-05-17-0019-RVW

Hayward, J., Horton, T. R., Pauchard, A., and Nunez, M. A. (2015). A single ectomycorrhizal fungal species can enable a Pinus invasion. *Ecology* 96, 1438–1444. doi: 10.1890/14-1100.1

Herren, C. M., and McMahon, K. D. (2018). Keystone taxa predict compositional change in microbial communities. *Environ. Microbiol.* 20, 2207–2217. doi: 10.1111/1462-2920.14257

Ho, Y.-P., Tan, C. M., Li, M.-Y., Lin, H., Deng, W.-L., and Yang, J.-Y. (2013). The AvrB_AvrC domain of AvrXccC of *Xanthomonas campestris* pv. campestris is required to elicit plant defense responses and manipulate ABA homeostasis. *Mol. Plant-Microbe Interact.* 26, 419–430. doi: 10.1094/MPMI-06-12-0164-R

Hu, L., Robert, C. A., Cadot, S., Zhang, X., Ye, M., Li, B., et al. (2018). Root exudate metabolites drive plant-soil feedbacks on growth and defense by shaping the rhizosphere microbiota. *Nat. Commun.* 9:2738. doi: 10.1038/s41467-018-05122-7

Huang, L., Yin, X., Sun, X., Yang, J., Rahman, M., Chen, Z., et al. (2018). Expression of a grape VqSTS36-increased resistance to powdery mildew and osmotic stress in *Arabidopsis* but enhanced susceptibility to *Botrytis cinerea* in *Arabidopsis* and tomato. *Int. J. Mol. Sci.* 19:E2985. doi: 10.3390/ijms19102985

Hussain, S. S., Mehnaz, S., and Siddique, K. H. (2018). "Harnessing the plant microbiome for improved abiotic stress tolerance," in *Plant Microbiome: Stress Response*, eds D. Egamberdieva and P. Ahmad (Singapore: Springer), 21–43. doi: 10.1007/978-981-10-5514-0_2

Jacobs, S., Zechmann, B., Molitor, A., Trujillo, M., Petutschnig, E., Lipka, V., et al. (2011). Broad spectrum suppression of innate immunity is required for colonization of *Arabidopsis thaliana* roots by the fungus *Piriformospora indica*. *Plant Physiol.* 156, 726–740. doi: 10.1104/pp.111.176446

Jha, P., Panwar, J., and Jha, P. N. (2018). Mechanistic insights on plant root colonization by bacterial endophytes: a symbiotic relationship for sustainable agriculture. *Environ. Sustain.* 1, 25–38. doi: 10.1007/s42398-018-0011-5

Jiang, C.-J., Shimono, M., Sugano, S., Kojima, M., Yazawa, K., Yoshida, R., et al. (2010). Abscisic acid interacts antagonistically with salicylic acid signaling pathway in rice–magnaporthe grisea interaction. *Mol. Plant-Microbe Interact.* 23, 791–798. doi: 10.1094/MPMI-23-6-0791

Junior, M. d. A. L., Lima, A., Arruda, J., and Smith, D. (2005). Effect of root temperature on nodule development of bean, lentil and pea. *Soil Biol. Biochem.* 37, 235–239. doi: 10.1016/j.soilbio.2004.07.032

Kalladan, R., Lasky, J. R., Chang, T. Z., Sharma, S., Juenger, T. E., and Verslues, P. E. (2017). Natural variation identifies genes affecting drought-induced abscisic acid accumulation in *Arabidopsis thaliana*. *Proc. Natl. Acad. Sci. U.S.A.* 114, 11536–11541. doi: 10.1073/pnas.1705884114

Kazan, K., and Lyons, R. (2014). Intervention of phytohormone pathways by pathogen effectors. *Plant Cell* 26, 2285–2309. doi: 10.1105/tpc.114.125419

Kennedy, N., Brodie, E., Connolly, J., and Clipson, N. (2004). Impact of lime, nitrogen and plant species on bacterial community structure in grassland microcosms. *Environ. Microbiol.* 6, 1070–1080. doi: 10.1111/j.1462-2920.2004.00638.x

Kikuchi, K., Matsushita, N., Suzuki, K., and Hogetsu, T. (2007). Flavonoids induce germination of basidiospores of the ectomycorrhizal fungus *Suillus bovinus*. *Mycorrhiza* 17, 563–570. doi: 10.1007/s00572-007-0131-8

Koo, A. J., Gao, X., Daniel Jones, A., and Howe, G. A. (2009). A rapid wound signal activates the systemic synthesis of bioactive jasmonates in *Arabidopsis*. *Plant J.* 59, 974–986. doi: 10.1111/j.1365-313X.2009.03924.x

Koornneef, A., Leon-Reyes, A., Ritsema, T., Verhage, A., Den Otter, F. C., Van Loon, L., et al. (2008). Kinetics of salicylate-mediated suppression of jasmonate signaling reveal a role for redox modulation. *Plant Physiol.* 147, 1358–1368. doi: 10.1104/pp.108.121392

Koscielny, C., Hazebroek, J., and Duncan, R. (2018). Phenotypic and metabolic variation among spring *Brassica napus* genotypes during heat stress. *Crop Pasture Sci.* 69, 284–295. doi: 10.1071/CP17259

Kotak, S., Larkindale, J., Lee, U., von Koskull-Döring, P., Vierling, E., and Scharf, K.-D. (2007). Complexity of the heat stress response in plants. *Curr. Opin. Plant Biol.* 10, 310–316. doi: 10.1016/j.pbi.2007.04.011

Laan, P. (1934). Effect of ethylene on growth hormone formation in *Avena* and *Vicia*. *Rec. Trav. Botan. Neerl* 31, 691–742.

Lebeis, S. L., Paredes, S. H., Lundberg, D. S., Breakfield, N., Gehring, J., McDonald, M., et al. (2015). Salicylic acid modulates colonization of the root microbiome by specific bacterial taxa. *Science* 349, 860–864. doi: 10.1126/science.aaa8764

Lemanceau, P., Blouin, M., Muller, D., and Moënne-Loccoz, Y. (2017). Let the core microbiota be functional. *Trends Plant Sci.* 22, 583–595. doi: 10.1016/j.tplants.2017.04.008

Li, C., Schilmiller, A. L., Liu, G., Lee, G. I., Jayanty, S., Sageman, C., et al. (2005). Role of β-oxidation in jasmonate biosynthesis and systemic wound signaling in tomato. *Plant Cell* 17, 971–986. doi: 10.1105/tpc.104.029108

Li, Z., Fu, J., Zhou, R., and Wang, D. (2018). Effects of phenolic acids from ginseng rhizosphere on soil fungi structure, richness and diversity in consecutive monoculturing of ginseng. *Saudi J. Biol. Sci.* 25, 1788–1794. doi: 10.1016/j.sjbs.2018.07.007

Liao, H. L., Chen, Y., and Vilgalys, R. (2016). Metatranscriptomic study of common and host-specific patterns of gene expression between pines and their symbiotic ectomycorrhizal fungi in the genus suillus. *PLoS Genet.* 12:e1006348. doi: 10.1371/journal.pgen.1006348

Liu, H., Carvalhais, L. C., Schenk, P. M., and Dennis, P. G. (2018). Activation of the salicylic acid signalling pathway in wheat had no significant short-term impact on the diversity of root-associated microbiomes. *Pedobiologia* 70, 6–11. doi: 10.1016/j.pedobi.2018.08.001

Massalha, H., Korenblum, E., Malitsky, S., Shapiro, O. H., and Aharoni, A. (2017). Live imaging of root-bacteria interactions in a microfluidics setup. *Plant Biol.* 114, 4549–4554. doi: 10.1073/pnas.1618584114

Mayak, S., Tirosh, T., and Glick, B. R. (2004). Plant growth-promoting bacteria that confer resistance to water stress in tomatoes and peppers. *Plant Sci.* 166, 525–530. doi: 10.1016/j.plantsci.2003.10.025

Mendes, R., Kruijt, M., De Bruijn, I., Dekkers, E., van der Voort, M., Schneider, J. H., et al. (2011). Deciphering the rhizosphere microbiome for disease-suppressive bacteria. *Science* 332, 1097–1100. doi: 10.1126/science.1203980

Mersmann, S., Bourdais, G., Rietz, S., and Robatzek, S. (2010). Ethylene signalling regulates accumulation of the *FLS2* receptor and is required for the oxidative burst contributing to plant immunity. *Plant Physiol.* 154, 391–400. doi: 10.1104/pp.110.154567

Meyer, K. M., and Leveau, J. H. (2012). Microbiology of the phyllosphere: a playground for testing ecological concepts. *Oecologia.* 168, 621–629. doi: 10.1007/s00442-011-2138-2

Micallef, S. A., Shiaris, M. P., and Colón-Carmona, A. (2009). Influence of *Arabidopsis thaliana* accessions on rhizobacterial communities and natural variation in root exudates. *J. Exp. Bot.* 60, 1729–1742. doi: 10.1093/jxb/erp053

Mikiciński, A., Sobiczewski, P., Puławska, J., and Maciorowski, R. (2016). Control of fire blight (*Erwinia amylovora*) by a novel strain 49M of *Pseudomonas graminis* from the phyllosphere of apple (*Malus* spp.). *Eur. J. Plant Pathol.* 145, 265–276. doi: 10.1007/s10658-015-0837-y

Mönchgesang, S., Strehmel, N., Schmidt, S., Westphal, L., Taruttis, F., Müller, E., et al. (2016). Natural variation of root exudates in *Arabidopsis thaliana*-linking metabolomic and genomic data. *Sci. Rep.* 6:29033. doi: 10.1038/srep29033

Nascimento, F. X., Rossi, M. J., and Glick, B. R. (2018). Ethylene and 1-Aminocyclopropane-1-carboxylate (ACC) in plant–bacterial interactions. *Front. Plant Sci.* 9:114. doi: 10.3389/fpls.2018.00114

Nath, M., Bhatt, D., Prasad, R., and Tuteja, N. (2017). "Reactive oxygen species (ROS) metabolism and signaling in plant-mycorrhizal association under biotic and abiotic stress conditions," in *Mycorrhiza-Eco-Physiology, Secondary Metabolites, Nanomaterials*, eds A. Varma, R. Prasad, and N. Tuteja (Cham: Springer), 223–232.

Naylor, D., DeGraaf, S., Purdom, E., and Coleman-Derr, D. (2017). Drought and host selection influence bacterial community dynamics in the grass root microbiome. *ISME J.* 11:2691. doi: 10.1038/ismej.2017.118

Neal, A. and Ton, J. (2013). Systemic defense priming by *Pseudomonas putida* KT2440 in maize depends on benzoxazinoid exudation from the roots. *Plant Signal. Behav.* 8:e22655. doi: 10.4161/psb.22655

Neal, A. L., Ahmad, S., Gordon-Weeks, R., and Ton, J. (2012). Benzoxazinoids in root exudates of maize attract *Pseudomonas putida* to the rhizosphere. *PLoS ONE* 7:e35498. doi: 10.1371/journal.pone.0035498

Niu, B., Paulson, J. N., Zheng, X., and Kolter, R. (2017). Simplified and representative bacterial community of maize roots. *Proc. Natl. Acad. Sci. U.S.A.* 114, E2450–E2459. doi: 10.1073/pnas.1616148114

Oberholster, T., Vikram, S., Cowan, D., and Valverde, A. (2018). Key microbial taxa in the rhizosphere of sorghum and sunflower grown in crop rotation. *Sci. Total Environ.* 624, 530–539. doi: 10.1016/j.scitotenv.2017.12.170

Oikawa, A., Ishihara, A., Hasegawa, M., Kodama, O., and Iwamura, H. (2001). Induced accumulation of 2-hydroxy-4, 7-dimethoxy-1, 4-benzoxazin-3-one glucoside (HDMBOA-Glc) in maize leaves. *Phytochemistry* 56, 669–675. doi: 10.1016/S0031-9422(00)00494-5

Ojuederie, O., and Babalola, O. (2017). Microbial and plant-assisted bioremediation of heavy metal polluted environments: a review. *Int. J. Environ. Res. Publ. Health* 14:1504. doi: 10.3390/ijerph14121504

Ordal, G. W., Villani, D. P., and Rosendahl, M. S. (1979). Chemotaxis towards sugars by *Bacillus subtilis*. *Microbiology* 115, 167–172. doi: 10.1099/00221287-115-1-167

Paine, R. T. (1966). Food web complexity and species diversity. *Am. Natur.* 100, 65–75. doi: 10.1086/282400

Paine, R. T. (1969). The pisaster-tegula interaction: prey patches, predator food preference, and intertidal community structure. *Ecology* 50, 950–961. doi: 10.2307/1936888

Pandey, P., Ramegowda, V., and Senthil-Kumar, M. (2015). Shared and unique responses of plants to multiple individual stresses and stress combinations: physiological and molecular mechanisms. *Front. Plant Sci.* 6:723. doi: 10.3389/fpls.2015.00723

Pangesti, N., Reichelt, M., van de Mortel, J. E., Kapsomenou, E., Gershenzon, J., van Loon, J. J., et al. (2016). Jasmonic acid and ethylene signaling pathways regulate glucosinolate levels in plants during rhizobacteria-induced systemic resistance against a leaf-chewing herbivore. *J. Chem. Ecol.* 42, 1212–1225. doi: 10.1007/s10886-016-0787-7

Pangesti, N., Vandenbrande, S., Pineda, A., Dicke, M., Raaijmakers, J. M., and Van Loon, J. J. (2017). Antagonism between two root-associated beneficial *Pseudomonas* strains does not affect plant growth promotion and induced resistance against a leaf-chewing herbivore. *FEMS Microbiol. Ecol.* 93:fix038. doi: 10.1093/femsec/fix038

Pappas, M. L., Broekgaarden, C., Broufas, G. D., Kant, M. R., Messelink, G. J., Steppuhn, A., et al. (2017). Induced plant defences in biological control of arthropod pests: a double-edged sword. *Pest Manage. Sci.* 73, 1780–1788. doi: 10.1002/ps.4587

Pieterse, C. M., Van der Does, D., Zamioudis, C., Leon-Reyes, A., and Van Wees, S. C. (2012). Hormonal modulation of plant immunity. *Annu.*

Rev. Cell Dev. Biol. 28, 489–521. doi: 10.1146/annurev-cellbio-092910-154055

Plett, J. M., Daguerre, Y., Wittulsky, S., Vayssières, A., Deveau, A., Melton, S. J., et al. (2014). Effector MiSSP7 of the mutualistic fungus *Laccaria bicolor* stabilizes the Populus JAZ6 protein and represses jasmonic acid (JA) responsive genes. *Proc. Natl. Acad. Sci. U.S.A.* 111, 8299–8304. doi: 10.1073/pnas.1322671111

Preece, C., and Peñuelas, J. (2016). Rhizodeposition under drought and consequences for soil communities and ecosystem resilience. *Plant Soil* 409, 1–17. doi: 10.1007/s11104-016-3090-z

Pye, M. F., Dye, S. M., Resende, R. S., MacDonald, J. D., and Bostock, R. M. (2018). Abscisic acid as a dominant signal in tomato during salt stress predisposition to *Phytophthora* root and crown rot. *Front. Plant Sci.* 9:525. doi: 10.3389/fpls.2018.00525

Qin, S., Zhang, Y.-J., Yuan, B., Xu, P.-Y., Xing, K., Wang, J., et al. (2014). Isolation of ACC deaminase-producing habitat-adapted symbiotic bacteria associated with halophyte *Limonium sinense (Girard) Kuntze* and evaluating their plant growth-promoting activity under salt stress. *Plant Soil* 374, 753–766. doi: 10.1007/s11104-013-1918-3

Ripple, W. J., Larsen, E. J., Renkin, R. A., and Smith, D. W. (2001). Trophic cascades among wolves, elk and aspen on Yellowstone National Park's northern range. *Biol. Conserv.* 102, 227–234. doi: 10.1016/S0006-3207(01)00107-0

Rottjers, L., and Faust, K. (2018). Can we predict microbial keystones? *Nat. Rev. Microbiol.* 17:193. doi: 10.1038/s41579-018-0132-y

Ruhe, J., Agler, M. T., Placzek, A., Kramer, K., Finkemeier, I., and Kemen, E. M. (2016). Obligate biotroph pathogens of the genus albugo are better adapted to active host defense compared to niche competitors. *Front. Plant Sci.* 7:820. doi: 10.3389/fpls.2016.00820

Sah, S. K., Reddy, K. R., and Li, J. (2016). Abscisic acid and abiotic stress tolerance in crop plants. *Front. Plant Sci.* 7:571. doi: 10.3389/fpls.2016.00571

Sangwan, V., Örvar, B. L., Beyerly, J., Hirt, H., and Dhindsa, R. S. (2002). Opposite changes in membrane fluidity mimic cold and heat stress activation of distinct plant MAP kinase pathways. *Plant J.* 31, 629–638. doi: 10.1046/j.1365-313X.2002.01384.x

Santos-Medellín, C., Edwards, J., Liechty, Z., Nguyen, B., and Sundaresan, V. (2017). Drought stress results in a compartment-specific restructuring of the rice root-associated microbiomes. *MBio* 8, e00764–17. doi: 10.1128/mBio.00764-17

Sasse, J., Martinoia, E., and Northen, T. (2018). Feed your friends: do plant exudates shape the root microbiome? *Trends Plant Sci.* 23, 25–41. doi: 10.1016/j.tplants.2017.09.003

Scharf, K.-D., Berberich, T., Ebersberger, I., and Nover, L. (2012). The plant heat stress transcription factor (Hsf) family: structure, function and evolution. *Biochim. Biophys. Acta* 1819, 104–119. doi: 10.1016/j.bbagrm.2011.10.002

Schilmiller, A. L., Koo, A. J., and Howe, G. A. (2007). Functional diversification of acyl-coenzyme A oxidases in jasmonic acid biosynthesis and action. *Plant Physiol.* 143, 812–824. doi: 10.1104/pp.106.092916

Shade, A., Peter, H., Allison, S. D., Baho, D., Berga, M., Bürgmann, H., et al. (2012). Fundamentals of microbial community resistance and resilience. *Front. Microbiol.* 3:417. doi: 10.3389/fmicb.2012.00417

Shah, J. (2003). The salicylic acid loop in plant defense. *Curr. Opin. Plant Biol.* 6, 365–371. doi: 10.1016/S1369-5266(03)00058-X

Sharon, A., Fuchs, Y., and Anderson, J. D. (1993). The elicitation of ethylene biosynthesis by a *Trichoderma xylanase* is not related to the cell wall degradation activity of the enzyme. *Plant Physiol.* 102, 1325–1329. doi: 10.1104/pp.102.4.1325

Siddikee, M. A., Chauhan, P., Anandham, R., Han, G.-H., and Sa, T. (2010). Isolation, characterization, and use for plant growth promotion under salt stress, of ACC deaminase-producing halotolerant bacteria derived from coastal soil. *J. Microbiol. Biotechnol.* 20, 1577–1584. doi: 10.4014/jmb.1007.07011

Singh, S., Najar, G., and Singh, U. (2012). Phosphorus management in field pea (*Pisum sativum*)-rice (*Oryza sativa*) cropping system under temperate conditions. *Indian J. Agric. Sci.* 82:494.

Sinha, R., Gupta, A., and Senthil-Kumar, M. (2016). Understanding the impact of drought on foliar and xylem invading bacterial pathogen stress in chickpea. *Front. Plant Sci.* 7:902. doi: 10.3389/fpls.2016.00902

Smalle, J., Haegman, M., Kurepa, J., Van Montagu, M., and Van Der Straeten, D. (1997). Ethylene can stimulate *Arabidopsis* hypocotyl elongation in the light. *Proc. Natl. Acad. Sci. U.S.A.* 94, 2756–2761. doi: 10.1073/pnas.94.6.2756

Soka, G., and Ritchie, M. (2015). Arbuscular mycorrhizal symbiosis, ecosystem processes and environmental changes in tropical soils. *Appl. Ecol. Environ. Res.* 13, 229–245. doi: 10.15666/aeer/1301_229245

Song, S., Huang, H., Gao, H., Wang, J., Wu, D., Liu, X., et al. (2014). Interaction between MYC2 and ETHYLENE INSENSITIVE3 modulates antagonism between jasmonate and ethylene signaling in *Arabidopsis*. *Plant Cell* 26, 263–279. doi: 10.1105/tpc.113.120394

Stanley, C. E., and van der Heijden, M. G. A. (2017). Microbiome-on-a-chip: new frontiers in plant-microbiota research. *Trends Microbiol.* 25, 610–613. doi: 10.1016/j.tim.2017.05.001

Stirling, G. R. (2017). "Biological control of plant-parasitic nematodes," in *Diseases of Nematodes* (CRC Press), 103–150.

Sukumar, P. (2010). *The role of auxin and ethylene in adventitious root formation in Arabidopsis and tomato* (Ph.D. thesis). Wake Forest University, Winston-Salem, NC, United States.

Takatsuji, H., and Jiang, C.-J. (2014). "Plant hormone crosstalks under biotic stresses," in *Phytohormones: A Window to Metabolism, Signaling and Biotechnological Applications*, eds L.-S. Tran and S. Pal (New York, NY: Springer), 323–350.

Thao, N. P., Khan, M. I. R., Thu, N. B. A., Hoang, X. L. T., Asgher, M., Khan, N. A., et al. (2015). Role of ethylene and its cross talk with other signaling molecules in plant responses to heavy metal stress. *Plant Physiol.* 169, 73–84. doi: 10.1104/pp.15.00663

Timm, C. M., Carter, K. R., Carrell, A. A., Jun, S.-R., Jawdy, S. S., Vélez, J. M., et al. (2018). Abiotic stresses shift belowground populus-associated bacteria toward a core stress microbiome. *MSystems* 3, e00070–17. doi: 10.1128/mSystems.00070-17

Tripathi, P., Rabara, R. C., Reese, R. N., Miller, M. A., Rohila, J. S., Subramanian, S., et al. (2016). A toolbox of genes, proteins, metabolites and promoters for improving drought tolerance in soybean includes the metabolite coumestrol and stomatal development genes. *BMC Genomics* 17:102. doi: 10.1186/s12864-016-2420-0

Trivedi, P., Delgado-Baquerizo, M., Trivedi, C., Hamonts, K., Anderson, I. C., and Singh, B. K. (2017). Keystone microbial taxa regulate the invasion of a fungal pathogen in agro-ecosystems. *Soil Biol. Biochem.* 111, 10–14. doi: 10.1016/j.soilbio.2017.03.013

van der Voort, M., Kempenaar, M., van Driel, M., Raaijmakers, J. M., and Mendes, R. (2016). Impact of soil heat on reassembly of bacterial communities in the rhizosphere microbiome and plant disease suppression. *Ecol. Lett.* 19, 375–382. doi: 10.1111/ele.12567

Vos, C., Schouteden, N., Van Tuinen, D., Chatagnier, O., Elsen, A., De Waele, D., et al. (2013). Mycorrhiza-induced resistance against the root–knot nematode *Meloidogyne incognita* involves priming of defense gene responses in tomato. *Soil Biol. Biochem.* 60, 45–54. doi: 10.1016/j.soilbio.2013.01.013

Wagner, M. R., Lundberg, D. S., Tijana, G., Tringe, S. G., Dangl, J. L., and Mitchell-Olds, T. (2016). Host genotype and age shape the leaf and root microbiomes of a wild perennial plant. *Nat. Commun.* 7:12151. doi: 10.1038/ncomms12151

Wang, J., Tao, F., An, F., Zou, Y., Tian, W., Chen, X., et al. (2017). Wheat transcription factor TaWRKY70 is positively involved in high-temperature seedling plant resistance to *Puccinia striiformis f.* sp. tritici. *Mol. Plant Pathol.* 18, 649–661. doi: 10.1111/mpp.12425

Wei, L., Jian, H., Lu, K., Filardo, F., Yin, N., Liu, L., et al. (2016). Genome-wide association analysis and differential expression analysis of resistance to *Sclerotinia* stem rot in *Brassica napus*. *Plant Biotechnol. J.* 14, 1368–1380. doi: 10.1111/pbi.12501

Whitaker, B. K., Reynolds, H. L., and Clay, K. (2018). Foliar fungal endophyte communities are structured by environment but not host ecotype in *Panicum virgatum* (switchgrass). *Ecology* 99, 2703–2711. doi: 10.1002/ecy.2543

White, R. (1979). Acetylsalicylic acid (aspirin) induces resistance to tobacco mosaic virus in tobacco. *Virology* 99, 410–412. doi: 10.1016/0042-6822(79)90019-9

Whitham, T. G., Schweitzer, J. A. S., Shuster, S. M. S., Imp, G. I. N. A. M. W., Fischer, D. G. F., Bailey, J. K. B., et al. (2003). Community and Ecosystem Genetics : a consequence of the extended phenotype special feature. *Ecology* 84, 559–573. doi: 10.1890/0012-9658(2003)084[0559:CAEGAC]2.0.CO;2

Xiong, L., and Yang, Y. (2003). Disease resistance and abiotic stress tolerance in rice are inversely modulated by an abscisic acid–inducible mitogen-activated protein kinase. *Plant Cell* 15, 745–759. doi: 10.1105/tpc.008714

Xu, L., Naylor, D., Dong, Z., Simmons, T., Pierroz, G., Hixson, K. K., et al. (2018). Drought delays development of the sorghum root microbiome and enriches for monoderm bacteria. *Proc. Natl. Acad. Sci. U.S.A.* 115, E4284–E4293. doi: 10.1073/pnas.1717308115

Yang, Y., M. Pollard, A., Höfler, C., Poschet, G., Wirtz, M., Hell, R., et al. (2015). Relation between chemotaxis and consumption of amino acids in bacteria. *Mol. Microbiol.* 96, 1272–1282. doi: 10.1111/mmi.13006

Yang, Y.-X., Ahammed, G., Wu, C., Fan, S.-Y., and Zhou, Y.-H. (2015). Crosstalk among jasmonate, salicylate and ethylene signaling pathways in plant disease and immune responses. *Curr. Protein Peptide Sci.* 16, 450–461. doi: 10.2174/1389203716666150330141638

Yuan, Z., Druzhinina, I. S., Labbé, J., Redman, R., Qin, Y., Rodriguez, R., et al. (2016). Specialized microbiome of a halophyte and its role in helping non-host plants to withstand salinity. *Sci. Rep.* 6:32467. doi: 10.1038/srep32467

Zandalinas, S. I., Mittler, R., Balfagón, D., Arbona, V., and Gómez-Cadenas, A. (2018). Plant adaptations to the combination of drought and high temperatures. *Physiol. Plant.* 162, 2–12. doi: 10.1111/ppl.12540

Ze, X., Duncan, S. H., Louis, P., and Flint, H. J. (2012). *Ruminococcus bromii* is a keystone species for the degradation of resistant starch in the human colon. *ISME J.* 6, 1535–1543. doi: 10.1038/ismej.2012.4

Zhang, G., Sun, Y., Sheng, H., Li, H., and Liu, X. (2018). Effects of the inoculations using bacteria producing ACC deaminase on ethylene metabolism and growth of wheat grown under different soil water contents. *Plant Physiol. Biochem.* 125, 178–184. doi: 10.1016/j.plaphy.2018.02.005

Zhu, J.-K. (2002). Salt and drought stress signal transduction in plants. *Annu. Rev. Plant Biol.* 53, 247–273. doi: 10.1146/annurev.arplant.53.091401.143329

Conflict of Interest Statement: The authors declare that the research was conducted in the absence of any commercial or financial relationships that could be construed as a potential conflict of interest.

frontiers in Plant Science

ORIGINAL RESEARCH
published: 25 July 2019
doi: 10.3389/fpls.2019.00955

Improved Powdery Mildew Resistance of Transgenic *Nicotiana benthamiana* Overexpressing the *Cucurbita moschata CmSGT1* Gene

Wei-Li Guo[1,2], Bi-Hua Chen[1,2], Yan-Yan Guo[1,2], He-Lian Yang[1,2], Jin-Yan Mu[1,2], Yan-Li Wang[1,2], Xin-Zheng Li[1,2] and Jun-Guo Zhou[1,2]*

[1] School of Horticulture Landscape Architecture, Henan Institute of Science and Technology, Xinxiang, China, [2] Henan Province Engineering Research Center of Horticultural Plant Resource Utilization and Germplasm Enhancement, Xinxiang, China

Powdery mildew (PM), which is mainly caused by *Podosphaera xanthii*, is a serious biotrophic pathogen disease affecting field-grown and greenhouse-grown cucurbit crops worldwide. Because fungicides poorly control PM, the development and cultivation of PM-resistant varieties is critical. A homolog of *SGT1* (*suppressor of the G2 allele of skp1*), which encodes a key component of the plant disease-associated signal transduction pathway, was previously identified through a transcriptomic analysis of a PM-resistant pumpkin (*Cucurbita moschata*) inbred line infected with PM. In this study, we have characterized this *SGT1* homolog in *C. moschata*, and investigated its effects on biotic stress resistance. Subcellular localization results revealed that CmSGT1 is present in the nucleus. Additionally, *CmSGT1* expression levels in the PM-resistant material was strongly induced by PM, salicylic acid (SA) and hydrogen peroxide (H_2O_2). In contrast, SA and H_2O_2 downregulated *CmSGT1* expression in the PM-susceptible material. The ethephon (Eth) and methyl jasmonate (MeJA) treatments upregulated *CmSGT1* expression in both plant materials. The constitutive overexpression of *CmSGT1* in *Nicotiana benthamiana* (*N. benthamiana*) minimized the PM symptoms on the leaves of PM-infected seedlings, accelerated the onset of cell necrosis, and enhanced the accumulation of H_2O_2. Furthermore, the expression levels of *PR1a* and *PR5*, which are SA signaling transduction markers, were higher in the transgenic plants than in wild-type plants. Thus, the transgenic *N. benthamiana* plants were significantly more resistant to *Erysiphe cichoracearum* than the wild-type plants. This increased resistance was correlated with cell death, H_2O_2 accumulation, and upregulated expression of SA-dependent defense genes. However, the chlorosis and yellowing of plant materials and the concentration of bacteria at infection sites were greater in the transgenic *N. benthamiana* plants than in the wild-type plants in response to infections by the pathogens responsible for bacterial wilt and scab. Therefore, *CmSGT1*-overexpressing *N. benthamiana* plants were hypersensitive to these two diseases. The results of this study may represent valuable genetic information for the breeding of disease-resistant pumpkin varieties, and may also help to reveal the molecular mechanism underlying CmSGT1 functions.

Keywords: *Cucurbita moschata* Duch., powdery mildew, *CmSGT1*, functional analysis, *N. benthamiana*

OPEN ACCESS

Edited by:
Valentina Fiorilli,
University of Turin, Italy

Reviewed by:
Yan Xu,
Northwest A&F University, China
Stefano Pavan,
University of Bari Aldo Moro, Italy

****Correspondence:***
Xin-Zheng Li
lxz2283@126.com

Specialty section:
This article was submitted to Plant Microbe Interactions, a section of the journal Frontiers in Plant Science

Received: *24 April 2019*
Accepted: *09 July 2019*
Published: *25 July 2019*

Citation:
Guo W-L, Chen B-H, Guo Y-Y, Yang H-L, Mu J-Y, Wang Y-L, Li X-Z and Zhou J-G (2019) Improved Powdery Mildew Resistance of Transgenic Nicotiana benthamiana Overexpressing the Cucurbita moschata CmSGT1 Gene. Front. Plant Sci. 10:955. doi: 10.3389/fpls.2019.00955

INTRODUCTION

The genus Cucurbita is composed of several species, including the cultivated *Cucurbita moschata* Duch., *Cucurbita pepo* L., *Cucurbita maxima* Duch., and several wild species. Pumpkins (*C. moschata*) are valued for their fruit and seeds. Additionally, they are rich in vitamins, amino acids, flavonoids, phenolics, and carbohydrates, and possess medicinal properties, including anti-diabetic, anti-oxidant, anti-carcinogenic, and anti-inflammatory activities (Wang et al., 2002; Yadav et al., 2010). In China alone, the annual yield of pumpkin, squash, and gourds is 8,051,495 t (i.e., approximately 22.68% of the global yield) from a harvested area of 438,466 ha (i.e., 17.42% of the global area) (Food and Agriculture Organization, 2017)[1]. Cucurbit powdery mildew (PM) is a serious disease affecting field-grown and greenhouse-grown cucurbit crops worldwide. The disease is mainly caused by *Podosphaera xanthii* (formerly known as *Sphaerotheca fuliginea*), which is a biotrophic plant pathogen (Perez-Garcia et al., 2009; Fukino et al., 2013). Fungicide applications poorly control PM and the long-term use of pesticides may lead to increased environmental pollution and the residual chemicals on food crops may be harmful for humans and animals. Therefore, studying the mechanism underlying PM resistance and exploiting the resistance genes to breed resistant varieties represents an effective way to control PM in pumpkin.

To date, there has been relatively little research on pumpkin ($2n = 2x = 40$), especially at the molecular level, which has seriously hindered developments in the fields of molecular biology and genetics. We previously conducted a RNA sequencing analysis of pumpkin inbred line highly resistant to PM (inbred line "112-2") and identified 4,716 differentially expressed genes, including genes encoding broad-spectrum disease-resistance/susceptibility proteins [PR protein, ubiquitin, heat shock protein and Mildew Locus O (MLO)], reactive oxygen scavengers (peroxidase, superoxide dismutase, and catalase), signal transduction molecules serine/threonine protein kinase, and transcription factors (WRKY, TGA, and MYB). Additionally, candidate disease-resistance genes, such as *WRKY21*, *MLO3*, and *SGT1*, were identified (Guo et al., 2018). One of the genes cloned from the transcriptome was a homolog of *Cucumis melo SGT1* (*suppressor of the G2 allele of skp1*). The expression of this *SGT1* homolog was highly upregulated in PM-resistant material at 6 h after an inoculation with the PM fungus, but not in PM-susceptible material. However, pumpkin *SGT1* has not been functionally characterized regarding its potential involvement in the defense response to PM.

The SGT1 protein was originally defined in yeast, in which it interacts with SKP1, which is a component of the Skp1/CDC/F-box protein E3 ubiquitin ligase complex (Kitagawa et al., 1999). The SGT1 protein contains three functional domains, namely the tetratricopeptide repeat (TPR), CHORD SGT1 (CS), and the SGT1-specific sequence (SGS) (Kumar and Kirti, 2015). SGT1 is closely related to the disease resistance mediated by the plant resistance (*R*) genes. The silencing or mutation of *NbSGT1* from *Nicotiana benthamiana* (*N. benthamiana*) can lead to reduction of steady-state levels of R proteins and the loss of the mediated resistance, and *AtSGT1a* overexpression can contribute positively to resistance triggered by the NB-LRR type R proteins, and can complement for loss of *AtSGT1b* in auxin signaling (Muskett and Parker, 2003; Azevedo et al., 2006). A previous study revealed that *NbSGT1* overexpression in *N. benthamiana* accelerates the development of the hypersensitive response (HR) during *R*-mediated disease resistance (Wang et al., 2010). Additionally, *Hv-SGT1* overexpression in wheat enhances the resistance to PM, which is correlated with increased levels of reactive oxygen intermediates at the pathogen entry sites (Xing et al., 2013). Furthermore, PsoSGT1 from *Prunus sogdiana* appears to interact with molecular chaperones (RAR1 and HSP90) to activate a nucleotide-binding domain and leucine-rich repeat-containing (NB-LRR)-type protein that confers disease resistance (Zhu et al., 2017). The regulation of NB-LRR-type protein stability or substrate degradation to maintain the balance between the activation and inhibition of plant defense responses (Meldau et al., 2011; Hoser et al., 2013), contributes to the RXLR elicitor-induced HR-related cell necrosis (Xiang et al., 2017).

The recent release of the pumpkin genome provided an opportunity for an additional screening for disease-resistance genes (Sun et al., 2017). In this study, on the basis of the above-mentioned transcriptome analysis that identified differentially expressed genes responsive to PM, we functionally characterized the pumpkin homolog of *SGT1* (designated as *CmSGT1*). The transcription of *CmSGT1* in the PM-resistant inbred line "112-2" was strongly induced by PM, salicylic acid (SA), hydrogen peroxide (H_2O_2), ethephon (Eth), and methyl jasmonate (MeJA). Transgenic *N. benthamiana* plants that constitutively overexpressed *CmSGT1* exhibited increased resistance to PM and were hypersensitive to bacterial wilt and scab.

RESULTS

Cloning of *CmSGT1* and Subcellular Localization the Encoded Protein

Pumpkin PM-related candidate genes identified in a transcriptome were reported previously (Guo et al., 2018). One of the isolated clones exhibited 89% identity at the nucleotide level to *C. melo SGT1*. A full-length clone of this homolog was obtained, and the gene was named *CmSGT1* and submitted to GenBank (accession number MH105820). The *CmSGT1* gene comprised 1,206 bp, which included a 1,080-bp open reading frame (ORF) encoding 360 amino acids. The predicted polypeptide was basic, with a pI of 5.32, and a molecular mass of 40.3 kDa. An alignment of the deduced CmSGT1 amino acid sequence with homologous sequences is presented in **Supplementary Figure S1**. At the amino acid level, CmSGT1 was highly similar to the SGT1 from the following plant species: *Cucumis melo* (CmSGT1, 84.4% identity), and *Cucumis sativus* (CsSGT1, 82.5% identity), *N. benthamiana* (NbSGT1.1 and NbSGT1.2, 89.5% identity), and *Arabidopsis thaliana* (AtSGT1a and AtSGT1b, 75.2% identity). The CmSGT1 sequence contained three conserved domains, namely TPR, CS, and SGS.

[1] http://www.fao.org/faostat/en/#data/QC

The subcellular localization of CmSGT1 was assessed with a CmSGT1-GFP fusion protein that was produced in *A. thaliana* protoplasts under the control of the 35S CaMV promoter. The GFP signal in protoplasts producing GFP alone was detected in the cytoplasm and nucleus (**Figure 1**), whereas the signal from the CmSGT1-GFP fusion protein was detected exclusively in the nucleus.

Expression of *CmSGT1* in Pumpkin Seedlings in Response to PM and Exogenous Treatments

A qRT-PCR assay was completed to analyze the *CmSGT1* expression patterns in PM-resistant inbred line "112-2" and PM-susceptible cultivar "JJJD" treated with PM, H_2O_2, SA, abscisic acid (ABA), Eth, and MeJA (**Figure 2**). The expression data were normalized against that of the β-*actin* gene and were recorded relative to the *CmSGT1* transcript level in the water-sprayed control "JJJD" plants at 0 hour post-inoculation (hpi).

The *CmSGT1* expression level in "112-2" plants were upregulated by PM (except at 24 h), H_2O_2, and SA treatments, with the PM-induced expression level at 3 hpi upregulated by 6.62-fold. In contrast, the ABA treatment essentially had no effect. The expression of *CmSGT1* in "JJJD" plants was inhibited by H_2O_2, SA, and ABA (except at 24 h) treatments, with irregular expression-level changes induced by PM. After the Eth treatment, the *CmSGT1* expression level was significantly higher in the "112-2" and "JJJD" seedlings than in the water-treatment control (CK) seedlings (except at 48 h), with peak levels occurring at 24 h (i.e., 10.2-fold and 4.5-fold increases in "112-2" and "JJJD" seedlings, respectively). In response to the MeJA treatment, *CmSGT1* expression levels were higher in "112-2" (except at 48 h) and "JJJD" (except at 3 h) seedlings than in CK seedlings. The results indicated that SA, and H_2O_2 upregulated *CmSGT1* expression in inbred line "112-2" (PM-resistant material), but downregulated *CmSGT1* expression in cultivar "JJJD" (PM-sensitive material). Moreover, Eth and MeJA induced *CmSGT1* expression regardless of PM susceptibility.

Improved PM Resistance of *CmSGT1*-Overexpressing *N. benthamiana* Plants

Firstly, transcript level of the high homology (*NbSGT1*) modulated by the overexpression of *CmSGT1* under normal conditions was determined by qRT-PCR. Compared to wild type (WT) plants, the expression of the homologous genes was not basically altered in transgenic plants when grown in normal condition (**Figure 3**), indicating that overexpression of pumpkin *CmSGT1* gene has no obvious effect on *NbSGT1* transcript in *N. benthamiana*. The *CmSGT1* gene was not detected in WT plants.

The disease severity at 10 days post-inoculation (dpi) was 78% lower for the transgenic plants than for the CK plants (**Table 1**). Powdery mildew symptoms were detectable on infected WT seedlings at 7 dpi, and the infected spots were chlorotic at 28 dpi. In contrast, the PM symptoms were undetectable and relatively slight at 7 and 28 dpi, respectively, in the *CmSGT1*-overexpressing transgenic plants (**Figure 4A**). A comparison of the leaves of PM-infected WT and transgenic plants revealed more blue spots displayed by the trypan blue staining, on the transgenic leaves than on the WT leaves at 4 dpi, although blue spots were developing on the WT leaves. The blue spots on the transgenic leaves expanded at 5 and 7 dpi, and were bigger than those of WT leaves, implying that the overexpression of *CmSGT1* in transgenic plants accelerated cell death following a PM infection (**Figure 4B**). Moreover, there were more brown spots manifested by the DAB staining, on the transgenic leaves than on the WT leaves at 1 dpi. These brown spots reflected the accumulation of H_2O_2, and were darker brown and larger at 3 dpi. At 5 dpi, the brown spots lightened in the infected plants, but were more intense in the transgenic plants than the spots in the WT plants. The results indicated that the overexpression of *CmSGT1* promoted the accumulation of H_2O_2 in transgenic plants infected with PM (**Figure 4C**).

Expression of Signal-Related Genes in Transgenic *N. benthamiana* Plants

To investigate the signal transduction pathways affected by CmSGT1 during plant defense responses to PM, the expression levels of five signaling-associated genes (*NPR1*, *PR5*, *PR1a*, *PAL*, and *PDF1.2*) in the SA, JA, and ET signal transduction pathways were analyzed by qRT-PCR for the *CmSGT1*-overexpressing transgenic and WT *N. benthamiana* plants, with water-treated WT plants at 0 hpi serving as the control samples (**Figure 5**). The *NPR1*, *PAL* (except at 120 h), and *PR5* expression levels were lower in the transgenic and WT plants infected with PM than in the CK plants, implying that PM inhibited the expression of these genes. The *PR1a* expression level was higher in the PM-infected transgenic plants than in the CK plants (i.e., 68.3-fold at 120 h), whereas the *PR1a* level was lower in the PM-infected WT plants than in the CK plants. The *PDF1.2* expression levels in the PM-infected transgenic plants were lower at 12 hpi and higher at 48 hpi than in the CK plants, with no differences thereafter. Thus, in response to the PM infection, the *NPR1*, *PAL* (except at 24 and 48 h), and *PDF1.2* (except at 48 h) expression levels were significantly lower in the transgenic plants than in the WT plants, whereas the opposite pattern was observed for the *PR1a*, and *PR5* expression levels. These results implied that the overexpression of *CmSGT1* in *N. benthamiana* upregulates the expression of *PR1a*, and *PR5*, which are involved in SA defense signal transduction. Furthermore, the increased PM resistance of the transgenic *N. benthamiana* plants appears to be related to the upregulated expression of these genes.

Compromised Resistance of Transgenic *N. benthamiana* Plants to Bacterial Diseases

To analyze the effect of *CmSGT1* on other plant diseases, two common bacterial pathogens causing bacterial wilt (*Ralstonia solanacearum*) and scab (*Xanthomonas euvesicatoria*) were injected into *N. benthamiana* plants (**Figure 6**). At 6 days after inoculation with *R. solanacearum* and *X. euvesicatoria*,

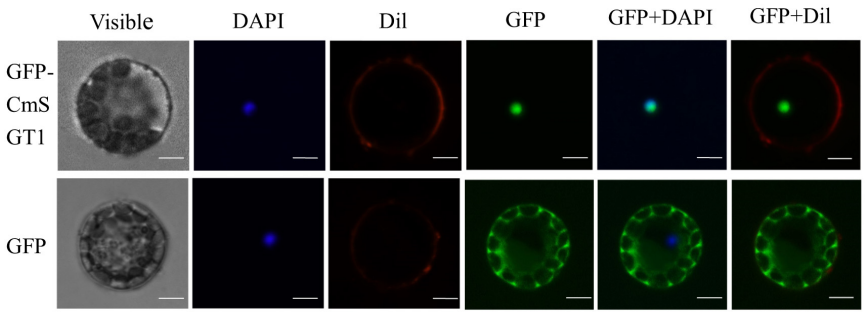

FIGURE 1 | The subcellular localization of pumpkin CmSGT1. The fused pBI221-GFP- CmSGT1 and pBI221-GFP constructs were introduced into *Arabidopsis* protoplast by polyethylene glycol (PEG)-mediated protoplast transformation. The fluorescent signals were detected using a confocal fluorescence microscope. Scale bars = 5 μm.

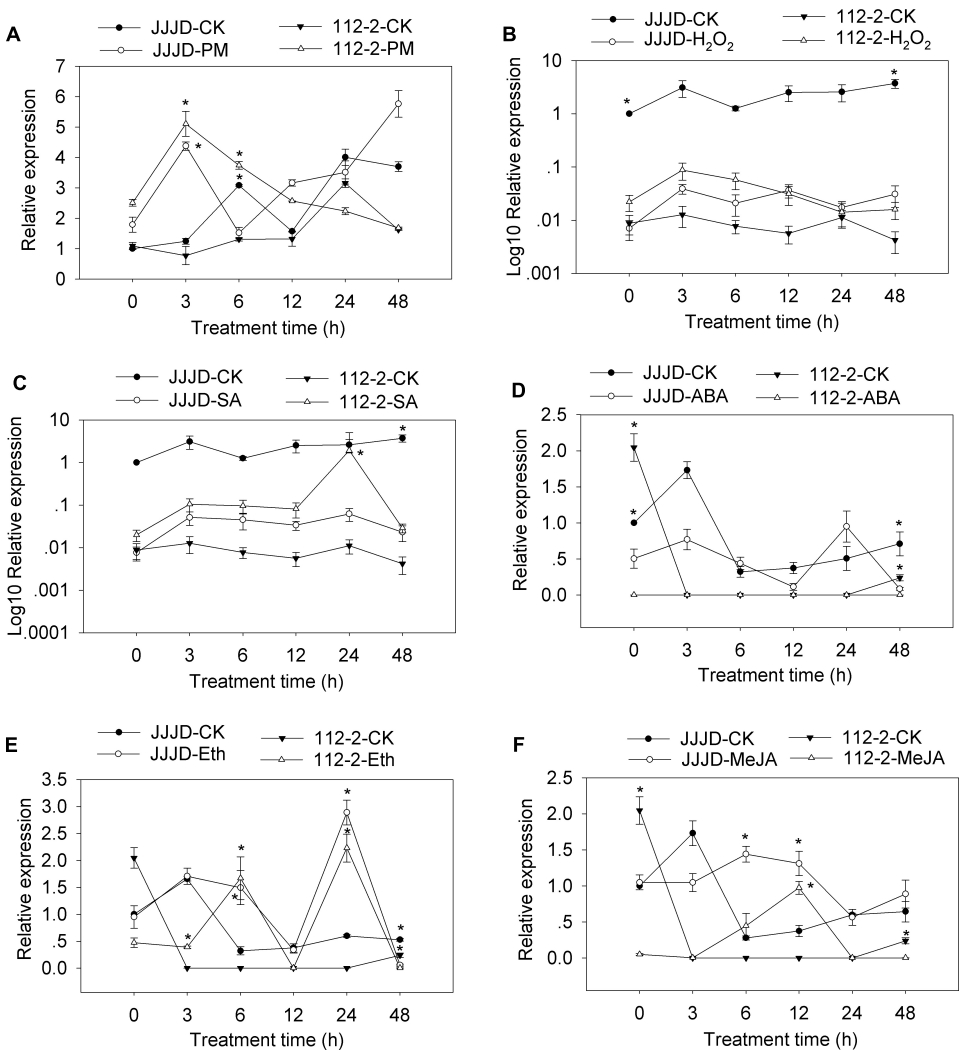

FIGURE 2 | *CmSGT1* expression in response to powdery mildew and exogenous hormones. The pumpkin seedlings were sprayed with a spore suspension **(A)**, exogenous H_2O_2 **(B)**, SA **(C)**, ABA **(D)**, Eth **(E)** and MeJA **(F)**. The pumpkin β-*actin* gene was used as an internal reference gene for qRT-PCR. The transcript level of *CmSGT1* in the susceptible cultivar "JJJD" at 0 h is used as control (quantities of calibrator) and was assumed as 1. The relative gene expression in B and C (*Y*-axis) was transformed to a $\log_{10}$ scale. The values are the means ± SEs of three biological replicates. Data between treatments (112-2-treatment vs. 112-2-CK and JJJD- treatment vs. JJJD-CK) were analyzed by one-way ANOVA and * denotes statistical significance at $p < 0.05$.

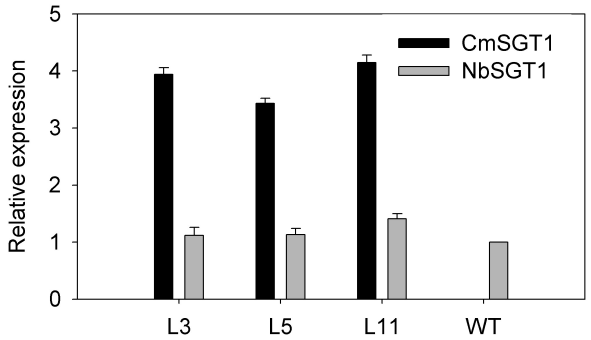

FIGURE 3 | Relative expression of *CmSGT1* and *NbSGT1* in transgenic or wild-type plants under normal growth conditions. *N. benthamiana* encodes *NbSGT1* isoform. L3, L5, and L11 are three independent transgenic lines that overexpress *CmSGT1*. Three biological triplicates were averaged and Bars indicate standard error of the mean. Data (*NbSGT1* expression in transgenic lines vs. *NbSGT1* expression in wild-type plants) were analyzed by one-way ANOVA and unmarked * denotes no statistical differences at $p < 0.05$.

TABLE 1 | Disease severity of leaves of *N. benthamiana* seedlings infected with powdery mildew.

Materials	Disease severity (*in vitro* leaf)
L3	7.90 ± 1.23
L5	8.60 ± 1.31
L11	9.00 ± 1.01
WT	38.80 ± 2.41*

Data are mean values (±SD) of at least three independent experiments. "" indicates significantly different values between treatments ($p < 0.05$). L3, L5, and L11 are three independent transgenic lines that overexpress CmSGT1.*

the chlorosis and yellowing of the sixth leaf veins was greater for transgenic *N. benthamiana* plants than for the WT plants. Additionally, there were 5.94- and 21.1-times more the concentration of bacterial wilt and scab bacteria, respectively, in the transgenic plants than in the WT plants. Yellowing was also observed between the veins of the 12th leaf in transgenic *N. benthamiana* plants, and there were 13.3- and 8.28-times more *R. solanacearum* and *X. euvesicatoria* bacteria, respectively, in the transgenic plants than in the WT plants. These observations suggested that the overexpression of *CmSGT1* in *N. benthamiana* decreases the resistance to bacterial wilt and scab.

DISCUSSION

In this study, we isolated a novel pumpkin *SGT1* gene, which was designated as *CmSGT1*. The predicted amino acid sequence was 89 and 82% identical to the NbSGT1.1 and CsSGT1 sequences, respectively. In *A. thaliana* and *N. benthamiana*, SGT1 encodes three functional domains (TPR, CS, and SGS) that are essential for SGT1 activity (Peart et al., 2002; Noël et al., 2007). In this study, the CmSGT1-GFP fusion protein was localized to the nucleus in *A. thaliana* protoplasts, which was inconsistent with the results of earlier studies involving SGT1 in other plant species (Xing et al., 2013; Liu et al., 2016). This inconsistency may be related with low identity (*Haynaldia villosa* HvSGT1, 64.0% identity; pepper CaSGT1, 63.7% identity) or the number of transformed cells examined. *Arabidopsis SGT1b* fused to Cerulean localized to the cytosol, but could be seen in nuclei of 25% of 55 transformed cells examined (Noël et al.,2007), and translocation of the SGT1/SRC2-1 complex from the plasma membrane and cytoplasm to the nuclei is required in pepper upon the inoculation of *Phytophthora capsici* (Liu et al., 2016), suggesting the movement of SGT1 between the cytosol and nucleus.

The interplay among complex signaling networks, including various pathways regulated by phytohormones, such as SA, JA, ethylene (ET) and ABA, considerably influences plant resistance to diseases. An earlier investigation proved that *HvSGT1* expression levels substantially increase following treatments with H_2O_2 and MeJA, slightly increase following exposure to ET or ABA, and are unchanged in response to SA (Xing et al., 2013). In the current study, SA and H_2O_2 treatments considerably upregulated *CmSGT1* expression in the PM-resistant inbred line "112-2", but downregulated *CmSGT1* expression in the PM-susceptible material. The expression of *CmSGT1* in both materials was upregulated by Eth and MeJA treatments. Recent reports indicated that *SGT1* expression may be induced by phytopathogens, such as *Blumeria graminis* in wheat and *P. capsici* in pepper (Xing et al., 2013; Liu et al., 2016). In this study, the *CmSGT1* expression in inbred line "112-2" was induced by PM. Additionally, the overexpression of *CmSGT1* in transgenic *N. benthamiana* plants decreased the disease index by 78%, accelerated cell necrosis, and increased the accumulation of H_2O_2. These results indicated that the PM resistance of the transgenic *N. benthamiana* plants was enhanced, likely because of the changes to the HR-related cell necrosis and H_2O_2 accumulation. Our findings are consistent with the results of an earlier study that revealed that H_2O_2 accumulation and the subsequent cell death usually lead to the resistance to diseases caused by biotrophic pathogens (Li et al., 2011). Moreover, SGT1 helps mediate cell death during compatible and incompatible plant–pathogen interactions, suggesting that SGT1 is an essential component of common signaling pathways responsible for cell death (Cuzick et al., 2009; Uppalapati et al., 2010; Wang et al., 2010). The silencing of the pepper *SGT1* gene adversely affects HR-related cell death, prevents H_2O_2 accumulation, and downregulates HR-related and SA/JA-dependent marker gene expression levels, and influences the PcINF1/SRC2-1-induced pepper defense response by SGT1 interacting with SRC2-1 (Liu et al., 2016).

The *PDF1.2* gene is important for the JA/ET-dependent signaling pathway. The disease-associated *NPR1* gene (non-expresser of PR1) affects various disease-resistance signal transduction pathways, and encodes one of the important transcription factors downstream of SA. The SA-dependent disease-resistance signal transduction pathway can be divided into NPR1-dependent and NPR1-independent transduction pathways (Gao and Zhang, 2012). The *PAL*, *PR1a*, and *PR5* expression levels are markers of the SA signaling pathway. In wheat, HvSGT1 activates PM resistance mechanisms through JA-dependent defense pathways and suppresses the activities

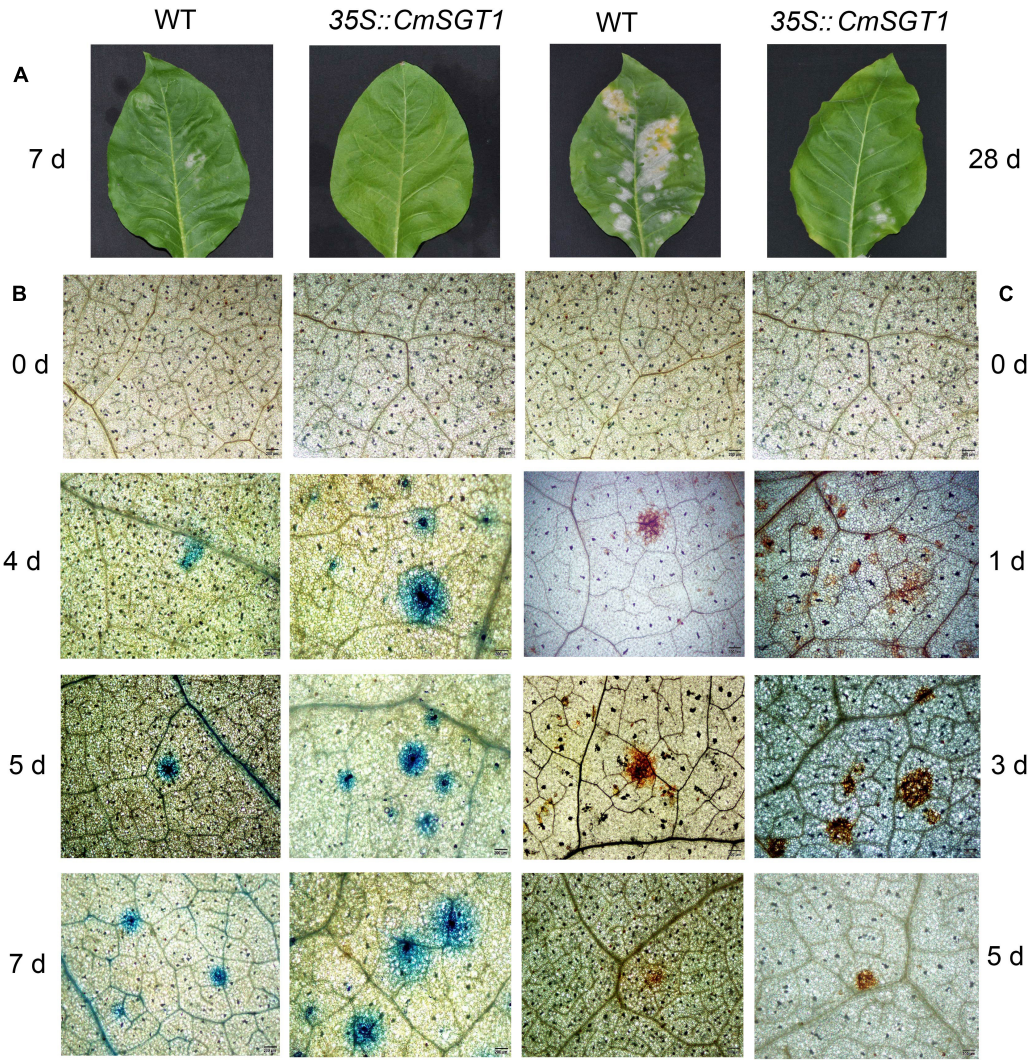

FIGURE 4 | The pathogenic symptoms, trypan blue and DAB staining of *N. benthamiana* leaves treated with powdery mildew. The pathogenic symptoms of transgenic *N. benthamiana* and WT at 7 and 28 days post-inoculation **(A)**; trypan blue staining was performed to visualize cell death **(B)**; DAB staining was performed to visualize H_2O_2 accumulation **(C)**. Scale bars = 200 μm.

of SA-dependent defense pathways (Xing et al., 2013). In the current study, following a PM infection, the *NPR1*, *PAL*, and *PDF1.2* expression levels were lower in the transgenic plants than in the WT plants, whereas the opposite pattern was observed for the *PR1a* and *PR5* expression levels. This suggests that in the SA pathway, the transactivation of *NPR1* is unaffected by CmSGT1, whereas the transactivation of *PR1a*, and *PR5* is dependent on CmSGT1. Additionally, CmSGT1 does not directly affect the JA/ET-dependent defense pathway to regulate *PDF1.2* expression. We propose that *CmSGT1* activates stress-resistance mechanisms through SA-dependent defense pathways without inducing *NPR1* and *PAL* expression levels, but suppresses the activities of JA/ET-dependent defense pathways. Therefore, we speculate that CmSGT1 positively regulates the H_2O_2 and SA pathways. Moreover, H_2O_2 might directly transfer the SA signal to regulate the expression of downstream response genes in the *CmSGT1*-overexpressing transgenic plants infected with PM. In NPR1-dependent SA signal transduction pathways, the activation of *PR* genes needs NPR1 and TGA transcription factor binding to identify its promoters (Fan and Dong, 2002; Spoel and Dong, 2012). The equivalent mutation in NPR1 abolishes its ability to bind SA and promotes SA-induced defense gene expression (Ding et al., 2018). We speculated that whether there is the relation of the downregulation of *NPR1* and SA-mediated transcriptional activation of *PR* genes or not. Notably, the phenotypes and genes in *CmSGT1*-overexpressing transgenic *N. benthamiana* plants infected with *N. benthamiana* PM might not be exactly the same as those regulated by *CmSGT1* in *C. moschata* in response to cucurbit PM. Further studies will be necessary to reveal biological functions for *CmSGT1* in *C. moschata* infected with PM.

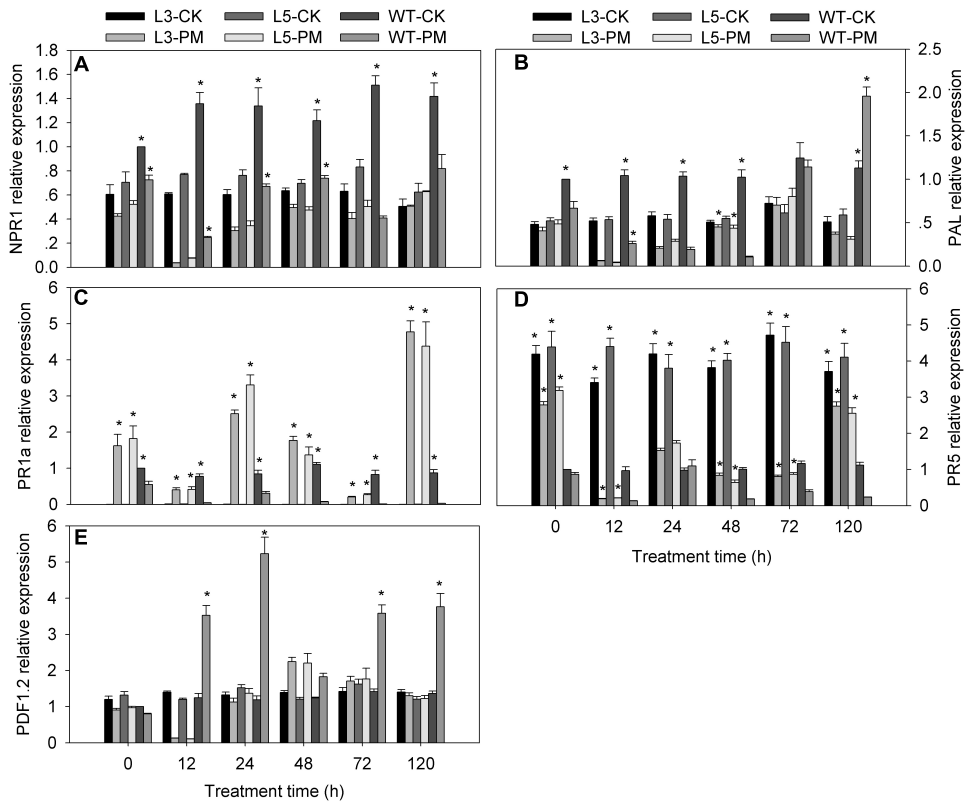

FIGURE 5 | Expression of signal-related genes in transgenic and wild-type plants treated with powdery mildew. The samples of two genetically modified *N. benthamiana* lines were used to analyze the genes expression by qRT-PCR. **(A)** *NtNPR1*; **(B)** *NtPAL*; **(C)** *NtPR1a*; **(D)** *NtPR5*; **(E)** *NtPDF1.2*. L3/5-CK represents transgenic *N. benthamiana* L3 or L5 line grown under normal conditions; L3/5-PM represents transgenic *N. benthamiana* L3 or L5 line infected with powdery mildew; WT-CK represents wild-type plants grown under normal conditions; WT-PM represents wild-type plants infected with powdery mildew. *N. benthamiana NtEF1-*α gene (AF120093) was used as an internal control for normalization of different cDNA samples. The expression levels of signal-related genes in wild-type plants at 0 h were used as control (quantities of calibrator) and were assumed as 1. Three biological triplicates per line were averaged and Bars indicate standard error of the mean. Data between transgenic plants and WT plants (L3/5-PM vs. WT-PM and L3/5-CK vs. WT-CK) were analyzed by one-way ANOVA and "*" denotes statistical significance at $p < 0.05$.

Two globally important diseases that affect *N. benthamiana*, bacterial wilt and scab, are caused by the necrotrophic *R. solanacearum* and the hemi-biotrophic *X. euvesicatoria*, respectively. There are differences in the resistance mechanisms and patterns of fungal development for biothophic (*P. xanthii*) and necrotrophic (*R. solanacearum*) pathogens. Recent studies confirmed that SGT1 promotes the resistance to biotrophic pathogens, while suppressing the resistance to necrotrophic and hemibiotrophic pathogens. Silencing of *SGT1* compromised resistance to the barley and *H. villosa* biothoph *B. graminis* (Shen et al., 2003; Xing et al., 2013) and the wheat biotroph *Puccinia striiformis* (Scofield et al., 2005), while enhancing the resistance of *N. benthamiana* to the necrotrophic pathogen *Botrytis cinerea* (El Oirdi and Bouarab, 2007). A recent study involving *N. benthamiana* indicated silencing of *NbSGT1* compromised the protective effect of systemic acquired resistance-induced plants on neighboring plants against bacteria wilt caused by *R. solanacearum* (Cheol Song et al., 2016). In the current study, the chlorosis and yellowing of the infection sites on leaves were greater in transgenic *N. benthamiana* plants than in WT plants at 6 dpi. Additionally, there were substantially more concentration of bacterial wilt and scab bacteria in the transgenic plants than in the WT plants, indicating that the overexpression of *CmSGT1* in *N. benthamiana* adversely affects the resistance to bacterial wilt and scab, which differs from the effects of *CmSGT1* overexpression on the resistance to PM. Consequently, SGT1 may function differently depending on the plant–pathogen combinations with diverse effectors and R proteins.

In conclusions, the results of this study indicate that the overexpression of *CmSGT1* may increase the PM resistance, but decrease bacterial wilt and scab resistance, in transgenic *N. benthamiana* plants. Additionally, *CmSGT1* overexpression may improve PM resistance by enhancing HR-related cell death and H_2O_2 accumulation and upregulating the expression of SA-mediated defense-response genes. Further analyses of the *CmSGT1* gene may be useful for characterizing biotic stress signaling pathways and for the genetic engineering of novel pumpkin cultivars. The results described herein may be relevant for future biotechnology-based

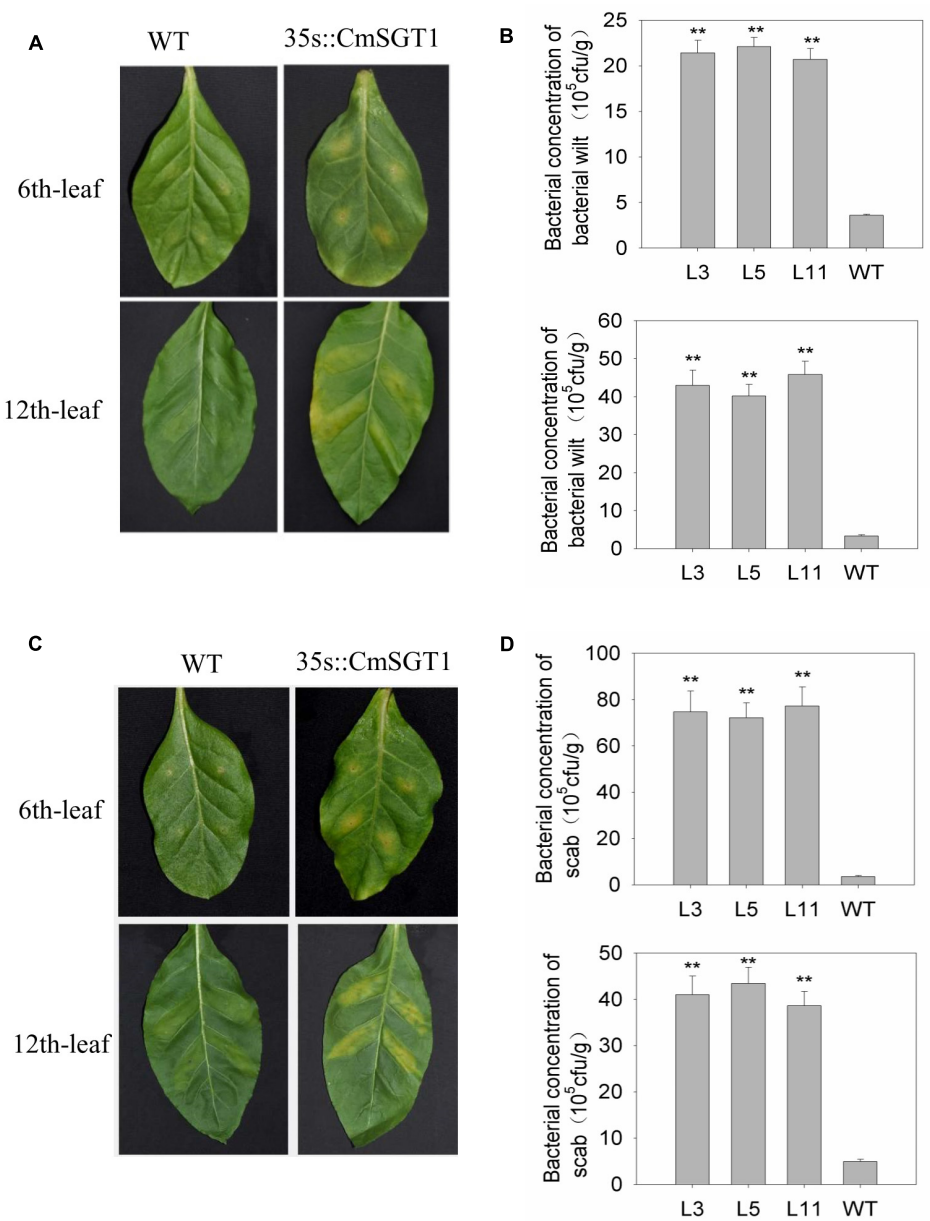

FIGURE 6 | The resistance of *CmSGT1* in transgenic and wild-type plants to *N. benthamiana* bacterial wilt and scab. **(A)** pathogens symptoms of the 6th-upper and 12th-upper leaf injection sites was injected with bacterial wilt bacteria with a needle-removed syringe. **(B)** concentration bacteria of the 6th-upper and 12th-upper leaf injection sites was injected with bacterial wilt bacteria with a needle-removed syringe. **(C)** pathogens symptoms of the 6th-upper and 12th-upper leaf injection sites was injected with scab bacteria with a needle-removed syringe. **(D)** concentration bacteria of the 6th-upper and 12th-upper leaf injection sites was injected with scab bacteria with a needle-removed syringe. "**" denotes significant differences between WT and transgenic plants at $p < 0.01$.

investigations and the molecular breeding of pumpkins and related plant species.

MATERIALS AND METHODS

Plant Materials and Treatments

Pumpkin (*C. moschata*) inbred line "112-2" and cultivar "Jiujiangjiaoding" (abbreviated "JJJD"), which are resistant and susceptible to PM, respectively, were provided by the Henan Institute of Science and Technology, Xinxiang, Henan, China (Zhou et al., 2010). Pumpkin seeds were germinated and the resulting seedlings were grown as previously described (Guo et al., 2018). Seedlings at the three-leaf stage were treated as follows. The PM infection was initiated as described by Guo et al. (2018). Specifically, conidia were collected from the leaves of pumpkin plants naturally infected with PM in a local greenhouse. Seedlings were sprayed with a freshly prepared spore suspension

(10^6 spores/ml) or an exogenous signaling molecule or hormone, including 1.5 mM H_2O_2, 100 μM SA, 100 μM ABA, 100 μM MeJA, 0.5 g/L Eth. Moreover, water alone was used for the control treatment (CK). The treated seedlings were maintained in a growth chamber with a 15-h light (28°C)/9-h dark (18°C) cycle (5,500 lux light intensity) and harvested after 0, 3, 6, 12, 24, and 48 h to examine the *CmSGT1* expression pattern. At each time point, two young leaves were collected from the upper parts of four seedlings (i.e., one sample), wrapped in foil, frozen in liquid nitrogen, and stored at −80°C. The treatments were arranged in a randomized complete block design, with three biological replicates.

Isolation of *CmSGT1* cDNA Clone and Sequence Analysis

The *SGT1* homolog expressed sequence tag (GenBank accession number SRR5369792) was identified in a PM-resistant pumpkin seedling transcriptome by Guo et al. (2018). The full-length ORF of the *SGT1* homolog was obtained with the cDNA fragment of this homolog used as a probe, as previously described (Guo et al., 2014). The theoretical molecular weight (Mw) and isoelectric point (pI) were calculated with the ExPASy Compute pI/Mw tool (Bjellqvist et al., 1993). Sequence data were analyzed with the ClustalW program (Thompson et al., 1994). The NCBI databases were screened for homologous sequences with the default parameters of the BLAST program[2] (Altschul et al., 1997).

Subcellular Localization Analysis of CmSGT1

The *CmSGT1* ORF (without the termination codon) was ligated into the pBI221-GFP vector for the subsequent production of a green fluorescent protein (GFP)-tagged CmSGT1 fusion protein. Polyethylene glycol was used during the transformation of *A. thaliana* protoplasts with the recombinant plasmid (Lee et al., 2013). The subcellular localization of CmSGT1 was determined based on the GFP signal, which was detected with the confocal fluorescence microscope (UltraVIEW VoX, Olympus, Japan) under excitation wavelength 488 nm and captured light wavelength range 448–508 nm. The cell membrane and nucleus were stained with 1,1′-dioctadecyl-3,3,3′,3′-tetramethylindocarbocyanine perchlorate (Dil) and 2-(4-Amidinophenyl)-6-indolecarbamidine dihydrochloride (DAPI), respectively.

Generation of *CmSGT1*-Overexpressing Transgenic *N. benthamiana* Plants

Pumpkin are known to be one of the plants most refractory for transformation. To date, only two reports on transformation in *C. moschata* existed using a combined method of vacuum infiltration and *Agrobacterium* infection (Nanasato et al., 2011; Nanasato and Tabei, 2015). So, we choose a heterologous overexpression assay in *N. benthamiana* instead of generating *C. moschata* transgenic plants. Forward and reverse primers with an added *Bam*H I site and *Kpn* I site, respectively, were used to amplify *CmSGT1*. The amplified sequence was then inserted into the pVBG2307 vector for the subsequent expression of *CmSGT1* under the control of the 35S cauliflower mosaic virus (CaMV) promoter. The recombinant plasmid was introduced into *Agrobacterium tumefaciens* GV3101 cells as previously described (Guo et al., 2014). The resulting *A. tumefaciens* cells were used to transform *N. benthamiana* plants according to a previously described leaf disk method (Li et al., 2012). The transgenic *N. benthamiana* plants were confirmed by examining the segregation ratio of the kanamycin selectable marker and by PCR analysis of *NPTII* and *CmSGT1*. T2 lines that produced 100% kanamycin-resistant plants in the T3 generation were considered as homozygous transformants. In each experiment, T2 generations of homozygous transgenic lines (L3, L5 and L11) were selected for further analysis. Similar phenotypes and results used for this study were observed in more than three independent lines of transgenic plants.

Primer Design

Details regarding all of the primers designed and used in this study are provided in **Supplementary Table S1**.

Analysis of Transgenic *N. benthamiana* Plants Infected With Powdery Mildew

Conidia were collected from *N. benthamiana* leaves naturally infected with *Erysiphe cichoracearum* DC., which causes PM. Transgenic *N. benthamiana* seedlings at the five-leaf stage were used for phenotypic analyses. Specifically, the petiole of the second leaf from the top of the seedlings was wrapped with cotton moistened with water. The leaf was placed on a porcelain tray containing filter paper, after which it was sprayed with a spore suspension (10^6 spores/ml). The tray was then covered with film to maintain humidity. At 10 dpi, disease severity of leaves *in vitro* was calculated as $[(5A + 4B + 3C + 2D + E)/5F] \times 100$ according to Ishii et al. (2001). Additionally, the first fully expanded true leaf of the transgenic and WT plants were sprayed with the above-mentioned spore suspension and sampled after 0, 12, 24, 48, 72, and 120 hpi, frozen in liquid nitrogen, stored at −80°C and used for extraction of total RNA. On the other hand, these leaves were harvested symmetrically along the sides of the main vein after 0, 1, 3, 4, 5, and 7 days to examine of cell death and H_2O_2 accumulation. The treatments were arranged in a randomized complete block design with three replicates.

Leaves from the transgenic *N. benthamiana* seedlings were stained with 3, 3′-diaminobenzidine (DAB) and trypan blue staining as previously described (Choi et al., 2012) to analyze H_2O_2 accumulation and cell death. For DAB staining, whole leaves were immersed in DAB solution (1 mg/ml, pH 5.7) and incubated overnight (almost 8 h) in darkness. Leaves were then de-stained three times with 95% ethanol. Regarding trypan blue staining, whole leaves were boiled in a lactophenol-ethanol trypan blue solution (10 ml lactic acid, 10 ml glycerol, 10 g phenol, 30 ml absolute ethanol, and 10 mg trypan blue dissolved in 10 ml distilled water) for 10 min and then maintained at room temperature overnight. Leaves were de-stained with 2.5 g/ml chloral hydrate in distilled water.

[2]http://www.ncbi.nlm.nih.gov/blast

Analysis of Transgenic *N. benthamiana* Plants Infected With Bacterial Wilt and Scab

The sixth and twelfth leaf from the top of transgenic *N. benthamiana* seedlings were inoculated with bacterial solutions (10^8 cfu/ml). Specifically, the bacterial solutions were injected into the underside of leaves between the lateral veins with a syringe lacking a needle. Each leaf was inoculated in four places. The petiole of leaves placed on a porcelain plate was wrapped with water-saturated degreased cotton, after which the plate was covered with film to maintain humidity and then incubated at 28°C with a 16-h light/8-h dark cycle. Water was periodically added to the cotton to maintain an appropriate moisture level. Experiments were done in triplicate for each line. After a 6-day incubation, the concentration of bacteria at the injection sites was determined as follows. The injection sites were sampled with a circular perforator (1 cm diameter) and ground in aseptic water (0.1 g added to 0.9 ml water). The ground material was serially diluted to produce the 10^2-fold, 10^3-fold, and 10^4-fold diluents. A 0.1-ml aliquot of the 10^3-fold, 10^4-fold, and 10^5-fold diluents were added to a petri dish containing NA medium. The medium was incubated upside down at 28°C. Plates with 30–300 colonies were considered ideal. The bacterial concentration was calculated with the following formula: colony average × 10 × dilution/g.

Quantitative Real-Time PCR Analysis

The RNA extraction, first-strand cDNA synthesis and quantitative real-time (qRT-PCR) were completed as described by Guo et al. (2015). Relative gene expression levels were determined with the $2^{-\Delta\Delta CT}$ method. Total RNA was extracted from the leaves of pumpkin seedlings treated with various stresses or distilled water for 0, 3, 6, 12, 24, or 48 h as described above. The β-*actin* gene was used as an internal control, because it was confirmed as a suitable reference gene for normalizing of gene expression levels in pumpkin (Wu and Cao, 2010). On the other hand, total RNA was extracted from *CmSGT1*-overexpressing transgenic and WT *N. benthamiana* seedlings to examine the expression of five hormone-related genes (*NtNPR1*, *NtPR1a*, *NtPR5*, *NtPDF1.2*, and *NtPAL*) and *N. benthamiana* isoform (*NbSGT1*). The *N. benthamiana NtEF1*-α gene (AF120093) was included in the assays as an internal control.

Statistical Analyses

Values were expressed as the mean ± standard error of three independent determinations. Data were compared by analysis of variance (ANOVA) using a one-way ANOVA, and differences between WT and transgenic plants were tested by a *post hoc* comparison test (Student–Newman–Keuls) at $p < 0.05$ with SPSS 19.0 for Windows (SPSS Inc., Chicago, IL, United States).

DATA AVAILABILITY

The datasets generated for this study can be found in NCBI, MH105820.

AUTHOR CONTRIBUTIONS

W-LG and Y-YG conceived and designed the experiments. W-LG and B-HC performed the experiments. J-YM and H-LY analyzed the data. Y-LW, J-GZ, and X-ZL contributed reagents, materials, and analysis tools. W-LG wrote the manuscript.

FUNDING

This work was supported by National Natural Science Foundation of China (No. 31401876), Henan High-level Talent Introduction and Training Special Foundation (No. 103020218003/008), and Natural Science Foundation of Henan Province (No. 162300410110).

ACKNOWLEDGMENTS

We thank Guizhou Academy of Tobacco Sciences researcher Hancheng Wang for providing tobacco *E. cichoracearum* and Liwen Bianji, Edanz Editing China (www.liwenbianji.cn/ac) for editing the English text of a draft of this manuscript.

SUPPLEMENTARY MATERIAL

The Supplementary Material for this article can be found online at: https://www.frontiersin.org/articles/10.3389/fpls.2019.00955/full#supplementary-material

FIGURE S1 | Amino acid sequences alignment of pumpkin CmSGT1 with others. The three conserved domains (TPR, CS, and SGS) are shown by thin underlines. The genes included are CmSGT1 (*Cucumis melo* L., XP_008439299.1) and CsSGT1 (*Cucumis sativus* L., XP_004140745.1) AtSGT1A (*Arabidopsis*, AT4G23570.3) and AtSGT1B (*Arabidopsis*, AT4G11260.1), NbSGT1.1 (*N. benthamiana*, AF516180) and NbSGT1.2 (*N. benthamiana*, AF516181).

TABLE S1 | Primers used in this investigation.

REFERENCES

Altschul, S. F., Madden, T. L., Schaffer, A. A., Zhang, J., Zhang, Z., and Miller, W. (1997). Gapped BLAST and PSI-BLAST: a new generation of protein database search programs. *Nucleic Acids Res.* 25, 3389–3402. doi: 10.1093/nar/25.17.3389

Azevedo, C., Betsuyaku, S., Peart, J., Takahashi, A., Noël, L., Sadanandom, A., et al. (2006). Role of SGT1 in resistance protein accumulation in plant immunity. *EMBO J.* 25, 2007–2016. doi: 10.1038/sj.emboj.7601084

Bjellqvist, B., Hughes, G. J., Pasquali, C., Paquet, N., Ravier, F., Sanchez, J. C., et al. (1993). The focusing positions of polypeptides in immobilized pH gradients can be predicted from their amino acid sequences. *Electrophoresis* 14, 1023–1031. doi: 10.1002/elps.11501401163

Cheol Song, G., Sim, H. J., Kim, S. G., and Ryu, C. M. (2016). Root-mediated signal transmission of systemic acquired resistance against above-ground and below-ground pathogens. *Ann. Bot.* 118, 821–831. doi: 10.1093/aob/mcw152

Choi, D. S., Hwang, I. S., and Hwang, B. K. (2012). Requirement of the cytosolic interaction between PATHOGENESIS-RELATED PROTEIN10 and LEUCINE-RICH REPEAT PROTEIN1 for cell death and defense signaling in pepper. *Plant Cell* 24, 1675–1690. doi: 10.1105/tpc.112.095869

Cuzick, A., Maguire, K., and Hammond-Kosack, K. E. (2009). Lack of the plant signaling component SGT1b enhances disease resistance to Fusarium culmorum in Arabidopsis buds and flowers. *New Phytol.* 181, 901–912. doi: 10.1111/j.1469-8137.2008.02712.x

Ding, Y., Sun, T., Ao, K., Peng, Y., Zhang, Y., Li, X., et al. (2018). Opposite roles of salicylic acid receptors NPR1 and NPR3/NPR4 in transcriptional regulation of plant immunity. *Cell* 6, 173–203. doi: 10.1016/j.cell.2018.03.044

El Oirdi, M., and Bouarab, K. (2007). Plant signalling components EDS1 and SGT1 enhance disease caused by the necrotrophic pathogen Botrytis cinerea. *New Phytol.* 175, 131–139. doi: 10.1111/j.1469-8137.2007.02086.x

Fan, W., and Dong, X. (2002). In vivo interaction between NPR1 and transcription factor TGA2 leads to salicylic acid–mediated gene activation in Arabidopsis. *Plant Cell* 14, 1377–1389. doi: 10.1105/tpc.001628

Fukino, N., Yoshioka, Y., Sugiyama, M., Sakata, Y., and Matsumoto, S. (2013). Identification and validation of powdery mildew (*Podosphaera xanthii*)-resistant loci in recombinant inbred lines of cucumber (*Cucumis sativus* L.). *Mol. Breed.* 32, 267–277. doi: 10.1007/s11032-013-9867-3

Gao, L. J., and Zhang, Y. X. (2012). Effects of salicylic acid on the expression of SOD, PPO Isozymes and NPR1 in Pear. *Acta Hortic. Sin.* 40, 41–48.

Guo, W. L., Chen, B. H., Chen, X. J., Guo, Y. Y., Yang, H. L., Li, X. Z., et al. (2018). Transcriptome profiling of pumpkin (*Cucurbita moschata* Duch.) leaves infected with powdery mildew. *PLoS One* 13:e0190175. doi: 10.1371/journal.pone.0190175

Guo, W. L., Chen, R. G., Du, X. H., Zhang, Z., Yin, Y. X., Gong, Z. H., et al. (2014). Reduced tolerance to abiotic stress in transgenic Arabidopsis overexpressing a Capsicum annuum multiprotein bridging factor 1. *BMC Plant Biol.* 14:138. doi: 10.1186/1471-2229-14-138

Guo, W. L., Wang, S. B., Chen, R. G., Chen, B. H., Du, X. H., Yin, Y. X., et al. (2015). Characterization and expression profile of CaNAC2 pepper gene. *Front. Plant Sci.* 6:755. doi: 10.3389/fpls.2015.00755

Hoser, R., Zurczak, M., Lichocha, M., Zuzga, S., Dadlez, M., Samuel, M. A., et al. (2013). Nucleocytoplasmic partitioning of tobacco N receptor is modulated by SGT1. *New Phytol.* 200, 158–171. doi: 10.1111/nph.12347

Ishii, H., Fraaije, B. A., Sugiyama, T., Noguchi, K., Nishimura, K., and Takeda, T. (2001). Occurrence and molecular characterization of Strobilurin resistance in cucumber powdery mildew and downy mildew. *Phytopathology* 91, 1166–1171. doi: 10.1094/PHYTO.2001.91.12.1166

Kitagawa, K., Skowyra, D., Elledge, S. J., Harper, J. W., and Hieter, P. (1999). SGT1 encodes an essential component of the yeast kinetochore assembly pathway and a novel subunit of the SCF ubiquitin ligase complex. *Mol. Cell.* 4, 21–33. doi: 10.1016/s1097-2765(00)80184-7

Kumar, D., and Kirti, P. B. (2015). Pathogen-induced SGT1 of Arachis diogoi induces cell death and enhanced disease resistance in tobacco and peanut. *Plant Biotechnol. J.* 13, 73–84. doi: 10.1111/pbi.12237

Lee, M. H., Lee, Y., and Hwang, I. (2013). "*In Vivo* localization in arabidopsis protoplasts and root tissue," in *G Protein-Coupled Receptor Signaling in Plants. Methods in Molecular Biology (Methods and Protocols)*, Vol. 1043, ed. M. Running (Totowa, NJ: Humana Press).

Li, A., Zhang, R., Pan, L., Tang, L., Zhao, G., Zhu, M., et al. (2011). Transcriptome analysis of H2O2-treated wheat seedlings reveals a H2O2-responsive ratty acid desaturase gene participating in powdery mildew resistance. *PLoS One* 6:e28810. doi: 10.1371/journal.pone.0028810

Li, Z., Wang, S., Tao, Q., Pan, J., Si, L., Gong, Z., et al. (2012). A putative positive feedback regulation mechanism in CsACS2 expression suggests a modified model for sex determination in cucumber (*Cucumis sativus* L.). *J. Exp. Bot.* 63, 4475–4484. doi: 10.1093/jxb/ers123

Liu, Z. Q., Liu, Y. Y., Shi, L. P., Yang, S., Shen, L., Yu, H. X., et al. (2016). SGT1 is required in PcINF1/SRC2-1 induced pepper defense response by interacting with SRC2-1. *Sci. Rep.* 6:21651. doi: 10.1038/srep21651

Meldau, S., Baldwin, I. T., and Wu, J. (2011). For security and stability: SGT1 in plant defense and development. *Plant Signal. Behav.* 6, 1479–1482. doi: 10.4161/psb.6.10.17708

Muskett, P., and Parker, J. (2003). Role of SGT1 in the regulation of plant R gene signaling. *Microbes Infect.* 5, 969–976. doi: 10.1016/s1286-4579(03)00183-7

Nanasato, Y., Konagaya, K., Okuzaki, A., Tsuda, M., and Tabei, Y. (2011). *Agrobacterium*-mediated transformation of kabocha squash (*Cucurbita moschata* Duch) induced by wounding with aluminum borate whiskers. *Plant Cell Rep.* 30, 1455–1464. doi: 10.1007/s00299-011-1054-6

Nanasato, Y., and Tabei, Y. (2015). Cucumber (*Cucumis sativus* L.) and kabocha squash (*Cucurbita moschata* Duch). (eds) *Agrobacterium* protocols. *Methods Mol. Biol.* 1223, 299–310. doi: 10.1007/978-1-4939-1695-5_24

Noël, L. D., Cagna, G., Stuttmann, J., Wirthmüller, L., Betsuyaku, S., Witte, C.-P., et al. (2007). Interaction between SGT1 and cytosolic/nuclear HSC70 chaperones regulates Arabidopsis immune responses. *Plant Cell* 19, 4061–4076. doi: 10.1105/tpc.107.051896

Peart, J. R., Lu, R., Sadanandom, A., Malcuit, I., Moffett, P., Brice, D. C., et al. (2002). Ubiquitin ligase-associated protein SGT1 is required for host and nonhost disease resistance in plants. *Proc. Natl. Acad. Sci. U.S.A.* 99, 10865–10869. doi: 10.1073/pnas.152330599

Perez-Garcia, A., Romero, D., Fernandez-Ortuno, D., Lopez-Ruiz, F., De-Vicente, A., and Tores, J. A. (2009). The powdery mildew fungus *Podosphaera fusca* (synonym *Podosphaera xanthii*), a constant threat to cucurbits. *Mol. Plant Pathol.* 10, 153–160. doi: 10.1111/j.1364-3703.2008.00527.x

Scofield, S. R., Huang, L., Brandt, A. S., and Gill, B. S. (2005). Development of a virus-induced gene-silencing system for hexaploid wheat and its use in functional analysis of the Lr21-mediated leaf rust resistance pathway. *Plant Physiol.* 138, 2165–2173. doi: 10.1104/pp.105.061861

Shen, Q. H., Zhou, F., Bieri, S., Haizel, T., and Shirasu, K. (2003). Recognition specificity and RAR1/SGT1 dependency in barley Mla disease resistance alleles to the powdery mildew fungus. *Plant Cell* 15, 732–744. doi: 10.1105/tpc.009258

Spoel, S. H., and Dong, X. (2012). How do plants achieve immunity? Defence without specialized immune cells. *Nat. Rev. Immunol.* 12, 89–100. doi: 10.1038/nri3141

Sun, H., Wu, S., Zhang, G., Jiao, C., Guo, S., Ren, Y., et al. (2017). Karyotype stability and unbiased fractionation in the paleo-allotetraploid Cucurbita genomes. *Mol. Plant* 10, 1293–1306. doi: 10.1016/j.molp.2017.09.003

Thompson, J. D., Higgins, D. G., and Gibson, T. J. (1994). CLUSTAL W: improving the sensitivity of progressive multiple sequence alignment through sequence weighting, position-specific gap penalties and weight matrix choice. *Nucleic Acids Res.* 22, 4673–4680. doi: 10.1093/nar/22.22.4673

Uppalapati, S. R., Ishiga, Y., Ryu, C. M., Ishiga, T., Wang, K., Noël, L. D., et al. (2010). SGT1 contributes to coronatine signaling and *Pseudomonas* syringae pv. Tomato disease symptom development in tomato and Arabidopsis. *New Phytol.* 189, 83–93. doi: 10.1111/j.1469-8137.2010.03470.x

Wang, K., Uppalapati, S. R., Zhu, X., Dinesh-Kumar, S., and Mysore, K. S. (2010). SGT1 positively regulates the process of plant cell death during both compatible and incompatible plant-pathogen interactions. *Mol. Plant Pathol.* 11, 597–611. doi: 10.1111/j.1364-3703.2010.00631.x

Wang, P., Liu, J. C., and Zhao, Q. Y. (2002). Studies on nutrient composition and utilization of pumpkin fruit. *J. Inner Mongolia Agric. Univ.* 23, 52–54.

Wu, T., and Cao, J. (2010). Molecular cloning and expression of a bush related CmV1, gene in tropical pumpkin. *Mol. Biol. Rep.* 37, 649–652. doi: 10.1007/s11033-009-9505-7

Xiang, J., Li, X., Yin, L., Liu, Y., Zhang, Y., Qu, J. J., et al. (2017). A candidate rxlr effector from plasmopara viticola can elicit immune responses in nicotiana benthamiana. *BMC Plant Biol.* 17:75. doi: 10.1186/s12870-017-1016-4

Xing, L., Qian, C., Cao, A., Li, Y., Jiang, Z., Li, M., et al. (2013). The Hv-SGT1 gene from Haynaldia villosa contribute to resistances towards both biotrophic and hemi-biotrophic pathogens in common wheat (*Triticum aestivum* L.). *PLoS One* 8:e72571. doi: 10.1371/journal.pone.0072571

Yadav, M., Jain, S., Tomar, R., Prasad, G. B. K. S., and Yadav, H. (2010). Medicinal and biological potential of pumpkin: an updated review. *Nutr. Res. Rev.* 23, 184–190. doi: 10.1017/S0954422410000107

Zhou, J. G., Hu, H. L., Li, X. Z., Zhou, R. J., and Zhang, H. R. (2010). Identification of a resource of powdery mildew resistance in *Cucurbita moschata*. *Acta Hortic.* 871, 141–146. doi: 10.17660/actahortic.2010.871.17

Zhu, X., Xiao, K., Cui, H., and Hu, J. (2017). Overexpression of the Prunus sogdiana NBS-LRR subgroup gene PsoRPM2 promotes resistance to the root-knot nematode meloidogyne incognita in tobacco. *Front. Microbiol.* 8:2113. doi: 10.3389/fmicb.2017.02113

Conflict of Interest Statement: The authors declare that the research was conducted in the absence of any commercial or financial relationships that could be construed as a potential conflict of interest.

Advantages of publishing in Frontiers

OPEN ACCESS
Articles are free to read for greatest visibility and readership

FAST PUBLICATION
Around 90 days from submission to decision

HIGH QUALITY PEER-REVIEW
Rigorous, collaborative, and constructive peer-review

TRANSPARENT PEER-REVIEW
Editors and reviewers acknowledged by name on published articles

Frontiers
Avenue du Tribunal-Fédéral 34
1005 Lausanne | Switzerland

Visit us: www.frontiersin.org
Contact us: info@frontiersin.org | +41 21 510 17 00

REPRODUCIBILITY OF RESEARCH
Support open data and methods to enhance research reproducibility

DIGITAL PUBLISHING
Articles designed for optimal readership across devices

FOLLOW US
@frontiersin

IMPACT METRICS
Advanced article metrics track visibility across digital media

EXTENSIVE PROMOTION
Marketing and promotion of impactful research

LOOP RESEARCH NETWORK
Our network increases your article's readership